

Sponsors



WASEDA University

Waseda University



The Committee of Battery Technology
The Electrochemical Society of Japan



Japan Association of Chemical Sensors
The Electrochemical Society of Japan

The Committee of Capacitor Technology
The Electrochemical Society of Japan

Nano and Micro Fabrication Division
The Electrochemical Society of Japan

Division of Electronics

The Surface Finishing Society of Japan

Exhibitors



Ivium Technologies



YAMAMOTO-MS



Metrohm



Tokyo Instruments

Kawaguchi Support

Kawaguchi Support

Lasertec

Lasertec Corporation



Yoshino Denka Kogyo



Hokuto Denko



Hohsen Corp



Ametek



Toyo Corp

International Society of Electrochemistry
Chemin du Closelet 2
1006 Lausanne
Switzerland

Copyright © 2018

All rights reserved. No part of this work may be reproduced, stored in a retrieval system or transmitted in any form or by any means, electronic, mechanical, photocopying, recording or otherwise, without prior written permission of the Publisher.

No responsibility is assumed by the Publisher for any injury and/or damage to persons or property as a matter of product liability, negligence or otherwise, or from any use or operation of any methods, products, instructions or ideas contained in the material herein.

Printed in Japan

Program of the
22nd Topical Meeting
of the
International Society of
Electrochemistry

Materials Engineering and Process Optimization at
Electrified Solid/Liquid Interfaces

15-18 April 2018
Tokyo, Japan

Organized by:
Division 4 Electrochemical Materials Science
Division 5 Electrochemical Process Engineering and Technology
ISE Region Japan



Organizing Committee

Mario Ferreira, *University of Aveiro, Portugal*

Takayuki Homma, *Waseda University, Japan (co-chair)*

Chi Chang Hu, *National Tsing Hua University, Taiwan*

Susumu Kuwabata, *Osaka University, Japan (co-chair)*

Sudipta Roy, *University of Strathclyde, Glasgow, UK*

Giovanni Zangari, *University of Virginia, USA*

Local Organizing Committee

Takayuki Homma, *Waseda University, Japan*

Toshiyuki Momma, *Waseda University, Japan*

Tetsuya Osaka, *Waseda University, Japan*

Masahiro Kunimoto, *Waseda University, Japan*

Table of Contents

Preliminary pages.....	i - iv
<i>Oral presentation program</i>	
Monday morning.....	2
Monday afternoon.....	3
Tuesday morning.....	15
Tuesday afternoon.....	19
Wednesday morning.....	28
Wednesday afternoon.....	34
<i>Poster presentation program</i> 41	
Session 1 on Monday	11:10 to 12:40
	s1-001 to s1-043
	s5-001 to s5-004
Session 2 on Tuesday	12:40 to 14:00
	s2-001 to s2-031
	s3-001 to s3-001
	s4-001 to s4-013
	s5-005 to s5-006
Session 3 on Wednesday	12:40 to 14:00
	s3-002 to s3-048
Index.....	65

Social Events

Sunday 15 April 2018

Okuma Garden House

17:00

Welcome Reception

Monday 16 April 2018

M. Ibuka Memorial Hall

09:30 to 09:50

Opening Ceremony

Chaired by: Takayuki Homma

Tuesday 17 April 2018

Rihga Royal Hotel Tokyo in the «Diamond Banquet Hall»

18:30

Banquet

Wednesday 18 April 2018

M. Ibuka Memorial Hall

16:20

Closing Ceremony

Monday 16 April 2018 - Morning

Keynotes

M. Ibuka Memorial Hall

Chaired by: Susumu Kuwabata

09:50 to 10:30 Keynote

Richard Alkire (Chemical and Biomolecular Engineering, University of Illinois, Urbana, USA)

Making Science Work: The Need for New Electrochemical Engineering Methods

10:30 to 11:10 Keynote

Hiroyuki Nishide (Applied Chemistry, Waseda University, Tokyo, Japan)

Redox Polymers as an Electrode-active Material

Monday 16 April 2018 - Afternoon

Materials engineering for energy devices: batteries & capacitors

M. Ibuka Memorial Hall

Chaired by: Hiroki Nara and Virginija Kepeniene

12:40 to 13:10 Invited

Stefano Passerini (Helmholtz Institute Ulm, Karlsruhe Institute of Technology, Ulm, Germany), Dominic Bresser

Nanostructures for Combined Conversion/Alloying Materials as Lithium-ion Anodes

13:10 to 13:30

Jernej Bobnar (Department of Materials Chemistry, National Institute of Chemistry, Ljubljana, Slovenia), Rémi Dedryvère, Robert Dominko, Boštjan Genorio, Gregor Kapun, Matic Lozinšek, Christian Njé

Fluorinated reduced graphene oxide as protective layer on lithium surface for batteries application

13:30 to 13:50

Motoko Nagasaki (Graduate School of Urban Environmental Sciences, Tokyo Metropolitan University, Tokyo, Japan), Kiyoshi Kanamura, Takuya Masuda, Hirokazu Munakata, Kei Nishikawa

Surface Analysis of Li metal Anode in Lithium Metal Rechargeable Battery Using $\text{Li}_4\text{Mn}_5\text{O}_{12}$ as Cathode

13:50 to 14:10

David Peralta (Battery Materials Laboratory, CEA Grenoble, Grenoble, France), Didier Bloch, Adrien Boulineau, Carole Bourbon, Jean-François Colin, Frederic Fabre, Sebastien Patoux, Jeremie Salomon

$\text{LiNi}_1/3\text{Mn}_1/3\text{Co}_1/3\text{O}_2$ submicronic particles to improve the power performances of Li-ion batteries

14:10 to 14:30

Yi-Shiuan Wu (Battery Research Center of Green Energy, Ming Chi University of Technology, New Taipei City, Taiwan)

Three-dimensional porous graphene-wrapped silicon nanoparticles composite anode with nanofiber composite PET separator for lithium-ion batteries

Materials engineering for energy devices: fuel cells & energy carriers

M. Ibuka Memorial Hall*Chaired by: Akimitsu Ishihara and Yoshitaka Aoki***14:30 to 14:50**

Shun Kobayashi (Clean Energy Research Center, University of Yamanashi, Kofu, Japan), Makoto Aoki, Junji Inukai, Teppei Kawamoto, Toshihiro Kondo, Ryo Shirasaka, Kohei Suda, Hiroyuki Uchida, Mitsuru Wakisaka
Multilateral Analyses of Pt-skin/Pt₃Co(111) Single Crystal Electrode with Extremely High Activity for the Oxygen Reduction Reaction

14:50 to 15:10

Virginija Kepeniene (Department of Catalysis, Center for Physical Sciences and Technology, Vilnius, Lithuania), Eugenijus Norkus, Raminta Stagniunaite, Loreta Tamasauskaite Tamasiunaite
Carbon Based Cobalt Catalysts for Oxygen Reduction Reaction

15:10 to 15:30

Jet-Sing Lee (iCeMS, Kyoto University, Kyoto, Japan), Satoshi Horike, Susumu Kitagawa
Alloy-Doped Carbons Derived from Porous Coordination Polymers for Oxygen Reduction Reaction

15:30 to 15:50

Coffee Break

15:50 to 16:20 Invited

Hasuck Kim (Department of Energy Science and Engineering, DGIST, Daegu, Korea), Pandian Ganesan, Sangaraju Shanmugam, Won-kyo Suh, Seunghee Woo
Preparation of Low Loading Pt Catalysts for Oxygen Reduction in Low Temperature Fuel Cells

16:20 to 16:40

Yoshiki Konno (Surface Finishing Technology Lab, Kyoto Municipal Inst. of Industrial Technology and Culture, Kyoto, Japan), Tomio Nagayama, Toshihiro Nakamura, Kaname Okura, Takayo Yamamoto
Formation of Nanoporous Spinel Ferrite Electrocatalysts by Anodizing of Electroplated Iron Alloys

16:40 to 17:00

Akimitsu Ishihara (Institute of Advanced Sciences, Yokohama National University, Yokohama, Japan), Masazumi Arao, Hideto Imai, Shunsuke Kasamatsu, Masashi Matsumoto, Koichi Matsuzawa, Shigenori Mitsushima, Takaaki Nagai, Ken-ichiro Ota, Osamu Sugino, Yoshiyuki Yamamoto

Oxygen reduction activity of titanium oxide-based compounds as non-platinum cathode for PEFCs

17:00 to 17:20

Shih-Cheng Chou (Materials Science and Engineering, National Chiao Tung University, Hsinchu, Taiwan)

Core-Shell $\text{Co}_3\text{O}_4@\text{Pt}$ on Mildly Oxidized Graphene Oxide for Oxygen Electro-Reduction in an Alkaline Electrolyte

17:20 to 17:40

Arumugam Sivanantham (Energy Science and Engineering, Daegu Gyeongbuk Institute of Science & Technology (DGIST), Daegu, Korea), Sangaraju Shanmugam

Co@NC Core-Shell as an Efficient and Ultra-Durable Oxygen Electrode in Water Electrolyzer

17:40 to 18:00

Yoshitaka Aoki (Faculty of Engineering, Hokkaido University, Sapporo, Japan), Hiroki Habazaki, Damian Kowalski

ORR activity of epitaxial and polycrystalline $\text{La}_{0.7}\text{Sr}_{0.3}\text{Mn}_{1-x}\text{Ni}_x\text{O}_3$ thin films fabricated by pulsed laser deposition

18:00 to 18:20

Xingxing Chen (School of Chemical Engineering, University of Science and Technology Liaoning, Anshan, China), Xinning Huang, Huimin Liu, Zhenjie Lu, Justus Masa, Haoran Pan, Jun Wang, Tao Wang

Earth-Abundant Coal-based Porous Carbon as the High-Performance Bi-functional Oxygen Electrocatalyst

Materials engineering for energy devices: batteries & capacitors

Room 1

Chaired by: Shuehlin Yau and Chunyu Zhu

12:40 to 13:10 Invited

Luca Magagnin (Chemistry, Materials and Chemical Engineering, Politecnico di Milano, Milano, Italy), Alessandra Accogli, Luca Magagnin
Electrochemistry of Particulate Electrodes Based on Magnetite Aggregates

13:10 to 13:30

Shuehlin Yau (Chemistry, National Central University, Taoyuan, Taiwan)
The Au(111) - Supported Pt Monolayer as the Most Active Electrocatalyst
Toward Hydrogen Oxidation and Evolution in Sulfuric Acid

13:30 to 13:50

Ove Oll (Institute of Chemistry, University of Tartu, Tartu, Estonia), Enn Lust, Ove Oll
Electroreflectance Study of Thin-film Graphite | Ionic Liquid Interface:
Electro-optics of Electrical Double-Layer and Dielectric Capacitors

13:50 to 14:10

Chunyu Zhu (Division of Applied Chemistry, Hokkaido University, Sapporo, Japan)
Exothermic reaction promoted production of hierarchical porous carbon
for electrochemical energy storage and conversion

14:10 to 14:30

Thomas Rabbow (Vienna, Austria)
Physical Chemistry of Thermal Activation and Electrochemical Reactivity
of Carbon Felts

14:30 to 14:50

Ozlem Sel (LISE (Laboratoire Interfaces et Systèmes Electrochimiques), Sorbonne Universités, UPMC University Paris 06, Paris, France), Hubert Perrot
Fast Electrogravimetric Methods for Investigating Electrode/Electrolyte
Interfaces in Electrochemical Storage Devices: Application to Nanostructured Metal Oxide Thin Films

Materials engineering for energy devices: fuel cells & energy carriers

Room 1

Chaired by: Donald Tryk and Hiroataka Sato

14:50 to 15:10

Federico Calle-Vallejo (Institute of Theoretical and Computational Chemistry, Universitat de Barcelona, Barcelona, Spain), Aliaksandr Bandarenka

Optimizing Platinum Electrocatalysts for Various Reactions by Means of Coordination-Activity Plots

15:30 to 15:50

Coffee Break

15:50 to 16:20 Invited

Aliaksandr Bandarenka (Department of Physics, Technical University of Munich, Garching, Germany)

Identification of Catalytically Active Sites at Electrode Surfaces

16:20 to 16:40

Akichika Kumatani (Advanced Institute for Materials Research, Tohoku University, Sendai, Japan), Hiroki Ida, Tomokazu Matsue, Chiho Miura, Takeru Okada, Seiji Samukawa, Hitoshi Shiku, Yasufumi Takahashi

Spatially Resolved Electrochemical Analysis for Redox Activities of Graphene/Graphite Surface Structures

16:40 to 17:00

Donald Tryk (Fuel Cell Nanomaterials Center, University of Yamanashi, Kofu, Japan), Akihiro Iiyama, Hideto Imai, Junji Inukai, Shun Kobayashi, Toshihiro Kondo, Masashi Matsumoto, Guoyu Shi, Ryo Shirasaka, Hiroyuki Uchida, Mitsuru Wakisaka, Hiroshi Yano

Recent Progress in Theoretical Understanding of Anode and Cathode Catalysts in Polymer Electrolyte Fuel Cells

17:00 to 17:20

Dongil Lee (Department of Chemistry, Yonsei University, Seoul, Korea)

Electrocatalytic Applications of Atomically Precise Metal Nanoclusters

17:20 to 17:40

Lu Gan (Surface and Interface Kinetics Group, National Institute of Materials Science, Tsukuba City, Japan), Hideyuki Murakami, Isao Saeki, Tomoyuki Yamamoto

Formation Kinetics of Co-W-based Oxides from an Electroplated Alloy Coating on a Stainless Steel

17:40 to 18:00

Hiroataka Sato (School of Mechanical and Aerospace Engineering, Nanyang Technological University, Singapore, Singapore), Kee Chun Poon, Haibin Su, Desmond Tan, Thang Vo, Jing Zhan

Facile Electrochemical Synthesis of Electrocatalysts for Fuel Cell and Electroless Plating

18:00 to 18:20

Masanori Hayase (Mechanical Engineering, Tokyo University of Science, Noda, Japan), Toshimitsu Miyauchi, Ryo Shirai, Natasa Vasiljevic

Au-Pd-Pt Catalyst for Miniature Fuel Cells with Monolithically Fabricated Si Electrodes

18:20 to 18:40

Ivar Kruusenberg (Institute of Chemistry, University of Tartu, Tartu, Estonia), Galina Dobeleva, Katlin Kaare, Eugenijus Norkus, Loreta Tamasauskaite Tamasiunaite, Aleksandrs Volperts, Aivars Zurins

Design and Manufacturing of Highly Active Wood-Derived Carbon Materials for Low Temperature Fuel Cells

Materials engineering for energy devices: batteries & capacitors

Room 2

Chaired by: Wataru Sugimoto and Sosbi Shiraishi

12:40 to 13:10 Invited

Bruce Dunn (Materials Science and Engineering, UCLA, Los Angeles, USA)
The Design of Materials for High Rate Energy Storage

13:10 to 13:30

Hubert Perrot (LISE, Sorbonne University, Paris, France), Ozlem Sel
Investigations of various capacitive/faradaic materials through multi-scale coupled methods

13:30 to 13:50

Wataru Sugimoto (Center for Energy and Environmental Science, Shinshu University, Ueda, Japan), Sho Makino, Dai Mochizuki
Lithium pre-doping from aqueous solution for hybrid supercapacitors

13:50 to 14:10

Krzysztof Fic (Institute of Chemistry and Technical Electrochemistry, Poznan University of Technology, Poznan, Poland), Elzbieta Frackowiak, Mikolaj Meller
Redox Activity of Sulphur-based Electrolytes in Supercapacitor Application

14:10 to 14:30

Nathan Keilbart (Materials Science and Engineering, The Pennsylvania State University, University Park, USA), Ismaila Dabo, Shin'ichi Higai, Yasuaki Okada
Quantum-continuum Simulations of High Power Density Oxide Electrodes for Pseudocapacitive Energy Storage

14:30 to 14:50

Da-Je Hsu (Chemical Engineering, National Tsing Hua University, Hsinchu, Taiwan), Yu-Wen Chi, Chi-Chang Hu, Kun-Ping Huang
Electrochemical activation of graphene nanowalls synthesized by plasma-enhanced chemical vapor deposition for high-voltage organic EDLCs

14:50 to 15:10

Grzegorz Lota (Institute of Chemistry and Technical Electrochemistry, Poznan University of Technology, Poznan, Poland), Andreas Bund, Lukasz Kolanowski, Jaroslaw Wojciechowski

The Influence of Current Collector Corrosion on the Performance of Electrochemical Capacitors

15:10 to 15:30

Bebi Patil (Institute of Nano Science and Technology, Hanyang University, Seoul, Korea), Suhyun Ahn, Heejoon Ahn, Youngjin Jeong, Hyeonjun Song, Seongil Yu

Ultrahigh performance of a coaxial fiber-shaped asymmetric supercapacitor based on nanostructured MnO₂/CNT-web paper and Fe₂O₃/carbon fiber electrodes

15:30 to 15:50

Coffee Break

Chaired by: David Zitoun and Torsten Wagner

15:50 to 16:20 Invited

Soshi Shiraiishi (Graduate School of Science and Technology, Gunma University, Kiryu, Japan), Yoshikiyo Hatakeyama, Hidehiko Tsukada

Highly Durable Electrochemical Capacitors Using Seamless Activated-Carbon Electrode

16:20 to 16:40

Bunsho Ohtani (Institute for Catalysis, Hokkaido University, Sapporo, Japan), Yuma Murakami, Akio Nitta, Mai Takase, Mai Takashima

Energy-resolved Density of Electron Traps as a Novel Macroscopic Measure for Characterization of Metal-Oxide Powders

16:40 to 17:00

Torsten Wagner (Institute of Nano- and Biotechnologies, FH Aachen, Juelich, Germany), Lars Breuer, Michael J. Schoening, Farnoosh Vahidpour, Rene Welden

A light-addressable lab-on-a-chip platform

17:00 to 17:20

Hoang Anh Truong (Biomedical Engineering, Tohoku University, Sendai, Japan), Koichiro Miyamoto, Carl Frederik Werner, Tatsuo Yoshinobu

Multi-well sensor platform based on a partially etched structure of light-addressable potentiometric sensor

17:20 to 17:40

Kei Murakoshi (Department of Chemistry, Faculty of Science, Hokkaido University, Sapporo, Japan), Hiro Minamimoto, Shumpei Oikawa

Ultra-Fine Tuning of Plasmonic Properties for Au Nano-Structures *via* Electrochemical Method

17:40 to 18:00

Tsubasa Ishii (Department of System and Control Engineering, Tokyo Institute of Technology, Meguro-ku, Japan), Kenji Amaya

Development of Polarization Curve Evaluation System Using Inverse Analysis

18:00 to 18:20

Stijn F.L. Mertens (Institute of Applied Physics, TU Wien, Vienna, Austria)

Quantifying and Modifying Defects in 2D Materials by Metal Underpotential Deposition

18:20 to 18:40

David Zitoun (Department of Chemistry, Bar Ilan University, Ramat Gan, Israel), Masha Alesker, Istvan Bakos, Luba Burlaka, Qingying Jia, Sanjeev Mukerjee, Meital Shviro

Direct Evidence for the Bifunctional Hydrogen Oxidation Reaction Electrocatalysis in Alkaline Medium

Materials engineering for sensing, electronic and photonic devices

Room 3

Chaired by: Chi-Chang Hu and Shigeki Kuroiwa

12:40 to 13:10 Invited

Hiroshi Nishihara (Department of Chemistry, School of Science, The University of Tokyo, Tokyo, Japan)

Interfacial Synthesis of Functional Coordination Nanosheets

13:10 to 13:30

Tony Breton (MOLTECH-Anjou UMR CNRS 6200, University of Angers, Angers, France), Marius Cesbron, Christelle Gautier, Eric Levillain

Mixed Functional Monolayers prepared from Redox Controlled Diazonium Grafting

13:30 to 13:50

Maja Budanovic (Division of Chemistry and Biological Chemistry, Nanyang Technological University, Singapore, Singapore), Dzeneta Halilovic, Surendra Mahadevegowda, Miahiela C. Stuparu, Richard D. Webster

The Enhancement of Electron-Acceptor Properties of Extended Corannulenes

13:50 to 14:10

Priscila Valverde Armas (Chemical and Process Engineering, University of Strathclyde, Glasgow, United Kingdom), Todd Green, Sudipta Roy

Electro-dissolution of Copper from a Water-containing Deep Eutectic Solvent

14:10 to 14:30

Prem Pandey (Chemistry, Indian Institute of Technology (BHU), Varanasi, India)

Synthesis and Applications of Processable Prussian Blue Nanoparticles

14:30 to 14:50

Alexander Kuhn (ENSCBP, University of Bordeaux, Pessac, France), Laurent Bouffier, Neso Sojic, Dodzi Zigah

Optimization of asymmetric particle synthesis with bipolar electrochemistry

14:50 to 15:10

Falk Muench (Department of Materials and Interfaces, Weizmann Institute of Science, Rehovot, Israel), Tatyana Bendikov, Yishay Feldman, Ronit Popovitz-Biro, Israel Rubinstein, Alexander Vaskevich

Shape-Selective Electroless Plating of High Aspect Ratio Silver Nanoplatelet Films

15:30 to 15:50

Coffee Break

Chaired by: Naoki Fukumuro and Antoine Allanore

15:50 to 16:20 Invited

Wei-Ping Dow (Chemical Engineering, National Chung Hsing University, Taichung, Taiwan), Po-Fan Chan, I.-Hsuan Chang, Shih-Cheng Chang, Yi-Yung Chen, Chun-Hsiang Lo, Wei-Yang Zeng

Advanced Electroplating Technologies for 2.5D and 3D Chip Packaging Fabrication

16:20 to 16:40

Andrew Lodge (Chemistry, University of Southampton, Southampton, United Kingdom), Richard Beanland, Ruomeng Hang, Andrew Hector, Reza Kashtiban, Samantha Soulé, Kees de Groot

Electrodeposition of porous silica templates inside lithographically defined substrates for nanofabricated devices

16:40 to 17:00

Chi-Chang Hu (Department of Chemical Engineering, National Tsing Hua University, Hsin-Chu, Taiwan), Chun-Cheng Lin

Surface morphology and microstructure control of electrodeposited copper foils for high-frequency wireless devices and Li-ion batteries

Fabrication and diagnosis processes including theoretical analyses and modeling

17:00 to 17:20

Antoine Allanore (Department of Materials Science & Engineering, MIT, Cambridge, USA), Andrew Caldwell, Bradley Nakanishi

AC-voltammetry signals during electrodeposition and gas evolution in molten salts

17:20 to 17:40

Tso-Fu Mark Chang (Institute of Innovative Research, Yokohama, Japan), Chun-Yi Chen, Yi-Hsuan Chiu, Yung-Jung Hsu, Masato Sone

Hydro-Baric Effect on Cathodic Deposition of Titanium Dioxide and Tin Dioxide

17:40 to 18:00

Remigiusz Kowalik (Faculty of Non-Ferrous Metals, Kraków, Poland), Karolina Kolczyk, Dawid Kutyla, Anna Kwiecinska, Piotr Zabinski

Electrochemical Analysis of Cobalt and Selenium Codeposition Process from Acidic Solutions

18:00 to 18:20

Krzysztof Mech (Academic Centre for Materials and Nanotechnology, AGH University of Science and Technology, Krakow, Poland), Jean Paul Chopart, Konrad Szacilowski, Mirosław Wróbel, Piotr Zabinski

Co-deposition of nickel and palladium from ammonia based bath

18:20 to 18:40

Naoki Fukumuro (Department of Chemical Engineering and Materials Science, University of Hyogo, Himeji, Japan), Yuh Fukai, Ayumu Matsumoto, Shinji Yae

Hydrogen-Induced Structural Changes in Electrodeposited Metal Films

Tuesday 17 April 2018 - Morning

Keynotes

M. Ibuka Memorial Hall

Chaired by: Toshiyuki Momma

09:30 to 10:10 Keynote

Ulrich Stimming (Chemistry, Newcastle University, Newcastle upon Tyne, United Kingdom), Oliver Schneider, Lukas Seidl

In-situ Studies of Li- and Na- Intercalation Batteries

10:10 to 10:50 Keynote

Eiichiro Matsubara (Materials Science and Engineering, Kyoto University, Kyoto, Japan)

Efforts to Develop the Innovative Batteries in the NEDO RISING 2 Project

10:50 to 11:10

Coffee Break

Materials engineering for energy devices: batteries & capacitors

M. Ibuka Memorial Hall

Chaired by: Futoshi Matsumoto and Nae-Lih Wu

11:10 to 11:40 Invited

Masayoshi Watanabe (Department of Chemistry and Biotechnology, Yokohama National University, Yokohama, Japan)

Effect of Activity of Free Solvents in Concentrated Electrolytes on Electrochemical Energy Conversion Reactions

11:40 to 12:00

Daniel Bélanger (Chimie, Université du Québec à Montréal, Montréal, Canada), Laura Coustan

Electrochemistry in superconcentrated aqueous electrolytes

12:00 to 12:20

Minoru Mizuhata (Department of Chemical Science and Engineering, Kobe University, Kobe, Japan), Hideshi Maki, Masaki Matsui, Marie Takemoto

Dynamic properties on NMR spectroscopy for LiClO₄ /PC-DME solution coexisting with fumed silica filler

12:20 to 12:40

Futoshi Matsumoto (Department of Life and Materials Chemistry, Kanagawa University, Yokohama, Japan)

Application of porous electrodes prepared with picosecond pulsed laser to lithium ion battery

Materials engineering for energy devices: fuel cells & energy carriers

Room 1

Chaired by: Eiji Higuchi and Hee-Tak Kim

11:10 to 11:40 Invited

Karel Bouzek (Department of Inorganic Technology, University of Chemistry and Technology Prague, Prague, Czech Republic), Tomas Bystron, Martin Prokop

Aspects of Phosphoric Acid Presence in High-Temperature PEM Fuel Cell with Regard to the Pt Catalyst

11:40 to 12:00

Fabian Bienen (Electrochemical Energy Technology, German Aerospace Center, Stuttgart, Germany), K. Andreas Friedrich, Elias Klemm, Dennis Kopljar, Armin Löwe, Nobert Wagner

On the applicability of the capillary rise method for determining the internal wettability of gas-diffusion electrodes

12:00 to 12:20

Tilman Jurzinsky (Applied Electrochemistry, Fraunhofer Institute for Chemical Technology ICT, Pfaffzettel, Germany), Michael Bruns, Carsten Cremers, Eduardo Daniel Gomez Villa, Julia Melke, Frieder Scheiba

Improving the electrode-electrolyte link in high-temperature polymer electrolyte membrane fuel cells by catalyst support functionalization

12:20 to 12:40

Junichiro Otomo (Department of Environment Systems, The University of Tokyo, Kashiwa, Japan), Fumihiko Kosaka, Chien-I. Li, Akio Oikawa

Electrode Design and Performance Characteristics for Ammonia Electrochemical Synthesis with Proton-Conducting Solid Electrolyte Fuel Cells

Fabrication and diagnosis processes including theoretical analyses and modeling

Room 2

Chaired by: Sho Hideshima and Yasuo Yoshimi

11:10 to 11:40 Invited

Daniel Scherson (Department of Chemistry, Case Western Reserve University, Cleveland, USA), Zhange Feng, Nicholas Georgescu, Qi Han

New Advances in Ohmic Microscopy

11:40 to 12:00

Alexander Oleinick (CNRS-ENS-UPMC, UMR8640 Pasteur, CNRS, Paris, France), Christian Amatore, Oleksii Sliusarenko, Irina Svir

Reconstruction of Nanoparticle or Electroactive Nano-Component Distributions in Electrochemical Arrays based on Chronoamperometric Data

12:00 to 12:20

Shofu Matsuda (Department of Materials Science and Technology, Nagaoka University of Technology, Nagaoka, Niigata, Japan), Yoshiki Obu, Yuuki Okuda, Minoru Umeda

Electrochemical Characteristics of Triphenylamine Derivative by Microelectrode Voltammetry

12:20 to 12:40

Georg Gorbatovski (Institute of Chemistry, University of Tartu, Tartu, Estonia), Erik Anderson, Enn Lust, Ove Oll

Specific Adsorption from an Ionic Liquid: *In Situ* STM and Impedance Study of Iodide Ion Adsorption from a Pure Halide Ionic Liquid at Bismuth Single Crystal Planes

Materials engineering for sensing, electronic and photonic devices

Room 3

Chaired by: Kazuhiro Fukami and Jan Macak

11:10 to 11:40 Invited

Mario Ferreira (Department of Materials Science and Engineering, Campus Santiago, Aveiro, Portugal), Joao Tedim, Mikhail Zheludkevich

Smart Nano/Micro-structured Coatings for Corrosion Protection, Anti-Fouling Application and Sensing

11:40 to 12:00

Chularat Wattanakit (Vidyasirimedhi Institute of Science and Technology, (VISTEC), Rayong, Thailand), Sunpet Assavapanumat, Alexander Kuhn, Veronique Lapeyre, Jumras Limtrakul, Somkiat Nokbin, Chompunuch Warakulwit, Thittaya Yutthalekha

Highly Enantioselective Electrosynthesis at Mesoporous Chiral Metal Surfaces

12:00 to 12:20

Christelle Gautier (Laboratoire MOLTECH-Anjou - UMR CNRS 6200, Université d'Angers, Angers, France), Olivier Aleveque, Sihame Bkhach, Eric Levillain

From solution to mixed self-assembled monolayers: enhancement or extinction of the properties?

12:20 to 12:40

Kazuhiro Fukami (Department of Materials Science and Engineering, Kyoto University, Kyoto, Japan), Takeshi Abe, Atsushi Kitada, Akira Koyama, Kuniaki Murase, Tetsuo Sakka

Acceleration of Ion Transport within Nanopore Caused by Confinement of Electrolyte Solution

Tuesday 17 April 2018 - Afternoon

Materials engineering for energy devices: batteries & capacitors

M. Ibuka Memorial Hall

Chaired by: Futoshi Matsumoto, and Nae-Lih Wu

14:00 to 14:20

Tokihiko Yokoshima (Research Organization of Nano and Life Innovation, Waseda University, Tokyo, Japan), Toshiyuki Momma, Hiroki Nara, Tetsuya Osaka, Taku Owada

Electrochemical Deposition Mechanism of Si-O-C Composite Anode from Propylene Carbonate Based Bath

14:20 to 14:40

Eduardo dos Santos Sardinha (Department of Chemistry, Carl-von-Ossietzky Universität Oldenburg, Oldenburg, Germany), Michael Sternad, Martin Wilkening, Gunther Wittstock

Scanning Electrochemical Microscopy Study of the Formation of Solid Electrolyte Interfaces and Lithiation on Silicon Electrodes

14:40 to 15:00

Lina Marcela Sepúlveda (Universidad de Antioquia, Medellín, Colombia), Juan Guillermo Castaño, Félix Echeverría

The Synthesis of TiO₂ Self-Ordering Nanocolumns on Al/Ti Layers by Two-Step Anodizing Process Using Etidronic Acid and Their Electrochemical Study by Cyclic Voltammetry

15:00 to 15:20

Song-Zhu S. Kure-Chu (Department of Materials Function and Design, Nagoya Institute of Technology, Nagoya, Japan), Takehiko Hihara, Nobuhiro Kawakami, Reona Miyazaki, Guoyi Tang, Hitoshi Yashiro, Yongda Ye

One-Process Fabrication of Nanostructured TiO₂-TiO-TiN/XO₂ Composite Films on Ti Foils toward High-Performance Anode Materials for Lithium Ion Batteries

15:20 to 15:40

Sayoko Shironita (Department of Materials Science and Technology, Nagaoka University of Technology, Nagaoka, Japan), Neil Ihsan, Kotaro Konakawa, Kenichi Souma, Minoru Umeda

Investigation of nitriding treated Ni-free stainless steel as current collector for 5V-class Li-ion secondary cell

15:40 to 16:00

Coffee Break

Chaired by: Minoru Mizuhata and Daniel Bélanger

16:00 to 16:20

Nae-Lih Wu (Chemical Engineering Department, National Taiwan University, Taipei, Taiwan)

Enhanced Performance of Li-Ion Battery Cathodes by Polymeric Artificial Solid-Electrolyte-Interphase Coatings

16:20 to 16:40

Jun Haruyama (CD-FMat, Advanced Industrial Science and Technology (AIST), Tsukuba, Japan), Tamio Ikeshoji, Minoru Otani

Li Insertion/Desorption Simulations at $\text{Li}_x\text{C}_6/\text{EC}$ (LiPF_6 1M) Interfaces Using Density Functional + Implicit Solvation Theory

16:40 to 17:00

Masashi Ishikawa (Department of Chemistry and Materials Engineering, Kansai University, Suita, Japan), Yukiko Matsui, Satoshi Uchida

Sulfur-Carbon Composite Electrodes and Effective Electrolytes for Rechargeable Li/S Batteries

17:00 to 17:20

Yunwen Wu (Graduate School of Advanced Science and Engineering, Waseda University, Tokyo, Japan), Toshiyuki Momma, Hiroki Nara, Tetsuya Osaka, Tokihiko Yokoshima

Potentiostatic Pre-lithiation for Preparing Lithium Sulfide Cathode

17:20 to 17:40

Sasan Ghashghaie (Department of Materials Science and Engineering, City University of Hong Kong, Hong Kong, China), Samson Ho-Sum Cheng, Jonathan Chi-Yuen Chung, Jie Fang, Robin Lok-Wang Ma, Hafiz Khurram Shahzad

Electric-Field Assisted Deposition of Carbon Nanostructures as a Binder-Free Approach to Fabricate High-Efficiency Li-S Batteries

17:40 to 18:00

Katarina Gavalierova (Dept of Physical Chemistry, Pavol Jozef Safarik University, Kosice, Slovakia), Pedro Gómez-Romero, Daniel Rueda, Andrea Straková Fedorková

Composite of S-MWCNTs-PPy-nanopipes as Cathode Material for Li-S Batteries

Materials engineering for energy devices: fuel cells & energy carriers

Room 1

Chaired by: Tilman Jurzinsky and Junichiro Otomo

14:00 to 14:20

Gumaa El-Nagar (Inst. of Chemistry and Biochemistry, Freie Berlin Universität, Berlin, Germany), Iver Lauer mann, Christina Roth

Efficient Direct Formic Acid Fuel Cells (DFAFCs) Anode Derived from Seafood Waste: Spillover Mechanism

14:20 to 14:40

Eiji Higuchi (Department of Applied Chemistry, Osaka Prefecture University, Sakai, Japan), Masanobu Chiku, Naoki Hiratsuka, Hiroshi Inoue

Preparation of Pd-deposited Spherical Ag Electrocatalysts and Their Application to Alkaline Fuel Cells

14:40 to 15:00

Hee-Tak Kim (Chemical and Biomolecular Engineering, KAIST, Daejeon, Korea)

Tuning the ionomer distribution in catalyst layer with scaling the ionomer aggregate size in dispersion for high performance PEMFC

15:00 to 15:20

Sana Ben Jadi (Chemistry, Faculty of Sciences - Ibn Zohr University, Agadir, Maroc), Zaynab Aouzal, El Arbi Bazzaoui, Mohammed Bazzaoui, Jadi, Mimouna Bouabdallaoui, Abdelqader El Guerraf, Abdelhadi El Jaouhari, Rongguang Wang

Effect of Conducting Polymers Coating on Nafion Methanol Crossover in Direct Methanol Fuel Cell (DMFC)

15:20 to 15:40

Raminta Stagniunaite (Department of Catalysis, Center for Physical Sciences and Technology, Vilnius, Lithuania), Virginija Kepeniene, Eugenijus Norkus, Loreta Tamasauskaite Tamasiunaite, Daina Upskuviene

Investigation of AuCeO₂/C as electrocatalyst for alkaline fuel cells

15:40 to 16:00

Coffee Break

Chaired by: Petr Krtil and Gumaa El-Nagar

16:00 to 16:30 Invited

Avner Rothschild (Materials Science and Engineering, Technion - Israel Institute of Technology, Haifa, Israel)

The rust challenge: Iron oxide photoelectrodes for solar water splitting

16:30 to 16:50

Petr Krtil (Low Dimension Systems, J. Heyrovsky Institute of Physical Chemistry, Prague, Czech Republic), Ivano Castelli, Ladislav Kavan, Monika Klusackova, Katerina Macounova, Roman Nebel, Jan Rossmesl

Activity and Selectivity Control of the Photo-electrochemical Behavior of Nanoparticulate n-semiconductors Based on Ti Oxides

16:50 to 17:10

Quinn Campbell (Materials Science and Engineering, The Pennsylvania State University, University Park, USA), Ismaila Dabo

Charge separation at electrified semiconductor-solution interfaces

17:10 to 17:30

Herman Kriegel (Institute of Materials Research, Helmholtz-Zentrum Geesthacht, Geesthacht, Germany), Iris Herrmann-Geppert, Thomas Klassen, Deirdre Olynick, Mauricio Schieda, Dmitriy Voronov

Effect of Structuring Geometry on the Photocurrent of Experimental Model Photoelectrode Surfaces

17:30 to 17:50

Yu-Chien Chueh (Chemical Engineering, National Cheng Kung University, Tainan, Taiwan), Chia-Yu Lin

Nanocomposite of CuBi_2O_4 and CuO as a highly efficient photocathode material for photoelectric hydrogen evolution

Fabrication and diagnosis processes including theoretical analyses and modeling

Room 2

Chaired by: Yumi Yoshida and Shofu Matsuda

14:00 to 14:20

Nelson Stradiotto (Institute of Chemistry, São Paulo State University (UNESP), Araraquara, Brazil), Daniel Rodrigues da Silva, José Luiz da Silva

Electrooxidation of polyphenols at a glassy carbon electrode modified with electrochemically reduced graphene oxide and Fe nanoparticles

14:20 to 14:40

Barbara Jachimiska (J. Haber Institute of Catalysis and Surface Chemistry, Polish Academy of Sciences, Krakow, Poland)

Self-Assembling Behavior of Proteins: Effect of the Interaction between Protein and Surface

14:40 to 15:00

Eduardo Luís Trindade da Silva (MagIC – Magnesium Innovation Centre, Helmholtz-Zentrum Geesthacht, Geesthacht, Germany), Filipe José Alves de Oliveira, Miguel Angelo Neto, Rui Ramos Ferreira e Silva, Mikhail Larionovich Zheludkevich

Boron Doped Diamond Microelectrodes as Amperometric Sensors for Studying Localized Corrosion on Mg and Mg Alloys

15:00 to 15:20

Yumi Yoshida (Faculty of Molecular Chemistry and Engineering, Kyoto Institute of Technology, Kyoto, Japan), Mao Fukuyama, Emi Kusakabe, Kohji Maeda, Yui Nakamura

Potential Stability of the Partially Oxidized Conducting Polymer-coated Electrode in Organic Phase for Application to an Amperometric Device

15:20 to 15:40

Yasuo Yoshimi (Department of Applied Chemistry, Shibaura Institute of Technology, Tokyo, Japan), Shunsuke Hayashi, Maki Seki, Rina Yamaguchi

Oil-assisted gate effect of molecularly imprinted polymer grafted directly on graphite particles in a paste electrode

15:40 to 16:00

Coffee Break

Materials engineering for sensing, electronic and photonic devices

Room 2

Chaired by: Yasushi Hasebe and Nelson Stradiotto

16:00 to 16:30 Invited

Tomokazu Matsue (Graduate School of Environmental Studies, Tohoku University, Sendai, Japan)

Nanoscale Electrochemical Imaging for Characterization of Functional Materials

16:30 to 17:00 Invited

Michael J. Schoening (Institute of Nano- and Biotechnologies (INB), FH Aachen, Juelich, Germany), Julio Arreola, Zaid Jildeh, Michael Keusgen, Jan Oberlaender, Patrick Wagner

MnO₂-based thin-film sensors for harsh environmental conditions

17:00 to 17:20

Lin-Chi Chen (Department of Bio-Industrial Mechatronics Engineering, National Taiwan University, Taipei, Taiwan), Yu-Fu Chen, Ching-Jung Yen

Electrodeposition of Polyaniline with High Hydrophobicity and Pseudo-capacitance for Multiplex Solid-contact Ion Sensing

17:20 to 17:40

Kenta Iitani (Graduate School of Medical and Dental Sciences, Tokyo Medical and Dental University, Tokyo, Japan), Takahiro Arakawa, Kohji Mitsubayashi, Koji Toma

Gas-imaging System (Sniff-cam) using NADH-dependent Alcohol Dehydrogenase for Assessment of Alcohol Metabolism

17:40 to 18:00

Yasushi Hasebe (Department of Life Science and Green Chemistry, Saitama Institute of Technology, Fukaya, Japan), Shin-ichi Seki, Yue Wang

Amperometric flow-through biosensor for uric acid using enzyme-modified carbon-felt based on oxidase and peroxidase-bi-enzyme system

Materials engineering for sensing, electronic and photonic devices

Room 3

Chaired by: Masatoshi Sakairi and Takashi Yanagishita

14:00 to 14:20

Mareike Haensch (Department of Chemistry, Carl von Ossietzky University Oldenburg, Oldenburg, Germany), Luis Balboa, Julian Behnken, Matthias Graf, Jörg Weissmüller, Gunther Wittstock

Nanoporous Gold - A Prototype for a Rational Design of Catalysts: Electrocatalysis and Transport

14:20 to 14:40

Takashi Yanagishita (Department of Applied Chemistry, Tokyo Metropolitan University, Tokyo, Japan), Masahiko Imaizumi, Toshiaki Kondo, Hideki Masuda

Preparation of Ordered Porous Alumina Spheres by Anodization of Small Al Particles

14:40 to 15:00

Shota Higashino (Graduate School of Energy Science, Kyoto University, Kyoto, Japan), Tetsuji Hirato, Takumi Ikenoue, Masao Miyake

Electrodeposition of Al-W Alloys and Surface Modification by Anodization

15:00 to 15:20

Masatoshi Sakairi (Faculty of Engineering, Hokkaido University, Sapporo, Japan), Toshiyuki Matsumoto

Fabrication of porous alumina filter by SF-MDC and etching

15:20 to 15:40

Dihia Benaoudia (ITODYS, University Paris Diderot, Paris, France),
Véronique Bennevault, Jalal Ghilane, Philippe Guégan, Jean-Christophe
Lacroix, Jérôme Mathé, Fabien Montel

Chemical nanopores modification for smart filters

15:40 to 16:00

Coffee Break

Chaired by: Ladislav Kavan and Chun-Yi Chen

16:00 to 16:20

Ladislav Kavan (Electrochemical Materials, J. Heyrovsky Institute of Physical
Chemistry, Prague, Czech Republic)

Electrochemical Characterization of Semiconducting Oxide Thin Films
for Energy Applications: Solar Cells, Fuels, Batteries and Beyond

16:20 to 16:40

Jan Macak (Center of Materials and Nanotechnologies, University of
Pardubice, Pardubice, Czech Republic), Milos Krbal, Jan Prikryl, Hanna
Sopha, Raul Zazpe

Anodic TiO₂ Nanotube Layers: Superior Photoelectrochemical Perfor-
mance due to Secondary Materials

16:40 to 17:00

Giovanni Zangari (Materials Science and Engineering, University of Virginia,
Charlottesville, USA), Rasin Ahmed

Growth of Bismuth Selenide by Electrodeposition and SILAR: Materials
for Photovoltaic and Photoelectrochemistry

17:00 to 17:20

Maryam Borghei (Bioproducts and Biosystems, Aalto University, Espoo, Finland)

Biobased aerogels of different surface charge as electrolyte interface in a quantum dot-sensitized solar cell

17:20 to 17:40

Chun-Yi Chen (Institute of Innovative Research, Tokyo Institute of Technology, Yokohama, Japan), Tso-Fu Mark Chang, Yi-Hsuan Chiu, Yung-Jung Hsu, Nobuhiro Matsushita, Mitsuo Niinomi, Kiyoshi Okada, Kazunari Ozasa, Masato Sone

Anodization of Ti-Nb-Ta-Zr-O Mixed-oxides Nanotube Arrays: A Promising Alternative Photoelectrode for Solar Conversion

Wednesday 18 April 2018 - Morning

Keynote

M. Ibuka Memorial Hall

Chaired by: Giovanni Zangari

09:30 to 10:10 Keynote

Yue Kuo (Thin Film Nano & Microelectronics Research Laboratory, Texas A&M University, College Station, USA), Noel Buckley

Electrochemical Reactions in Solid State Device Fabrication – Current and Future

Materials engineering for energy devices: batteries & capacitors

M. Ibuka Memorial Hall

Chaired by: Nathalie Herlin Boime and Kenji Kawaguchi

10:10 to 10:30

Nathalie Herlin Boime (IRAMIS, CEA CNRS UMR NIMBE, Saclay, France), John P. Alper, Pierre Bernard, Marion Chandesris, Antoine Desrues, N. Dufour, Cedric Haon

Interface Analysis of Si-based Anode in Li-ion Batteries through Electrochemical Impedance Spectroscopy and Equivalent Electrical Circuit Analysis

10:30 to 10:50

Fu-Ming Wang (Graduate Institute of Applied Science and Technology, National Taiwan University of Science and Technology, Taipei, Taiwan)

An Alternative Solution of Internal Short and Safety Problems in Lithium Ion Battery

10:50 to 11:10

Marketa Zukalova (Electrochemical Materials, J. Heyrovsky Institute of Physical Chemistry CAS, Prague, Czech Republic)

Novel synthesis of nanocrystalline $\text{Na}_2\text{Ti}_3\text{O}_7$ with improved performance for Na-ion batteries

11:10 to 11:30

Coffee Break

11:30 to 11:50

Daniel Stock (Institute of Physical Chemistry, Justus Liebig University Giessen, Giessen, Germany), Saustin Dongmo, Jürgen Janek, Daniel Schröder

Keeping anions where they belong: Increased cycling stability of zinc anodes with homogeneous anion-exchange ionomer coating

11:50 to 12:10

Ghonchek Kasiri Bidhendi (Energiespeicher- und Energiewandlersysteme, Universität Bremen, Bremen, Germany), Amir Bani Hashemi, Fabio La Mantia

Synthesis and Characterization of New Improved Copper Hexacyanoferrate Nanoparticles for Zinc-Ion Batteries

Materials engineering for energy devices: fuel cells & energy carriers

Room 1

Chaired by: Kenji Sakamaki and Piotr Zabinski

10:10 to 10:30

Kenji Sakamaki (Department of Applied Chemistry and Biochemistry, Fukushima College, National Institute of Technology, Iwaki, Fukushima, Japan), Haruka Endo, Ryoko Kato, Honoka Matsuda, Wakana Sakashita, Masataka Sato, Sayuri Usui, Ayana Watanabe

Photoelectrochemical Visible Light Zero Bias Hydrogen Generation with Membrane-Based Cells Designed for Decreasing Overall Water Electrolysis Voltage and Water Dissociation (18)

10:30 to 10:50

Roudabeh Valiollahi (Department of Science and Technology, Linköping University, Norrköping, Sweden), Xavier Crispin, Amritpal Singh, Mikhail Vagin, Igor Zozoulenko

Vapor Phase Polymerized PEDOT for Electrochemical Hydrogen Evolution Reaction

11:10 to 11:30

Coffee Break

11:30 to 11:50

Chuan Zhao (School of Chemistry, UNSW, Sydney, Australia)

Nanostructuring Earth Abundant Electrocatalysts for Water Splitting

11:50 to 12:10

Piotr Zabinski (Faculty of Non-Ferrous Metals, AGH University of Science and Technology, Krakow, Poland), Iwona Dobosz, Karolina Kolczyk, Remigiusz Kowalik, Dawid Kutyla

External Magnetic Field Assisted Electrodeposition of Co-Ru Nanorods for Water Splitting Reaction

12:10 to 12:30

Yan Shen (Wuhan National Laboratory for Optoelectronics, Huazhong University of Science and Technology, Wuhan, China), Minglei Tao, Mingkui Wang, Xin Xiao

Electronic Modulation of Transition Metal Phosphide *via* Doping as Efficient and pH-universal Electrocatalysts for Hydrogen Evolution Reaction

Materials engineering for sensing, electronic and photonic devices

Room 2

Chaired by: Takeo Hyodo and Bo Yao

10:10 to 10:30

Takeo Hyodo (Graduate School of Engineering, Nagasaki University, Nagasaki, Japan), Kai Kamada, Yasuhiro Shimizu, Mari Takamori, Taro Ueda
Potentiometric Carbon Monoxide Sensors Employing Anion-Conducting Polymer Electrolyte and Oxide-Based Sensing Electrodes

10:30 to 10:50

Deng Pan (School of Medical, Southeast University, Nanjing, China), Yanfei Shen

A Sandwiched Immunosensor for Highly Selective and Sensitive Detection of Alpha-fetoprotein by Using CdTe@SiO₂/GO Electrochemiluminescence Probe

10:50 to 11:10

Chih-Yu Lai (Bio-Industrial Mechatronics Engineering, National Taiwan University, Taipei, Taiwan), Lin-Chi Chen

EIS Detection of MUC1 with Two Symmetric Aptamer/Au Electrodes

11:10 to 11:30

Coffee Break

11:30 to 11:50

Kosuke Ino (Graduate School of Engineering, Tohoku University, Sendai, Japan), Mai Gakumasawa, Hitoshi Shiku, Mayuko Terauchi

Electrodeposition of patterned hydrogels using an LSI-based electrochemical devices for biosensing and cell culture

11:50 to 12:10

Emmanuel Iwuoha (Chemistry, SensorLab, University of Western Cape, Cape Town, South Africa), Usisipho Feleni, Laura Pacoste

Patterns in the Nanoamperometry of Breast Cancer Drug Metabolism

12:10 to 12:30

Bo Yao (Chemistry, Zhejiang University, Hangzh, China)

Sensitive Gold Electrode Biosensors Fabricated on Plastic Substrate

Development of micro to large scale reactors including process optimization and industrial applications

Room 3

Chaired by: Woonsup Shin

10:10 to 10:30

Kangwoo Cho (Division of Environmental Science and Engineering, Pohang University of Science and Technology, Pohang, Korea), Seok Won Hong, William Na

Photoelectrochemical Reactor for Degradation of Organic Compounds and Disinfection Based on Self-doped TiO₂ Nanotubes

10:30 to 10:50

Mary Elizabeth Wagner (Department of Materials Science and Engineering, Massachusetts Institute of Technology, Cambridge, USA), Antoine Allanore

Electrochemistry of Precious Metals in Molten Sulfides

10:50 to 11:10

Jaromir Hnat (Department of Inorganic Technology, University of Chemistry and Technology Prague, Prague, Czech Republic), Karel Bouzek, Roman Kodym, Jakub Rutrlé

Laboratory Zero-gap Alkaline Water Electrolyzer Stack: Development, Optimization and Mathematical Modeling

11:10 to 11:30

Coffee Break

11:30 to 11:50

Geir Martin Haarberg (Materials Science and Engineering, Norwegian University of Science and Technology, Trondheim, Norway), Babak Khalaghi, Ole Kjos, Tommy Mokkelbost

Reducing CO₂ Emissions from Aluminium Electrolysis Cells by Supplying Porous Anodes with Methane

11:50 to 12:10

Ying-Hsuan Chen (Interface Chemistry and Surface Engineering, Max-Planck-Institut fuer Eisenforschung GmbH, Dusseldorf, Germany), Andreas Erbe

The multiple roles of an organic corrosion inhibitor on copper investigated by a combination of electrochemistry-coupled optical *in situ* spectroscopies

12:10 to 12:30

Woonsup Shin (Chemistry, Sogang University, Seoul, Korea), Mijung Park

Electrochemical CO₂ to formic acid process based on dental amalgam electrode

Wednesday 18 April 2018 - Afternoon

Materials engineering for energy devices: batteries & capacitors

M. Ibuka Memorial Hall

Chaired by: Toshihiko Mandai and Alexandre Ponrouch

14:00 to 14:20

Kenji Kawaguchi (Organization for Research Initiatives and Development, Doshisha University, Kyoto, Japan), Tsukasa Gejo, Masatsugu Morimitsu
Polarization Behaviors and Cycle Performance of Air Electrode Using Water Repellent Film for Metal Hydride/Air Secondary Battery

14:20 to 14:40

Haoran Jiang (Department of Mechanical and Aerospace Engineering, The Hong Kong University of Science and Technology, Hong Kong, China), Wei Shyy, Maochun Wu, Jianbo Xu, Lin Zeng, Tianshou Zhao
Unraveling the Roles of Point Defects on Carbon Surfaces in Non-Aqueous Lithium-Oxygen Batteries

14:40 to 15:00

Tatsumi Ishihara (Department of Applied Chemistry, Faculty of Engineering, Kyushu University, Fukuoka, Japan), Shintaro Ida, Yuiko Inoishi, Takayashi Miyano
Mesoporous $\text{La}_{0.6}\text{Ca}_{0.4}\text{CoO}_3$ Perovskite Oxide for Oxygen Reduction and Oxygen Evolution Reaction for Reversible Zn-air Battery

15:00 to 15:20

Yi-Ting Lu (Chemical Engineering, National Tsing-Hua University, Hsin-Chu, Taiwan), Chi-Chang Hu
Enhanced Catalytic Performance of Ternary Spinel $\text{Fe}_x\text{Ni}_{1-x}\text{Co}_2\text{O}_4$ / Activated Carbon Composite for the Air Cathode of Rechargeable Zinc-Air Batteries

15:20 to 15:40

Sviatlana Lamaka (Department of Corrosion and Surface Technology, Magnesium Innovation Center, Helmholtz-Zentrum Geesthacht, Geesthacht, Germany)

Electrolyte Additives for Improving Performance of Primary Mg-Air Batteries

15:40 to 16:00

Toshihiko Mandai (Chemistry and Biological Sciences, Iwate University, Morioka, Japan), Mizuki Hatta, Tatsuya Takeguchi

Novel Oxygen- and Chloride-free Magnesium Salt for Magnesium Rechargeable Batteries

16:00 to 16:20

Alexandre Ponrouch (QES, ICMAB-CSIC, Bellaterra, Spain)

Electrodeposition and Development of Mg and Ca Metal Anodes

Materials engineering for energy devices: fuel cells & energy carriers

Room 1

Chaired by: Natasa Vasiljevic and Kensaku Nagasawa

14:00 to 14:20

Hiroshi Ito (Research Institute for Energy Conservation, Natl Inst of Adv Ind Sci and Tech (AIST), Tsukuba, Japan), Natsuki Kawaguchi, Tetsuo Munakata, Akihiro Nakano, Satoshi Someya

Pressurized Hydrogen Production with Anion Exchange Membrane Electrolysis

14:20 to 14:40

Natasa Vasiljevic (School of Physics, H.H. Wills Physics Lab, University of Bristol, Tyndal, Bristol, United Kingdom)

Exploiting Hydrogen-sorption for Deposition of Platinum on Palladium Films

14:40 to 15:00

Maria Valnice Boldrin Zanoni (Analytical Chemistry, UNESP, Araraquara, Brazil)

CO₂ Photoelectroreduction at TiO₂ Nanotubes Electrodes Decorated with Nanoparticle/Nanocubes Silver

15:00 to 15:20

Kensaku Nagasawa (Institute of Advanced Sciences, Yokohama National University, Yokohama, Japan), Yuta Inami, Junpei Koike, Yoshiyuki Kuroda, Shigenori Mitsushima, Ichiro Yamanaka

Electro-catalytic Performance in Toluene Hydrogenation Electrolyzer for Energy Carrier Synthesis

15:20 to 15:40

Stefan Ringe (Department of Chemical Engineering, Stanford University, Stanford, USA), Karen Chan, Jens Nørskov

Implications of Transport and pH-Effects on Electrocatalytic CO₂ Reduction

15:40 to 16:00

Dan Shan (School of Environmental and Biological Engineering, Nanjing University of Science and Technology, Nanjing, China), Wen-Li Xin

Two-dimensional porphyrin-based metal-organic frameworks: The enhanced electrocatalysis of CO₂ reduction in aqueous solution

16:00 to 16:20

Qingli Hao (School of Chemical Engineering, Nanjing University of Science and Technology, Nanjing, China), Jiawei Fan, Wu Lei, Haitao Ye

Novel Catalyst for Electroreduction of CO₂ to Ethanol

Materials engineering for energy devices: batteries & capacitors

Room 2

Chaired by: Ying-Chih Liao and Qiong Cai

14:00 to 14:20

Tatsuya Ando (International Center of Materials Nanoarchitectonics, National Institute for Materials Science, Tsukuba, Japan), Toyohiro Chikyow

Enhancement of Sensitivity and Accuracy of Aqua Droplet Detection

14:20 to 14:40

Ying-Chih Liao (Department of Chemical Engineering, National Taiwan University, Taipei, Taiwan), Bendix Ketelsen, Florian Schulz, Chun-Hao Su, Tobias Vossmeier, Mazlum Yesilmen

Highly Responsive Humidity Sensor Based on Gold Nanoparticle *via* Inkjet Printing Technology

14:40 to 15:00

Lin Zeng (HKUST Jockey Club Institute for Advanced Study, The Hong Kong University of Science and Technology, Hong Kong, China), Le Shi, Lei Wei, Jianbo Xu, Tianshou Zhao

Unravelling the Role of Oxygen-containing Functional Groups for Vanadium Electrochemistry

15:00 to 15:20

Abdulmonem Fetyan (Physical and Theoretical Chemistry, Freie Universität Berlin, Berlin, Germany), Igor Derr, Gumaa El-Nagar, Christina Roth

A Neodymium Oxide Nanoparticle-Doped Carbon Felt as Promising Electrode for Vanadium Redox Flow Batteries

15:20 to 15:40

Qiong Cai (Chemical and Process Engineering, University of Surrey, Guildford, United Kingdom)

Electrode Design for Redox Flow Batteries by Using a Three-Dimensional Multiphase Lattice Boltzmann Model

15:40 to 16:00

Matthäa Verena Holland-Cunz (Chemistry, Newcastle University, Newcastle upon Tyne, United Kingdom), Faye Cording, Robert Fleck, Jochen Friedl, Barbara Schrickler, Ulrich Stimming, Holger Wolfschmidt

Asymmetric Polyoxometalate Electrolytes for Redox Flow Batteries

16:00 to 16:20

Marcus Worsley (Physical and Life Sciences Directorate, Lawrence Livermore National Laboratory, Livermore, USA), Victor Beck, Juergen Biener, Swetha Chandrasekaran Chandrasekaran, Eric Duoss, Ryan Hensleigh, Anna Ivanovskaya, Yat Li, Tianyu Liu, Bryan Moran, Fang Qian, Yu Song, Michael Stadermann, Dan Tortorelli, Seth Watts, Todd Weisgraber, Bin Yao, Xiaoyu Zheng, Cheng Zhu

3D Printing 2D Materials-Based Electrodes for Electrochemical Energy Storage and Conversion

Materials engineering for sensing, electronic and photonic devices

Room 3

Chaired by: Kangwoo Cho and Jaromir Hnat

14:00 to 14:20

Md Zaved H. Khan (Chemistry and Chemical Engineering, Henan University, Kaifeng, China), Xiuhua Liu

Synthesis of a Novel Reduced Graphene Oxide-copper-tin (rGO-Cu-Sn) hybrid nanocomposite with Enhanced Electrochemical Performance for Modified Electrode

14:20 to 14:40

Ken-ichi Fukui (Materials Engineering Science, Graduate School Eng. Sci., Osaka University, Toyonaka, Japan), Ken-ichi Bando, Hiroo Miyamoto, Hiroaki Nato, Daijiro Okaue, Sakuroko Ono, Kouta Sakamoto, Taiki Sato, Jun Takeya, Ichiro Tanabe, Yasuyuki Yokota

Correlation between the Interfacial Structure and Carrier Mobility for Electric Double Layer - Organic FET using Ionic Liquid

14:40 to 15:00

Przemyslaw Data (Department of Physical Chemistry and Technology of Polymers, Silesian University of Technology, Gliwice, Poland), Heather Cole

Electropolymerized Xanthone-Triarylaminates for Used as TADF Emitters

15:00 to 15:20

Piret Pikma (Institute of Chemistry, University of Tartu, Tartu, Estonia), Eric Borguet, Parisa Yasini

Fabrication of Single Molecule Polycyclic Aromatic Hydrocarbon Switches at an Electrochemical Interface

15:20 to 15:40

Richard Beanland (Department of Physics, University of Warwick, Coventry, United Kingdom), Philip Bartlett, Ruomeng Huang, Reza Kashtiban, Gabriela Kissling, Kees de Groot

High-Density Ge₂Sb₂Te₅ Phase Change Memory by Electrodeposition

15:40 to 16:00

Gabriela Kissling (Physics and Astronomy, University of Southampton, Southampton, United Kingdom), Mohsin Aziz, Philip Bartlett, Andrew Hector, Gabriela Kissling, Andrew Lodge, Gill Reid, Wenjian Zhang

Electrodeposition of HgTe and related compounds from dichloromethane

16:00 to 16:20

Dongping Zhan (Chemistry, Xiamen University, Xiamen, China), Lianhuan Han, Zhong-Qun Tian, Zhao-Wu Tian

Electrochemical Micro/Nano-Machining on Semiconductor Wafers

Poster Presentations

Session 1 on Monday 11:10 to 12:40
s1-001 to s1-043
s5-001 to s5-004

Session 2 on Tuesday 12:40 to 14:00
s2-001 to s2-031
s3-001 to s3-001
s4-001 to s4-013
s5-005 to s5-006

Session 3 on Wednesday 12:40 to 14:00
s3-002 to s3-048

Materials engineering for energy devices: batteries & capacitors

s1-001**Po-Yu Chen** (Chemical Engineering, National Tsing Hua University, Hsinchu, Taiwan)

Optimization of Alkali Ion-intercalated Manganese Oxide for Asymmetric Supercapacitors

s1-002**Jie Fang** (Department of Materials Science and Engineering, City University of Hong Kong, Hong Kong, China), Samson Ho-Sum Cheng, Chi Yuen Chung, Sasan Ghoshghaie, Hafiz Khurram Shahzad, Robin Lok-Wang Ma

Electrochemical Impedance Spectroscopy Study of Lithium-Sulfur Batteries: Effects of Electrolyte/Sulfur Ratios

s1-003**Kensuke Fujiwara** (Graduate School of Engineering and Science, Shibaura Institute of Technology, Tokyo, Japan), Takahiro Ishizaki, Amane Kaneko, Hoonseung LeeEffect of Carbon-Based Cathode Materials on Charge-Discharge Performance of Aprotic Li-O₂ Battery**s1-004****Mathäa Verena Holland-Cunz** (Chemistry, Newcastle University, Newcastle upon Tyne, United Kingdom), Jochen Friedl, Ulrich Stimming

Heterogeneous and Homogenous Catalysis in an All-Vanadium Flow Battery

s1-005**Jingting Huang** (Graduate Institute of Environmental Engineering, National Taiwan University, Taipei, Taiwan), Chia-Hung HouElectrodeposited MnO₂//Polyaniline on Electrospun Carbon Nanofibers for Asymmetric Electrochemical Capacitor in Water Desalination**s1-006****Shota Inoguchi** (Department of Materials Science and Engineering, Kyoto University, Kyoto, Japan), Kazuhiro Fukami, Shota Inoguchi, Atsushi Kitada, Kuniaki Murase

HCP Metal Electrodeposition from Concentrated Aqueous Solution using a Hydrophobic Anion

s1-007**Heechan Jang** (Chemical Engineering, Tokyo Institute of Technology, Tokyo, Japan), Izumi TaniguchiSynthesis and Characterization of Carbon Modified Li₂MnP₂O₇/C Composites Prepared by Spray Pyrolysis

s1-008

Heechan Jang (Chemical Engineering, Tokyo Institute of Technology, Tokyo, Japan), Izumi Taniguchi

Synthesis and Electrochemical Characterization of Transition Metal Doped $\text{Li}_2\text{Fe}_{0.975}\text{M}_{0.025}\text{P}_2\text{O}_7/\text{C}$ (M=Co, Ni, or Cu)

s1-009

Ade Julistian (Chemical and Materials Engineering, National Chin-Yi University of Technology, Taichung, Taiwan), An-Ya Lo

Hydrothermal Synthesis of Copper Oxide and Carbon Nanotube (CuO/CNT) Nanocomposite to Enhance Supercapacitor Electrodes Performance

s1-010

Amane Kaneko (Department of Material Science and Engineering, Shibaura Institute of Technology, Tokyo, Japan), Takahiro Ishizaki, Hoonseung Lee, Camelia Miron, Yuta Wada

Electrocatalytic Activity for Oxygen Reduction Reaction of Nitrogen-containing Carbon Composites Synthesized *via* Solution Plasma Process

s1-011

Kazuki Kitta (Faculty of Science and Technology, Keio University, Yokohama, Japan), Hideto Imai, Yasushi Katayama, Tetsuo Nishida, Nobuyuki Serizawa, Naoki Tachikawa, Toshihiro Takekawa, Kazuki Yoshii

Influences of Lithium Species and Additional Cesium Ion on the Morphology of Lithium Deposited in Ionic Liquid Electrolytes

s1-012

Shinji Kondo (Department of Chemistry and Biotechnology, Yokohama National University, Yokohama, Japan), Kaoru Dokko, Shoshi Terada, Kazuhide Ueno, Masayoshi Watanabe

Effect of Divalent Cation in Highly Concentrated Aqueous Electrolytes for Li-Ion Batteries

s1-013

Na-Jung Kuo (Graduate Institute of Applied Science and Technology, National Taiwan University of Science and Technology, Taipei, Taiwan), Bing-Joe Hwang, Chun-Hong Kuo, Wei-Nien Su, Yi-Ying Tsai, Min-Hsin Yeh

Novel approaches to Synthesize S-PAN/FeS₂ Electrocatalyst for Hydrogen Evolution Reaction

s1-014

Ya-Ru Li (Chemical Engineering, Ming Chi University of Technology, New Taipei, Taiwan)

LiFePO₄/C Composite Cathode Materials with Different Types of Graphene Oxides and its Performance

s1-015

Sheng Chi Lin (Chemical Engineering, National Tsing-Hua University, Hsin-Chu, Taiwan), Chi-Chang Hu, Chen-Chi M. Ma

Asymmetric supercapacitors based on electrospun carbon nanofiber/sodium-pre-intercalated manganese oxide electrodes with high power and energy densities

s1-016

Xiaoxia Liu (Chemistry, Northeastern University, Shenyang, China), Xiang Cai, Yu Song

Partial Exfoliation of Graphite and its Integration with Pseudocapacitive Materials for Supercapacitor

s1-017

Yuta Masuda (Applied Chemistry, Waseda, Tokyo, Japan), Yasuhiro Fukunaka, Takayuki Homma, Tomohiro Otani

Effect of electrolyte flow on the evolution of microsteps during zinc electrodeposition

s1-018

Hisayoshi Matsushima (Faculty of Engineering, Hokkaido University, Sapporo City, Japan), Kei Nishikawa, Takaki Saitoh, Mikito Ueda

Application of Holographic Interferometric Microscope for Cu^{2+} Concentration Profile during Cu Electrodeposition in Magnetic Field

s1-019

Hiroki Nara (Research Organization for Nano and Life Innovation, Waseda University, Tokyo, Japan), Seongki Ahn, Toshiyuki Momma, Tetsuya Osaka, Tokihiko Yokoshima

Si-O-C powders with ultra-long cycle ability as anode materials in lithium ion batteries

s1-020

Fumihiko Nomura (Department of Life and Materials Chemistry, Kanagawa University, Yokohama, Japan)

Optimization of Calcination Temperature in Preparation of a High Capacity Li-rich Solid-Solution $\text{Li}[\text{Li}_{0.2}\text{Ni}_{0.18}\text{Co}_{0.03}\text{Mn}_{0.58}]\text{O}_2$ Material and its Cathode Performance in Lithium Ion Battery

s1-021

Ayano Ohama (Chemistry, Ochanomizu University, Bunkyo-ku, Japan), Toshihiro Kondo, Asako Niida, Kumar Sai Smaran

Pre-potential Cycling Effects of Lithium Deposition/Dissolution Processes Studied by Electrochemical Quartz Crystal Microbalance

s1-022

Yukihiro Okamoto (Chemistry and Biotechnology, Yokohama National University, Yokohama, Japan), Kaoru Dokko, Mahfuzul Hoque, Shoshi Terada, Kazuhide Ueno, Masayoshi Watanabe

N-doped Carbons Directly Synthesized from Protic Salts for Sodium Secondary Battery

s1-023

Tomohiro Otani (Department of Advanced Science and Engineering, Waseda University, Shinjuku, Japan), Yasuhiro Fukunaka, Takayuki Homma, Masato Nagata

Influences of ZnO Formation on Morphological Evolution of Zn Negative Electrode

s1-024

Habin Park (Department of Chemical Engineering, University of Seoul, Seoul, Korea), Jongwon Jung, Cheolsoo Jung, Sanghyeon Lee, Hansol Yong

Highly Thermal Stable Acetonitrile based Gel Polymer Electrolyte for 3.0 V Supercapacitor

s1-025

Satoshi Saito (Chemistry and Biotechnology, Yokohama National University, Yokohama, Japan), Tatsuhiko Horii, Yumi Kobayashi, Hisashi Kokubo, Kazumoto Miwa, Shimpei Ono, Caihong Wang, Masayoshi Watanabe

Effect of Photoisomerization Reaction in Electric Double Layer Transistor Using Photoresponsive Ionic Liquid

s1-026

Yuto Sato (Graduate School of Environmental Studies, Tohoku University, Sendai, Japan), Shinichi Komaba, Kei Kubota, Akichika Kumatani, Tomokazu Matsue, Hitoshi Shiku, Yasufumi Takahashi

Local Cyclic Voltammogram Mapping on Silicon-Carbon Composite Negative Electrodes for Lithium-ion Batteries

s1-027

Keisuke Shigenobu (Chemistry and Biochemistry, Yokohama National University, Yokohama, Japan), Kaoru Dokko, Azusa Nakanishi, Kazuhide Ueno, Masayoshi Watanabe

Redox-Active Solvate Ionic Liquids with Halide/Polyhalide Redox Couples

s1-028

Masahiro Shimizu (Materials Chemistry, Shinshu University, Nagano, Japan), Susumu Arai, Masaomi Horita, Ryosuke Yatsuzuka

Electrochemical Preparation of Roughened Current Collectors and Their Application to Sn Negative Electrode for Na-ion Batteries

s1-029

Sven Stauss (Inst. of Multidisciplinary Research for Advanced Materials, Tohoku University, Sendai, Japan), Itaru Honma, Naoki Tazawa

Investigation of Biocompatible Electrode Materials for Powering Ingestible Electronic Medical Devices

s1-030

Ulrich Stimming (Chemistry, Newcastle University, Newcastle upon Tyne, United Kingdom), Jochen Friedl

The Double Layer Capacitance of Room Temperature Ionic Liquids and the Influence of Water

s1-031

Manami Takata (Graduate School of Engineering, Hokkaido University, Hokkaido, Japan), Yoshitaka Aoki, Hiroki Habazaki, Cheong Kim, Chunyu Zhu

Nitrogen-Doped Carbon with Hierarchical Porous Structure as Electrocatalyst for Oxygen Reduction Reaction

s1-032

Pemika Teabnamang (Chemical Engineering, Chulalongkorn University, Bangkok, Thailand), Soraya Hosseini, Soorathep Kheawhom

Solid Polymer Electrolyte for Flexible Secondary Zinc-Air Batteries

s1-033

Eika Tomizawa (Chemistry, Ochanomizu University, Bunkyo-ku, Japan), Yuri Kondo, Toshihiro Kondo, Haruka Terasaki

Photo-electrochemical Characteristics of Porphyrin Containing Metal Organic Frameworks on Solid Surfaces

s1-034

Takashi Tsuda (Department of Materials and Life Chemistry, Kanagawa University, Yokohama, Japan), Nobuo Ando, Narumi Hayashi, Kaoru Itagaki, Futoshi Matsumoto, Naoto Mitsuhashi, Susumu Nakamura, Naohiko Soma, Toyokazu Tanabe

Fabrication of Porous Electrodes with a Picosecond Pulsed Laser and Improvement of the Rate Performance of a Porous Graphite Anode, LiFePO_4 and LiFePO_4 /Activated Carbon Cathodes

s1-035

Yoshiharu Uchimoto (Graduate School of Human and Environmental Studies, Kyoto University, Kyoto, Japan)

Improvement of lithium ion transportation at interface between LiFePO_4 and electrolyte by surface-nitrided treatment

s1-036

Yosuke Ugata (Department of Chemistry and Biotechnology, Yokohama National University, Yokohama, Japan), Kaoru Dokko, Shoshi Terada, Kazuhide Ueno, Daiki Watanabe, Masayoshi Watanabe, Jingjun Zhang

Highly Concentrated Mixed-Li Salt Electrolytes for High-Voltage Lithium-ion Batteries

s1-037

Koichi Ui (Department of Frontier Materials and Function Engineering, Graduate School of Engineering, Iwate University, Morioka, Japan), Toshihiko Mandai, Yushi Sato, Tatsuya Takeguchi

Analysis of Interface Behavior of Room-temperature Ionic Liquids / Air Electrodes in Lithium-Air Secondary Batteries

s1-038

Ronald Väli (Institute of Chemistry, University of Tartu, Tartu, Estonia), Meelis Härmas, Riinu Härmas, Alar Jänes, Enn Lust, Tavo Romann, Thomas Thomberg

How Sodium Storage Depends on Hard Carbon Structure?

s1-039

Jeng-An Wang (Chemical Engineering, National Tsing Hua University, Hsinchu, Taiwan)

Establishing ionic tunnels with WPU-PAAK GPE in electrode materials for supercapacitor

s1-040

Masato Yanagi (Department of Chemistry and Biotechnology, Yokohama National University, Yokohama, Japan), Ayumi Ando, Kaoru Dokko, Yoshiharu Matsumae, Azusa Nakanishi, Kenzo Obata, Kazuhide Ueno, Masayoshi Watanabe

Effect of Glyme/Li Salt Molar Ratios on Charge-Discharge Behavior of High Sulfur Loading Lithium-Sulfur Batteries

s1-041

Tien-Yu Yi (Chemical Engineering, National Tsinghua University, Hsinchu, Taiwan), Chi-Chang Hu

Graphene Electrodes Modification with an Elastic Structure by Partially Neutralized Acrylic Acid-Based Copolymer for Organic Supercapacitors

s1-042

Risa Yoshioka (Chemistry, Ochanomizu University, Bunkyo-ku, Japan), Toshihiro Kondo, Sayumi Sakai

Structural Study of Pt Ultra-thin Film on Ni Substrate Surface Prepared by Galvanic Replacement

s1-043

Ting-Hsuan You (Department of Chemical Engineering, National Tsing-Hua University, Hsinchu, Taiwan), Chi-Chang Hu

Designing binary Ru-Sn oxides with optimized performances for the air electrode of rechargeable zinc-air batteries

Materials engineering for energy devices: fuel cells & energy carriers

s2-001

Fuma Ando (Department of Materials and Life Chemistry, Kanagawa University, Yokohama, Japan)

Relationship between d-band Center of Dealloyed PtPb Ordered Intermetallic Nanoparticle Deposited on TiO₂/ Cup-Stacked Carbon Nanotube and ORR Activity in Acidic Aqueous Media

s2-002

Kornelija Antanaviciute (Department of Catalysis, Center for Physical Sciences and Technology, Vilnius, Lithuania), Arnas Naujokaitis, Eugenijus Norkus, Zita Sukackiene, Lukas Sumskas, Loreta Tamasauskaite Tamasiunaite, Jurate Vaiciuniene

Investigation of Hydrogen Generation on Cobalt-Manganese-Boron and Cobalt-Iron-Boron Catalysts from Borohydride Solution

s2-003

Kornelija Antanaviciute (Department of Catalysis, Center for Physical Sciences and Technology, Vilnius, Lithuania), Aldona Balciunaite, Arnas Naujokaitis, Eugenijus Norkus, Zita Sukackiene, Loreta Tamasauskaite Tamasiunaite, Jurate Vaiciuniene

Investigation of Electrochemical Activity of Cobalt-Manganese-Boron Catalysts Towards Ethanol and Borohydride Oxidation

s2-004

Gyeong Sook Bang (School of Electrical Engineering, KAIST, Daejeon, Korea), Sung-Yool Choi

Electrochemical characterization of solution-processed TMD thin films

s2-005

Wan-Ting Chiu (Materials Science and Engineering, Tokyo Institute of Technology, Yokohama, Japan), Tso-Fu Mark Chang, Chun-Yi Chen, Tomoko Hashimoto, Hiromichi Kurosu, Masato Sone

Co-deposition of Ni-P and P25 on Silk Textile by Supercritical CO₂ Promoted Electroless Plating for Flexible Photocatalyst Applications

s2-006

Tyler Enright (Physics, McGill University, Montreal, Canada), Connor Aiken, Peter Grutter, Aaron Mascaro, Yoichi Miyahara

Design of Combined Scanning Ion Conductance and Atomic Force Microscope Investigation of Lithium Iron Phosphate

s2-007

Atsushi Fukazawa (Graduate School of Environment and Information Sciences, Yokohama National University, Yokohama, Japan), Mahito Atobe, Yoshimasa Matsumura, Shigenori Mitsumura, Kensaku Nagasawa, Ken Takano

Electrocatalytic Hydrogenation of Toluene in a PEM Reactor: Influence of Catalyst Materials on the Process

s2-008

Ren-Hau Guo (Chemical Engineering, National Tsing Hua University, Hsinchu, Taiwan), Chi-Chang Hu

Dependence of surface adsorption status on electrode potentials for electrocatalytic reduction of CO₂ on Pd nanoparticles

s2-009

Jaromir Hnat (Department of Inorganic Technology, University of Chemistry and Technology Prague, Prague, Czech Republic), Karel Bouzek, Monika Drakselova, Michaela Plevova, Jan Zitka

Catalyst Coated Membrane for Efficient Alkaline Water Electrolysis

s2-010

Tepei Kawamoto (Fuel Cell Nanomaterials Center, University of Yamanashi, Kofu-Shi, Japan), Makoto Aoki, Junji Inukai, Taro Kimura, Takako Mizusawa, Norifumi Yamada

Distribution of Water inside Thin Nafion Film Analyzed by Neutron Reflectivity

s2-011

Virginija Kepeniene (Department of Catalysis, Center for Physical Sciences and Technology, Vilnius, Lithuania), Eugenijus Norkus, Algirdas Selskis, Loreta Tamasauskaite Tamasiunaite, Daina Upskuviene

Carbon-Supported Gold Catalysts for Ethanol Oxidation Reaction

s2-012

Hoyoung Kim (School of Integrative Engineering, Chung-Ang University, Seoul, Korea), Dong-Kwon Kim, Soo-Kil Kim, Seonhwa Oh, Hyanjoo Park

Highly Porous Non-precious Cathode Catalysts for Proton Exchange Membrane Water Electrolyzer

s2-013

Cheong Kim (Graduate School of Chemical Sciences and Engineering, Hokkaido University, Sapporo, Japan), Yoshitaka Aoki, Hiroki Habazaki, Chunyu Zhu

Nitrogen-containing Porous Carbon Electrocatalyst for Efficient Oxygen Reduction Reaction

s2-014

Ryo Kobayashi (Fuel Cell Nanomaterials Center, University of Yamanashi, Kofu, Japan), Akihiro Iiyama, Kakinuma Katsuyoshi, Makoto Uchida

Influence of Ionomer Content on Cell Performance and Load Cycle Durability of Membrane-Electrode Assemblies Using Pt/Nb-SnO₂ Cathode Catalyst Layers

s2-015

Gen Kojo (Department of Environment Systems, The University of Tokyo, Kashiwa, Japan), Yoshio Matsuzaki, Junichiro Otomo, Hiroshi Tadokoro

Evaluation of Anode-Supported Solid Oxide Fuel Cells using Lanthanum Tungstate as a Proton-Conducting Solid Electrolyte Membrane

s2-016

Tomoaki Kumeda (Graduate School of Engineering, Chiba University, Chiba, Japan), Nagahiro Hoshi, Masashi Nakamura

Interfacial Structure of Hydrophobic Cations Activating Oxygen Reduction Reaction on Pt(111) Electrode

s2-017

Dawid Kutyla (Department of Physical Chemistry and Metallurgy, AGH University of Science and Technology in Kraków, Krakow, Poland), Karolina Kolczyk, Remigiusz Kowalik, Anna Kwiecinska, Piotr Zabinski

Electrodeposition of Ni-Ru Alloys from Chloride Solutions - Morphology and Catalytic Study

s2-018

Yanyu Liang (College of Materials Science and Technology, Nanjing University of Aeronautics and Astronautics, Nanjing, China)

Controllable Construction of Core-Shell Polymer@Zeolitic Imidazolate Frameworks Fiber Derived Heteroatom-doped Carbon Nanofiber Network for Efficient Oxygen Electrocatalysis

s2-019

Kuan-Hua Liao (Chemical and Materials Engineering, National Chin-Yi University of Technology, Taichung, Taiwan), Jing-Shan Do, Ming-Liao Tsai

Glucose-oxygen Biofuel Cell Based on Anodizing Mesoporous Carbon as Support for Immobilizing Enzymes

s2-020

Andrew Lin (Department of Chemical and Materials Engineering, Chang Gung University, Taoyuan, Taiwan), Hsin-Wen Huang

Electro-catalysts used in Direct Ammonia Fuel Cell

s2-021

Momoka Nagamine (Chemistry, Adelphi University, Garden City, USA), Pawel Kryszynski, Magdalena Osial, Justyna Widera-Kalinowska

Synthesis, Photocatalytic Properties and Langmuir-Blodgett Film Photoelectrochemical Behavior of CdS and CdSe Nanoparticles of Hydrophilic or Hydrophobic Organic Shell

s2-022

Kanji Otsuji (Fuel Cell Nanomaterials Center, University of Yamanashi, Kofu, Japan), Kenji Miyatake, Manai Shimada, Makoto Uchida, Naoki Yokota, Natsumi Yoshimura

Performance Evaluation of Anion Exchange Membrane Fuel Cells Using Hydrocarbon Polymer Electrolytes

s2-023

Hyanjoo Park (School of Integrative Engineering, Chung-Ang University, Seoul, Korea), Hoyoung Kim, Dong-Kwon Kim, Soo-Kil Kim, Seonhwa Oh

Electrodeposited Pt Alloy Cathode Catalysts for High Temperature PEMFC

s2-024

Ryo Shimizu (Interdisciplinary Graduate School of Engineering, University of Yamanashi, Kofu, Japan), Alexander Eychmüller, Sebastian Henning, Juan Herranz, Katsuyoshi Kakinuma, Laura Kühn, Thomas Schmidt, Makoto Uchida

Evaluation of Unsupported Pt₃Ni Aerogels as PEFC Anode Catalysts under Hydrogen Starvation Conditions

s2-025

Miyu Shimura (Graduate School of Environmental Studies, Tohoku University, Sendai, Japan), Hiroki Ida, Akichika Kumatani, Tomokazu Matsue, Chiho Miura, Takeru Okada, Seiji Samukawa, Hitoshi Shiku, Ysufumi Takahashi

Nanoscale Electrochemical Imaging of Redox Activities on Metallic and Semiconducting Single-Walled Carbon Nanotubes

s2-026

Zita Sukackiene (Department of Catalysis, Center for Physical Sciences and Technology, Vilnius, Lithuania), Arnas Naujokaitis, Eugenijus Norkus, Loreta Tamasauskaite Tamasiunaite, Jurate Vaiciuniene

Investigation of Hydrogen Generation from Borohydride Solution on Noble-Metal-Free Cobalt Catalysts

s2-027

Zita Sukackiene (Department of Catalysis, Center for Physical Sciences and Technology, Vilnius, Lithuania), Kornelija Antanaviciute, Aldona Balciunaite, Arnas Naujokaitis, Eugenijus Norkus, Loreta Tamasauskaite Tamasiunaite, Jurate Vaiciuniene

Cobalt-Boron-Iron/Copper Catalysts for Low-Temperature Fuel Cells

s2-028

Yumi Wang (Chemistry, Chungbuk National University, Cheongju, Korea), Jongwon Kim

Effect of Nanoporous Structure and Ir Modification on Electrocatalytic Oxygen Evolution Reaction

s2-029

Yu-Ching Weng (Department of Chemical Engineering, Feng Chia University, Taichung, Taiwan), Ke-Jih Ciou

Screening of Indium Cadmium Sulfur-based Photocatalysts and Characterization of Efficient Photocatalysts

s2-030

Naohito Yamada (Graduate School of Chemical Sciences and Engineering, Hokkaido University, Sapporo, Japan), Yoshitaka Aoki, Hiroki Habazaki, Damian Kowalski, Yuki Sato, Chunyu Zhu

Improved dispersion of Co_3O_4 nanoparticles on platelet carbon nanofibers for oxygen reduction reaction

s2-031

Naoki Yoshihara (Department of Chemical Engineering, Fukuoka University, Fukuoka, Japan), Masaru Noda, Hiroki Saito

Electrochemical Reduction Reaction of Carbon Dioxide on the Exfoliated Single-Crystal Copper Membranes

Materials engineering for sensing, electronic and photonic devices

s3-001

Fethi Bedioui (Unite de Technologies Chimiques et Biologiques pour la Sante, Chimie ParisTech-PSL Research University/CNRS, Paris, France), Helene Bertrand, Vincent Ching, Marc Fontecave, Sophie Griveau, Regis Guillot, Naomi Perugio Holland, Clotilde Policar, Cyrine Slim, Xia Wang

Rhenium Complexes Based on 2-Pyridyl-1,2,3-Triazole Ligands: a New Class of CO₂ Reduction Catalysts

s3-002

Sana Ben Jadi (Chemistry, Faculty of Sciences - Ibn Zohr University, Agadir, Maroc), Zaynab Aouzal, El Arbi Bazzaoui, Mohammed Bazzaoui, Mimouna Bouabdallaoui, Abdelqader El Guerraf, Abdelhadi El Jaouhari, Rongguang Wang

Non-Polluting Process for Plastic Metallization

s3-003

Maria Valnice Boldrin Zanoni (Analytical Chemistry, UNESP, Araraquara, Brazil)

Electrochemically Gating of Low Molecular Weight Analytes through Self-Doped TiO₂ Nanotubes

s3-004

Po-Yu Chen (Medicinal and Applied Chemistry, Kaohsiung Medical University, Kaohsiung, Taiwan), Yi-An Shao

Voltammetric Study and Electrodeposition of Copper with Electrocatalytic Activity to Nitrate Reduction from a Hydrophobic Brønsted Acidic Amide-Type Ionic Liquid Using Copper Oxides as the Copper Source

s3-005

Jou Hsuan Chu (Bio-Industrial Mechatronics Engineering, National Taiwan University, Taipei, Taiwan), Lin-Chi Chen

Functionalized Conducting Polymer Electrodes for Cardiac Troponin I Aptasensor Fabrication

s3-006

Loanda R. Cumba (School of Chemical Sciences, Dublin City University, Dublin, Ireland), Craig Banks, Robert Forster

Mechanical Activation by Polishment of Screen-Printed Electrodes

s3-007

Przemyslaw Data (Department of Physical Chemistry and Technology of Polymers, Silesian University of Technology, Gliwice, Poland), Piotr Pander, Marharyta Vasylieva

Electrochemical and Spectroelectrochemical Analysis of Pyridine Derivatives as Materials for Optoelectronic Applications

s3-008

Asuka Hayashi (Applied Chemistry, Waseda University, Tokyo, Japan), Takayuki Homma, Masahiro Kunimoto, Yuta Sato, Masahiro Yanagisawa

Development of Silica Microlens Array Sensor for *in situ* SERS Analysis of Electrode Reaction Processes

s3-009

Li-Cheng Ho (Bio-Industrial Mechatronics Engineering, National Taiwan University, Taipei, Taiwan), Lin-Chi Chen, Chi-Han Lu

Effects of Anion Doping on the Surface Hydrophobicity and Pseudo-capacitance of a Poly(3,4-ethylenedioxythiophene) Solid Contact

s3-010

Jong-In Hong (Department of Chemistry, Seoul National University, Seoul, Korea)

Electrochemiluminescent Chemodosimetric Sensors for Selective Detection of Homocysteine

s3-011

Huan-Ping Jhong (Department of Chemical Science and Technology, Tokushima University, Tokushima, Japan), Wei-Hung Chiang, Yusuke Fuchiwaki, Toshihiko Harada, Shunsuke Isoai, Masashi Kurashina, Masahiro Uchimaru, Chen-Hao Wang, Mikito Yasuzawa

Immobilization of Nanocarbons and Glucose Oxidase by Electrodeposition Method for Glucose Sensor Fabrication

s3-012

Mana Kambe (Department of Applied Chemistry, Waseda University, Tokyo, Japan), Shogo Hashimoto, Takayuki Homma, Siggı Wodarz, Giovanni Zangari

Analysis of Electrodeposition Process of $L1_0$ -Ordered FePtCu Nanodot Arrays

s3-013

Yuka Kashimata (Applied Chemistry, Waseda University, Tokyo, Japan), Takayuki Homma, Masahiro Kunimoto, Yuta Sato, Masahiro Yanagisawa

Fabrication of plasmon sensor with Ag@TiO₂ core-shell nanoparticles for surface-enhanced Raman scattering

s3-014

Chang Su Kim (Advanced Functional Thin Films Department, Korea Institute of Materials Science, Changwon, Korea)

Silver nanowire based flexible electrodes with improved optical properties

s3-015

Karolina Kolczyk (Faculty of Non-Ferrous Metals, University of Science and Technology, Krakow, Poland), Remigiusz Kowalik, Dawid Kutyla, Anna Kwiecinska, Piotr Zabinski, Wojciech Zborowski

Metallization of 3D prints by magnetic coatings in electroless and electro-deposition processes

s3-016

Masato Komoda (Department of Pure and Applied Chemistry, Faculty of Science, Tokyo University of Science, Noda, Japan), Yoshinao Hoshi, Masayuki Itagaki, Isao Shitanda

Fabrication of Fully Screen-printed Reference Electrode using Silica Gel Inks

s3-017

Kohei Kumagai (Engineering, Osaka University, Osaka, Japan)

Developments of novel semiconductor nanoparticles stabilized with metal-organic frameworks (MOFs)

s3-018

Shigeki Kuroiwa (Research Organization for Nano and Life Innovation, Waseda University, Tokyo, Japan), Sho Hideshima, Katsunori Horii, Naoto Kaneko, Hiroataka Minagawa, Toshiyuki Momma, Takuya Nakanishi, Keishi Ohashi, Tetsuya Osaka, Ryota Takibuchi, Iwao Waga

Detection of Mental Stress Biomarker by Aptamer-Immobilized Field-Effect Transistor Sensor

s3-019

Hsin-Yi Lee (Scientific Research Division, National Synchrotron Radiation Research Center, Hsinchu, Taiwan), Jenh-Yih Juang, Man-Ling Lin

High mobility transparent conductive Al-doped ZnO thin films grown by atomic layer deposition

s3-020

Kwan Hyi Lee (Center for Biomaterials, KIST, Seoul, Korea), Jungmok Seo, Tae Wha Seong

Electrochemical Sensing of Cathepsin L Activity *via* H3-functionalized Biosensor

s3-021

Nai-Chang Lo (Department of Chemistry, National Cheng Kung University, Tainan, Taiwan), I.-Wen Sun

One-Pot Fabrication of Nanoporous Pd-Au *via* Electrochemical Alloying/Dealloying in Chlorozincate Ionic Liquid

s3-022

Ko-Ichiro Miyamoto (Department of Electronic Engineering, Tohoku University, Sendai, Japan), Daisuke Suzuki, Shigeyasu Uno, Carl Frederik Werner, Yuhki Yanase, Tatsuo Yoshinobu

Visualization of the barrier function of an epithelial cell layer by chemical imaging sensor and its future application

s3-023

Tadashi Mori (Dept Applied Chemistry, School of Advanced Engineering, Kogakuin University, Nakano, Hachioji, Japan), Hidetaka Asoh, Hideki Hashimoto

Formation of Porous Alumina Films by DC-Bipolar Anodization

s3-024

Yusuke Muramatsu (Department of Applied Chemistry, Kogakuin University, Nakano, Hachioji, Japan), Hidetaka Asoh, Hideki Hashimoto

Influence of Electrolysis Conditions on Anodic Exfoliation of Graphite in Sulfuric Acid

s3-025

Asep Sugih Nugraha (Nanoscience and Nanoengineering, Waseda University, Tokyo, Japan), Toru Asahi, Yusuke Yamauchi

Electrochemical Synthesis of Mesoporous Gold-Copper Alloy Films with Vertical Mesochannels

s3-026

Aditya Febry Nurpratama (Chemical and Materials Engineering, National Chin-Yi University of Technology, Taichung, Taiwan), Jing-Shan Do, Ming-Liao Tsai

Highly Sensitive Amperometric Formaldehyde Gas Sensor Based on Nafion®/Pt/Au/Al₂O₃ Electrode: Optimizing Electrode Preparation

s3-027

Yusuke Onabuta (Department of Applied Chemistry, Waseda University, Tokyo, Japan), Takayuki Homma, Masahiro Kunimoto, Hiromi Nakai

First-Principles Study of Reaction Mechanism of Reducing Agents on Ni and Cu in Electroless Deposition Processes

s3-028

Hao-Jen Pai (School of Engineering, Tohoku University, Sendai, Japan),
Kosuke Ino, Takehiro Onodera, Hitoshi Shiku

Respiration Assay of Co-culture Cell Spheroid Using an LSI-based Electrochemical Device

s3-029

Sandra Pluczyk (Department of Physical Chemistry and Technology of Polymers, Silesian University of Technology, Gliwice, Poland), Przemyslaw Data, Heather Higginbotham, Satoshi Minakata, Youhei Takeda

Electrochemical and Spectroelectrochemical Properties of Phosphorus-Containing Organic Materials

s3-030

Hiroyuki Saito (Mechanical Engineering, Tokyo Denki University, Tokyo, Japan)

Measurement of Tin Oxide Thickness with Sequential Electrochemical Reduction Analysis

s3-031

Junji Sasano (Department of Mechanical Engineering, Toyohashi University of Technology, Toyohashi, Japan), Masanobu Izaki, Yuya Kojima, Kentaro Nishiyama, Takuya Sakai, Seiji Yokoyama

Anodic Electrodeposition of Tungsten Oxide Hydrate Films from Tungstate-Citrate Complex Solutions

s3-032

Michael J. Schoening (Institute of Nano- and Biotechnologies (INB), FH Aachen, Juelich, Germany), Melanie Jablonski, Claudia Koch, Arshak Poghossian, Christina Wege

TMV nanoparticles as enzyme carriers for biosensor applications

s3-033

Minji Seo (Department of Chemistry, Chungbuk National University, Cheongju, Korea), Jongwon Kim

Determination of As(III) at Nanoporous Gold Electrode by Square Wave Voltammetry

s3-034

Yanyan Song (Department of Chemistry, Northeastern University, Shenyang, China), Zhida Gao, Xiaoxia Jian, Yongfang Qu

Au@g-C₃N₄ Decorated TiO₂ Nanotube Arrays: Visible-Light Triggered Photoelectrochemical Platforms for H₂O₂ Sensing

s3-035

Misaki Sugie (Applied Chemistry, Waseda University, Tokyo, Japan),
Takayuki Homma, Mikiko Saito, Hidefumi Takahashi, Ichiro Terasaki

Effect of Metal Additives on Electrodeposited Bi-Sb-Te Films for Micro
Thermoelectric Devices

s3-036

Chia-Liang Sun (Department of Chemical and Materials Engineering, Chang
Gung University, Taoyuan, Taiwan), Chia-Heng Kuo, Cheng-Hsuan Lin

Synthesis of Graphene Oxide Nanoribbons and Their Photoelectrochemi-
cal Measurements

s3-037

Yuichi Takasaka (Department of Chemical Engineering and Materials
Science, University of Hyogo, Himeji, Japan), Ryo Fujii, Naoki Fukumuro,
Kotaro Higashi, Ayumu Matsumoto, Susumu Sakamoto, Shinji Yae

Effects of Atomic Diffusion on Electroless Ni-P Film/Epitaxial Gold Na-
noparticles/Silicon Wafer Interface

s3-038

Jeerakit Thangphatthanarungruang (Chemistry, Srinakharinwirot
University, Bangkok, Thailand), Chuleekorn Chotsuwan, Rawiwan
Laocharoensuk, Aroonsri Ngamaroonchote, Weena Siangproh

A Novel Graphene/Nafion Screen-Printed Electrode for the Simultaneous
Determination of Fat-Soluble Vitamins by Square-Wave Voltammetry

s3-039

Priscila Valverde Armas (Chemical and Process Engineering, University of
Strathclyde, Glasgow, United Kingdom), Todd Green, Sudipta Roy

Effect of Water on Cu Electrodeposition from a Water-containing Deep
Eutectic Solvent

s3-040

Torsten Wagner (Institute of Nano- and Biotechnologies, FH Aachen,
Juelich, Germany), Michael J. Schoening, Patrick Wagner, Rene Welden

Fabrication and evaluation of light-addressable electrodes for the integra-
tion in lab-on-a-chip systems

s3-041

Guang-Ren Wang (Materials Science and Engineering, National Chiao Tung
University, Hsinchu, Taiwan), Pei-Sung Hung

Three-Dimensional Ordered Macro/Meso Porous Composite Materials in
Electrode Array Configuration for Gas Sensing Applications

s3-042

Mengyun Wang (Electronic Engineering, Tohoku University, Sendai, Japan), Koichiro Miyamoto, Hoang Anh Truong, Carl Frederik Werner, Tatsuo Yoshinobu

Gas-Imaging Sensor Based on Metal Oxide and Field Effect Structure

s3-043

Yu-Ching Weng (Department of Chemical Engineering, Feng Chia University, Taichung, Taiwan), Wei Peng

Bimetallic Pt-based Sensor for Oxygen Detection

s3-044

Fu-Ren Xiao (Department of Chemical Engineering, National Taiwan University, Taipei, Taiwan), Ying-Chih Liao, Chun-Hao Su

Porous Nanocomposite for Highly Sensitive Pressure Sensor

s3-045

Ying-Fang Xu (Chemical and Materials Engineering, National Chin-Yi University of Technology, Taichung, Taiwan), Jing-shan Do, Ming-Liao Tsai

Solid-state Planar Amperometric CO Gas Sensor Based on Nafion®/Porous Pd/Au(Sputtering)/Al₂O₃

s3-046

Jia-De Yan (Department of Bio-Industrial Mechatronics Engineering, National Chung Hsing University, Taichung, Taiwan), Yu-Fen Kuo, Ching-Chou Wu

Development of Third Generation Glucose Biosensors Based on Organic Metal Particles of *in Situ* Synthesis

s3-047

Tetsuya Yasuda (Applied Chemistry, Waseda University, Tokyo, Japan), Takayuki Homma, Masahiro Kunimoto, Futa Yamaguchi, Masahiro Yanagisawa

In-situ analysis for interaction of additives for electrodeposition in through silicon *via* using surface enhanced Raman scattering

s3-048

Koichiro Yoshitoku (Applied Chemistry, Waseda, Tokyo, Japan), Takayuki Homma, Hinako Matsuo, Mikiko Saito, Hidefumi Takahashi, Ichiro Terasaki

Morphology Control of Electrodeposited ZnO Patterns for Micro Thermoelectric Devices

Fabrication and diagnosis processes including theoretical analyses and modeling

s4-001

Chun-Hsien Chen (Department of Chemistry, National Taiwan University, Taipei, Taiwan), Ching-Hwa Ho, Er-Chien Horng, Han Hsiao, Hsu-Fu Hsu, Wei-Ling Hua, Chih-Hsun Lin, Geng-Min Lin, Tsai-Hui Wang, Wei-Chen Yen
Electrochemical Mapping of Transmission Spectra for Electron Transporting through Single-Molecule Junctions

s4-002

Yu-Sheng Chuang (Department of Bio-Industrial Mechatronics Engineering, National Chung Hsing University, Taichung, Taiwan), Ching-Chou Wu, Hao-Yu Yen
Electrochemical Impedance Spectroscopy for Detection of Single Nucleotide Polymorphism by Using S1 Nuclease

s4-003

Ronggui Du (Department of Chemistry, Xiamen University, Xiamen, China), Zichao Guan, Haipeng Wang, Xia Wang
Fabrication of Ag/SnO₂/TiO₂ Nanotube Films for Photoelectrochemical Cathodic Protection of Stainless Steel

s4-004

Ken Hashigata (Materials Science and Engineering, Tokyo Institute of Technology, Yokohama, Japan), Tso-Fu Mark Chang, Chun-Yi Chen, Toshifumi Konishi, Katsuyuki Machida, Kazuya Masu, Masato Sone, Haochun Tang, Daisuke Yamane
Electroplating of Gold on Titanium Substrate: Method to Deposit Defect-Free Film

s4-005

Takeshi Kinoshita (Department of Chemical Engineering and Materials Science, University of Hyogo, Himeji, Japan), Naoki Fukumuro, Ayumu Matsumoto, Shinji Yae, Ayano Yokoyama
Analysis of Hydrogen Adsorption and Incorporation during Electrodeposition of Platinum Films

s4-006

Mikiko Saito (Research Organization for Nano and Life Innovation, Waseda University, Tokyo, Japan), Hidemichi Fujiwara, Takayuki Homma, Tomohiro Ishii
Effect of Supporting Electrolyte on Electrochemical Production of Cu Nanoparticles

s4-007

Tomoya Sasaki (Graduate School of Engineering, Osaka University, Suita-shi, Yamadaoka, Japan), Susumu Kuwabata, Tsukasa Torimoto, Tetsuya Tsuda, Taro Uematsu

Real-time observation of Au nanoparticles formation process using ionic liquid-sputtering method

s4-008

Yuta Suzuki (Science of Environment and Mathematical Modeling, Doshisha University, Kyotanabe, Japan), Yasuhiro Fukunaka, Takuya Goto, Yoshihide Sakanaka

Electrodeposition of Li at Propylene Carbonate / Ga(l) Interface

s4-009

Irina Svir (Chemistry, Ecole Normale Supérieure, Paris, France), Christian Amatore, Alexander Oleinick

Two Important Examples of Accurate Simulation of Complex Electrochemical Problems by KISSA-software

s4-010

Haochun Tang (Innovative Institute of Research, Tokyo Institute of Technology, Yokohama, Japan), Tso-Fu Mark Chang, Chun-Yi Chen, Toshifumi Konishi, Katsuyuki Machida, Kazuya Masu, Masato Sone, Daisuke Yamane

Pulse Current Electrodeposition of Ultrahigh Strength Nanocrystalline Au-Cu Alloys

s4-011

Kohei Watanabe (Graduate School of Engineering and Science, Shibaura Institute of Technology, Tokyo, Japan)

Corrosion Resistance of Boehmite Based Films Prepared on Al-Mg-Si Alloy by Steam Coating

s4-012

Carl Frederik Werner (Department of Electronic Engineering, Tohoku University, Sendai, Japan), Koichiro Miyamoto, Michael J. Schöning, Torsten Wagner, Tatsuo Yoshinobu

Effect of light intensity towards the signal of a light-addressable potentiometric sensor

s4-013

Takahiro Yamamoto (Materials Science and Engineering, Tokyo Institute of Technology, Yokohama, Japan), Tso-Fu Mark Chang, Chun-Yi Chen, Toshifumi Konishi, Katsuyuki Machida, Kazuya Masu, Masato Sone, Daisuke Yamane

Effects of Current Density on Mechanical Properties of Electroplated Nickel with High Speed Sulfamate Bath

Development of micro to large scale reactors including process optimization and industrial applications

s5-001

Daisuke Baba (School of Advanced Science and Engineering, Tsukuba, Japan), Toru Asahi, Yusuke Yamauchi

Electrochemical Synthesis of Mesoporous Nickel Films by Using Polymeric Micelles

s5-002

Kangwoo Cho (Division of Environmental Science and Engineering, Pohang University of Science and Technology, Pohang, Korea), Chong Min Chung, Kazuo Yamamoto

Fouling Behavior of Electrooxidation-membrane Bioreactor (EO-MBR) Coupled with Non-woven Fabric prefiltration

s5-003

Yuki Maeda (Department of Materials Science and Engineering, Kyoto University, Kyoto, Japan), Kazuhiro Fukami, Tatsuya Hinoki, Atsushi Kitada, Sosuke Kondo, Kuniaki Murase

Corrosion Behavior of 3C-SiC with Irradiation-Induced Defects

s5-004

Yutaro Norikawa (Institute of Advanced Energy, Kyoto University, Uji, Japan), Tomoyuki Awazu, Masatoshi Majima, Toshiyuki Nohira, Koma Numata, Kouji Yasuda

Electrodeposition of Ti Films in Water-Soluble KF-KCl Molten Salt

s5-005

Risako Tanii (Faculty of Engineering, Hokkaido University, Sapporo, Japan), Hisayoshi Matsushima, Ryota Ogawa, Mikito Ueda

Measurement of Deuterium Isotope Separation Factor By Combined Electrolysis Fuel Cell

s5-006

Jiachao Yao (College of Environment, Zhejiang University of Technology, Hangzhou, China), Jiade Wang

Simultaneous Removal of COD and Total Nitrogen for Wastewater Treatment Using Electrochemical Method

Index

A

- Abe, Takeshi, (*Tue s4*)12:20
 Accogli, Alessandra, (*Mon s1*)12:40
 Ahmed, Rasin, (*Tue s3*)16:40
 Ahn, Heejoon, (*Mon s1*)15:10
 Ahn, Seongki, *s1-019*
 Ahn, Suhyun, (*Mon s1*)15:10
 Aiken, Connor, *s2-006*
 Alesker, Masha, (*Mon s4*)18:20
 Aleveque, Olivier, (*Tue s3*)12:00
 Alkire, Richard, (*Mon 00*)09:50
 Allanore, Antoine, (*Mon s4*)17:00, (*Wed s5*)10:30
 Alper, John P., (*Wed s1*)10:10
 Alves de Oliveira, Filipe José, (*Tue s4*)14:40
 Amatore, Christian, (*Tue s4*)11:40, *s4-009*
 Amaya, Kenji, (*Mon s4*)17:40
 Anderson, Erik, (*Tue s4*)12:20
 Ando, Ayumi, *s1-040*
 Ando, Fuma, *s2-001*
 Ando, Nobuo, *s1-034*
 Ando, Tatsuya, (*Wed s3*)14:00
 Antanaviciute, Kornelija, *s2-002*, *s2-003*, *s2-027*
 Antanaviciute, Kornelija
 Aoki, Makoto, (*Mon s2*)14:30, *s2-010*
 Aoki, Yoshitaka, *s1-031*, (*Mon s2*)17:40, *s2-013*, *s2-030*
 Aouzal, Zaynab, (*Tue s2*)15:00, *s3-002*
 Arai, Susumu, *s1-028*
 Arakawa, Takahiro, (*Tue s3*)17:20
 Arao, Masazumi, (*Mon s2*)16:40
 Arreola, Julio, (*Tue s3*)16:30
 Asahi, Toru, *s3-025*, *s5-001*
 Asoh, Hidetaka, *s3-023*, *s3-024*
 Assavapanumat, Sunpet, (*Tue s3*)11:40
 Atobe, Mahito, *s2-007*
 Awazu, Tomoyuki, *s5-004*
 Aziz, Mohsin, (*Wed s3*)15:40
- B
- Baba, Daisuke, *s5-001*
 Bakos, Istvan, (*Mon s4*)18:20
 Balboa, Luis, (*Tue s3*)14:00
 Balcuinaite, Aldona, *s2-003*, *s2-027*
 Bandarenka, Aliaksandr, (*Mon s2*)14:50, (*Mon s2*)15:50
 Bando, Ken-Ichi, (*Wed s3*)14:20
 Bang, Gyeong Sook, *s2-004*
 Bani Hashemi, Amir, (*Wed s1*)11:50
 Banks, Craig, *s3-006*
 Bartlett, Philip, (*Wed s3*)15:20, (*Wed s3*)15:40
 Bazzaoui, El Arbi, (*Tue s2*)15:00, *s3-002*
 Bazzaoui, Mohammed, (*Tue s2*)15:00, *s3-002*
 Beanland, Richard, (*Mon s3*)16:20, (*Wed s3*)15:20
 Beck, Victor, (*Wed s1*)16:00
 Bedioui, Fethi, *s3-001*
 Behnken, Julian, (*Tue s3*)14:00
 Bélanger, Daniel, (*Tue s1*)11:40
 Ben Jadi, Sana, (*Tue s2*)15:00, *s3-002*
 Benaoudia, Dihia, (*Tue s3*)15:20
 Bendikov, Tatyana, (*Mon s3*)14:50
 Bennevault, Véronique, (*Tue s3*)15:20
 Bernard, Pierre, (*Wed s1*)10:10
 Bertrand, Helene, *s3-001*
 Bienen, Fabian, (*Tue s2*)11:40
 Biener, Juergen, (*Wed s1*)16:00
 Bkhach, Sihame, (*Tue s3*)12:00
 Bloch, Didier, (*Mon s1*)13:50
 Bobnar, Jernej, (*Mon s1*)13:10
 Boldrin Zaroni, Maria Valnice, (*Wed s2*)14:40, *s3-003*
 Borghei, Maryam, (*Tue s3*)17:00
 Borguet, Eric, (*Wed s3*)15:00
 Bouabdallaoui, Mimouna, (*Tue s2*)15:00, *s3-002*
 Bouffier, Laurent, (*Mon s3*)14:30
 Boulineau, Adrien, (*Mon s1*)13:50
 Bourbon, Carole, (*Mon s1*)13:50
 Bouzek, Karel, (*Tue s2*)11:10, (*Wed s5*)10:50, *s2-009*
 Bresser, Dominic, (*Mon s1*)12:40
 Breton, Tony, (*Mon s3*)13:10
 Bruns, Michael, (*Tue s2*)12:00
 Buckley, Noel, (*Wed*)09:30

Budanovic, Maja, (*Mon s3*)13:30
 Bund, Andreas, (*Mon s1*)14:50
 Burlaka, Luba, (*Mon s4*)18:20
 Bystron, Tomas, (*Tue s2*)11:10

C

Cai, Qiong, (*Wed s1*)15:20
 Cai, Xiang, *s1-016*
 Caldwell, Andrew, (*Mon s4*)17:00
 Calle-Vallejo, Federico, (*Mon s2*)14:50
 Campbell, Quinn, (*Tue s2*)16:50
 Castaño, Juan Guillermo, (*Tue s1*)14:40
 Castelli, Ivano, (*Tue s2*)16:30
 Cesbron, Marius, (*Mon s3*)13:10
 Chan, Karen, (*Wed s2*)15:20
 Chan, Po-Fan, (*Mon s3*)15:50
 Chandesris, Marion, (*Wed s1*)10:10
 Chandrasekaran, Swetha Chandrasekaran,
 (*Wed s1*)16:00
 Chang, I.-Hsuan, (*Mon s3*)15:50
 Chang, Shih-Cheng, (*Mon s3*)15:50
 Chang, Tso-Fu Mark, (*Mon s4*)17:20, (*Tue s3*)17:20, *s2-005, s4-004, s4-010, s4-013*
 Chen, Chun-hsien, *s4-001*
 Chen, Chun-Yi, (*Mon s4*)17:20, (*Tue s3*)17:20, *s2-005, s4-004, s4-010, s4-013*
 Chen, Lin-Chi, (*Tue s3*)17:00, (*Wed s3*)10:50, *s3-005, s3-009*
 Chen, Po-Yu, *s1-001, s3-004*
 Chen, Xingxing, (*Mon s2*)18:00
 Chen, Yi-Yung, (*Mon s3*)15:50
 Chen, Ying-Hsuan, (*Wed s5*)11:50
 Chen, Yu-Fu, (*Tue s3*)17:00
 Cheng, Samson Ho-Sum, (*Tue s1*)17:20, *s1-002*
 Chi, Yu-Wen, (*Mon s1*)14:30
 Chiang, Wei-Hung, *s3-011*
 Chiku, Masanobu, (*Tue s2*)14:20
 Chikyow, Toyohiro, (*Wed s3*)14:00
 Ching, Vincent, *s3-001*
 Chiu, Wan-Ting, *s2-005*
 Chiu, Yi-Hsuan, (*Mon s4*)17:20, (*Tue s3*)17:20
 Cho, Kangwoo, (*Wed s5*)10:10, *s5-002*
 Choi, Sung-Yool, *s2-004*
 Chopart, Jean Paul, (*Mon s4*)18:00
 Chotsuwan, Chuleekorn, *s3-038*
 Chou, Shih-Cheng, (*Mon s2*)17:00

Chu, Jou Hsuan, *s3-005*
 Chuang, Yu-Sheng, *s4-002*
 Chung, Chong Min, *s5-002*
 Chung, Jonathan Chi-Yuen, (*Tue s1*)17:20,
 (*Tue s2*)17:30, *s1-002*
 Ciou, Ke-Jih, *s2-029*
 Cole, Heather, (*Wed s3*)14:40
 Colin, Jean-François, (*Mon s1*)13:50
 Cording, Faye, (*Wed s1*)15:40
 Coustan, Laura, (*Tue s1*)11:40
 Cremers, Carsten, (*Tue s2*)12:00
 Crispin, Xavier, (*Wed s2*)10:30
 Cumba, Loanda R., *s3-006*

D

da Silva, Daniel Rodrigues, (*Tue s4*)14:00
 da Silva, José Luiz, (*Tue s4*)14:00
 Dabo, Ismaila, (*Mon s1*)14:10, (*Tue s2*)16:50
 Data, Przemyslaw, (*Wed s3*)14:40, *s3-007, s3-029*
 de Groot, Kees, (*Mon s3*)16:20, (*Wed s3*)15:20
 Dedryvère, Rémi, (*Mon s1*)13:10
 Derr, Igor, (*Wed s1*)15:00
 Desrués, Antoine, (*Wed s1*)10:10
 Do, Jing-Shan, *s2-019, s3-026, s3-045*
 Dobeles, Galina, (*Mon s2*)18:20
 Dobosz, Iwona, (*Wed s2*)11:50
 Dokko, Kaoru, *s1-012, s1-022, s1-027, s1-036, s1-040*
 Dominko, Robert, (*Mon s1*)13:10
 Dongmo, Saustin, (*Wed s1*)11:30
 dos Santos Sardinha, Eduardo, (*Tue s1*)14:20
 Dow, Wei-Ping, (*Mon s3*)15:50
 Drakselova, Monika, *s2-009*
 Du, Ronggui, *s4-003*
 Dufour, N., (*Wed s1*)10:10
 Dunn, Bruce, (*Mon s1*)12:40
 Duoss, Eric, (*Wed s1*)16:00

E

Echeverría, Félix, (*Tue s1*)14:40
 El Guerraf, Abdelqader, (*Tue s2*)15:00, *s3-002*
 El Jaouhari, Abdelhadi, (*Tue s2*)15:00, *s3-002*

El-Nagar, Gumaa, (*Tue s2*)14:00, (*Wed s1*)15:00

Endo, Haruka, (*Wed s2*)10:10

Enright, Tyler, *s2-006*

Erbe, Andreas, (*Wed s5*)11:50

Eychmüller, Alexander, *s2-024*

F

Fabre, Frederic, (*Mon s1*)13:50

Fan, Jiawei, (*Wed s2*)16:00

Fang, Jie, (*Tue s1*)17:20, *s1-002*

Feldman, Yishay, (*Mon s3*)14:50

Feleni, Usisipho, (*Wed s4*)11:50

Feng, Zhange, (*Tue s4*)11:10

Ferreira e Silva, Rui Ramos, (*Tue s4*)14:40

Ferreira, Mario, (*Tue s3*)11:10

Fetyan, Abdulmonem, (*Wed s1*)15:00

Fic, Krzysztof, (*Mon s1*)13:50

Fleck, Robert, (*Wed s1*)15:40

Fontecave, Marc, *s3-001*

Forster, Robert, *s3-006*

Frackowiak, Elzbieta, (*Mon s1*)13:50

Friedl, Jochen, (*Wed s1*)15:40, *s1-004*,
s1-030

Friedrich, K. Andreas, (*Tue s2*)11:40

Fuchiwaki, Yusuke, *s3-011*

Fujii, Ryo, *s3-037*

Fujiwara, Hidemichi, *s4-006*

Fujiwara, Kensuke, *s1-003*

Fukai, Yuh, (*Mon s4*)18:20

Fukami, Kazuhiro, (*Tue s4*)12:20, *s1-006*,
s5-003

Fukazawa, Atsushi, *s2-007*

Fukui, Ken-ichi, (*Wed s3*)14:20

Fukumuro, Naoki, (*Mon s4*)18:20, *s3-037*,
s4-005

Fukunaka, Yasuhiro, *s1-017*, *s1-023*, *s4-008*

Fukuyama, Mao, (*Tue s4*)15:00

G

Gakumasawa, Mai, (*Wed s3*)11:30

Gan, Lu, (*Mon s2*)17:20

Ganesan, Pandian, (*Mon s2*)15:50

Gao, Zhida, *s3-034*

Gautier, Christelle, (*Mon s3*)13:10, (*Tue s3*)12:00

Gavalirova, Katarina, (*Tue s1*)17:40

Gejo, Tsukasa, (*Wed s1*)14:00

Genorio, Bostjan, (*Mon s1*)13:10

Georgescu, Nicholas, (*Tue s4*)11:10

Ghashghaie, Sasan, (*Tue s1*)17:20, *s1-002*

Ghilane, Jalal, (*Tue s3*)15:20

Gomez Villa, Eduardo Daniel, (*Tue s2*)12:00

Gómez-Romero, Pedro, (*Tue s1*)17:40

Gorbatovski, Georg, (*Tue s4*)12:20

Goto, Takuya, *s4-008*

Graf, Matthias, (*Tue s3*)14:00

Green, Todd, (*Mon s3*)15:10, *s3-039*

Griveau, Sophie, *s3-001*

Grueter, Peter, *s2-006*

Guan, Zichao, *s4-003*

Guégan, Philippe, (*Tue s3*)15:20

Guillot, Regis, *s3-001*

Guo, Ren-Hau, *s2-008*

H

Haarberg, Geir Martin, (*Wed s5*)11:30

Habazaki, Hiroki, (*Mon s2*)17:40, *s1-031*,
s2-013, *s2-030*

Haensch, Mareike, (*Tue s3*)14:00

Härmas, Meelis, *s1-038*

Härmas, Riinu, *s1-038*

Halilovic, Dzeneta, (*Mon s3*)13:30

Han, Lianhuan, (*Wed s3*)16:00

Han, Qi, (*Tue s4*)11:10

Hang, Ruomeng, (*Mon s3*)16:20

Hao, Qingli, (*Wed s2*)16:00

Haon, Cedric, (*Wed s1*)10:10

Harada, Toshihiko, *s3-011*

Haruyama, Jun, (*Tue s1*)16:20

Hasebe, Yasushi, (*Tue s3*)17:40

Hashigata, Ken, *s4-004*

Hashimoto, Hideki, *s3-023*, *s3-024*

Hashimoto, Shogo, *s3-012*

Hashimoto, Tomoko, *s2-005*

Hatakeyama, Yoshikiyo, (*Mon s1*)15:50

Hatta, Mizuki, (*Wed s1*)15:40

Hayase, Masanori, (*Mon s2*)18:00

Hayashi, Asuka, *s3-008*

Hayashi, Narumi, *s1-034*

Hayashi, Shunsuke, (*Tue s4*)15:20

Hector, Andrew, (*Mon s3*)16:20, (*Wed s3*)15:40

Henning, Sebastian, *s2-024*

Hensleigh, Ryan, (*Wed s1*)16:00

Herlin Boime, Nathalie, (*Wed s1*)10:10

Herranz, Juan, *s2-024*
 Herrmann-Geppert, Iris, (*Tue s2*)17:10
 Hideshima, Sho, *s3-018*
 Higai, Shin'ichi, (*Mon s1*)14:10
 Higashi, Kotaro, *s3-037*
 Higashino, Shota, (*Tue s3*)14:40
 Higginbotham, Heather, *s3-029*
 Higuchi, Eiji, (*Tue s2*)14:20
 Hihara, Takehiko, (*Tue s1*)15:00
 Hinoki, Tatsuya, *s5-003*
 Hirato, Tetsuji, (*Tue s3*)14:40
 Hiratsuka, Naoki, (*Tue s2*)14:20
 Hnat, Jaromir, (*Wed s5*)10:50, *s2-009*
 Ho, Ching-Hwa, *s4-001*
 Ho, Li-Cheng, *s3-009*
 Holland-Cunz, Matthäa Verena, *s1-004*,
 (*Wed s1*)15:40
 Homma, Takayuki, *s1-017*, *s1-023*, *s3-008*,
s3-012, *s3-013*, *s3-027*, *s3-035*, *s3-047*,
s3-048, *s4-006*
 Hong, Jong-In, *s3-010*
 Hong, Seok Won, (*Wed s5*)10:10
 Honma, Itaru, *s1-029*
 Hoque, Mahfuzul, *s1-022*
 Horii, Katsunori, *s3-018*
 Horii, Tatsuhiro, *s1-025*
 Horike, Satoshi, (*Mon s2*)15:10
 Horita, Masaomi, *s1-028*
 Horng, Er-Chien, *s4-001*
 Hoshi, Nagahiro, *s2-016*
 Hoshi, Yoshinao, *s3-016*
 Hosseini, Soraya, *s1-032*
 Hou, Chia-Hung, *s1-005*
 Hsiao, Han, *s4-001*
 Hsu, Da-Je, (*Mon s1*)14:30
 Hsu, Hsu-Fu, *s4-001*
 Hsu, Yung-Jung, (*Mon s4*)17:20, (*Tue*
s3)17:20
 Hu, Chi-Chang, (*Mon s1*)14:30, (*Mon*
s3)16:40, (*Wed s1*)15:00, *s1-015*, *s1-041*,
s1-043, *s2-008*
 Hua, Wei-Ling, *s4-001*
 Huang, Hsin-Wen, *s2-020*
 Huang, Jingting, *s1-005*
 Huang, Kun-Ping, (*Mon s1*)14:30
 Huang, Ruomeng, (*Wed s3*)15:20
 Huang, Xinning, (*Mon s2*)18:00

Hung, Pei-Sung, *s3-041*
 Hwang, Bing-Joe, *s1-013*
 Hyodo, Takeo, (*Wed s3*)10:10

I

Ida, Hiroki, (*Mon s2*)16:20, *s2-025*
 Ida, Shintaro, (*Wed s1*)14:40
 Ihsan, Neil, (*Tue s1*)15:20
 Itani, Kenta, (*Tue s3*)17:20
 Iiyama, Akihiro, (*Mon s2*)16:40, *s2-014*
 Ikenoue, Takumi, (*Tue s3*)14:40
 Ikeshoji, Tamio, (*Tue s1*)16:20
 Imai, Hideto, (*Mon s2*)16:40, (*Mon*
s2)16:40, *s1-011*
 Imaizumi, Masahiko, (*Tue s3*)14:20
 Inami, Yuta, (*Wed s2*)15:00
 Ino, Kosuke, (*Wed s3*)11:30, *s3-028*
 Inoguchi, Shota, *s1-006*, *s1-006*
 Inoishi, Yuiko, (*Wed s1*)14:40
 Inoue, Hiroshi, (*Tue s2*)14:20
 Inukai, Junji, (*Mon s2*)14:30, (*Mon*
s2)16:40, *s2-010*
 Ishihara, Akimitsu, (*Mon s2*)16:40
 Ishihara, Tatsumi, (*Wed s1*)14:40
 Ishii, Tomohiro, *s4-006*
 Ishii, Tsubasa, (*Mon s4*)17:40
 Ishikawa, Masashi, (*Tue s1*)16:40
 Ishizaki, Takahiro, *s1-003*, *s1-010*
 Isoai, Shunsuke, *s3-011*
 Itagaki, Kaoru, *s1-034*
 Itagaki, Masayuki, *s3-016*
 Ito, Hiroshi, (*Wed s2*)14:00
 Ivanovskaya, Anna, (*Wed s1*)16:00
 Iwuoha, Emmanuel, (*Wed s4*)11:50
 Izaki, Masanobu, *s3-031*

J

Jablonski, Melanie, *s3-032*
 Jachimska, Barbara, (*Tue s4*)14:20
 Jänes, Alar, *s1-038*
 Janek, Jürgen, (*Wed s1*)11:30
 Jang, Heechan, *s1-007*, *s1-008*
 Jeong, Youngjin, (*Mon s1*)15:10
 Jhong, Huan-Ping, *s3-011*
 Jia, Qingying, (*Mon s4*)18:20
 Jian, Xiaoxia, *s3-034*
 Jiang, Haoran, (*Wed s1*)14:20
 Jildeh, Zaid, (*Tue s3*)16:30

Juang, Jenh-Yih, *s3-019*
 Julistian, Ade, *s1-009*
 Jung, Cheolsoo, *s1-024*
 Jung, Jongwon, *s1-024*
 Jurzinsky, Tilman, (*Tue s2*)12:00

K

Kaare, Katlin, (*Mon s2*)18:20
 Kakinuma, Katsuyoshi, *s2-024*
 Kamada, Kai, (*Wed s3*)10:10
 Kambe, Mana, *s3-012*
 Kanamura, Kiyoshi, (*Mon s1*)13:30
 Kaneko, Amane, *s1-003*, *s1-010*
 Kaneko, Naoto, *s3-018*
 Kapun, Gregor, (*Mon s1*)13:10
 Kasamatsu, Shunsuke, (*Mon s2*)16:40
 Kashimata, Yuka, *s3-013*
 Kashtiban, Reza, (*Mon s3*)16:20, (*Wed s3*)15:20
 Kasiri Bihendi, Ghoncheh, (*Wed s1*)11:50
 Katayama, Yasushi, *s1-011*
 Kato, Ryoko, (*Wed s2*)10:10
 Katsuyoshi, Kakinuma, *s2-014*
 Kavan, Ladislav, (*Tue s3*)16:00, (*Tue s2*)16:30
 Kawaguchi, Kenji, (*Wed s1*)14:00
 Kawaguchi, Natsuki, (*Wed s2*)14:00
 Kawakami, Nobuhiro, (*Tue s1*)15:00
 Kawamoto, Teppei, (*Mon s2*)14:30, *s2-010*
 Keilbart, Nathan, (*Mon s1*)14:10
 Kepeniene, Virginija, (*Mon s2*)14:50, (*Tue s2*)15:20, *s2-011*
 Ketelsen, Bendix, (*Wed s3*)14:20
 Keusgen, Michael, (*Tue s3*)16:30
 Khalaghi, Babak, (*Wed s5*)11:30
 Khan, Md Zaved H., (*Wed s3*)14:00
 Kheawhom, Soorathep, *s1-032*
 Khurram, Hafiz Khurram, *s1-002*
 Kim, Chang Su, *s3-014*
 Kim, Cheong, *s1-031*, *s2-013*
 Kim, Dong-Kwon, *s2-012*, *s2-023*
 Kim, Hasuck, (*Mon s2*)15:50
 Kim, Hee-Tak, (*Tue s2*)14:40
 Kim, Hoyoung, *s2-012*, *s2-023*
 Kim, Jongwon, *s2-028*, *s3-033*
 Kim, Soo-Kil, *s2-012*, *s2-023*
 Kimura, Taro, *s2-010*
 Kinoshita, Takeshi, *s4-005*

Kissling, Gabriela, (*Wed s3*)15:20, (*Wed s3*)15:40
 Kitada, Atsushi, *s1-006*, (*Tue s4*)12:20, *s5-003*
 Kitagawa, Susumu, (*Mon s2*)15:10
 Kitta, Kazuki, *s1-011*
 Kjos, Ole, (*Wed s5*)11:30
 Klassen, Thomas, (*Tue s2*)17:10
 Klemm, Elias, (*Tue s2*)11:40
 Klusackova, Monika, (*Tue s2*)16:30
 Kobayashi, Ryo, *s2-014*
 Kobayashi, Shun, (*Mon s2*)14:30, (*Mon s2*)16:40
 Kobayashi, Yumi, *s1-025*
 Koch, Claudia, *s3-032*
 Kodym, Roman, (*Wed s5*)10:50
 Koike, Junpei, (*Wed s2*)15:00
 Kojima, Yuya, *s3-031*
 Kojo, Gen, *s2-015*
 Kokubo, Hisashi, *s1-025*
 Kolanowski, Lukasz, (*Mon s1*)14:50
 Kolczyk, Karolina, (*Mon s4*)17:40, (*Wed s2*)11:50, *s2-017*, *s3-015*
 Komaba, Shinichi, *s1-026*
 Komoda, Masato, *s3-016*
 Konakawa, Kotaro, (*Tue s1*)15:20
 Kondo, Shinji, *s1-012*
 Kondo, Sosuke, *s5-003*
 Kondo, Toshiaki, (*Tue s3*)14:20
 Kondo, Toshihiro, *s1-021*, *s1-033*, *s1-042*, (*Mon s2*)14:30, (*Mon s2*)16:40
 Kondo, Yuri, *s1-033*
 Konishi, Toshifumi, *s4-004*, *s4-010*, *s4-013*
 Konno, Yoshiki, (*Mon s2*)16:20
 Kopljar, Dennis, (*Tue s2*)11:40
 Kosaka, Fumihiko, (*Tue s2*)12:20
 Kowalik, Remigiusz, (*Mon s4*)17:40, (*Wed s2*)11:50, *s2-017*, *s3-015*
 Kowalski, Damian, (*Mon s2*)17:40, *s2-030*
 Koyama, Akira, (*Tue s4*)12:20
 Krbal, Milos, (*Tue s3*)16:20
 Kriegel, Herman, (*Tue s2*)17:10
 Krtil, Petr, (*Tue s2*)16:30
 Kruusenberg, Ivar, (*Mon s2*)18:20
 Kryszynski, Pawel, *s2-021*
 Kubota, Kei, *s1-026*
 Kühn, Laura, *s2-024*

- Kuhn, Alexander, (*Mon s3*)14:30, (*Tue s3*)11:40
 Kumagai, Kohei, *s3-017*
 Kumatani, Akichika, (*Mon s2*)16:20, *s1-026*, *s2-025*
 Kumeda, Tomoaki, *s2-016*
 Kunimoto, Masahiro, *s3-008*, *s3-013*, *s3-027*, *s3-047*
 Kuo, Chia-Heng, *s3-036*
 Kuo, Chun-Hong, *s1-013*
 Kuo, Na-Jung, *s1-013*
 Kuo, Yu-Fen, *s3-046*
 Kuo, Yue, (*Wed*)09:30
 Kurashina, Masashi, *s3-011*
 Kure-Chu, Song-Zhu S., (*Tue s1*)15:00
 Kuroda, Yoshiyuki, (*Wed s2*)15:00
 Kuroiwa, Shigeki, *s3-018*
 Kurosu, Hiromichi, *s2-005*
 Kusakabe, Emi, (*Tue s4*)15:00
 Kutyla, Dawid, (*Mon s4*)17:40, (*Wed s2*)11:50, *s2-017*, *s3-015*
 Kuwabata, Susumu, *s4-007*
 Kwiecinska, Anna, (*Mon s4*)17:40, *s2-017*, *s3-015*
- L**
- La Mantia, Fabio, (*Wed s1*)11:50
 Lacroix, Jean-Christophe, (*Tue s3*)15:20
 Lai, Chih-Yu, (*Wed s3*)10:50
 Lamaka, Sviatlana, (*Wed s1*)15:20
 Laocharoensuk, Rawiwan, *s3-038*
 Lapeyre, Veronique, (*Tue s3*)11:40
 Larionovich Zheludkevich, Mikhail, (*Tue s4*)14:40
 Lauermann, Iver, (*Tue s2*)14:00
 Lee, Dongil, (*Mon s2*)17:00
 Lee, Hoonseung, *s1-003*, *s1-010*
 Lee, Hsin-Yi, *s3-019*
 Lee, Jet-Sing, (*Mon s2*)15:10
 Lee, Kwan Hyi, *s3-020*
 Lee, Sanghyeon, *s1-024*
 Lei, Wu, (*Wed s2*)16:00
 Levillain, Eric, (*Mon s3*)13:10, (*Tue s3*)12:00
 Li, Chien-I., (*Tue s2*)12:20
 Li, Ya-Ru, *s1-014*
 Li, Yat, (*Wed s1*)16:00
 Liang, Yanyu, *s2-018*
- Liao, Kuan-Hua, *s2-019*
 Liao, Ying-Chih, (*Wed s3*)14:20, *s3-044*
 Limtrakul, Jumras, (*Tue s3*)11:40
 Lin, Andrew, *s2-020*
 Lin, Cheng-Hsuan, *s3-036*
 Lin, Chia-Yu, (*Tue s2*)17:30
 Lin, Chih-Hsun, *s4-001*
 Lin, Chun-Cheng, (*Mon s3*)16:40
 Lin, Geng-Min, *s4-001*
 Lin, Man-Ling, *s3-019*
 Lin, Sheng Chi, *s1-015*
 Liu, Huimin, (*Mon s2*)18:00
 Liu, Tianyu, (*Wed s1*)16:00
 Liu, Xiaoxia, *s1-016*
 Liu, Xiuhua, (*Wed s3*)14:00
 Lo, An-Ya, *s1-009*
 Lo, Chun-Hsiang, (*Mon s3*)15:50
 Lo, Nai-Chang, *s3-021*
 Lodge, Andrew, (*Mon s3*)16:20, (*Wed s3*)15:40
 Löwe, Armin, (*Tue s2*)11:40
 Lota, Grzegorz, (*Mon s1*)14:50
 Lozinsek, Matic, (*Mon s1*)13:10
 Lu, Chi-Han, *s3-009*
 Lu, Yi-Ting, (*Wed s1*)15:00
 Lu, Zhenjie, (*Mon s2*)18:00
 Lust, Enn, (*Mon s1*)13:30, (*Tue s4*)12:20, *s1-038*
- M**
- Ma, Chen-Chi M., *s1-015*
 Ma, Robin Lok-Wang, (*Tue s1*)17:20, *s1-002*
 Macak, Jan, (*Tue s3*)16:20
 Machida, Katsuyuki, *s4-004*, *s4-010*, *s4-013*
 Macounova, Katerina, (*Tue s2*)16:30
 Maeda, Kohji, (*Tue s4*)15:00
 Maeda, Yuki, *s5-003*
 Magagnin, Luca, (*Mon s1*)12:40
 Mahadevegowda, Surendra, (*Mon s3*)13:30
 Majima, Masatoshi, *s5-004*
 Maki, Hideshi, (*Tue s1*)12:00
 Makino, Sho, (*Mon s1*)13:30
 Mandai, Toshihiko, (*Wed s1*)15:40, *s1-037*
 Masa, Justus, (*Mon s2*)18:00
 Mascaro, Aaron, *s2-006*
 Masu, Kazuya, *s4-004*, *s4-010*, *s4-013*
 Masuda, Hideki, (*Tue s3*)14:20

- Masuda, Takuya, (*Mon s1*)13:30
Masuda, Yuta, *s1-017*
Mathé, Jérôme, (*Tue s3*)15:20
Matsubara, Eiichiro, (*Tue 00*)10:10
Matsuda, Honoka, (*Wed s2*)10:10
Matsuda, Shofu, (*Tue s4*)12:00
Matsue, Tomokazu, (*Mon s2*)16:20, (*Tue s3*)16:00, *s1-026, s2-025*
Matsui, Masaki, (*Tue s1*)12:00
Matsui, Yukiko, (*Tue s1*)16:40
Matsumae, Yoshiharu, *s1-040*
Matsumoto, Ayumu, (*Mon s4*)18:20, *s3-037, s4-005*
Matsumoto, Futoshi, *s1-034*
Matsumoto, Masashi, (*Mon s2*)16:40
Matsumoto, Toshiyuki, (*Tue s3*)15:00
Matsumura, Yoshimasa, *s2-007*
Matsuo, Hinako, *s3-048*
Matsushima, Hisayoshi, *s1-018, s5-005*
Matsushita, Nobuhiro, (*Tue s3*)17:20
Matsuzaki, Yoshio, *s2-015*
Matsuzawa, Koichi, (*Mon s2*)16:40
Mech, Krzysztof, (*Mon s4*)18:00
Melke, Julia, (*Tue s2*)12:00
Meller, Mikolaj, (*Mon s1*)13:50
Mertens, Stijn F.L., (*Mon s4*)18:00
Minagawa, Hirotaka, *s3-018*
Minakata, Satoshi, *s3-029*
Minamimoto, Hiro, (*Mon s3*)17:20
Miron, Camelia, *s1-010*
Mitsubayashi, Kohji, (*Tue s3*)17:20
Mitsubishi, Naoto, *s1-034*
Mitsumura, Shigenori, *s2-007*
Mitsushima, Shigenori, (*Mon s2*)16:40, (*Wed s2*)15:00
Miura, Chiho, (*Mon s2*)16:20, *s2-025*
Miwa, Kazumoto, *s1-025*
Miyahara, Yoichi, *s2-006*
Miyake, Masao, (*Tue s3*)14:40
Miyamoto, Hiroo, (*Wed s3*)14:20
Miyamoto, Koichiro, (*Mon s3*)17:00, *s3-022, s3-042 s4-012*
Miyano, Takayashi, (*Wed s1*)14:40
Miyatake, Kenji, *s2-022*
Miyachi, Toshimitsu, (*Mon s2*)18:00
Miyazaki, Reona, (*Tue s1*)15:00
Mizuhata, Minoru, (*Tue s1*)12:00
Mizusawa, Takako, *s2-010*
Mochizuki, Dai, (*Mon s1*)13:30
Mokkelbost, Tommy, (*Wed s5*)11:30
Momma, Toshiyuki, (*Tue s1*)14:00, (*Tue s1*)17:00, *s1-019, s3-018*
Montel, Fabien, (*Tue s3*)15:20
Moran, Bryan, (*Wed s1*)16:00
Mori, Tadashi, *s3-023*
Morimitsu, Masatsugu, (*Wed s1*)14:00
Muench, Falk, (*Mon s3*)14:50
Mukerjee, Sanjeev, (*Mon s4*)18:20
Munakata, Hirokazu, (*Mon s1*)13:30
Munakata, Tetsuo, (*Wed s2*)14:00
Murakami, Hideyuki, (*Mon s2*)17:20
Murakami, Yuma, (*Mon s3*)16:20
Murakoshi, Kei, (*Mon s3*)17:20
Muramatsu, Yusuke, *s3-024*
Murase, Kuniaki, (*Tue s4*)12:20, *s5-003, s1-006*
- N**
- Na, William, (*Wed s5*)10:10
Nagai, Takaaki, (*Mon s2*)16:40
Nagamine, Momoka, *s2-021*
Nagasaki, Motoko, (*Mon s1*)13:30
Nagasawa, Kensaku, (*Wed s2*)15:00, *s2-007*
Nagata, Masato, *s1-023*
Nagayama, Tomio, (*Mon s2*)16:20
Nakai, Hiromi, *s3-027*
Nakamura, Masashi, *s2-016*
Nakamura, Susumu, *s1-034*
Nakamura, Toshihiro, (*Mon s2*)16:20
Nakamura, Yui, (*Tue s4*)15:00
Nakanishi, Azusa, *s1-027, s1-040*
Nakanishi, Bradley, (*Mon s4*)17:00
Nakanishi, Takuya, *s3-018*
Nakano, Akihiro, (*Wed s2*)14:00
Nara, Hiroki, (*Tue s1*)14:00, (*Tue s1*)17:00, *s1-019*
Nato, Hiroaki, (*Wed s3*)14:20
Naujokaitis, Arnas, *s2-002, s2-003, s2-026, s2-027*
Nebel, Roman, (*Tue s2*)16:30
Neto, Miguel Angelo, (*Tue s4*)14:40
Ngamaroonchote, Aroonsri, *s3-038*
Niida, Asako, *s1-021*
Niinomi, Mitsuo, (*Tue s3*)17:20
Nishida, Tetsuo, *s1-011*

Nishide, Hiroyuki, (*Mon 00*)10:30
 Nishihara, Hiroshi, (*Mon s3*)12:40
 Nishikawa, Kei, (*Mon s1*)13:30, *s1-018*
 Nishiyama, Kentaro, *s3-031*
 Nitta, Akio, (*Mon s3*)16:20
 Njel, Christian, (*Mon s1*)13:10
 Noda, Masaru, *s2-031*
 Nohira, Toshiyuki, *s5-004*
 Nokbin, Somkiat, (*Tue s3*)11:40
 Nomura, Fumihiko, *s1-020*
 Norikawa, Yutaro, *s5-004*
 Norkus, Eugenijus, (*Mon s2*)14:50, (*Mon s2*)18:20, (*Tue s2*)15:20, *s2-002*, *s2-003*, *s2-011*, *s2-026*, *s2-027*
 Nugraha, Asep Sugih, *s3-025*
 Numata, Koma, *s5-004*
 Nurpratama, Aditya Febry, *s3-026*
 Nørskov, Jens, (*Wed s2*)15:20

O

Obata, Kenzo, *s1-040*
 Oberlaender, Jan, (*Tue s3*)16:30
 Obu, Yoshiki, (*Tue s4*)12:00
 Ogawa, Ryota, *s5-005*
 Oh, Seonhwa, *s2-012*, *s2-023*
 Ohama, Ayano, *s1-021*
 Ohashi, Keishi, *s3-018*
 Ohtani, Bunsho, (*Mon s3*)16:20
 Oikawa, Akio, (*Tue s2*)12:20
 Oikawa, Shumpei, (*Mon s3*)17:20
 Okada, Kiyoshi, (*Tue s3*)17:20
 Okada, Takeru, (*Mon s2*)16:20, *s2-025*
 Okada, Yasuaki, (*Mon s1*)14:10
 Okamoto, Yukihiko, *s1-022*
 Okaue, Daijiro, (*Wed s3*)14:20
 Okuda, Yuuki, (*Tue s4*)12:00
 Okura, Kaname, (*Mon s2*)16:20
 Oleinick, Alexander, (*Tue s4*)11:40, *s4-009*
 Oll, Ove, (*Mon s1*)13:30, (*Tue s4*)12:20
 Olynick, Deirdre, (*Tue s2*)17:10
 Onabuta, Yusuke, *s3-027*
 Ono, Sakuroko, (*Wed s3*)14:20
 Ono, Shimpei, *s1-025*
 Onodera, Takehiro, *s3-028*
 Osaka, Tetsuya, *s1-019*, (*Tue s1*)14:00, (*Tue s1*)17:00, *s3-018*
 Osial, Magdalena, *s2-021*
 Ota, Ken-ichiro, (*Mon s2*)16:40

Otani, Minoru, (*Tue s1*)16:20
 Otani, Tomohiro, *s1-017*, *s1-023*
 Otomo, Junichiro, (*Tue s2*)12:20, *s2-015*
 Otsuji, Kanji, *s2-022*
 Owada, Taku, (*Tue s1*)14:00
 Ozasa, Kazunari, (*Tue s3*)17:20

P

Pacoste, Laura, (*Wed s4*)11:50
 Pai, Hao-Jen, *s3-028*
 Pan, Deng, (*Wed s3*)10:30
 Pan, Haoran, (*Mon s2*)18:00
 Pander, Piotr, *s3-007*
 Pandey, Prem, (*Mon s3*)14:10
 Park, Habin, *s1-024*
 Park, Hyanjoo, *s2-012*, *s2-023*
 Park, Mijung, (*Wed s5*)12:10
 Passerini, Stefano, (*Mon s1*)12:40
 Patil, Bebi, (*Mon s1*)15:10
 Patoux, Sebastien, (*Mon s1*)13:50
 Peng, Wei, *s3-043*
 Peralta, David, (*Mon s1*)13:50
 Perrot, Hubert, (*Mon s1*)13:10, (*Mon s1*)14:30
 Perugio Holland, Naomi, *s3-001*
 Pikma, Piret, (*Wed s3*)15:00
 Plevova, Michaela, *s2-009*
 Pluczyk, Sandra, *s3-029*
 Poghossian, Arshak, *s3-032*
 Policar, Clotilde, *s3-001*
 Ponrouch, Alexandre, (*Wed s1*)16:00
 Poon, Kee Chun, (*Mon s2*)17:40
 Popovitz-Biro, Ronit, (*Mon s3*)14:50
 Prikryl, Jan, (*Tue s3*)16:20
 Prokop, Martin, (*Tue s2*)11:10

Q

Qian, Fang, (*Wed s1*)16:00
 Qu, Yongfang, *s3-034*

R

Rabbow, Thomas, (*Mon s1*)14:10
 Reid, Gill, (*Wed s3*)15:40
 Ringe, Stefan, (*Wed s2*)15:20
 Romann, Tavo, *s1-038*
 Rossmeisl, Jan, (*Tue s2*)16:30
 Roth, Christina, (*Tue s2*)14:00, (*Wed s1*)15:00
 Rothschild, Avner, (*Tue s2*)16:00

Roy, Sudipta, (*Mon s3*)15:10, *s3-039*
 Rubinstein, Israel, (*Mon s3*)14:50
 Rueda, Daniel, (*Tue s1*)17:40
 Rutrle, Jakub, (*Wed s5*)10:50

S

Saeki, Isao, (*Mon s2*)17:20
 Sai Smaran, Kumar, *s1-021*
 Saito, Hiroki, *s2-031*
 Saito, Hiroyuki, *s3-030*
 Saito, Mikiko, *s3-035, s3-048, s4-006*
 Saito, Satoshi, *s1-025*
 Saitoh, Takaki, *s1-018*
 Sakai, Sayumi, *s1-042*
 Sakai, Takuya, *s3-031*
 Sakairi, Masatoshi, (*Tue s3*)15:00
 Sakamaki, Kenji, (*Wed s2*)10:10
 Sakamoto, Kouta, (*Wed s3*)14:20
 Sakamoto, Susumu, *s3-037*
 Sakanaka, Yoshihide, *s4-008*
 Sakashita, Wakana, (*Wed s2*)10:10
 Sakka, Tetsuo, (*Tue s4*)12:20
 Salomon, Jeremie, (*Mon s1*)13:50
 Samukawa, Seiji, (*Mon s2*)16:20, *s2-025*
 Sasaki, Tomoya, *s4-007*
 Sasano, Junji, *s3-031*
 Sato, Hirotaka, (*Mon s2*)17:40
 Sato, Masataka, (*Wed s2*)10:10
 Sato, Taiki, (*Wed s3*)14:20
 Sato, Yuki, *s2-030*
 Sato, Yushi, *s1-037*
 Sato, Yuta, *s3-008, s3-013*
 Sato, Yuto, *s1-026*
 Scheiba, Frieder, (*Tue s2*)12:00
 Scherson, Daniel, (*Tue s4*)11:10
 Schieda, Mauricio, (*Tue s2*)17:10
 Schmidt, Thomas, *s2-024*
 Schneider, Oliver, (*Tue 00*)09:30
 Schoening, Michael J., (*Tue s3*)16:30,
s3-032, s3-032, s3-040, s4-012
 Schricker, Barbara, (*Wed s1*)15:40
 Schröder, Daniel, (*Wed s1*)11:30
 Schulz, Florian, (*Wed s3*)14:20
 Seidl, Lukas, (*Tue 00*)09:30
 Seki, Maki, (*Tue s4*)15:20
 Seki, Shin-Ichi, (*Tue s3*)17:40
 Sel, Ozlem, (*Mon s1*)13:10, (*Mon s1*)14:30
 Selskis, Algirdas, *s2-011*

Seo, Jungmok, *s3-020*
 Seo, Minji, *s3-033*
 Seong, Tae Wha, *s3-020*
 Sepúlveda, Lina Marcela, (*Tue s1*)14:40
 Serizawa, Nobuyuki, *s1-011*
 Shahzad, Hafiz Khurram, (*Tue s1*)17:20
 Shan, Dan, (*Wed s2*)15:40
 Shanmugam, Sangaraju, (*Mon s2*)15:50,
*(Mon s2)*17:20
 Shao, Yi-An, *s3-004*
 Shen, Yan, (*Wed s2*)12:10
 Shen, Yanfei, (*Wed s3*)10:30
 Shi, Guoyu, (*Mon s2*)16:40
 Shi, Le, (*Wed s1*)14:40
 Shigenobu, Keisuke, *s1-027*
 Shiku, Hitoshi, (*Mon s2*)16:20, (*Wed*
s3)11:30, *s1-026, s2-025, s3-028*
 Shimada, Manai, *s2-022*
 Shimizu, Masahiro, *s1-028*
 Shimizu, Ryo, *s2-024*
 Shimizu, Yasuhiro, (*Wed s3*)10:10
 Shimura, Miyu, *s2-025*
 Shin, Woonsup, (*Wed s5*)12:10
 Shirai, Ryo, (*Mon s2*)18:00
 Shiraiishi, Soshi, (*Mon s1*)15:50
 Shirasaka, Ryo, (*Mon s2*)14:30, (*Mon*
s2)16:40
 Shironita, Sayoko, (*Tue s1*)15:20
 Shitanda, Isao, *s3-016*
 Shviro, Meital, (*Mon s4*)18:20
 Shyy, Wei, (*Wed s1*)14:20
 Siangproh, Weena, *s3-038*
 Singh, Amritpal, (*Wed s2*)10:30
 Sivanantham, Arumugam, (*Mon s2*)17:20
 Slim, Cyrine, *s3-001*
 Sliusarenko, Oleksii, (*Tue s4*)11:40
 Sojic, Neso, (*Mon s3*)14:30
 Soma, Naohiko, *s1-034*
 Someya, Satoshi, (*Wed s2*)14:00
 Sone, Masato, (*Mon s4*)17:20, (*Tue*
s3)17:20, *s2-005, s4-004, s4-010, s4-013*
 Song, Hyeonjun, (*Mon s1*)15:10
 Song, Yanyan, *s3-034*
 Song, Yu, *s1-016, (Wed s1)*16:00
 Sopha, Hanna, (*Tue s3*)16:20
 Soulé, Samantha, (*Mon s3*)16:20
 Souma, Kenichi, (*Tue s1*)15:20

- Stadermann, Michael, (*Wed s1*)16:00
 Stagniunaite, Raminta, (*Mon s2*)14:50,
 (*Tue s2*)15:20
 Stauss, Sven, *s1-029*
 Sternad, Michael, (*Tue s1*)14:20
 Stimming, Ulrich, (*Tue*)09:30,
 (*Wed s1*)15:40, *s1-004*, *s1-030*
 Stock, Daniel, (*Wed s1*)11:30
 Stradiotto, Nelson, (*Tue s4*)14:00
 Straková Fedorková, Andrea, (*Tue s1*)17:40
 Stuparu, Miahuela C., (*Mon s3*)13:30
 Su, Chun-Hao, (*Wed s3*)14:20, *s3-044*
 Su, Haibin, (*Mon s2*)17:40
 Su, Wei-Nien, *s1-013*
 Suda, Kohei, (*Mon s2*)14:30
 Sugie, Misaki, *s3-035*
 Sugimoto, Wataru, (*Mon s1*)13:30
 Sugino, Osamu, (*Mon s2*)16:40
 Suh, Won-kyo, (*Mon s2*)15:50
 Sukackiene, Zita, *s2-002*, *s2-003*, *s2-026*,
s2-027
 Sumskas, Lukas, *s2-002*
 Sun, Chia-Liang, *s3-036*
 Sun, I.-Wen, *s3-021*
 Suzuki, Daisuke, *s3-022*
 Suzuki, Yuta, *s4-008*
 Svir, Irina, (*Tue s4*)11:40, *s4-009*
 Szacilowski, Konrad, (*Mon s4*)18:00
- T**
- Tachikawa, Naoki, *s1-011*
 Tadokoro, Hiroshi, *s2-015*
 Takahashi, Hidefumi, *s3-035*, *s3-048*
 Takahashi, Yasufumi, (*Mon s2*)16:20,
s1-026, *s2-025*
 Takamori, Mari, (*Wed s3*)10:10
 Takano, Ken, *s2-007*
 Takasaka, Yuichi, *s3-037*
 Takase, Mai, (*Mon s3*)16:20
 Takashima, Mai, (*Mon s3*)16:20
 Takata, Manami, *s1-031*
 Takeda, Youhei, *s3-029*
 Takeguchi, Tatsuya, (*Wed s1*)15:40, *s1-037*
 Takekawa, Toshihiro, *s1-011*
 Takemoto, Marie, (*Tue s1*)12:00
 Takeya, Jun, (*Wed s3*)14:20
 Takibuchi, Ryota, *s3-018*
- Tamasauskaite Tamasiunaite, Loreta, (*Mon s2*)14:50, (*Mon s2*)18:20, (*Tue s2*)15:20,
s2-002, *s2-003*, *s2-011*, *s2-026*, *s2-027*
 Tan, Desmond, (*Mon s2*)17:40
 Tanabe, Ichiro, (*Wed s3*)14:20
 Tanabe, Toyokazu, *s1-034*
 Tang, Guoyi, (*Tue s1*)15:00
 Tang, Haochun, *s4-004*, *s4-010*
 Taniguchi, Izumi, *s1-007*, *s1-008*
 Tanii, Risako, *s5-005*
 Tao, Minglei, (*Wed s2*)12:10
 Tazawa, Naoki, *s1-029*
 Teabnamang, Pemika, *s1-032*
 Tedim, Joao, (*Tue s3*)11:10
 Terada, Shoshi, *s1-012*, *s1-022*, *s1-036*
 Terasaki, Haruka, *s1-033*
 Terasaki, Ichiro, *s3-035*, *s3-048*
 Terauchi, Mayuko, (*Wed s3*)11:30
 Thangphatthanarungruang, Jeerakit, *s3-038*
 Thomborg, Thomas, *s1-038*
 Tian, Zhao-Wu, (*Wed s3*)16:00
 Tian, Zhong-Qun, (*Wed s3*)16:00
 Toma, Koji, (*Tue s3*)17:20
 Tomizawa, Eika, *s1-033*
 Torimoto, Tsukasa, *s4-007*
 Tortorelli, Dan, (*Wed s1*)16:00
 Trindade da Silva, Eduardo Luís, (*Tue s4*)14:40
 Truong, Hoang Anh, (*Mon s3*)17:00, *s3-042*
 Tryk, Donald, (*Mon s2*)16:40
 Tsai, Ming-Liao, *s2-019*, *s3-026*, *s3-045*
 Tsai, Yi-Ying, *s1-013*
 Tsuda, Takashi, *s1-034*
 Tsuda, Tetsuya, *s4-007*
 Tsukada, Hidehiko, (*Mon s1*)15:50
- U**
- Uchida, Hiroyuki, (*Mon s2*)14:30, (*Mon s2*)16:40
 Uchida, Makoto, *s2-014*, *s2-022*, *s2-024*
 Uchida, Satoshi, (*Tue s1*)16:40
 Uchimaru, Masahiro, *s3-011*
 Uchimoto, Yoshiharu, *s1-035*
 Ueda, Mikito, *s1-018*, *s5-005*
 Ueda, Taro, (*Wed s3*)10:10
 Uematsu, Taro, *s4-007*
 Ueno, Kazuhide, *s1-012*, *s1-022*, *s1-027*,
s1-036, *s1-040*

Ugata, Yosuke, *s1-036*
 Ui, Koichi, *s1-037*
 Umeda, Minoru, (*Tue s4*)12:00, (*Tue s1*)15:20
 Uno, Shigeyasu, *s3-022*
 Upskuviene, Daina, (*Tue s2*)15:20, *s2-011*
 Usui, Sayuri, (*Wed s2*)10:10

V

Väli, Ronald, *s1-038*
 Vagin, Mikhail, (*Wed s2*)10:30
 Vaiciuniene, Jurate, *s2-002*, *s2-003*, *s2-026*, *s2-027*
 Valiollahi, Roudabeh, (*Wed s2*)10:30
 Valverde Armas, Priscila, (*Mon s3*)15:10, *s3-039*
 Vasiljevic, Natasa, (*Mon s2*)18:00, (*Wed s2*)14:20
 Vaskevich, Alexander, (*Mon s3*)14:50
 Vasylieva, Marharyta, *s3-007*
 Vo, Thang, (*Mon s2*)17:40
 Volperts, Aleksandrs, (*Mon s2*)18:20
 Voronov, Dmitriy, (*Tue s2*)17:10
 Vossmeier, Tobias, (*Wed s3*)14:20

W

Wada, Yuta, *s1-010*
 Waga, Iwao, *s3-018*
 Wagner, Mary Elizabeth, (*Wed s5*)10:30
 Wagner, Nobert, (*Tue s2*)11:40
 Wagner, Patrick, (*Tue s3*)16:30, *s3-040*
 Wagner, Torsten, *s3-040*, *s4-012*
 Wakisaka, Mitsuru, (*Mon s2*)14:30, (*Mon s2*)16:40
 Wang, Caihong, *s1-025*
 Wang, Chen-Hao, *s3-011*
 Wang, Fu-Ming, (*Wed s1*)10:30
 Wang, Guang-Ren, *s3-041*
 Wang, Haipeng, *s4-003*
 Wang, Jeng-An, *s1-039*
 Wang, Jiade, *s5-006*
 Wang, Jun, (*Mon s2*)18:00
 Wang, Mengyun, *s3-042*
 Wang, Mingkui, (*Wed s2*)12:10
 Wang, Rongguang, (*Tue s2*)15:00, *s3-002*
 Wang, Tao, (*Mon s2*)18:00
 Wang, Tsai-Hui, *s4-001*
 Wang, Xia, *s3-001*, *s4-003*

Wang, Yue, (*Tue s3*)17:40
 Wang, Yumi, *s2-028*
 Warakulwit, Chompunuch, (*Tue s3*)11:40
 Watanabe, Ayana, (*Wed s2*)10:10
 Watanabe, Daiki, *s1-036*
 Watanabe, Kohei, *s4-011*
 Watanabe, Masayoshi, (*Tue s1*)11:10, *s1-012*, *s1-022*, *s1-025*, *s1-027*, *s1-036*, *s1-040*
 Wattanakit, Chularat, (*Tue s3*)11:40
 Watts, Seth, (*Wed s1*)16:00
 Webster, Richard D., (*Mon s3*)13:30
 Wege, Christina, *s3-032*
 Wei, Lei, (*Wed s1*)14:40
 Weisgraber, Todd, (*Wed s1*)16:00
 Weissmüller, Jörg, (*Tue s3*)14:00
 Welden, Rene, *s3-040*
 Weng, Yu-Ching, *s2-029*, *s3-043*
 Werner, Carl Frederik, (*Mon s3*)17:00, *s3-022*, *s3-042*, *s4-012*
 Widera-Kalinowska, Justyna, *s2-021*
 Wilkening, Martin, (*Tue s1*)14:20
 Wittstock, Gunther, (*Tue s3*)14:00, (*Tue s1*)14:20
 Wodarz, Sigg, *s3-012*
 Wojciechowski, Jaroslaw, (*Mon s1*)14:50
 Wolfschmidt, Holger, (*Wed s1*)15:40
 Woo, Seunghee, (*Mon s2*)15:50
 Worsley, Marcus, (*Wed s1*)16:00
 Wrobel, Miroslaw, (*Mon s4*)18:00
 Wu, Ching-Chou, *s3-046*, *s4-002*
 Wu, Maochun, (*Wed s1*)14:20
 Wu, Nae-Lih, (*Tue s1*)16:00
 Wu, Yi-Shiuan, (*Mon s1*)14:10
 Wu, Yunwen, (*Tue s1*)17:00

X

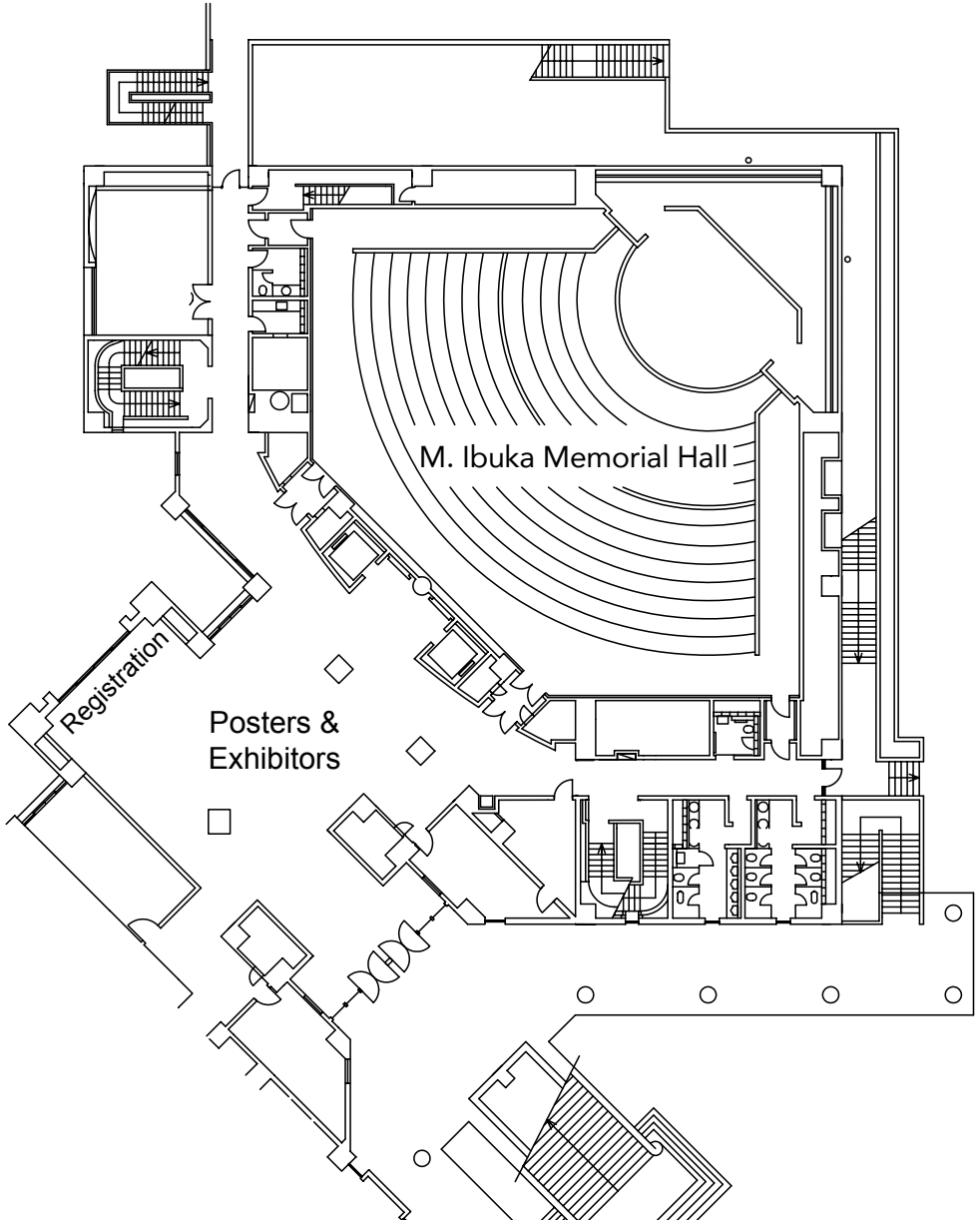
Xiao, Fu-Ren, *s3-044*
 Xiao, Xin, (*Wed s2*)12:10
 Xin, Wen-Li, (*Wed s2*)15:40
 Xu, Jianbo, (*Wed s1*)14:20, (*Wed s1*)14:40
 Xu, Ying-Fang, *s3-045*

Y

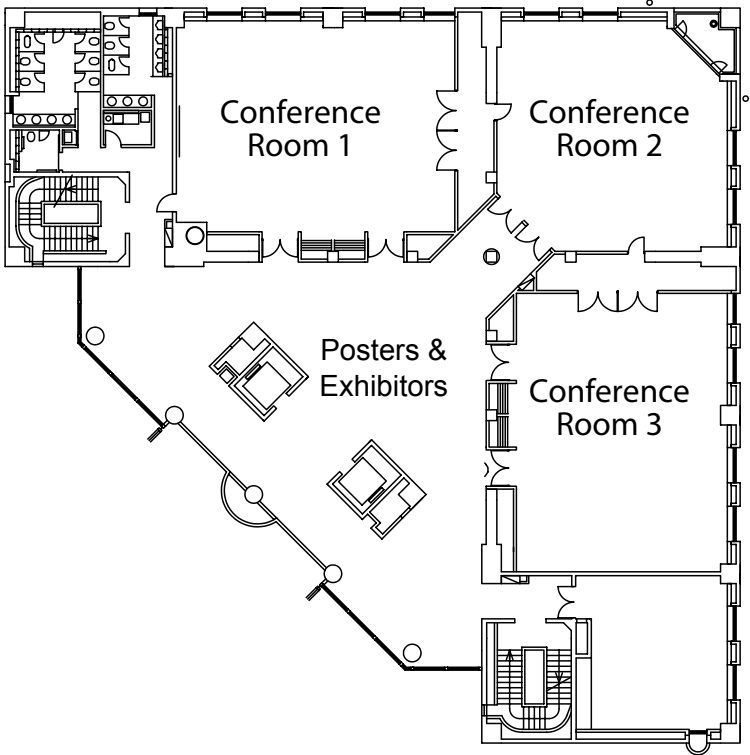
Yae, Shinji, (*Mon s4*)18:20, *s3-037*, *s4-005*
 Yamada, Naohito, *s2-030*
 Yamada, Norifumi, *s2-010*
 Yamaguchi, Futa, *s3-047*

- Yamaguchi, Rina, (*Tue s4*)15:20
Yamamoto, Kazuo, *s5-002*
Yamamoto, Takahiro, *s4-013*
Yamamoto, Takayo, (*Mon s2*)16:20
Yamamoto, Tomoyuki, (*Mon s2*)17:20
Yamamoto, Yoshiyuki, (*Mon s2*)16:40
Yamanaka, Ichiro, (*Wed s2*)15:00
Yamane, Daisuke, *s4-004, s4-010, s4-013*
Yamauchi, Yusuke, *s3-025, s5-001*
Yan, Jia-De, *s3-046*
Yanagi, Masato, *s1-040*
Yanagisawa, Masahiro, *s3-008, s3-013, s3-047*
Yanagishita, Takashi, (*Tue s3*)14:20
Yanase, Yuhki, *s3-022*
Yano, Hiroshi, (*Mon s2*)16:40
Yao, Bin, (*Wed s1*)16:00
Yao, Bo, (*Wed s4*)12:10
Yao, Jiachao, *s5-006*
Yashiro, Hitoshi, (*Tue s1*)15:00
Yasini, Parisa, (*Wed s3*)15:00
Yasuda, Kouji, *s5-004*
Yasuda, Tetsuya, *s3-047*
Yasuzawa, Mikito, *s3-011*
Yatsuzuka, Ryosuke, *s1-028*
Yau, Shuehlin, (*Mon s1*)13:10
Ye, Haitao, (*Wed s2*)16:00
Ye, Yongda, (*Tue s1*)15:00
Yeh, Min-Hsin, *s1-013*
Yen, Ching-Jung, (*Tue s3*)17:00
Yen, Hao-Yu, *s4-002*
Yen, Wei-Chen, *s4-001*
Yesilmen, Mazlum, (*Wed s3*)14:20
Yi, Tien-Yu, *s1-041*
Yokoshima, Tokihiko, *s1-019, (Tue s1)14:00, (Tue s1)17:00*
Yokota, Naoki, *s2-022*
Yokota, Yasuyuki, (*Wed s3*)14:20
Yokoyama, Ayano, *s4-005*
Yokoyama, Seiji, *s3-031*
Yong, Hansol, *s1-024*
Yoshida, Yumi, (*Tue s4*)15:00
Yoshihara, Naoki, *s2-031*
Yoshii, Kazuki, *s1-011*
Yoshimi, Yasuo, (*Tue s4*)15:20
Yoshimura, Natsumi, *s2-022*
Yoshinobu, Tatsuo, (*Mon s3*)17:00, *s3-022, s3-042, s4-012*
Yoshioka, Risa, *s1-042*
Yoshitoku, Koichiro, *s3-048*
You, Ting-Hsuan, *s1-043*
Yu, Seongil, (*Mon s1*)15:10
Yutthalekha, Thittaya, (*Tue s3*)11:40
- ## Z
- Zabinski, Piotr, (*Mon s4*)17:40, (*Mon s4*)18:00, (*Wed s2*)11:50, *s2-017, s3-015*
Zangari, Giovanni, (*Tue s3*)16:40, *s3-012*
Zazpe, Raul, (*Tue s3*)16:20
Zborowski, Wojciech, *s3-015*
Zeng, Lin, (*Wed s1*)14:20, (*Wed s1*)14:40
Zeng, Wei-Yang, (*Mon s3*)15:50
Zhan, Dongping, (*Wed s3*)16:00
Zhan, Jing, (*Mon s2*)17:40
Zhang, Jingjun, *s1-036*
Zhang, Wenjian, (*Wed s3*)15:40
Zhao, Chuan, (*Wed s2*)11:30
Zhao, Tianshou, (*Wed s1*)14:20, (*Wed s1*)14:40
Zheludkevich, Mikhail, (*Tue s3*)11:10
Zheng, Xiaoyu, (*Wed s1*)16:00
Zhu, Cheng, (*Wed s1*)16:00
Zhu, Chunyu, (*Mon s1*)13:50, *s1-031, s2-013, s2-030*
Zigah, Dodzi, (*Mon s3*)14:30
Zitka, Jan, *s2-009*
Zitoun, David, (*Mon s4*)18:20
Zozoulenko, Igor, (*Wed s2*)10:30
Zukalova, Marketa, (*Wed s1*)10:50
Zurins, Aivars, (*Mon s2*)18:20

Waseda University International Conference Center Floor 1: M. Ibuka Memorial Hall



Waseda University International Conference Center Floor 3: Rooms 1-3



Making Science Work: The Need for New Electrochemical Engineering Methods

Richard Alkire
University of Illinois
Urbana, IL USA
r-alkire@illinois.edu

Electrochemical phenomena control the existence and movement of charged species in the bulk as well as across interfaces between ionic, electronic, semiconductor, photonic, and dielectric materials. The pervasive occurrence of electrochemical phenomena may be seen in many nanoscale and biological systems, energy systems, microelectronic and photovoltaic devices, green processes and natural systems.

During the past several decades, the electrochemical field has benefited from a suite of remarkable new experimental and computational capabilities. These provide the ability to create precisely characterized systems for fundamental study; to monitor behavior at unprecedented levels of sensitivity, atomic resolution, and chemical specificity; and to predict behavior with new theories and improved computational abilities. These capabilities have revolutionized fundamental scientific understanding of interfacial and catalytic processes, as well as contributed to the present rapid pace of discovery of novel materials and devices.

Future trends in electrochemical engineering will be influenced by the need to provide molecular manipulation as an engineering design focus. Engineering approaches are needed that couple traditional current- and potential-distribution methods with molecular-scale events in order to predict behavior accurately, and to design technological systems for which quality control resides at the molecular scale.

The existing technology base of the electrochemical field is massive. For economic reasons, most traditional large-scale processes are driven to transport-limited rates. Therefore, for many decades, engineering methods focused on predicting how ohmic and/or mass transport phenomena influence the potential field between electrodes and the current distribution along electrode surfaces. More recently, mathematical modeling of electrochemical systems has expanded to include additional phenomena at multiple time- and length-scales, as well as the presence of adjoining phases and interfaces/films between them. Today, sophisticated continuum models based primarily on differential-algebraic equations dominate the extensive literature and, for many applications, commercial software is available.

When combined with experimental observations, mathematical models can today often serve as the hypothesis for the *scientific method*, and thus contribute to the advance of fundamental scientific understanding. However, an *engineering method* is essential for advancing important applications toward development and market entry. This is where new electrochemical engineering methods are needed. Such engineering methods find use, for example, to identify what limits the path forward from discovery to product, to find the thermodynamic limit, to provide a system-wide view from the outset, to guide prediction and scale-up, to optimize for control of uncertainty and risk. For these methods, highly efficient numerical algorithms are needed to obtain error bars and parameter sensitivities for comparison of experimental data with numerical simulations over wide ranges of length- and time-scales.

To accomplish these goals, we need more scientists and engineers pursuing the engineering method. Close collaborations with industry can play an important role in balancing between ‘blue sky curiosity’ and ‘targeted design.’ In addition, there are many advances in other disciplines, which can inform the electrochemical community. For example, the rapid advance of high performance computing and data-driven insights will surely benefit some complex applications for which ‘rules of thumb’ or ‘pretty pictures’ no longer suffice. New easy-to-use engineering methods that link small-scale events to macroscopic processes will be helpful optimizing materials selection. The development and reduction to routine use of these and other re-usable methods will provide engineering tools needed for next-generation design and control of electrochemical systems, and will open the way to exploiting and controlling self-assembly during processing.

Electrochemical Reactions in Solid State Device Fabrication – Current and Future

Yue Kuo and Noel Buckley*

Texas A&M University, Thin Film Nano & Microelectronics Research Laboratory
Artie McFerrin Department of Chemical Engineering, College Station, TX 77843-3122, USA
yuekuo@tamu.edu

*University of Limerick, Department of Physics and Energy, Limerick, V94 T9PX, IE

Materials, processes, and device characteristics are three critical elements for the success of solid state devices, such as microelectronics and optoelectronics, as shown in Figure 1. Furthermore, in real applications, the device and product structures are critical to the choice of composition materials as well as the optimized fabrication process. Conventionally, dry processes, such as CVD, sputtering, plasma etching, and ion implantation, are used in solid state device fabrication. However, some electrochemical reactions, such as anodization and copper plating, have been used in the process for many years. Optoelectrochemical reactions have also been demonstrated in fabrication some devices.

In this talk, the author will make a systematic review on requirements of solid state devices with respect to structures, operation physics, and reliability. Then, based on above criteria, possible applications of electrochemical reactions on device and product fabrications are discussed. Advantages and challenges in satisfying manufacturing, performance, and reliability requirements are discussed. For some nano dimension structures, the electrochemical reaction process may be more suitable than the conventional process with respect to costs of equipment and operation.

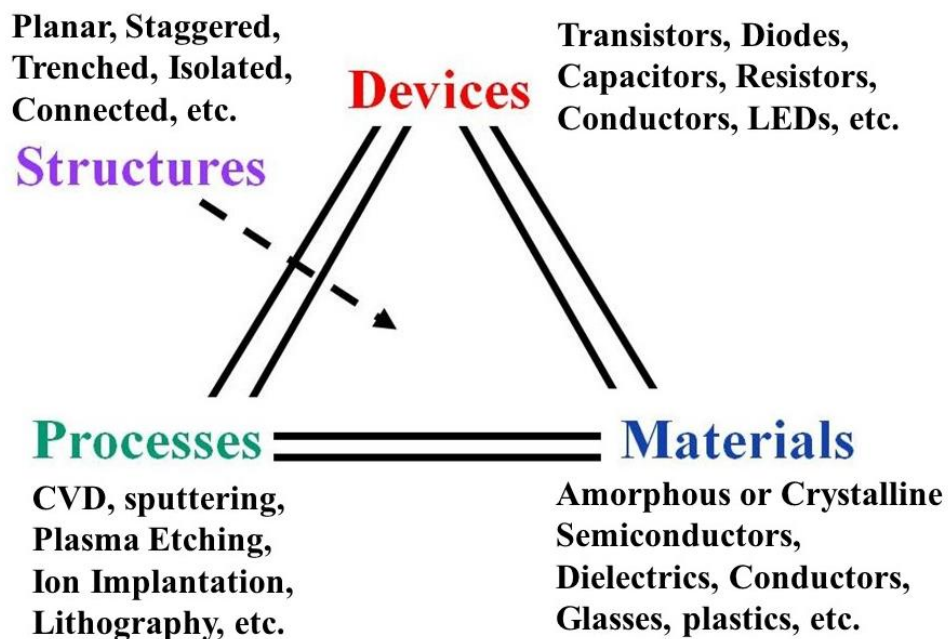


Fig. 1. Materials, processes, devices, and structures relationships in solid state device and products.

Redox Polymers as an Electrode-active Material

Hiroyuki Nishide

Waseda University

Shinjuku, Tokyo 165-8895, Japan

nishide@waseda.jp

Organic redox polymers are a series of aliphatic polymers bearing robust nitroxide, triarylamminium, phenoxy, viologen, quinone, etc as electron-releasing and -gaining sites per their repeating unit. They are characterized by both a dense population of the redox site and a rubbery state with the coexistence of small amount of electrolytes, to allow very fast self-exchanging reaction among the redox sites with the driving force of concentration gradient, and to provide efficient charge-transport and -storage throughout the polymers. The very high charge-transporting capability within the purely organic polymers led to the tremendously large current density beyond 100 mA/cm² and long distance for the thickness of 50 μm. Organic-based, high-power and flexible rechargeable devices are the application examples. Output voltages of the electrodes corresponded to redox potentials of the redox groups and were tunable with their molecular designing. Effect of the polymers on redox mediation of conventional cathode-active materials such as LFP and LCO will be also described.

In-situ Studies of Li- and Na- Intercalation Batteries

Lukas Seidl¹, Oliver Schneider¹ and Ulrich Stimming^{1,2}

¹*Electrochemistry Group, Institute of Informatics VI, Technical University Munich, Germany*

²*Chemistry - School of Natural and Environmental Sciences, Bedson Building, Newcastle University,*

Newcastle upon Tyne, NE1 7RU, United Kingdom

ulrich.stimming@ncl.ac.uk

The SEI layer plays an important role in the operation of Li-ion intercalation batteries. Yet, the processes of SEI formation and of intercalation are still not well understood on the molecular level. Scanning probe techniques are capable of analysing these processes under in-situ conditions.

The SEI-formation on graphitic electrodes operated as an Li⁺-ion battery anode in a standard 1 M LiPF₆ EC/DMC (1 : 1) electrolyte has been studied using in-situ electrochemical scanning tunnelling microscopy (EC-STM)¹. Two different modes of in situ study were applied, one, which allowed to follow topographic and crystallographic changes (solvent co-intercalation, graphite exfoliation, SEI precipitation on the HOPG basal plane) of the graphite electrode during SEI-formation, and the second, which gave an insight into the SEI precipitation on the HOPG basal plane in real time. From the in situ EC-STM studies, not only conclusions about the SEI-topography could be drawn, but also about the formation mechanism and the chemical composition, which strongly depend on the electrode potential. It was shown that above 1.0 V vs. Li/Li⁺ the SEI-formation is still reversible, since the molecular structure of the solvent molecules remains intact during an initial reduction step. During further reduction, the molecular structures of the solvents are destructed, which causes irreversible charge losses.

The reversible intercalation of solvated Na-ions into graphite and the concomitant formation of ternary Na-graphite intercalation compounds (GICs) is studied by EC-STM and other in-operando techniques². Linear ethylene glycol dimethyl ether homologes ("glymes") G_x with x+1 O-atoms were used as solvents, where x is 1-4. The intercalation mechanism of Na⁺(G_x)_y-complexes was investigated with the focus on phase transitions and diffusion rates of the Na⁺(G_x)_y-complexes inside the graphite lattice. For the four shortest glymes (G1 to G4), it is found by XRD that an intermediate stage 2 Na-GIC (NaC₄₈) is formed upon partial sodiation of the graphite electrode. At full sodiation a stage 1 Na-GIC (NaC₁₈, 112 mAh g⁻¹) is obtained for G1, G2 and G4, while the G3-system is also forming a stage 1 Na-GIC but with less Na incorporated (NaC₃₀, 70 mAh g⁻¹). Phase transitions of a battery electrode upon ion-intercalation are visualised by STM on the atomic scale for the first time. In addition, local diffusion rates of the intercalated species inside the electrode were determined, a unique approach to determining kinetic effects in batteries on the atomic scale. The formation of a solid electrolyte interphase (SEI) is observed in EC-STM.

- 1) Lukas Seidl, Sladjana Martens, Jiwei Ma, Ulrich Stimming, Oliver Schneider "[In-Situ Scanning Tunneling Microscopy of the SEI Formation on Graphite Electrodes for Li-Ion Batteries](#)" *Nanoscale*, 2016, **8**, 14004;
- 2) L. Seidl, N. Bucher, E. Chu, S. Hartung, S. Martens, O. Schneider and U. Stimming, "[Intercalation of solvated Na-ions into graphite](#)", *Energy Environ. Sci.*, 2017, **10**, 1631.

Efforts to Develop the Innovative Batteries in the NEDO RISING2 Project

Eiichiro Matsubara

*Department of Materials Science and Engineering, Kyoto University
Yoshida-honmachi, Sakyo-ku, Kyoto, Japan, 606-8507
matsubara.eiichiro.6z@kyoto-u.ac.jp*

We will verify batteries with an energy density of 500 Wh/kg for commercial production of rechargeable batteries in 2030 in the NEDO (New Energy and Industrial Technology Development Organization) project “R & D of promoting practical implementation of innovative batteries”, popularly known as “RISING2”. The two innovative battery groups depending on the charge carriers, that is, the anode-ion-driven battery group and the cathode-ion-driven group, and the advanced analysis group are organized in RISING2. Core research bases are centralized in Office of Society-Academia Collaboration for Innovation, Kyoto University and Kansai Center, National Institute of Advanced Industrial Science and Technology (AIST). And 18 universities and research institutes all through Japan are located as the satellite research bases. 10 automobile and electric companies, etc. are sending transferred researchers and engineers to the core bases.

Zinc metal-air batteries and fluoride-ion-driven nano-interface controlled batteries where hydroxide ions and fluoride ions are charge carriers, respectively, are studied as the anion-ion-driven innovative batteries in the Kyoto University core base. The very high energy density is theoretically expected in the zinc metal-air battery since a positive electrode active material oxygen is taken from the outside of the system and high safety is secured because its solution is water system. In addition, a low cost battery may be constructed with common metal zinc. Although the zinc-air batteries have been studied for long time, there have been still some problems on cycle performance in both zinc and air electrodes. In the zinc metal-air battery team, improvement of durability of zinc electrodes based on the concept of controlling solubility of zinc in the electrolyte, establishment of longer life battery performance of the graphite air electrode, and enhancement of electro catalytic activity of metal-oxide catalysts have been studied.

Since monovalent fluoride ions are used as a charge carrier in the fluoride-ion-driven nano-interface controlled battery, its input/output battery performance may be better than those of the polyvalent metal ion-driven or oxide ion-driven batteries. The research history of this battery is relatively short and many unsolved problems exist. In the present project, we study on establishment of a method to control solubility of metal fluorides and morphology of precipitation of metal from metal fluoride and metal fluoride from metal in positive and negative electrodes in battery reactions. And we are also searching new electrolytes with good fluoride-ion conductivity and excellent high-potential durability.

Lithium-sulfur batteries and lithium-nano-interface controlled conversion-type batteries where lithium ions are charge carriers are studied as the cation-ion-driven innovative batteries in the Kansai Center, AIST. Both battery systems show the largest theoretical weight energy density in closed systems and consist of low cost materials. Thus, we expect to design high battery performance and inexpensive batteries. Although the history of research is long, we have still some problems, such as cycle degradation and dissolution of sulfur, etc. In these teams, the cause of cycle degradation and control of dissolution of sulfur are clarified to find a clue of their solution.

In the present project, the advanced analysis group is organized to solve the problems of the operand innovative batteries by exploring the mechanism of battery reaction from the atomic level to nano-, meso- and micro-scopic levels by applying synchrotron x-ray radiation, neutron scattering, NMR spectroscopy, electrochemical measurement, transmission electron microscopy, Raman spectroscopy and computer science. For example, the spatial resolution of high energy confocal x-ray diffraction technique with synchrotron radiations in SPring-8 has been largely improved to observe a depth profile of a battery reaction in a working composite electrode. Using neutron radiography and diffraction, reaction inhomogeneity in a storage battery for a vehicle has been observed. By using pulse x-rays from the synchrotron ring, we are challenging to explore catastrophic battery reactions of active materials just after insertion of a nail to a model battery. This will provide us knowledge of battery safety.

In the present talk, I will introduce some examples of the innovative battery analyses in collaboration with the innovative battery R & D groups.

A light-addressable lab-on-a-chip platform

T. Wagner^{1,2}, L. Breuer¹, R. Welden¹, F. Vahidpour¹, M.J. Schöning^{1,2}

¹ *FH Aachen, Campus Jülich, Institute of Nano- and Biotechnologies (INB), 52428 Jülich, Germany*

² *Research Center Jülich, Institute of Complex Systems (ICS-8, Bioelectronics), 52425 Jülich, Germany
torsten.wagner@fh-aachen.de*

In the fields of lab-on-a-chip devices, the attribute light-addressability describes the usage of light to stimulate respectively trigger a sensor and actuator functions, by means of a focused light beam. Light-addressability has several advantages over conventional methods. The light beam can be easily modified in shape, size and its position, to address precisely areas of interest. With transparent cover materials or substrates, light can be utilized to trigger sensor and actuator units directly within a microfluidic set-up. The usual and often complex sealing and encapsulation steps for the otherwise needed wires and connections can be omitted. This simplifies, both production and handling. Reducing the number of elements, materials and openings, in direct contact with the analyte under test, helps further to reduce the risk of potential contamination and hence, measurements under sterile environments can be performed more easily. In addition, the wavelength of the light source, the light intensity, as well as the pulse timing can be precisely controlled, which enables an exact control of the underlying processes and mechanisms for the particular light-addressable technologies.

In this work we will introduce a new developed lab-on-a-chip platform, which integrates light-addressable potentiometric sensors (LAPS) as sensing elements, light-addressable electrodes (LAE) as electrochemical actuator elements and light-addressable hydrogels as micro-valves. All of these elements are integrated in a microfluidic set-up.

Furthermore, we will introduce the necessary developments of the required programmable light-sources, discuss challenges during the integration steps to combine different light-addressable technologies and give an outlook on potential applications.

Nanostructures for Combined Conversion/Alloying Materials as Lithium-ion Anodes

Stefano Passerini and Dominic Bresser

*Helmholtz Institute Ulm (HIU) Helmholtzstrasse 11, 89081 Ulm, Germany
Karlsruhe Institute of Technology (KIT), P.O. Box 3640, 76021 Karlsruhe, Germany*

Email: stefano.passerini@kit.edu

Despite the unique combination of exceptional energy and power density, making lithium-ion batteries the state-of-the-art electrochemical energy storage technology for small- and large-scale applications [1], further improvement is needed for realizing lightweight and small-sized batteries to achieve, for instance, in case of electric vehicles extended driving ranges without requiring tremendous additional load. For this reason, alternatives to the classic intercalation chemistry are attracting great attention. With respect to the anode, these are so far mainly alloying [2] and conversion materials [3]. Both, however, suffer from intrinsic issues, including extensive volume variations and large voltage hystereses, as in particular in case of the former and the latter, respectively [2,3]. Recently, an additional class of anode materials has gained steadily increasing attention, combining these two lithium storage mechanisms in a single compound: conversion/alloying materials (CAMs) [4].

Herein, a comprehensive overview on this new material class will be provided, starting from a brief summary of the major strengths and issues related to pure alloying and conversion electrodes, subsequently introducing the two approaches to realize CAMs while highlighting some recent results, before finally summarizing their potential advantages and the remaining challenges.

Potential Stability of the Partially Oxidized Conducting Polymer-coated Electrode in Organic Phase for Application to an Amperometric Device

Yumi Yoshida^{a*}, Emi Kusakabe^a, Yui Nakamura^a, Mao Fukuyama^{b,c}, Kohji Maeda^a

^a*Faculty of Molecular Chemistry and Engineering, Kyoto Institute of Technology
Matsugasaki, Sakyo, Kyoto 606-8585, Japan*

^b*PRESTO, Japan Science and Technology Agency
4-1-8 Honcho, Kawaguchi, Saitama 332-0012, Japan*

^c*Institute of Multidisciplinary Research for Advanced Materials, Tohoku University
2-1-1 Katahira, Aoba-ku Sendai 980-8577, Japan
yyoshida@kit.ac.jp*

A solid electrode that can operate as both a reference electrode and a counter electrode—a reference/counter electrode—for an organic phase, Org, is necessary for the fabrication of a micro and/or thin layer cell with an organic membrane such as a liquid membrane-type ion-selective electrode, ISE, and an amperometric cell with the interface between aqueous phase, W and Org.

A conducting polymer-coated solid electrode has been one of candidates for use as a reference/counter electrode in Org. The conducting polymer has low solubility in Org and functions as an ion-electron transducer. In 1987-1988, the conducting polymer-coated electrode was applied to an all-solid ISE in which the inner solution was replaced by the conducting polymer, and there have been many reports on the all-solid ISE using the conducting polymer-coated electrode even in recent literature, as shown in several reviews. Recently, amperometric ISEs and a coulometric thin layer cell using the conducting polymer-coated electrode have been proposed and used for the realization of stripping voltammetry and absolute determination of redox-inactive ions. However, these ISE and electrolysis cells with the conducting polymer-coated electrode have rarely been used in practical applications even though various applications of the conducting polymer-coated electrode have been proposed.

Low stability and poor reproducibility of the electrode potential are the most serious problems for the conducting polymer-coated electrode. Poly(3,4-ethylenedioxythiophene), PEDOT, is a chemically stable conducting polymer that improves the potential stability of the all-solid ISE; however, slow potential drift and a shift of the absolute value of the electrode potential in an aqueous standard solution have been observed for this ISE. The factors related to the potential stability and reproducibility of the conducting polymer-coated electrode have been extensively discussed on the basis of the redox capacitance of the conducting polymer or the irreversibility of the ionic transfer between the polymer and the selective membrane.

In the present work, the potential stability and potential reproducibility of the conducting polymer-coated under open circuit or current-flowing were examined in hydrophobic Orgs for longer period by focusing on the oxidized conditions of the conducting polymer. The oxidized conditions and the formal potential of the conducting polymer were evaluated from the dependence of the absorption spectra of the conducting polymer on the applied potential. The partially oxidized PEDOT electrode was applied to amperometric device for the ion transfer between aqueous sample solution and organic membrane.

Interfacial Synthesis of Functional Coordination Nanosheets

Hiroshi Nishihara

Department of Chemistry, School of Science, The University of Tokyo
7-3-1 Hongo, Bunkyo-ku, Tokyo 113-0033, Japan
nishihara@chem.s.u-tokyo.ac.jp

A new type of two-dimensional (2D) materials, coordination nanosheets (CONASHs) comprising metal ions and organic π -ligands have attracted much recent attention because of their unique physical and chemical properties [1-3]. We have developed interfacial reaction to synthesize high-quality CONASH films. For example, a liquid–liquid interfacial reaction of nickel(II) acetate in an aqueous phase with benzenhexathiol in an organic phase produced electro-conducting multilayered sheets containing bis(dithiolato)nickel moieties with one micrometer thickness (Fig. 1a). A single-layer nanosheet with 0.6 nm thickness was successfully synthesized using a gas–liquid interfacial reaction. Modulation of the oxidation state and the electronic conductivity of the coordination nanosheet was achieved using redox reactions. Bis(dithiolato)palladium nanosheet was prepared by a modified interfacial method inhibiting the formation of Pd nanoparticles.

A series of multilayered coordination nanosheets comprising 1,3,5-tris(4(2,2':6',2''-terpyridyl)phenyl)benzene and iron(II) or cobalt(II) ions was synthesized by liquid/liquid interfacial coordination reactions (Fig. 1b). The resultant bis(terpyridine)metal nanosheet had a flat, smooth morphology and was several hundreds of nanometers thick. Upon its deposition on an indium tin oxide (ITO) electrode, the nanosheets underwent a reversible and robust redox reaction ($\text{Fe}^{3+}/\text{Fe}^{2+}$ or $\text{Co}^{2+}/\text{Co}^{+}$) accompanied by a distinctive color change. Electrochromism was achieved in a solidified device composed of the nanosheet, a pair of ITO electrodes, and a polymer-supported electrolyte. The combination of Fe^{2+} and Co^{2+} nanosheets in one device deposited on each ITO electrode demonstrated dual-electrochromic behavior. Bis(terpyridine)zinc nanosheets exhibit photoluminescence properties.

Coordination nanosheets featuring a photoactive bis(dipyrrinato)zinc(II) complex motif were also prepared by an interfacial reaction between a three-way dipyrrin ligand and zinc(II) ions (Fig. 1c). The bis(dipyrrinato)zinc(II) nanosheet deposited on a SnO_2 electrode functions as a photoanode in a photoelectric conversion system.

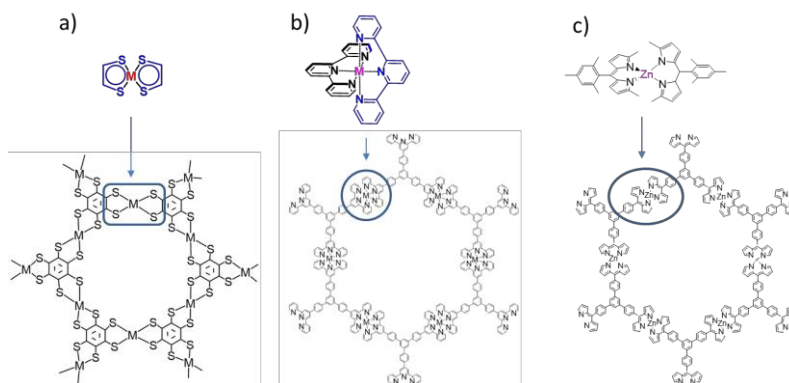


Fig.1. Coordination nanosheets of bis(dithiolato)metal (a), bis(terpyridine)metal (b), and bis(dipyrrinato)zinc complexes

References

- [1] R. Sakamoto, K. Takada, X. Sun, T. Pal, T. Tsukamoto, E. J. H. Phua, A. Rapakousiou, K. Hoshiko, H. Nishihara, *Coord. Chem. Rev.* **2016**, 320-321, 118, and the references therein.
- [2] H. Maeda, R. Sakamoto, H. Nishihara, *Langmuir* **2016**, 32, 2527 (Feature Article), and the references therein.
- [3] H. Maeda, R. Sakamoto, H. Nishihara, *Coord. Chem. Rev.* **2017**, 346, 139, and the references therein.

Nanoscale Electrochemical Imaging for Characterization of Functional Materials

Tomokazu Matsue

Graduate School of Environmental Studies, Tohoku University
6-6-11-605 Aramaki, Aoba, Sendai 980-8579, Japan
matsue@bioinfo.che.tohoku.ac.jp

Electrochemical imaging [1] is an emerging technology to understand localized functions of various materials because unique functions of biomaterials, energy materials, and other materials are in many cases based on electrochemical phenomena. Electrochemical imaging is categorized into two basic ways; the imaging using micro/nanoelectrode arrays and scanning micro/nanoelectrochemical probes. In this presentation, I will show basic outlines and recent progress of nanoscale electrochemical imaging of the two categories.

1. Electrochemical imaging using microelectrode arrays.

Microelectrode arrays have been frequently used to attain device-based electrochemical imaging. It is, however, difficult to arrange many microelectrodes into small areas because of limited spaces for connection pads for external control units. To solve this drawback, we have developed a new electrode array for imaging. It is called a local redox cycling-based electrochemical (LRC-EC) device [2], based on detection of local redox cycling events between adjacent two microelectrodes. The LRC-EC device has been successfully applied for imaging of gene expression from single cells and high-throughput detection of differentiation of Embryonic stem (ES) cells. Also, we developed a CMOS-based LSI (BioLSI) for rapid, highly-sensitive, comprehensive analysis [3] and applied to imaging of biomaterials, live cells, cell aggregates, small aquatic organisms.

2. Electrochemical Imaging using scanning electrochemical probes

Although a scanning electrochemical microscope (SECM) has become popular, the distance control between the probe and sample has still been a big challenge to improve the temporal resolution and sensitivity. We adopted voltage-switching mechanisms to attain high resolution bioimaging in SECM systems and applied to simultaneous imaging of topography and electrochemical responses live cells [4]. We also incorporated an ion-conductance feedback for nanoelectrochemical imaging and applied to rapid, non-invasive bioimaging of live cells [5]. This system affords information on dynamic changes of nanostructures of cell membrane surfaces. Capacitive currents can also be used for feedback signal to control the distance. We incorporated this feedback mechanism to develop a nano-scanning electrochemical cell microscope (SECCM) and applied to characterization of localized battery materials with resolution of less than 100 nm [6]. The technique measures electrode topography and different electrochemical properties simultaneously, and the information can be combined with complementary microscopic techniques to reveal new perspectives on structure and activity. The nanoscale SECCM (NanoSECCM) exhibit highly spatially heterogeneous electrochemistry at the nanoscale, both within secondary particles and at individual primary nanoparticles, which is highly dependent on the local structure and composition. We also applied NanoSECCM to characterize functional 2D materials.

References

[1] Y. Takahashi et al., *Anal. Chem.*, 2017, 89, 342; K. Ino et al., *Cur. Opinion Electrochem.*, in press. [2] Z. Y. Lin et al., *Angew. Chem. Int. Ed.*, 2009, 48, 2044; K. Ino et al., *Angew. Chem. Int. Ed.*, 51, 2012, 6648; *Anal. Chem.*, 2014, 86, 2989. [3] K. Y. Inoue et al., *Lab Chip*, 2013, 12, 3481; *Lab. Chip.*, 2015, 15, 848; K. Ino et al., *Angew. Chem. Int. Ed.*, 2017, 56, 6818. [4] Y. Takahashi et al., *PNAS*, 2012, 109, 11540. [5] Y. Takahashi et al., *JACS.*, 2010, 132, 10118; *Angew. Chem. Int. Ed.*, 2011, 50, 9638; Y. Nashimoto et al., *ACS Nano*, 2016, 10, 6915; H. Ida et al. *Anal. Chem.*, 2017, 89, 6016. [6] Y. Takahashi et al., *Nature Commun.*, 2014, 5, 6450.

MnO₂-based thin-film sensors for harsh environmental conditions

M.J. Schöning^{1,3}, J. Oberländer^{1,2}, J. Arreola^{1,2}, Z. Jildeh^{1,4}, M. Keusgen², P. Wagner⁴

¹ FH Aachen, Campus Jülich, Institute of Nano- and Biotechnologies (INB), 52428 Jülich, Germany

² Philipps-University Marburg, Institute of Pharmaceutical Chemistry, 35032 Marburg, Germany

³ Research Center Jülich, Institute of Complex Systems (ICS-8, Bioelectronics), 52425 Jülich, Germany

⁴ Katholieke Universiteit Leuven, Departement Natuurkunde en Sterrenkunde, Afdeling Zachte Materie en Biofysica, 3001 Leuven, Belgium
schoening@fh-aachen.de

In food industry, gaseous hydrogen peroxide (H₂O₂) serves as a common sterilization agent to sterilize beverage cartons on aseptic filling machines. H₂O₂ possesses different advantages over conventional chemical sterilization media (e.g., chlorine or peracetic acid) such as high microbicidal and sporicidal activity in a short exposure time (due to radical formation, especially at elevated temperatures). Moreover, it decomposes into the environmental-friendly end products water vapor and oxygen [1]. The sterilization process, however, is performed under harsh environmental conditions (high temperatures and high H₂O₂ concentrations).

Several types of calorimetric gas sensors have been developed in our laboratory to monitor sterilization processes of beverage cartons in real time [2-4]. The sensing principle of these calorimetric gas sensors relies on the determination of the decomposition energy (exothermic heat reaction), when H₂O₂ is decomposed on the catalytically active sensor surface. For sensor operation, a differential set-up of two temperature sensors is applied: One of the sensors is passivated with a H₂O₂-resistant polymer, whereas the second temperature sensor is covered with a catalyst to force the decomposition of H₂O₂. Various catalytic materials have been investigated such as manganese(IV)-oxide, platinum and palladium. In case of a polymer-based thin-film sensor, the flexible substrate even enables positioning of the sensor chip inside beverage packages. In combination with a wireless readout system, online monitoring of the sterilization processes could be demonstrated.

In industrial environment, the evaluation of this sterilization process is commonly done by laborious and time-consuming microbiological challenge tests. Recently, a spore-based biosensor chip (spores of *Bacillus atrophaeus*) was introduced allowing a rapid process control [5,6]. The biosensor exposure to the H₂O₂ sterilization process causes alterations on the immobilized microorganisms. Impedance measurements at different sensor states are recorded as electrical quantification.

- Les paramètres requis sont manquants ou erronés.**
1. I. A. Ansari and A. K. Datta, An overview of sterilization methods for packaging materials used in aseptic packaging systems, Food and Bioproducts Processing, vol. 81, (2003) 57-65.
 2. N. Näther, L.M. Juarez, R. Emmerich, J. Berger, P. Friedrich and M.J. Schöning, Detection of hydrogen peroxide (H₂O₂) at exposed temperatures for industrial processes, Sensors, vol. 6, (2006) 308-317.
 3. P. Kirchner, J. Oberländer, P. Friedrich, J. Berger, G. Rysstad, M. Keusgen and M.J. Schöning, Realisation of a calorimetric gas sensor on polyimide foil for applications in aseptic food industry, Sensors and Actuators B, vol. 170, (2012) 60-66.
 4. P. Kirchner, J. Oberländer, H.-P. Suso, G. Rysstad, M. Keusgen and M.J. Schöning, Monitoring the microbicidal effectiveness of gaseous hydrogen peroxide in sterilisation processes by means of a calorimetric gas sensor, Food Control, vol. 31, (2013) 533-538.
 5. J. Oberländer, A. Bromm, L. Wendeler, H. Iken, M. Palomar Duran, A. Greeff, P. Kirchner, M. Keusgen and M.J. Schöning, Towards a biosensor to monitor the sterilisation efficiency of aseptic filling machines, Physica Status Solidi A, vol. 212(6), (2015) 1299-1305.
 6. J. Arreola, J. Oberländer, M. Mätzkow, M. Keusgen and M.J. Schöning, Surface functionalization of spore-based biosensors with organosilanes, Electrochimica Acta, vol. 241, (2017) 237-241.

Electrochemical CO₂ to formic acid process based on dental amalgam electrode

Woonsup Shin and Mijung Park

Department of Chemistry, Sogang University, Seoul 121-742, Korea
shinws@sogang.ac.kr

CO₂-to-Formate or Formic Acid Process is one of the actively pursuing CCU technologies. The dental amalgam is formed on the porous copper foam for fast conversion of CO₂ at a high current density in flowing condition. We succeeded in producing formate of 1.2 M concentration for 30 hrs electrolysis using 9 cm x 9 cm electrode. The current efficiency of 80~90% was obtained at 50 mA/cm² and at 100 mA/cm². The continuous electrolysis could be operated for more than a month. The produced formate could be converted to formic acid efficiently followed by the process of the addition of sulfuric acid. The developed process is currently applied to build a pilot system of 500 kg/day conversion unit in Hadong power plant in Korea. We'll discuss the current status and the future development of the process.

Activity and Selectivity Control of the Photo- electrochemical Behavior of Nanoparticulate n-semiconductors Based on Ti Oxides

Petr Krtil, Roman Nebel, Monika Klusáčková, Kateřina Minhová Macounová, Ladislav Kavan, Ivano Castelli*, Jan Rossmeisl*

*J. Heyrovsky Institute of Physical Chemistry, Academy of Sciences of the Czech Republic
Dolejškova 3, Prague, Czech Republic*

**Department of Chemistry, University of Copenhagen, Universitetsparken 5, 2100 København Ø,
Denmark.*

Petr.Krtil@jh-inst.cas.cz

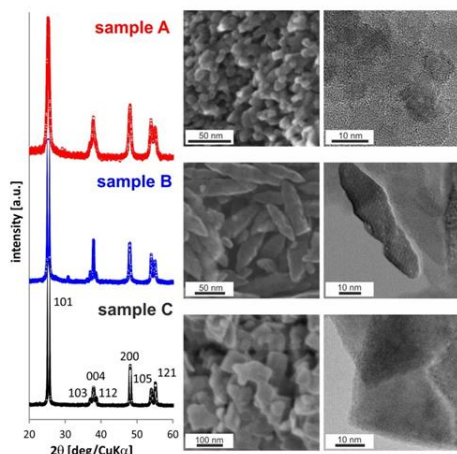


Figure 1 Powder X-ray diffraction patterns (left) and SEM images (middle) and HRTEM images (right) of anatase samples differing in the nanocrystal shape. The sample assignment is given in the Figure annotation. The SEM images were taken on the catalysts attached to the electrodes; the HRTEM images correspond to as prepared catalysts after calcination

Photo-electrochemical water splitting represents one of the key processes needed for successful utilization of renewable energy sources for distributed generation, storage and use of energy[1]. The research related to the electrochemical and photo-electrochemical splitting of water is primarily motivated by electricity storage in hydrogen. The overall process itself, however, is limited by the kinetically sluggish oxygen evolution reaction (OER). Although the surface sensitivity of the oxygen evolution on conductive oxides is well established the concept of surface control in steering the photoelectrochemical activity of semiconductors has not yet been explored.

This paper compares activity and selectivity of different surface orientations of the three representative n-semiconductors based on oxides of Ti - TiO₂ – anatase, SrTiO₃ and BaTiO₃ in the nanocrystalline forms with preferential surface orientation when the surface orientation of different samples was achieved from high resolution TEM micrographs as shown in Fig. 1. The selectivity of different surface structures of various Ti oxide based n-semiconductors in photo-electrochemical water splitting will be compared based using on-line mass spectroscopic detection (DEMS). The relative amount of oxygen normalized by the passed charge will be used to quantify the

ability of the surface structures to enter oxygen evolution of radical forming reaction sequences (see Fig. 2). The significant differences in the amount of the produced oxygen on different surface structures is attributed to a competition between electron and hole charge transfer at the semiconductor/electrolyte interface. The observed tendencies can be rationalized with help of the DFT calculation assuming the nanocrystalline electrode behaves electronically as macroscopic object [2] (i.e. the formation of SC layer is not hindered by the dimensions of the individual nanocrystals). The DEMS selectivity data will be matched against the photoelectrocatalytic behavior of the single crystals namely at different pH values and in different electrolytes.

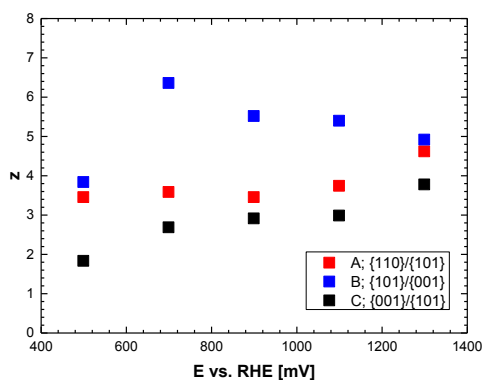


Figure 2 DEMS based average number of electrons needed to evolve one molecule of oxygen as a function of the applied potential on different anatase photocatalysts illuminated in acid (pH=1) electrolyte solution. The sample colour coding is the same as in Figure 1.

[1] Lewis NS, Nocera DG, *Proc. Natl. Acad. Sci. U.S.A.*, 103 (2006) 15729.

[2] Bisquert J, Garcia-Belmonte G, Fabregat-Santiago F, *J. Solid State Electrochem.*, 3(1999) 337.

Exploiting Hydrogen-sorption for Deposition of Platinum on Palladium Films

Dr Natasa Vasiljevic

School of Physics, University of Bristol

H.H. Wills Physics Laboratory, Tyndall Avenue, Bristol BS8 1TL, UK

n.vasiljevic@bristol.ac.uk

Among different electrochemical methods developed for the design of Pt-bimetallic electrocatalysts, surface limited redox replacement (SLRR) has an important place.[1] The SLRR method enables successful epitaxial deposition of Pt monolayers, thin films and nanoclusters with atomic scale control that cannot be matched by any other method. The method utilises the underpotentially deposited (UPD) epitaxial layer of metal as a sacrificial layer that is replaced by a more noble Pt through surface-limited galvanic replacement reaction. Besides Cu UPD and Pb UPD based SLRR growth, it has been demonstrated that hydrogen UPD can be successfully used for Pt thin films growth.[2] The H-UPD SLRR approach has been recently extended to other metals such as Pd well known for its unique H-sorption behavior.[3, 4]

Here we will present an electrochemical Quartz Crystal Microbalance (EQCM) and in-situ Scanning Tunneling Microscopy (STM) study of Pt electrodeposition on Pd ultra-thin films based on the galvanic displacement of a controlled amount of sacrificially pre adsorbed or absorbed hydrogen. The study will be focused on the growth of Pt on 2ML and 10 ML epitaxial Pd films electrodeposited of Au because of notable differences in their structure and H absorption behavior.[5] For example, 2ML Pd films are pseudomorphic and do not feature absorption of hydrogen, while 10 ML Pd films maintain the epitaxial structure with the underlying Au and feature energetically separated H (ad and ab) sorption processes.

The SLRR replacement kinetics and the reaction stoichiometry were investigated by EQCM. On 2ML Pd films, Pt deposition showed the expected deposition efficiency (2:1 H to Pt). On 10ML Pd samples, the SLRR deposition resulted in the higher amount of Pt deposition per growth cycle, and more prolonged replacement transients with the transport limited replacement kinetics. X-ray Photoemission Spectroscopy was used for the analysis of surface composition of Pt-10ML Pd/Au, and the in-situ Scanning Tunneling Microscopy demonstrated the quasi- 2D epitaxial growth. Electrochemical characterisation of Pt-10ML Pd/Au films showed faster H absorption with more reversible behavior than on corresponding Pd film. Conventional electrochemical methods have been used to further examine the unexpected effect of Pt coverage and structure on the kinetics of H-absorption.

References:

- [1] N. Dimitrov, Recent Advances in the Growth of Metals, Alloys, and Multilayers by Surface Limited Redox Replacement (SLRR) Based Approaches, *Electrochimica Acta*, 209 (2016) 599-622.
- [2] J. Nutariya, M. Fayette, N. Dimitrov, N. Vasiljevic, Growth of Pt by surface limited redox replacement of underpotentially deposited hydrogen, *Electrochimica Acta*, 112 (2013) 813-823.
- [3] P.J. Cappillino, J.D. Sugar, F. El Gabaly, T.Y. Cai, Z. Liu, J.L. Stickney, D.B. Robinson, Atomic-layer electroless deposition: a scalable approach to surface-modified metal powders, *Langmuir*, 30 (2014) 4820-4829.
- [4] I. Achari, S. Ambrozik, N. Dimitrov, Electrochemical Atomic Layer Deposition of Pd Ultrathin Films by Surface Limited Redox Replacement of Underpotentially Deposited H in a Single Cell, *The Journal of Physical Chemistry C*, 121 (2017) 4404-4411.
- [5] M. Baldauf, D.M. Kolb, A Hydrogen Adsorption and Absorption study with ultrathin Pd overlayers on Au(111) and Au(100), *Electrochimica Acta*, 38 (1993) 2145-2153.

The Design of Materials for High Rate Energy Storage

Bruce Dunn

Department of Materials Science and Engineering

University of California, Los Angeles

bdunn@ucla.edu

The prospect of developing materials with the energy density of batteries and the power density and cycle life of electrical double-layer capacitors is an exciting direction that has yet to be realized. With these materials there is the promise of achieving charging in minutes to storage levels comparable to battery electrode materials. This paper will review our work on using Li^+ insertion in Nb_2O_5 as a model system in which to achieve high rate energy storage. This research has established a basis for intercalation processes in which the rate of charge storage is determined by surface-like kinetics rather than semi-infinite diffusion as occurs with battery materials. Another important feature with this mechanism is that the structure does not undergo a first-order phase transition upon Li^+ insertion. In addition, we have found that nanostructuring of materials leads to high rate energy storage because of the large number of surface sites for charge storage or because phase transitions are suppressed. In research to date, we have used nanostructuring to create electrode materials that retain high capacity for lithium at charging rates of 1 to 2 minutes. The results presented in this paper provide a basis for developing a variety of materials systems and a new generation of energy storage devices which possess both high energy density and high power density.

Li Insertion/Desorption Simulations at $\text{Li}_x\text{C}_6/\text{EC}$ (LiPF_6 1M) Interfaces Using Density Functional + Implicit Solvation Theory

Jun Haruyama, Tamio Ikeshoji, Minoru Otani
National Institute of Advanced Industrial Science and Technology (AIST)
1-1-1 Umezono, Tsukuba, Ibaraki 305-8568, Japan
haruyama-jun@aist.go.jp

Development of a stable energy storage device is a fundamental approach to solve energy-related issues. Lithium-ion batteries (LIBs) are one of the most promising candidates because of their high energy density and long cycle life. The main factor limiting the performance of LIB is regarded as charge transfer reactions at electrode/electrolyte interfaces. Although the detailed mechanism of electrochemical reaction of solid/liquid interface is dependent on several elemental subreactions, electrochemical impedance spectroscopic measurements revealed that the charge-transfer resistance mainly comes from Li^+ desolvation process at the interface. [1, 2]

We focused on Li insertion/desorption processes at the interface between a graphite anode and EC (LiPF_6 1M) electrolyte; they are conventional LIB components. We applied density functional theory (DFT) + effective screening medium (ESM) method [3] combined with reference interaction site method (RISM): ESM-RISM simulation. [4] Namely, the graphite surface (Li_xC_6 slab + additional Li^+) and liquid solution (EC LiPF_6 1M) are represented as quantum mechanical and implicit classical solvation, respectively (see Figure 1). Therefore, the distribution function of the classical solvation automatically formulates the solvation/desolvation structures in the Li insertion/desorption processes. Additionally, ESM-RISM formulation can define the inner solvation potential; the electrode potential applied in Li insertion/ desorption simulation is possibly interpreted into the experimental Li/Li⁺ potentials.

In the presentation, we will explain the details of the ESM-RISM simulation, and introduce the energy profiles of the Li insertion/desorption path at the LiC_6/EC LiPF_6 interface. We will also discuss the activation energies of the insertion process with respect to x of Li_xC_6 ($x=0, 0.5, 1$), the graphite tilt angles (30 and 90 degrees), and Li/Li⁺ potentials if possible.

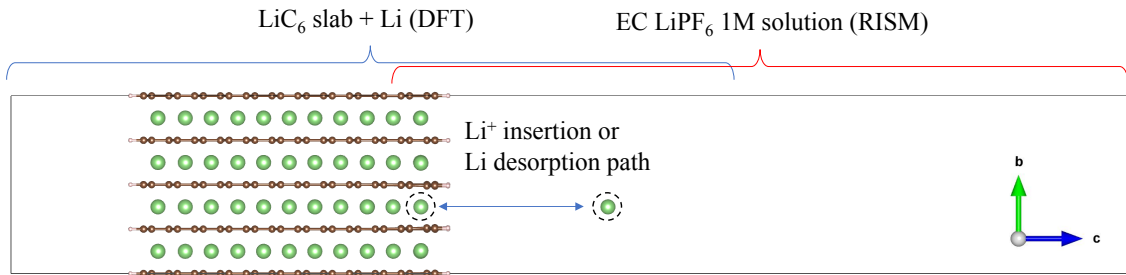


Fig. 1: LiC_6/EC LiPF_6 interface for Li insertion/desorption simulation. The graphite surface (Li_xC_6 slab + additional Li^+) and liquid solution (EC LiPF_6 1M) are treated within DFT and RISM, respectively.

- [1] T. Abe, H. Fukuda, Y. Iriyama, and Z. Ogumi, *J. Electrochem. Soc.* **151**, A1120 (2004).
- [2] K. Xu, A. von Cresce, and U. Lee, *Langmuir* **26**, 11538 (2010).
- [3] M. Otani and O. Sugino, *Phys. Rev. B* **73**, 115407 (2006).
- [4] S. Nishihara and M. Otani, *Phys. Rev. B* **96**, 115429 (2017).

Growth of Bismuth Selenide by Electrodeposition and SILAR: Materials for Photovoltaic and Photoelectrochemistry

Rasin Ahmed, Giovanni Zangari

Department of Materials Science and Engineering, University of Virginia

Bismuth selenide (Bi_2Se_3) is a semiconductor which presents two distinct crystalline phases, the first a seemingly stable rhombohedral structure, and the second, metastable, with orthorhombic phase. The two phases exhibit different band gap, 0.35 eV for the former and 1.25 eV for the latter, and show interesting optical, thermoelectric and topological electronic properties. Thin films of Bi_2Se_3 were grown by electrodeposition from an acidic electrolyte, with and without a surfactant and under both galvanostatic or potentiostatic conditions. The orthorhombic phase is obtained by growing at room temperature, while the rhombohedral one is obtained by growing at higher temperature (60°C) or upon gentle annealing. Under optimized deposition parameters, and using simultaneous heating and electrolyte stirring, smooth and thick films can be obtained. Morphological characterization from films grown without a surfactant evidences the formation of compact, uniform and smooth layers, attributed to the growth of small grains of ~50 nm. In contrast, films grown with a surfactant exhibit much smoother films. Structural characterization shows formation of a metastable orthorhombic phase with traces of a rhombohedral phase. The films grow initially with a rhombohedral crystalline structure, which progressively changes to orthorhombic, likely due to the accumulation of internal stresses and successive stress relaxation. In addition, a full recrystallization to the rhombohedral structure can be achieved by using short time and low temperature thermal treatments.

Bi_2Se_3 nanoparticles were grown by solution-processed SILAR method at room temperature. By increasing the SILAR deposition cycles from 15 to 60, only a partial coverage of the FTO substrates was achieved. Study of XRD patterns were inconclusive in identifying a distinct crystalline structure for SILAR deposited Bi_2Se_3 . Raman spectroscopy revealed evidence of a strong third A_1^3 vibrational mode for Bi_2Se_3 at 162.6 cm^{-1} besides the two modes, E_g^2 (136.3 cm^{-1}) and A_{1g}^2 (179.1 cm^{-1}). This suggests the existence of a mixed phase in SILAR deposited Bi_2Se_3 . Upon annealing at 100°C in vacuum, a rhombohedral crystalline phase was revealed, verified by both XRD pattern and Raman spectrum. The optical absorbance spectra of Bi_2Se_3 deposited on FTO substrates were determined, showing a gradual red shift of the long wavelength cutoff due to increasing the deposition cycles. The optical bandgap of the deposited Bi_2Se_3 nanoparticles was observed to vary between 1.39 eV (for $\text{Bi}_2\text{Se}_3_{15}$) and 0.66 eV (for $\text{Bi}_2\text{Se}_3_{90}$). To further clarify the observed bandgap using UPS study we found that the Fermi level position in Bi_2Se_3 is 0.74 eV above the valence band maxima (VBM), consistent with our calculated bandgap value of 0.8 eV.

The ability to synthesize materials with different band gaps is here exploited by growing graded materials that may generate internal electric fields to guide the flow of charge carriers. More generally, a combination of such materials may be successfully exploited to the construction of low cost, efficient novel devices based on thermoelectric, optical or electronic technologies.

Novel Catalyst for Electroreduction of CO₂ to Ethanol

Haitao Ye, Jiawei Fan, Wu Lei, Qingli Hao

School of Chemical Engineering, Nanjing University of Science and Technology, Nanjing 210094, China

E-mail: qinglihao@njust.edu.cn

Due to the large-scale consumption of fossil fuel, the increased CO₂ concentration in the atmosphere are associated with greenhouse effect and climate change, which have gained increasing research attention [1,2]. Therefore, the possibly captured CO₂ can be a potentially useful feedstock if it is converted into other hydrocarbon products. Electrochemical reduction is one of efficient methods for CO₂ utilization and recycling, which may be carried out at moderate temperature and atmospheric pressure. It also shows relatively high product selectivity compared with other reduction methods, such as chemical and thermochemical methods. However, the high over-potential for the electroreduction of CO₂ is the critical bottleneck. By now, various electrocatalysts have been shown to enable CO₂ reduction at low overpotentials, which include metals, metal compounds, and other nanostructures, especially for copper based catalysts. The main conversion products are CO, CH₄, HCOOH, and C1-related chemicals. The higher carbon-containing products have only been found in case of copper-related electrocatalysts used. Herein, we reported a novel catalyst of cobalt/graphene nanocomposites for the electrochemical reduction of CO₂ to ethanol with a high selectivity and a low overpotential. The XRD, TEM, XPS, Raman characterizations were used to confirm the chemical structure and morphology. The electrochemical performance of the cobalt/graphene catalyst was investigated systematically. A high efficiency towards CO₂ electroreduction to ethanol has been found, which is attributed to the synergistic effect of two components. This work highlights the importance of combination of non-copper nanoparticles with carbon on its catalytic activities. It also provides a strategy to design efficient catalysts for CO₂ electroreduction to higher carbon products in the future.

Acknowledgements

The work was supported by the National Natural Science Foundation of China (Nos. 21576138, 51572127), China-Israel Cooperative Program (S2016G5243), and the program for Science and Technology Innovative Research Team in Universities of Jiangsu Province, China.

Reference

- [1] Gao, S., et al., *Partially oxidized atomic cobalt layers for carbon dioxide electroreduction to liquid fuel*. *Nature*, 2016. **529**(7584): p. 68-71.
- [2] Costentin, C., M. Robert, and J.M. Saveant, *Catalysis of the electrochemical reduction of carbon dioxide*. *Chem Soc Rev*, 2013. **42**(6): p. 2423-36.

Fluorinated reduced graphene oxide as protective layer on lithium surface for batteries application

Jernej Bobnar^{1,2}, Matic Lozinšek³, Gregor Kapun¹, Christian Njel^{4,5}, Rémi Dedryvère^{4,5}, Boštjan Genorio², Robert Dominko^{1,2,5}

¹National Institute of Chemistry, Hajdrihova 19, SI-1001, Ljubljana, Slovenia

²University of Ljubljana, Faculty of Chemistry and Chemical Technology, Večna pot 113, SI-1001, Ljubljana, Slovenia

³Jožef Stefan Institute, Jamova cesta 39, SI-1000, Ljubljana, Slovenia

⁴CNRS / Univ. Pau & Pays Adour, Institute of Analytical Sciences and Physical Chemistry for Environment and Materials, IPREM – UMR 5254, 64000, Pau, France

⁵ALISTORE - European Research Institute, 33 rue Saint-Leu, Amiens 80039 Cedex, France

E-mail (Jernej Bobnar): jernej.bobnar@ki.si

Metallic lithium is one of the most promising anode materials for batteries applications. It is inherently lightweight, it has high theoretical capacity and it offers high energy density. The main drawback of metallic lithium is its unstable solid electrolyte interface (SEI), resulting in high surface area lithium (HSAL) growth. HSAL can be suppressed by different approaches including preparation of artificial SEI on lithium surface. Artificial SEI can be prepared by *in situ* technique with suitable additive in electrolyte such as LiNO_3 ,^[1] or by *ex situ* technique by pretreatment of lithium surface with protective layer before assembling electrochemical cell. Protective layer should be highly Li-ion conductive, electronically insulative, as thin as possible, and with high Young's modulus. Graphene derivatives meet all these requirements, thus they are ideal materials for protective layer application.^[2,3]

In present work, fluorinated reduced graphene oxide (FGI) was investigated as protective layer on lithium surface in order to suppress HSAL. Protective layer was studied in Li-symmetrical cell and full cell configurations with two different cathodes (LFP and Li-sulfur) in carbonate and ether based electrolytes. To confirm HSAL growth suppression, scanning electron microscopy (SEM), focused-ion beam-scanning electron microscopy (FIB-SEM), X-ray photoelectron spectroscopy (XPS) and electrochemical measurements were used.^[4]

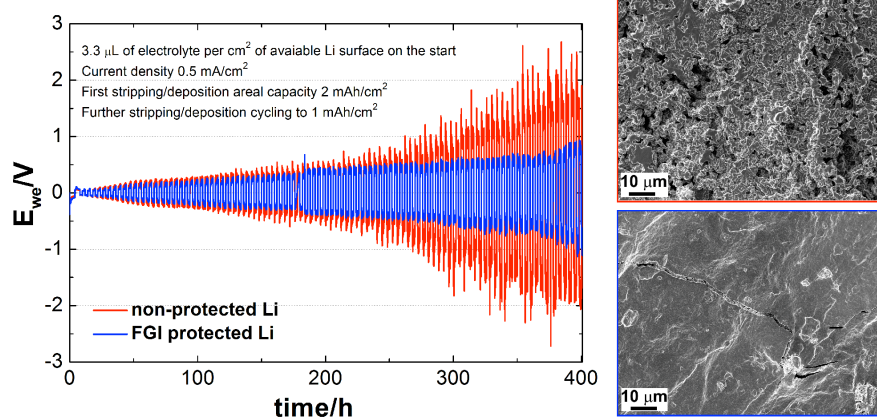


Figure 1. Voltage versus time curves for Li-symmetrical cell and post-mortem morphology of non-protected and FGI protected anode.

Acknowledgement

The presented work is part of HELiS project which receives funding from the European Union's Horizon 2020 research and innovation programme under Grant Agreement No 666221.

References:

- [1] D. Aurbach, E. Pollak, R. Elazari, G. Salitra, C. S. Kelley, J. Affinito, *J. Electrochem. Soc.* **2009**, *156*, A694.
- [2] Q. Tang, Z. Zhou, Z. Chen, *Nanoscale* **2013**, *5*, 4541.
- [3] F. Yao, F. Güneş, H. Q. Ta, S. M. Lee, S. J. Chae, K. Y. Sheem, C. S. Cojocaru, S. S. Xie, Y. H. Lee, *J. Am. Chem. Soc.* **2012**, *134*, 8646.
- [4] J. Bobnar, M. Lozinšek, G. Kapun, C. Njel, R. Dedryvère, B. Genorio, R. Dominko, Submitted.

Enhancement of Sensitivity and Accuracy of Aqua Droplet Detection

Tatsuya Ando, Jin Kawakita, and Toyohiro Chikyow
National Institute for Materials Science
1-1, Namiki, Tsukuba 305-0044, Japan
ANDO.Tatuya@nims.go.jp

Small water droplets derived from environment such as moisture cause phenomena such as corrosion of metal and fogging of glass while the degree of these phenomena varies depending on the particle diameter. Although the hygrometer can measure the amount of moisture, it cannot distinguish the size of moisture, i.e. diameter of adhering droplet. On the other hand, optical techniques can discriminate the size of water droplets while many of them are relatively huge because optical source and detector are required. Therefore, the authors have developed a sensor that detect invisibly small water droplet and distinguish its particle size with high accuracy and high speed. This sensor uses narrow lines (arrays) made of dissimilar metals arranged with gaps of 0.5 to 10 μm as electrodes and serves as the principle of measuring the galvanic current generated when a water droplet come in contact with adjacent electrodes like a bridge between the electrodes. In addition, the relationship between the change with time of the droplet's shape contacted with the sensor and the response current from the sensor was clarified. From this clarification, it was inferred that the discriminated size of water droplet, i.e. accuracy of sensor, and response current value, i.e. sensitivity of sensor, depend on the wettability between the sensor surface and the water droplet. In this research, the hydrophilicity and the hydrophobicity of the sensor surface were controlled for the purpose of enhancing the sensitivity and accuracy of the sensor when the microdroplet was in contact.

In the sensor, the substrate was a silicon wafer, the surface of which was covered with a silica layer. Fine interconnections (arrays) made of dissimilar metals were alternately arranged on the substrate to form an opposing comb structure, which were used as the electrodes. The combination of dissimilar metals was Al and Au. The electrode was 1 μm in width and 0.2 μm in thickness and the gap between the adjacent electrodes was 0.5 to 10 μm . The number of electrodes' pair was 50. Two kinds of polymers termed as PM and GL in this study were formed between the electrodes. Sensor surface was observed by using an optical microscope. The contact angle of droplet on the sample was measured. The response current from the sensor was measured at a minimum measurement interval of 0.2 sec by using a measuring device installed on the observation stage of the optical microscope. Water droplets were introduced to the surface of the moisture sensor using a sprayer (water droplet size: about 1 to 8 μm).

Fig. 1 shows optical microscopic images obtained when water droplets were sprayed on the surface of the sensor with and without the polymer formation. When polymers were formed on the surface of the sensor substrate, the sensor surface was changed to both hydrophobicity and

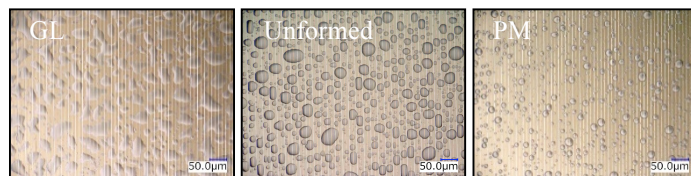


Fig. 1 Microscopic images of water droplet on sensor surface with polymer formation.

hydrophilicity by forming PM and GL, respectively. From these images, the projected area and the number of waterdrops were estimated. Fig. 2 shows the relationship among the contact angle, the projected area of the water droplet and the response current of the sensor. When the contact angle was small, the average value and distribution of projected area and the sensor response tend to increase. This is because as the wettability (hydrophilicity) increases, the area of the waterdrop covering (bridging) the electrode increases, leading to enhancing sensor sensitivity. On the other hand, when the contact angle was large, the area of the water droplet and its distribution became small. As a result, the wettability was low while the (hydrophobicity)

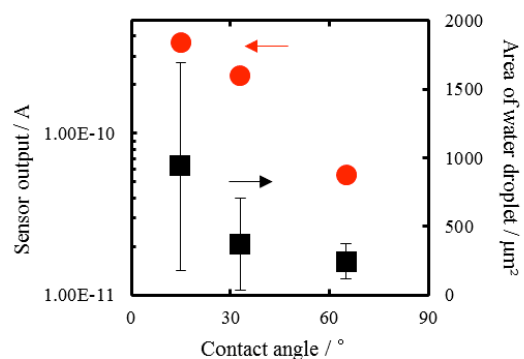


Fig. 2 Relation among contact angle, sensor output and projected area of water droplet.

was increased, it is suggested that the accuracy of discriminating the waterdrop diameter by the sensor can be enhanced.

One-Process Fabrication of Nanostructured TiO₂-TiO-TiN/XO₂ Composite Films on Ti Foils toward High-Performance Anode Materials for Lithium Ion Batteries

Song-Zhu S. Kure-Chu^{a,*}, Yongda Ye^{a,c}, Nobuhiro Kawakami^b, Reona Miyazaki^a, Takehiko Hihara^a, Hitoshi Yashiro^b, Guoyi Tang^c

^a Department of Materials Function and Design, Nagoya Institute of Technology
Gokiso, Showa, Nagoya, Aichi, 466-8555 Japan

^b Department of Chemistry and Bio-Sciences, Iwate University
Ueta 4-3-5, Morioka, Iwate, 020-8551 Japan

^c Advanced Materials Institute, Graduate School at Shenzhen, Tsinghua University
Shenzhen, Guangdong, 518055, China

*corresponding author: chusongz@nitech.ac.jp

Lithium-ion batteries (LIBs) have been widely used as power sources in many electric/electronic products such as cellular phones, digital cameras, portable computers, as well as electric vehicles (EVs) and hybrid electric vehicles (HEVs). To meet the ever-expanding needs for lithium-ion battery industry, it is highly desirable to explore new electrode materials with higher power density and satisfied lifetime cycles. TiO₂ material is considered as a promising potential anode candidate to replace conventional graphite electrodes for improving the safety of LIBs, because of its satisfied thermal stability and, more importantly, the relatively high working potential (1.7 V vs. Li/Li⁺) that eliminates dendrite lithium electrodeposition during charge/discharge process.

In this study, we first present a 3D nanoporous TiO₂-TiO-TiN composite film on Ti sheets, which are formed by anodization in nitric-based aqueous electrolytes. Then, we report a novel TiO₂-TiO-TiN/XO₂ (X = Sn, Mo) composite film by a hybrid anodization in acidic solutions containing Sn, Mo, V ions. Both of the composite films were formed in one-process anodization. The microstructures, chemical composition, and crystalline structure of the anodized specimens before and after annealing were investigated FE-SEM, TEM (FIB), XRD, XPS, and GD-OES. Moreover, the charge-discharge performances of various nanostructured composite films on Ti foils were investigated as binder-free anode materials for Li ion secondary batteries.

The nanoporous anodic titania films that formed in NO₃⁻-based solutions consisted of amorphous TiO₂, polycrystalline cubic TiO, and a small amount of TiN. The nanoporous TiO₂-TiO-TiN composite films exhibited the highest discharge capacity of 440 μAh cm⁻² upon ~800-nm-thick film and a high Coulombic efficiency close to 100%. Moreover, the Sn and Mo elements that included in nanoporous TiO₂-TiO-TiN films existed as multivalent metallic oxides. The detail results will be reported on meeting.

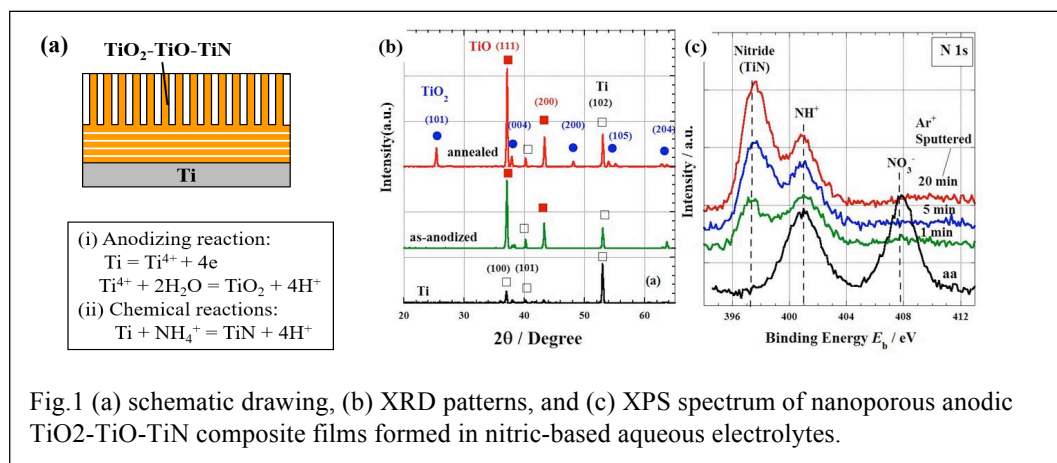


Fig.1 (a) schematic drawing, (b) XRD patterns, and (c) XPS spectrum of nanoporous anodic TiO₂-TiO-TiN composite films formed in nitric-based aqueous electrolytes.

Gas-imaging System (Sniff-cam) using NADH-dependent Alcohol Dehydrogenase for Assessment of Alcohol Metabolism

Kenta Iitani¹, Koji Toma², Takahiro Arakawa² and Kohji Mitsubayashi^{1,2,*}

¹Graduate School of Medical and Dental Sciences, Tokyo Medical and Dental University

1-5-45 Yushima, Bunkyo-ku, Tokyo, 113-8510, Japan

²Institute of Biomaterials and Bioengineering, Tokyo Medical and Dental University

2-3-10 Kanda-Surugadai, Chiyoda-ku, Tokyo, 101-0062, Japan

*m.bdi@tmd.ac.jp

Volatile organic compounds (VOCs) in exhaled breath or skin gas have been attracting a lot of attention because some of them reflect diseases or metabolisms. Understanding concentration distributions, release sites and release dynamics of these VOCs is expected to lead to methods for noninvasive disease screening and assessment of metabolisms. In this study, we developed a gas-imaging system (Sniff-cam) for visualization of the distribution of gaseous ethanol (EtOH) and acetaldehyde (AcH) in real-time, and it was applied to breath and skin gas after drinking for assessment of alcohol metabolism.

In order to visualize EtOH and AcH, alcohol dehydrogenase (ADH)-mediated reaction was used. This reaction progressed to both oxidation of EtOH and reduction of AcH depending on a buffer solution pH. The ADH Sniff-cam was composed of an ultraviolet (UV)-light emitting diode (LED) array sheet, a highly sensitive camera, and a gas-permeable ADH-immobilized mesh as shown in figure 1. A reduced form of nicotinamide adenine dinucleotide (NADH) was used as a coenzyme in the redox reaction because it had the autofluorescence property: the emission was at 490 nm and excitation was at 340 nm wavelengths. Therefore, imaging of EtOH (or AcH) was carried out by measuring the increase (or decrease) of fluorescence intensity of NADH on the ADH-immobilized mesh. In addition, an image differentiation analysis method that calculated a fluorescence changing rate was employed to improve a temporal response of the Sniff-cam and to visualize a concentration change of AcH in real-time.

In the characterization of the ADH Sniff-cam by standard gaseous samples, dynamic ranges to EtOH and AcH were determined as 0.5–150 ppm and 0.1–10 ppm, respectively, which encompassed the concentrations of both volatiles in breath after drinking. Selectivity of the ADH Sniff-cam was also validated by the results showing no response to common compounds in breath after drinking. Finally, the ADH Sniff-cam was applied to imaging of EtOH and AcH in exhaled breath and skin gas after drinking. As the results, differences of EtOH and AcH concentrations in breath which were attributed to genetic polymorphism of aldehyde dehydrogenase type 2 (ALDH2) of the subjects were observed. ALDH2 inactive subjects showed a higher concentration of EtOH and AcH (146 and 8.5 ppm) than the active (82 and 3.2 ppm). The results were in good agreement with a previous report⁽¹⁾. Furthermore, distribution of EtOH and AcH transpired from the skin surface could be observed by the ADH Sniff-cam. These results indicate that the Sniff-cam holds the potential for noninvasive disease screening and metabolism assessment.

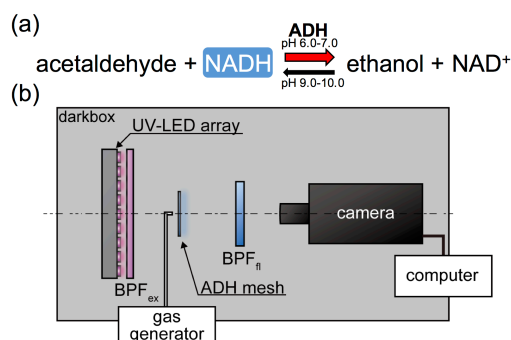


Figure 1. (a) Detection principle of EtOH and AcH and (b) a schematic illustration of the Sniff-cam.

Reference

- (1) Mitsubayashi, K. et al. "Bioelectronic sniffers for ethanol and acetaldehyde in breath air after drinking". *Biosens. Bioelectron.* **20**, pp.1573–1579 (2005).

Multi-well sensor platform based on a partially etched structure of light-addressable potentiometric sensor

Hoang Anh Truong¹, Carl Frederik Werner², Koichiro Miyamoto², Tatsuo Yoshinobu^{1,2}

¹Department of Biomedical Eng. and ²Department of Electronic Eng., Tohoku Univ.

Tohoku university, Department of Biomedical Engineering, Yoshinobu Laboratory
6-6-05, Aoba, Aramaki, Aoba-ku, Sendai 980-8579 Japan

E-mail : truonganh@ecei.tohoku.ac.jp

In clinic diagnosis, a simultaneous measurement of a plurality of samples in a single step is advantageous for reduction of time and cost required. The light-addressable potentiometric sensor (LAPS) [1] offers a platform to integrate a large number of measurement spots on a single sensor plate, which can be individually and simultaneously accessed by addressing light beams. In our previous study [2], we developed a partially-etched structure of LAPS, in which the back surface of the sensor plate was etched to realize higher spatial resolution, larger photocurrent signal and wider frequency bandwidth. In this study, we propose to apply the partially etched structure on the front surface for sensing, so that, in addition to the said advantages, each of the etched region serves as a defined well to accommodate a sample solution. These wells are also applicable to incubation of biological samples, etc.

Figure 1 illustrates the measurement of plurality of samples by a LAPS sensor plate with a multi-well structure. The sensor plate was made by partially Si etching of a 200- μm -thick n-type Si (100) substrate with 25% Tetramethylammonium hydroxide (TMAH) at 92-94°C. As a pH-sensitive surface, a 130 nm-thick SiO₂ layer was formed on the partially etched surface. A thin Ti/Au film was evaporated on both edges of the front surface, where the SiO₂ film was partially removed by 5% HF using a photolithographically patterned resist. Each etched region is loaded with 2-4 μL solution contacted with a platinum wire coated with Ag/AgCl. The wells can be addressed either one by one with a scanning light beam or simultaneously with a plurality of light beams modulated at different frequencies.

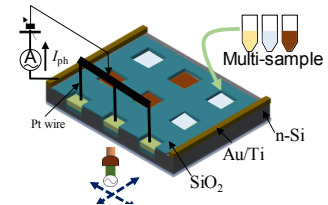


Figure 1. Schematic illustration of a multi-sample measurement by a single LAPS.

Figure 2(a) shows the photocurrent-bias voltage curve for a series of pH3, 5, 7 and 9, measured in one of the 9 wells. Figure 2(b) shows the calibration plots for the 9 wells, in which the bias voltage corresponding to the inflection point of each curve is plotted as a function of pH, show a pH sensitivity of 32 ± 2 mV/pH.

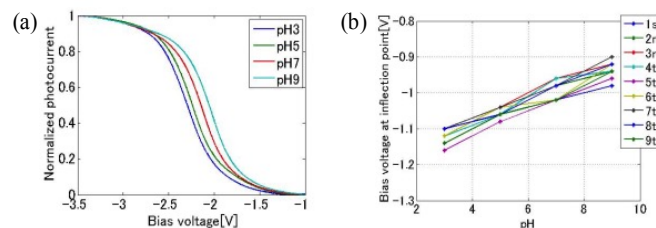


Figure 2. (a) Photocurrent-voltage curves of an etched region. (b) Inflection points vs. pH value in each well.

In

conclusion, the partially etched LAPS sensor plate with SiO₂ sensing surface was fabricated, which is expected to have the advantages of multi-sample measurement, larger photocurrent signal, robustness and fabrication simplicity of fabrication.

Acknowledgement

The authors appreciate the financial support of the Japan Science Society and the technical support of the Institute of Nano- and Biotechnologies (INB), Aachen University of Applied Sciences.

References

- [1] D. G. Hafeman, et al., Science 240, pp.1182-1185, 1988.
- [2] H. Truong, et al., presented at *Engineering of Functional Interfaces (EnFI) 2017*, Marburg, Germany,

28–29 August, 2017.

Preparation of Low Loading Pt Catalysts for Oxygen Reduction in Low Temperature Fuel Cells

Hasuck Kim^{1,2}, Seunghee Woo¹, Won-kyo Suh², Pandian Ganesan², and Sangaraju Shanmugam²

¹Department of Chemistry, Seoul National University, Seoul 08826, Korea

²Department of Energy Science and Engineering, DGIST, Daegu 42988, Korea
hasuckim@snu.ac.kr

The Fuel cells have been receiving considerable interests as power sources for small electronic devices to large vehicles and power for residents because they exhibit high energy efficiency and are environmentally friendly. Despite these advantages, fuel cells in general need to overcome not only technical, but also economical barriers for wide applications. In order to realize the wide use of fuel cells, the performance of fuel cells has to be improved. Catalysts, support, MEA preparation, membrane, and bipolar plates are the materials involved for possible improvement.

Catalysts are the core of concerns. They have to show high activity towards fuel cell reactions especially towards oxygen reduction reaction (ORR) and methanol oxidation reaction and enough stability for extended usage. [1] Also efficient use of catalyst can reduce the over-all cost. One of ways to enhance and improve the efficiency is to increase the number of triple-phase boundaries, where catalyst meets reactant and conductive (electronic as well as ionic) sites and uniform distribution of catalysts.

In this respect, works performed in our group for fuel cell catalysts will be summarized, they are preparation of catalysts by galvanostatic pulse electrodeposition of Pt-Co on Nafion-bonded carbon layer (Fig.) [2,3] and uniform distribution of nano-size Pt-Ni on various carbon supports for ORR.

Catalysts prepared by the electrochemical deposition show a significant improvement in performance even though the amount of metal is far less than conventional experiments. It is due to the utilization of catalysts were improved significantly because the deposition of metal occurred only on the surface.

Also, the ORR activity of Pt–Ni supported on graphene (G) was compared with Pt–Ni on Vulcan carbon XC-72 (VXC) and carbon nanotubes (CNT). Among the three evaluated catalysts, Pt–Ni/graphene showed the highest ORR activities, and all Pt–Ni alloy catalysts followed the direct 4-electron pathway. The ORR specific activity decreased in the order of Pt–Ni/G > Pt–Ni/VXC > Pt–Ni/CNT. Also, Pt–Ni/graphene catalysts showed the highest methanol resistance. However, the Pt–Ni/G catalysts suffered from the accelerated stability test (AST) [4]. It could be due to the dissolution and agglomeration occurred when the Pt based nanoparticles were exposed to an acidic environment. Improvement of the stability and durability of noble metal catalysts for fuel cells should be considered in future studies.

Details of experimental procedures and results will be discussed.

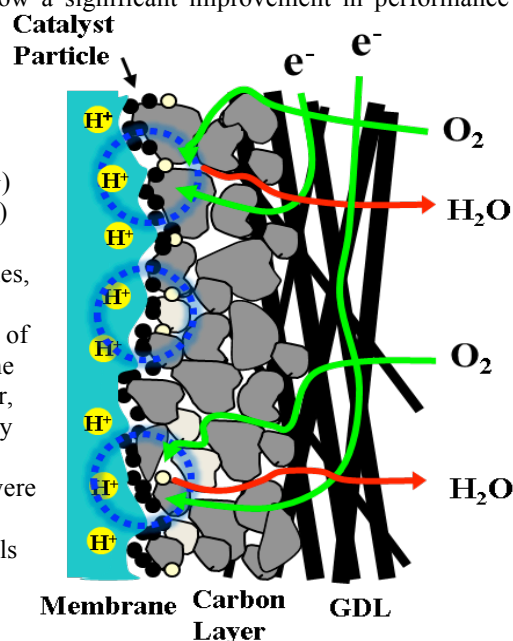


Fig. Electrochemical Deposition.

References

- [1] H. A. Gasteiger, S. S. Kocha, B. Sompalli, F. T. Wagner, *Applied Catalysis B: Environmental*, 2005, **56**, 9-35.
- [2] S. Woo, I. Kim, J. K. Lee, S. Bong, J. Lee, H. Kim, *Electrochim. Acta*, 2011, **56**, 3036-3041.
- [3] Y. Ra, J. Lee, I. Kim, S. Bong, H. Kim, *J. Power Sources*, 2009, **187**, 363-370.
- [4] Won-kyo Suh, Pandian Ganesan, Byungrak Son, Hasuck Kim, and Sangaraju Shanmugam, *Int. J. Hydrogen Energies*, 2016, **41**, 12983-12994.

Potentiostatic Pre-lithiation for Preparing Lithium Sulfide Cathode

Yunwen Wu^a, Toshiyuki Momma^{a,b*}, Tokihiko Yokoshima^b, Hiroki Nara^b, and Tetsuya Osaka^{a,b}

a Graduate School of Advanced Science and Engineering, Waseda University, 3-4-1, Okubo, Shinjuku-ku, Tokyo 169-8555, Japan;

b Research Organization for Nano & Life Innovation

Waseda University, 5-1-3, Wasedaturumakicho, Shinjuku-ku, Tokyo 162-0041, Japan

e-mail address: momma@waseda.jp

Introduction

The lithium rich lithium sulfide (Li_2S) with high theoretical capacity (1165 mAh g^{-1}) is considered as an alternate cathode material for next-generation Li-ion batteries[1]. Making Li_2S cathode by using the commercial Li_2S powder[2] synthesized Li_2S by the thermochemical methods[3] are the main two approaches reported to obtain Li_2S cathode. However, the dissolution of the intermediate product, polysulfide in the electrolyte and the low electrical conductivity of the Li_2S bulk will cause poor electrochemical performance of the Li_2S cathode. In addition, the high sensitivity of Li_2S to moisture in air impede the operability and give rise to the fabrication cost. Under this circumstance, it is important to find a new way to make Li_2S cathode which is easy operate and has better electrochemical performance. In this study, a novel potentiostatic pre-lithiation method based on the sulfur/ Ketjen Black (S/KB) cathode in a beaker cell is reported.

Experimental

The S/KB composite was mixed in a weight ratio of 1:1 after a heating process at 155°C . The S cathode was prepared by mixing S/KB composite:PvDF= 90:10 wt%. The S/KB cathode is used as the working electrode and a Li metal is used as the counter electrode. The pre-lithiation process was conducted at the constant potential from the range of 0.8 V to 1.2 V. The cutoff capacity was conducted from 1000 mAh g^{-1} to 1700 mAh g^{-1} . 1M bis(trifluoromethanesulfonyl)imide (LiTFSI) in Triglyme (G3) was used as the bath solution. Coin type 2032 cells were assembled in an Ar filled glove box. The electrolyte was fabricated by dissolve LiTFSI in dioxolane (DOL)/Dimethoxyethane (DME) (1:1 vol ratio) with 1% lithium nitrate. 25 μm thick polypropylene porous film was used as the separator. The galvanostatic charge discharge tests of the metallic metal free full cells were conducted using a charge discharge system (TOSCAT-3100, Toyo system).

Results and Discussion

We studied the effective potentiostatic pre-lithiation method for the S/KB cathode in a beaker cell by adjusting the bath solution, pre-lithiation potential and cutoff capacity. Firstly, the bath solution is studied due to the high trend of polysulfides to dissolve in the large amount of electrolyte. It is found that in the DOL/DME bath, the pre-lithiated cathode showed poor charge capacity, which indicates most of the active material was run away in the bath solution. In the ionic liquid G3 bath, it showed remarkably increased specific capacity. Secondly, $\text{Li}_2\text{S}/\text{KB}$ cathode made at different pre-lithiation potential of 0.8V, 1.0V, 1.2 V, 1.5 V and 2.0 V are studied. It is proved that at a cutoff capacity of 1000 mAh g^{-1} , the pre-lithiation potential at 1.2 V shows the highest specific capacity.

Lastly, we increased the cutoff capacity from 1000 mAh g^{-1} to 1700 mAh g^{-1} , the capacity of the fabricated $\text{Li}_2\text{S}/\text{KB}$ was increased to 800 mAh g^{-1} in the first discharge at 0.05 C-rate. By XPS analysis, the S2p peak was composed of Li_2S and Li_2S_2 , which indicates the un-fully pre-lithiation state of the cathode. Figure 1 shows the cycling performance of the fabricated $\text{Li}_2\text{S}/\text{KB}$ at the optimized conditions, from which stable cyclability with a capacity retention of 560 mAh g^{-1} at 100th cycle at 0.2 C-rate can be confirmed.

Acknowledgement

This work is supported by Advanced Low Carbon Technology Research and Development Program (JST-ALCA) Special Priority Research Area "Next-generation Rechargeable Battery".

References

- [1] Y. Son, J.-S. Lee, Y. Son, J.-H. Jang, J. Cho, *Advanced Energy Materials*, 5 (2015) n/a-n/a.
- [2] F. Wu, J.T. Lee, E. Zhao, B. Zhang, G. Yushin, *ACS Nano*, 10 (2016) 1333-1340.
- [3] J. Liu, H. Nara, T. Yokoshima, T. Momma, T. Osaka, *Electrochimica Acta*, 183 (2015) 70-77.

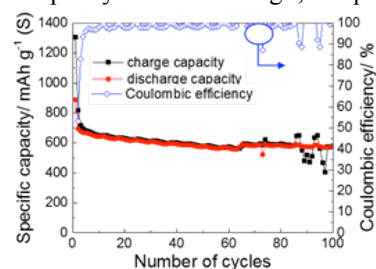


Figure 1. Cycling performance of the $\text{Li}_2\text{S}/\text{KB}$ cathode fabricated by potentiostatic pre-lithiation at 0.2 C-rate.

Electronic Modulation of Transition Metal Phosphide via Doping as Efficient and pH-universal Electrocatalysts for Hydrogen Evolution Reaction

Yan Shen*, Xin Xiao, Leiming Tao, Mingkui Wang

Wuhan National Laboratory for Optoelectronics, Huazhong University of Science and Technology
Wuhan 430074, P. R. China
cica_sheny@mail.hust.edu.cn

It is highly desirable to develop efficient and low-cost catalysts to minimize the overpotential of hydrogen evolution reaction (HER) for large-scale hydrogen production from electrochemical water splitting.^[1] Doping foreign element into the host catalysts has been proposed as an effective approach to optimize the electronic characteristics of catalysts and thus improve their electrocatalytic performance.^[2,3] Herein we for the first time report doped transition Metal Phosphide on self-supported conductive carbon cloth as a robust HER electrocatalyst, which exhibits extremely low overpotential and superior long-term durability for HER over a wide pH range, outperforming most recently reported transition metal-based phosphides. We believe that the doping engineering opens up new opportunities to improve the HER catalytic activity of transition metal phosphides through regulating their physiochemical and electrochemical properties. Furthermore, the material design present in this work broadens our vision to fabricate noble-metal free catalysts for other important reactions in electrochemical energy conversion and storage.

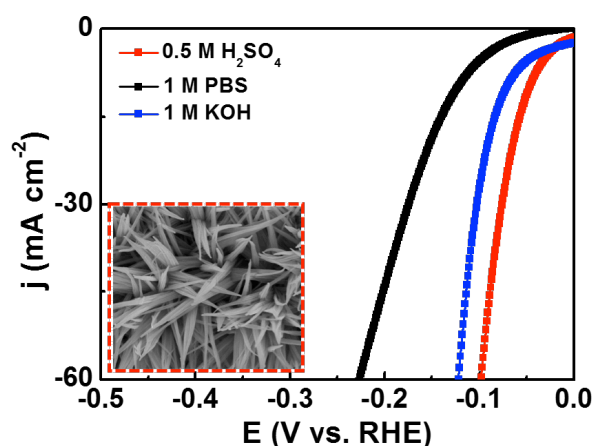


Fig. 1. The electrochemical activity of doped transition Metal Phosphide for HER over a wide pH range.

References

1. X. X. Zou, Y. Zhang, Chem. Soc. Rev., 2015, **44**, 5148-5180.
2. D. Y. Wang, M. Gong, H. L. Chou, C. J. Pan, H. A. Chen, Y. P. Wu, M. C. Lin, M. Y. Guan, J. Yang, C. W. Chen, Y. L. Wang, B. J. Hwang, C. C. Chen, H. J. Dai, J. Am. Chem. Soc., 2015, **137**, 1587-1592.
3. H. F. Liang, A. N. Gandi, D. H. Anjum, X. B. Wang, U. Schwingenschlögl, H. N. Alshareef, Nano Lett., 2016, **16**, 7718-7725.

Amperometric flow-through biosensor for uric acid using enzyme-modified carbon-felt based on oxidase and peroxidase-bienzyme system

Yasushi Hasebe¹, Yue Wang², Shin-ichi Seki¹

¹ Department of Life Science and Green Chemistry, Faculty of Engineering, Saitama Institute of Technology, 1690 Fusaiji, Fukaya, Saitama, 369-0293, Japan

² School of Chemical Engineering, University of Science and Technology Liaoning, 185 Qianshan Middle Road, High-tech-zone, Anshan 114501, Liaoning, China
hasebe@sit.ac.jp

Carbon felt (CF) is a micro-electrode ensemble of micro-carbon fiber (ca. 7 μm diameter) that possesses a three-dimensional random structure. The CF has high conductivity and a large effective surface area, which allows large measurable current density and high electrolytic efficiency. In addition, a high porosity of CF (> 90 %) permits a low diffusion barrier of solution-flow. Therefore, along with other electro-active porous materials, CF is useful for the electrochemical flow-through detector. Compared with other porous electrode materials, CF has the following advantages: (1) inexpensive; (2) physically and mechanically stable; (3) can be easily handled; and (4) can be easily manufactured into arbitrary shapes. Therefore, the immobilization of catalysts on the CF surface has enabled the development of highly selective electrochemical flow sensors. In previous studies, we reported that coadsorption of horseradish peroxidase (HRP) and thionine (Th) onto CF is effective for developing a highly sensitive bioelectrocatalytic flow-through detector for the amperometric determination of hydrogen peroxide (H_2O_2) [1, 2]. In this case, the coadsorbed Th played an important role in facilitating the direct electron transfer between the HRP-active heme-center and the CF electrode surface [1,2]. Furthermore, the resulting HRP/Th-CF-based flow-through detector exhibited an excellent operational stability (repetitive 100 sample injection of 100 μM H_2O_2 induced no serious current decrease, and the RSD was 0.41–1.21% ($n = 100$)). Strong interactions between the HRP molecule and the CF surface may contribute to this stable response. In addition, this HRP/Th-CF-based flow-through detector has excellent sensitivity toward H_2O_2 (detection limit, 0.02 μM). Therefore, the combination of this HRP/Th-CF-based H_2O_2 flow-detector and oxidases, which produce H_2O_2 during their catalyzed reactions, could enable the development of various flow-biosensors for the determination of the substrates of oxidases.

Uric acid is a final product of the purine-metabolic pathway, and its detection is clinically important in the diagnosis of diseases caused by the disorder of purine biosynthesis and/or purine catabolism (e.g., gout, hyperuricemia, Lesch–Nyhan syndrome and cardiovascular disease). Uricase (EC. 1.7.3.3. urate oxidase, UOx) catalyzes the oxidative transformation of uric acid to allantoin with concomitant conversion of molecular oxygen to H_2O_2 . In this study, we prepared uricase (UOx), HRP and Th-coadsorbed CF (UOx/HRP/Th-CF) to fabricate an electrochemical uric acid biosensor. As shown in Fig. 1, H_2O_2 produced enzymatically during the UOx-catalyzed oxidation of uric acid is electrochemically detected by HRP/Th-CF-based detector at -50 mV vs. Ag/AgCl. The main purpose of this study is as follows: (1) optimization of UOx and HRP adsorption conditions; (2) optimization of operational conditions; (3) evaluation of the analytical performance of the UOx/HRP/Th-CF-based uric acid biosensor; and (4) determination of uric acid in human serum and urine using the present bienzyme-modified CF-based uric acid biosensor.

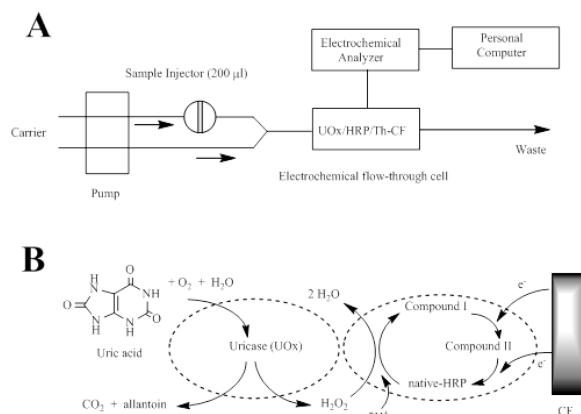


Fig. 1 Schematic diagram (A) and detection scheme (B) of UOx/HRP/Th-CF-based flow biosensor.

References

- [1] Y. Yue, Y. Hasebe, *Anal. Sci.*, 27 (4), 401-407 (2011).
- [2] Y. Yue, Y. Hasebe, *Anal. Sci.*, 27 (6), 605-612 (2011).

Electrooxidation of Polyphenols at a Glassy Carbon Electrode Modified with Electrochemically Reduced Graphene Oxide and Fe Nanoparticles

Daniel Rodrigues da Silva, José Luiz da Silva, Nelson Ramos Stradiotto

*Instituto de Química de Araraquara – Universidade Estadual Paulista “Júlio de Mesquita Filho” UNESP
R. Prof. Francisco Degni, 55- Quitandinha – Araraquara (SP), Brazil.
nrstradi@gmail.com, danielrsl00@gmail.com, silva_jl@iq.unesp.br*

Electrooxidation of polyphenols was performed at a glassy carbon electrode (GCE) modified with electrochemically reduced graphene oxide (ERGO) and Fe nanoparticles (FeNP). This class of organic compounds grew in research interest in the last decades due to their antioxidant, antimutagenic, and anticarcinogenic properties in addition to their capability to prevent cardiovascular pathologies¹. Phenolic acids derived from hydroxybenzoic acid (gallic, and vanillic acids) and hydroxycinnamic acid (caffeic, p-coumaric, and ferulic acids), and flavonols (quercetin and rutin) were studied. Electrochemical experiments were conducted with an Ag/AgCl (KCl 3 mol L⁻¹) reference electrode and a platinum wire as counter-electrode. Graphene oxide was electrochemically reduced on GCE surface by applying -1.4 V for 500 seconds. Optimum condition for electrodeposition of FeNP was achieved by applying -1.3V to a 1 mmol L⁻¹ FeCl₃ in 0.1 mol L⁻¹ KCl until a charge of 25 mC was detected. Techniques such as SEM-FEG, EDS and EDX were employed for GCE-ERGO-FeNP electrode characterization and provided information on surface composition and morphology. SEM images showed the adhesion of nanoparticles over ERGO layers, thus, increasing surface area of the electrode. Peaks of carbon, oxygen, sodium and iron were detected and it was revealed that deposited nanoparticles were constituted of several iron oxides such as Fe₂O₃, FeOOH and FeO. EIS data showed that charge-transfer resistance (R_{ct}) was decreased of 88%, from 957 Ω to 118 Ω, after modification of GCE with ERGO and FeNP, providing a faster electron transfer at electrolyte-electrode interface. CV experiments showed that a shift of anodic peak potential (E_{pa}) to more negative values coupled with an increase of anodic peak currents (I_{pa}) occurred at the modified sensor when compared to a bare GCE. Different mass transfer electrode processes took place during electrooxidation of tested polyphenols: diffusion-controlled (gallic, and caffeic acids), adsorption-controlled (vanillic acid) and adsorption-diffusion mixed-controlled (p-coumaric, and ferulic acids, quercetin and rutin). Oxidation of studied polyphenols occurred at potentials (all in V) of: 0.22, gallic acid; 0.31, caffeic acid; 0.47, quercetin; 0.48, rutin; 0.67, vanillic acid; 0.68, p-coumaric acid; and 0.72, ferulic acid. Only caffeic acid exhibited a reversible redox process at GCE-ERGO-FeNP. Ferulic acid displayed changes in cyclic voltammogram profile after the first scan due to formation of the same quinone generated after caffeic acid oxidation. Fouling of the electrode surface was observed after successive scans due to the high tendency of adsorption of the analytes. Pulsed amperometric detection was employed in order to reactivate the sensor and solve this issue. A three pulse sequence was used and consisted of the detection potential, corresponding to E_{pa} of each studied analyte (E1), a more positive potential (E2 = 1.1 V) for oxidation of generated products and a more negative potential (E3 = -0.1 V) to reduce products that could still be adsorbed on GCE-ERGO-FeNP surface and to renew it for a new pulse sequence. Analytical curves presented linear ranges that varied from 1.5 10⁻⁶ (rutin) to 1.1 10⁻² (caffeic acid). Limits of detection were of (all in μmol L⁻¹): 58.1, gallic acid; 46.2, vanillic acid; 54.4, caffeic acid; 23.8, ferulic acid; 29.6, p-coumaric acid; 40.0, quercetin; 42.7, rutin. Amperometric sensitivities, in A L mol⁻¹, ranged from 0.036 (vanillic acid) to 0.76 (rutin). Electrode response time (in seconds) varied from 1.1 (rutin) to 4.0 (caffeic acid). Double step chronoamperometric experiments were performed to determine kinetic parameters regarding electrooxidation of tested analytes at GCE-ERGO-FeNP by Cottrell equation. Catalytic rate constants of studied polyphenols varied from 2.5 10⁶ (p-coumaric acid) to 7.9 10⁸ (quercetin), both in cm³ mol⁻¹ s⁻¹. Quercetin and rutin present multiple chelation sites in their molecular structures and, thus, interaction of these flavonols with the nanoparticles of GCE-ERGO-FeNP was higher in comparison with phenolic acids. Diffusion coefficients were also higher for flavonols due to their enhanced affinity with FeNP. This parameter ranged from 1.6 10⁻⁸ (gallic acid) to 1.2 10⁻² (rutin), both in cm² s⁻¹. Electrooxidation of polyphenols was achieved with a low cost sensor that presented faster and improved response than a bare GCE. Therefore, GCE-ERGO-FeNP poses as an excellent option for determination of this increasingly attractive class of organic compounds in several samples.

References:

¹ Bravo, L. Nutrition Reviews, v. 56, n. 11, p. 317-333, 1998.

Multiscale Modeling Framework for Supramolecular Structures, Nanomaterials, and Biomolecules

Andriy Kovalenko

*Mechanical Engineering Dept., University of Alberta, and National Institute for Nanotechnology
10-203 Donadeo Innovation Centre for Engineering, 9211-116 Str., Edmonton, AB, Canada T6G 1H9
andriy.kovalenko@ualberta.ca*

Molecular theory of solvation for nanostructures in both aqueous and non-aqueous solution, a.k.a. three-dimensional reference interaction site model (3D-RISM) with Kovalenko-Hirata (KH) closure relation¹⁻⁴ has been systematically developed and applied to a variety of compounds, supramolecules, and biomolecules in a number of solvents, mixtures, electrolyte and non-electrolyte solutions.³⁻¹¹ Based on the first principles of statistical mechanics, 3D-RISM-KH predicts solvation structure and thermodynamics of nanochemical and biomolecular systems, including their analytical long-range asymptotics. It yields high accuracy, efficiency, and applicability by multiscale coupling of methods at different space and time scales to provide fundamental understanding and prediction for nanomaterials and biomolecules.

This method was coupled with quantum chemistry,³⁻⁸ molecular dynamics,⁹⁻¹¹ and dissipative particle dynamics,¹² including examples of helical rosette nanotubes with tunable stability and hierarchy,⁹ water promoted supramolecular chirality inversion,¹⁰ formation and stability of self-assembling supramolecular structures of organic rosette nanotubes with ordered shells of inner and outer water,¹¹ and accurate and efficient dissipative particle dynamics of polymer chains with coarse-grained effective pair potential obtained from DRISM-KH theory.¹²

3D-RISM-KH molecular solvation was also coupled with Multi-Time-Step Molecular Dynamics and Generalized Solvation Force Extrapolation (MTS-MD/3D-RISM-KH/GSFE), providing quasidynamics description of biomolecules.¹³ Validation included folding of miniprotein in solution from fully extended to equilibrated state in 60 ns, which yielded acceleration by two orders of magnitude time scale as compared to 4-9 μ s protein folding in experiment.¹³

Recent developments and applications of 3D-RISM-KH consisted in multiscale coupling of quantum chemistry, molecular solvation theory, molecular dynamics, and dissipative particle dynamics.^{4,14,15} Multiscale methods framework yields dramatically improved accuracy, efficiency, and applicability by coupling models & methods on different scales and providing fundamental understanding and predictions.

References

- [1] Kovalenko, A.; Hirata, F. *J. Chem. Phys.*, 1999, 110, 10095; 2000, 112, 10391; 2000, 112, 10403.
- [2] Kovalenko, A. In: *Molecular Theory of Solvation*. Hirata, F. (Ed.) Series: Understanding Chemical Reactivity, Kluwer, Dordrecht, 2003, Vol. 24, pp.169–275.
- [3] Kovalenko, A. *Pure Appl. Chem.*, 2013, 85, 159.
- [4] Kovalenko, A. Multiscale Modeling of Solvation. In: *Springer Handbook of Electrochemical Energy*, pp. 95-139. Breitkopf, C.; Swider-Lyons, K. (Eds.) Springer-Verlag Berlin Heidelberg, 2017, 1016p.
- [5] Gusarov, S.; Ziegler, T.; Kovalenko, A. *J. Phys. Chem. A*, 2006, 110, 6083.
- [6] Casanova, D.; Gusarov, S.; Kovalenko, A.; Ziegler, T. *J. Chem. Theory Comput.*, 2007, 3, 458.
- [7] Kaminski, J.W.; Gusarov, S.; Wesolowski, T.A.; Kovalenko, A. *J. Phys. Chem. A*, 2010, 114, 6082.
- [8] Malvaldi, M.; Bruzzzone, S.; Chiappe, C.; Gusarov, S.; Kovalenko, A. *J. Phys. Chem. B*, 2009, 113, 3536.
- [9] Moralez, J.; Ruez, J.; Yamazaki, T.; Motkuri, R. K.; Kovalenko, A.; Fenniri, H. *J. Am. Chem. Soc.* 2005, 127, 8307.
- [10] Johnson, R.S.; Yamazaki, T.; Kovalenko, A.; Fenniri, H. *J. Am. Chem. Soc.*, 2007, 129, 5735.
- [11] Yamazaki, T.; Fenniri, H.; Kovalenko, A. *Chem. Phys. Chem.*, 2010, 11, 361.
- [12] Kobryn, A. E.; Nikolić, D.; Lyubimova, O.; Gusarov, S.; Kovalenko, A. *J. Phys. Chem. B*, 2014, 118, 12034.
- [13] Omelyan, I.; Kovalenko, A. *J. Chem. Theory Comput.*, 2015, 11, 1875.
- [14] S. Hlushak and A. Kovalenko, *J. Phys. Chem. C*, 2017, 121, 22092
- [15] Kovalenko, A.; Gusarov, S. *Phys. Chem. Chem. Phys.*, 2017, DOI: 10.1039/c7cp05585d.

Electrode design for redox flow batteries by using a three-dimensional multiphase lattice Boltzmann model

Qiong Cai^{1*}, Duo Zhang¹, Oluwadamilola O. Taiwo², Vladimir Yufit², Nigel Brandon², Sai Gu¹

¹ Department of chemical and process engineering, Faculty of Engineering and Physical Sciences, University of Surrey, Guildford, GU2 7XH, United Kingdom

² Department of Earth Science & Engineering, Faculty of Engineering, Imperial College London, South Kensington Campus, London, SW7 2AZ, United Kingdom

*Corresponding Author. Email: q.cai@surrey.ac.uk

Redox flow batteries (RFBs) have emerged as a promising technology for large-scale storage of intermittent power generated from renewable energy sources due to its advantages such as scalability, decoupling of energy and power, and high energy efficiency. However, to make it technologically and economically viable, advancement is needed to improve the performance (i.e. power and energy density) and reduce cost. In this paper, we report our efforts in understanding the fundamental mechanisms in redox flow battery electrodes using computational modelling, which is important for improving the performance. A three-dimensional (3D) multiphase lattice Boltzmann model [1-2] has been developed at University of Surrey to simulate the transport mechanisms of gases, liquid electrolyte flow, species and charge in the porous electrodes of RFBs. An electrochemical model based on the Butler-Volmer equation is used to provide species and charge coupling at the surface of active electrode. We apply this model first to simulate an all vanadium RFB and demonstrate that this model is able to capture the multiphase flow phenomenon and predict the local concentration for different species, over-potential and current density profiles under charge/discharge conditions [2]. The partial wetting of the solid electrode surface due to the trap of gas bubbles in the liquid electrolyte is also observed; the effect of the wetting area of the solid electrode surface on the electrochemical performance is investigated. It is found that the electrochemical performance of positive half-cell is reduced with air bubbles trapped inside the electrode.

To prove the validity of the developed LBM model, the simulation results are compared with the experimental data based on the same electrode structures. Three electrode structures (SGL paper, Freudenberg paper, Cloth paper) are reconstructed from X-ray computed tomography (CT). These electrodes are used in an organic RFB based on TEMPO. The results indicate that different electrode structure with different pore size distribution and specific surface area will result in significant differences in battery performance. From simulation result, the electrode based on cloth paper shows better performance comparing with other two electrodes, which is consistent with the experimental results. The electrode over-potential and pressure drop values are derived from the model, which are in good agreement with the values from experimental measurement. The comparison shows that validity of the model. In the future, the developed 3D lattice Boltzmann model can be used as a design tool to optimize the electrode structure of redox flow batteries.

References

- [1] Duo Zhang, Qiong Cai, Sai Gu, Three-dimensional lattice-Boltzmann model for liquid water transport and oxygen diffusion in cathode electrode of PEM fuel cell with electrochemical reaction, under review by *Electrochimica Acta*.
- [2] Duo Zhang, Qiong Cai, Oluwadamilola O. Taiwo, Vladimir Yufit, Nigel P. Brandon, Sai Gu, The effect of wetting area in carbon paper electrode on the performance of vanadium redox flow batteries: A three-dimensional lattice Boltzmann study, under review by *Electrochimica Acta*.

Redox Activity of Sulphur-based Electrolytes in Supercapacitor Application

Krzysztof Fic, Mikolaj Meller, Elzbieta Frackowiak

Institute of Chemistry and Technical Electrochemistry, Poznan University of Technology

Berdychowo 4, 60965 Poznan, Poland

krzysztof.fic@put.poznan.pl

Several forms of activated carbons have already been implemented and widely investigated as electrodes for electrochemical capacitors. Aqueous solutions based on inorganic salts demonstrated effective operating voltages around 1.6 V, and several interesting strategies have been furthermore implemented to improve these systems, including redox activity of the electrolyte.

This work is focused on the electrochemical performance of the activated carbon electrodes operating in various electrolytes containing sulphur-based species. Since sulphate (SO_4^{2-})-based aqueous solutions have already been widely investigated, this study will discuss the electrolytes with containing $\text{S}_2\text{O}_3^{2-}$, SO_3^{2-} and S^{2-} anions and their interaction with a carbon electrode. The results obtained clearly indicated that sulphur plays an important role in the charge accumulation process and has an excellent redox chemistry. Dependently on the electrolyte pH, the ionic specimen might be easily reduced or oxidized and perfectly preserves the activated carbon surface against oxidation. Moreover, the affinity of sulphur to the carbon surface promotes a sulphur-carbon bonding and creates additional redox active site on the electrode surface.

A variety of electrochemical methods used in the study confirmed that a specific formulation of the electrolyte with sulphur-based redox shuttle might remarkably enhance the electrode capacitance (up to 300 F g^{-1}) and the operating voltage (up to 2.0 V). Moreover, *operando* Raman spectroscopy proved that sulphur-carbon bond is reversibly created while the charge transfer occurs. Furthermore, high energy density (ca. 26 Wh kg^{-1}) maintained at excellent power rates (1 kW kg^{-1}) has been preserved during 10 000 charge/discharge cycles with reversibility of 97%.

The IMMOCAP project (GA 759603) funded by European Research Council (ERC-StG-2017) is acknowledged.

Self-Assembling Behavior of Proteins: Effect of the Interaction between Protein and Surface

B. Jachimska^{1*}, K. Tokarczyk¹, K. Kubiak-Ossowska², P. Komorek¹, S. Swiatek¹, P. Mulheran²

¹*J. Haber Institute of Catalysis and Surface Chemistry, PAS, Niezapominajek 8,
30-239 Krakow, Poland, *ncjachim@cyf-kr.edu.pl*

²*Department of Chemical Engineering and Process Engineering, University of Strathclyde,
Glasgow, G11XJ, UK*

The properties of the adsorbed protein layer are highly dependent on the shape, effective charge and structure of the protein as these factors influence surface affinity, protein surface coverage, and hydration of the layer. Also, the polarity, hydrophobicity and surface roughness affect the reversibility of the protein adsorption process. Preferred binding orientation has been confirmed as a result of the protein surface interactions induced by the heterogeneous surface of protein molecules, which can further affect protein conformational transitions, orientation or deformation [1-4].

Analysis of the experimental data shows that there are still inconsistent opinions about the mechanism of protein adsorption concerning adsorption kinetics, structural reorientation or conformation, and protein aggregation whether in a solution or on the surface [1-4]. As protein adsorption depends on several factors, which many are irreversible processes consequently producing various final effects for the same protein. Therefore, the development of new research techniques makes it possible to study adsorption with increasing accuracy: from measurements of adsorption kinetics at high protein concentrations to detect even a single protein molecule adsorbed on a surface. It is also possible to trace changes in the orientation and structural properties of proteins in the adsorbed state. Development of theoretical methods makes it possible to determine the interaction of protein molecules with a surface and to visualize the whole process at the atomic level that is not available experimentally. Simulations can show not only how proteins adsorb to the surfaces, but also provide an understanding of what the driving forces are and how they can be controlled through surface chemistry [5-6]. A combination of experimental studies with theoretical calculations should enable continued progress in the understanding of the behavior of proteins on solid surfaces and how bioactivity can be preserved by retaining the protein secondary and tertiary structures.

Multidimensional research using advanced in-situ measurement techniques and molecular dynamics (MD) simulations allows conducting a multifaceted study of the protein structure formation and quantitative description of the mechanisms governing the phenomena of protein adsorption on the surface. The mechanisms of interaction of functional materials with different types of proteins present in the plasma, together with the analysis of conformational changes and reorganization of protein structures on the functional surfaces have great cognitive value. It will also contribute to a better understanding of the physicochemical mechanisms of creating protein layers with controlled architecture and functionality.

Acknowledgement: This work was supported by Grant NCN OPUS 2016/23/B/ST5/02788

- [1] B. Jachimska, A. Pajor, *Bioelectrochemistry*, 2012, 87, 136-146
- [2] B. Jachimska, A. Kozłowska, A. Pajor-Swierzy, *Langmuir*, 2012, 28, 11502-11510
- [3] B. Jachimska, M. Wasilewska, Z. Adamczyk, *Langmuir*, 2008, 24, 6866-6872
- [4] B. Jachimska, K. Tokarczyk, M. Łapczyńska, A. Puciul-Malinowska, S. Zapotoczny, *Colloids and Surfaces A*, 489, 2016, 163-172
- [5] K. Kubiak-Ossowska, B. Jachimska, P. Mulheran, *PCCP*, 2015, 17, 37, 24070-77
- [6] K. Kubiak-Ossowska, K. Tokarczyk, B. Jachimska, P. Mulheran, *J. Phys. Chem. B*, 2017, 121, 3975-3986

New Advances in Ohmic Microscopy

Daniel A. Scherson, Zhange Feng, Nicholas S. Georgescu, Qi Han
Department of Chemistry Case Western Reserve University
Cleveland, OH 44106,
Daniel.scherson@case.edu

The measurement of local electrostatic potentials in electrolyte solutions with reference electrodes has been known and indeed widely exploited for many decades. Particularly noteworthy in the area of physical electrochemistry are the contributions of Miller and Bellavance,¹ for studies of the current distribution to a rotating disk electrode, Lillard *et al.*² and Orazem, Vivier, and Tribollet^{3,4} for impedance spectroscopy, and those of Amatore *et al.*^{5,6} for mapping concentrations profiles of redox-active species in solution. To be presented are implementations of this strategy for monitoring the current distribution at a composite electrode by measuring the local difference in electrostatic potential, $\Delta\phi_{\text{sol}}$.

The Au-disk Pt–Ir ring electrode was constructed by filling the orifice of a Pt : Ir (95 : 5) electron microscope aperture (Ted Pella, Inc.) with molten Au. The resulting piece was then cast in epoxy and subsequently polished to expose a Au disk 1.2 mm in diameter surrounded by a Pt–Ir ring 2 mm outside diameter (see panel b, Fig. 1). Cyclic voltammetry curves were recorded in the range -0.2 to 1.4 V at a scan rate of 10 V/s, while acquiring $\Delta\phi_{\text{sol}}$ as a function of time from either two single barrel, or a double barrel (175 μm edge to edge distance μ -ref electrodes).

Shown in Fig 1 are representative measurements of the effects of current distribution on the local electrostatic potential in solution, performed with the tip of a double-barrel capillary housing the μ -ref electrodes placed at a fixed distance of 50 μm from the surface while scanning the potential of the Pt–Ir ring Au disk electrode at 10 V/s for various points along its radius. As a cursory examination of these curves indicates, the features observed for the tip placed along the center line of the Au disk displays mostly, but not exclusively, Au-like voltammetric characteristics, which then decrease in intensity as the tip is displaced away from the center, while at the same time, the curves attain features characteristic of Pt. In fact, no Au features from the center disk could be gleaned for the data collected at the outermost edge. This demonstrates the sensitivity to the local electrostatic environment and therefore the overall effectiveness of this technique.

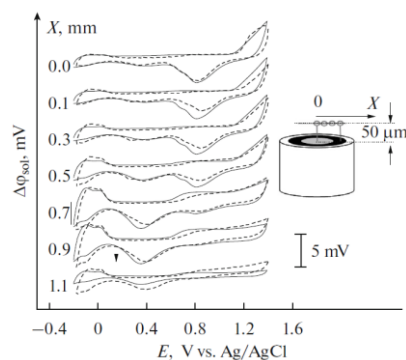


Figure 1. Plots of $\Delta\phi_{\text{sol}}$ vs. E acquired with the double barrel capillary while the working electrode was scanned at 10 V/s, where each of the curves represents data collected with the tip placed along a line parallel to the surface of the ring disk intersecting the center of the disk ($X = 0$), at a fixed distance from the surface, i.e. 50 μm .

References

1. Miller, B.; Bellavance, M. I. *J. Electrochem. Soc.* 1973, 120, 42.
2. Lillard, R. S.; Moran, P. J.; Isaacs, H. S. *J. Electrochem. Soc.* 1992, 139, 1007.
3. Frateur, I.; Bayet, E.; Keddad, M.; Tribollet, B. *Electrochem. Commun.* 1999, 1, 336.
4. Frateur, I.; Huang, V. M.; Orazem, M. E.; Tribollet, B.; Vivier, V. J. *Electrochem. Soc.* 2007, 154, C719.
5. Amatore, C.; Pebay, C.; Scialdone, O.; Szunerits, S.; Thouin, L. *Chem. & Eur. J.* 2001, 7, 2933.
6. Amatore, C.; Szunerits, S.; Thouin, L. *Electrochem. Commun.* 2000, 2, 248.

Electrolyte Additives for Improving Performance of Primary Mg-Air Batteries

Sviatlana Lamaka, B. Vaghefinazari, L. Wang, M. Deng, D. Höche, D. Snihirova, M.L. Zheludkevich

*Magnesium Innovation Center, Helmholtz-Zentrum Geesthacht,
Max-Planck Str. 1, Geesthacht, 21502, Germany*
Sviatlana.Lamaka@hzg.de

The development of cheap, long-lasting and environmentally innocuous energy storage devices is a topic of high industrial and social demand. In this respect, magnesium batteries might be a viable alternative to lithium or nickel counterparts. Unfortunately, wide commercialization of Mg-air primary batteries is still limited due to the high tendency of anode material to self-corrosion.

Our recent studies have indicated the efficient ways to control the degradation of Mg-anode material in aqueous electrolytes [1-4]. The talk will introduce a novel concept of controlling anode degradation for tuning the discharge process and to stabilize battery voltage. Aspects of hydrogen formation, requirements to the additives and to the anode material will be discussed. The increased voltage can be achieved via shifting the equilibrium towards magnesium dissolution by adding organic additives into the aqueous electrolyte. Such additives have twofold influence: efficiently prevent formation of insoluble precipitates at the electrode surface, increasing the specific energy at higher current densities, and suppress detrimental self-corrosion of magnesium anode.

[1] D. Höche, S.V. Lamaka, M.L. Zheludkevich, Electrolyte additives for magnesium air batteries, European Patent Application 16187152.0, **2016**.

[2] D. Höche, C. Blawert, S.V. Lamaka, N. Scharnagl, C. Mendis, M.L. Zheludkevich, The effect of iron re-deposition on the corrosion of impurity-containing magnesium, *Physical chemistry chemical physics: PCCP*, 18 (**2016**) 1279-1291.

[3] S.V. Lamaka, D. Höche, R.P. Petruskas, C. Blawert, M.L. Zheludkevich, A new concept for corrosion inhibition of magnesium: Suppression of iron re-deposition, *Electrochemistry Communications*, 62 (**2016**) 5-8.

[4] S.V. Lamaka, B. Vaghefinazari, D. Mei, R.P. Petruskas, D. Höche, M.L. Zheludkevich, Comprehensive screening of Mg corrosion inhibitors, *Corrosion Science*, 128 (**2017**) 224-240.

The rust challenge: Iron oxide photoelectrodes for solar water splitting

Avner Rothschild*

Dep. Mater. Sci. & Eng., Technion – Israel Inst. of Technology, Haifa, Israel

*E-mail: avner@mt.technion.ac.il

Photoelectrochemical (PEC) water splitting is a promising route for solar energy conversion to hydrogen. It produces clean hydrogen that can be used for refueling fuel cell electric vehicles or serve as a feedstock for the production of drop-in liquid fuels by CO₂ hydrogenation or ammonia via the Haber–Bosch process. The greatest challenges towards PEC solar water splitting technology lay in the selection and optimization of stable photocatalytic materials for water photo-oxidation, and the design of scalable PEC devices that produce hydrogen at a competitive cost. Iron oxide (α -Fe₂O₃, hematite) is one of few materials meeting the basic selection criteria for stable photoanodes, but its poor charge transport properties and fast recombination present challenges for efficient charge separation and collection. We investigate the root causes underlying the limitations of hematite photoanodes using thin film layered structures that serve as ideal model systems for systematic investigations of the effect of doping,¹ orientation,² device configuration³ and other control parameters on PEC properties. In addition, we also explore advanced light management schemes to enhance the light harvesting efficiency in ultrathin (10-30 nm) films using interference,⁴ scattering⁵ and plasmonic effects,⁶ as well as the effect of solar concentration on the PEC performance.⁷ Our most recent results on the effect of doping on the magnetic states at the surface of hematite films,⁸ and wavelength-dependent lifetime of photogenerated charge carriers⁹ will be presented to stimulate further discussion during the workshop.

References:

1. Deo Malviya et al., *J. Mater. Chem. A* **4**, 3091–3099 (2016).
2. Grave et al., *J. Phys. Chem. C* **120**, 28961–28970 (2016).
3. Kay et al., *ACS Energy Lett.* **1**, 827–833 (2016).
4. Dotan et al., *Nature Mater.* **12**, 158-164 (2013).
5. Niv et al., *J. Mater. Chem. A* **4**, 3043–3051 (2016).
6. Gross Koren et al., *J. Phys. Chem. C* **120**, 15042–15051 (2016).
7. Segev et al., *Adv. Energy Mater.* **6**, 1500817 (2016).
8. Ellis et al., *Phys. Rev. B* **96**, 094426 (2017).
9. Kay et al., *J. Phys. Chem. C* (2017, DOI: 10.1021/acs.jpcc.7b09472)

The Influence of Current Collector Corrosion on The Performance of Electrochemical Capacitors

Grzegorz Lota^a, Jarosław Wojciechowski^a, Łukasz Kolanowski^a, Andreas Bund^b

^a Poznan University of Technology, Institute of Chemistry and Technical Electrochemistry, Berdychowo 4, 60-965 Poznan, Poland

^b Technische Universitat Ilmenau, Electrochemistry and Electroplating Group, Gustav-Kirchhoff-Straße 6, 98693 Ilmenau, Germany

grzegorz.lota@put.poznan.pl

In this work the influence of current collectors corrosion on the performance of electrochemical capacitors are presented. Current collectors, which are made of 316L stainless steel, undergo corrosion processes in the aqueous electrolytes [1-4]. They dissolve to form a thin passive oxide film. This phenomenon has a huge impact on the supercapacitors working parameters such as voltage, working potentials of single electrodes, self-discharge as well as the internal resistance and cycling stability [5]. The most commonly utilized aqueous electrolytes are 1 M H₂SO₄, 1 M KI, 1 M Na₂SO₄, 1 M KOH and 6 M KOH.

Electrochemical measurements were performed in three-electrode Swagelok[®] cells with five different electrolytes and corresponding reference electrodes. Open circuit potential vs time, linear polarization, electrochemical impedance spectroscopy, cyclic voltammetry and galvanostatic charge/discharge measurements were made. The surface of the current collectors as well as the corrosion products were characterized using scanning electron microscopy, energy-dispersive X-ray spectroscopy, Raman spectroscopy and atomic force microscopy.

The physicochemical and electrochemical studies of 316L stainless steel confirm the relationship between the choice of one of the above electrolytes and the quality and thickness of the resulting passive oxide film. The thinnest and thermodynamically most stable layer is formed in neutral solutions such as 1 M KI and 1 M Na₂SO₄. This phenomenon has a direct impact on the ability to expand the operating voltage, as well as decrease capacitance and inhibit the self-discharge phenomenon of the supercapacitors. The thickest and most porous oxide layers are formed in acidic and alkaline solutions where the dissolution process of steel components such as iron, chromium, nickel and molybdenum is the fastest. In addition, these elements in large amounts pass into the electrolyte solution in the form of ions, thus taking an active part in charging the electrode electrical double layer of electrochemical capacitor. Acid and alkaline electrolytes allow to increase capacitance, decrease voltage and accelerate self-discharge phenomena. This has a destructive effect on the life of the current collector and the entire device.

References

- [1] N. Perez, *Electrochemistry and Corrosion Science*, Kluwer Academic Publishers, Boston, 2004.
- [2] E. McCafferty, *Introduction to Corrosion Science*, Springer, New York, 2010.
- [3] Y. Waseda, S. Suzuki, *Characterization of Corrosion Products on Steel Surfaces*, Springer, Berlin, 2006.
- [4] H. Kaesche, *Corrosion of Metals: Physicochemical Principles and Current Problems*, Springer-Verlag, Berlin, 2003.
- [5] J. Wojciechowski, Ł. Kolanowski, A. Bund, G. Lota, The influence of current collector corrosion on the performance of electrochemical capacitors, *J. Power Sources* 368 (2017) 18-29.

Acknowledgements

This work was financially supported by the National Science Centre of Poland granted on the basis of the decision number DEC-2013/10/E/ST5/00719.

Effect of Structuring Geometry on the Photocurrent of Experimental Model Photoelectrode Surfaces

H. Kriegel¹, M. Schieda¹, I. Herrmann-Geppert¹, D. Voronov², D. L. Olynick², T. Klassen^{1,2}

1. Helmholtz-Zentrum Geesthacht, Institute of Materials Research, Max-Planck-Str. 1, 21502 Geesthacht, Germany

2. Helmut-Schmidt-University, Holstenhofweg 85, 22043 Hamburg, Germany

3. Lawrence Berkeley National Laboratory, One Cyclotron Road, Berkeley, CA 94720, USA
mauricio.schieda@hzg.de

In photoelectrochemical water splitting cells, the electrode/electrolyte interface must enable light absorption and carrier generation by the electrode, offering a large reactive surface area but limiting surface recombination.

While surface structuring is a generally accepted strategy to improve the electrode performance, most electrode manufacturing methods allow only minimal variation in surface structuring geometry, which does not permit a systematic understanding of surface structuring effects on performance.

Using nanofabrication methods, we are developing a library of experimental model photoelectrodes in order to investigate the influence of surface structuring geometry on photoelectrochemical performance. We present an update on performance trends for model electrodes prepared by atomic layer deposition of TiO₂ on silicon substrates previously structured with series of surface features with different geometries: lines, pillars, or holes.

Photoelectrochemical characterization is performed in order to identify the optimal structural parameters. For a series of electrode surfaces structured with the same geometry, at a moderate surface-feature height, a distinctive photocurrent optimum is generally observed. Higher structures result in a decrease in photocurrent. The performance drop is more significant for shorter periods (distance between two features). For very long periods, the maximum achievable photocurrents are lower than for short and medium periods. While in all cases surface recombination is significant, it is not the main factor determining performance trends.

Additionally, experimentally acquired UV-Vis spectra are in good agreement with finite difference time domain (FDTD) calculations of spectral reflectance. This enables the use of simulated data to better understand the absorption and generation processes in these model photoelectrodes.

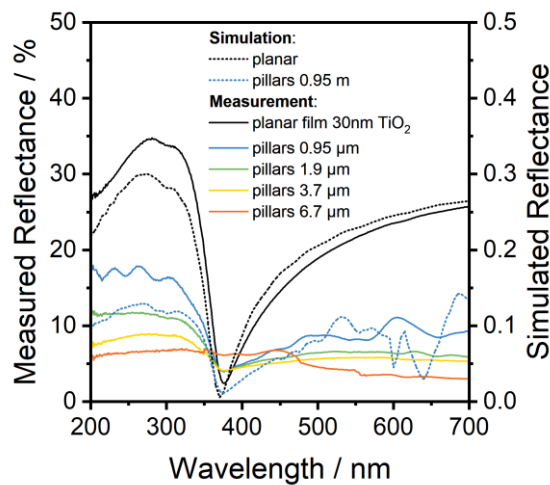


Figure 1. Integrated diffuse reflectance spectra of a series of p⁺⁺Si substrates, structured with pillars of period=800 nm, and coated with 60 nm of ALD-grown TiO₂.

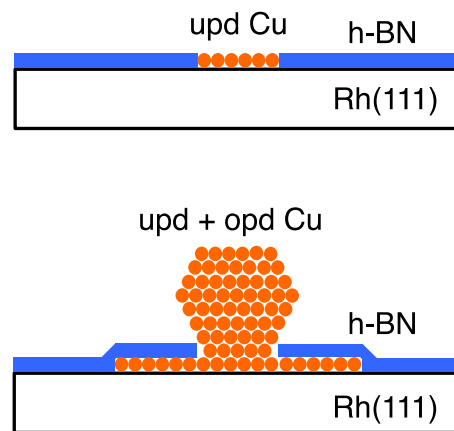
Quantifying and Modifying Defects in 2D Materials by Metal Underpotential Deposition

Stijn F. L. Mertens

*TU Wien, Institute of Applied Physics
Wiedner Hauptstraße 8-10/134, 1040 Vienna, Austria
mertens@iap.tuwien.ac.at; stmerten@gmail.com*

The number density and size of defects in 2D materials such as graphene and hexagonal boron nitride (h-BN) are decisive for many of the materials' properties. Even though growth procedures are often optimised to minimise defect density, facile quantification remains important. Direct visualisation of defects using scanning probe microscopies is possible, but cannot be scaled to macroscopic areas.

Here, it is demonstrated how metal underpotential deposition (upd) may find use as a general tool to determine the collective defect area in hybrids between 2D materials and various substrate metals. By investigating copper upd on a monolayer of h-BN on Rh(111), we explore how this process can be used to quantify the defects in the h-BN monolayer that form during its chemical vapour deposition. In addition, the upd signature allows assessing the potential window of the h-BN/metal hybrid, which is important to explore its functionality under ambient and electrochemical conditions. Importantly, upd itself does not alter the defect area on repeated cycling. Overpotential deposition, on the other hand, is shown to have significant consequences on the defect area. We show that this non-innocent Cu electrodeposition involves intercalation originating at initial defects, causing irreversible delamination of the h-BN layer; this effect therefore may be used for 2D material nanoengineering.



References: *Nature* 534, 676 (2016); *Electrochim. Acta* 246, 730 (2017)

Electrochemical Analysis of Cobalt and Selenium Codeposition Process from Acidic Solutions

Anna Kwiecińska, Karolina Kołczyk, Dawid Kutyla, Piotr Żabiński, Remigiusz Kowalik
AGH University of Science and Technology, Faculty of Non-Ferrous Metals
al. A. Mickiewicza 30, 30-059 Krakow, Poland,
rkowalik@agh.edu.pl

The electrochemical deposition of transition metal chalcogenides thin films has received recently much attention due to their potential applications in electrocatalysis. Among them the special attention is focused on cobalt-selenium system. Usually, thin films of these materials are prepared by hydrothermal synthesis or high temperature and vacuum techniques. However electrodeposition has been found to be a very good and low-cost method to fabricate thin polycrystalline films of these compounds.

The electrodeposition of thin films of polycrystalline Co-Se system from aqueous baths was studied. The experiments were carried out following the thermodynamic analysis. A conventional three-electrode cell: Cu as working electrode, Pt-sheet as counter electrode and Saturated Calomel Electrode (SCE) as reference electrode was used. The electrodeposition mechanism of pure elements Se, Co and Co-Se phases on copper substrate was studied by chronoamperometry, cyclic voltammetry and hydrodynamic techniques. Additionally, chronoamperometry and cyclic voltammetry were combined with electrochemical quartz crystal microbalance to analyze this process in details.

Thin films were deposited potentiostatically on copper substrate. The influence of potential deposition, H_2SeO_3 and CdSO_4 concentration, pH and bath temperature on the chemical composition of the films was discussed. The formation of Co-Se intermetallic phases was confirmed by X-ray diffraction. The chemical composition of the deposits was determined by XRF and EDS analysis. Morphology of the deposits was examined by scanning electron microscopy.

This work was supported by the Polish National Center of Science under grant 2016/21/B/ST8/00431.

Direct Evidence for the Bifunctional HOR electrocatalysis in alkaline medium

Masha Alesker, Meital Shviro, Luba Burlaka, David Zitoun

Bar Ilan University, Department of Chemistry, Bar Ilan Institute of Technology and Advanced Materials (BINA), Ramat Gan, 52900, Israel.

Istvan Bakos

Institute of Materials and Environmental Chemistry, Hungarian Academy of Sciences, Budapest, Hungary

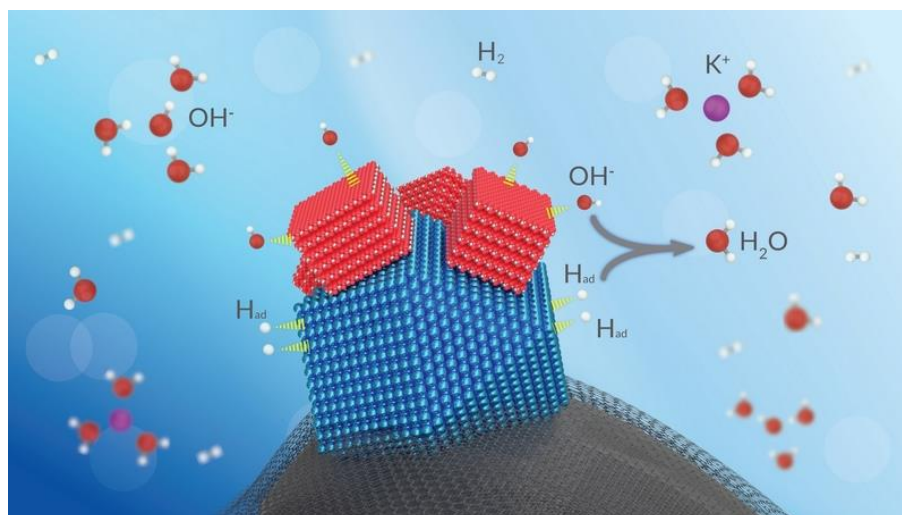
Qingying Jia, Sanjeev Mukerjee

*Department of Chemistry and Chemical Biology
Northeastern University, Boston, MA 02115*

Investigation of the hydrogen oxidation reaction (HOR) in alkaline media has been pursued in the past few years side by side with the development of Alkaline exchange membrane fuel cells (AEMFCs). We have developed a family of platinum-free bimetallic catalysts.[1,2] The catalysts are synthesized through novel synthetic approaches to allow the control at the nanoscale of two phases, one responsible for the hydrogen binding and the other one for hydroxide binding. [3]

A detailed investigation of the catalysts by advanced electron microscopies show the interconnections between the two phases: Pd metal and NiOOH. The in-situ study of the catalysts has been carried on by operando X-Ray absorption spectroscopy collected on a synchrotron light source at the K-edge of Ni and Pd.

This study emphasizes the importance of tuning the interface of the electrocatalyst and opens way to improve the activity of HOR catalysts in alkaline medium (scheme 1 below).



Scheme of the bifunctional HOR mechanism on C/Pd/NiOOH electrocatalyst

[1] *Pd/Ni Synergistic Activity for Hydrogen Oxidation Reaction in Alkaline Conditions* Istvan Bakos, Andras Paszternak, David Zitoun *Electrochimica Acta*, **2015**, 176, 1074-1082

[2] *Palladium/Nickel Bifunctional Electrocatalyst for Hydrogen Oxidation Reaction in Alkaline Membrane Fuel Cell* Masha Alesker, Miles Page, Meital Shviro, Gregory Gershinsky, Yair Paska, Dario Dekel, David Zitoun *Journal of Power Sources* **2016**, 304, 332-339

[3] *Method for fabricating multi-metallic hydrogen oxidation electrocatalyst materials*, Provisional appl. no.: 62/541,810 David Zitoun, Masha Alesker, Meital Shviro

Sulfur-Carbon Composite Electrodes and Effective Electrolytes for Rechargeable Li/S Batteries

Masashi Ishikawa, Yukiko Matsui, Satoshi Uchida
Department of Chemistry and Materials Engineering
Faculty of Chemistry Materials and Bioengineering
Kansai University
3-3-35 Yamate-cho, Suita 564-8680, Japan
masaishi@kansai-u.ac.jp

Sulfur (S) has a high theoretical capacity (1,672 mAh g⁻¹) and is abundantly available and inexpensive material. There are, however, several problems limiting S performance in a positive electrode. A major problem is the behavior of lithium polysulfide (Li₂S_n) intermediates, which are formed during charge and discharge processes, may dissolve into an electrolyte³. If dissolution of Li₂S_n occurs, this should lead to a rapid capacity decay and a decrease in stability by a redox shuttle reaction.

It is difficult to solve these problems as far as only elemental S is used, so it is proposed to synthesize S-composites for stabilization of S derivatives. In previous work, S-composites with mesoporous activated carbon and conductive polymers with S and S-graphene have been extensively studied, and these systems show relatively high cycle stability. However, these electrodes still have a problem of insufficient charge-discharge efficiency. This is ascribed to the redox shuttle of dissolving Li₂S_n intermediates, and as far as we know, there is no practical method that completely prevents the dissolution of Li₂S_n intermediates with these electrodes. Therefore, in recent years, other studies have been conducted to completely prevent the dissolution of Li₂S_n intermediates by using different host materials for S and different cell design; they are composites of S with microporous activated carbon or organic substances and all-solid Li-S batteries¹⁻⁵. These technologies can completely suppress the dissolution of a Li₂S intermediate, so that it is known that not only their capacity retention but also their charge-discharge efficiency is stabilized⁶. However, these electrodes have a problem in energy density because their micropore volume is still low, meaning low S loading⁶.

In this work, we synthesized a S-composite based on microporous alkali-activated carbon with high porous volume and tested positive electrode performance of the S-composite. As a result, we achieved both improvement of cycling characteristics by preventing Li₂S_n dissolution and an increase in S loading. Also in this study, to increase S loading into microporous carbon as well as avoid dissolution of Li₂S₄₋₈ we designed micropore-rich activated carbon with high surface area and pore volume, which was obtained by activation of azulmic carbon (AZC) precursor as a nitrogen (N)-doped carbon. The AZC was a carbonized product from azulmic acid (AZA) that was obtained by polymerization of hydrocyanic acid (H-C≡N) under a high temperature. We would suggest that our activated AZC is promising material as positive S electrode matrix for the next-generation rechargeable Li batteries.

This work was partly supported by “Advanced Low Carbon Technology Research and Development Program, Specially Promoted Research for Innovative Next Generation Batteries (ALCA-SPRING)” from Japan Science and Technology Agency (JST). We thank Mr. Takuya Takahashi for his contribution in the early stage of our work.

Reference

1. S. Zheng, P. Han, Z. Han, H. Zhang, Z. Tang, and J. Yang, *Scientific Reports*, **4**, 4842 (2014).
2. Z. Li, L. Yuan, Z. Yi, Y. Sun, Y. Liu, Y. J. iang, Y. Shen, Y. Xin, Z. Zhang, and Y. Huang, *Adv. Energy Mater.*, **4**, 1301473 (2014).
3. B. Zhang, X. Qin, G. R. Li, and X. P. Gao, *Energy Environ. Sci.*, **3**, 1531 (2010).
4. L. Wang, X. He, J. Li, M. Chen, J. Gao, and C. Jiang, *Electrochim. Acta*, **72**, 114 (2012).
5. T. Kobayashi, Y. Imade, D. Shishihara, K. Homma, M. Nagao, R. Watanabe, T. Yokoi, A. Yamada, R. Kanno, and T. Tatsumi, *J. Power Sources*, **182**, 621 (2008).
6. T. Takahashi, M. Yamagata, and M. Ishikawa, *Prog. Nat. Sci.*, **25**, 612 (2015).

Design and Manufacturing of Highly Active Wood-Derived Carbon Materials for Low Temperature Fuel Cells

Ivar Kruusenberg^{a,*}, Kätlin Kaare^a, Aleksandrs Volperts^b, Galina Dobeļe^b, Aivars Zurins^b, Loreta Tamasauskaite-Tamasiunaite^c, Eugenijus Norkus^c.

^aInstitute of Chemistry, University of Tartu
Ravila 14a, 50411 Tartu, Estonia

^bLatvian State Institute of Wood Chemistry, Dzerbenes street 27, Riga LV-1006, Latvia

^cState research institute Center for Physical Sciences and Technology, Savanorių ave. 231, LT-02300 Vilnius, Lithuania

*ivar.kruusenberg@ut.ee

Fuel cells are considered to be one of the most promising future energy source that could be a good alternative to the fossil-fuel technology. But the biggest problem lies in the poor kinetics of oxygen reduction reaction (ORR) at the cathode. Currently, Pt and its alloys are the most active electrocatalysts for the ORR [1]. Pt is very expensive and rare and on the other hand Pt-free catalysts are far cheaper and show acceptable efficiency. N-doped carbons are the most investigated metal-free ORR catalysts [2]. As an alternative we aim to develop wood-based carbon catalysts for low-temperature fuel cells. This research was performed in co-operation with Horizon Pulp & Paper Ltd, one of the biggest cellulose manufacturer in Eastern-Europe, to demonstrate the great potential of cellulose and wood industry residues as catalyst and catalyst support materials for the fuel cells.

In this work carbonized commercial cellulose, activated wood-based carbon and black liqueur were doped with cheap nitrogen precursor, dicyandiamide (DCDA). The doping was done by pyrolysing samples at 800 °C in the presence of DCDA. The mass ratio of samples-to-DCDA was 1:20 or 1:10. For electrochemical characterisation the glassy carbon (CG) electrodes were modified with synthesized catalysts and the experiments were carried out in 0.1 M KOH solution employing rotating disk electrode (RDE) method. For modifying the electrodes, a suspension (4 mg ml⁻¹) was made in isopropanol, containing 0.25% of Tokuyama ionomer AS-04.

Activated wood-based carbon (1:20) showed a good activity after milling and secondary pyrolysis at 800 °C. Fig. 1 presents the ORR polarization curve of N-doped wood-based catalyst in comparison to the commercial Pt-catalysts. Overall electrocatalytic activity of N-doped wood-based catalyst material in alkaline media, was higher than that of commercial 20% Pt catalyst. The number of electrons transferred per O₂ molecule (*n*) at different potentials was calculated from the Koutecky-Levich equation. *n* was 4, in wide range of potentials which is advantageous from the potential fuel cell application point of view. The results obtained in this work show that even wood-based carbon materials can have a great potential for fuel cell application.

References

1. K. Vignarooban, J. Lin, A. Arvay, S. Kolli, I. Kruusenberg, K. Tammeveski, L. Munukutla, A.M. Kannan, Chinese Journal of Catalysis 36 (2015) 458.
2. Q. Liu, C. Chen, F. Pan, Electrochim. Acta. 170 (2015) 234.

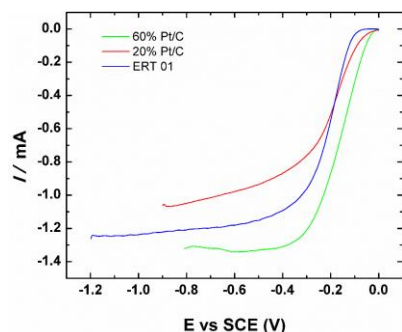


Fig. 1. Comparison of RDE results for oxygen reduction on different catalysts in O₂-saturated 0.1 M KOH. $v = 10 \text{ mV s}^{-1}$. $\omega = 1900 \text{ rpm}$.

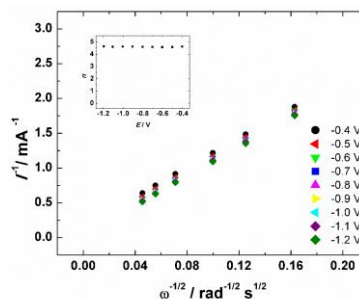


Fig. 2. Koutecky-Levich plots for oxygen reduction on wood-based carbon modified electrode in 0.1 M KOH at various potentials. The inset shows the potential dependence of *n*.

Investigations of various capacitive/faradaic materials through multi-scale coupled methods

H. Perrot^{1,2} and O. Sel^{1,2}

¹*Sorbonne Universités, UPMC University Paris 06, UMR 8235, Laboratoire Interfaces et Systèmes Electrochimiques, F-75005, Paris, France*

²*CNRS, UMR 8235, LISE, F-75005, Paris, France*

e-mail address: hubert.perrot@upmc.fr

Capacitive or faradaic materials are often used as thin films coating the metallic electrode in various applications like energy storage, energy conversion, biosensors domains. Charge transport, charge transfer reactions or electro-adsorption phenomena must play key roles in the electrochemical response of these electroactive films. It is commonly admitted that the oxidation process or anodic potential applied to such a film requires either a cation expulsion or an anion entry to compensate for the positive charges formed inside the film. However, it has been shown that these processes in electroactive films are accompanied, not only by the exchange of ions with the electrolyte solution but also by solvent exchanges. As electroneutrality is required, it is generally assumed that the field-assisted transport of charged species is more rapid than the transport of neutral species and, consequently, solvation equilibria can be only slowly established. Therefore, the equilibria associated with electronic, ionic, and solvation processes may be established on quite different time scales, but, at long enough time scales, thermodynamics will prevail and processes will attain a state of global equilibrium. However, the relative rates of all the processes involved in the charge compensation are still an open question for capacitive and faradaic materials.

Different techniques can be used to investigate ionic and solvent transfer and transport in electroactive materials. As the models employed are largely dependent on the techniques used to test them, different approaches can be used. The electrochemical investigation of electroactive films, in terms of voltammetry and electrochemical impedances, takes into account the charged species involved in the electrochemical process of the film. The addition of gravimetric investigations thanks to quartz crystal microbalances allows the solvent interaction to be attained. In order to discriminate the contribution of each involved species, charged or not, a multi scale coupling method of characterization was developed by coupling a fast quartz crystal microbalance to electrochemical impedances measurements [1]. More precisely, ac-electrogravimetry allows the mass response to a small potential perturbation to be analyzed thanks to this fast quartz crystal microbalance used in dynamic regime. Thus, ac-electrogravimetry was employed to characterize ions and solvent motion at the film/electrolyte interface during the electrochemical reactions of electroactive material [2]. This technique was already fruitful in several domains: ionic and solvent insertion in inorganic films (Prussian Blue [3]), conducting polymer layers (polypyrrole [4]), taking account the film porosity [5], in PEMFC [6] and more recently in films based on carbon nanotubes [7].

References

- [1] E. Calvo, K. Kanazawa, H. Perrot et Y. Jimenez, "Combination of Quartz Crystal Microbalance with other Techniques", edited by A. Arnau 2nd édition, Springer, 2008, p307.
- [2] C. Gabrielli and H. Perrot, "ac-electrogravimetry investigation in electroactive thin films", edited by M. Schlesinger, Springer, 2009, p151-231.
- [3] "Ac-Electrogravimetry Study of Electroactive Thin Films: I. Application to Prussian Blue", C. Gabrielli, J. J. García-Jareño, M. Keddad, H. Perrot and F. Vicente, *J. Phys. Chem. B*, 106(2002)3182.
- [4] "Ac-Electrogravimetry Study of Electroactive Thin Films. II- Application to Polypyrrole ", C. Gabrielli, J. J. García-Jareño, M. Keddad, H. Perrot and F. Vicente, *J. Phys. Chem. B*, 106(2002)3192.
- [5] "Redox switching of heteropolyanions entrapped in Polypyrrole films investigated by ac-electrogravimetry", L. To Thi Kim, C. Debiemme-Chouvy, C. Gabrielli and H. Perrot, *Langmuir*, 28(38)(2012)13746.
- [6] "Proton Transport Properties in Hybrid Membranes investigated by ac-electrogravimetry", L. To Thi Kim, O. Sel, C. Debiemme-Chouvy, C. Gabrielli, C. Laberty-Robert, H. Perrot and C. Sanchez, *Electrochem. Com.*, 12(2010)1136.
- [7] "Gravimetric and dynamic deconvolution of global EQCM response of carbon nanotube based electrodes by Ac-electrogravimetry" F. Escobar-Teran, A. Arnau, J.V. Garcia, Y. Jiménez, H. Perrot, O. Sel, *Electrochem Comm*, 2016, 70, 73.

Electro-dissolution of Copper from a Water-containing Deep Eutectic Solvent

Priscila Valverde Armas^a, Todd Green^b, Sudipta Roy^c

^{a,b,c}Department of Chemical and Process Engineering, Strathclyde University

James Weir building, 75 Montrose Street, 4th Floor, Scotland-United Kingdom, G1 1XJ

^apriscila.valverde-armas@strath.ac.uk, ^btodd.green@strath.ac.uk, ^csudipta.roy@strath.ac.uk

Due to growing environmental regulations, alternatives to aqueous systems such as Ionic Liquids (ILs) have been examined for the electrodeposition of metals. Over other types of ILs, deep eutectic solvents (DESs) are substances tolerant to water and stable under ambient conditions. Although DESs are hygroscopic chemicals, most of metal electrodeposition studies have been carried out either from dry DES systems or neglecting their intrinsic water content. Likewise, scarce studies have concentrated on anodic processes from DESs. Since water cannot be avoided in a real electrodeposition process and it is likely that not only metal electrodeposition also electro-dissolution proceed from a hydrated electrolyte, the effect of water on both cathodic and anodic processes requires thorough investigation.

Until now, our group has studied the electrodeposition of Cu from water-containing ‘ethaline’ which is a DES obtained by mixing choline chloride and ethylene glycol. Since Cu electroplating has been studied extensively from aqueous systems, this is a convenient ‘model’ system to compare the results with the existing literature. It has been established that ‘ethaline’ can adsorb up to 15 wt% of H₂O over a month period. Also, water reduced the viscosity of the liquid which promotes the diffusivity of Cu²⁺ ions. As a result, the limiting currents of the process increased, which was indicative of the enhanced mass transport of the electroactive species. However, the plated films became less uniform and differences in morphology were found. The oxidation of a solvent may occur when inert anodes are used during metal electrodeposition [1]. Furthermore, DESs can be electrochemically decomposed and form chlorinated by-products [2]. On the other hand, the use of soluble anodes remains as a viable option. In this line, the second phase of this work has concentrated on the electrochemical dissolution of soluble Cu anode from hydrated ‘ethaline’.

The experiments were performed in a divided electrochemical cell at 25 °C without agitation. The working electrode was a Cu rod, the counter electrode (CE) was a Cu rotating disk (99.999% of purity, A=1.18 cm²) and a Ag wire was the reference electrode, inserted in a fritted glass tube containing pure ‘ethaline’ to avoid etching by the CuCl₂. Copper anodes were galvanostatically dissolved in pure ‘ethaline’ and in the electrolyte containing 1, 3, 6, 10 and 15 wt% of H₂O. The DES electrolyte comprised 0.2 M CuCl₂·2H₂O in ‘ethaline’. The applied anodic current density was set at 2.84 mA/cm² during a dissolution time of 1 or 2 h. Thereafter, samples of the liquid were taken to study the anodic species using Ultraviolet-Visible spectroscopy. The CE was weighted before and after dissolution to compute the ‘apparent’ valence of dissolution and the potential at which Cu was dissolved was monitored.

Cu when electrochemically dissolved in ‘ethaline’ at different water content formed cuprous species in the solution, e.g. CuCl₂⁻ or CuCl₃⁻. These results are corroborated by the potential at which Cu is dissolved where only Cu⁺ ions can be produced (Fig 1). The ‘apparent’ valence of dissolution in pure ethaline/water solutions was nearly the unit. However, this ‘apparent’ valence in the electrolyte was <1, which means that a superimposed reaction may occur. A simple corrosion model that explains this superimposed reaction will be discussed.

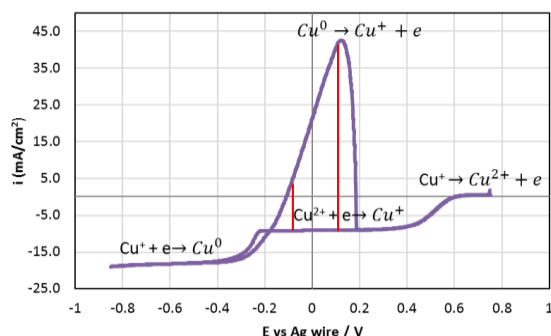


Fig. 1 Polarisation data of Cu using Pt electrode at 25°C, scan rate of 5 mV/s from 0.2 M CuCl₂·2H₂O in ‘ethaline’.

[1] D. Yue, Y. Jia, J. Sun, Y. Jing, J. Electrochim. Acta 65 (2012) 30-36.

[2] K. Haerens, E. Matthijs, K. Binnemans, B. Bruggen, Green Chem. 11 (2009), 1357-1365.

Fast Electrogravimetric Methods for Investigating Electrode/Electrolyte Interfaces in Electrochemical Storage Devices: Application to Nanostructured Metal Oxide Thin Films

Ozlem Sel^{1,2} and Hubert Perrot^{1,2}

¹Sorbonne Universités, UPMC University Paris 06, UMR 8235, Laboratoire Interfaces et Systèmes Electrochimiques, F-75005, Paris, France

²CNRS, UMR 8235, LISE, F-75005, Paris, France

e-mail address: ozlem.sel@upmc.fr

The need for new materials with improved ion transfer properties continues to be one of the main pressing concerns in energy storage/conversion materials research. In accompanying this search for optimal materials, appropriate characterization tools to assess key parameters of newly developed materials are required. Particularly, the morphology dependent performance, and kinetic or dynamic aspects of ion transfer behaviour of metal oxide electrodes is not very well understood. In the literature, the insertion of ions in metal oxide electrodes was investigated by *in situ* and *ex situ* characterization techniques, including electrochemical and gravimetric methods [1-3]. However, none of these methods alone provides the information on the exact identification of the inserted ionic species, their dynamics of transfer at the interfaces, as well as the role of electrolyte composition and the effect of ions solvation on the charge compensation phenomena. Therefore, in this work, an alternative characterization tool was proposed which couples fast quartz crystal microbalance (QCM) and electrochemical impedance spectroscopy (EIS) (*ac*-electrogravimetry) [4-8]. This method has recently been employed for studying transfer and transport phenomena in materials for (pseudo)capacitive charge storage [5-8]. This coupled method, so called *ac*-electrogravimetry differs from classical EQCM and measures the usual electrochemical impedance, $\Delta E/\Delta I(\omega)$, and the mass variations of the film under a sinusoidal potential perturbation, $\Delta m/\Delta E(\omega)$, simultaneously. This coupling has the ability to detect the contribution of the charged or uncharged species and to separate the anionic, cationic, and the free solvent contributions during the various (pseudo)capacitive processes. These features make the *ac*-electrogravimetry as an attractive and appropriate tool to investigate transfer/transport phenomena of charged and uncharged species in ion insertion materials. As pertinent examples, the adaptation of *ac*-electrogravimetry to evaluate the ion (Li^+ , Na^+ ...) transfer in nanostructured metal oxide (MnO_2 etc.) based thin films will be discussed in detail. Metal oxide thin films were synthesized by electrodeposition methods and the ion transfer properties (Li^+ and Na^+ in aqueous and acetonitrile solutions) were investigated by electrochemical quartz crystal microbalance (EQCM) and *ac*-electrogravimetry. Our study identifies the involvement of several charged species (Li^+ , Na^+ and their solvated counterparts) in the charge compensation, and solvent molecules indirectly contribute to the process. The results of the study indicate that the transfer resistances of the cations, especially that of larger solvated cations are much lower when the metal oxide films are mesoporous, probably due to the increased surface area and pore volume created by mesoporous morphology facilitating the larger charged species transfer. This qualitative and quantitative study of ionic and nonionic species contribution in the charge compensation process, together with dynamic information of their interfacial transfer further proves the advantageous nature of nanostructuring of metal oxide films for potential applications.

References

- [1] Toupin, M.; Brousse, T.; Belanger, D. *Chem. Mater.* **2004**, *16*, 3184.
- [2] Kanoh, H.; Tang, W.; Makita, Y.; Ooi, K. *Langmuir* **1997**, *13*, 6845.
- [3] Kuo, S-L.; Wu, N-L. *J. Electrochem. Soc.* **2006**, *153*, A1317.
- [4] Gabrielli, C.; García-Jareño, J. J.; Keddou, M.; Perrot, H.; Vicente, F. *J. Phys. Chem. B* **2002**, *106*, 3182.
- [5] Ridruejo Arias, C.; Debiemme-Chouvy, C.; Gabrielli, C.; Laberty-Robert, C.; Pailleret, A.; Perrot, H.; Sel, O. *J. Phys. Chem. C* **2014**, *118*, 26551.
- [6] Razzaghi, F.; Deviemme-Chouvy, C.; Pillier, F.; Perrot, H.; Sel, O. *Phys. Chem. Chem. Phys.* **2015**, *17* (22), 14773.
- [7] Escobar-Teran, F.; Arnau, A.; Garcia, J.V.; Jiménez, Y.; Perrot, H.; Sel, O. *Electrochem. Comm.* **2016**, *70*, 73.
- [8] Goubaa, H.; Escobar-Teran, F.; Ressam, I.; Gao, W.; El Kadib, A.; Lucas, I. T.; Raihane, M.; Lahcini, M. Perrot, H.; Sel, O. *J. Phys. Chem C* **2017**, *121*, 9370.

Asymmetric Polyoxometalate Electrolytes for Redox Flow Batteries

J. Friedl^{1*}, M. V. Holland-Cunz^{1*}, F. Cording¹, B. Schricker², R. Fleck, H. Wolfschmidt², U. Stimming¹;

*These authors contributed equally

¹ Newcastle University, Chemistry, School of Natural and Environmental Sciences, Bedson Building,
NE17RU, Newcastle upon Tyne, United Kingdom

² Siemens AG, CT REE ENS PTS-DE, 91058 Erlangen, Germany

ulrich.stimming@newcastle.ac.uk

Electrochemical storage of energy is a valuable asset for the integration of intermittent renewable energy sources such as wind and solar power. Redox flow batteries (RFBs) are the only type of battery in which the energy content and the power output can be scaled independently, offering flexibility for applications such as frequency regulation and load levelling. In addition, degradation of RFBs should be limited because the electrodes do not undergo conversion or intercalation reactions. The energy of a RFB is stored in dissolved redox shuttles in its electrolytes. However, while the advantages of the flow battery concept are undisputed, there is no agreement on the best (electro-) chemistry yet. The four oxidation states of vanadium (V^{2+} , V^{3+} , VO^{2+} , VO_2^+) and inexpensive organic molecules are strong contenders, but face their individual challenges. The main drawbacks of the vanadium RFB are the sluggish kinetics of the V^{2+}/V^{3+} and the VO^{2+}/VO_2^+ redox reaction which limit the current density and therefore the power density [1]. Catalysis of the half-cell reactions has been investigated mostly by introducing oxygen containing functional groups onto the graphitic electrodes; but those only catalyse the V^{2+}/V^{3+} redox reaction and have no influence on or even impede the VO^{2+}/VO_2^+ redox reaction [2,3]. Another type of redox chemistry that can be employed in RFBs are polyoxometalates (POMs). POMs form a class of discrete transition metal-oxide nanoclusters, are prepared from metals and offer versatile electrochemistry [4].

In this study we investigate two polyoxometalates (POMs), $[SiW_{12}O_{40}]^{4-}$ and $[PV_{14}O_{42}]^{9-}$, as redox-active species for RFBs [5]. We show that these POMs exhibit fast redox kinetics (electron transfer constant $k_0 = 4 \cdot 10^{-2} \text{ cm s}^{-1}$ for $[SiW_{12}O_{40}]^{4-}$), which is four orders of magnitude faster than that of the vanadium redox reactions employed in the VRFB [1], thereby enabling high power densities. They undergo multi-electron electron transfer, realising a high capacity per molecule. There was no cross-contamination through the cation exchange membrane observed which eliminates self-discharge. Additionally the investigated POMs are chemically and electrochemically stable as shown by *in-situ* NMR. In flow battery studies the theoretical capacity (10.7 Ah L^{-1}) could be achieved under operating conditions. The cell showed a capacity fade of 0.16% per cycle when the cell was cycled for 14 days with current densities from 30 to 60 mA cm^{-2} due to the presence of oxygen within the system. The lost capacity could be replenished by adding a reducing agent to the catholyte which showed no sign of degradation after 155 cycles.

[1] Friedl, J.; Stimming, U., *Electrochim. Acta* 2017, **227**, 235–245.

[2] Fink, H.; Friedl, J.; Stimming, U., *J. Phys. Chem. C* 2016, **120**, 15893–15901.

[3] Friedl, J.; Bauer, C. M.; Rinaldi, A.; Stimming, U., *Carbon N. Y.* 2013, **63**, 228–239.

[4] Friedl, J.; Al-Oweini, R.; Herpich, M.; Keita, B.; Kortz, U.; Stimming, U., *Electrochim. Acta* 2014, **141**, 357–366.

[5] Friedl, J.*; Holland-Cunz, M. V.*; Cording, F.; Pfanschilling, F.; Wills, C.; MacFarlane, W.; Schricker, B.; Fleck, R.; Wolfschmidt, H.; Stimming, U., submitted.

Mesoporous $\text{La}_{0.6}\text{Ca}_{0.4}\text{CoO}_3$ Perovskite Oxide for Oxygen Reduction and Oxygen Evolution Reaction for Reversible Zn-air Battery

Tatsumi Ishihara^{a,b}, Takayoshi Miyano^b, Yuiko Inoishi^b, and Shintaro Ida^{a,b}

^aDepartment of Applied Chemistry, Faculty of Engineering, Kyushu University

^bInternational Institute for Carbon Neutral Energy Research (WPI-I²CNER)

Motoooka 744, Nishi-ku, Fukuoka, 819-0395, Japan

ishihara@cstf.kyushu-u.ac.jp

Metal-air battery can theoretically achieve much higher energy densities than that Li ion batteries, which are currently in wide use as an electrical source for mobile devices because the half-cell can work as a battery. Several metals have been investigated for use as the anode of metal-air batteries, and Li metal has the largest gravimetric energy density.¹⁾ However, from the perspectives of safety and cost, Zn is another attractive metal for metal-air batteries.²⁾ The Zn-air battery has already been commercialized as a non-rechargeable type battery, while for use as a rechargeable battery, reversibility and cycle stability are required for both the Zn anode and the air cathode. In this study, mesoporous LaCoO_3 doped with Ca was prepared by hard template method and applied for air electrode of Zn-air battery. It was unexpectedly found that introduction of mesoporous structure is highly effective for increasing cycle stability of air electrode. Mechanism of degradation of air electrode performance was also reported from oxidation of carbon binder during charge process which leads to large diffusion resistance.

Mesoporous $\text{La}_{0.6}\text{Ca}_{0.4}\text{CoO}_3$ (LCC) with large surface area was prepared using mesoporous SiO_2 (KIT-6) as a hard template for the procedure. In this method, the LCC precursor is deposited inside the one dimensional mesopores in KIT-6, calcined at 1073 K, followed by removal of the SiO_2 template with 2 M NaOH. Therefore, it is expected that prepared mesoporous materials by hard template method is consisted of nano particles or nanorods.

According to the XRD measurement and N_2 adsorption method, it was found that single phase of LaCoO_3 was obtained and the average pore size exists around 1.6 nm. Application of the prepared mesoporous LCC for air electrode of Zn-air battery was performed. The ORR and OER activity was measured over the mesoporous LCC perovskite oxide with a gas diffusion electrode (GDE). Figure 1 shows the overpotential of the air electrode as a function of the current density. The overpotential of bulk LCC and MnO_2 , which is generally used as the Zn-air electrode for commercialized Zn-air button cells are also plotted for comparison. Compared with the widely used MnO_2 catalyst, the ORR activity is almost the same for both bulk and mesoporous LCC, and even comparing with Pt/C which is well known active ORR catalyst, almost the same ORR activity is achieved. However, the overpotential for OER activity is much lower for LCC than for MnO_2 . Even comparing with Pt/C, LCC shows much smaller overpotential for OER reaction.

Zn- O_2 batteries with bulk LCC and mesoporous LCC as air catalysts were fabricated using 4 M KOH saturated with ZnO as an electrolyte and O_2 as oxidant. At $50\text{mA}/\text{cm}^2$, the observed potential and discharge capacity were 1.1 V and $750\text{mAh}/\text{g}_{\text{Zn}}$, respectively, which is 90% of theoretical value. However, the discharge capacity and the potential were decreased with the cycle number for both cells as shown in Fig.2. Considering the results for the cycling performance with the GDE, this decrease in discharge potential could be attributed to the decreased potential of the LCC air electrode. However, over 90 cycles, the cell with the mesoporous LCC air electrode had reasonable cycle stability, which suggests that mesoporous LCC is both active and stable as an air electrode for Zn-air batteries.

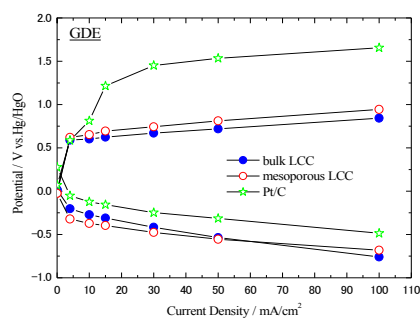


Fig. 1 Overpotential of air electrode as a function of current density

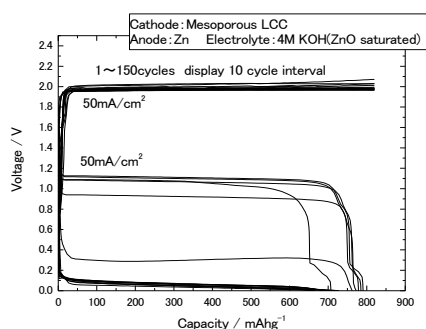


Fig.2 charge and discharge curves of Zn-air using mesoporous LCC for air electrode.

1) J.M. Tarascon, M. Armand, Nature, 2001, 414, 359.

2) Z.L. Wang, D. Xu, J.J. Xu and X.B. Zhang, Chem. Soc. Rev., 2014, 43, 7746

Electropolymerized Xanthone-Triarylamines for Used as TADF Emitters

Przemyslaw Data,^{1,2,3} Heather Cole²

¹ *Silesian University of Technology, Faculty of Chemistry, Department of Physical Chemistry and Technology of Polymers, 44-100 Gliwice, Strzody 9, Poland*

² *Durham University, Department of Physics, South Road, DH1 3LE, Durham, United Kingdom*

³ *Centre for Polymer and Carbon Materials of the Polish Academy of Sciences, Zabrze, Poland
przemyslaw.data@polsl.pl*

The OLED worldwide market is growing rapidly and Europe needs experts possessing a comprehensive knowledge and practical experience in this technology. OLED technology is used in small de-vices such as smart phones and tablets but also in high-end TVs and lighting, as OLEDs are still relatively expensive compared to LCD. But with research progressing towards lower cost and longer lifetime, together with a growing trend to use flexible displays in smartphones etc., the OLED market is growing fast. The organic light-emitting diodes (OLED) industry is very demanding in its search for new compounds that could be used as the emitter material or in transporting layers. The OLED devices are typically divided into fluorescence and phosphorescence devices. Fluorescence is a fast relaxation process, where the excited molecule in the excited singlet state returns to the ground state by emitting energy in the form of photons. In fluorescent OLEDs, emission arises from the only radiative decay of singlet excitons, are radiative triplet exciton decay is forbidden. The quantum efficiency of a fluorescent emitter based device, therefore, will be limited to 25% which means that the 75% triplet excitons will be lost. In order to increase the efficiency of devices, it is possible to link fluorescence and phosphorescence and get 100% efficiency by employing the TADF process. In this new type of delayed fluorescence emitters harvesting both singlet and triplet excited states to give 100% internal conversion of a charge into light gave the possibility to replace very expensive Ir based phosphors in OLEDs.

Here, we would like to present electrochemical and spectroelectrochemical investigation of three novel donor-acceptor-donor (D-A-D) materials, comprising of two diphenylamine (DPA) or modified DPA donors bonded to a single xanthone acceptor. Although a xanthone acceptor D-A-D derivative has been previously synthesised and used as a TADF materials with limited success, as well as used as a sky blue triplet harvester within a FRET-based electroluminescence device, these materials, XDPA, XNAP, XDPAOMe, have been specifically synthesised for electropolymerization in order to highlight a new design pathway for the creation of TADF polymeric materials.

Acknowledgements

This work was supported by the European Union's Horizon 2020 research and innovation programme under grant agreement No 691684

Chemical nanopores modification for smart filters

Dihia Benaoudia^{1,2}, Véronique Bennevault^{2,5}, Jérôme Mathé³,
Fabien Montel⁴, Jalal Ghilane¹, Philippe Guégan² and Jean-Christophe Lacroix¹

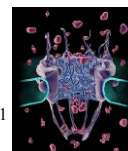


Fig. 1 Nuclear pore complex

¹Université Paris Diderot-Paris 7, Sorbonne Paris cité, Interfaces Traitement Organisation et Dynamique des Systèmes, 75205 Paris, France

²Université Pierre et Marie Curie-Paris 6, Sorbonne Universités, Institut Parisien de Chimie Moléculaire

³LAMBE, Université Evry, Université Paris-Saclay, CNRS, CEA, Université Cergy-Pontoise

⁴CNRS, Laboratoire de Physique, équipe Matière et Complexité, Ecole Normale Supérieure de Lyon

⁵Université Evry, 91025 Evry, France
dihia.benaoudia@univ-paris-diderot.fr

Filtration is a key process in chemical industry, water treatments and in biotechnology. It is crucial in emerging environment friendly technologies, which require to sort and to recycle efficiently and rapidly used materials and molecules. Filtration problems are numerous and can be classified according to the size and nature of the objects to be filtered (molecules, macromolecules, virus, particles, living cells), to the filters used (clothes, paper, sand, membranes). Active filtration devices, i.e. filters whose properties can be controlled by an external input, are of tremendous interest. Nuclear pore is an interesting source of inspiration for the elaboration of active filter answering to the pH or temperature. Such systems can be mimicked by the grafting of specific macromolecules in solid pores of diameter below 50 nm.

In this communication, we will describe the different steps to mimic such nuclear pore and to build a selective filter. For that, nanopores will be electrochemically grafted by a) molecules bearing various chemical functions deposited as compact ultrathin films (thickness below 5 nm) and b) by long macromolecules with hydrodynamic radius of 10 nm leading to a hairy nanopore. In both cases grafting, has been performed by diazonium electroreduction and the properties of the functionalized membrane has been studied by measuring DNA translocation through the nanopores by zeromode wave guide setup or by electrical measurements. [1]

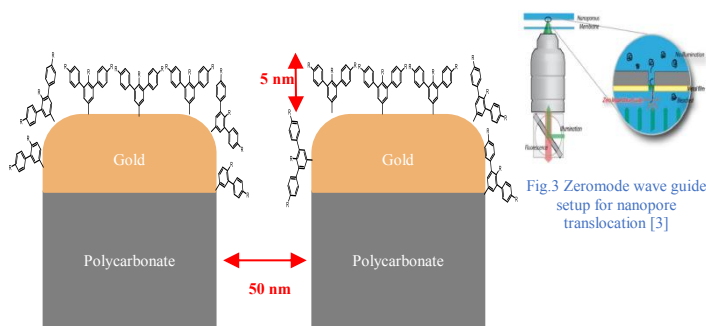


Fig. 2 Pore modification by diazonium salt reduction [2]

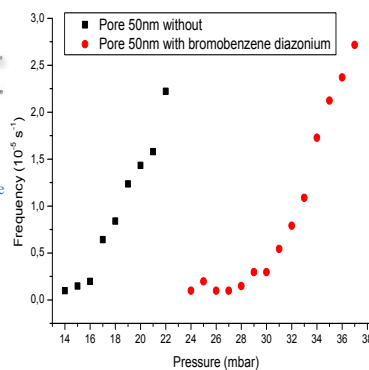


Fig. 4 Frequency of DNA translocation through nanopores

When using aminophenyl molecules having different chemical function we clearly demonstrate that DNA translocation can be tuned by the chemical functions deposited at the entrance of the nanopores. Indeed, we observed a clear shift of the curves DNA translocation frequency vs pressure towards higher pressures as compared to bare membranes (Fig. 4). Furthermore, this change can be related to the change of the effective radius of the pore due to the grafting. After that heterotelechelic poly (2-alkyl-2-oxazoline) has been synthesized and grafted [4]. Oxazoline brings a hydrophobicity control to the pore by the modulation of the lower critical solubility temperature (LCST) of those polymers. The first results toward active filter controlled by temperature will be described.

References

- [1] D W. Deamer* *Acc. Chem. Res.* **2002**, 35, 817-82
- [2] D. Bélanger, J. Pinson, *Chem. Soc. Rev.* **2011**, 40, 3995-4048
- [3] F. Montel*, *PhysRevLett.* **2014**, 113.028302
- [4] V. Bennevault-Celton*, *Aust. J. Chem.* **2012**, 65, 1145 1155

Core-Shell $\text{Co}_3\text{O}_4@\text{Pt}$ on Mildly Oxidized Graphene Oxide for Oxygen Electro-Reduction in an Alkaline Electrolyte

Shih-Cheng Chou, Yi-Chieh Hsieh, Wei-An Chung, Pu-Wei Wu*
Department of Materials Science and Engineering, National Chiao Tung University
Hsinchu 300, Taiwan, ROC
ppwu@mail.nctu.edu.tw

This research covers three different parts. The first part focuses on preparing two types of graphene oxides and exploring their potential as carbon supports for catalysis reaction; in the second part, we synthesize and characterize Co_3O_4 electrocatalysts impregnated on the graphene oxides, and determine their electrocatalytic activities; in the third part, we adopt a displacement reaction to form a Pt-shell structure on the Co_3O_4 and analyze its electrocatalytic activity for oxygen reduction reaction in an alkaline media.

Experimentally, first we utilize a modified Hummers' method to synthesize graphene oxides with different oxygenated groups. The presence of oxidized functional groups is confirmed by X-ray photoelectron spectroscopy. Then, we adopt a hydrothermal route to synthesize Co_3O_4 nanoparticles on the graphene oxide sheets. From literatures, this Co_3O_4 exhibits a greater ORR catalytic activity in alkaline medium. X-ray diffraction pattern is used to determine the crystallinity of Co_3O_4 nanoparticles. Lastly, we entail a mild reduction method to partially reduce the surface of Co_3O_4 nanoparticles to a thin layer of metallic Co encapsulating the Co_3O_4 nanoparticles, followed by a displacement reaction involving an immersion of the sample in a Pt electrolyte at 10°C so Pt is deposited on the surface of Co_3O_4 . We optimize relevant processing parameters to obtain desirable electrocatalytic ability toward oxygen reduction in an alkaline electrolyte. Comprehensive electrochemical analysis and materials characterization have been conducted and will be discussed.

Specific adsorption from an ionic liquid: *in situ* STM and impedance study of iodide ion adsorption from a pure halide ionic liquid at bismuth single crystal planes

Georg Gorbatovski, Ove Oll, Erik Anderson and Enn Lust
Institute of Chemistry, University of Tartu
Ravila 14A, 50411 Tartu, Estonia
georg.gorbatovski@ut.ee

Adsorption of particles, such as molecules or ions, is an important basis for many everyday phenomena, such as corrosion inhibition or chromatographic separation. With regard to electrochemical technology, it provides a basis for energy storage in supercapacitors as well as helps to mitigate many important faradic processes via the formation of the electrical double layer (EDL). However, in many cases, the particles themselves adsorb at the surface by chemical bonding interaction, thereby contributing to an effect called specific adsorption, which means that the adsorbed species can no longer be considered as part of the diffuse phase at a solid|liquid interface. Therefore, as part of the solid interface, they contribute strongly to the interfacial properties, such as energy storage, reactivity and interaction with other interfaces. It is of interest to look at such systems whereby there are no neutral particles within the liquid phase, such as ionic liquids (IL). Composed exclusively of ions, ILs constitute a large variety of liquidous electrolyte media that can be specifically tuned for an application in mind. This allows ILs to have a varied range of applications, such as electrolytes for energy storage, separation of ionic or organic species and catalyst media for organic synthesis. Although the formation of the EDL in ILs has been in the scientific focus for over a decade, there is still a lack of understanding with regard to the specific interaction of ions at IL|metal interfaces [1,2]. This is partially due to the difficulty in describing such interactions from a modelling perspective, as well as the complexity of the systems in electrochemical experiments.

To overcome these problems, both classical electrochemical methods (cyclic voltammetry and electrochemical impedance spectroscopy) as well as *in situ* scanning tunneling microscopy (STM) method have been applied to observe the interfacial structuring at IL|single crystal bismuth interfaces. Bi(hkl) electrodes have been chosen for the working electrodes due to their variable metallic properties and stable interfacial structure. The iodide ions adsorb at Bi interfaces forming densely packed monolayer structures that are stable in a wide range of electrochemical potential. Thus it is suggested that the electron transfer coefficient i.e. the number of electrons shared between the ions and the metal changes with potential, rather than the surface coverage of ions. This also results in the fact that considerably more charge can be accumulated at the interface. Dynamic cyclic voltammetry and *in situ* STM measurements show that while the Bi(111) single crystal plane is highly resistant to surface reconstruction processes, the more metallic Bi(001) and Bi(01 $\bar{1}$) planes do indeed reconstruct upon the variation of potential, but that those processes are both highly reversible and fast. Although full impedance equivalent scheme fitting procedure [3] was carried out in the same region of potentials, these surface reconstruction processes were not detected by either impedance nor cyclic voltammetry methods. This highlights the need for advanced imaging methods to supplement classical electrochemical techniques to fully understand the underlying interfacial processes.

Acknowledgements

This work was supported by the Estonian Ministry of Education and Research (projects no. IUT 20-13, PUT55, PUT1033 and PUT1107), and European Regional Development Fund (Estonian Centre of Excellence “Advanced materials and high-technology devices for energy recuperation systems”, TK141).

References

- [1] M.V. Fedorov, A.A. Kornyshev, Ionic liquids at electrified interfaces, *Chem. Rev.* 114 (2014) 2978–3036.
- [2] O. Oll, T. Romann, C. Siimenson, E. Lust, Influence of chemical composition of electrode material on the differential capacitance characteristics of the ionic liquid|electrode interface, *Electrochem. Commun.* 82 (2017) 39–42. doi:10.1016/j.elecom.2017.07.015.
- [3] O. Oll, C. Siimenson, K. Lust, G. Gorbatovski, E. Lust, Specific adsorption from an ionic liquid: impedance study of iodide ion adsorption from a pure halide ionic liquid at bismuth single crystal planes, *Electrochimica Acta.* 247 (2017) 910–919. doi:10.1016/j.electacta.2017.07.034.

Earth-Abundant Coal-based Porous Carbon as The High-Performance Bifunctional Oxygen Electrocatalyst

Huimin Liu¹, Xingxing Chen^{1*}, Zhenjie Lu¹, Haoran Pan¹, Jun Wang¹, Xinning Huang², Tao Wang³
Justus Masa⁴

¹ *Research Group of Functional Materials for New Energy, School of Chemical Engineering, University of Science and Technology Liaoning, 114051 Anshan, China*

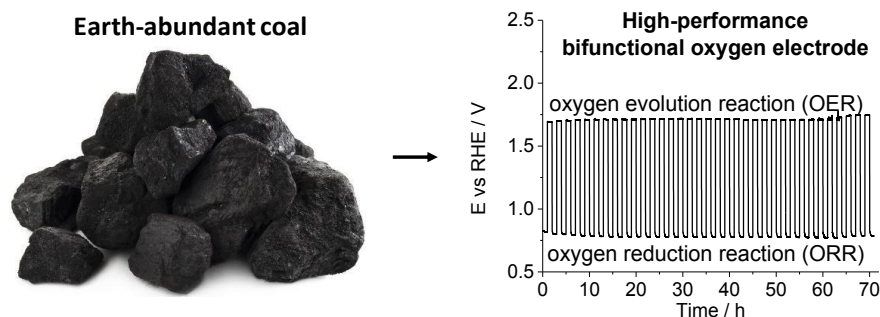
² *Engineering Training Center, University of Science and Technology Liaoning, Qianshan Road 185, 114051 Anshan, P. R. China*

³ *Key Laboratory of Energy Materials Chemistry, Institute of Applied Chemistry, Xinjiang University, 830046 Urumqi, China*

⁴ *Analytical Chemistry - Center for Electrochemical Sciences (CES), Ruhr-Universität Bochum, Universitätsstr. 150, 44780 Bochum, Germany*

* *Email-address: xingchenstar79@163.com*

Efficient bifunctional electrocatalysts for reversible oxygen electrodes are vitally important for realization of important future generation electrochemical energy conversion devices, such as regenerative fuel cells and rechargeable metal air batteries. Importantly, the electrocatalysts need not only be efficient but also inexpensive and source-abundant from the viewpoint of sustainability. Herein, we report active and stable bifunctional catalysts for oxygen electrodes obtained by pyrolysis of pristine coal in ammonia. The pyrolysis yielded nitrogen rich mesoporous graphitic carbon containing pyrrolic, pyridinic and quaternary groups, which demonstrated very good electrocatalysis of the oxygen reduction reaction (ORR) and the oxygen evolution reaction (OER) in 0.1 M NaOH. The optimized catalysts afford a stable round trip overvoltage than RuO₂, IrO₂ in the same solution thus unveiling a unique opportunity of directly transforming coal into a valuable catalyst without costly processing.



References

- [1] Xingxing Chen, Xinning Huang, Tao Wang, Stefan Barwe, Kunpeng Xie, Yasin Ugur Kayran, Daniela Wintrich, Wolfgang Schuhmann, Justus Masa, *Electrochimica Acta*, 2016, 222, 568-575.
- [2] Xingxing Chen, Jun Wang, Xinning Huang, Xuefei Zhao, Bingcai He, Penggao Liu, Tao Wang, Justus Masa, *Submitted*.

A real-time heparin monitor could be used to optimize the dosage of heparin during extracorporeal circulation procedures. This report describes the development of a graphite-paste (GP) electrode with molecularly imprinted polymer (MIP) grafted onto it. Heparin-imprinted poly (methacryloxyethyltriammonium chloride -*co*- acrylamide -*co*- methylenebisacrylamide) was grafted directly onto graphite particles. The grafted particles were thoroughly mixed with oil to fabricate the MIP-GP electrode. Traditional cyclic voltammetry was performed with the electrode in physiological saline or bovine whole blood containing 5 mM ferrocyanide and 0-8 units/mL heparin. The current intensity increased with heparin concentration. The current was insensitive to chondroitin sulfate C (CSC), which is a heparin analog. The contact angle of saline drop was decreased by addition of heparin but insensitive to CSC. The current and the contact angle at non-imprinted polymer (NIP)-grafted electrode was insensitive to heparin. Thus, the increase of the current is thought to increase by expansion of surface area by pushing into oil into the bulk of the electrode by specific interaction between MIP and the template. The sensitivity in blood is almost same as that in saline. The new sensing method using carbon paste electrode grafted directly with MIP would actualize new sensor which can be use in whole blood.

Lithium pre-doping from aqueous solution for hybrid supercapacitors

Wataru Sugimoto, Sho Makino, Dai Mochizuki
Shinshu University, Center for Energy and Environmental Science
Tokida 3-15-1 Ueda 386-8567 JAPAN
wsugi@shinshu-u.ac.jp

Lithium pre-doping process is necessary for lithium ion capacitors. Conventional pre-doping is conducted by using sacrificial Li metal in the cell, which leads to dead space after the Li pre-doping process. We have developed a hybrid supercapacitor based on aqueous electrolytes and carbon anode by using a water stable solid electrolyte [1,2]. For the pre-doping process our original recipe was to pre-dope graphite with Li in a separate cell, disassemble the cell, take out the Li pre-doped graphite (Li_xC_6) and re-assemble with gel electrolyte and solid electrolyte (Li_xC_6 | gel electrolyte | solid electrolyte). Here we will present our latest results on pre-doping from aqueous phase, which drastically simplifies the fabrication procedure.

The alginate gel was prepared following literature [3] and 0.5 M LiFSI/P13FSI was impregnated into the gel (alg-LiFSI/P13FSI) and vacuum dried. A water stable lithium conducting glass ceramic ($\text{Li}_{1+x+y}(\text{Ti},\text{Ge})_{2-x}\text{Al}_x\text{Si}_y\text{P}_{3-y}\text{O}_{12}$ ($x \sim 0.25$, $y \sim 0.3$); Ohara Inc., Japan, hereafter denoted as LTAP) was used as the solid electrolyte. A graphite electrode, alg-LiFSI-P13FSI, and LTAP were laminated into a pouch cell with a window cut out to allow LTAP to contact the aqueous electrolyte.

Electrochemical impedance spectroscopy of the non-doped protected graphite electrode was conducted in 1.0 M Li_2SO_4 (25°C) with a Pt mesh counter electrode. The resistance was $225 \Omega \text{ cm}^2$. Aqueous phase Li pre-doping was conducted by using activated carbon fiber (ACF) electrode as the counter electrode in 1.0 M Li_2SO_4 . Pre-doping was conducted at 1/20 C. The electrode potential of the pristine graphite electrode was 0.40 V vs RHE. The potential drops as the pre-doping proceeds reaches -2.67 V vs RHE when the capacity is $600 \text{ mAh (g-carbon)}^{-1}$. After a number of full doping/un-doping break-in cycles, the protected anode was un-doped until $100 \text{ mAh (g-carbon)}^{-1}$. The electrode potential was -2.56 V vs RHE and thus is suitable as an anode for hybrid supercapacitor.

After the pre-doping process, the ACF electrode was then connected to a new ACF electrode and the hybrid capacitor properties were characterized. Galvanostatic charge/discharge was conducted between 3.7 and 2.7 V. The discharge curves showed the capacity of the cathode was $20.2 \text{ mAh (g-carbon)}^{-1}$ and capacitance as $84.5 \text{ (g-carbon)}^{-1}$. The results show that aqueous phase pre-doping can be conducted for our hybrid supercapacitor, thus allowing elimination of using Li metal during the fabrication process.

- 1) S. Makino, Y. Shinohara, T. Ban, W. Shimizu, K. Takahashi, N. Imanishi, and W. Sugimoto, *RSC Adv.*, **2**, 12144 (2012).
- 2) S. Makino, R. Yamamoto, S. Sugimoto, and W. Sugimoto, *J. Power Sources*, **326**, 711 (2016).
- 3) M. Yamagata, K. Soeda, S. Yamazaki, and M. Ishikawa, *Electrochem. Solid-State Lett.*, **14**, A165 (2011).

The multiple roles of an organic corrosion inhibitor on copper investigated by a combination of electrochemistry-coupled optical in situ spectroscopies

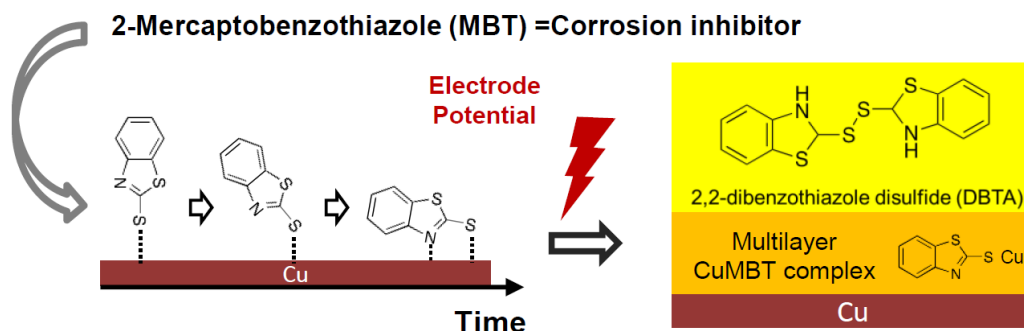
Ying-Hsuan Chen¹, Andreas Erbe^{1,2}

¹Department of Interface Chemistry and Surface Engineering, Max-Planck-Institut für Eisenforschung GmbH, Max-Planck-Straße 1, 40237 Düsseldorf, Germany

²Department of Materials Science and Engineering, NTNU, Norwegian University of Science and Technology, 7491 Trondheim, Norway
y.h.chen@mpie.de

2-Mercaptobenzothiazole (MBT) is known as one of the most effective organic corrosion inhibitors of copper for 40 years. During the inhibition process, MBT is supposed to react with copper forming a passivating layer (CuMBT complex) to prevent further corrosion [1]. The complex electrochemical and chemical processes between copper, electrolyte, copper oxides, and the inhibitor films are not fully understood, in particular, how the passivating layer forms and why it is so protective.

In this work, the interaction of MBT with copper in alkaline solution was investigated by in situ infrared (IR) and Raman spectroscopy, and in situ spectroscopic ellipsometry, coupled to cyclic voltammetry (CV). The attenuated total reflection (ATR) technique was applied in IR spectroscopy to study MBT during electrochemical processes at the solid/liquid interface [2]. At negative potentials, MBT monolayers relax on a minute time scale through MBT reorientation, leading to MBT-copper binding via S and N-atoms. After copper dissolution becomes thermodynamically feasible, including at open circuit, formation of a multilayer CuMBT complex sets in, in which thiol dominates over thione. As electrode potential increased, it was shown that multilayer films effectively inhibited oxide formation according to the disappearance of oxide related peak in Raman spectra. At positive potentials, MBT oxidatively dimerises to 2,2'-dibenzothiazole disulfide (DBTA), which remains protective [3].



References:

- [1] M. Finšgar, J. Jackson, *Corros. Sci.* 86 (2014) 17–41.
- [2] S. Nayak, P.U. Biedermann, M. Stratmann, A. Erbe, *Phys. Chem. Chem. Phys.* 15 (2013) 5771–5781.
- [3] Y.-H. Chen, A. Erbe, *Corros. Sci.*, submitted.

Facile Electrochemical Synthesis of Electrocatalysts for Fuel Cell and Electroless Plating

Jing Zhan¹, Desmond C. L. Tan¹, Kee Chun Poon¹, Thang D. T. Vo¹, Haibin Su², Hiroataka Sato¹
¹*School of Mechanical & Aerospace Engineering*, ²*School of Material Science & Engineering*
Nanyang Technological University, Singapore
hirosato@ntu.edu.sg

There are lots of electrocatalysts developed to date especially for the fuel cell reactions including oxygen reduction, oxidation of hydrogen and alcohols. However, most of the developed catalysts need harsh conditions such as very high temperature, vacuum environment and long synthesis reaction, which put the catalysts away from the practical use, and still conventional platinum loaded carbon (Pt/C) is the most or only practically used catalysts for fuel cell.

Our group has developed a remarkably facile electrocatalyst synthesis method, refereed as to 'step-wise electroless deposition' which uses only two separate solutions: metal ion solution and reduction agent solution. A substrate is alternatively dipped into these solutions for seconds, and metal ion adsorbed on the substrate surface is reduced to the metal by the electrons discharged from the oxidation of reduction agent. Consequently after repeating the sequential dipping, metal nanoparticles are formed over the substrate surface. Total operation time is up to 10 min and no harsh condition is required the deposition process is operated at ambient temperature and under atmosphere. By introducing mixture of different metal ion solutions, we can synthesize even alloy electrocatalysts.

Interestingly, by using hypophosphite or dimethylaminoborane (DMAB) as reduction agent, phosphorus (P) or boron (B) can be doped into deposited metal nanoparticle, which could change the microstructure or binding energy and lead to change in catalytic activity. For example, we synthesized P doped palladium (Pd) nanoparticle by the stepwise electroless deposition and found they had amorphous state in microstructure and exhibited very high catalytic activity for oxygen reduction and oxidation of formic acid.^{1,2} On the other hand, we computationally modeled B doped Pd and found it is highly active for enhancing oxygen reduction reaction due to negative shift of surface core level of Pd.³ The stepwise electroless deposition allows to fabricate the modeled B-doped Pd catalyst and we have also experimentally confirmed the high catalytic activity.

We built up a machine to automate the stepwise electroless deposition toward combinatorial chemistry like electrocatalyst synthesis and evaluation. The machine will allow us to systematically and efficiently survey varieties of electrocatalysts with different compositions and sizes for various electrochemical reactions.

For electroless plating based process to metalize non-conductive substrate, we need to form densely packed metal (usually Pd, a few $\mu\text{g}/\text{cm}^2$) nanoparticle catalyst over the substrate surface conventionally. We introduced graphene oxide into the catalyzation process to form reduced graphene oxide layer over the surface to make it relatively conductive. We then successfully reduced the catalyst loading down to a few $10^{-2} \mu\text{g}/\text{cm}^2$.⁴

1. K. C. Poon *et al.*, *Journal of the American Chemical Society*, 136(14), 5217 (2014).
2. K. C. Poon *et al.*, *Chemical Communications*, 52, 3556-3559 (2016).
3. T. T. V. Doan, *et al.* *Angewandte Chemie International Edition*, 55, 6842-6847 (2016).
4. J. Zhan *et al.*, *Chemical Communications*, 53(66), 9198-201 (2017).

High-Density Ge₂Sb₂Te₅ Phase Change Memory by Electrodeposition

R. Huang¹, G. P. Kissling², R. Kashtiban³, P. N. Bartlett², C. H. de Groot¹, R. Beanland³

¹ ECS, University of Southampton, SO17 1BJ, UK

² School of Chemistry, University of Southampton, SO17 1BJ, UK

³ Physics Department, University of Warwick, Coventry CV4 7AL, UK
 chdg@soton.ac.uk, R.Beanland@warwick.ac.uk

Non aqueous electrodeposition of Ge₂Sb₂Te₅ phase change memory provides a scalable method for the filling of confined cells of high aspect ratio nanostructures. In previous proof-of-concept measurements, we demonstrated the ability of electrodeposition to successfully create nanoscale sized phase change memory devices with the deposition of GST on TiN electrodes being the key process step. An electrolyte system based on compatible tetrabutylammonium chlorometallate sources in non-aqueous solvents is used [1]. Here we present a new two dimensional, architecture for future non-volatile high-density memory applications suitable for electrodeposition. As core structures, passive crossbar arrays were fabricated by combining lithography, followed by e-beam lithography for the confined cells and electrodeposition processes, offering immense scaling potential and high aspect ratio nanostructures filling. The crossbar arrays of Fig 1 consist of two terminal devices, with as a minimum an electrode/GST/electrode structure. Inclusion of a selector diode by electrodeposition at the cross points is envisaged. The word lines that provide contact to each individual cell cause an ohmic voltage drop. Critically though, the total electrodeposition current (charge) scales with the feature size in the same proportion as the resistance of the lines. The total IR drop is hence independent of the feature size and allows further scaling to sub 10nm device sizes. The word lines are all connected together during the electrodeposition process allowing a single common applied voltage but are separated during the dicing process Fig. 2. Transmission Electron Microscopy (TEM) of the individual cells will be discussed.

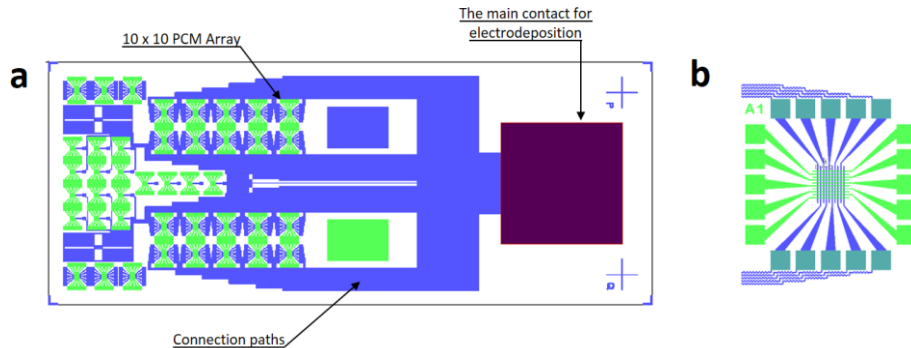


Figure 1. Design with different memory cells and electrodeposition contacts with a zoom on a 10x10 array

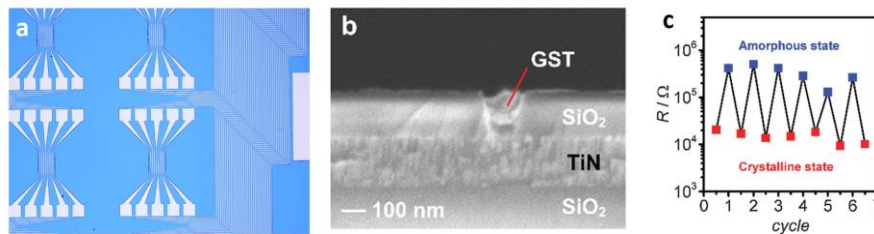


Figure 2. (a) Optical micrographs after depositing the bottom electrode and (b) SEM Cross sectional images of electrodeposited GST in 100 nm and (c) Repeated resistance measurements of a 100 nm GST memory cell [1].

[1] P. N. Bartlett, et. al., Mater. Horiz., (2015), 2, 420-426

This work was funded by EPSRC Programme Grant EP/N035437/1 Advanced Devices by ElectroPlating (ADEPT) and EPSRC (EP/I010890/1)

Preparation of Ordered Porous Alumina Spheres by Anodization of Small Al Particles

Takashi Yanagishita, Masahiko Imaizumi, Toshiaki Kondo, and Hideki Masuda
Tokyo Metropolitan University
1-1 Minamiosawa, Hachioji, Tokyo, Japan
yanagish@tmu.ac.jp

Nanoporous particles have been growing interest for their various applications. There have been a large number of methods for the preparation of nanoporous particles so far. However, in most cases, it is difficult to prepare the nanoporous particles with controlled geometrical structures. In our previous reports, we described a process for the preparation of nanoporous spheres based on the anodization of metal small spheres [1, 2]. The nanoporous spheres could be obtained by anodization of close-packed metal particles in an acidic solution. Nanoporous hollow spheres could be also formed by the selective dissolution of residual metals. The small hollow spheres obtained by this process have a unique geometrical structure composed of a porous oxide layer with an inner hollow cavity. One important advantage of this process is that it enables control of the dimensions of the porous structures by simply adjusting anodizing conditions. In the present report, we describe the preparation of nanohole spheres with ordered hole arrangement by two-step anodization of Al small particles. Two-step anodization process can generate highly ordered anodic porous alumina from the surface on the surface of Al substrate [3]. Obtained ordered porous alumina spheres are expected to be useful for various applications.

In the present study, we used Al small particles as starting materials. Al particles were anodized in 0.3M oxalic acid under a constant voltage of 40 V. After the selective removal of oxide layer formed by first anodization, a second anodization was carried out under the same anodizing conditions. During the second anodization step, the ordered porous alumina layer was formed on the surface of small Al particles

Figure 1 shows the SEM images of ordered anodic porous alumina spheres. From SEM images shown in Fig. 1, ordered anodic porous alumina was observed on the surface of Al particles. The hole interval was 100 nm. The hole size and depth could be controlled by adjusting the preparation conditions. Ordered porous alumina hollow spheres were also obtained by selective removal of residual Al using an etching. The ordered anodic porous spheres obtained by the present process are expected to be used in various application fields requiring controlled geometrical structures with a large surface area.

References

- [1] T. Yanagishita, K. Nishio, and H. Masuda, *Appl. Phys. Express*, **1**, 084001 (2008).
- [2] T. Yanagishita, M. Imaizumi, T. Kondo, and H. Masuda, *RSC Adv.*, **5**, 41830 (2015).
- [3] H. Masuda and M. Satoh, *Jpn. J. Appl. Phys.*, **35**, L126 (1996).

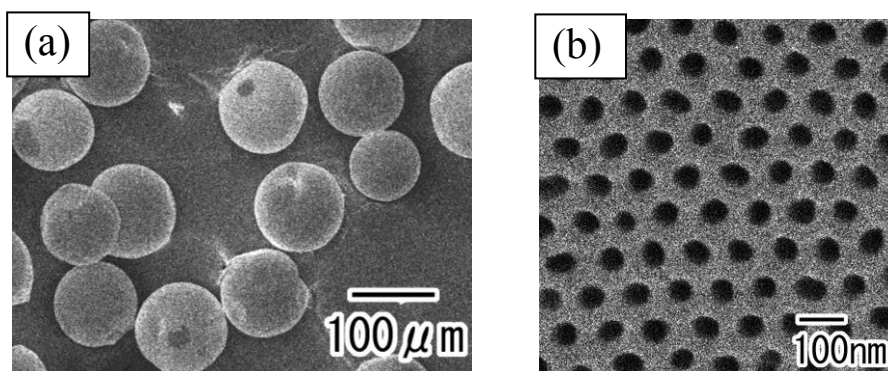


Figure 1. SEM images of ordered anodic porous alumina spheres: (a) low-magnification and (b) high-magnification images.

Electrochemical Deposition Mechanism of Si-O-C Composite Anode from Propylene Carbonate Based Bath

Tokihiko Yokoshima¹, Taku Owada², Hiroki Nara¹, Toshiyuki Momma^{1,2,3}, Tetsuya Osaka^{1,2,3}

¹ Research organization of Nano and Life Innovation, Waseda University

² Graduate School of Advanced Science and Engineering, Waseda University

³ Kagami Memorial Res. Inst. For Materials Sci. and Tech., Waseda University

Shinjuku-ku, Tokyo, 169-8555, Japan

e:-mail address: momma@waseda.jp

Si-based materials are one of the most promising anode materials for lithium secondary batteries because of high theoretical capacity. Despite that, pure Si anodes rapidly degradate due to significant volume change during charge-discharge cycles. We have proposed Si-O-C composite anode, which is composed of Si, O and C, synthesized by non-aqueous electrodeposition technique as a long life Si anode¹. It has been supposed that Si-O-C composite is consisted of inorganic (SiO_x) and organic (solvent decomposition) phase. Properties of the electrodeposited inorganic-organic composite were effected by its formation stages², so analysis of deposition process is very important to realize high performance anode materials of the inorganic-organic composite. Herein this work was focused on detailed investigation about the formation stages of the Si-O-C composite and relationship between these stages and properties.

0.5 M TBAClO₄ and 0.5 M SiCl₄ were dissolved in propylene carbonate (PC) for electrolyte. Before the electrodeposition, Cu substrate was degreased and acid rinsed in air and degreased in inert atmosphere. Electrodeposition was proceeded galvanostatically with -1.0 mA cm⁻². Scanning electron microscopy with energy dispersive X-ray spectroscopy (SEM-EDX) and X-ray photoelectron spectroscopy (XPS) were used to characterize deposit. Charge-discharge cycle test for deposit was carried out by preparing half-cell.

Figure 1 shows the potential profile of the electrodeposition of Si-O-C composite. In Figure 1, three plateaus at 2.2 V, 1.5 V, 1.2 V vs. Li/Li⁺ were observed, existing three electrodeposition stages of Si-O-C composite including two initial stages. From XPS analysis, products at 2.2 V, 1.5 V and 1.2 V plateaus were compounds of Si-O, Si-O and Si-O-C, respectively. From voltammetric analysis, PC and SiCl₄ were electrochemically reduced at potentials less than 1.5 V and 1.2 V vs. Li/Li⁺, respectively, therefore it is thought that Si-O-C composite was formed from the reductant of both PC and SiCl₄. On the other hand, products at 2.2 V and 1.5 V were derived from chemical decomposition of SiCl₄, because potentials were higher than SiCl₄ reduction potential. The various investigation of the deposition condition implied that the initial stage of deposits affect the cycle performance of the deposits, which would be caused by the difficulty of peeling off from the substrate. So it was thought that different interfacial microstructure caused by different initial stages of formation effected the adhesion strength.

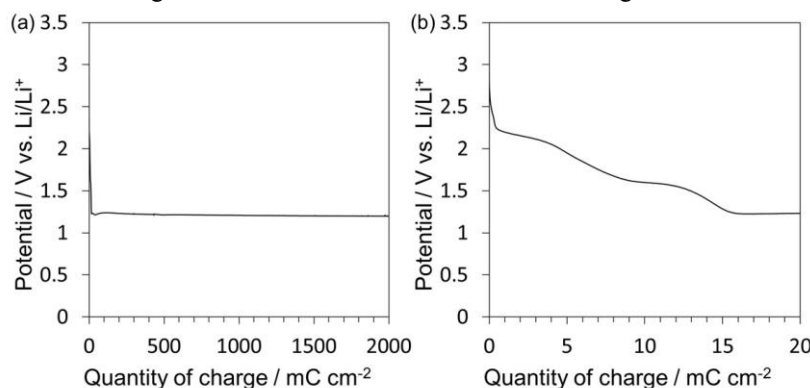


Figure 1. (a)Entire, (b)initial potential profile during galvanostatic electrodeposition of Si-O-C composite

1. Momma, T., Aoki, S., Nara, H., Yokoshima, T., Osaka, T. *Electrochem. commun.* **2011**, 13, 969–972.

2. Jeong, M., Yokoshima, T., Nara, H., Momma, T., Osaka, T. *J. Electrochem. Soc.* **2014**, 161, 3025–3031.

Acknowledgements.

This work is partly supported by Advanced Low Carbon Technology Research and Development Program Special Priority Research Area “Next-generation Rechargeable Battery” (ALCA-Spring) from the Japan Science and Technology Agency (JST), Japan.

Electroreflectance Study of Thin-film Graphite | Ionic Liquid Interface: Electro-optics of Electrical Double-Layer and Dielectric Capacitors

Ove Oll and Enn Lust

Institute of Chemistry, University of Tartu

Ravila 14a, Tartu, 50411 Estonia

ove.oll@ut.ee

Detailed understanding of the interface between graphitic carbon materials and concentrated electrolytes is of great importance for the rational design of novel high energy and power density supercapacitors and graphene based dielectric capacitors[1,2]. It is of interest to describe how the limitation of electronic surface states of semimetal electrodes influences the dielectric part of the electrical double-layer (edl) via the modulation of optical properties dependent on applied voltage.

A novel technique of *in situ* infrared absorption (IRA) spectroscopy for the study of thin film graphite electrodes has been developed[3] and is applied for the study of the graphite | 1-ethyl-3-methylimidazolium tetrafluoroborate (EMImBF₄) ionic liquid interface as a model supercapacitor and graphite | polydicyanamide (PDCA) interface as a dielectric capacitor. The surface specificity of the technique, as well as the plasmonic enhancement properties of the electrode are demonstrated. The IRA results show that, unlike previous theoretical considerations of the edl between semimetals and electrolytes, the strong interaction between the electronic and ionic part of the edl is of fundamental importance for the description of semimetal interfaces[4]. Together with the data provided by *in situ* electroreflectance [3] technique of the electronic and energetic structure of the graphite electrode and differential capacitance-potential dependence of the graphite|EMImBF₄ system, it is demonstrated that the screening of excess surface charge by the ionic liquid is strongly correlated with the potential dependent electronic properties of the electrode surface states. While the increase of the energy of surface electronic states is linear with respect to applied bias in case of the graphite | EMImBF₄ system, it is shown that for the graphite | PDCA dielectric capacitor the increase of relative surface state absorption peaks is independent on the passivation potential (dielectric film thickness) applied. Instead, for thicker layers of PDCA both initial (nonpolarized) and polarized (fully charged) state electronic absorption bands shift toward higher energy, while the difference between the two states is constant. This helps to explain the fundamental differences between the two electrochemical energy storage devices, but also to design novel, high power and energy density capacitors[5].

Acknowledgements

This work was supported by the Estonian Ministry of Education and Research (projects no. IUT 20-13, PUT55, PUT1033 and PUT1107), and European Regional Development Fund (Estonian Centre of Excellence “Advanced materials and high-technology devices for energy recuperation systems”, TK141).

References

- [1] T. Romann, O. Oll, P. Pikma, K. Kirsimäe, E. Lust, 4–10 V capacitors with graphene-based electrodes and ionic liquid electrolyte, *J. Power Sources*. 280 (2015) 606–611.
- [2] T. Romann, O. Oll, P. Pikma, H. Tamme, E. Lust, Surface chemistry of carbon electrodes in 1-ethyl-3-methylimidazolium tetrafluoroborate ionic liquid—an *in situ* infrared study, *Electrochimica Acta*. 125 (2014) 183–190.
- [3] O. Oll, T. Romann, E. Lust, An infrared study of the few-layer graphene | ionic liquid interface: Reintroduction of *in situ* electroreflectance spectroscopy, *Electrochem. Commun.* 46 (2014) 22–25.
- [4] O. Oll, T. Romann, C. Siimenson, E. Lust, Influence of chemical composition of electrode material on the differential capacitance characteristics of the ionic liquid|electrode interface, *Electrochem. Commun.* 82 (2017) 39–42.
- [5] T. Romann, E. Lust, O. Oll, Method of Forming a Dielectric Through Electrodeposition on an Electrode for a Capacitor, WO/2016/050761, 2016.

Reducing CO₂ Emissions from Aluminium Electrolysis Cells by Supplying Porous Anodes with Methane

Geir Martin Haarberg¹, Babak Khalaghi¹, Ole Kjos² and Tommy Mokkelbost²

¹Department of Materials Science and Engineering, Norwegian University of Science and Technology, N-7491 Trondheim, Norway

²SINTEF Materials and Chemistry, N-7465 Trondheim, Norway

geir.martin.haarberg@ntnu.no

One of the main drawbacks of the current aluminium production process is the excessive amount of CO₂ emissions from the electrolysis cells. There have been numerous studies to tackle this problem; mainly based on the idea of developing an inert oxygen evolving anode. However, no inert anode material has been developed for industrial operation so far [1]. A new concept has been suggested where anodes are supplied with methane and the anodic reaction is changed [2, 3]. As a result, electrochemical oxidation of methane takes place at the anode instead of or in parallel to the consumption of carbon anodes. This leads to significant reduction in the CO₂ emissions from the electrolysis cell.

Based on this new idea, laboratory experiments were carried out and different porous graphites were tested as anode material for such an application. Flow properties of the anodes, such as air-permeability and pore size distribution, were measured to determine the optimum condition for the establishment of the three-phase boundary between methane, the electrolyte and the anode which in turn, determines the effectiveness of electrochemical oxidation of methane. Besides, galvanostatic electrolysis experiments were carried out and the variations of cell voltage, carbon consumption and level of HF above the electrolyte were measured during electrolysis. Of all the graphite materials tested, the sample with a porosity of 12% and pore size mainly in the range of 1-10 μm showed the best performance and up to 35% reduction in the anode consumption was achieved. It showed that methane effectively participated in the anode process. The effects of key parameters are discussed.

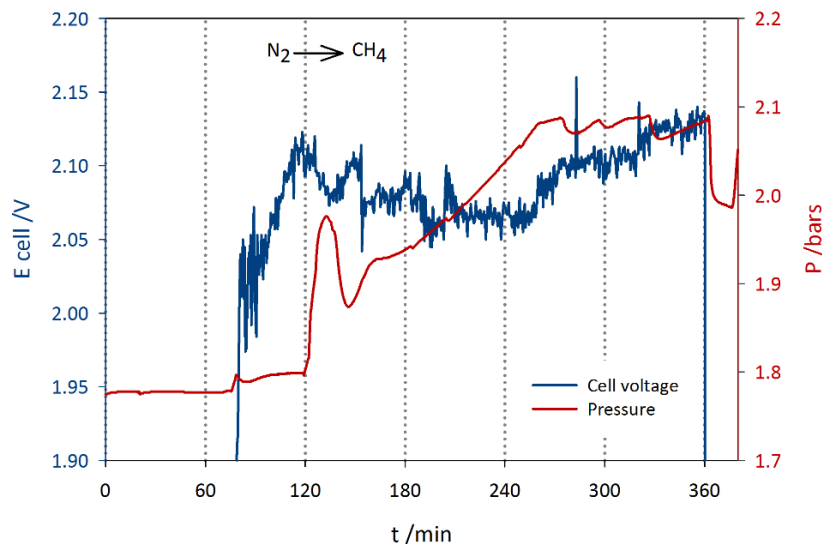


Figure 1. Cell voltage variations and pressure changes during galvanostatic electrolysis. The anode gas was changed from nitrogen to methane at $t = 120$ min.

[1] R.P. Pawlek, *Light Metals* 2014, 1309-1313.

[2] S. Xiao, T. Mokkelbost, O. Paulsen, A.P. Ratvik, G.M. Haarberg, *Metallurgical and Materials Transactions B: Process Metallurgy and Materials Processing Science* 44(5) (2013) 1311-1316.

[3] G.M. Haarberg, B. Khalaghi, T. Mokkelbost, *Faraday Discussions* 190 (2016) 71-84.

Electrodeposition of porous silica templates inside lithographically defined substrates for nanofabricated devices

Andrew W. Lodge, Samantha Soulé, Andrew .L. Hector, Ruomeng Hang, Kees de Groot, Reza J. Kashtiban and Richard Beanland

Chemistry, University of Southampton, SO17 1BJ, United Kingdom

Electronics and Computer Science, University of Southampton, SO17 1BJ, United Kingdom

Department of Physics, University of Warwick, Coventry, CV4 7AL, United Kingdom

a.w.lodge@soton.ac.uk

There has been much recent interest in applications of nanowires in electronic devices. In the EPSRC-funded Advanced Devices by Electroplating project (EP/N035437/1) we are working on the electrodeposition of functional materials such as thermoelectrics,¹ infrared detectors² and phase change memory.³ In some cases, appropriate templates for nanowire deposition can be directly fabricated using lithographic methods. For feature sizes below 10 nm or with longer aspect ratios than are available lithographically, vertically aligned hexagonal mesoporous silica is an appealing prospect.

Aligned mesoporous silica has been electrodeposited onto surfaces such as TiN or ITO using the electrochemically assisted surfactant assembly method.⁴ This method combines ordering of surfactant assemblies under the effect of an electric field with localised silica electrodeposition. In this work we take it a step further and electrodeposit aligned silica into features that have been e-beam patterned into silica films on conductive substrates. The effects of feature size and geometry on the formation of the hexagonal micelles and alignment of the pores have been investigated. The diameter of the pores formed can be fine-tuned by changing the surfactant concentration or adding swelling agents.

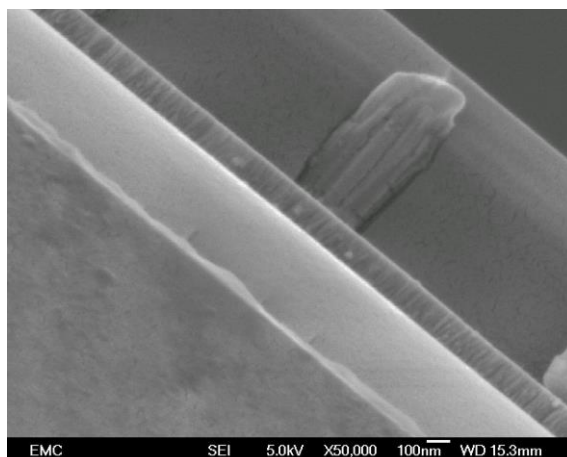


Figure 1: silica electrodeposited inside a pore of an e-beam lithographed substrate.

This work was funded by EPSRC Programme Grant EP/N035437/1, Advanced Devices by ElectroPlaTing (ADEPT). The work was carried out by an interdisciplinary team of researchers based at the Universities of Southampton, Nottingham and Warwick, UK.

References

- 1 L. Trahey, C. R. Becker and A. M. Stacy, *Nano Lett.*, 2007, **7**, 2535–2539.
- 2 K. M. Chahrouh, N. M. Ahmed, M. R. Hashim, N. G. Elfadill and M. Bououdina, *Sensors Actuators, A Phys.*, 2016, **239**, 209–219.
- 3 W. Lu and C. M. Lieber, *Nat. Mater.*, 2007, **6**, 841.
- 4 A. Goux, M. Etienne, E. Aubert, C. Lecomte, J. Ghanbaja and A. Walcarius, *Chem. Mater.*, 2009, **21**, 731–741.

Dynamic properties on NMR spectroscopy for LiClO₄/PC-DME solution coexisting with fumed silica filler

Minoru Mizuhata, Marie Takemoto, Hideshi Maki, Masaki Matsui

Department of Chemical Science and Engineering, Graduate School of Engineering, Kobe University
1-1 Rokkodai-cho, Nada, Kobe 657-8501 Japan
mizuhata@kobe-u.ac.jp

For various electrochemical devices in practical use, porous solid materials are widely fabricated for holding electrolyte solutions. It is reported that electrolyte solutions related to ion-solvent interaction indicate different properties by coexistence of solid phase[1], and an elucidation of liquid phase properties of solid-liquid interface in the non-aqueous electrolyte solution system is important for improving the performance of energy storage devices such as lithium ion batteries(LIBs). In addition, in late years the study of new electrolyte materials used highly-concentrated electrolytes attracts attention. In this study, we used non-aqueous binary electrolyte mixed with fumed silica as model system of filler materials for LIBs, and investigated a selective interaction with solvent molecules, dependence on Li⁺ ion concentration and DME mixture ratio, due to the influence of solid-liquid interface in NMR spectroscopy.

Samples were prepared LiClO₄ -propylene carbonate(PC)-1,2-dimethoxyethane (DME) solution in Ar glove box in the concentration range below 1 M and fumed silica(FS) (200 ± 50 m² g⁻¹) in NMR tube. A content of liquid phase were ranged from 90-100 vol% by gravimetry. We measured ¹H and ⁷Li NMR spectroscopy (Varian INOVA 400; 9.39T) , spin-lattice relaxation time; T₁ measurements, and spin-spin relaxation time ;T₂ measurements (XiGo Nanotools Acorn area ; 0.3T).

The result of ¹H NMR spectroscopy measurement of 1 mol/L PC-DME/FS (DME=45 mol%) samples indicated in Fig. 1. (The minute peak around 4.6 ppm was derived from ¹H of H₂O contained in D₂O in the outer tube.) Sharp peaks were observed in both PC and DME in the case only for liquid phase. In both PC and DME signals, broad signals were confirmed under the existence solid-phase. It was shown that the dynamic property of solvent molecules largely decreased in comparison with the case only for liquid phases. The liquid content dependences of ¹H NMR detection ratios of 1 mol/L PC-DME/FS (DME=45 mol%) were shown in Fig. 2. The ¹H NMR detection ratios are determined by the ratio of the overall signal intensity due to PC-DME for the sample without solid-phase and that for the sample with solid phase. Peak intensity is the sum of total of each proton of solvent molecules. The solid line represented the theoretical value of detected amount of PC and DME by ¹H NMR.

The detected amount of PC and DME molecules decreased compared to solid line. It indicates that solvent molecules have low mobility due to being restricted by solids. The integrated intensity value of ¹H in DME is much smaller than the total integrated intensity value of PC and DME. It suggests that the mobility of DME molecules were restricted than that of PC molecules in PC-DME/FS system. We will also discussed the relaxation phenomena in this system.

This study was supported by the JST Core Research for Evolutional Science and Technology (CREST).

【Reference】

- [1] M. Mizuhata et al., *J. Mol. Liq.*, **83**, 179, (1999).
- [2] Wu Li, J. R. Dahn, D. S. Wainwright, *Science*, **264**, 1115, (1994).

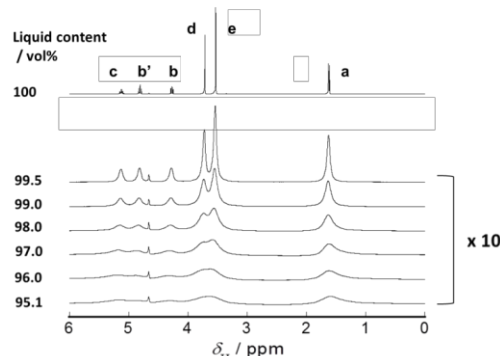


Fig. 1 Liquid content dependence of the ¹H NMR spectra for FS + 1 mol/L LiClO₄/PC-DME (DME=45 mol%) systems.

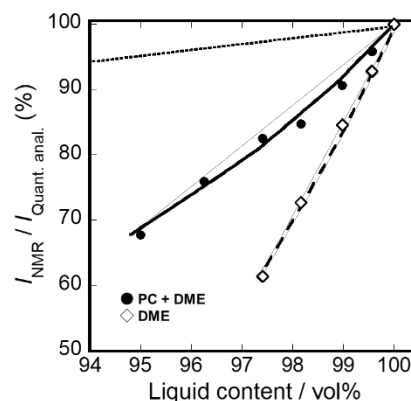


Fig. 2 Liquid content dependence of the ¹H NMR detection ratios for FS + 1 mol/L LiClO₄/PC-DME (DME=45 mol%) systems.

Laboratory zero-gap alkaline water electrolyzer stack: Development, optimization and mathematical modeling

Jaromír Hnát, Jakub Rutrle, Roman Kodým, Karel Bouzek
University of Chemistry and Technology Prague
Technická 5, 166 28, Prague 6-Dejvice, Prague, Czech Republic
hnatj@vscht.cz

Water electrolysis represents the most widely used method of water splitting under hydrogen and oxygen evolution. It separates the overall reaction into two half-cell reactions in which hydrogen and oxygen are released from molecule of water by individual electrode reactions. Such separation is necessary in order to reach high product purity and process efficiency, as well as to operate the process safely. Three different technologies of water electrolysis for hydrogen production are generally considered. These are (i) alkaline, (ii) proton exchange membrane (PEM) and (iii) high temperature water electrolysis. Main advantage of the PEM system represents high process intensity and flexibility. Besides acidic character of the process connected with high mobility of protons in the water environment represents one of the main reasons of its superior performance zero-gap construction of the PEM electrolysis cells. This is related to the availability of the perfluorinated sulfonated (PFSA) materials to be used as a polymer electrolyte and electrode compartment separator in one. Alkaline water electrolysis represents industrially established technology which, on the other hand, was not subject of significant development for several decades. The most desired step in future development of this technology represents replacement of diaphragm type separator of electrode compartments by anion selective polymer electrolyte membrane. Such a setup allows utilizing of the zero-gap construction also in the case of alkaline water electrolysis. As one of the consequences KOH electrolyte concentration can be reduced, which increases safety and flexibility of the process. At the same time, due to the reduced conductivity of the liquid electrolyte, importance of the parasitic currents is in contrast to the traditional stack arrangement reduced.

This contribution reports on development of an alkaline water electrolyzer stack operating with homogeneous anion selective polymer membranes based on the block copolymer of styrene-ethylene-butylene-styrene (PSEBS) functionalized by 1,4-diazabicyclo[2.2.2]octane (DABCO) functional groups. Ni foam was used for the electrodes construction, both blank and as the support of the catalytic layer based on non-platinum metals.

Both, experimental studies and mathematical modelling were used to optimize distribution channels and flow plate design with respect to homogeneity of flow distribution, effective gas phase removal and elimination of the parasitic currents. Performance of the optimized stack was evaluated in terms of voltage/current efficiency and produced gases purity. Results show that the application of the homogenous anion selective membrane represents promising way how to increase the intensity of the alkaline water electrolysis under milder conditions when compare to the industrial operational conditions.

Acknowledgement

Financial support of this research by the Ministry of the Industry and Trade of the Czech Republic under the project No. FV10529 is gratefully acknowledged.

Novel Oxygen- and Chloride-free Magnesium Salt for Magnesium Rechargeable Batteries

Toshihiko Mandai, Mizuki Hatta, and Tatsuya Takeguchi

Department of Chemistry and Biological Sciences, Faculty of Science and Engineering, Iwate University
4-3-5 Ueda, Morioka, 020-8551 Japan
mandai@iwate-u.ac.jp

Magnesium rechargeable batteries (MRBs) are an emerging class of energy storage systems as alternative to Li batteries owing to the fascinating properties of magnesium metal anode, such as large volumetric capacity (3833 mAh cm^{-3}), comparatively low electrode potential (-2.37 V vs. SHE), and large natural abundance. Inherent chemical stability of magnesium metal even upon exposure to air combined with remarkable cycling stability is indeed attractive for mass production of highly safe rechargeable batteries. One of the most critical barriers for materialization of MRBs is a lack of suitable electrolyte materials compatible with both magnesium metal anode and applicable cathode. The ethereal solutions of magnesium chloride complexed with strong Lewis acid or other reagents, such as AlCl_3 ,^{1,2} CrCl_3 ,³ and $\text{Mg}(\text{TFSA})_2$,^{4,5} often serve as potential electrolytes for MRBs because they support reversible magnesium plating/stripping with extremely low overpotential. In such electrolytes, chloride effectively breaks the passivation film on the magnesium surface. The presence of chloride however causes poor anodic stability and severe corrosion of various battery substrates,^{6,7} making these electrolytes unapplicable to practical batteries. The active electrolytes without chloride are strongly required.

Sluggish electrochemical reactivity of magnesium metal anode in typical electrolyte solutions mainly caused by the surface passivation film. Such insulating film leads to extremely large overpotential in magnesium plating/stripping process. The main components of this surface film is magnesium oxide, and the source of oxygen is considered to be come from anions. Here we propose the novel magnesium salt, magnesium 4,5-dicyano-2-trifluoromethylimidazolate ($\text{Mg}(\text{TDI})_2$), as an oxygen- and chloride-free ingredient which potentially unable to form oxide-based passivation film on the magnesium surface, owing to the absence of oxygen in the molecular structure. The magnesium salt with the TDI anion was successfully synthesized for the first time according to the literature for the synthesis of LiTDI .⁸ X-ray crystallography on the synthesized salts revealed the formation of a hexa-coordinated complex salt $[\text{Mg}(\text{TDI})_2(\text{AN})_2(\text{H}_2\text{O})_2]$ (**1**) for the magnesium-based system while a tetra-coordinated dimer $[\text{Li}_2(\text{TDI})_2(\text{AN})_2]$ (**2**) was found for the lithium-based counterpart (Figure 1).⁹ The electrolyte solution, where **1** was dissolved in dimethoxyethane, followed by removal of coordinated solvents, showed somewhat reversible electrochemistry of magnesium plating/stripping on Pt electrode with very small overpotential for the stripping process. This result suggests that the plated magnesium is not passivated in our electrolyte solution, thus the oxygen-free TDI anion is likely compatible with magnesium metal anode. The detailed electrochemical properties will be presented.

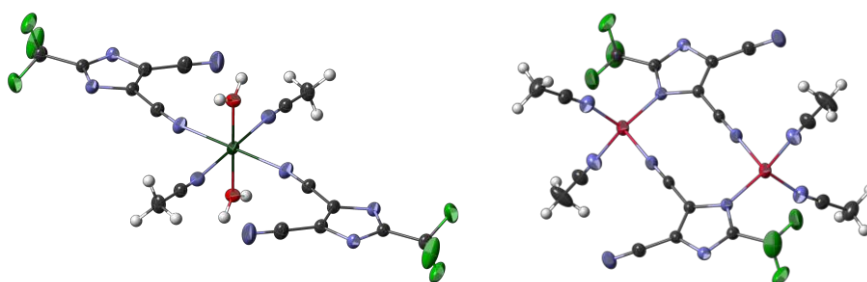


Figure 1. Thermal ellipsoid models of (left) Mg- and (right) Li-based TDI complexes. Thermal ellipsoids are drawn at 50% probability level. Gray, C; white, H; dark green, Mg; pink, Li; red, O; blue, N; light green, F.

References

- 1) D. Aurbach et al., *J. Electrochem. Soc.*, 2002, **149**, A115; 2) R. E. Doe et al., *Chem. Commun.* 2014, **50**, 243; 3) J. H. Ha et al., *J. Mater. Chem. A*, 2016, **4**, 7160; 4) I. Shterenberg et al., *J. Electrochem. Soc.*, 2015, **162**, A7118; 5) T. Mandai et al., *J. Mater. Chem. A*, 2017, **5**, 3152; 6) S. Yagi et al., *J. Electrochem. Soc.*, 2013, **160**, C83; 7) J. Muldoon et al., *Energy Environ. Sci.*, 2013, **6**, 482; 8) L. Niedzicki et al., *Electrochim. Acta*, 2010, **55**, 1450; 9) T. Mandai et al., *in manuscript*.

Acknowledgement: Authors gratefully thank to ALCA-SPRING (JST) for their financial support.

CO₂ Photoelectroreduction at TiO₂ Nanotubes Electrodes Decorated with Nanoparticle/Nanocubes Silver

João A. L. Perini, Livia M. Christovam, Lilian D. M. Torquato, Maria Del Pilar T. Sotomayor, Sidney J.

L. Ribeiro, Maria V. Boldrin Zanoni*

Institute of Chemistry, São Paulo State University (UNESP), Araraquara, São Paulo, Brazil

Rua Prof. Francisco Degni, 55, 14800-060

*boldrinv@iq.unesp.br

The conversion of CO₂ to higher value-added compounds (methanol, ethanol, formic acid, methane, and others) is a subject of great importance nowadays due to problems generated by the increase of the emission of carbon dioxide in the atmosphere. The present work aims preparing, characterizing and testing semiconductor nanotubes Ti/TiO₂ (NT) electrodes modified by coating of silver nanoparticles (NP) and its performance in the photoelectrocatalytic reduction of CO₂. Considering that the photoelectrocatalytic reduction of CO₂ on the Ti/TiO₂ surface is very small due to the lack of visible-light response and high recombination of electron-hole pair leading to low quantum efficiency of the process, the use of silver NP as cocatalyst at the NT Ti/TiO₂ surface could enhance the CO₂ photoconversion [1] due its capture of electron properties. Silver was deposited on the surface of Ti/TiO₂NT by two different methods: (1) Electrodeposition of Ag onto the Ti/TiO₂NT by electrochemical reduction at -0.70 V vs Ag/AgCl during 15 s in an electrochemical cell containing AgNO₃ 0.01 M in NaNO₃ 0.1 mol L⁻¹ and (2) Impregnation of Ag nanocubes (NC) on Ti/TiO₂NT by using dopamine (13 mM) as mediator in a tris-buffer (10 mmol L⁻¹ pH 8.6) during 8 h [2]. The photoelectrocatalytic reduction was carried out by using 170 mL of 0.1 M mol L⁻¹ Na₂SO₄, at 1 atm pressure saturated with CO₂ for 1 h, using Ti/TiO₂NT-Ag as photocathode, irradiated with UV/Vis light for 60 min at potential -0.6 V. An electrode of dimensionally stable anode (DSA) was used as a counter electrode and an Ag|AgCl (KCl 3 M) as reference electrode. Methanol generation was monitored by GC-FID after extraction using a solid-phase microextraction fiber. The formation of methanol under Ti/TiO₂NT electrode was irrelevant for one hour of reaction, achieving only 0.045 mM. On the other hand, with the addition of silver NC or NP on the surface of Ti/TiO₂NT, the formation of methanol was enhanced 8.1 and 7.1 times, respectively (**Figure 1**). Therefore, it is concluded that modification of TiO₂NT with silver nanoparticles/nanocubes, is efficient for the generation of methanol, since this metal acts as cocatalysts of TiO₂ semiconductor.

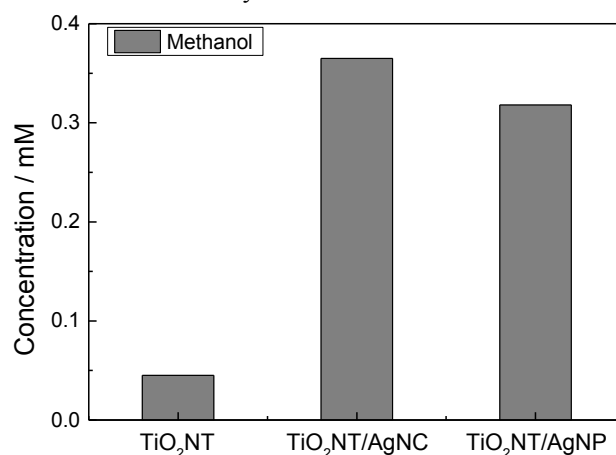


Figure 1. Evaluation of products formed after 60 min of photoelectrocatalytic CO₂ reduction in 0.1 M Na₂SO₄, at 1 atm pressure, potential -0.6 V at: Ti/TiO₂NT, Ti/TiO₂NT/AgNC (silver nanocubes) and Ti/TiO₂NT/AgNP (silver nanoparticles) electrodes.

References

K. Kočí, K. Matějů, L. Obalová, S. Krejčíková, Z. Lacný, D. Plachá, L. Čapek, A. Hospodková, O. Šolcová, *Appl. Catal. B* 2010, 96, 239 – 244.

G. Loget, J.E. Yoo, A. Mazare, L. Wang, P. Schmuki, *Electrochem. Commun.* 2015, 52, 41 – 44.

Synthesis and Characterization of New Improved Copper Hexacyanoferrate Nanoparticles for Zinc-Ion Batteries

Ghoncheh Kasiri, Amir Bani Hashemi, Fabio La Mantia
Energiespeicher- und Energiewandlersysteme, Universität Bremen
Bibliothekstr. 1, 28359 Bremen,
kasiri@uni-bremen.de

The demand for large-scale energy storage is rapidly growing, driven by the interest in increasing the percentage of electrical energy produced by means of renewable sources, such as wind and solar power. In order to reach more than 20% renewable sources, it is necessary to develop new energy storage systems with lower capital cost and intrinsic higher safety [1-3].

In 2015, we have developed an aqueous zinc-ion battery based on copper hexacyanoferrate (CuHCF) with an average discharge potential of 1.73 V and capacity retention of 96.3% after 100 cycles in 20 mM zinc sulfate (ZnSO_4) [4]. To reach high power density, higher concentration of ZnSO_4 in solution needs to be used. As the concentration of the electrolyte was raised to 100 mM ZnSO_4 , the life cycle of the zinc-ion battery was significantly decreased to less than 200 cycles, due to the formation of a new phase upon cycling [5]. Therefore, improving the structure of active material to reduce the number of defects in the CuHCF lattice is a primary of importance in order to obtain a prolonged cycle life. The objective of this work is optimizing the synthesis route by acting on different synthesis parameters.

We observed that by changing the synthesis parameters we could influence significantly the performances of the system and it was possible to reach an energy retention after 1000 cycles equal to 87%. In other words, that the battery could be stable up to 1500 cycles, thus reaching the performances of a classic high power lithium-ion battery. The power performances confirmed that the copper hexacyanoferrate zinc-ion battery is well designed for stationary applications and for short-time storage of the solar and wind power.

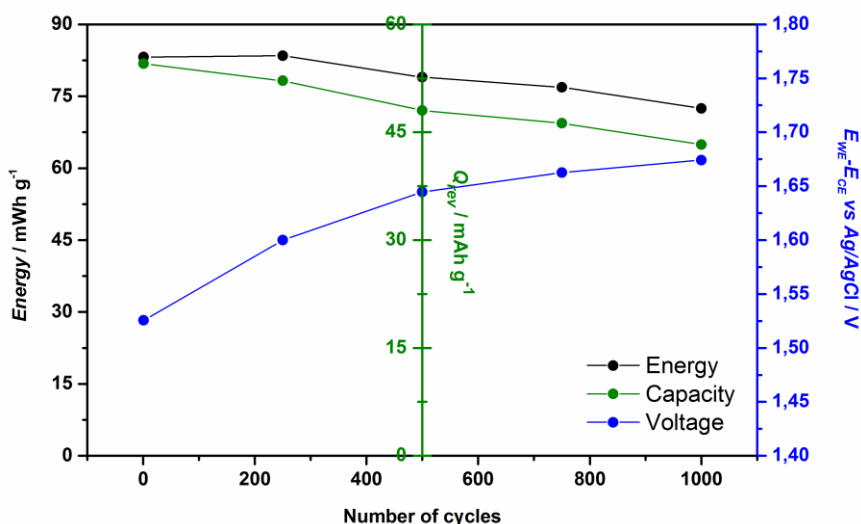


Fig. 1. Evolution of Energy, Capacity and Potential provided by new CuHCF synthesized powder at 1C rate in 100 mM ZnSO_4 .

References

- [1] Z. Yang, et al., Chem. Rev., 111, 3577 (2011).
- [2] G. Soloveichik, Annu. Rev. Chem. Biomol. Eng. 2 (2011) 503–527.
- [3] Wessells, et al. ACS nano 6.2 (2012): 1688-1694.
- [4] Trócoli, et al. ChemSusChem 8.3 (2015): 481-485.
- [5] Kasiri, et al. Electrochimica Acta 222 (2016): 74-83.

Patterns in the Nanoamperometry of Breast Cancer Drug Metabolism

Emmanuel Iwuoha, Usisipho Feleni and Luara Pacoste

SensorLab, University of Western Cape

4th Floor Chemical Sciences Building, Robert Sobukwe Road, Bellville, Cape Town, 7535, South Africa

eiwuoha@uwc.ac.za

Differences are known to exist in the responses of patients to the selective estrogen receptor modulators, tamoxifen (TAM) and toremifene (TOR), which are among the most prescribed breast cancer treatment drugs. These differences include the amount of drug that can cause drug toxicity due to overdose or non-response to treatment due to rapid clearance of drug and its active metabolites. Oncologist, pharmacologists and biomedical analysts have been seeking suitable protocols that will reliably determine breast cancer patients' metabolic classification (as slow, regular or rapid metabolisers). Cytochrome P450 (CYP) enzymes, which metabolise TAM and TOR in the liver microsomes, exhibit genetic polymorphism. That has been the basis for developing gene-based protocols for determining whether a patient exhibits impaired, extensive or rapid metabolism. Current genotype-based tests for the drug-response patterns of breast cancer patients are expensive and omit the contribution of other factors. Amperometric sensing tests, involving nanobiosensors prepared with CYP enzymes and biocompatible quantum dots have been developed, for the determination of inter-individual metabolic response patterns for TAM and TOR.

Ultra-high performance of a coaxial fiber-shaped asymmetric supercapacitor based on nanostructured MnO₂/CNT-web paper and Fe₂O₃/carbon fiber electrodes

Bebi Patil^a, Suhyun Ahn^b, Seongil Yu^b, Hyeonjun Song^c, Youngjin Jeong^c, Heejoon Ahn^{*a,b}

^a Institute of Nano Science and Technology, Hanyang University, Seoul 04763, South Korea

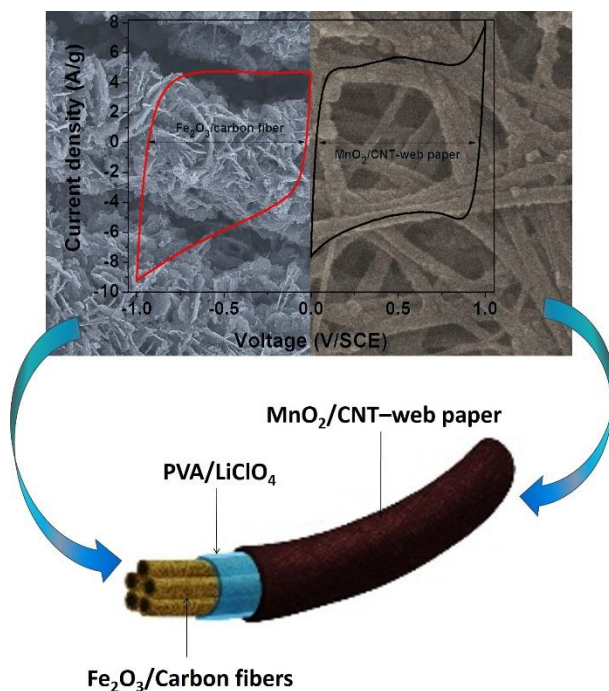
^b Department of Organic and Nano Engineering, Hanyang University, Seoul 04763, South Korea

^c Department of Organic Materials and Fiber Engineering, Soongsil University, Seoul 07027, South Korea

Corresponding Author

E-mail: ahn@hanyang.ac.kr (Prof. H. Ahn)

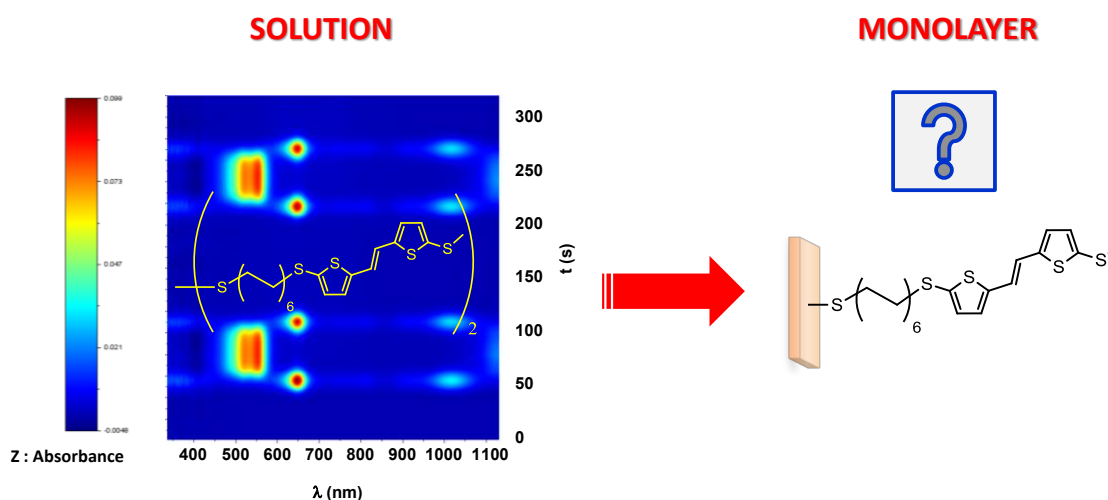
The fiber-shaped supercapacitor is a promising energy storage device in wearable and portable electronics because of its high flexibility, small size, and light weight. However, most of the reported fiber-shaped supercapacitors have exhibited low capacitance and energy density due to the limited surface area between the two fiber electrodes and operating voltage range. Herein, we successfully developed a coaxial fiber-shaped asymmetric supercapacitor (CFASC) made from MnO₂/CNT-web paper as a cathode coupled with Fe₂O₃/carbon fiber as an anode with a high operating voltage of 2.2 V. The prepared CFASC device showed a high volumetric energy density of 0.43 mWh cm⁻³ at a power density of 0.02 W cm⁻³, which is appreciably higher than those of most reported fiber-shaped supercapacitors. Additionally, CFASC exhibited good rate capability, long cycle life, and high volumetric capacitance (0.67 F cm⁻³) with excellent flexibility. The promising performance of CFASC illustrated its potential for portable and wearable energy storage devices.



From solution to mixed self-assembled monolayers: enhancement or extinction of the properties?

Christelle Gautier, Sihame Bkhach, Olivier Alévêque, Eric Levillain
Laboratoire MOLTECH-Anjou, UMR CNRS 6200,
2 boulevard Lavoisier, 49045 Angers, FRANCE
christelle.gautier@univ-angers.fr

Self-assembled monolayers (SAMs), which have the advantage of giving simple, organized and reproducible surfaces, constitute an ideal system suitable for the study of interfacial phenomena. These assets make them surfaces of choice to understand how a specific property observed in solution can be conserved, exalted or attenuated towards the confined environment that is the monolayer. The work presented concerns the electrochemical study, coupled or not with spectroscopy, of electroactive mixed monolayers on gold. The objective is to study reactions coupled to electron transfer when the redox precursor is immobilized on a surface. The electroactive groups of interest retained are tetrathiafulvalene (TTF) and thienylenevinylene (TV), molecules known to give intermolecular interactions at the oxidized state.



The spectroelectrochemical study of TTF-based and TV-based SAMs at different surface coverages made it possible to understand how the absorption properties of materials evolved, with comparison to the ones already characterized in solution.

Nanocomposite of CuBi_2O_4 and CuO as a highly efficient photocathode material for photoelectrochemical hydrogen evolution

Yu-Chien Chueh, Chia-Yu Lin

Department of Chemical Engineering, National Cheng Kung University

No.1, University Road, Tainan City 70101, Taiwan

cyl44@mail.ncku.edu.tw

We report on the fabrication of nanocomposite of CuBi_2O_4 and CuO modified electrode, which consists of CuBi_2O_4 nanodendrites decorated with CuO nanoparticles ($\text{nanoCuBi}_2\text{O}_4|\text{CuO}$), and the application of the fabricated $\text{nanoCuBi}_2\text{O}_4|\text{CuO}$ as a photocathode in photoelectrochemical (PEC) hydrogen generation. $\text{nanoCuBi}_2\text{O}_4|\text{CuO}$ was prepared by firstly electrodepositing BiOI nanosheets (nanoBiOI) onto the FTO substrate, followed by chemical conversion of nanoBiOI into $\text{nanoCuBi}_2\text{O}_4|\text{CuO}$ by dropcasting a Cu^{2+} precursor solution onto nanoBiOI and subsequent thermal treatment. As revealed in Figure 1a, without drop-casting the Cu^{2+} precursor solution, nanoBiOI was converted into Bi_2O_3 after thermal treatment. However, with the increase in the dosage of Cu^{2+} solution for the conversion process, the decrease in the intensity of the diffraction peaks belonging to Bi_2O_3 and the appearance of diffraction peaks belonging to $\text{nanoCuBi}_2\text{O}_4$ and CuO were noticed. Finally, with sufficient dose ($\geq 30 \mu\text{L cm}^{-2}$) of Cu^{2+} solution, Bi_2O_3 was completely removed. Figures 1b-e show the SEM images of the resultant electrodes converted from the nanoBiOI template with various dosages of the Cu^{2+} solution. The as-prepared nanoBiOI consists of vertically accumulated nanosheets with sheet thickness and length of ~ 20 nm and ~ 800 nm, respectively (data not shown). In addition, without adding the Cu^{2+} solution, the resultant electrode, *i.e.*, Bi_2O_3 , loses the integrity of the nanosheets structure of the nanoBiOI template and is composed of submicron-sized particles. Nevertheless, with adding the Cu^{2+} solution, the converted material reserved the porous nanostructure of the nanoBiOI template, and with higher dosage of the Cu^{2+} solution, more nanoparticles, presumably CuO nanoparticles (*vide infra*), attached the surface of $\text{nanoCuO-CuBi}_2\text{O}_4$ was observed. Nevertheless, when the dosage of the Cu^{2+} containing precursor solution was further increased to $50 \mu\text{L cm}^{-2}$, so much CuO nanoparticles formed, from excess dose of Cu^{2+} precursor solution, that the pores of the $\text{nanoCuBi}_2\text{O}_4|\text{CuO}$ was almost completely covered with CuO nanoparticulate layer. The preliminary PEC characterization (Figure 1f) indicates that $\text{nanoCuBi}_2\text{O}_4|\text{CuO}$ fabricated with $30 \mu\text{L cm}^{-2}$ of Cu^{2+} precursor solution showed superior photostability than other samples; after 1 h light illumination, the photocurrent density, at 0.5 V vs RHE in Na_2SO_4 (0.1 M, pH 7), of $\text{nanoCuBi}_2\text{O}_4|\text{CuO}$ remained about 40% of its initial value. Further optimization on its PEC properties by interfacing with hydrogen evolution catalyst is under investigation.

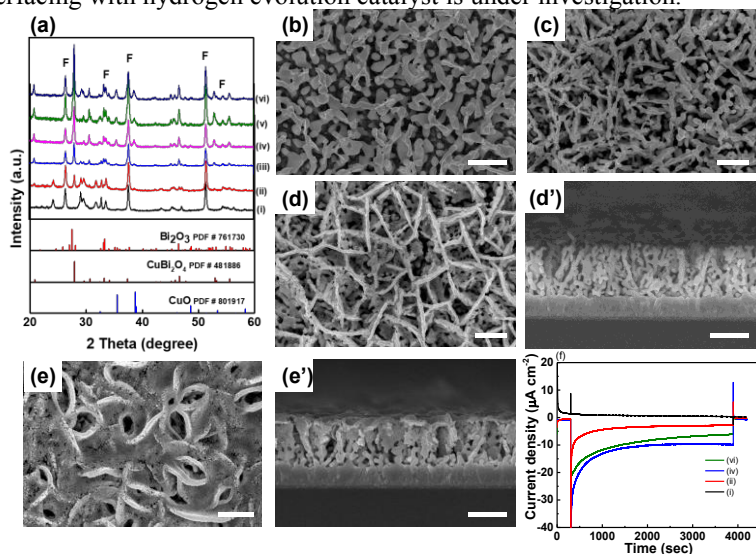


Figure 1 (a) XRD, (b-e) SEM images, and (f) chronoamperograms, recorded at an applied potential of 0.5 V vs. RHE, of the samples prepared by dropcasting a Cu^{2+} precursor solution with different dosages ($\mu\text{L cm}^{-2}$): (i, b) 0, (ii, c) 10, (iii) 20, (iv, d, d') 30, (v) 40, (vi, e, e') 50. Scale bar: 1 μm .

Physical Chemistry of Thermal Activation and Electrochemical Reactivity of Carbon Felts

Thomas J. Rabbow

Schuppengasse 32/24/3, 1230 Vienna, Austria

thomas.rabbow@gmx.de

Carbon felts are utilized as electrodes in many industrial electrochemical applications like flow batteries or supercapacitors. To adjust the wettability of the graphitic material and to improve the charge transfer, the felts are regularly activated. Among many different techniques thermal activation is widespread and typically used as a benchmark process.

In this work the processes during thermal activation and its electrochemical characterization methods are critically reviewed. The kinetic and thermodynamic basics of thermal activation in air are studied and there is experimental evidence that thermal activation is a combined process of both defect formation at the carbon lattice on the fibers surface and subsequent oxidation with burn off. The generation of defects is analyzed by changes of electrochemical double layer capacitance *EDLC*, total surface area *TSA* and by calculation of active surface area *ASA*. The activation energy for defect formation exceeds that for carbon oxidation to CO and CO₂ by far and therefore it is only possible to generate a sufficient amount of defects at comparable low temperatures when the burn off is minimized at the same time.

On the background of a characterization by *EDLC*, *TSA* and *ASA* the electrochemical reactivity of untreated and activated carbon felts is studied by cyclic voltammetry CV and electrochemical impedance spectroscopy EIS for outer- and inner-sphere charge transfer complexes. Whereby it is possible to estimate the surface area of planar electrodes by using CV of outer sphere complexes this cannot be applied to carbon felts, since the boundary conditions for diffusion and reaction have to be described by a thin film model. In contrast to many findings in the recent literature there is a clear evidence found that the constraints of diffusion during CV of inner and outer sphere reaction prohibit in general a description by Randles-Ševčík equation. At low scan rates the macro porosity of the felts causes a finite diffusion constraint, which is expressed during CV in peak separation ΔE_p well below the limit for planar macro-electrodes with semi-infinite diffusion conditions ($2.218 RT/nF$). For an outer sphere reaction (1 mM Co(III) phenantroline in 1 M KCl) the strong uptake of surface area *TSA* and number of defects *ASA* after activation has practically no influence on the reactivity and current densities. In the case of an outer sphere mechanism obviously only the projected surface area of the fibers is relevant since the currents during CV remain unchanged for untreated and activated felts which however can easily show a ten-fold increase of *TSA*. For a complex with inner sphere mechanism (V^{2+}/V^{3+} at various concentrations in 1.6 M H₂SO₄) there is a clear inverse proportional correlation of the charge transfer resistance to the number of defects *ASA* as estimated by *EDLC* and *TSA*, which had been shown earlier for other carbon based thin film electrodes. The results make it advisable to reconsider the diffusion constraints of thin film electrodes for an electrochemical characterization of carbon felts by cyclic voltammetry or impedance spectroscopy.

Fabrication of porous alumina filter by Sf-MDC and etching

Masatoshi Sakairi¹⁾, Toshiyuki Matsumoto²⁾

¹⁾*Faculty of Engineering, Hokkaido University,
Kita-13, Nishi-8, Kita-ku, Sapporo, Japan
msakairi@eng.hokudai.ac.jp*

²⁾*Graduate School of Engineering, Hokkaido University,
Kita-13, Nishi-8, Kita-ku, Sapporo, Japan*

In recently, porous type anodic aluminum oxide (porous alumina) films have been attracted much attention. The size and length of the pores can be controlled by the anodizing conditions, such as voltage, temperature and composition of electrolytes. A formation of area selective porous alumina film was achieved by mask process, however, these techniques present disadvantage in the complex processes involved. A solution flow-type micro-droplet cell with co-axial dual capillary tubes (Sf-MDC) has been applied to form porous alumina films locally^{1,2)}. It is, however, not elucidate possibility to form through hole type porous alumina layer. The purpose of this experiment is to form porous alumina filter locally with Sf-MDC and electro-chemical etching.

Highly pure aluminum sheets with 110 μm thickness were used for specimens. The specimens were ultrasonically cleaned in both ethanol and highly purified water for 300 s and then an electropolishing was carried out in 13.6 kmol m^{-3} CH_3COOH / 2.56 kmol m^{-3} HClO_4 at 28 V for 150 s at 278 K. The electropolished specimens were, then, cleaned with acetone and highly purified water. The specimen was set on the stage, and the specimen temperature during the anodizing was controlled by a Peltier device at 333 K. The solution for the anodizing was 0.22 kmol m^{-3} $(\text{COOH})_2$. A Pt wire with 50 μm in diameter was used as counter electrode and the Pt wire was inserted into the inner capillary tube. A droplet of electrolyte was formed at the tip of the inner capillary tube, and then the droplet of electrolyte was put in contact with the specimen surface. A constant voltage of 50 V was applied between the specimen and Pt wire during anodizing. The moving speed of the specimen was controlled by XYZ stage. Through hole was formed by dipping the anodized specimens in 0.5 kmol m^{-3} NaOH. The surface and cross section of the specimens were examined by optical microscope and SEM.

There was lighter line part in the surface optical microscope images and the thickness of the line part was increases with increasing repetition number. A nano-size ordered pores were observed by SEM surface and cross sectional observation. After treatment of through hole formation, porous alumina with through hole was fabricated locally.

References

- 1) T. Yamaguchi and M. Sakairi, Journal of the Surface Finishing Society of Japan, 385-390, 65 (2014).
- 2) M. Sakairi, F. Nishino, and R. Itzinger, Surface and Interface Analysis, 48, 921-925 (2016)

Keeping anions where they belong: Increased cycling stability of zinc anodes with homogeneous anion-exchange ionomer coating

Daniel Stock, Saustin Dongmo, Jürgen Janek, Daniel Schröder
Institute of Physical Chemistry, Justus-Liebig-University Giessen
Center of Materials Research, Justus-Liebig-University Giessen
Heinrich-Buff-Ring 17, Giessen, Germany
Daniel.Schroeder@phys.chemie.uni-giessen.de

Low cost, abundance and recyclability are some of the appealing advantages of Zn-based secondary batteries.¹ Especially, Zn-air batteries become a promising candidate for energy storage in electronic applications combining high specific energy density, environment friendliness and safe operation.^{1,2}

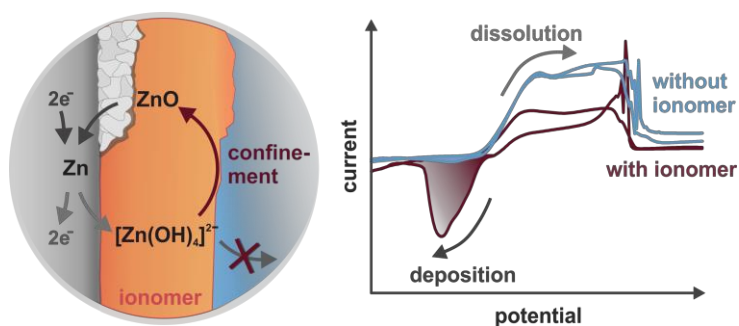
However, secondary Zn-based batteries possess limited cycling stability, which is related to complex and intertwined issues at anode and cathode.^{1,3}

Focusing on the Zn anode, one major issue arises from the high solubility of oxidized zinc species in the alkaline electrolyte resulting in electrode shape change and loss of active material during repeated discharge and charge.⁴

We present a homogeneous coating with an anion-exchange ionomer on top of the electrode to confine the oxidized zinc species. Ideally, the confinement of oxidized zinc species as zinc oxide interlayer reduces the shape change of the electrode and keeps the active material as close as possible at its place of origin.

Continuous cyclic voltammetry measurements on Zn model electrodes with anion-exchange ionomer coating denote the prevention of the loss of oxidized zinc species into the bulk electrolyte during zinc dissolution and increased amount of restored zinc during zinc deposition. In addition, X-ray photoelectron spectroscopy depth profiling was used to prove the formation of a zinc oxide interlayer between the anion-exchange ionomer and the surface of the zinc electrode indicating that hydroxide ions are able to pass the coating layer and react as intended, while migration of oxidized zinc species into the bulk electrolyte is hindered. Moreover, the changes in the morphology of cycled Zn anodes with anion-exchange ionomer coating were investigated using scanning electron microscopy and evidence repeated zinc dissolution and deposition processes at the interface between anion-exchange ionomer and zinc surface without degradation of the anion-exchange ionomer.

All in all, applying an anion-exchange ionomer coating increases the achievable cycle number of the Zn model electrode by up to six times demonstrating the benefit of ion-selective electrode coatings to improve their cycling stability.



References

- (1) Fu, J.; Cano, Z. P.; Park, M. G.; Yu, A.; Fowler, M.; Chen, Z. Electrically Rechargeable Zinc–Air Batteries: Progress, Challenges, and Perspectives. *Adv. Mater.* **2017**, *29* (7), 1604685.
- (2) Pei, P.; Wang, K.; Ma, Z. Technologies for Extending Zinc-Air Battery's Cyclelife: A Review. *Appl. Energy* **2014**, *128*, 315–324.
- (3) Schröder, D.; Arlt, T.; Krewer, U.; Manke, I. Analyzing Transport Paths in the Air Electrode of a Zinc Air Battery Using X-Ray Tomography. *Electrochem. commun.* **2014**, *40*, 88–91.
- (4) Hampson, N. a.; Tarbox, M. J. The Anodic Behavior of Zinc in Potassium Hydroxide Solution. *J. Electrochem. Soc.* **1963**, *110* (2), 95.

Synthesis of a Novel Reduced Graphene Oxide-copper-tin (rGO-Cu-Sn) hybrid nanocomposite with Enhanced Electrochemical Performance for Modified Electrode

M. Z. H. Khan and X. Liu*

College of Chemistry and Chemical Engineering, Henan University, Kaifeng 475004, China

*Corresponding Author: Prof. Dr. Liu Xiuhua (liuxiuhua@henu.edu.cn)

Now-a-days, graphene-metal nanoparticles based hybrid nanocomposites are attractive to effectively tune the intrinsic properties of inorganic semiconductors. We report a simple and facile one-step chemical reduction method for the preparation of a reduced graphene oxide-copper-tin (rGO-Cu-Sn) hybrid nanocomposite. The as-synthesized materials were well characterized with the aid of various techniques and used to modify indium tin oxide (ITO) semiconductor electrode. The scanning electron microscopy (SEM) and X-ray powder diffraction (XRD) observations indicate that Cu nanocubes and Sn nanoparticles, with an average diameter of 100 nm and 10 nm respectively, are anchored on rGO sheets. Electrochemical tests show that as-synthesized rGO-Cu-Sn hybrid nanocomposite modified ITO electrode (ITO/rGO-Cu-Sn) confirmed the high charge mobility to accelerate the electron transport efficiency by creating additional conduction paths for electrochemical reaction. Such study may provide insight into the usage of the rGO-Cu-Sn hybrid nanocomposite for electrocatalytic and photovoltaic applications.

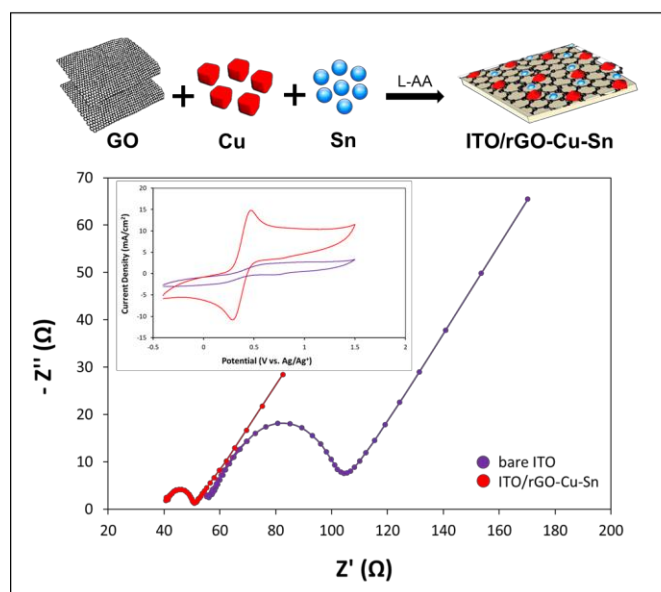


Figure 1: As-prepared rGO-Cu-Sn hybrid nanocomposite modified ITO electrode and their electrochemical performance

Polarization Behaviors and Cycle Performance of Air Electrode Using Water Repellent Film for Metal Hydride/Air Secondary Battery

Kenji Kawaguchi^{1*}, Tsukasa Gejo², and Masatsugu Morimitsu^{2,3**}

¹Organization for Research Initiatives and Development,

²Department of Science of Environment and Mathematical Modeling,

³Department of Environmental Systems Science,

Doshisha University

1-3 Tatara-miyakodani, Kyotanabe, Kyoto 610-0394, Japan

*kkawaguc@mail.doshisha.ac.jp, **mmorimit@mail.doshisha.ac.jp

A metal hydride/air secondary battery is expected as one of the next generation energy storage devices showing a higher energy density than LIB, because the active mass of the air electrode is oxygen in air so, which means no limitation on the discharge capacity of the air electrode. We have been developing the MH/air secondary battery using A_2B_7 type of hydrogen storage alloys at the negative electrode, and our previous results have demonstrated that a high energy density of 897 Wh/L and a high current discharge at 1000 mA are possible with the lab-scale cell, of which the maximum capacity is 2.5 Ah [1-3]. The polarization and cycle performance of the battery strongly depends on the air electrode, at which water is produced with oxygen reduction during discharge and water is decomposed to release oxygen during charge, suggesting that the volume of water in the electrolyte, *e.g.*, a concentrated KOH solution, changes during the operation. Under the situation, the air electrode should keep pore spaces for oxygen diffusion and block the electrolyte to go out through the air electrode. In this work, the preparation procedure and conditions of the air electrode with a PTFE film attached on the air side were examined and the polarization behaviors for oxygen evolution and reduction of the obtained air electrode were investigated by cyclic voltammetry and charge-discharge cycle test.

The air electrode comprised carbon powders as the conducting material, $Bi_{2-x}Ru_xO_{7-z}$ as the bifunctional catalyst, and PTFE as the binder [4]. Carbon powders, oxide catalysts and aqueous dispersion of PTFE particles were directly mixed, then the mixture was rolled and pressed on a nickel mesh to form a sheet, and the obtained sheet was finally calcined at 370 °C under nitrogen atmosphere [1-4]. A porous PTFE film was attached to the air electrode by the roll press method, and the conditions of the roll pressure and clearance between two rolls were examined. The polarization behaviors and the charge-discharge cycle performance of the air electrode were examined by cyclic voltammetry and constant current cycle test using a three-electrode cell, in which one side of the air electrode was exposed to air and the other side to 6 mol/L KOH solutions.

The polarization for oxygen evolution and reduction of the air electrode attached with the PTFE film was almost the same as that of that without the film, suggesting no influence on oxygen permeability of the air electrode by the attached film. The cycle performance of the air electrodes demonstrated that the PTFE film was effective to suppress the flooding of the electrolyte and the increase in polarization during the charge-discharge cycles, compared to the air electrode without the film. We will also present the cycle performance of the metal hydride/air secondary battery using the air electrode attached with the PTFE film.

This work was done under “Advanced Low Carbon Technology Research and Development Program (ALCA)” of Japan Science and Technology Agency (JST).

References

1. C. Baba, K. Kawaguchi, and M. Morimitsu, *Electrochemistry*, **83**, 855 (2015).
2. T. Gejo, K. Kawaguchi, and M. Morimitsu, The 56th Battery Symposium, #1G21, Nagoya (2015).
3. K. Kawaguchi, S. Terui, and M. Morimitsu, PRiME 2016, Abs#75, Honolulu (2016).
4. K. Kawaguchi, Y. Ujino, and M. Morimitsu, 232nd ECS Meeting, Abs#464, National Harbor (2017).

Energy-resolved Density of Electron Traps as a Novel Macroscopic Measure for Characterization of Metal-Oxide Powders

Bunsho Ohtani, Akio Nitta, Yuma Murakami, Mai Takase and Mai Takashima

¹Institute for Catalysis and ²Graduate School of Environmental Science, Hokkaido University and

³Graduate School of Engineering, Muroran Institute of Technology

¹Sapporo 001-0021, ²Sapporo 060-0810 and ³Muroran 050-8585, Japan

ohtani@cat.hokudai.ac.jp

Although organic compounds are practically identified by their elemental compositions and nuclear magnetic resonance (NMR) patterns, metal-oxide powders cannot be identified by bulk composition and crystalline structure. Such a difference between molecules and powders is attributable to existence of both surface and bulk are to be identified for powders. What has been conventionally evaluated as structural properties of metal-oxide powders is crystal phase, primary particle diameter, secondary particle diameter and specific surface area, but those properties reflect only bulk composition or size. In other words, a lack of sufficient analytical method that enables measurement of a property reflecting surface structure has prevented characterization and thereby identification of metal-oxide powders. In this study, we focus on energy-resolved density of electron traps (ERDT) located mainly on the surface of metal-oxide powders, and evaluate ERDT in various particulate samples as a function of energy from valence-band top (VBT) by reversed double-beam photoacoustic spectroscopy (RDB-PAS), in which photoabsorption of trapped electrons directly excited from valence band to electron traps by scanned continuous light is measured by PAS [1].

Representative ERDT patterns of titania powders are shown in Fig. 1. Conduction-band bottom (CBB) depending on the crystalline phase and total density of electron traps increasing with increase in the specific surface area indicate that CBB and total density of electron traps can reflect bulk composition and bulk size, respectively. On the other hand, ERDT patterns of TIO-1 and TIO-13 seem to be clearly different. This result indicates that ERDT can reflect surface structural property. By calculating degree of coincidence ζ , multiplied by each degree of coincidence for ERDT pattern matching, total density of electron traps (shown in \diamond in units of $\mu\text{mol g}^{-1}$) and CBB position, some given pairs of two samples which are made by the same manufacturing method show higher ζ values than those of other pairs. Therefore, it is suggested that an ERDT/CBB pattern can be a fingerprint for metal-oxide powders. Evaluation of VBT by observing ERDT of mixture sample is also discussed.

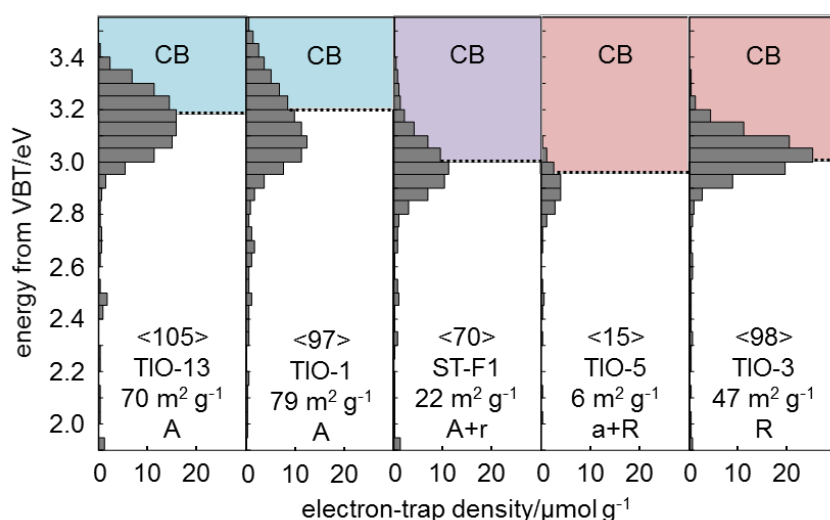


Fig. 1 Representative ERDT/CBB patterns as energy function from VBT for titania powders.

[1] A. Nitta, M. Takase, M. Takashima, N. Murakami, B. Ohtani, *Chem. Commun.*, 52, 12096-12099 (2016). [2] A. Nitta, M. Takashima, N. Murakami, M. Takase, B. Ohtani, *Electrochim. Acta*, in revision.

Three-dimensional porous graphene-wrapped silicon nanoparticles composite anode with nanofiber composite PET separator for lithium-ion batteries

¹Yi-Shiuan Wu, ^{1,2}Chun-Chen Yang, ^{1,2}Zong-Han Wu, ^{1,2}Chao-Nan Wei, ^{1,2}Min-Yen Yang
¹Battery Research Center of Green Energy, Ming Chi University of Technology (MCUT)
²Department of Chemical Engineering, Ming Chi University of Technology (MCUT)
 #84 Gungjuan Rd., Taishan Dist., New Taipei City 24301, Taiwan, R.O.C.
yishiuan@mail.mcut.edu.tw

In this paper, silicon nanoparticles (SiNPs, ~50 nm in diameter)/reduced graphene oxide (rGO, 100–300 nm in thickness)/carbon (SiNPs/rGO/C) composite anodes have been successfully synthesized, characterized and examined for lithium-ion batteries (LIBs). In Figure 1, nano-porous (pore size: ~50 nm) SiNPs/rGO/C composite microspheres (average diameter: ~2 μm) were obtained by dispersing SiNPs encapsulated into the rGO inter-layers via ball milling, spray drying and sintering techniques, leading to significant enhancements of electrical conductivity before and after SiNPs pulverization, as shown in Figure 2. Compared with a commercialized PE separator (Asahi®), as shown in Figure 3 inset, the as-prepared SiNPs/rGO/C composite anodes assembled with a homemade nanofiber composite PET separator exhibited higher C-rate capability with reversible specific capacities ($Q_{sp,PET}$: 1311, 1250, 1106, 906 and 825 mAh g⁻¹ vs. $Q_{sp,PE}$: 1159, 1129, 903, 707 and 678 mAh g⁻¹ at various current densities of 100, 200, 400, 800 and 1000 mA g⁻¹, respectively). After cycling at 400 mA g⁻¹ for 100 cycles (Figure 3), the SiNPs/rGO/C composite anodes containing a PET composite separator also showed the enhanced specific capacity by 34% ($Q_{sp,ave,PET}$ vs. PE: 1008 mAh g⁻¹ vs. 754 mAh g⁻¹) and higher capacity retention (CR%_{PET} vs. PE: ~100% vs. ~93%), which are better than those in the previous literature (CR%: 73–90%, Table 1) [1–5]. The afore-mentioned results can be attributed to the synergistic effects of the SiNPs/rGO/C composite anode associated with the homemade nanofiber composite PET separator.

Keywords: silicon nanoparticles, reduced graphene oxide, lithium-ion batteries, spray drying, nanofiber composite PET separator.

References:

1. R.C. de Guzman et al., J. Power Sources 246 (2014) 335.
2. S.H. Park et al., Chem. of Mater. 27 (2015) 457.
3. X. Li et al., New J. Chem. 40 (2016) 8961.
4. M. Tokur et al., Electrochim. Acta 216 (2016) 312.
5. K. Zhang et al., RSC Adv. 7 (2017) 24305.

Table 1. Comparisons of the SiNPs/rGO anodes.

Anode [ref.]	Binder	Separator /Electrolyte additive	CR % (100 cyc.)	R _t ohm
Si(50 nm)/rGO [1]	PAA	/+EC+DMC+VC	73 @0.5 A g ⁻¹	20
Si(100 nm)/rGO [2]	PAA	/+EC+DMC+FEC	-	251
Si(60 nm)/rGO [3]	CMC	PP /+EC+DEC+VC	79 @0.2 A g ⁻¹	50
Si(130 nm)/rGO [4]	PVDF	PP /+EC+DEC+DMC	77 @0.1 A g ⁻¹	60
Si(100 nm)/rGO [5]	CMC+SBR	PP /+EC+DEC	90 @0.5 A g ⁻¹	30
Si(50 nm)/rGO [MCUT]	PVDF	Asahi (PE) /+FEC+DMC PET composite /+FEC+DMC	93 @0.4 A g ⁻¹ 100 @0.4 A g ⁻¹	23 18

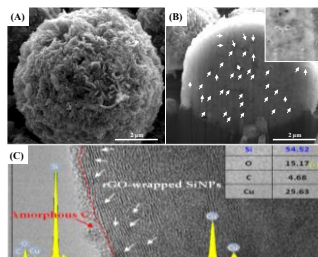


Figure 1. (A), (B) SEM micrographs and (C) TEM image of the nano-porous SiNPs/rGO/C composite microspheres.

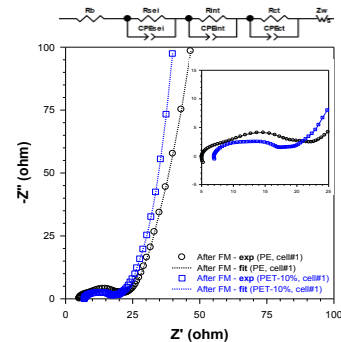


Figure 2. EIS of the SiNPs/rGO/C composite anodes with two different separators (PE vs. PET).

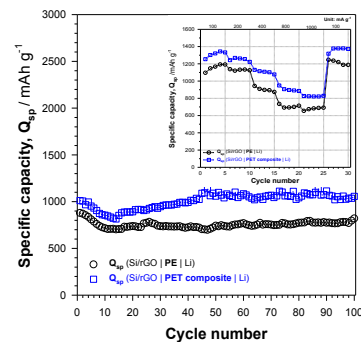


Figure 3. C-rate profile (inset) and long-term cycling of the SiNPs/rGO/C composite anodes.

Fabrication of Single Molecule Polycyclic Aromatic Hydrocarbon Switches at an Electrochemical Interface

Piret Pikma^{a,b}, Parisa Yasini^b, Eric Borguet^b

^a*Institute of Chemistry, University of Tartu, Ravila 14A, Tartu 50411, Estonia*

^b*Department of Chemistry, Temple University, 1901 N. 13th Street, Philadelphia, 19122 PA, USA*
piret.pikma@ut.ee

Molecular-scale electronic devices are often constructed by wiring a single molecule between two metal electrodes using mechanically controlled break junctions (BJ) in a scanning tunneling microscope (STM) [1]. One of the possible applications of single molecules is as a switch to control nanoscale electrical circuits and for the detection of chemical species. Molecules which exist in two or more states that could be interconverted by external stimuli, *e.g.* potential, and that can exhibit different conductive states may have critical roles in information storage in molecular electronics.

Polycyclic aromatic hydrocarbons (PAH) are of interest from a theoretical point of view as well as a practical standpoint as functional organic materials. One attractive feature of PAH is that the difference between the molecule's highest energy occupied molecular orbital (HOMO) and its lowest energy unoccupied molecular orbital (LUMO) values, can be tuned by the number of aromatic rings [2]. Charge transport through metal–molecule–metal junctions has been investigated by measuring the conductance (or resistance) as a function of molecular length. In general, the resistance across such junctions gives rise to an exponential decay of measured conductance with increasing molecular length [3].

In this study *in situ* STM imaging and STM break junction techniques, supported by cyclic voltammetry, were applied to investigate the adsorption and conductivity properties of naphthalene, 2,6-naphthalenedicarboxylic acid, anthracene, and tetracene (Figure 1) on an Au(111) single crystal electrode and their dependence on the applied surface potential. Ordered structures were observed by STM at potentials more negative than the zero charge potential and were accompanied by the observation of a high molecular conductivity in STM-BJ measurements. When the applied surface potential was gradually changed from more negative than the potential of zero charge (pzc) to more positive than the pzc, it was observed that the ordered structures disappear, accompanied by the loss of the high molecular conductivity feature in STM-BJ measurements.

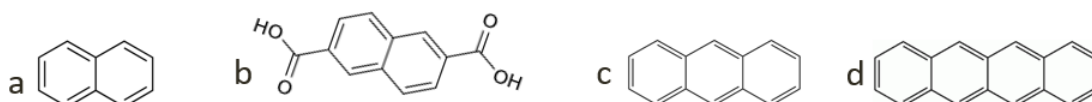


Figure 1. Molecular structures of investigated molecules: naphthalene (a) 2,6-naphthalenedicarboxylic acid (b), anthracene (c) and tetracene (d).

The data, which was analyzed based on the influence of the applied surface potential, the structure of the chosen molecules, and the HOMO-LUMO gap, revealed that the chosen molecules could be used as ON/OFF switches with the external stimuli being the applied surface potential. Additionally, it was observed that the conductance for these PAH molecules decreases as the molecules increase in size, while the HOMO-LUMO gap actually decreases.

References:

- [1] I. Gomez, Y. Mercier, M. Reguero, *J. Phys. Chem. A*, 110 (2006) 11455-11461
- [2] M. Watanabe, Y.J. Chang, S.-W. Liu, T.-H. Chao, K. Goto, Md. M. Islam, C.-H. Yuan, Y.-T. Tao, T. Shinmyozu, T.J. Chow, *Nat. Chem.*, 4 (2012) 574–578
- [3] Z. Li, T.-H. Park, J. Rawson, M.J. Therien, E. Borguet, *Nano Lett.*, 12 (6) (2012) 2722-2727

Electrochemistry of Particulate Electrodes Based on Magnetite Aggregates

Alessandra Accogli, Luca Magagnin
Dip. Chimica, Materiali e Ing. Chimica G. Natta, Politecnico di Milano
Via Mancinelli, 7 – 20131 Milano - Italy
luca.magagnin@polimi.it

In current research, micro and nanoparticulate electrode materials have taken their place because they offer a large internal surface area with respect to the macroscopic dimensions of such electrodes [1]. The nano-impact method is a powerful tool that enables the characterization of individual particulate nano-objects in solution and study of their reactivity [2]. A three electrodes setup system working as a standard electrochemical cell is typically used. Magnetite (Fe₃O₄) nanoparticles with the strongest saturation magnetization of all naturally occurring iron oxides, combined with properties such as low toxicity, good biocompatibility, high stability, and low production costs, have attracted a lot of interest [3]. There is also substantial interest in their use as magnetic fluids, in data storage, in catalysis, and as electrode materials. In this work, magnetite micro and nanoparticles have been synthesized by chemical precipitation method in presence of surfactants or functional organic polymer. The use of surfactants to stabilize these synthesized nanoparticles is crucial, as Fe₃O₄ nanoparticles have high surface energies and tend to aggregate. They also have high chemical activity. Magnetite particles are used as particulate electrode in different fluid and characterized into a three electrodes cell in order to evaluate their electrochemical behavior. A deeper understanding of the particulate electrode has been performed in situ on supported particles through electrochemical AFM/STM measurements, highlighting the behavior of the single aggregate. Together with the charge transfer characterization as a function of particles size and concentration, functionalization and fluid composition, practical applications of the particulate electrodes will be presented. Specifically, the use of particulate electrodes in the electrochemical metal recovery, showing the ions adsorption properties of magnetite particles as a function of surface functionalization and their electrochemical reduction at the magnetic fluid/current collector interphase, in the production of electrochemical sensors for glucose detection and in the development of semi-solid electrodes for improving the performances of lithium ions batteries.

References

1. V. Noack, H. Weller, A. Eychmüller, J. Phys. Chem. B, 106 (2002) 8514-8523
2. S.V Sokolov et al., Phys.Chem.Chem.Phys., 19 (2017) 28
3. K. Murugappan, ChemElectroChem, 1 (2014) 1211 – 1218

Aspects of Phosphoric Acid Presence in High-Temperature PEM Fuel Cell with Regard to the Pt Catalyst

Martin Prokop, Tomas Bystron, Karel Bouzek
University of Chemistry and Technology Prague
Technicka 5, Prague 6, 16628, Czech Republic
bouzekk@vscht.cz

High-temperature proton exchange membrane fuel cell (HT PEM FC) represents interesting device for conversion of chemical (of H₂ and O₂) to electric energy. Its operating temperature lies in the range of 120-200 °C. Due to this fact, sulfonated perfluorinated type membrane cannot be used as a polymer electrolyte. Instead, polymeric membrane (typically polybenzimidazole based) doped with phosphoric acid is the material of the choice, as it ensures required proton conductivity between the electrodes under operating conditions. Application of the phosphoric acid has significant impact on the resulting properties and behaviour of the cell. Important part of them relates to the interaction of phosphoric acid present in the system with Pt catalyst present in the catalytic layer.

The interactions of the phosphoric acid with the catalyst represent a complex problem. It involves: (i) redox changes of phosphoric acid, (ii) sorption of phosphoric acid and oxoacids of phosphorus resulting from the changes mentioned in the previous point on the catalyst surface and (iii) degradation of the Pt catalyst.

Redox changes of the phosphoric acid in the operating cell may be attributed to its interaction with hydrogen on the Pt electrocatalyst at the anode side of the cell. It leads to formation of phosphorus compounds, such as H₃PO₃ (eventually also H₃PO₂) and adsorbed phosphorus, characterised by different stability and reactivity in the system. Interaction of the selected phosphorus compounds with the Pt catalyst was studied for a broad range of conditions, including those relevant to the HT PEM FC operation. Also activity of the catalyst towards oxygen reduction reaction, as well as transport parameters of oxygen in the phosphoric acid, under conditions relevant to the HT PEM FC operation were determined. For this purpose, an innovative technique based on the modified rotating disk electrode was developed and tested. These experiments provided a deeper insight into the complex issue of electrochemistry of oxoacids of phosphorus on the Pt electrode.

Subsequently, the impact of the HT PEM FC operational conditions on the stability of the carbon black supported Pt catalyst was studied by means of a single cell experiments. For this purpose, the cell was operated under constant voltage conditions for the defined period of time. Impact of the exposure to the various operational conditions was evaluated ex-situ by means of HR TEM, XRD and SAXS. Evolution of the catalyst particles size distribution and thus of its active surface with respect to the time and conditions of exposure were evaluated. This information is important for evaluation of Pt catalyst degradation kinetics and it will be used later in the mathematical model of HT PEM FC stack which is currently being developed.

The results obtained represent an interesting contribution towards understanding of the processes occurring inside the HT PEM FC during its operation. They, thus, allow more accurate and targeted optimisation of this technology.

Acknowledgement

Financial support of this research by the Grant Agency of the Czech Republic under the project No. 18-10493J is gratefully acknowledged.

Formation of Nanoporous Spinel Ferrite Electrocatalysts by Anodizing of Electroplated Iron Alloys

Yoshiki Konno, Tomio Nagayama, Takayo Yamamoto, Kaname Okura, Toshihiro Nakamura
Kyoto Municipal Institute of Industrial Technology and Culture, Surface Finishing Technology Lab.
91 Chudoji Awata-Cho, Shimogyo-ku, Kyoto, Japan
E-mail: konno@tc-kyoto.or.jp

Oxygen reduction / evolution reactions (ORR/OER) play important roles in many kinds of energy conversion and storage technologies, including metal-air batteries, fuel cells and electrolysis. The reactions are traditionally require the use of highly efficient catalysts based on platinum group elements (e. g. Pt, IrO₂, RuO₂). The scarcity of those elements limits their practical use in mass production. Therefore, extensive studies have been carried out for the inexpensive and efficient electrocatalysts composed of earth-abundant metals. Spinel-type ferrite oxides, based on ubiquitous iron element, are one of the candidates as alternative and low-cost electrocatalysts for ORRs and OERs [1].

The traditional synthesis of spinel compounds generally follows a solid-state route that involves grinding and calcination of a mixture of oxides, nitrates or carbonates. However, the traditional method requires elevated temperature and prolonged process times. Furthermore, for fabrication of catalytic layer, the catalysts need to be mechanically milled, mixed with polymer binder and carbon additives, and coated on current collector, which restricts the reduction of the process cost.

In this study, we present a low cost and suitable processing to mass production of electrocatalyst by using electrodeposition followed by anodizing and annealing to fabricate spinel ferrite binary oxides M_xFe_{3-x}O₄ (M=Mn, Ni) layers with nanoporous structures. We also investigate the electrocatalytic OER and ORR performances of the nanoporous oxides formed on Fe-M deposits of various compositions using electrochemical methods.

Copper or iron plates (YAMAMOTO-MS Co., Ltd.) were used as substrates. Electrodeposition was carried out in aqueous solution of metal sulfate and chloride salts containing trisodium citrate and ammonium chloride. Subsequent anodizing were performed at a constant voltage of 40 V with Pt mesh counter electrode in ethylene glycol electrolyte containing 0.1 mol dm⁻³ NH₄F and 0.5 mol dm⁻³ H₂O. Post annealing were treated under nitrogen atmosphere at 673 K for 30 minutes.

Formation of Fe-Mn films was deposited in the range of Mn content from 6 to 90 wt%. Porous anodic films were formed on Fe-Mn deposits with Mn compositions of about 30 wt% or less.

ORR and OER performances were investigated with electrochemical polarization in 0.1 mol dm⁻³ KOH (Figure. 1 a, b). The onset potential for ORR on porous oxide of Fe-30 wt% Mn deposit (p-Fe-Mn oxide) is remarkably positive from that on porous Fe₃O₄ (p-Fe₃O₄) formed on pure iron, which indicates that p-Fe-Mn oxide have higher activity for ORR (Fig. 1 a). Further its onset is relatively near the onset of efficient Pt electrode, therefore p-Fe-Mn oxide could be promising electrocatalysts for ORR. The onset potential for OER is negative from that of p-Fe₃O₄ (Fig. 1 b). Thus, OER activity of p-Fe-Mn oxide is also higher than that of p-Fe₃O₄. Since the porous oxide formed on Fe-Mn deposit shows good activity in both reactions, it could be cost-effective electrode for ORR and OER.

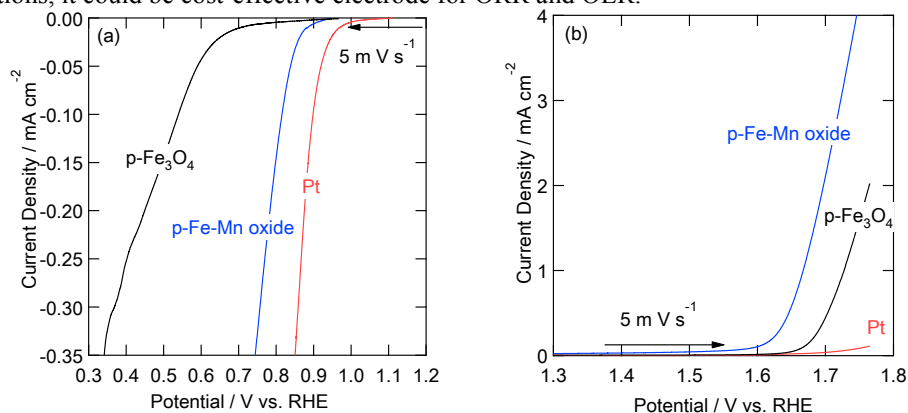


Figure 1. Polarization curves of the porous oxide on Fe-30 wt% Mn, porous Fe₃O₄ on iron, and Pt for (a) ORR and (b) OER measurements in 0.1 mol dm⁻³ KOH at room temperature.

[1] M. Li, Y. Xiong, X. Liu, X. Bo, Y. Zhang, C. Han, L. Guo, *Nanoscale*, 7 (2015) 8920.

Highly Responsive Humidity Sensor Based on Gold Nanoparticle via Inkjet Printing Technology

Chun-Hao Su¹, M. Yesilmen², B. Ketelsen², F. Schulz² T. Vossmeier² and Ying-Chih Liao^{1*}

¹*Department of Chemical Engineering, National Taiwan University, Taipei 10617, Taiwan*

²*Institute of Physical Chemistry, University of Hamburg, Grindelallee 117, 20146 Hamburg, Germany*

Address: No. 1, Sec. 4, Roosevelt Rd., Taipei 10617, Taiwan (R.O.C.)

e-mail address: liaoy@ntu.edu.tw

Accurate humidity measurement plays a vital role in many industrial applications and personal health monitoring. A variety of humidity sensing technologies have been developed, such as resistance, capacitive, optics and surface acoustic wave technology. Among these methods, resistive sensors have simple structure, low cost, high sensitivity and rapid response compared to other technology. However, the production of humidity sensors often has cumbersome steps. Therefore, inkjet printing technology, a direct-writing method which can precisely deposit liquid thin film patterns effectively, is utilized to fabricate humidity sensors.

In this research, a gold nanoparticle thin film is inkjet-printed on a flexible substrate over an interdigital carbon paste electrode to detect humidity. With proper ink formulation and particle suspension, gold nanoparticles(GNP) with well-defined mixed ligand layers of α -methoxypoly(ethylene glycol)- ω -(11-mercaptoundecanoate)(PEGMUA) and 11-mercaptoundecanoic acid(MUA) are printed to form uniform thin films on printed electrodes for humidity sensing. With the help of great precision in liquid deposition, the thicknesses of the printed gold nanoparticle thin films can be accurately controlled by the number of printed layers. Because mixed ligand layer can quickly absorb water vapor molecules, the wetted GNP film shows fast electrical resistance response to humidity. After fixed on a mask, the sensor not only can detect exhalation and inhalation, but also can distinguish normal breathing and rapid breathing. The sensitivity, stability and repeatability with potential applications of the printed sensors will be carefully examined to demonstrate the feasibility of printed sensors for quick and accurate determination of humidity. This study demonstrates the feasibility of the proposed printing process for not only humidity sensing but also for health monitoring.

Oxygen reduction activity of titanium oxide-based compounds as non-platinum cathode for PEFCs

Akimitsu Ishihara,¹ Takaaki Nagai,² Masazumi Arao,³ Masashi Matsumoto,³ Yoshiyuki Yamamoto,⁴ Shusuke Kasamatsu,⁴ Koichi Matsuzawa,² Osamu Sugino,⁴ Hideto Imai,³ Shigenori Mitsushima,^{1,2} and Ken-ichiro Ota²

¹ Institute of Advanced Sciences, Yokohama National University, 79-5 Tokiwadai, Hodogaya-ku, Yokohama, Kanagawa, Japan

² Green Hydrogen research Center, Yokohama National University, 79-5 Tokiwadai, Hodogaya-ku, Yokohama, Kanagawa, Japan

³ Device Analysis Department, NISSAN ARC,LTD., 1 Natsushima-cho, Yokosuka, 237-0061, Japan

⁴ Institute for Solid State Physics, University of Tokyo, 5-1-5 Kashiwanoha, Chiba, Japan
Ishihara-akimitsu-nh@ynu.ac.jp

Polymer electrolyte fuel cells are expected for the residential and transportable applications, especially for the automobile use, due to their high power density and low operating temperature. In order to commercialize the fuel cell vehicles widely, the development of a non-noble metal cathode is strongly required. We focused on group 4 and 5 metal oxides, which are well known as valve metals, as stable oxygen reduction reaction (ORR) catalysts because they are stable even in acidic and oxidative atmosphere. However, these oxides are generally insulators. In order to create active sites for oxygen reduction reaction, these oxides should be modified by the formation of the oxygen vacancies and/or the substitution of foreign atoms. In this study, we have tried to apply niobium-doped titanium oxides to the cathode catalysts to clarify the generation of the ORR activity.

We used carbon nano-tubes (CNTs) as supports to have sufficient electronic conductivity of the catalyst powder. Nb-doped TiO₂ nano-particles were dispersed on the CNT by hydrolysis method to make the precursor. The weight ratio of CNT: TiO₂:Nb₂O₅ was adjusted to be 20 : 4 : 1. The precursor was heat-treated for 10 min under 4%H₂/Ar at 600, 700, 800 and 900°C. The crystalline structure of the catalysts was analyzed by XRD (Rigaku Ultima IV, X-ray Source: Cu K α). In order to estimate the distortion of the crystalline structure, the lattice volume of the anatase phase was calculated. The ORR activities were measured in an acidic electrolyte of 0.1 M H₂SO₄ using a three-electrode cell (reference electrode is a reversible hydrogen electrode, RHE; counter electrode is a glassy carbon).

Figure 1 shows the potential-current curves of the Nb-doped TiO₂/CNTs prepared at various temperatures. The Nb-doped TiO₂/CNT prepared at 800°C had highest activity among them. Figure 2 shows the dependence of the ORR current density at 0.7 V on the lattice volume of the anatase phase of the samples. The ORR current increased with increasing lattice volume, indicating that the distortion of the anatase phase might be essential for the generation of the ORR activity of the titanium oxide-based cathodes.

Acknowledgements

The authors thank New Energy and Industrial Technology Organization (NEDO) for financial support. This research was supported by Strategic International Research Cooperative Program, Japan Science and Technology Agency (JST). This work was conducted under the auspices of the Ministry of Education, Culture, Sports, Science and Technology (MEXT) Program for Promoting the Reform of National Universities.

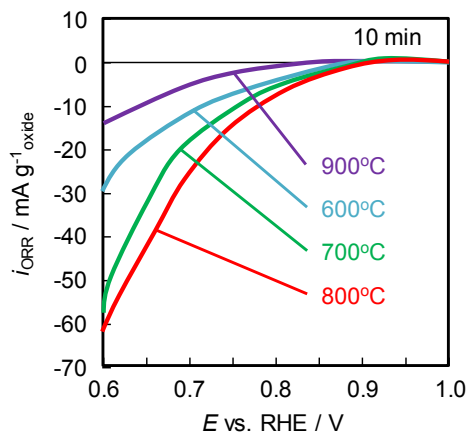


Fig.1 Potential-ORR current curves of Nb doped TiO₂/CNTs.

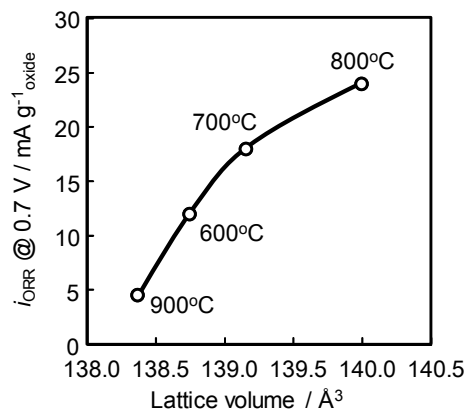


Fig.2 Dependence of ORR current at 0.7 V on lattice volume of Nb doped TiO₂/CNTs.

Two-dimensional porphyrin-based metal-organic frameworks: The enhanced electrocatalysis of CO₂ reduction in aqueous solution

Wen-Li Xin, Dan Shan*

*School of Environmental and Biological Engineering, Nanjing University of Science and Technology,
Nanjing 210094, P. R. China
Email address: danshan@njust.edu.cn*

The electrocatalytic CO₂ reduction reaction (CO₂RR) is of considerable interest because of its potential for both the storage of intermittent renewable energy from wind and solar, and the conversion into value-added fuels and other chemicals in a sustainable manner. Two-dimensional (2D) materials are known to be useful in catalysis. In this work, iron-tetraphenylporphyrin (FeTCPP) was used to synthesize 2D Fe-MOFs by the solvothermal reaction of Zn(NO₃)₂·6H₂O and FeTCPP in N,N-dimethylformide (DMF). To enhance the electrocatalytic performance, MoS₂ quantum dots (MQDs) were introduced during the above solvothermal reaction at 80 °C, the final 2D hybrid materials Fe-MOFs@MQDs were obtained. The comparative study of the electrocatalytic CO₂ reduction was performed. The synergistic effect of electrocatalysis from Fe-MOFs and MQDs was investigated. This effect is ascribed to the particular environment created by the aqueous medium at the catalytic site of the combined catalyst that facilitates the adsorption and further reaction of CO₂.

Reference

[1] Xinming Hu *et al.* Enhanced catalytic activity of cobalt porphyrin in CO₂ electroreduction upon immobilization on carbon materials. *Angew. Chem. Int. Ed.* **2017**, 56, 6468-6472.

Acceleration of Ion Transport within Nanopore Caused by Confinement of Electrolyte Solution

Kazuhiro Fukami,¹ Akira Koyama,¹ Kitada Atsushi,¹ Tetsuo Sakka,² Takeshi Abe,² and Kuniaki Murase¹

¹ Department of Materials Science and Engineering, Kyoto University, Kyoto 606-8501, Japan

² Department of Energy and Hydrocarbon Chemistry, Kyoto University, Kyoto 615-8510, Japan
fukami.kazuhiro.2u@kyoto-u.ac.jp

Conducting and/or semiconducting nanoporous materials attract keen attention as electrodes for electrochemical reactions. In order to achieve ultra-high surface area, the pore size must be tuned as small as possible, with keeping the porosity as high as possible. As a drawback of miniaturization of pores at the scale of nanometers, ionic conductivity within nanopore significantly decreases because of the difficulty in mass-transfer within nanopore [1]. A strategy for the enhancement of mass-transfer within nanopore has been desired so far.

As one of the promising strategies, we focus on the tuning of hydration properties of electrode surface as well as solutes (ions) [2-4]. In order to experimentally investigate the rate of ion transport in nanopore, we adopt electrodeposition as a model system for the evaluation. This is because the number density of nanoparticles deposited and their distribution indirectly give information of mass-transfer of metallic ions in confined nanopore. In the present study, electrochemical deposition of platinum is studied in detail for the purpose mentioned above.

Figure 1 shows time development of potential measured during the deposition of platinum. An exponential increase in potential is detected when flat silicon is used as the working electrode. The utilization of porous silicon results in a different behavior. At the initial stage of the deposition, an increase in potential is observed. This is very much similar to the result on flat silicon. After this stage, the potential shows a plateau for a while, and followed by a gradual increase to a higher potential. Close inspection of the cross-sectional views of samples after platinum deposition clearly indicated that the potential plateau is caused by the penetration of platinum complex anion into the nanopore of porous silicon. Once the supply of platinum complex anion reaches to the bottom of nanopore, the plateau ceases and the potential increase restarts. Therefore, one can evaluate the penetration rate of platinum complex anions into the nanopore of porous silicon by measuring the length of the potential plateau. When the pore size is ~ 30 nm, the potential plateau continues for 5 min. With decreasing the pore size from 30 nm to 15 nm, the plateau becomes 12 min. This result is understandable according to the diffusion model. However, the plateau is extremely short when using porous silicon with ~ 4 nm in diameter. In the ~ 4 nm pore, the plateau continues only for 2 min, suggesting that the penetration of platinum complex anions is extremely fast.

In our previous study, it was reported that the platinum complex anion is strongly accumulated when using the 4 nm pore. This accumulation is caused by a hydrophobic interaction between porous silicon and the complex. The results shown in the present study indicate that there exists a clear relation between the accumulation and the acceleration of mass-transfer within nanopore.

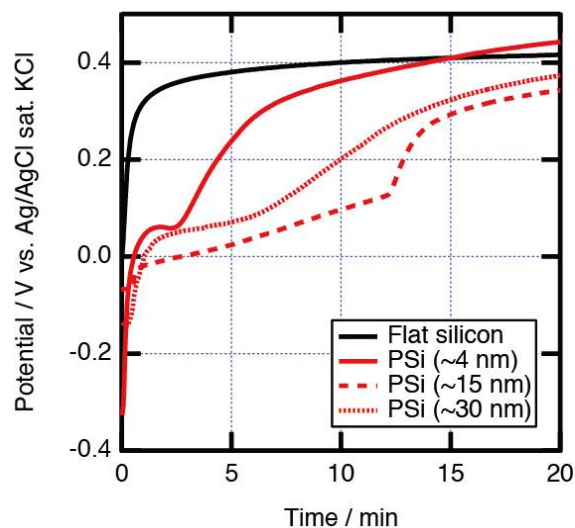


Figure 1. Time development of potential during platinum deposition. When using porous electrodes, potential plateau is observed. The potential plateau is caused by the penetration of platinum complex anions into nanopore.

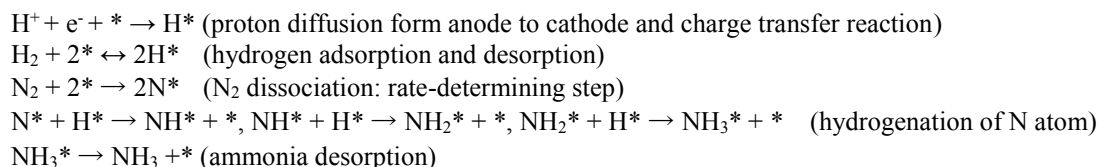
References

- [1] T. Fukutsuka et al., *Electrochim. Acta*, **199**, 380 (2016).
- [2] K. Fukami et al., *Chem. Phys. Lett.*, **542**, 99 (2012).
- [3] K. Fukami et al., *J. Chem. Phys.*, **138**, 094702 (2013).
- [4] A. Koyama et al., *J. Phys. Chem. C*, **119**, 19105 (2015).

Electrode Design and Performance Characteristics for Ammonia Electrochemical Synthesis with Proton-Conducting Solid Electrolyte Fuel Cells

Junichiro Otomo*, Fumihiko Kosaka, Akio Oikawa and Chien-I Li
Department of Environment Systems, Graduate School of Frontier Sciences,
The University of Tokyo
5-1-5 Kashiwanoha, Kashiwa, Chiba 277-8563, Japan
* otomo@k.u-tokyo.ac.jp

Nowadays ammonia attracts great attention as a promising green energy carrier/storage medium of hydrogen because of high energy density and easy liquefaction. In this report, we discussed a direct electrochemical synthesis of ammonia using proton-conducting solid electrolyte fuel cells with yttrium-doped barium cerate (BCY) in terms of electrode design and performance characteristics. In our previous studies, metal catalysts such as Ru and Fe were investigated in terms of electrode design, i.e., nanoparticle formation [1, 2] and cermet structures [3] for the electrode catalysts were tested. As for metal nanoparticle catalyst, we used Ru-doped BaCe_{0.9}Y_{0.1}O₃ (BCYR) [2]. The formation of 1–10 nm Ru nanoparticles on the BCYR surface was observed after a heat-treatment in a reducing atmosphere. Ammonia formation rate per active amount of Ru nanoparticles with BCYR showed good performance, but ammonia formation rate per electrode area was still low (~10⁻¹¹ mol/s cm²). In this study, to improve the electrode performance further, we rather focused on cermet electrodes of Fe-BCY and Ru-BCY prepared by the infiltrated method, in which BCY particle networks were covered by Ru or Fe catalyst. When supplying pure N₂ to the cathode side, ammonia formation was observed with an increase in cathodic polarization, but slow ammonia formation rate was observed (~10⁻¹¹ mol/s cm²). On the other hand, significant improvement of ammonia formation rate with cathodic polarization was observed when supplying a N₂/H₂ gaseous mixture to the cathode side. With Fe-BCY electrode, ammonia formation rate increased with an increase in cathodic potential at high temperatures > 650°C. Moreover, further improvement of ammonia formation rate was observed with K addition in Fe-BCY electrode and the rate exceeded 10⁻¹⁰ mol/s cm² at higher potentials than 500 mV. Dissociation of N₂ molecule on Fe catalyst will be a rate-determining step, which may be promoted by cathodic polarization. A kinetic model proposed based on the following mechanism can explain the experimental results adequately.



With Ru-BCY electrode, the extent of promotion for ammonia formation rate in a N₂/H₂ gaseous mixture was not so significant in comparison with that of Fe-BCY electrode. The reason is probably due to a reverse reaction, i.e., ammonia decomposition reaction on Ru-BCY electrode. For further improvement, the electrode structures (thickness and Ru loading amount) should be optimized, which can also increase Faraday efficiency.

Acknowledgements

This work was supported by CREST, Japan Science and Technology Agency (JPMJCR1441).

References

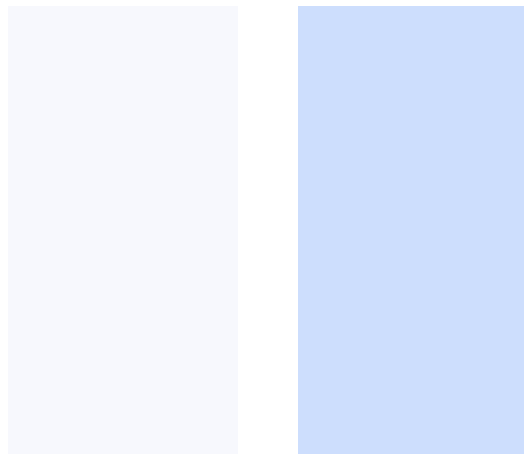
- [1] J. Otomo, N. Noda, F. Kosaka, ECS Trans., 68(1), 2663 (2015).
- [2] F. Kosaka, T. Nakamura, J. Otomo. J. Electrochem. Soc., 164(13) F1323 (2017).
- [3] F. Kosaka, T. Nakamura, A. Oikawa, J. Otomo, ACS Sus. Chem. Eng. 5(11) 10439 (2017).

Development of Polarization Curve Evaluation System Using Inverse Analysis

Tsubasa Ishii and Kenji Amaya

Department of Systems and Control Engineering, School of Engineering, Tokyo Institute of Technology
2-12-1-W8-36, O-okayama, Meguro-ku, Tokyo, 152-8550, Japan
tishii@a.sc.e.titech.ac.jp

A novel method to identify accurate polarization characteristics for ion concentration dependent electrochemical reaction was developed. This method identifies a polarization curve which is dependent of ion concentration on the surface of an electrode. Since the concentration of the electrode surface cannot be measured directly, a rotating disk electrode is used to control and evaluate the concentration at the electrode surface.¹ However, when the concentration becomes nonuniform on the electrode,^{2,3} the method for evaluating the concentration-dependent characteristic of the polarization curve has not been established. In the proposed method, an inverse problem approach is applied to evaluate the concentration dependent characteristic of the polarization curves. As the observation information of this inverse problem, total currents on the electrode are measured with various bulk concentration. The unknown polarization curve is expressed with parametric piecewise linear function. The fluid velocity field and the concentration field around the electrode are modeled by the Navier-Stokes equation and the advection-diffusion equation. These equations are solved by the finite volume method and the total currents are calculated as shown in fig. 1. By minimizing the difference between experimental and simulational currents, inverse analysis for identifying the concentration dependent characteristic of the polarization curve is performed. In order to verify the proposed method, identification using both phantom data and experimental data were performed. The verification result as shown in fig. 2 showed the good accuracy of the method.



a) Velocity field b) Concentration field

Fig. 1 The results of simulation around the electrode

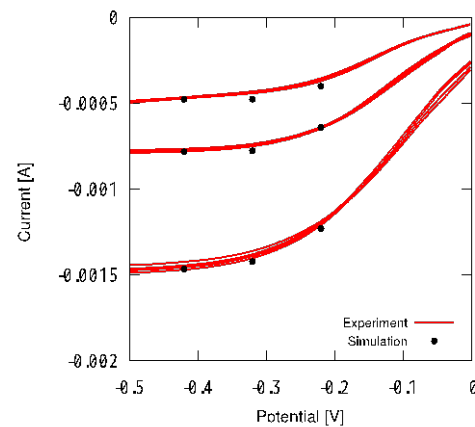


Fig. 2 Comparison of experiment data and simulation result using identified polarization curves

References

- (1) A. J. Bard and L. R. Faulkner, (2000), *Electrochemical Methods: Fundamentals and Applications*, 2nd ed, New York: John Wiley & Sons
- (2) T. P. Moffat and D. Josell, Extreme Bottom-Up Superfilling of Through-Silicon-Vias by Damascene Processing: Suppressor Disruption, Positive Feedback and Turing Patterns, *Journal of The Electrochemical Society*, 159(2012), pp. D208–D216.
- (3) D. Josell and T. P. Moffat, Superconformal Bottom-Up Nickel Deposition in High Aspect Ratio Through Silicon Vias, *Journal of The Electrochemical Society*, 163(2016), pp. D322–D331.

Electro-catalytic Performance in Toluene Hydrogenation Electrolyzer for Energy Carrier Synthesis

Kensaku Nagasawa¹, Junpei Koike², Yuta Inami³, Ichiro Yamanaka³, Yoshiyuki Kuroda², and Shigenori Mitsushima^{1,2}

¹*Institute of Advanced Sciences, Yokohama National University, 79-5 Tokiwadai, Hodogaya-ku, Yokohama 240-8501, Japan*

²*Green Hydrogen Research Center, Yokohama National University, 79-5 Tokiwadai, Hodogaya-ku, Yokohama 240-8501, Japan*

³*School of Materials and Chemical Technology, Tokyo Institute of Technology, 2-12-1 Ookayama, Meguro-ku, Tokyo 152-8550, Japan*
nagasawa-kensaku-st@ynu.ac.jp

Introduction

The hydrogen electrosynthesized using renewable energy such as wind or solar power has been expected as the green energy to solve global warming. The large-scale hydrogen transport and storage system has been considered the important technology to solve the regional and horary imbalance of energy supply in global scale. We have studied the high-efficient electrolytic direct-hydrogenation of toluene with water decomposition for the organic hydride system^{1,2}. This method has the advantages of small theoretical decomposition voltage with no exothermic heat loss compare with the conventional 2-step hydrogenation with the water electrolysis. In this study, we have investigated the electrocatalytic performance of Pt/C, PtRu/C and IrRu/C cathode catalysts using toluene hydrogenation electrolyzer to improve electrochemical reaction.

Experimental

Anode, cathode, and proton exchange membrane (PEM) were used DSE[®](De Nora Permelec ltd) for the oxygen evolution, carbon paper (10BC, SGL carbon ltd.) applied Pt/C(TEC10E50E, TKK), PtRu/C(TEC61E54, TKK) or IrRu/C catalyst with ionomer, and Nafion 117[®], respectively. Reversible hydrogen electrode (RHE) was set in the anode compartment. The carbon paper was loaded the 0.02 mg cm⁻² of Pt by the impregnation method before electrocatalyst coating. The cathode was hot-pressed on the PEM at 120 °C and 1 MPa for 3 min to fabricate a membrane cathode assembly. During the electrolyzer operation, the anode and cathode compartments were circulated 1 mol dm⁻³ H₂SO₄ at 10 ml min⁻¹ and 10% toluene–methylcyclohexane at 5 ml min⁻¹, respectively. The electrochemical measurements were chronoamperometry and electrochemical impedance spectroscopy (EIS) at 60 or 80°C.

Results and discussion

Figure 1 shows the cathode polarization curves 60 and 80°C. The order of cathode potential was IrRu/C>PtRu/C>Pt/C at the both of 60 and 80°C, and IrRu/C showed the best performance in all cathode catalysts. Especially, the advantage of cathode performance for IrRu/C was larger at 80°C than at 60°C. On the other hand, the difference of cathode potential between Pt/C and PtRu/C at 80°C was significantly smaller than 60°C. High performance of IrRu/C might originated from the selective catalytic-functions, which are the H_{ad} generation on Ir atomic-surface from the migrated proton and the toluene hydrogenation on Ru atomic-surface with the H_{ad} supplied from Ir atomic surface with synergetic effect, while the role of Pt and Ru of PtRu/C would not so clear³.

Acknowledgements

This work was supported by New Energy and Industrial Technology Development Organization (NEDO). The Institute of Advanced Sciences (IAS) in YNU is supported by the MEXT Program for Promoting Reform of National Universities.

References

1. S. Mitsushima, Y. Takakuwa, K. Nagasawa, Y. Sawaguchi, Y. Kohno, K. Matsuzawa, Z. Awaludin, A. Kato, and Y. Nishiki, *Electrocatalysis*, 7, 127 (2016).
2. K. Nagasawa, A. Kato, Y. Nishiki, Y. Matsumura, M. Atobe, S. Mitsushima, *Electrochim. Acta* 246, 459 (2017).
3. Y. Inami, H. Ogihara, I. Yamanaka, *ChemistrySelect*, 2, 1939 (2017).

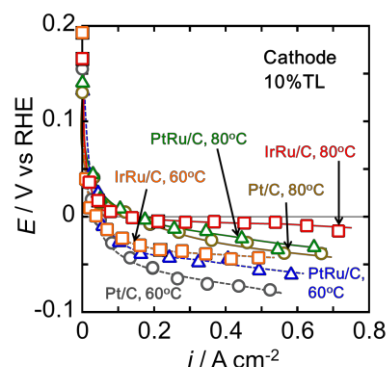


Figure 1 cathode polarization curves with 10 % toluene concentration at 60 and 80°C.

Ultra-Fine Tuning of Plasmonic Properties for Au Nano-Structures via Electrochemical Method

Shumpei Oikawa, and Hiro Minamimoto, and Kei Murakoshi
Department of Chemistry, Faculty of Science, Hokkaido University,
060-0810, Sapporo, Hokkaido, Japan
kei@sci.hokudai.ac.jp

Under the illumination of the visible or near-infrared light onto metal nano-structures, the unique optical properties can be appeared due to the excitation of the localized surface plasmon resonance (LSPR). Especially for the case of the dimer structure, the strong light energy concentration at its gap is induced and, thus, the various applications have been expected. It is well known that the characteristics of the dimer strongly depend on its shape and gap distance. Very interestingly, when the gap distance is down to sub-nm, the intensity of the generated nearfield at the gap is extremely enhanced. In addition to this, with the gap distance of less than 1 nm, the charge transfer plasmon (CTP) and the bonding quadrupole plasmon (BQP) which can suppress the light scattering are generated because of the effect of the tunneling electrons [1]. From these backgrounds, it can be expected that the precise control of the gap distance can be applied for many various nano-photonics technologies, such as photovoltaic devices. Although many nano-fabrication technique has been established, the sub-nm scale structure control is still a challenge. As our previous study, we have succeeded in reversible control of the Au nano-dimer structures with atomic resolution via electrochemical under potential method [2]. Moreover, we have also tried to control of the gap distance through electrochemical Au oxidation reaction [3]. In this study, for the further investigation of the previous technique, we have attempted to establish the novel approach for the control of the gap distance and the shape of well-defined Au nano-dimer structures in a single nanometer scales by the control of the electrochemical oxidation reaction. For the detail discussion about the optical property depending on the structure change, in-situ electrochemical dark-field microscopic measurements were conducted.

Well-defined Au nanodimer structures were fabricated on a conductive glass substrate using the electron beam lithography method. Figure 1a and b shows the prepared Au nano-briged structures obtained before and after electrochemical dissolution. The time series scattering spectra obtained during electrochemical reactions were collected via the dark-field microscopy observation (Fig. 1b). The electrode potential was set to 0.74 V vs. Ag/AgCl for the dissolution of Au. SEM images clearly prove the formation of the gap between Au nanoparticles. From the time series scattering spectra of Au nanodimer, the drastic optical property changes has been observed at the polarization time of around 400 s. Considering the strong suppression of the light scattering at 420 s, this optical property change would be corresponded to the plasmon mode change from charge transfer mode to bonding dipolar mode caused and the appearance of the BQP mode by the formation of the sub-nm gap at Au nanodimer. Consequently, we now believe that our method would become a useful tool for controlling the shape and the gap distance between Au nanoparticles in a single nanometer scales.

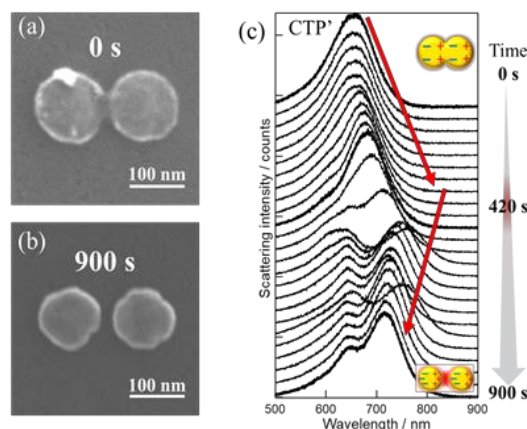


Figure 1. SEM images of Au nanodisk dimer obtained (a) before ($t = 0$ sec) and (b) after dissolving ($t = 900$ sec). WE, CE and RE were prepared Au nanodisk substrate, Pt and Ag/AgCl, respectively. Electrolyte solution was 10 mM KBr aq. Thickness, gap distance of Au nanodisk dimer are 50 nm and -5 nm, respectively. The diameter of single Au nanodisk is 125 nm. (c) The time series scattering spectra collected during Au dissolution.

References

- [1] K. J. Savage, *et al.*, *Nature*, 491 (2012), 574, S. A. Maier *et al.*, *Nano Lett.*, 12 (2012), 1683.
- [2] S. Oikawa, H. Minamimoto, and K. Murakoshi, *Chem. Lett.*, 46 (2017), 1148.
- [3] S. Oikawa, H. Minamimoto, X. Li, and K. Murakoshi, *Nanotechnology*, *in press*, doi: 10.1088/1361-6528/aa9e78.

Electrodeposition of patterned hydrogels using an LSI-based electrochemical devices for biosensing and cell culture

Kosuke Ino¹, Mayuko Terauchi², Mai Gakumasawa¹, Hitoshi Shiku^{1,2}

¹ Graduate School of Engineering, Tohoku University, 6-6-11-406, Aoba-ku, Aramaki-aza Aoba, Sendai 980-8579, Japan

² Graduate School of Environmental Studies, Tohoku University, 6-6-11-604, Aoba-ku, Aramaki-aza Aoba, Sendai 980-8579, Japan

kosuke.ino@tohoku.ac.jp

We previously reported a large-scale integration (LSI) device (Fig. 1), which is designated as a Bio-LSI device [1], for cell analysis based on amperometry. Since 400 electrochemical sensors are incorporated into the device with a 250- μm pitch, the device can be applied for real-time electrochemical imaging [2]. In previous studies, the device was successfully applied for electrochemical imaging of cell activity of cell spheroids, such as cell differentiation of embryonic stem cells and dopamine release from neuron-like cells. In addition, the device was applied for simultaneous imaging of enzyme and respiration activities in these cell spheroids [3]. Since the each sensor can control concentrations of chemicals on the electrode, the device can be applied for another bioapplications. In the present study, the device was applied to fabricate hydrogels with designed shapes for biosensing and cell culture.

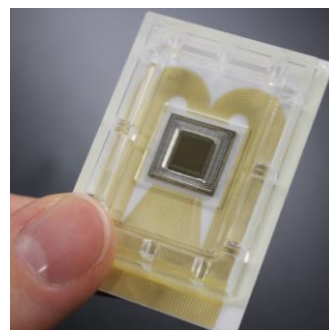


Fig. 1 Device image.

Hydrogels are widely utilized for biosensing and tissue engineering. We previously reported three-dimensional (3D) hydrogels using electrodeposition [4]. Since a potential can be applied at desired sensors on the LSI device, in the present method, designed hydrogels were electrodeposited on the device. For hydrogel electrodeposition, we utilized an anodic method to deposit chitosan hydrogels reported by the group in University of Maryland reported [5]. In the method, reactive chlorine species (e.g., HOCl) is generated via the electrolysis of chloride, so that chitosan is oxidized to form chitosan hydrogels on the electrode. As a demonstration, two-dimensional patterned hydrogels were fabricated. On the device with the hydrogels, mammalian cells were cultured, so that patterned cell sheets were successfully fabricated. Thus, the device with the hydrogels is useful as a cell culture platform. In addition, 3D complex hydrogels were also fabricated on the device by sequential formation of designed hydrogels. The hydrogels will be utilized for fabrication of 3D tissue organs. As another application for biosensing, the hydrogel fabrication was utilized for local enzyme modification, such as glucose oxidase (GOx) and horseradish peroxidase (HRP). The enzyme-modified device was successfully applied for detection of glucose and H_2O_2 . In the future, the enzyme-modified device will be utilized for cell analysis. Thus, the local hydrogel fabrication on the device is useful for bioapplications.

Acknowledgements: This work was partially done in the Matsue lab in Tohoku University. This work was supported in part by supported by the Special Coordination Funds for Promoting Science and Technology, Creation of Innovation Centers for Advanced Interdisciplinary Research Areas Program from the Japan Science and Technology Agency.

References

- [1] Inoue KY et al., Advanced LSI-based amperometric sensor array with light-shielding structure for effective removal of photocurrent and mode selectable function for individual operation of 400 electrodes, *Lab Chip*, 15, 848, 2015.
- [2] Ino K et al., Electrochemical motion tracking of microorganisms using a large-scale integration (LSI)-based amperometric device, *Angew. Chem. Int. Ed.*, 56, 6818, 2017.
- [3] Kanno et al., Electrochemicolor imaging using an LSI-Based device for multiplexed cell assays, *Anal. Chem.*, in press. DOI: 10.1021/acs.analchem.7b03042.
- [4] Ozawa F et al., Cell sheet fabrication using RGD peptide-coupled alginate hydrogels fabricated by an electrodeposition method, *Chem. Lett.*, 46, 605, 2017.
- [5] Gray KM et al., Electrodeposition of a biopolymeric hydrogel: potential for one-step protein electroaddressing. *Biomacromolecules*, 13, 1181, 2012.

ORR activity of epitaxial and polycrystalline $\text{La}_{0.7}\text{Sr}_{0.3}\text{Mn}_{1-x}\text{Ni}_x\text{O}_3$ thin films fabricated by pulsed laser deposition

Yoshitaka Aoki, Damian Kowalski, Hiroki Habazaki
Faculty of Engineering, Hokkaido University
N13W8 Kita-ku, Sapporo, 060-8628 Japan
y-aoki@eng.hokudai.ac.jp

In recent years, zinc-air secondary batteries have attracted much attention as an alternative to lithium ion batteries due to the exclusively high energy density. A large overvoltage of the oxygen reduction reaction (ORR) and the oxygen evolution reaction (OER) at the air electrode is one of issues for zinc-air batteries to be technologically-viable. Precious metals, such as Pt and Ru have been known to be a good electrocatalysts for these electrode reactions, however, for the natural resource scarcity, it is desirable to realize the high catalytic activity by using more abundant transition metals. Hence it is strongly motivated to develop a noble-metal-free electrode with high catalytic activity for OER and ORR. In recent years, a number of perovskite type transition metal oxides have been studied for ORR and/or OER electrocatalysts, and some of them have been found to be promising for air electrode materials of zinc-air batteries. However, in many of them, fundamental catalytic mechanisms including active sites or rate-limiting steps for the catalytic reaction are remained unclear. Perovskite-type manganese $\text{La}_{0.7}\text{Sr}_{0.3}\text{Mn}_{1-x}\text{Ni}_x\text{O}_3$ (LSMN; $x = 0 - 0.5$) are one of candidates of air electrode catalysts due to their excellent ORR electrocatalytic activity. Recently, we demonstrated that the ORR activity of $\text{La}_{0.7}\text{Sr}_{0.3}\text{Mn}_{1-x}\text{Ni}_x\text{O}_3$ is dependent on x and the highest activity is achieved at $x = 0.1$. Furthermore, 4-electron-transfer ORR reaction is driven on the phase with $x=0.1$ under potentials below 0.85 V vs. RHE without aids of carbon. Hence, it is of fundamental and of technological important to figure out the catalytic mechanism of the perovskite phase. In this study, epitaxial and polycrystalline LSMN thin film electrodes were prepared by the PLD method and the ORR activity was investigated by combining electrochemical measurements and XPS analysis.

LSMN powder was synthesized by Pechini method. The obtained LSMN powders were mixed with a sintering aid, and the green pellets were prepared by uniaxially-press at 20 MPa, and were sintered at 1200 ° C for 12 h in air, which results in a dense sintered disc with relative density of > 97%. These sintered discs are used as a target for pulsed-laser-deposition (PLD). $\text{La}_{0.7}\text{Sr}_{0.3}\text{Mn}_{0.9}\text{Ni}_{0.1}\text{O}_3$ thin films (30 nm thickness) were deposited on a 0.5wt% Nb-doped SrTiO₃ (NSTO) single crystal (100) or a gold plate by PLD under optimized conditions. The obtained thin film was evaluated by XRD, AFM, XPS, TEM and the like. The thin film electrode was mounted on the rotor for the rotating disk electrode measurements. ORR and OER polarization measurements were carried out using an Hg/HgO reference electrode under oxygen saturation conditions in 4M KOH electrolyte solution.

From the XRD and TEM measurements, it was confirmed that LSMN thin film was epitaxially grown on NSTO substrate with a growth orientation of (011). On the other hand, the thin film deposited on the Au substrate was polycrystalline. EDX measurement reveal that the chemical composition of both films is identical to the target, and XPS measurement confirms that the valence states of Mn in both were quite similar each other and are equivalent to that of the powder sample. When the epitaxial film was potentiostatically polarized at 0.4 V vs RHE under O₂-saturation, the ORR current increased with the polarization time, and after 1 hour, the current reached to twice of the initial current flows. On the other hand, when a similar experiment was conducted on a polycrystalline film, very small increment was observed. XPS clarified that Mn valence state in the epitaxial film was reduced by the cathodic polarization, suggesting that such low valence Mn sites would play an important role for the ORR reaction.

Co@NC Core-Shell as an Efficient and Ultra-Durable Oxygen Electrode in Water Electrolyzer

Arumugam Sivanantham, Sangaraju Shanmugam*

Department of Energy Science & Engineering, Daegu Gyeongbuk Institute of Science & Technology (DGIST), Daegu, 42988, Republic of Korea.

E-mail: sangarajus@dgist.ac.kr.

Oxygen electrode widely plays a key role in the various renewable energy technologies, such as batteries, fuel cells and water electrolyzers.^[1] Water electrolysis is an efficient and eco-friendly method to produce the alternative clean energy of H₂ fuel for the universal energy applications. So, the development of remarkable oxygen electrode is a new challenge in the advanced materials and energy research.^[2] Recently, we developed the Prussian blue analogue-derived nitrogen-doped nanocarbon (NC) layer-trapped, cobalt-rich, core-shell nanostructured (Co@NC) electrocatalysts as a promising oxygen anode catalyst in the water electrolysis.^[3] The core-shell Co@NC electrocatalyst exhibits a remarkable oxygen evolution activity (OER) and stability as compared to the different commercial noble electrocatalysts of IrO₂ and RuO₂ during alkaline water electrolysis. The core-shell Co@NC/Nickel foam oxygen electrode shows overpotential of 330 mV at the current density of 10 mA cm⁻², which is lower than that of IrO₂/Nickel foam and RuO₂/Nickel foam oxygen electrode, including an ultra-durability of over 400 h at 10 mA cm⁻². One step close to the real water electrolysis, the conventional water electrolyzer has constructed using the commercial Pt/C/Ni foam electrode as a cathode with core-shell Co@NC-anode. It delivers 10 mA cm⁻² at a cell voltage of 1.59 V, which is 70 mV lower than that of the noble IrO₂-anode replaced water electrolyzer in alkaline electrolyte (Fig.1a). Over the long-term chronopotentiometry durability testing, the core-shell Co@NC-anode electrolyzer shows only 60 mV cell voltage loss (4%) even after 350 h of continuous cell operation at 10 mA cm⁻² current density (Fig. 1b). But, the IrO₂-anode water electrolyzer shows 230 mV (14%) cell voltage loss at a short term water electrolysis of 95 h, which indicates core-shell Co@NC is a suitable oxygen electrode to replace noble metal based anodes in alkaline water electrolysis. In conclusion, our findings indicate that the Prussian blue analogue is a class of metal(s) unified (small) organic ligands that can be used to derive metal-rich, N-doped nanocarbon layer surrounded, core-shell electrocatalysts with single and multiple active centers.

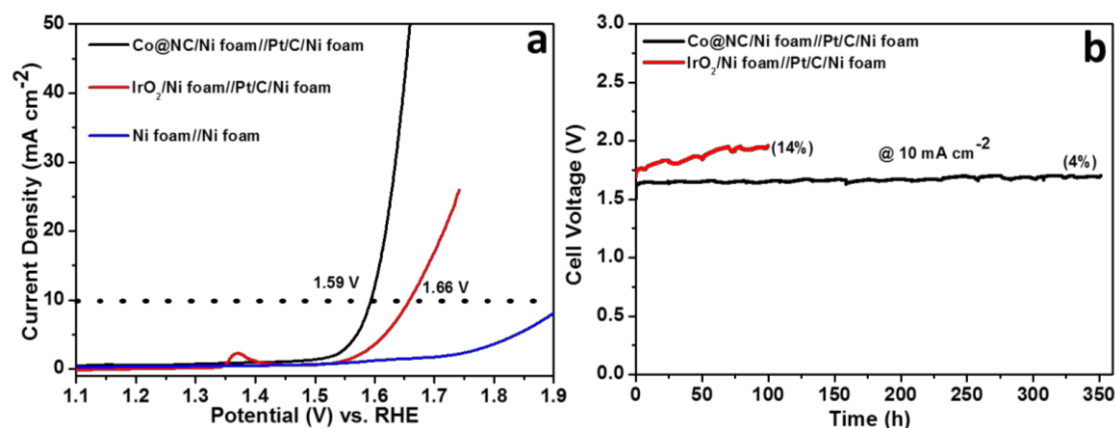


Figure. Water Electrolysis: (a) Linear Sweep Voltammograms (LSVs) and (b) Chronopotentiometry durability test @ 10 mA cm⁻².

References:

1. P. G. Bruce, S. A. Freunberger, L. J. Hardwick, J. M. Tarascon, *Nature Mater.*, 2012, 11, 19.
2. A. Sivanantham, P. Ganesan, S. Shanmugam, *Adv. Funct. Mater.*, 2016, 26, 4661.
3. A. Sivanantham, P. Ganesan, L. Estevez, B. P. McGrail, R. K. Motkuri, S. Shanmugam, *Adv. Energy Mater.*, 2017, DOI: 10.1002/aenm.201702838.

Exothermic reaction promoted production of hierarchical porous carbon for electrochemical energy storage and conversion

Chunyu Zhu, Manami Takata, Cheong Kim, Jinhui Cao, Yoshitaka Aoki, and Hiroki Habazaki
Hokkaido University
Kita-13, Nishi-8, Kita-ku, Sapporo 060-8628, Hokkaido, Japan
chunyu6zhu@eng.hokudai.ac.jp

To meet the growing demands for energy consumption and environmental conservation, the development of high-performance, low-cost and environment-friendly electrochemical energy storage and conversion devices, such as supercapacitors, lithium ion batteries and fuel cells, are becoming increasingly more important. The applications of different electrochemical energy storage and conversion devices in specific situations are all primarily reliant on the electrode materials, especially on carbon materials. Recently, porous carbon materials have attracted significant attentions in various electrochemical electrodes because of their attractive properties, such as ready abundance, chemical and thermal stability, easy processability. In particular, the well-designed hierarchical porous carbon (HPC), with three-dimensionally interconnected multi-pores of micro-, meso- and macropores, has been recognized as the most attractive electrode material for achieving high-performance supercapacitors, lithium ion battery anode, and oxygen reduction electrocatalyst. In such a hierarchical structure, the abundant micro- and mesopores provide high accessible surface areas and active sites for electrochemical reactions and processes, while the interconnected meso- and macropores facilitate the fast ion transport by supplying ion-buffering reservoirs and ion-transport pathways. In this circumstance, the development of simple, inexpensive and effective synthetic methods for preparing HPC with well-designed porosity is of great interest. Therefore, in this study, we will present our recent work on the preparation of HPC with well-controlled porosity by facile and effective processes, which are promoted by exothermic reactions, especially by employing biomass carbon resources. The applications of the HPC for supercapacitor, lithium ion battery anode, and oxygen reduction electrocatalyst will be demonstrated.

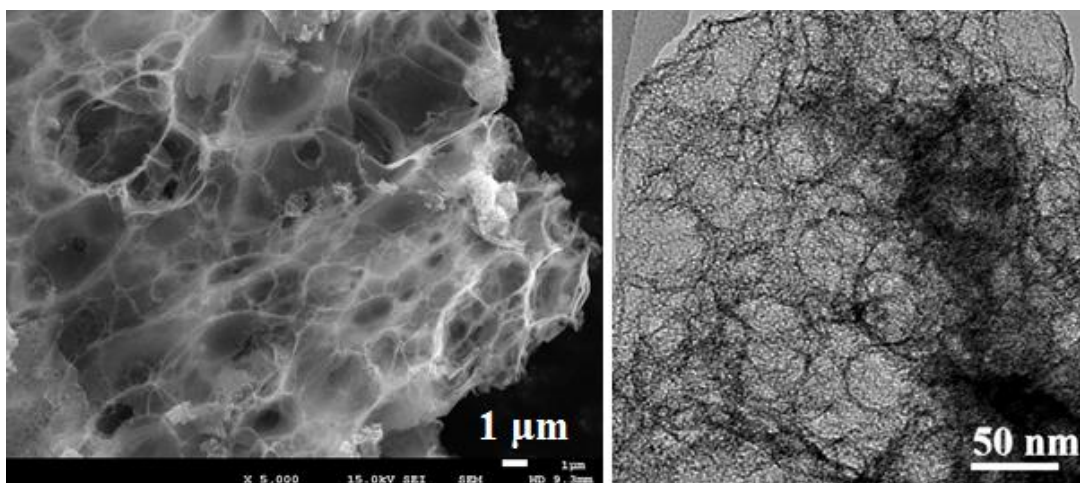


Figure. The typical SEM and TEM images of as-prepared HPC with hierarchical pore structure.

Reference:

1. C. Zhu, C. Kim, Y. Aoki, H. Habazaki. *Advanced Materials Interfaces*, 4 (2017) 1700583.
2. C. Zhu, Y. Aoki, H. Habazaki. *Particle & Particle Systems Characterization*, (2017) 1700296.
3. C. Zhu, T. Akiyama. *Green Chemistry*, 18 (2016) 2106-2114.

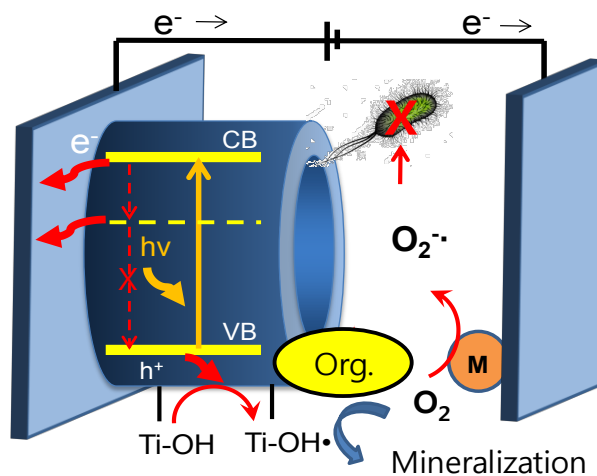
Photoelectrochemical Reactor for Degradation of Organic Compounds and Disinfection Based on Self-doped TiO₂ Nanotubes

Kangwoo Cho^{1,*}, William¹, Seok Won Hong²

¹ Division of Environmental Science and Engineering, Pohang University of Science and Technology (POSTECH), Pohang 790-784, Korea.

² Center for Water Resource Cycle Research, Korea Institute of Science and Technology, P.O. Box 131, Cheongryang, Seoul 130-650, Korea.
e-mail address: kwcho1982@postech.ac.kr (corresponding author)

Electrochemical self-doping or cathodization may prove to be a viable way to enhance the photoelectrochemical activities of TiO₂ for water treatment. We herein provide the proof-of-concept for reactors for degradation of organic compounds and disinfection, utilizing the self-doped titanium nanotube photoanode as a core component. The effects of primary doping conditions were systematically interrogated with respect to the physico-chemical properties and water treatment efficacy of titanium nanotube array (TNA). TNA prepared by anodization of Ti foil was subject to variable self-doping regimes and the rates of model organic compounds degradation and disinfection efficiency were assessed under photochemical (PC, UV or visible light), electrochemical (EC, potential bias of 1 V NHE), and photo-electrochemical (PEC) conditions. The self-doping of crystalline (anatase) TNA reduced the band gap to 2.4 eV (blue TNA), while the same sequence for amorphous TNA even further narrowed the gap to 1.4 eV (black TNA). The level of passed charge during the cathodization showed marginal influence. Depth profiles of X-ray photoelectron spectroscopy indicated that the dopants (Ti³⁺) were exclusively located on surface for the blue TNA, whereas they penetrated into the bulk tube structure for the black TNA which was accompanied with quasi-permanent lattice distortion as confirmed by X-ray diffraction patterns. Therefore, the electrical conductivity in terms of donor density was found to be greater for the black TNA. The buffering intensity of the cathodization electrolyte switch the relative level of proton intercalation in comparison with oxygen vacancy formation, which was demonstrated by time-of-flight and dynamic secondary ion mass spectrometry analysis. Consequently, the organics degradation was mostly faster on the black TNA, particularly in PC and PEC (with visible light) conditions. In contrast, the blue TNA allowed greater disinfection efficiency than the black one. The lower photocurrents of the blue TNA might be beneficial for the superoxide radical generation competing with the molecular hydrogen generation. The results of this study would broaden the usage of TiO₂ nanomaterials by tuning the physico-chemical characteristics depending on variable water treatment purposes (mineralization of organic compounds versus disinfection).



Spatially Resolved Electrochemical Analysis for Redox Activities of Graphene/Graphite Surface Structures

A. Kumatani^{1,2}, C. Miura², Y. Takahashi^{3,4}, T. Okada⁵, H. Ida², H. Shiku⁶, S. Samukawa^{1,5} and T. Matsue²

1. Advanced Institute for Materials Research (AIMR), Tohoku University, Japan.

2. Graduate School of Environmental Studies, Tohoku University, Japan.

3. Division of Electrical Engineering and Computer Science, Kanazawa University, Kanazawa, Japan.

4. Precursory Research for Embryonic Science and Technology (PRESTO),

Japan Science and Technology Agency (JST), Japan.

5. Institute for Fluid Science (IFS), Tohoku University, Japan.

6. Department of Applied Chemistry, Graduate School of Engineering, Tohoku University, Japan.

e-mail address: kumatani@bioinfo.che.tohoku.ac.jp, matsue@bioinfo.che.tohoku.ac.jp

Graphene, one atom thick of graphite layers, is known to have tremendous physical properties in energy harvesting applications by their high electrocatalytic reactions. One of keys to enhance their performance is to control their active structures precisely including their edges, defect and surface states at atomic level. In general, a conventionally available electrochemical characterization technique is applied in bulk sample by soaking the sample into electrolyte solution with reference and counter electrodes. It is therefore difficult to classify a key factor quantitatively at specified structures. In other words, a spatially resolved electrochemical analysis is necessary, which will be a sensitive measure for the electrochemical activities at atomic levels in graphene or other atomically thick energy materials.

In this study, to investigate local electrochemical activities on graphene/graphite surfaces under sub-micrometer scale, we have applied a self-developed scanning electrochemical cell microscopy with a 100 nm diameter single barrel nanopipette (SECCM) as a spatially resolved electrochemical characterization [1]. The SECCM utilizes a nanopipette filled with electrolyte and a quasi-reference/counter electrode (QRCE) as a probe. Once the pipette is proximately of the sample surface, a meniscus is made. The meniscus confines area where electrochemical activities are induced. For quantification of electrochemical activities in graphene/graphite surface structures, we have used a redox reaction of $\text{Ru}(\text{NH}_3)_6^{3+/2+}$ inside 5 mM hexaammine ruthenium chloride and 25 mM KCl in phosphate buffer or deionized water electrolyte as shown in Fig. 1(a). By applied voltage induced the redox reaction, we have visualized their electrochemical actives with both electrochemical and topographical information in Fig. 1 (b). The result showed that the mainly edges at graphene layers were more active than that at the basal plane. Moreover, the intensity of the redox reaction at the edges depended upon the number of layers, which was confirmed by the atomic force microscopy at the same measurement spot. At some area, the edge with two graphene layers were successfully measured. Additionally, by positioning the pipette at the area where the higher activities were observed, a cyclic voltammetry was also conducted at scan rate of 100 mV/s to compare the acuities between the edge and basal plane. Thus, the SECCM is a powerful spatially resolved electrochemical analysis for atomically control the surface structures in graphene.

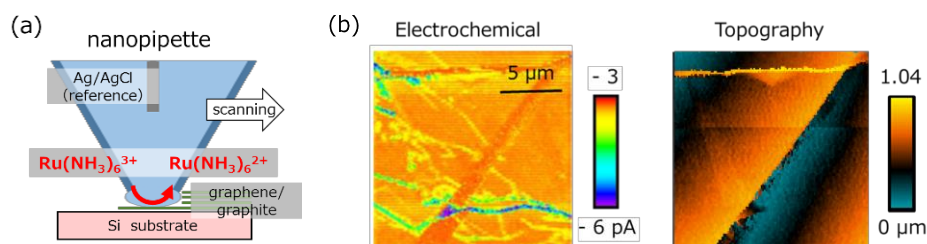


Fig.1 (a) A schematic of SECCM, (b) SECCM images of graphite/graphene surface: Electrochemical activities by redox reaction of $\text{Ru}(\text{NH}_3)_6^{3+/2+}$ (LEFT) and its topography (RIGHT)

Reference:

[1] Y. Takahashi, A. Kumatani *et al.*, Nat. Commun. 5:6450 (2014).

Recent Progress in Theoretical Understanding of Anode and Cathode Catalysts in Polymer Electrolyte Fuel Cells

Donald A. Tryk,^a Guoyu Shi,^a Shun Kobayashi,^a Ryo Shirasaka,^a Hiroshi Yano,^a Mitsuru Wakisaka,^b Junji Inukai,^a Toshihiro Kondo,^c Hiroyuki Uchida,^a Akihiro Iiyama,^a Masashi Matsumoto,^d and Hideto Imai^d

^aUniversity of Yamanashi, 4 Takeda, Kofu, Yamanashi 400-8510, Japan

^bToyama Prefectural University, 5180 Kurokawa, Imizu, Toyama 939-0398, Japan,

^cOchanomizu University, Ohtsuka, Bunkyo-ku, Tokyo 112-8610, Japan

^dDevice Analysis Department, Nissan ARC Ltd., 1, Natsushima, Yokosuka, Japan, 237-0061

Email address: donald@yamanashi.ac.jp

Recently, electrochemical data^{1,2} and a wide variety of in situ results, including FTIR³ and those employing synchrotron radiation⁴ have led to a deeper understanding of the Pt alloy catalysts used for the hydrogen oxidation reaction (HOR) and oxygen reduction reaction (ORR) in polymer electrolyte fuel cells (PEFCs). Density functional theory calculations have helped to explain the increasing order in HOR activity and CO tolerance: Pt < Pt-Ru < Pt-Ni < Pt-Co < Pt-Fe for alloys with specially stabilized Pt “skins” with x atomic layers, Pt_{xAL}-PtM/C.² Using realistic stepped (221) model surfaces, with (110) steps and (111) terraces, we have proposed a new type of metal-metal spillover mechanism, in which H₂ adsorbs dissociatively at the (110) steps and then diffuses to the (111) terraces, from which the 2H_{ad} desorb oxidatively to produce 2H⁺ (Fig. 1). This mechanism is supported by recent FTIR results for Pt_{xAL}-PtFe(221).³ In situ X-ray absorption spectroscopy (XAS) studies have led to a deeper understanding of both the structural and electronic properties of the nanoparticulate Pt_{xAL}-PtCo/C catalyst in comparison with Pt/C. All of the findings are consistent with the DFT calculations, including the weakened H and CO adsorption, and have also led to a better understanding of the H and CO bonding to these surfaces.

Recent work with Pt-Co(111) single crystals has shown a striking peak in activity for the ORR at the Pt-skin/Pt₇₃Co₂₇(111) surface, with a factor of 27 higher activity than that of a Pt(111) surface.⁵ Also, in situ surface X-ray scattering (SXS) measurements have indicated a highly distinctive sandwich structure in the surface Pt and Co underlayer, with grazing angle incidence photoelectron spectra showing significant charge transfer from Co to Pt, which is supported by the DFT calculations.

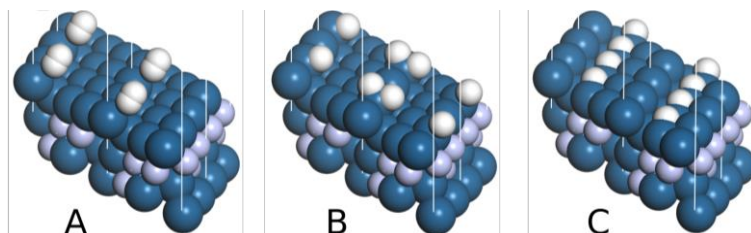


Figure 1. Atomic models of the Pt_{xAL}-PtCo(221) surface, showing (A) non-dissociative H₂ adsorption, (B) spontaneously dissociated 2H at the (110) step, and (C) 2H after diffusion to the (111) terraces.

This work was supported by the SPer-FC project from NEDO.

References

1. Shi, G.; Yano, H.; Tryk, D. A.; Watanabe, M.; Iiyama, A.; Uchida, H. *Nanoscale* **2016**, *8*, 13893-13897.
2. Shi, G.; Yano, H.; Tryk, D. A.; Iiyama, A.; Uchida, H. *ACS Catal.* **2017**, *7*, 267-274.
3. Ogihara, Y.; Yano, H.; Matsumoto, T.; Tryk, D.; Iiyama, A.; Uchida, H. *Catalysts* **2017**, *7*, 8.
4. Shi, G.; Yano, H.; Tryk, D. A.; Matsumoto, M.; Tanida, H.; Arao, M.; Imai, H.; Inukai, J.; Iiyama, A.; Uchida, H. *Catal. Sci. Tech.* **2017**, <https://doi.org/10.1039/C7CY01700F>.
5. Kobayashi, S.; Wakisaka, M.; Tryk, D. A.; Iiyama, A.; Uchida, H. *J. Phys. Chem. C* **2017**, *121*, 11234-11240.

Electrochemical Characteristics of Triphenylamine Derivative by Microelectrode Voltammetry

Shofu Matsuda, Yuuki Okuda, Yoshiki Obu, Minoru Umeda

Department of Materials Science and Technology, Graduate School of Engineering,
Nagaoka University of Technology, 1603-1 Kamitomioka, Nagaoka, Niigata 940-2188, Japan
mumeda@vos.nagaokaut.ac.jp

In the organic photoconductors for electrophotography such as digital copiers and laser-beam printers, triphenylamine and its derivatives are commonly used as a hole transport material. In recent years, they are expected to be employed in many functional organic devices. Hence, it is important to understand the stable state of the triphenylamine derivatives. In this study, we employed the 4-(2,2-diphenylethenyl)-*N,N*-bis(4-methylphenyl)-benzenamine (TPA) [1] and evaluated its electrochemical characteristics by microelectrode voltammetry.

We measured cyclic voltammograms of 5 mmol·dm⁻³ TPA in acetonitrile solution containing the supporting electrolyte of 0.1 mol·dm⁻³ tetraethylammonium perchlorate using Pt disk with the diameter of 300 μm and 10 μm, Pt coil, and Ag/AgCl as the working electrode, the counter electrode, and the reference electrode, respectively. The scan rate was 0.05 V·s⁻¹ and 1000 V·s⁻¹. The molecular orbital calculation of TPA was performed by the computational method using the software program Winmostar™ (X-Ability Co., Ltd.). For its structural optimization, a package of General Atomic and Molecular Electronic Structure System (GAMESS) was used.

In Fig. 1 (A), the first oxidation current is observed at ~0.85 V vs. Ag/AgCl along with a reduction current, which is indicative of the reversible electrode reaction. On the other hand, the second oxidation current is observed between 1.2 and 1.5 V vs. Ag/AgCl without a corresponding reduction current, implying that the reaction is irreversible. It should be noted that both of the first and second redox current peaks are observed in Fig. 1 (B). Based on the results of Fig. 2, the electronic state distribution is found to localize at the N-phenyl group and the C=CH group in the first and the second oxidation state of TPA, respectively. Therefore, this study demonstrated that the first oxidation state of TPA, which the electron distribution localizes at the N-phenyl group, is stable against the chemical reaction, while its second oxidation state, which the electron distribution localizes at the C=CH group, is unstable and would be broken by subsequent chemical reaction. Overall, the first oxidation state of TPA is suggested to show the stable hole conduction in organic photoconductors actually used in printing systems.

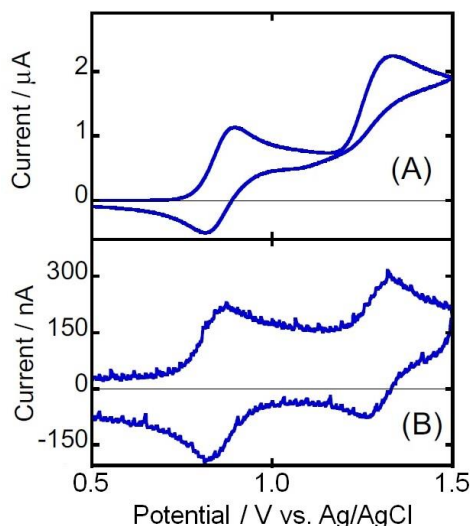


Fig. 1 Cyclic voltammograms of TPA at the scan rate of 0.05 V s⁻¹ (A) and 1000 V s⁻¹ (B).

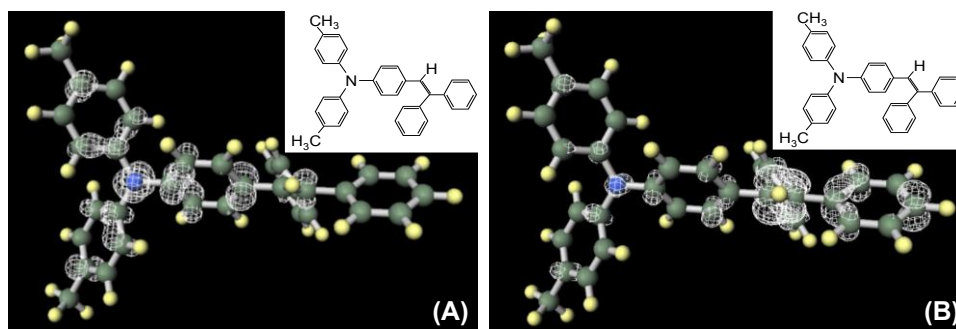


Fig. 2 The molecular orbitals of TPA at the energy level of the HOMO (A) and the second HOMO (B).

[1] T. Niimi, M. Umeda, *J. Phys. Chem. B* 106 (2002) 3657.

Electrochemistry of Precious Metals in Molten Sulfides

Mary Elizabeth Wagner, Antoine Allanore

Massachusetts Institute of Technology

77 Massachusetts Avenue, Cambridge, MA, USA 02139

mbwagner@mit.edu

Molten sulfides show promise as an alternative electrolyte for refining precious metals such as Au, Ag, and Pt. In the case of recycling from spent electronics, where these metals are used for data storage and conductivity, this provides a new, environmentally friendly way to recover these resources. Because of these metals' nobility in most systems, current recycling methods for electronic waste involve either hydrometallurgical or pyrometallurgical steps that are complicated, energy intensive, and harmful to the environment. However, recent results have shown molten sulfides can support stable electrochemical signals for the reduction of both Au and Ag.

Experimental data show that molten sulfides may act as a common solvent for both Au and Ag. Two solvents were tested and successfully demonstrated individual metal solubility comparable to their respective industrial solvents such as aqua regia or nitric acid. Na₂S-ZnS (54 mol% Na₂S at 800°C) and BaS-Cu₂S (80 mol% BaS at 1300 °C) were demonstrated to be successful solvents. Electrochemical experiments have shown that Na₂S-ZnS is a stable supporting electrolyte that can allow for the oxidation of Ag at the anode and the reduction of Ag ions into Ag metal at the cathode. Likewise, Na₂S-ZnS can also act as a successful supporting electrolyte for the electrowinning of Au ions in the molten sulfide into Au metal at the cathode.

Current work focuses on defining the electrochemical nature of Ag and Au in molten sulfide electrolytes, including the thermodynamics and kinetics of the reaction, how Ag and Au complex with molten sulfides, and where Ag and Au are placed on the reactivity series for sulfides with respect to other metals such as Cu and Fe. Progress made in thermodynamic modeling of high temperature systems, as well as experimental results that demonstrate the viability of molten sulfides as a new route for electronic waste recycling, will be discussed.

Electrodeposition of Al–W Alloys and Surface Modification by Anodization

Shota Higashino, Masao Miyake, Takumi Ikenoue, and Tetsuji Hirato
Graduate School of Energy Science, Kyoto University
Yoshida-honmachi, Sakyo-ku, Kyoto, 606-8501, Japan
higashino.shota.84u@st.kyoto-u.ac.jp

Aluminum–tungsten (Al–W) alloys have attracted significant attention as corrosion-protective coatings for reactive materials such as Mg alloys[1–4]. Recently, we reported that dense Al–W alloy films with high W content can be electrodeposited from 1-ethyl-3-methylimidazolium chloride (EMIC)–aluminum chloride (AlCl₃) ionic liquids containing tungsten (II) chloride, W₆Cl₁₂[3, 4].

In this study, we explored the feasibility of anodizing Al–W alloys, with the aim of enhancing their corrosion resistance and mechanical strength as well as providing the films with additional functionalities. Anodization is a well-known surface modification technique for Al metal. Anodization of Al metal yields a porous Al₂O₃ layer on its surface, and enhances the corrosion resistance and mechanical strength of the Al material. Anodization of Al–W alloys should yield a porous Al₂O₃ layer containing WO₃. WO₃ is a photocatalytic material sensitive to visible light and catalyzes the decomposition of organic compounds under visible light illumination. Therefore, the electrodeposition and anodization of Al–W alloy films can yield corrosion-protective coatings with additional self-cleaning functionalities. We also investigated the microstructure and other physical properties of the porous layer obtained by anodization of the Al–W alloy films under different conditions.

Al–W alloy films containing ~12 at.% W were electrodeposited in an EMIC–AlCl₃ ionic liquid containing W₆Cl₁₂. Anodization of the Al–W alloy films was performed in a 0.3 mol/L oxalic acid solution. The scanning electron microscope images of the films revealed that pores with diameters of <30 nm were formed. The anodized films displayed bright interference colors, which varied depending on anodization conditions. The corrosion resistance and mechanical strength of the anodized films were investigated by anodic polarization and nano-indentation, respectively. The anodized films showed significantly higher pitting-corrosion potential and hardness than pure Al metal. These results indicate that anodization of Al–W alloys is beneficial for their practical applications.

References

- [1] T. Tsuda, Y. Ikeda, T. Arimura, M. Hirogaki, A. Imanishi, S. Kuwabata, G. R. Stafford, and C. L. Hussey, *J. Electrochem. Soc.*, **161**, D405 (2014).
- [2] K. Sato, H. Matsushima, and M. Ueda, *ECS Trans.*, **75**, 305 (2016).
- [3] S. Higashino, M. Miyake, H. Fujii, A. Takahashi, and T. Hirato, *J. Electrochem. Soc.*, **164**, D120 (2017).
- [4] S. Higashino, M. Miyake, A. Takahashi, Y. Matamura, H. Fujii, R. Kasada, and T. Hirato, *Surf. Coat. Technol.*, **325**, 346 (2017)

Surface Analysis of Li metal Anode in Lithium Metal Rechargeable Battery using $\text{Li}_4\text{Mn}_5\text{O}_{12}$ as Cathode

Motoko Nagasaki¹, Takuya Masuda², Kei Nishikawa², Hirokazu Munakata¹, Kiyoshi Kanamura¹

¹Graduate School of Urban Environmental Sciences, Tokyo Metropolitan University, 1-1 Minami-Ohsawa Hachioji, Tokyo 192-0397, Japan

²National Institute for Materials Science, 1-1, Namiki, Tsukuba 305-0044, Japan
mnagasaki@inorg777.apchem.ues.tmu.ac.jp

The surface of the Li metal anode obtained from Li / 3DOM (1 mol dm^{-3} LiPF_6 / EC) / $\text{Li}_4\text{Mn}_5\text{O}_{12}$ laminate cells before and after charge and discharge cycle were analyzed by X-ray photoelectron spectroscopy (XPS). The XPS spectra indicate that the products of electrolyte components, like LiF , $\text{Li}_x\text{PF}_y\text{O}_z$, and the organic compounds containing ketone, ether and hydrocarbon structures exist on the surface of Li metal anode after discharge and charge cycle. The structural model for the Li metal surface was proposed based on our XPS study.

1. Introduction

The Li metal is a desired anode material because of its low oxidation-reduction potential and high capacity density (3861 mA h g^{-1}). Unfortunately, the Li metal anode has not been utilized in practical rechargeable batteries because of dendritic lithium deposits formed during discharge and charge cycles. The dendritic lithium metal results in low cycleability and poor safety. In this study, chemical state of Li metal anode surface obtained from Li metal rechargeable battery using $\text{Li}_4\text{Mn}_5\text{O}_{12}$ as cathode was analyzed with XPS to investigate a relationship between surface state of anode and rechargeability Li metal rechargeable battery.

2. Experimental

The laminate cells were assembled in an Ar-filled glove box to avoid the reaction with air. $\text{Li}_4\text{Mn}_5\text{O}_{12}$ electrode ($\text{Li}_4\text{Mn}_5\text{O}_{12}$ (Toshiba manufacturing Co., Ltd): acetylene black : PVdF = 80:10:10), Li metal foil (thickness of 20 μm) on Cu foil (thickness of 10 μm), the membrane made of polyimide which has three-dimensionally ordered macro-porous structure (3DOM separator) and ethylene carbonate (EC) containing 1 mol dm^{-3} LiPF_6 were used as cathode, anode, separator and electrolyte, respectively. After 200 discharge and charge cycles at 1 C rate, cells were disassembled and the Li metal anodes were washed with dimethyl carbonate. The surface analysis for Li metal anode was conducted by XPS using ULVAC-PHI Versa Probe II. The Li metal anodes were transferred to the chamber of XPS equipment by using the transfer vessel without air exposure. An Al-K α line was used as an x-ray source. In order to minimize the buildup of electrical charge during XPS measurements, charge compensation was performed using the neutralizer and the ion gun. The surface of cycled Li metal was compared with that of non-cycled one.

3. Results and discussion

Figure 1 shows the XPS spectra for surface of Li metal anode obtained from non-cycled and 200 cycled laminate cells in (1) Li 1s, (2) C 1s, (3) O 1s and (4) F 1s regions. The peak at 55.4 eV is attributed to LiF , Li_2O , LiOH , and/or Li_2CO_3 . The peaks corresponding to these components are too close to be separated individually. Therefore, these peaks are gathered into one peak as the other Li components in this study.

In the case of non-cycled Li metal surface, the peaks corresponding to Li metal, ketone and hydrocarbon structure (derived from EC), and LiPF_6 were observed. The peaks corresponding to hydroxide at 532.5 eV in the O 1s region was observed, so that the peak at 55.4 eV is assigned to LiOH . These results indicate that LiOH , electrolyte components and Li metal exist on the surface of Li metal anode before charge and discharge cycles.

In the case of 200 cycled Li metal surface, the peaks corresponding to LiF , $\text{Li}_x\text{PF}_y\text{O}_z$, carbonate, ketone or aldehyde, ether, hydrocarbon, alkyl-lithium, Li_2O and C_xLi_y were observed. The peaks corresponding to carbonate, ketone or aldehyde, ether, hydrocarbon, alkyl-lithium are derived from reduced products of solvent EC. For example, Li_2CO_3 and $(\text{CH}_2\text{OCO}_2\text{Li})_2$ were reported as the major reduction products of EC⁽¹⁾⁽²⁾. The peaks corresponding to LiF , $\text{Li}_x\text{PF}_y\text{O}_z$ are derived from reduction products of LiPF_6 . LiF , PF_5 and POF_3 were reported as the reduction products of LiPF_6 ⁽³⁾⁽⁴⁾, for example. Li_2O and C_xLi_y are considered as reaction products during discharge and charge cycles. These results indicate that reduction products of electrolyte exist on the surface of Li metal anode after charge and discharge cycles. More quantitative and detail discussion from XPS analysis will be given in the presentation.

[References]

- 1) Tao Li, et al., Chemical Physics Letters, **317**, 421 (2000)
- 2) Y Wang, et al., J. Am. Chem. Soc., **123**, 11708 (2001)
- 3) K. Kanamura, et al., J. Electrochem. Soc., **141**, 2379 (1994)
- 4) H. Lee, et al., J. Electrochem. Soc., **152**, A1193 (2005)

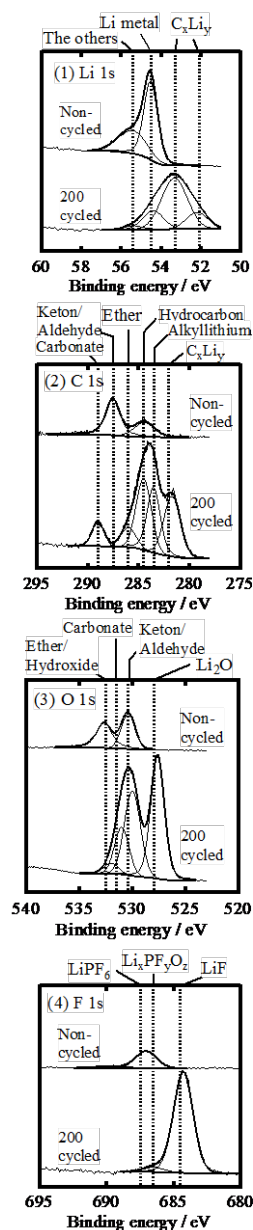


Figure 1 XPS spectra for surface of Li metal anode obtained from non-cycled and 200 cycled laminate cells in (1) Li 1s, (2) C 1s, (3) O 1s and (4) F 1s regions.

Formation Kinetics of Co-W-based Oxides from an Electroplated Alloy Coating on a Stainless Steel

Lu GAN⁽¹⁾⁽³⁾, Isao SAEKI⁽²⁾ Hideyuki MURAKAMI⁽¹⁾⁽³⁾, Tomoyuki YAMAMOTO⁽¹⁾,
(1) *Waseda University* (2) *Muroran Institute of Technology* (3) *National Institute for Materials Science*
1-2-1, Sengen, Tsukuba-City, 305-0047, Japan
GAN.Lu@nims.go.jp

1. Introduction.

A solid oxide fuel cell (SOFC) is categorized as an intermediate temperature (650–800 °C) fuel cell which is one of the most potential power source for next generation because of its high efficiency and relatively low cost. Individual SOFC units are connected in a stack with electronically conducting plates called interconnects. Recently, Cr-based ferritic stainless steels, which have a thermal expansion coefficient close to that for the SOFC system, have become of interest to SOFC developers because of their relatively low cost and ease of manufacturing. These steels, however, form relatively thick chromia (Cr_2O_3) scales at high temperature which would form volatile $\text{CrO}_2(\text{OH})_2$ and CrO_3 , resulting in poisoning the cathode materials. Also the chromia scale has very poor electrical conductivity, thus, increases the resistance of the system. One approach to improve the stainless steel interconnects and enhance SOFC lifetime is to apply a coating that may reduce the Cr outward penetration as well as modify the conductivity properties of the oxide.

In previous works, we have found the Co-W alloy showed a good barrier property at 800 °C that the Co-W oxide would block Cr outward penetration and control the Cr oxide accumulated upon the substrate, thus improved both the conductivity and oxidation properties. In this research, we have electroplated Co-5at% W film on ferritic stainless steel, then conducted 750 and 850 °C oxidation test for 1000 hours. Formation kinetics of oxide layers is investigated with thermodynamic calculations. TEM observation and EELS analysis have also been conducted to understand the Cr-blocking mechanism.

A commercially used type 430 steel was cut into small coupons with dimensions of $20 \times 15 \times 0.5$ mm. Thin Co was deposited on the coupons with a strike electroplating solution. Electrodeposition of the Co-W alloy was carried out with a prepared acidic bath. The cathodic current density and electroplating time was adjusted to obtain a 10- μm -thick Co-W layer (85 g m^{-2}). The composition of Co-W electroplating was measured with an energy dispersive X-ray fluorescent analyzer (XRF-1800, HITACHI). The samples were oxidized at 750 and 850 °C in air for the oxidation time $t_{\text{ox}} = 1000$ h. The mass gain of the samples was calculated using the mass of the specimens before and after oxidation exposed for every 100 hour. The morphology of the specimens was observed by scanning electron microscopy (S-4700, HIRACHI), and elemental distribution along the depth direction was analyzed with an energy dispersive X-ray spectrometer. The interface of Co-W oxide and Cr oxide was analyzed by transmission electron microscopy (JEM-2800F, JEOL). And the valence and electrical structure was characterized by electron energy loss spectroscopy.

The oxidation behaviors at 750–850 °C of type 430 stainless steels, with electroplated Co-W alloy coatings, was studied. The results are summarized as follows:

1. At both 750 and 850 °C, the CoWO_4 layers were formed. Up to 850 °C, the Co-W oxide structure was stable, and the Cr barrier properties by the formation of CoWO_4 effectively worked.
2. The crystal structure has been analyzed. The CoWO_4 would grow to large cells while the Cr oxide remained small size approximately amorphous.
3. Lattice structure as well as the interface between CoWO_4 and Cr oxide has been analyzed. The different structure and the volume shift of octahedral void in CoWO_4 could result to a higher active energy for Cr cation's penetration.
4. Electron energy loss spectrums of each layer have been obtained. The EELS result showed a clear boundary between Co-W oxide and Cr oxide. The valence of Co, Cr and Fe has been confirmed.

AC-voltametry signals during electrodeposition and gas evolution in molten salts

Andrew Caldwell, Brad Nakanishi and Antoine Allanore

Department of Materials Science and Engineering - Massachusetts Institute of Technology

77 Massachusetts Avenue, Office 13-5066

Cambridge, MA 02139-4307 (USA)

allanore@mit.Edu

AC-voltametry is a well-established technique for electroanalytical chemistry in low temperature electrolytes, which application in molten salts for metal electrodeposition or gas evolution has been very limited. In the context of identifying thermodynamic electrochemical reaction potentials in high temperature molten electrolytes, our group has found AC-voltametry as revigorated by Prof. A. Bond a very valuable tool. This work presents an overview of AC-voltametry, followed by experimental results obtained in molten oxides, sulfides and chlorides, for both metal deposition and gas evolution. Examples of metal deposition and electrochemistry include molten alumina at 2100K, europia dissolved in molten calcia, aluminium deposition in molten chlorides and copper deposition in molten sulfides. Gas evolution studies encompass oxygen evolution in molten alumina and chlorine evolution in molten chlorides. The obtained results are discussed in the framework of the available electrochemistry theory, enabling to pinpoint the value and limitations of the technique.

Effect of Conducting Polymers Coating on Nafion Methanol Crossover in Direct Methanol Fuel Cell (DMFC)

S. Ben Jadi¹, Z. Aouzal², A. El Jaouhari¹, M. Bouabdallaoui², A. El Guerraf², E.A. Bazzaoui², R. Wang³, M. Bazzaoui¹

¹ LME, Faculty of sciences, Ibn Zohr University, 80 000 Agadir, Morocco

² LCM, Faculty of sciences, Mohammed 1^{er} University, 60 000 Oujda, Morocco

³ Department of Mechanical Systems Engineering, Faculty of Engineering, Hiroshima Institute of Technology, 2-1-1 Miyake, Saeki-ku, Hiroshima 731-5193, Japan
e-mail address: sanabencji@gmail.com

Nafion membranes are highly used as proton exchange membranes for Direct Methanol Fuel cell. However, despite their advantageous characteristics of (high proton conductivity, operating temperature and mechanical strength) the leakage of methanol through Nafion membranes from the anode to the cathode compartment causes depletion of fuel cell energy.

In this work Nafion membranes were modified by chemical polymerization of aniline and pyrrole for different polymerization time (1h to 24h). The permeability was studied by electrochemical oxidation of the permeated methanol for Nafion-polyaniline and Nafion-polypyrrole, using the unmodified Nafion as a reference. Results showed a reduction of permeated methanol estimated to 40% for overall the modified membranes. By way of comparison, best resistance to methanol leakage was observed for Nafion-Polypyrrole even for low modification time. Modified membranes have been characterized by several techniques such as FTIR, XPS, MEB, proton conductivity by impedance electrochemical spectroscopy, water uptake (WU) and methanol uptake (MU).

Keywords: Nafion, Conductive polymer, Direct methanol fuel cell.

Electrodeposition and Development of Mg and Ca Metal Anodes

A. Ponrouch

Affiliation Institut de Ciència de Materials de Barcelona (ICMAB-CSIC)

Campus UAB, E-08193 Bellaterra, Catalonia, (Spain)

aponrouch@icmab.es

Various metals have been used as battery anodes in electrochemical cells ever since the birth of batteries with Volta's pile and also in the first commercialized primary (Zn/MnO₂, Leclanché 1866) and secondary (Pb/acid, Planté 1859) batteries. The idea and prospects of building a technology based on lithium are much more recent, as it required moving away from aqueous electrolytes. However, the first Li-MoS₂ cells with specific energy two or three times higher than the current Ni/Cd or Pb/acid cells were withdrawn from the market after safety difficulties were experienced with overheating on recharge related to dendrite growth. As an alternative, secondary Li-ion batteries avoiding the use of lithium metal anodes were commercialized by Sony in 1991. In contrast with Li metal anode, electrodeposition of Mg and Ca does not seem to be plagued with dendrite formation.^{1,2} In addition to the low cost of the raw materials (\$5000/ton, \$100/ton and \$265/ton for Li₂CO₃, CaCO₃ and MgO₂, respectively), such alternative technologies would benefit from high standard reduction potentials (ca. -2.87 V and -2.37 V vs NHE for Ca and Mg, respectively, as compared to -3 V for Li) and high theoretical electrochemical capacities (both gravimetric and volumetric) for the metal electrode, while relying on the 5th (Ca) and 8th (Mg) most abundant elements on the Earth's crust, respectively, whereas Li is the 25th). These metals are thus interesting candidates as anodes in rechargeable batteries.

Pioneering research work by Aurbach et al.^{3,4} allowed to conclude that the electrochemical behavior of Ca and Mg metal anodes in conventional organic electrolytes is surface-film controlled, as is the case for Li, but Ca and Mg plating is virtually impossible, which was attributed to the lack of divalent cation transport through the passivation layer (solid electrolyte interphase or SEI). Therefore, research has been focusing on electrolyte formulation in which no SEI is formed. Recently Ca plating and stripping through a stable SEI layer has been demonstrated, setting out the basis for the development of new electrolytes for divalent cation based batteries with high resilience upon oxidation.² The effect of several factors influencing the Ca deposition/stripping will be presented. Also, the reliability of the so called half-cell configuration in which Mg or Ca pseudo reference and counterelectrodes are used will be discussed and a systematic evaluation of the non-polarizability and stability in the electrolytic environment will be presented for these metal electrodes.⁵

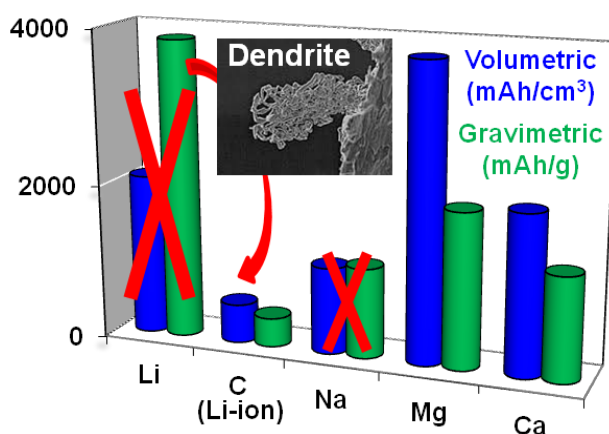


Figure 1. Theoretical gravimetric and volumetric capacities for different anodes: metals and Li-ion.

References:

- [1] M. Matsui, *J. Power Sources*, 196 (2011) 7048.
- [2] A. Ponrouch, C. Frontera, F. Bardé, M.R. Palacín, *Nat. Mater.* 15 (2016) 169.
- [3] D. Aurbach, R. Skaletsky, Y. Gofer, *J. Electrochem. Soc.* 138 (1991) 3536.
- [4] Z. Lu, A. Schechter, M. Moshkovich, D. Aurbach, *J. Electroanal. Chem.* 466 (1999) 203.
- [5] D.S. Tchitchekova, D. Monti, P. Johansson, F. Bardé, A. Randon-Vitanova, M. R. Palacín, A. Ponrouch, *J. Electrochem. Soc.* 164 (2017) A1384.

Smart Nano/Micro-structured Coatings for Corrosion Protection, Anti-Fouling Application and Sensing

Mário G.S. Ferreira, João Tedim, Mikhail Zheludkevich

*Department of Materials and Ceramic Engineering / CICECO, University of Aveiro, Campus Santiago,
3810-193 Aveiro, Portugal
mgferreira@ua.pt*

The active corrosion protection of metallic substrates can be achieved by addition of corrosion inhibitors to protective coatings. However, direct mixing of an inhibitor with coating formulations can lead to important drawbacks decreasing barrier properties of the coating and diminishing activity of the inhibitor. Also, soluble inhibitors can cause phenomena like osmotic blistering or be leached out spontaneously to the environment, which limits long-term performance and is environmentally pernicious. To overcome this problem and have controlled release of inhibitor different strategies of inhibitors storage in nanocontainers have been developed in order to produce smart self-healing coatings.

In this work novel protective nanostructured coatings with self-healing ability are presented. This effect is obtained on the basis of nanocontainers that release entrapped corrosion inhibitors in response to local pH changes or presence of corrosive species. The development of new nanocontainers for organic and inorganic corrosion inhibitors achieved is described, especially the most promising from industrial point of view, based on Layered Double Hydroxides (LDH). The combination of different nanocontainers in the same coating system has proved to be effective to accomplish further functions as antifouling and sensing.

Keywords: smart coatings, corrosion, anti-fouling.

Identification of Catalytically Active Sites at Electrode Surfaces

Aliaksandr Bandarenka

Technical University of Munich, Department of Physics, James-Frank-Str. 1, D-85748 Garching, Germany

e-mail: bandarenka@ph.tum.de

The activity of electrocatalysts is mostly determined by the properties of specific surface sites with optimal adsorption properties for reaction intermediates. However, identification of such catalytic centers is not a trivial task. In the presentation several examples related to experimental [1-3] and theoretical [4] identification of those catalytic centers will be given. While new theoretical approaches can be relatively simple, they require experimental confirmation. The latter can be in some cases done under reaction conditions using common electrochemical scanning tunneling microscopes (see Figure 1) [1].

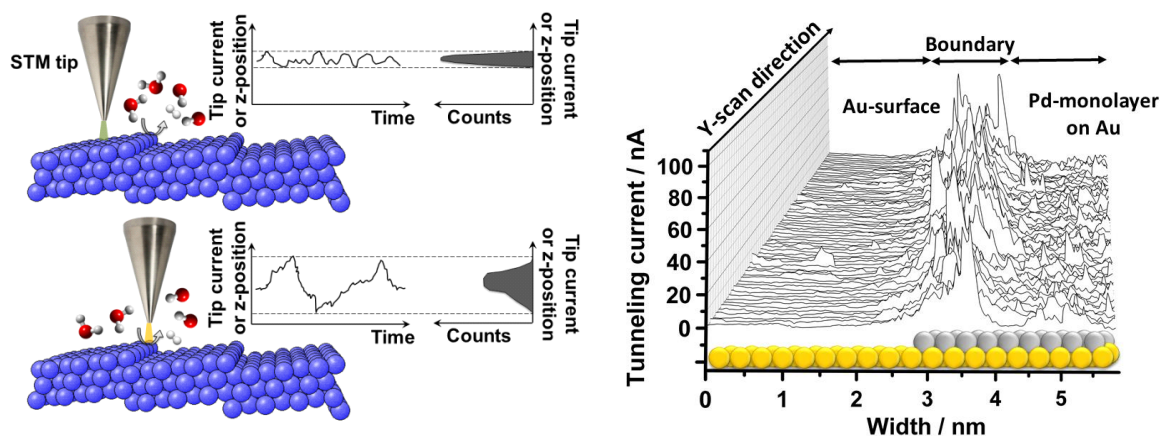


Figure 1. (Left) A scheme explaining the concept of revealing of electrocatalytic surface sites using electrochemical scanning tunneling microscopy: the increased tunneling current noise is likely to appear when the tunneling barrier is changed with time by the frequently approaching reactants and reaction products, considering a scenario in which a step edge is more active than the sites at the terrace. (Right) electrochemical scanning tunneling microscopy line scans of a boundary between a Pd island and the Au substrate under hydrogen evolution reaction conditions in 0.1 M H₂SO₄ [1].

References

- [1] J.H.K. Pfisterer⁽¹⁾, Y. Liang⁽¹⁾, O. Schneider, A.S. Bandarenka. Direct instrumental identification of catalytically active surface sites // **Nature** 549 (2017) 74–77.
- [2] J. Tymoczko, F. Calle-Vallejo, W. Schuhmann, A.S. Bandarenka. Making the hydrogen evolution reaction in polymer electrolyte membrane electrolyzers even faster // **Nature Communications** 7 (2016) 10990
- [3] F. Calle-Vallejo, M. Pohl, D. Reinisch, D. Loffreda, P. Sautet, A.S. Bandarenka. Why conclusions from platinum model surfaces do not necessarily lead to enhanced nanoparticle catalysts for the oxygen reduction reaction // **Chemical Science** 8 (2017) 2283-2289
- [4] F. Calle-Vallejo⁽¹⁾, J. Tymoczko⁽¹⁾, V. Colic, Q.H. Vu, M.D. Pohl, K. Morgenstern, D. Loffreda, P. Sautet, W. Schuhmann, A.S. Bandarenka. Finding optimal surface sites on heterogeneous catalysts by counting nearest neighbors // **Science** 350 (2015) 185-189.

Scanning Electrochemical Microscopy Study of the Formation of Solid Electrolyte Interfaces and Lithiation on Silicon Electrodes

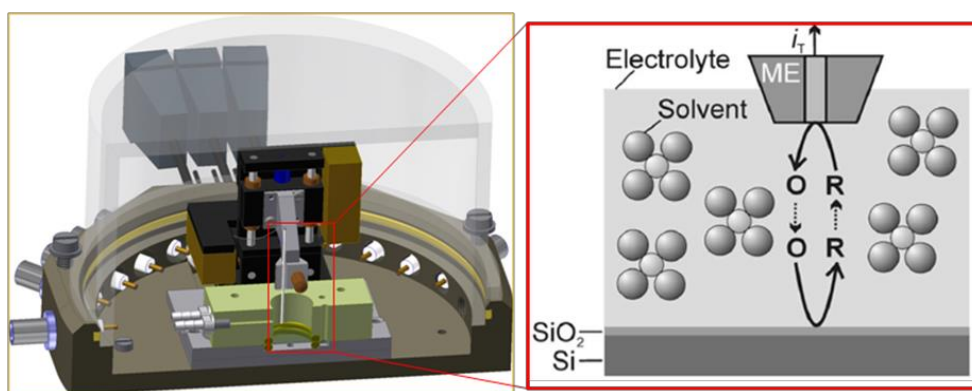
E. dos Santos Sardinha^a, M. Sternad^b, M. Wilkening^b, G. Wittstock^a

^a Carl von Ossietzky University of Oldenburg, School of Mathematics and Natural Sciences, Institute of Chemistry, D-26111 Oldenburg, Germany

^b Graz University of Technology (NAWI Graz), Christian Doppler Laboratory for Lithium Batteries, Institute for Chemistry and Technology of Materials, A-8010 Graz, Austria

eduardo.dos.santos.sardinha@uni-oldenburg.de

Silicon is considered as one of the promising alternatives to graphite as negative electrode material in lithium-ion batteries due to its wide abundance, low voltage and high theoretical gravimetric capacity.¹ The electron transfer at Si was characterized using the feedback mode of scanning electrochemical microscopy (SECM) and 2,5-di-tert-butyl-1,4-dimethoxybenzene as redox mediator. Approach curves and images demonstrate that the electron transfer rate constants at pristine Si are relatively small due to the native SiO₂ surface layer. In addition, the electron transfer rate constants show local variations because of the heterogeneous coverage of SiO₂.²



After removal of the SiO₂ surface layer by an HF treatment, the surface shows high positive feedback currents indicative of the absence of a solid electrolyte interphase (SEI). The formation of the SEI and the lithiation process could be studied in situ by scanning the potential of the Si electrodes in intervals from the open circuit value to 0.5 V and to 0 V vs. Li|Li⁺ respectively.³

For the SEI investigation the scan was periodically interrupted to record approach curves for the characterization of the interfacial kinetics at intermediate stages of SEI formation. This is an interesting aspect because the formation of the SEI depends on the reductions of electrolyte components.

Upon going to lower potentials Li is alloyed with Si. The integrity of the SEI is challenged due to the strong volume expansion upon lithiation of Si. By intermittent recording of the linear sweep and cyclic voltammograms with slow scan rates (30-10 μV/s), the voltammetric features can be directly correlated to the build-up of the SEI if an effect on the interfacial kinetics is evident from the SECM approach curves.

SECM imaging in the feedback mode provides also an impression on the homogeneity of the surface layers at different phases of their formation.

References:

1. M. N. Obrovac, L. Christensen. *Electrochem. Solid State Lett.*, **7**, (2004) A93.
2. H. Bülter, M. Sternad, E. dos Santos Sardinha, J. Witt, C. Dosche, M. Wilkening, G. Wittstock; *J. Electrochem. Soc.* 163 (2016) A504-A512.
3. M. Sternad, M. Forster, M. Wilkening; *Sci. Rep.* **6** (2016) 31712.

Composite of S-MWCNTs-PPy-nanopipes as Cathode Material for Li-S Batteries

Katarína Gavalierová¹, Andrea Straková Fedorková¹, Daniel Rueda², Pedro Gómez-Romero²

¹ Department of Physical Chemistry, Faculty of Science, Pavol Jozef Safarik University in Košice, Moyzesova 11, 040 01 Košice, Slovakia

² Catalan Institute of Nanoscience and Nanotechnology, UAB Campus, Bellaterra (Barcelona) 08193, Spain

katarina.gavalierova@gmail.com

Nowadays, the demand for energy storage devices is increasing rapidly. Lithium-sulfur batteries (Li-S) belong to the next-generation of these devices and are very attractive because of the highest theoretical specific capacity of sulfur (1675 mAh/g), not to mention the cost effectiveness and non-toxicity of sulphur [1].

We report the synthesis of S-MWCNTs-PPy-nanopipes as a cathode material for Li-S batteries. The synthesis was accomplished using a simple chemical oxidative polymerization of pyrrole monomer by adding the anions azo dye methyl orange (MO) and FeCl₃. To characterize the cathode material cyclic voltammetry, galvanostatic charge/discharge measurements or electrochemical impedance spectroscopy were carried out.

As shown in Fig. 1, MWCNTs formed agglomerates among the PPy-nanopipes. Our goal was to accommodate sulfur inside these agglomerates to control volumetric increase during the charge/discharge process. Homogeneous sulfur distribution in PPy-nanopipes and also in MWCNTs agglomerates was confirmed by EDX elemental map analysis and by TEM. STEM analysis confirmed a presence of sulphur inside the MWCNT tube. The improved electrochemical performance of S-MWCNTs-PPy-nanopipes was attributed to the stable network between the sulfur and MWCNTs-PPy-nanopipes that effectively facilitates Li⁺ ion diffusion which inhibited shuttle effect. Combination of PPy-nanopipes and MWCNTs provides additional conductivity and delivers extra capacity.

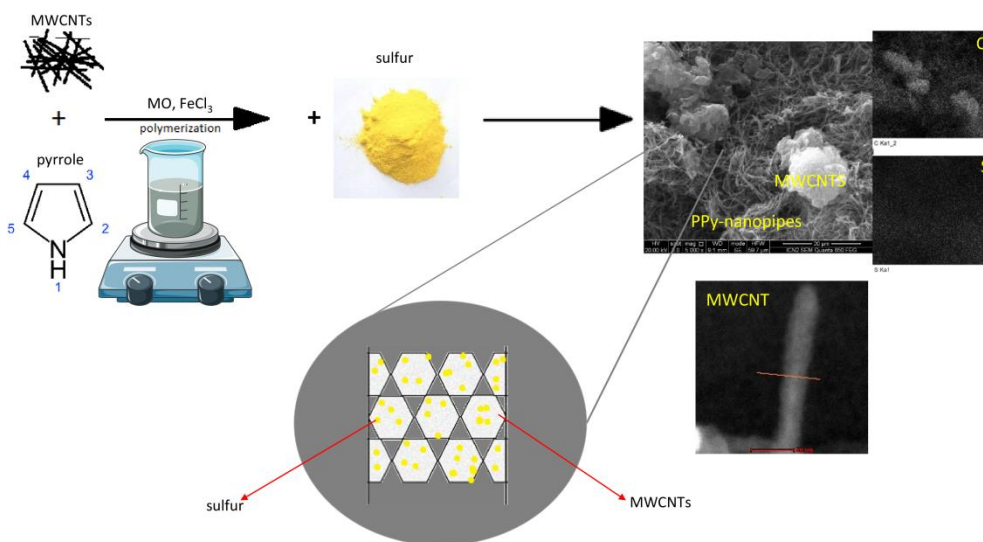


Fig. 1 Schematic representation of sample preparation and characterization, SEM image and elemental map of carbon and sulfur distribution for S-MWCNTs-PPy-nanopipes sample.

Acknowledgement

This research was sponsored by the NATO Science for Peace and Security Programme under grant 985148 and by the project VEGA 1/0074/17.

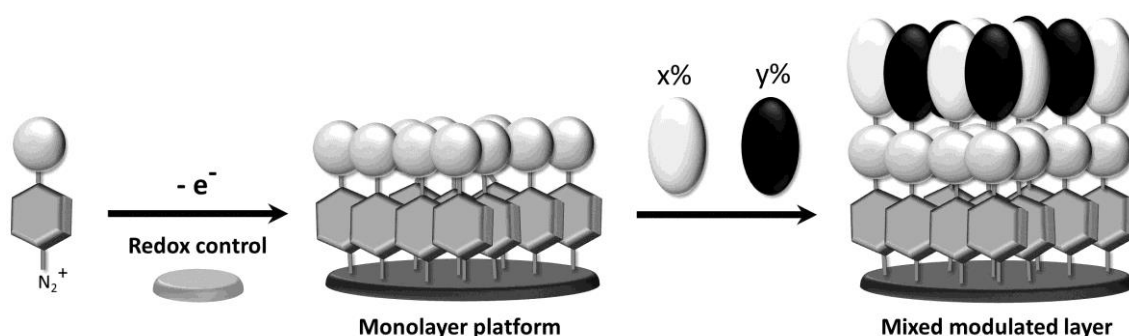
References

- [1] Xinhe Zhang, Bo Jin, Linlin Li, Tuo Cheng, Huanhuan Wang, Peiming Xin, Xingyou Lang, Chuncheng Yang, Wang Gao, Yongfu Zhu, Qing Jiang, *Journal of Electroanalytical Chemistry*, 780 (2016), 26-31.

Mixed Functional Monolayers prepared from Redox Controlled Diazonium Grafting

Tony Breton, Marius Cesbron, Eric Levillain, Christelle Gautier
Laboratoire MOLTECH-Anjou, Université d'Angers – CNRS
2 Boulevard Lavoisier 49045, Angers Cedex, France.
tony.breton@univ-angers.fr

Grafting of organic structures using the diazonium chemistry is a recognized method for obtaining functionalized surfaces.¹ Various conducting materials as metals and carbon can be modified in aprotic or aqueous media, and provide covalently tethered layers. The efficiency of this grafting process rests upon the high reactivity of the aryl radicals produced at the electrode-solution interface. This reactivity leads to the generation of disorganized polyaryl layers via the radical attack of already grafted aryl species on the surface. We recently developed a simple and useful control strategy to limit the radical polymerization by adding appropriate concentration of 2,2-diphenylpicrylhydrazyl (DPPH) in the deposition solution.^{2,3} This approach, previously assumed to be based on the radical capture of highly reactive aryl intermediates via the scavenging activity of DPPH, actually rests on redox cross reactions involving its electro-reduced form. A simple numerical approach, developed to model the inhibition process, accurately reflects the grafting control observed as function of the potential applied for the diazonium deposition. To confirm the redox nature of this control, our approach was successfully extended to the use of electro-reducible substituted benzoquinones instead of DPPH. The surface functionalization limitation was found dependent on the gap between the redox potentials of the diazonium salt and the benzoquinone used. A concentration effect of the reductive mediator was clearly evidenced, offering the possibility to modulate the surface coverage/thickness of the organic layer depending on the targeted application. This study demonstrates that the grafting control can be extended to the use of every stable electro-reducible mediator for which the redox potential is lower than the diazonium one.



Our approach was applied to the preparation of controlled mixed organic layer for which the ratio of functional moieties can be freely modulated. Electrochemical properties and interfacial reactivity of those modified surface were found dependent on the organic layer structure and thickness.⁴ This approach opens the way for the monolayer attachment of a wide variety of molecules or biomolecules and should offer promising prospects in forthcoming research on nanomaterials.

References:

- (1) Pinson, J.; Podvorica, F. *Chemical Society Reviews* **2005**, *34*, 429.
- (2) Breton, T.; Levillain, E.; Menanteau, T.; Downard, A. J. *Physical Chemistry Chemical Physics* **2015**, *17*, 13137.
- (3) Breton, T.; Downard, A. J. *Australian Journal of Chemistry* **2017**, *70*, 960.
- (4) Menanteau, T.; Dabos-Seignon, S.; Levillain, E.; Breton, T. *ChemElectroChem* **2017**, *4*, 278.

Optimizing Platinum Electrocatalysts for Various Reactions by Means of Coordination-Activity Plots

Federico Calle-Vallejo, Aliaksandr Bandarenka
Universitat de Barcelona
Carrer de Marti i Franques 1, 08028, Barcelona, Spain
f.calle.vallejo@ub.edu

Electrocatalysts usually contain several types of sites that contribute differently to the overall catalytic activity. Therefore, rational optimization of catalytic activity requires first the identification of the most active sites, followed by maximization of their presence using suitable synthesis procedures. However, in practice this is an extraordinarily challenging process, especially for multifaceted materials and nanostructures, and usually contradictory conclusions are found in the literature.

Focusing on Pt electrocatalysts, in this talk I will first present “generalized coordination numbers” (GCN), which can accurately describe adsorption-energy trends for a wide variety of sites on extended surfaces and nanoparticles of different sizes and shapes [1, 2].

Moreover, I will show that “coordination-activity plots” based on such geometric descriptors are not only able to identify the optimal adsorption energies of key intermediates but also outline the geometric configuration of optimal sites. In particular, I will compare computational and experimental results for the following three electrocatalytic reactions:

I) Oxygen reduction reaction [3, 4], for which concave sites with large generalized coordination numbers are most active (GCN ~ 8.3).

II) Hydrogen evolution reaction [5, 6], for which concave sites are also most active (GCN ~ 7.7), but the active sites are different from those of oxygen reduction.

III) CO oxidation reaction [7], for which convex sites with small generalized coordination numbers are most active (GCN ~ 5.4).

References

- [1] F. Calle-Vallejo, J.I. Martínez, J.M. Garcia-Lastra, P. Sautet, D. Loffreda, *Angew. Chem. Int. Ed.*, 53 (2014) 8316-8319.
- [2] F. Calle-Vallejo, P. Sautet, D. Loffreda, *J. Phys. Chem. Lett.*, (2014) 3120-3124.
- [3] F. Calle-Vallejo, J. Tymoczko, V. Colic, Q.H. Vu, M.D. Pohl, K. Morgenstern, D. Loffreda, P. Sautet, W. Schuhmann, A.S. Bandarenka, *Science*, 350 (2015) 185-189.
- [4] F. Calle-Vallejo, M.D. Pohl, D. Reinisch, D. Loffreda, P. Sautet, A.S. Bandarenka, *Chem. Sci.*, 8 (2017) 2283-2289.
- [5] J. Tymoczko, F. Calle-Vallejo, W. Schuhmann, A.S. Bandarenka, *Nat. Commun.*, 7 (2016) 10990.
- [6] M.D. Pohl, S. Watzele, F. Calle-Vallejo, A.S. Bandarenka, *ACS Omega*, 2 (2017) 8141-8147.
- [7] F. Calle-Vallejo, M.D. Pohl, A.S. Bandarenka, *ACS Catal.*, (2017) 4355-4359.

Photoelectrochemical Visible Light Zero Bias Hydrogen Generation with Membrane-Based Cells Designed for Decreasing Overall Water Electrolysis Voltage and Water Dissociation (18)

Kenji Sakamaki, Ayana Watanabe, Honoka Matsuda, Sayuri Usui, Wakana Sakashita, Ryoko Kato, Haruka Endo, and Masataka Sato
 Chemistry Course, Department of Applied Chemistry and Biochemistry,
 Fukushima College, National Institute of Technology, Fukushima 980-8034, Japan
 sakenji@fukushima-nct.ac.jp

The Honda-Fujishima effect is a milestone in the history of advanced hydrogen generation and artificial photosynthesis [1]. In their following paper, chemical bias served as electromotive force leads to increase quantum efficiency for hydrogen production under sunlight [2]. Thus, in a series of papers, membrane-based cells designed for decreasing overall water electrolysis voltage and water dissociation have been created to control and supply active reaction species for water splitting, which are the crucial prerequisite for achieving an efficient photoelectrochemical (PEC) hydrogen generation. In the first stage, we have developed a renewable acid-base three-compartment cell with a combination of cation (basic) and anion (acidic) exchange membranes (electrolytes) bridging a neutral electrolyte. We have accomplished 0.7 V onset hydrogen generation and visible light zero bias water splitting using Fe₂O₃. Extending our concept, in the second stage, we have created a two-compartment cell (2CC) separated by bipolar membrane (BPM) sandwich through-holed electrodes assembly (BPMEA-2CC) and carried out hydrogen generation derived from water dissociation based on golden rule for sustainable water splitting [3].

A decisive advantage of BPMEA-2CC is that all electrolytes used are sustainable, because reaction starts from water dissociation in the junction of BPM [4]. The opposite directional charge separation of H⁺ and OH⁻ induces inner chemical bias (ICB) within BPM, which reduce water electrolysis voltage. Further advantage is that many possible anolyte-catholyte combinations induce outer chemical bias (OCB). Therefore, dual chemical bias (ICB & OCB) reduces overall water electrolysis voltage. We have accomplished hydrogen generation derived from water dissociation with BPMEA-2CC with OER active dimensionally stable anode (DSA, De Nora Permelec) having lower oxygen overpotential, breaking the theoretical 1.23 V for water splitting at room temperature [3].

We have applied the BPMEA-2CC to zero bias photocell. As a through-holed n-type photoelectrode (THPE), anatase TiO₂ for a model to demonstrate our concept was fabricated by anodization. Illumination of light to photocell (Fig), anolyte (water or base) | THPE | BPM | Pt | catholyte (water or acid), we have succeeded in measuring photocurrent from distilled water without any external bias. The magnitude of photocurrent enhances with an increase of OCB, water-water < water-acid < base-acid. Further importance is that flat band potential of n-type oxide semiconductor shifts to negative potential direction with an increase of the pH of anolyte. Luminous intensity dependent PEC voltammetry curves suggest that the rate-determining step is the migration process of H⁺ and OH⁻ in the BPM. Currently, our research efforts are focused on PEC zero bias hydrogen generation with supercontinuum solar light using BPMEA-2CC with THPE and metal nanoparticle. Formation of visible light responsive THPE and BPM modification for plasmon-induced water dissociation are now underway.

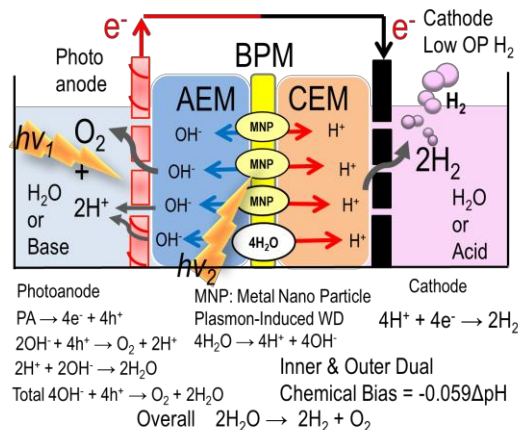


Fig. Photoanode – (MNP-BPM) – HER active electrode assembly

- [1] A. Fujishima and K. Honda, *Nature*, **238**, 37 (1972).
- [2] A. Fujishima, K. Kohayakawa and K. Honda, *J. Electrochem. Soc.*, **122**, 1487 (1975).
- [3] M. Sato, Y. Kamo and K. Sakamaki, *MRS Proceedings* Vol. **1601** (2013), H. Endo, M. Sato, Y. Kamo, and K. Sakamaki, *65th ISE*, Lausanne, Switzerland, ise 141164 (2014), K. Sakamaki et al., *66th ISE*, Taipei, Taiwan, ise 151283 (2015), K. Sakamaki et al., *2017 International Conference on Artificial Photosynthesis (ICARP2017)*, Kyoto, March 2-5 (2017), H. Matsuda et al., *97th annual meeting of CSJ*, 3A6-05, (2017), K. Sakamaki et al., *68th ISE*, Providence, RI, USA, ise171503, (2017).
- [4] V. J. Frilette, *J. Phys. Chem.*, **60**, 435 (1956).

Multilateral Analyses of Pt-skin/Pt₃Co(111) Single Crystal Electrode with Extremely High Activity for the Oxygen Reduction Reaction

Shun Kobayashi,^a Makoto Aoki,^b Mitsuru Wakisaka,^c Teppei Kawamoto,^a Ryo Shirasaka,^a Kohei Suda,^a Junji Inukai,^a Toshihiro Kondo,^d and Hiroyuki Uchida^a

^a University of Yamanashi, 4 Takeda, Kofu 400-8510, Japan,

^b Kobe University, 1-1 Rokkodai-cho, Nada-ku, Kobe 658-8501, Japan

^c Toyama Prefectural University, 5180 Kurokawa, Imizu, Toyama 939-0398, Japan,

^d Ochanomizu University, Ohtsuka, Bunkyo-ku, Tokyo 112-8610, Japan

Email address: g17dg003@yamanashi.ac.jp (S. Kobayashi)

Bimetallic alloys of Pt such as Pt-Co, Pt-Ni, and Pt-Fe exhibit higher activity for the oxygen reduction reaction (ORR) than that of pure Pt in polymer electrolyte fuel cells.^{1,2} It is essential to understand the mechanism of improvement of the ORR activity of these alloys. Very recently, at a series of (111), (100), and (110) faces of Pt_{100-x}Co_x single crystal electrodes with well-controlled Co content x, we found that the values of kinetically-controlled area-specific current densities (j_k) for the ORR increased in the order (100) < (110) << (111): Pt-skin/Pt₇₃Co₂₇(111) exhibited the highest j_k value, which was about 27 times larger than that on pure Pt(111).³ In the present work, we have multilaterally analyzed the Pt-skin layer and the underlying alloy of the Pt-skin/Pt₃Co(111) single crystal electrode (with very high ORR activity quite close to the maximum value) in 0.1 M HClO₄ electrolyte solution.

The Pt₃Co(111) single crystals were prepared in the same manner as described in our previous work.³ They were annealed at 1273 K for 1 h in H₂, resulting in the formation of Pt-skin layer on the surface. It was clearly observed in a high-resolution image of in-situ scanning tunneling microscopy (STM) for the Pt₇₆Co₂₄(111) in N₂-purged 0.1 M HClO₄ that the (111) terrace of Pt-skin was atomically flat, without corrugations in height.

Next, we analyzed the layer-by-layer compositions of a Pt-skin/Pt₃Co(111) single crystal electrode by in-situ surface X-ray scattering (SXS). As shown in Fig. 1, the topmost surface layer was found to consist of pure Pt (98 at%) with one atomic layer thickness. It is striking that cobalt was enriched in the 2nd layer up to 98 at%, while the Co contents in the 3rd and 4th layers were slightly smaller than that in the bulk. By angle-resolved, grazing-incidence X-ray photoelectron spectroscopy, the Co in the subsurface layers was found to be positively charged, suggesting an electron transfer from Co into the Pt-skin layer, i.e., the electronic modification of the Pt-skin layer (d-band center downshift). The extremely high activity for the ORR at the Pt-skin/Pt₃Co(111) single crystal is correlated with this specific surface structure.

This work was supported by the SPER-FC project from NEDO and a Grant-in-Aid (No. 25410007) for Scientific Research from MEXT of Japan. The synchrotron radiation experiments were performed as projects approved by the Photon Factory Advisory Committee (PAC No. 2016G059) and by the Japan Synchrotron Radiation Research Institute (2016A1184 and 2016B1551).

References

1. T. Toda, H. Igarashi, H. Uchida, M. Watanabe, *J. Electrochem. Soc.* **1999**, *146*, 3750-3756.
2. V. R. Stamenkovic, B. S. Mun, K. J. J. Mayrhofer, P. N. Ross, N. M. Markovic, J. Rossmeisl, J. Greeley, J. K. Nørskov, *Angew. Chem. Int. Ed.* **2006**, *45*, 2897-2901.
3. S. Kobayashi, M. Wakisaka, D. A. Tryk, A. Iiyama, H. Uchida, *J. Phys. Chem. C* **2017**, *121*, 11234-11240.

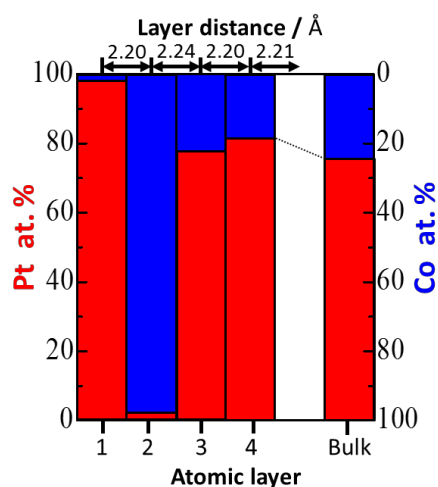


Figure 1. Alloy composition from the top surface to the bulk of the Pt-skin/Pt₇₅Co₂₅(111) single crystal electrode in N₂-purged 0.1 M HClO₄ at 0.4 V vs. RHE and 298 K.

Shape-Selective Electroless Plating of High Aspect Ratio Silver Nanoplatelet Films

Falk Muench,^a Alexander Vaskevich,^a Ronit Popovitz-Biro,^b Tatyana Bendikov,^b Yishay Feldman,^b Israel Rubinstein^{a†}

Weizmann Institute of Science, Department of Materials and Interfaces, 7610001 Rehovot

Weizmann Institute of Science, Chemical Research Support, 7610001 Rehovot

e-mail address: muench@ma.tu-darmstadt.de / Alexander.Vaskevich@weizmann.ac.il

† I. R. passed away on October 21, 2017.

Open-porous, free-standing metal nanostructure assemblies display a privileged class of functional materials, which simultaneously provide desired properties such as large surface area, high conductivity, tunable reactivity / selectivity, efficient diffusive access, mechanical robustness, and long-term stability [1]. Solution-based deposition methods represent particularly important routes toward such materials [2]: They enable direct surface functionalization without separate nanostructure fabrication, isolation, transfer and assembly steps, and ensure a good connection with the underlying substrate.

While auto-catalytic plating displays a convenient method for preparing high quality metal films, it commonly does not yield anisotropic nanostructures of defined crystallinity [3, 4]. In this contribution, we show how this limitation can be overcome, using an Fe(III) tartrate surfactant to deposit films composed of high aspect ratio silver nanoplatelets. The approach is applicable to a wide range of substrate materials, is compatible with curved surfaces, proceeds quickly, and only relies on stock chemicals.

The nanostructures follow a complex and unusual growth pattern, starting from one-dimensional, jagged nanobelts, which are transformed into nanoplatelets by space-filling growth. Contrary to colloidal syntheses, the nanoplatelet thickness increases discontinuously, via the formation of stacked, aligned layers. Diffusion-limited growth conditions can be used to realize porous, dendritic nanoplatelets.

Aside presenting strategies to modify the product morphology, we explore the application potential of the nanoplatelet films in flow and (electro)catalysis.

Finally, the highly porous, conductive Ag nanoplatelet films can serve as support material, allowing outfitting them with new functionalities. Using solution-based deposition reactions, we demonstrate how they can be decorated with secondary materials on the nanoscale, while fully maintaining their microscale architecture (Fig. 1).

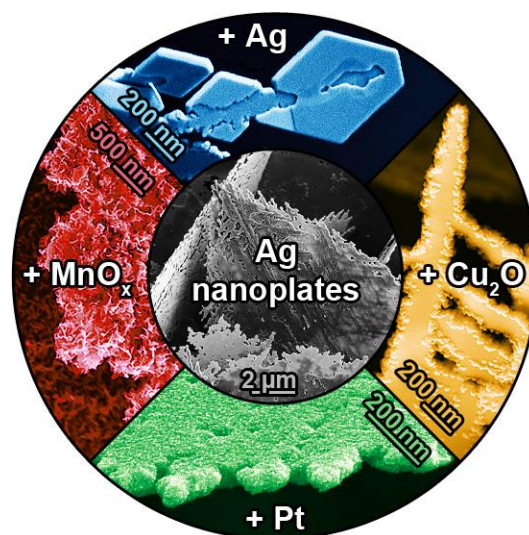


Figure 1. SEM images of Ag nanoplate films in pristine form (center), and in modified variants, using solution-based reactions to decorate them with various materials.

[1] C. Zhu, D. Du, A. Eychmüller, Y. Lin, *Chem. Rev.* 115 (2015) 8896 – 8943

[2] J. Kim, Z. Li, I. Park, *Lab. Chip* 11 (2011) 1946 – 1951

[3] F. Muench, S. Schaefer, L. Hagelüken, L. Molina-Luna, M. Duerrschabel, H.-J. Kleebe, J. Brötz, A. Vaskevich, I. Rubinstein, W. Ensinger, *ACS Appl. Mater. Interfaces* 9 (2017) 31142 – 31152

[4] X. Zhao, F. Muench, S. Schaefer, J. Brötz, M. Duerrschabel, L. Molina-Luna, H.-J. Kleebe, S. Liu, W. Ensinger, *Electrochem. Commun.* 65 (2016) 39 – 43

Anodic TiO₂ Nanotube Layers: Superior Photoelectrochemical Performance due to Secondary Materials

Hanna Sopha, Milos Krbal, Raul Zazpe, Jan Prikryl, Jan M. Macak
*Center of Materials and Nanotechnologies, Faculty of Chemical Technology, University of Pardubice,
Nam. Cs. Legii 565, 530 02 Pardubice, Czech Republic*
e-mail address: jan.macak@upce.cz

The self-organized TiO₂ nanotube layers have attracted considerable scientific and technological interest over the past 10 years, which are motivated for their possible range of applications including photo-catalysis, solar cells, hydrogen generation and biomedical uses [1]. The synthesis of 1D TiO₂ nanotube structure is carried out by a conventional electrochemical anodization of Ti sheet. The main drawback of TiO₂ is its applicability in the UV light (wavelengths < 390 nm). In order to enhance the efficiency, TiO₂ has been doped by N [2] or C [3] to shift its absorption into the visible light.

Except of an increase of the visible light response, one of the remaining major issues for TiO₂ is to achieve efficient charge carrier separation. Recently, it has been shown that ultrathin surface coatings of TiO₂ by materials such as TiO₂ [4], Al₂O₃ [5], ZnO [6, 7] or CdS [8] annihilates electron traps at the TiO₂ surface and thus increases the concentration of the photo-generated charge carriers.

The presentation will focus in detail on the coating of the nanotube arrays by various materials using ALD, with focus on TiO₂ coatings that are very beneficial for superior photocatalytic performance.

The deposited materials influence strongly photo-electrochemical properties of nanotube layers. Experimental details and some very recent photocatalytic [4], sensing [7] and solar cell [8] results will be presented and discussed.

References:

1. J. M. Macak et al., *Curr. Opin. Solid State Mater. Sci.* 1-2 (2007) 3.
2. C. Burda et al., *Nano Lett.* 3 (2003) 1049.
3. S. Sakthivel et al., *Angew. Chem. Int. Ed.* 42 (2003) 4908.
4. H. Sopha et al., *Appl. Mater. Today* 9 (2017) 104.
5. Q. Gui, *ACS Appl. Mater. Interfaces*, 6 (2014) 17053
6. A. Ghobadi et al., *Sci. Rep.* 6 (2016) 30587
7. S. Ng et al. *Adv. Eng. Mater.* DOI: 10.1002/adem.201700589.
8. M. Krbal et al., *Nanoscale* 9 (2017) 7755

Preparation of Pd-deposited Spherical Ag Electrocatalysts and Their Application to Alkaline Fuel Cells

Eiji Higuchi, Naoki Hiratsuka, Masanobu Chiku and Hiroshi Inoue

Department of Applied Chemistry, Graduate School of Engineering, Osaka Prefecture University
Sakai, Osaka 599-8531, Japan
e-higuchi@chem.osakafu-u.ac.jp

The investigation on electrocatalysts for oxygen reduction reaction (ORR) is important for energy applications such as fuel cells and air-metal batteries. In alkaline fuel cells, inexpensive transition metals can be used as electrocatalysts in place of Pt and Pd, which is the greatest advantage. Ag is a promising substitute for Pt and Pd because it is not so expensive and its ORR mechanism in alkaline media is similar to Pt and Pd. However, Ag is less active in ORR than Pt and Pd. Several research groups found that PdAg and Ag₄Pd had higher activity and stability for ORR in alkaline media compared to Ag [1, 2]. In this study, to improve ORR activity in alkaline media for commercial spherical Ag particles with size of ca. 0.5 μm, we developed a modification technique of Pd on the Ag particle surface, in which Pd was deposited on the spherical Ag particles (Pd/Ag) by immersing commercial spherical Ag particles in perchloric acid solutions containing different concentrations of Pd²⁺. The prepared Pd/Ag catalysts whose Pd mole fraction was 0.09 – 0.52 were characterized by various spectroscopic and electrochemical methods, and evaluated ORR activity per unit mass of Pd (mass activity; MA).

A 0.1 M HClO₄ solution containing 48 mM AgClO₄ was added into a 0.1 M HClO₄ solution containing 8 mM PdCl₄²⁻ to form Pd(ClO₄)₂, and AgCl as a byproduct was filtered out. The resultant Pd(ClO₄)₂ solution was added into a 0.1 M HClO₄ aqueous solution including the Ag particles, and then stirred at 60 °C for 1 h. The Pd mole fraction for Pd/Ag catalysts was controlled by the concentration of Pd(ClO₄)₂ solution. After suction filtration, the residue was washed with ultrapure water and ethanol, followed by drying.

The SEM image showed that a Pd/Ag particle had numerous holes because Ag dissolved with the Pd deposition. The size of the Ag particles was maintained even after Pd deposition. In the Pd 3d core level spectrum for the Pd/Ag catalyst, the double peaks for metallic Pd shifted to the lower binding energies. The X-ray diffraction (XRD) pattern of the Pd/Ag (Fig. 1) exhibited that the Pd(111) peak was not observed, but the Ag(111) peak shifted to higher angles. These results suggest that deposited Pd was alloyed with Ag.

In cyclic voltammogram of the Pd/Ag/GC in Ar-saturated 1 M KOH, the peak due to the Ag₂O reduction was weakened, suggesting that the oxidation of the Ag surface was inhibited due to the Pd deposition. In addition, the reduction peak of PdO for Pd/Ag/GC was observed at more negative potential than the Pd electrode. MA for Pd/Ag/GC was evaluated by rotating disk electrode method. Fig. 2 shows MA at -0.10 V in O₂-saturated 1 M KOH for Ag/GC and Pd/Ag/GC. Pd/Ag/GC exhibited higher MA than Ag/GC. These results suggest that the alloying of Pd with Ag enhanced the ORR activity.

References

- [1] Q. He and E. J. Cairns, *J. Electrochem. Soc.*, **162**, F1504 (2015).
- [2] D. A. Slanac, W. G. Hardin, K. P. Johnston, and K. J. Stevenson, *J. Am. Chem. Soc.*, **134**, 9812 (2012).

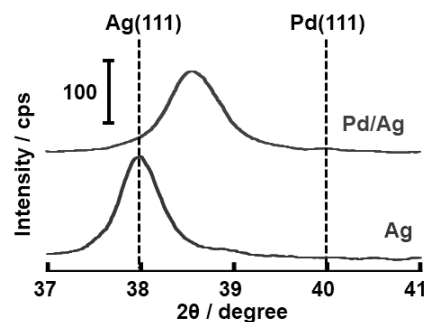


Fig. 1 XRD patterns for Ag and Pd/Ag.

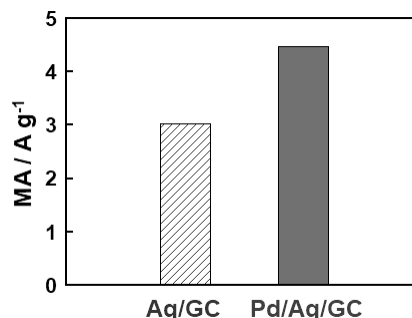


Fig. 2 MAs for Ag/GC and Pd/Ag/GC.

Synthesis and Applications of Processable Prussian blue Nanoparticles

Prem C. Pandey

*Department of Chemistry, Indian Institute of Technology (BHU), Varanasi-221005, India
pcpandey.apc@iitbhu.ac.in*

Abstract

The present report describes the new approaches to synthesize Prussian blue Nanoparticles having efficient catalytic activity in developing PB based devices. The controlled conversion of single precursor, potassium hexacyanoferrate, into Prussian blue nanoparticles in the presence of organic reagents is demonstrated. The use of organic reagent control the nucleation process yielding Prussian blue nanoparticles suitable for developing modified electrodes having efficient electrocatalytic ability. As developed Prussian blue nanoparticles also display homogeneous catalysis similar to that of peroxidase enzyme. Four different systems namely; (1) 3-aminopropyltrimethoxysilane and cyclohexanone, (2) tetrahydrofuran hydroperoxide, (3) tetrahydrofuran and hydrogen peroxide and (4) polyethylenimine; are reported for controlled conversion of potassium hexacyanoferrate into Prussian blue nanoparticles. The modified electrode made from as developed Prussian blue nanoparticles display excellent PB character with electron transfer rate constant to the order of 32.1 s^{-1} and simultaneously could be explored as peroxidase mimetic with K_m value to the order of $< 1 \text{ mM}$. The present synthetic approach could also be explored to incorporate Prussian blue nanoparticles in mesoporous matrix for many practical applications. The as reported process also enable the controlled synthesis of noble metal nanoparticles introducing new route for yielding Prussian blue-noble metal nanoparticle nanocomposite that manipulate the catalytic/electrocatalytic activity for targeted system. The role of polyethylenimine and formaldehyde are demonstrated in this presentation.

Optimization of asymmetric particle synthesis with bipolar electrochemistry

A.Kuhn*, L. Bouffier, D. Zigah, N. Sojic

University of Bordeaux, CNRS UMR 5255, Bordeaux INP, Site ENSCBP, 16 avenue Pey Berland, 33607 Pessac, France

**kuhn@enscbp.fr*

During the last decade, it has been demonstrated that bipolar electrochemistry (BPE) has some remarkable advantages over conventional electrochemistry when used in the context of material science. The key benefits of BPE are, among others, simultaneous wireless addressing of thousands of objects, and a straightforward experimental set-up in order to break the symmetry of a chemical system [1-4]. This somewhat unconventional way of performing electrochemical experiments therefore undergoes currently a true renaissance not only in the frame of micro- and nanotechnology, but also in various other scientific domains [5]. In this lecture, we will illustrate with some very recent results that the concept is indeed extremely powerful and opens the door to completely new approaches for modifying the solid/liquid interface, which are impossible with classic electrochemistry [6-11].

1. F. Mavré et al. *Anal. Chem.* 82 (2010) 8766
2. G. Loget et al. *Anal. Bioanal. Chem.* 400 (2011) 1691
3. S. E. Fosdick et al. *Angew. Chem. Int. Ed.* 52 (2013) 10438
4. G. Loget et al. *Acc. Chem. Res.* 46 (2013) 2513
5. A. Kuhn et al. *ChemElectroChem* 3 (2016) 351
6. S. Tiewcharoen et al. *Angew.Chem.Int.Ed.* 56 (2017) 11431
7. L. Bouffier et al. *ChemPhysChem* 18 (2017) 2637
8. B. Gupta et al. *Angew.Chem.Int.Ed.* 56 (2017) 14183
9. B. Gupta et al. *Adv. Funct. Mater.* (2018) 1705825
10. Z. Ali Fattah et al. *Appl.Mater.Today* 9 (2017) 259
11. L. Bouffier et al. *Electroanalytical Chemistry: A Series of Advances, Volume 27*, eds. A.J. Bard, C.G. Zoski, 2017, CRC Press, Taylor&Francis Group, 2017, ISBN 9781138034181

Boron Doped Diamond Microelectrodes as Amperometric Sensors for Studying Localized Corrosion on Mg and Mg Alloys

Eduardo L. Silva¹, Miguel A. Neto², Rui F. Silva², Filipe J. Oliveira², Mikhail L. Zheludkevich^{1,2}

¹*MagIC – Magnesium Innovation Centre, Helmholtz-Zentrum Geesthacht*

Max-Planck Str. 1, 21502 Geesthacht, Germany

²*Department of Materials and Ceramics Engineering/CICECO, University of Aveiro*

3810-193 Aveiro, Portugal

eduardo.trindade@hzg.de

The demand for magnesium and related alloys has been increasing over the last decade, partly driven by Mg properties such as high strength-to-weight ratio or biocompatibility, which can easily integrate solutions for social and environmental challenges such as controlling CO₂ emissions or developing biodegradable orthopedic devices. However, being the least noble of all structural metals, the high corrosion rate observed on Mg-based materials is a major drawback, and still requires better control and understanding, especially due to the impact of transition metal impurities such as Fe, Ni, Cu and Zn, even in trace amounts in the ppm range.

Localized corrosion techniques such as SVET (Scanning Vibrating Electrode Technique), SIET (Scanning Ion-Selective Electrode Technique), and microamperometry can provide high lateral resolution measurements of corrosion related variables such as ionic current density, pH, dissolved oxygen (DO) and metal cations, by scanning the electrolyte solution near the metal surface. Depending on the local level of impurities, or the specific microstructure of each alloy, macro and micro galvanic corrosion are common on Mg, resulting in accelerated dissolution of the Mg matrix and abundant hydrogen evolution. As an example, a 2 mm² Mg (99.9%) surface immersed in NaCl 0.5 M can be completely corroded in less than two hours. Hence, besides adequate selectivity and detection limit, it is important that microprobes also exhibit fast response time and long term stability, especially for the case of surface mapping.

Boron-doped diamond microelectrodes are solid state sensors that can be synthesized by CVD (Chemical Vapour Deposition) and exhibit properties such as high signal-to-noise ratio, wide potential window (~3V), high chemical stability, resistance to fouling, long term stability and fast response time (< 0.1 s per point) [1]. In this work BDD microelectrodes were used in order to demonstrate different angles of Mg corrosion that are usually overlooked. Although being the main species involved in the cathodic reaction for other alloy systems, dissolved oxygen is considered to be an irrelevant species during the corrosion of Mg. By using BDD microelectrodes operating in the amperometric mode on a SVET equipment, a significant lowering of DO concentration was found in uncorroded areas of Mg (99.9%) immersed in NaCl 0.5 M. In simultaneous measurements with SVET and a DO-sensitive micro-optode, it was shown that such DO depletion is associated with areas of cathodic activity. While there is compelling evidence that water reduction is the main cathodic process during Mg corrosion, it was demonstrated that DO is actually an influential species, although to a lesser extent. This evidence suggests that in other environments, such as physiological conditions, where the fluid composition is radically different from a simple chloride solution, variations in the local concentration of oxygen might contribute for the regulation of the overall biodegradation of a magnesium-based implant. In the second part of this work, BDD microelectrodes were applied for the reduction of transition metal ions released during the corrosion of Mg (99.9%) during corrosion in NaCl 0.5 M, particularly Ni (II), at deposition potentials between -1.3 and -1.5 V vs Ag|AgCl. SEM and EDS were used to investigate both the compounds deposited on the microelectrode surface and the corrosion products on the corroded Mg sample, showing that similar Ni-rich compounds can be found in the microelectrode and in the periphery of surface cracks on the Mg surface. These results are in good agreement with a recently proposed mechanism [2] of oxidation and redeposition of transition metal impurities, which may act as moving cathodes during Mg corrosion.

Hence, this work demonstrates how properties such as fast response time and wide potential window in aqueous solution, allow the fast mapping of DO over large Mg surfaces, as well as the reduction of aqueous species at distinct potentials at the BDD surface, at a potential range that would be problematic with more common electrode materials due to the strong rate of hydrogen evolution.

[1] E. L. Silva, A. C. Bastos, M. A. Neto, A. J. S. Fernandes, R. Silva, M. G. S. Ferreira, M. L. Zheludkevich, F. Oliveira, *Sens. Act. B*, 204 (2014) 544-551

[2] D. Höche, C. Blawert, S. V. Lamaka, N. Scharnagl, C. Mendis, M. L. Zheludkevich, *Phys. Chem. Chem. Phys.*, 18 (2016) 1279-1291

Highly Enantioselective Electrosynthesis at Mesoporous Chiral Metal Surfaces

Chularat Wattanakit¹, Thittaya Yuthalekha¹, Sunpet Assavapanumat^{1,2}, Veronique Lapeyre², Somkiat Nokbin³, Chompunuch Warakulwit³, Jumras Limtrakul¹ and Alexander Kuhn²

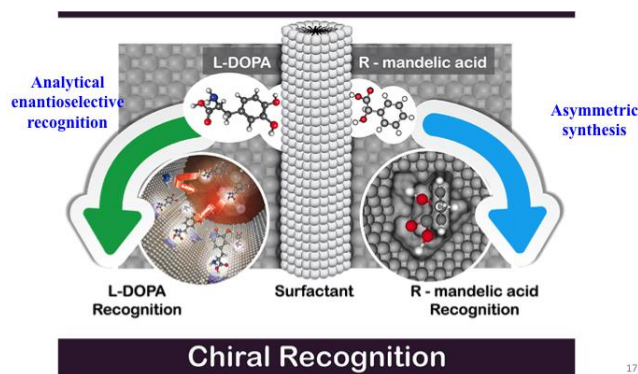
¹Vidyasirimedhi Institute of Science and Technology, Rayong 21210, Thailand.

²Univ. de Bordeaux, CNRS, ISM, UMR 5255, Pessac, France.

³Department of Chemistry, Faculty of Science, Kasetsart University, Bangkok 10900, Thailand

e-mail: chularat.w@vistec.ac.th

Enantioselective recognition and asymmetric synthesis of enantiomers are crucial scientific challenges due to a large number of potential applications, in particular, sensing and catalysis. We report here the elaboration of chiral imprinted mesoporous metal, obtained by the electrochemical reduction of platinum salts in the simultaneous presence of a liquid crystal phase and chiral template molecules [1, 2]. The chiral encoded mesoporous metal perfectly retains the chiral information after removal of the template and shows a very significant discrimination between two enantiomers when using these materials as electrodes in Differential Pulse Voltammetry. Interestingly, such nanostructured metals are also able to break the symmetry during the electrochemical synthesis of mandelic acid as a model molecule [3, 4]. The R/S ratio of the synthesis product is higher than unity when using (R)-imprinted electrodes and vice versa for the (S)-imprinted ones. In addition, we could demonstrate that by optimizing the electrochemical synthesis parameters it is possible to achieve very high enantiomeric excess (>90 %) [5]. Therefore, these designer surfaces open new promising horizons not only for electroanalysis, but also for efficient enantioselective electrosynthesis.



Scheme 1 Illustration of enantioselective recognition and asymmetric synthesis at mesoporous chiral metal surfaces

References

- [1] C. Wattanakit, Y. Bon Saint Côme, V. Lapeyre, P. A. Bopp, M. Heim, S. Yadnum, S. Nokbin, C. Warakulwit, J. Limtrakul, A. Kuhn, *Nat. Comm.* 2014, 5:3325.
- [2] T. Yuthalekha, C. Warakulwit, J. Limtrakul, A. Kuhn, *Electroanalysis*, 2015, 27: 2209.
- [3] T. Yuthalekha, C. Wattanakit, V. Lapeyre, S. Nokbin, C. Warakulwit, J. Limtrakul, A. Kuhn, *Nat. Comm.* 2016, 7:12678.
- [4] C. Wattanakit, *Current Opinion in Electrochemistry*, 2017, 7:54–60.
- [5] C. Wattanakit, T. Yuthalekha, S. Assavapanumat, V. Lapeyre, A. Kuhn, *Nat. Comm.* 2017, in press, DOI: 10.1038/s41467-017-02190-z.

Hydrogen-Induced Structural Changes in Electrodeposited Metal Films

Naoki Fukumuro^{1,*}, Yuh Fukai², Ayumu Matsumoto¹, Shinji Yae¹

¹ Department of Chemical Engineering and Materials Science, Graduate School of Engineering, University of Hyogo, 2167 Shosha, Himeji, Hyogo, 671-2280, Japan

² Institute of Industrial Science, The University of Tokyo

4-6-1 Komaba, Meguro-ku, Tokyo, 153-0041, Japan

*fukumuro@eng.u-hyogo.ac.jp

The behavior of hydrogen in electrodeposited metal films plays a critical role in the structural changes. Thermal desorption spectroscopy (TDS) can discriminate between different hydrogen trap sites in metals (i.e., regular interstitial sites, vacancies, voids, etc.) from distinct desorption temperatures. The TDS study revealed that superabundant vacancies (SAVs) were formed in metals under high hydrogen pressures and temperatures, and in electrodeposited metals as well [1]. Over the past decade, we have investigated the atomistic state and behavior of hydrogen in 10 kinds of electrodeposited metal films by the TDS measurements. This paper describes the hydrogen-induced structural changes observed notably in several electrodeposited metal films of high hydrogen concentrations.

We previously reported that the room-temperature grain growth was observed in electrodeposited Cu films with higher hydrogen concentrations [2]. For the Cu films electrodeposited from a sulfate bath containing additives ($x = \text{H}/\text{Cu} = 5.4 \times 10^{-4}$), a chloride bath containing citric acid ($x = 45.7 \times 10^{-4}$), ethylenediamine (EDA)-complex bath ($x = 98.2 \times 10^{-4}$), and ethylenediaminetetraacetic acid (EDTA)-complex bath ($x = 78.1 \times 10^{-4}$), the grain growth proceeded as hydrogen desorption proceeded during 7~21 days after deposition. On the other hand, such grain growth was not observed in the Cu films with lower hydrogen concentrations electrodeposited from an acid sulfate bath ($x = 0.8 \times 10^{-4}$) and a pyrophosphate bath ($x = 0.2 \times 10^{-4}$).

In the case of Pd films electrodeposited from an ammonium chloride bath containing citric acid, different structural changes depending on the hydrogen concentration were observed with hydrogen desorption at room temperature [3]. For the Pd films with higher hydrogen concentrations ($x = \text{H}/\text{Pd} \geq 0.058$), fine grains became large columnar grains, and a large-grained Cu-Pd interlayer was formed by interdiffusion between the Cu substrate and the Pd film. On the other hand, for the Pd films with lower hydrogen concentrations ($x \leq 0.040$), the lattice contraction and grain growth proceeded as hydrogen desorption proceeded. Such lattice contraction can only be explained in terms of hydrogen-induced SAV formation [4].

In the case of Pt films electrodeposited from a dinitrosulfatoplatinate(II) bath, the hydrogen concentration was extremely high ($x = \text{H}/\text{Pt} = 0.10$), which remained almost unchanged 30 days after deposition at room temperature [5]. The lattice parameter contracted slightly (~0.3%) and many nano-voids were observed in the fine-grained texture of Pt film (Fig. 1). The lattice contraction decreased and the pronounced grain growth occurred with hydrogen desorption by low temperature heat treatments (~500 K).

The primary cause of these structural changes may be ascribed to the formation of hydrogen-induced SAVs.

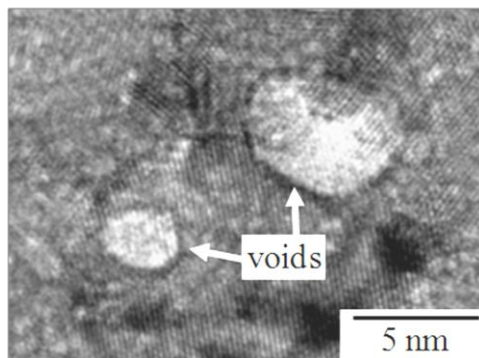


Fig. 1 TEM image of electrodeposited Pt film.

Acknowledgement

This work was partly supported by JSPS KAKENHI Grant Number JP17K06864.

References

- [1] Y. Fukai, M. Mizutani, S. Yokota, M. Kanazawa, Y. Miura, T. Watanabe, *J. Alloys Compd.*, 356-357 (2003) 270.
- [2] N. Fukumuro, H. Yoshida, T. Yamazaki, Y. Fukai, S. Yae, *J. Japan. Inst. Met. Mater.*, 80 (2016) 736.
- [3] N. Fukumuro, M. Yokota, S. Yae, H. Matsuda, Y. Fukai, *J. Alloys Compd.*, 580 (2013) S55.
- [4] Y. Fukai, *Phys. Scr.*, T103 (2003) 11.
- [5] N. Hisanaga, N. Fukumuro, S. Yae, H. Matsuda, *ECS Trans.*, 50(48) (2013) 77.

3D Printing 2D Materials-Based Electrodes for Electrochemical Energy Storage and Conversion

Victor A. Beck¹, Todd Weisgraber¹, Anna N. Ivanovskaya¹, Swetha Chandrasekaran¹, Cheng Zhu¹, Bin Yao², Yu Song², Tianyu Liu², Fang Qian¹, Ryan Hensleigh³, Bryan D. Moran¹, Seth E. Watts¹, Dan A. Tortorelli¹, Eric B. Duoss¹, Juergen Biener¹, Michael Stadermann¹, Xiaoyu Zheng³, Yat Li², Marcus A. Worsley¹

¹*Lawrence Livermore National Laboratory, 7000 East Ave, Livermore, California, United States*

²*University of California – Santa Cruz, Santa Cruz, California, United States*

³*Virginia Polytechnic Institute and State University, Blacksburg, Virginia, United States*
worsley1@llnl.gov

Two-dimensional (2D) nanomaterials, such as graphene and transition metal dichalcogenides, hold extraordinary promise for application in a number of electrochemical technologies. Electrochemical energy storage (EES) devices, such as lithium-ion batteries, flow batteries, and supercapacitors, in particular, have seen 2D materials integrated into various components with exciting results. In general, EES devices are emerging as primary power sources for global efforts to shift energy dependence from limited fossil fuels towards sustainable and renewable resources. These EES devices, while renowned for their high energy or power densities, portability, and long cycle life, are still facing significant performance hindrance due to manufacturing limitations. One major obstacle is the ability to engineer macroscopic components that possess designed and highly resolved microstructures with optimal performance, via controllable and scalable manufacturing techniques. 3D printing covers several additive manufacturing methods that enable well-controlled creation of functional materials with 3D architectures, representing a promising approach for fabrication of next-generation EES devices with high performance. Here, we present recent work to a) develop modeling and optimization algorithms that determine the optimal electrochemical cell geometries for various performance objectives (e.g. maximize current, minimize pressure drop, etc.) and b) fabricate 3D functional electrodes utilizing 3D printing-based methodologies. Specifically, the framework of the 3D printing techniques such as projection microstereolithography and direct ink writing are described, as well as the details of respective feedstock development efforts. Finally, characterization of the 3D-printed electrodes and their performance in various EES applications (e.g. supercapacitors and batteries) will be compared with predicted performance and discussed.

This work was performed under the auspices of the U.S. Department of Energy by Lawrence Livermore National Laboratory under Contract DE-AC52-07NA27344.

Type the title single-spaced in 14-point Times Roman bold, upper and lower case and NOT in ALL CAPITAL letters.

Type the author(s) name(s) single-spaced in 10-point Times Roman regular.

Type the affiliation(s) and address(es) single-spaced in 10-point Times Roman italic.

Type the body of the abstract text (including references and tables) single-spaced in 10-point Times Roman regular.

Paper Size: A4 (21.0 x 29.7 cm)

Margins

Top: 30.0 mm

Bottom: 30.0 mm

Sides: 30.0 mm

Tuning the ionomer distribution in catalyst Layer with scaling the ionomer aggregate size in dispersion for high performance PEMFC

Gisu Doo[†], Ji Hye Lee[§], Seongmin Yuk[†], Sungyu Choi[†], Dong-Hyun Lee[†], Dong Wook Lee[†], Hyun Gyu Kim[†], Sung Hyun Kwon[§], Seung Geol Lee[§], Hee-Tak Kim[†],

[†]Department of Chemical and Biomolecular Engineering, Korea Advanced Institute of Science and Technology (KAIST), Daejeon 34141, Republic of Korea

[§]Department of Organic Material Science and Engineering, Pusan National University, Busan 46241, Republic of Korea
heetak.kim@kaist.ac.kr

With the demands for better performance of polymer electrolyte membrane fuel cells, studies on controlling the distribution of ionomers have recently gained interest. Here, we present a tunable ionomer distribution in the catalyst layer (CL) with dipropylene glycol (DPG) and water mixtures as ionomer dispersion medium. Dynamic light scattering and molecular dynamics simulation demonstrate that, by increasing the DPG content in the dispersion, the size of the ionomer aggregates in the dispersion is exponentially reduced due to the higher affinity of DPG for the backbone of Nafion ionomers. The ionomer distribution of the resulting CLs dictates the dimensional feature of the ionomer dispersion. Although the ionomer distribution becomes more uniform with increasing the DPG content, an optimal power performance is obtained at a DPG content of 50 wt% regardless of feed humidity due to balanced proton and mass transports. As a guide for tuning the ionomer distribution, we suggest that the ionomer aggregates in the dispersion with a size close to that of the Pt/C aggregates form a highly connected ionomer network and maintain a porosity in the catalyst/ionomer aggregate resulting in high power performance.

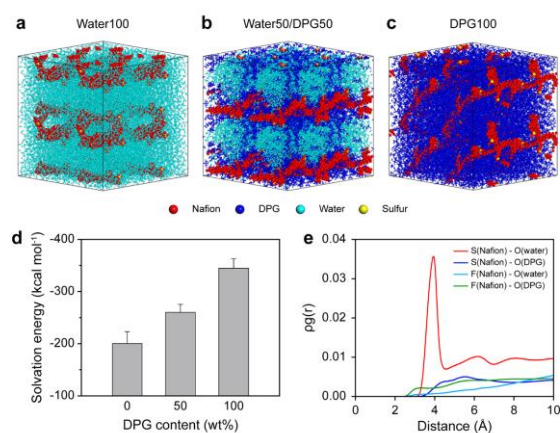


Figure 1. Equilibrium structures with a 2 x 2 x 2 supercell of Nafion ionomer in (a) water, (b) water/DPG (50/50) mixture and (c) DPG solvent. The red, blue and cyan colors denote the Nafion ionomer, DPG and water molecules, respectively. Sulfur atoms of the Nafion ionomer are represented by yellow colors for clarity. (d) The solvation energies of the Nafion ionomers in each solvent system and (e) radial distribution functions of the Nafion ionomer in water/DPG (50/50) mixture solvent.

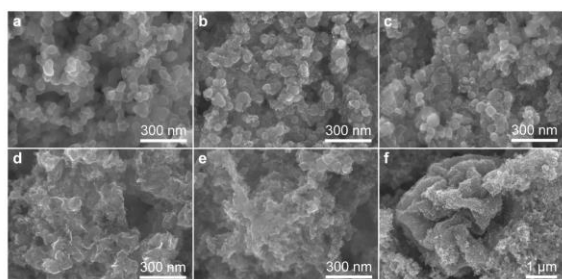


Figure 2. SEM image of the catalyst layer fabricated with (a) DPG 100 wt% (b) DPG 70 wt% (c) DPG 50 wt% (d) DPG 30 wt% (e-f) DPG 0wt% aqueous dispersions. TEM images of the catalyst layer fabricated with (a) DPG 100 wt% (b) DPG 70 wt% (c) DPG 50 wt% (d) DPG 30 wt% (e-f) DPG 0wt% aqueous dispersions

Pressurized Hydrogen Production with Anion Exchange Membrane Electrolysis

Hiroshi Ito¹, Natsuki Kawaguchi^{1,2}, Satoshi Someya^{1,2}, Tetsuo Munakata^{1,2}, Akihiro Nakano¹

¹ National Institute of Advanced Industrial Science and Technology (AIST)

1-2-1 Namiki, Tsukuba 305-8564, Japan

² Graduate School of Frontier Sciences, The University of Tokyo

5-1-5 Kashiwa-no-ha, Kashiwa 277-8563, Japan

ito.h@aist.go.jp

In attempting the renewable energy use promotion, the role of hydrogen as the energy carrier has become very important for buffering fluctuated and intermittent power from renewable energy sources. As the conversion device from renewable energies into hydrogen (H₂), a water electrolyzer is simply and most realistic. There have been two major existing technologies for water electrolyzers; alkaline (solution) electrolysis and proton exchange membrane (PEM) electrolysis. Among them, the PEM system is promising technology due to its high efficiency and flexibility. Technical advantages of the PEM system are mainly attributed to the membrane potential and cell structure. One of major drawbacks of PEM electrolysis is high capital cost per power. The acidic environment of PEM limits the material of cell components (bipolar plates and current collectors) and the catalyst to titanium (Ti) and PGM, respectively. The use of these precious materials is one of major reasons of high stack cost of the PEM electrolyzer. The material restriction for the cell components should be relieved, when a membrane performing under alkaline (basic) conditions was applied. In particular, there is a possibility that the material of bipolar plates is changed from Ti to cheaper material such as stainless steel. Recently, several research groups demonstrated a new electrolysis technology using alkaline anion exchange membrane (AEM) [1-3].

In this study, we tried pressurized hydrogen production using the AEM electrolyzer. In our lab, a small scale (electrode area = 25cm²) AEM electrolytic cell was fabricated with AEM, carbon paper GDL (cathode), and nickel form GDL (anode), where Pt/C and CuCoO_x was applied for cathode and anode catalyst, respectively. The cell was operated at 50 °C and an electrolytic solution (10 wt.-%-K₂CO₃ aq) was circulated only at the anode side. Hydrogen pressure of cathode compartment (P_{H_2}) was controlled with a back pressure valve. Fig.1 shows the current density (i) – cell voltage (V_{cell}) characteristics under different P_{H_2} (1.0, 5.0, and 8.5 bar (abs)). It was proven that the pressure dependency on the i - V characteristics was limited under the present range of P_{H_2} . Hydrogen permeation flux through the membrane was also measured.

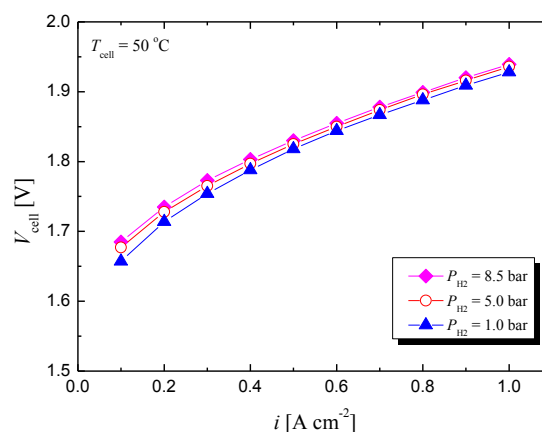


Fig. 1 : Current density (i) – cell voltage (V_{cell}) characteristics during AEM electrolysis under different pressures of hydrogen(P_{H_2}).

References

- [1] L. Xiao et al. Energy Environ. Sci.2 (2012) 7869.
- [2] S. H. Ahn et al. J. Mater. Chem. 22 (2012) 15153.

[3] C. C. Pavel et al. *Angew. Chem. Int. Ed.* 53 (2014) 1378.

Investigation of nitriding treated Ni-free stainless steel as current collector for 5V-class Li-ion secondary cell

Sayoko Shironita¹, Neil Ihsan¹, Kotaro Konakawa¹, Kenichi Souma^{1,2}, Minoru Umeda^{1,*}

¹ Nagaoka University of Technology, 1603-1, Kamitomioka, Nagaoka, Niigata 940-2188, Japan

² Hitachi Industrial Equipment Systems Co., Ltd, 3 Kanda Neribe, Chiyoda, Tokyo 101-0022, Japan

* mameda@vos.nagaokaut.ac.jp

Li-ion secondary cells have been widely used as a power sources in portable electronic devices and electric vehicles, and further higher operating voltage and higher capacity are required. To realize higher operating voltage, it is necessary to develop a cathode current collector material with high corrosion resistance. In our previous study, it is found that a corrosion resistance of Ni-free stainless steel in an acid aqueous solution is improved by a nitriding heat treatment [1]. Therefore, in this study, the corrosion resistance as the cathode current collector of the nitriding treated Ni-free stainless steel was electrochemically evaluated.

The Ni-free stainless steel SUS445 was nitrided by a heat treatment in N₂ atmosphere at 1473 K for 4 h. The nitriding treated stainless steel is SUS445N. Electrochemical measurement was conducted using a T-type three electrode glass cell. The working electrodes were SUS445N and Al plate. Li foils were used as counter and reference electrodes. The electrolyte was 1 mol dm⁻³ LiPF₆/ethylene carbonate (EC) + dimethyl carbonate (DMC) (1:1v/v%). All electrochemical measurements were performed in Ar atmosphere using a glove box. SUS445N was conducted a potential sweep for 30 min in a range of 0-5 V vs. Li/Li⁺ prior to measure cyclic voltammogram.

Figure 1 shows the cyclic voltammograms of SUS445N and Al in 1 mol dm⁻³ LiPF₆/EC+DMC. In addition, the cyclic voltammograms of LiCoO₂ [2] and LiNi_{0.5}Mn_{1.5}O₄ [3] of the cathode active material are shown in Fig. 1. The Li-ion extraction and insertion of LiCoO₂ and LiNi_{0.5}Mn_{1.5}O₄ take place at 3.7-4.2 V vs. Li/Li⁺ and 4.5-5.2 V vs. Li/Li⁺, respectively. Al is stable until 4.3 V vs. Li/Li⁺, but the dissolution of Al occurs at more positive potential than 4.3 V vs. Li/Li⁺. In the case of LiCoO₂, Al can be used as the cathode current collector. However, Al cannot be used in the case of LiNi_{0.5}Mn_{1.5}O₄. On the other hand, the nitriding treated SUS445N is stable until 5.5 V vs. Li/Li⁺. Therefore, it was found that SUS445N possesses a potential as the cathode current collector material for Li-ion secondary cell.

References

- [1] Y. Yu, S. Shironita, K. Nakatsuyama, K. Souma, M. Umeda, *Appl. Surf. Sci.*, **388**, 234-238 (2016).
- [2] K. Dokko, M. Mohamedi, Y. Fujita, T. Itoh, M. Nishizawa, M. Umeda, I. Uchida, *J. Electrochem. Soc.*, **148**, A422-A426 (2001).
- [3] K. Dokko, N. Anzue, Y. Makino, M. Mohamedi, T. Itoh, M. Umeda, I. Uchida, *Electrochemistry*, **71**, 1061-1063 (2003).

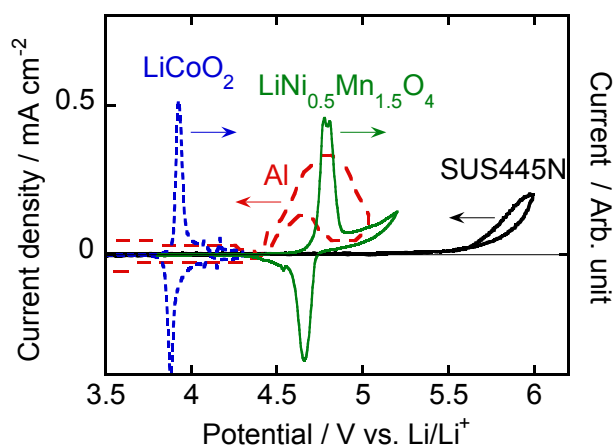


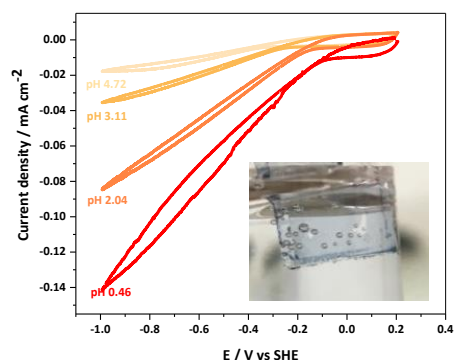
Fig. 1 Cyclic voltammograms of SUS445N (solid line) and Al (broken line) in 1 mol dm⁻³ LiPF₆/EC+DMC (1:1v/v%). Sweep rate: 10 mV s⁻¹. Cyclic voltammograms of Li-ion extraction and insertion at LiCoO₂ (dotted line)^[2] and LiNi_{0.5}Mn_{1.5}O₄ (solid line)^[3].

Vapor Phase Polymerized PEDOT for Electrochemical Hydrogen Evolution Reaction

Roudabeh Valiollahi, Mikhail Vagin, Amritpal Singh, Igor Zozoulenko, Xavier Crispin
*Laboratory of Organic Electronics, Department of Science and Technology, Linköping University, SE-601 74
Norrköping, Sweden*
roudabeh.valiollahi@liu.se

Ever increasing demand for clean and renewable energy sources initiated a research area to explore fossil-free fuels and energy sources. Due to their high energy efficiency, fuel cells as energy conversion devices are candidates for producing electricity from chemical energy carriers like hydrogen. Hydrogen is the common fuel for fuel cells which can be produced by electrochemical water splitting in an electrolyzer by reducing protons to molecular hydrogen. Since the hydrogen evolution reaction (HER) naturally has sluggish kinetics, electrocatalysts play a key role to increase the rate and efficiency of this reaction. One option is to use precious metal catalysts, such as platinum, palladium, *etc.* The precious metal's prohibitive cost and source scarcity hinder their practical usage as catalyst in large scale electrolyzers. Thus, it is of great importance to introduce and develop efficient and low-cost catalysts based on non-noble metals.

In this context, organic conductors such as conducting polymers are of interest and have not been investigated in details. One interesting candidate is Poly(3,4-ethylenedioxythiophene) (PEDOT) a highly conductive, electrochemically stable and cost-effective polymer. Previous studies showed that PEDOT had some electrochemical activity for hydrogen evolution reaction¹⁻³ but the role of the underlying electrodes was not clear. In the present work, we studied the fundamental HER electrochemistry on vapor phase polymerized (VPP) PEDOT. The PEDOT thin film electrode was polymerized on a glass substrate in order to rule out competitive substrate effects. The figure shows cyclic voltammograms of the hydrogen evolution on PEDOT in different pHs. The studies showed that PEDOT is an active catalyst material for the HER and that the polymer activity can be optimized by a variety of parameters. Theoretical studies also have been done to investigate the probable mechanism of HER on PEDOT film.



Cyclic voltammogram of HER on PEDOT/glass in H₂SO₄ at different pHs. Potential sweep rate: 5 mVs⁻¹. Inset: Typical photo of produced hydrogen bubbles on the electrode surface

References

1. B. Winther-Jensen, K. Fraser, C. Ong, M. Forsyth and D. R. MacFarlane, *Adv. Mater.*, 2010, **22**, 1727-1730.
2. R. K. Pandey and V. Lakshminarayanan, *J. Phys. Chem. C*, 2010, **114**, 8507-8514.
3. H. T. Xu, Z. Q. Jiang, H. J. Zhang, L. Liu, L. Fang, X. Gu and Y. Wang, *ACS Energy Lett.*, 2017, **2**, 1099-1104.

Electric-Field Assisted Deposition of Carbon Nanostructures as a Binder-Free Approach to Fabricate High-Efficiency Li-S Batteries

S. Ghashghaie, H. S. Cheng, ?, ?, ?

Affiliation

Address

Sghashgh a2-c@my.cityu.edu.hk

Compared with the conventional li-ion batteries, lithium-sulfur (Li-S) batteries have been recognized as one of the most promising energy storage systems for the next-generation of lithium batteries regarding their high theoretical specific capacity (1675 mAhg^{-1}) and energy density (2600 Whkg^{-1}) [1]. In the present study, the multi-step electrophoretic deposition (EPD) method [2] was successfully employed as a facile approach to deposit a layered structure of conductive agents on the surface of Al sheet (as current collector). For this purpose, uniform DC electric fields in the range of 20-100 V were applied to stable suspensions of carbon black and MWCNTs in acetone for certain durations to obtain crack-free uniform layers. In the first step, a thick layer of carbon black was deposited on Al sheet serving as a 3-D framework for the following CNT layer. The obtained Al/CB/CNT cathode was impregnated with sulfur using a facile vapor-phase infusion technique at 200°C on hot plate. The galvanostatic charge-discharge profiles of the coin cells containing liquid organic electrolyte and lithium metal anode exhibited an initial discharge capacity of around 1000 mAhg^{-1} along with an improved capacity retention rate after up to 50 cycles and coulombic efficiency of 94% at 0.1 C. The obtained results clearly show that cathode structures with significantly high discharge capacity and enhanced cycling behavior can be fabricated by simultaneous application of EPD technique and the sulfur vapor infusion method. The rate-capability tests carried out at 0.1C, 0.5C, 1C, and 2C also revealed relatively high cyclability of the cells. As a result, the EPD method can be applied as a facile binder-free and flexible method to fabricate layered/composite cathode structures for Li-S batteries.

[1] X. Zhanga, H. Xieb, C.-S. Kimc, K. Zaghibc, A. Maugerd, C.M. Juliend, *Mater Sci Eng R Rep*, 121 (2017) 1–29.

[2] M. Diba, D. W. H. Fam, A. R. Boccaccini, and M. S. P. Shaffer, *Prog. Mater. Sci.*, 82 (2016) 83–117.

Au-Pd-Pt Catalyst for Miniature Fuel Cells with Monolithically Fabricated Si Electrodes

Masanori Hayase^a, Ryo Shira^a, Toshimitsu Miyauchi^a, Natasa Vasiljevic^b

^aTokyo University of Science

2641 Yamazaki, Noda, Chiba, Japan

^bUniversity of Bristol

mhayase@rs.noda.tus.ac.jp

We have developed miniature fuel cells with monolithically fabricated Si electrodes. In the fuel cells, two Si electrodes with porous Pt catalyst layer, in which amount of Pt was $3.6\text{mg}/\text{cm}^2$, were hot-pressed onto either side of a PEM (polymer electrolyte membrane), and the prototype fuel cells showed promising performances of over $500\text{mW}/\text{cm}^2$ peak power at 313K with $\text{H}_2\text{-O}_2$. However, recent improvements of Li-ion battery are lowering expectation to the miniature fuel cells. The advantage of the fuel cell, i.e. clean and efficient energy source, should be strengthened.

Bio-mass is an ultimate energy source, and hydrogen can be produced by gasification of the bio-mass in reducing environment. But high CO concentration in the bio-mass derived hydrogen is inevitable. Catalyst poisoning by CO is problematic. We found that our Pd-Pt catalyst obtained by using UPD (Underpotential deposition) -SLRR (Surface limited redox replacement) had promising feature. Though the catalyst layer used only $6\mu\text{g}/\text{cm}^2$ of Pt, high tolerance to CO and high peak power were observed. But Pd and Pt are rare metals, and both amounts should be minimized. In this study, a novel Au-Pd-Pt multilayer catalyst is proposed as shown in figure 1. Though Au is also a precious metal, reserve of Au is much larger than Pd and Pt, and porous Au can be formed on a Si substrate by similar process to porous Pt.

There is no clear evidence, but it is assumed that high CO tolerance of the Pd-Pt catalyst is realized with sub-monolayer Pt on Pd. Hydrogen absorption or stress near the interface between Pd and Pt are sensitive to the number of atomic layer of Pd, and fine control of Pd and Pt deposition on Au is crucial. In our previous study, sub-monolayer Pt was deposited with Cu-UPD, but hydrogen also absorbs on some metal surfaces and forms atomic monolayer at slightly under the equilibrium potential. The H-UPD-SLRR can be performed just in an acidic plating bath containing Pd^{2+} or Pt^{4+} . There is no need to replace the plating bath, and repetition of the atomic layer deposition process will be easy. In this study, basic fabrication strategy of the Au-Pd-Pt multilayer catalyst using H-UPD-SLRR process was examined using Au wire. Preliminary results of cyclic voltammetry suggested that Pd and Pt were successfully deposited on Au wire, and optimum amount of Pd and Pt for the catalytic activity were discussed as shown in figure 2.

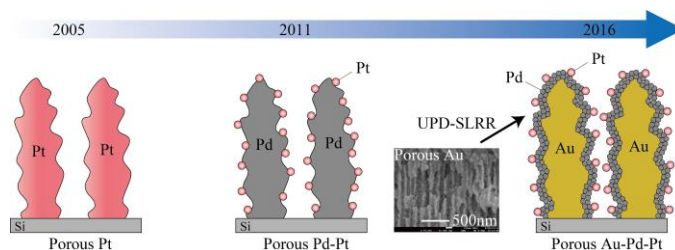


Figure 1. History of catalyst layers for our miniature fuel cells. In order to reduce Pt amount and obtain tolerance to CO, Au-Pd-Pt multilayer catalyst was proposed.

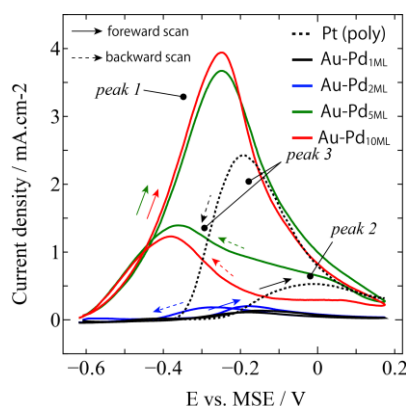


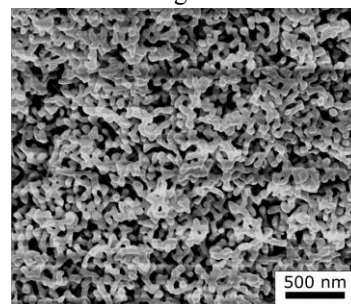
Figure 2. Cyclic voltammogram obtained in a formic acid solution. Pt, 1-10 ML Pd on Au were examined, and high CO tolerance was observed with 5 and 10 ML Pd on Au specimens.

Nanoporous Gold – A Prototype for a Rational Design of Catalysts: Electrocatalysis and Transport

Mareike Haensch¹, J. Behnken^{1,2}, L. Balboa¹, M. Graf³, J. Weissmüller^{3,4} and G. Wittstock¹

¹Carl von Ossietzky University of Oldenburg, Institute of Chemistry, Oldenburg, Germany; ²DLR Institute of Networked Energy Systems, Oldenburg, Germany; ³Hamburg University of Technology, Institute of Materials Physics and Technology, Hamburg, Germany; ⁴Helmholtz-Zentrum Geesthacht, Institute of Materials Research, Materials Mechanics, Geesthacht, Germany
mareike.haensch@uol.de

Nanoporous gold (NPG) is an interesting material for a wide range of applications such as (electro-) catalysis, sensing, energy storage and energy conversion due to its large surface-to-volume ratio, easy preparation, good electrical conductivity, high catalytic activity and chemical as well as structural flexibility. NPG is a nanoporous bulk material consisting of a bicontinuous network of pores and ligaments and it can be fabricated with a homogeneous structure up to several mm size. It can be obtained by dealloying a silver-gold alloy, either by free or by electrochemical corrosion. Although NPG consists mostly of pure gold, an amount of 1-3 at-% is Ag, the sacrificial metal. In addition to its very large surface-to-volume ratio, reactants inside the porous network have many more contacts with the pore walls than on a flat substrate which enhances the probability of a chemical reaction. By understanding the complex interplay of structure and properties, a rational design of NPG catalysts should be possible. Herein we are using electrochemical and spectroscopic methods to investigate NPG towards adsorbates, especially surface oxides and methanol oxidation, transport behavior inside the porous network and compositional changes during electrocatalysis.



The investigation of porous materials with electrochemical methods often faces transport limitations and concentration gradients in the pore space, which result in broad peaks in cyclic voltammograms unless the scan rate is extremely slow. The filling of the nanoporous material into a cavity microelectrode enables a more efficient mass transport and faster measurements. In this work we developed further the surface interrogation mode of scanning electrochemical microscopy (SECM) which was introduced for flat samples^[1] and investigated NPG inside cavity-microelectrodes to probe active sites. First we investigated electrochemically generated surface oxides^[2] with regard to detect adsorbates during methanol electro-oxidation. Digital simulations with COMSOL supported our findings.

To investigate mass transfer inside the porous network of NPG with different morphologies we used SECM approach curves to obtain relative effective diffusion coefficients. The experiments with ascorbic acid (as an example for a small organic molecule) show a strong influence of pore size on the transport and the obtained relative effective diffusion coefficient are in good agreement with estimates based on porosity and tortuosity derived from electron micrographs.

Furthermore, x-ray photoelectron spectroscopy (XPS) can be used to identify the composition of NPG and distribution of residual silver due to the chemical shift of Ag in NPG. The Ag 3d peak is shifted to lower binding energies the more diluted the silver is in the silver-gold alloy. After a calibration of the binding energy for different silver-gold alloys we could confirm earlier studies which showed that Ag is not homogeneously distributed in the material but forms Ag-rich regions.^[3] In addition, XPS showed that the electrochemical cycling in methanol-containing solution resulted in a compositional change of the NPG.^[4]

[1] J. Rodríguez-López, M. A. Alpuche-Avilés, A. J. Bard, *J. Am. Chem. Soc.* **2008**, *130*, 16985.

[2] M. Haensch, J. Behnken, L. Balboa, A. Dyck, G. Wittstock, *Phys. Chem. Chem. Phys.* **2017**, *19*, 22915.

[3] T. Krekeler, A. V. Straßer, M. Graf, K. Wang, C. Hartig, M. Ritter, J. Weissmüller, *Mater. Res. Lett.* **2017**, *1*.

[4] M. Graf, M. Haensch, J. Carstens, G. Wittstock, J. Weissmüller, *Nanoscale* **2017**, *9*, 17839.

Improving the electrode-electrolyte link in high-temperature polymer electrolyte membrane fuel cells by catalyst support functionalization

T. Jurzinsky¹, E. D. Gomez Villa^{1,2}, J. Melke³, M. Bruns^{2,4}, F. Scheiba², C. Cremers¹

1 Department for Applied Electrochemistry, Fraunhofer Institute for Chemical Technology ICT

Joseph-von-Fraunhofer-Straße 7, 76327 Pfanzelt, Germany

2 Institute for Applied Materials (IAM), Karlsruhe Institute of Technology (KIT)

Hermann-von-Helmholtz-Platz 1, 76344 Eggenstein-Leopoldshafen, Germany

3 Institute of Inorganic and Analytic Chemistry, University of Freiburg

Albertstraße 21, 79104 Freiburg, Germany

4 Karlsruhe Nano Micro Facility (KNMF), Karlsruhe Institute of Technology (KIT)

Hermann-von-Helmholtz-Platz 1, 76344 Eggenstein-Leopoldshafen, Germany

e-mail address: tilman.jurzinsky@ict.fraunhofer.de

High-temperature polymer electrolyte membrane fuel cells (HT-PEMFCs) are an emerging energy technology for efficient power generation from alcohol and hydrocarbon fuels and for combined heat and power (CHP) systems. The German-based company Elcore already introduced such systems to the market for the residential sector. The German company Fischer Eco-Solutions and its Danish sister Serenergy have demonstrated a HT-PEMFC solution on board of passenger Ship “MS Innogy” in Germany. The term high-temperature in HT-PEMFC refers to an operation temperature between 120 and 200 °C. This temperature range is higher than the one of the well-developed PEMFCs (approx. 80°C), but admittedly it is noticeably lower than for typical high-temperature fuel cells (e.g. solid oxide fuel cells) which operate at > 600 °C. Instead of a proton-exchange membrane such as Nafion typically used in PEMFCs, HT-PEMFCs make use of a H₃PO₄-doped Polybenzimidazole (PBI) membrane as electrolyte to be able to operate at temperatures higher than 120 °C.

A known advantage of HT-PEMFCs over PEMFCs is that HT-PEMFCs are less prone to catalyst poisoning from fuel impurities such as CO due to the higher temperature. At 80 °C, a carbon monoxide content of 25 ppm in the fuel supply results in a significant loss in cell performance [1]. On the other hand at 180 °C, even 2 to 5 % of carbon monoxide is bearable for the fuel cell [2,3]. Hence, there is no need of hydrogen purification for HT-PEMFCs, which makes them a suitable technology to be run with hydrogen originating from reforming processes. This is a valuable option especially if a hydrogen infrastructure is missing. On the downside, HT-PEMFCs lack of a suitable catalyst binder. While PEMFCs make use of the well-known Nafion as a binder, Su et al. reported that compared to a membrane electrode assembly (MEA) with PBI as binder the higher cell performance is reached by using PTFE as a binder in HT-PEMFC MEAs due to superior catalyst layer structure [4]. However, PTFE isn't a proton-conductive polymer. Therefore, the usage of PTFE in the catalyst layer leads to lowered Platinum catalyst utilization because parts of the Platinum are not electrolytically linked to the H₃PO₄-doped PBI membrane.

In this study, we present a novel way to improve the link between the catalyst and the H₃PO₄ electrolyte by functionalizing the catalyst support. By introducing Indazole groups to the surface of carbon nanotubes (CNTs), the functionalized catalyst support is able to interact with H₃PO₄ in a similar way as it is done in PBI membranes. The new material is able to integrate well with the gas diffusion layer (GDL) as well as the membrane thus allows for low interfacial resistance. The novel CNT material was physically characterized via thermogravimetric analysis coupled with mass spectrometry (TGA-MS), X-ray photoelectron spectroscopy (XPS) and near edge X-ray absorption fine structure (NEXAFS). Additionally, electrochemical measurements and contact angle experiments showed the property changes from non-functionalized to functionalized CNTs. Ultimately, Pt nanoparticles were applied onto Indazole-functionalized CNTs and the resulting catalyst was not only investigated regarding its activities for oxygen reduction and CO oxidation reactions, but also implemented into HT-PEMFC MEAs.

References

- [1] H.-F. Oetjen, V.M. Schmidt, U. Stimming, F. Trila, J. Electrochem. Soc. 143 (1996) 3838.
- [2] Q. Li, R. He, J.-A. Gao, J.O. Jensen, N.J. Bjerrum, J. Electrochem. Soc. 150 (2003) A1599.
- [3] S.K. Das, A. Reis, K.J. Berry, Journal of Power Sources 193 (2009) 691–698.
- [4] H. Su, S. Pasupathi, B. Bladergroen, V. Linkov, B.G. Pollet, International Journal of Hydrogen Energy 38 (2013) 11370–11378.

The Enhancement of Electron-Acceptor Properties of Extended Corannulenes

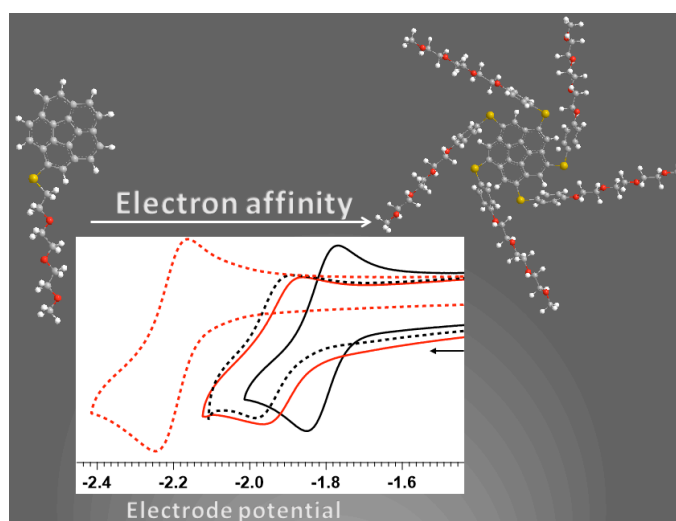
Maja Budanovic^a, Surendra Mahadevegowda^b, Dzeneta Halilovic^a, Mihaiela C. Stuparu^{a*}, Richard D. Webster^{a*}

^aNanyang Technological University, School of Physical and Mathematical Science; ^bNanyang Technological University, School of Biological Science

^a21 Nanyang Link, Singapore 637371; ^b60 Nanyang Drive, Singapore 637551

¹maja001@ntu.edu.sg; ²surendrahm@ntu.edu.sg; ³dzeneta001@ntu.edu.sg; ⁴webster@ntu.edu.sg; ⁵mstuparu@ntu.edu.sg;

Corannulenes, as bowl-shaped polycyclic aromatic hydrocarbons with high symmetry, have unique geometric and electronic properties¹. As a result of these properties, significant research has been conducted for industrial and academic purposes with the aim of designing new materials offering a wide range of applications, including electron acceptor molecules for active organic polymers and conductive charge-transfer complexes². One of the greater challenges encountered in supramolecular chemistry of corannulenes is the enhancement of their electron acceptor ability. Previous studies have shown that corannulenes can be modified with different substituents to alter their electronic and steric properties³. This changes the reduction potential and reaction kinetics involved that may increase electron affinity and lower the amount of energy needed for corannulene reduction. Studies performed on corannulene derivatives in dimethylformamide have shown that stilbene-like fluorinated substituents shift the reduction potentials towards less negative values, hence inducing greater electron affinity. From the electrochemical behavior of polycyclic aromatic sulfones and sulfides, it can be deduced that the presence of sulfur-containing substituents on the corannulene core shifts its redox potentials to less negative values by an electron-withdrawing inductive effect. All corannulene derivatives showed some degree of one-electron reversible reduction, whereas some corannulene derivatives exhibit reversibility in the second reduction process resulting in an EEC mechanism. Controlled potential electrolysis experiments showed that the first reduction process for corannulene results in reduced anion species stable under the timescale of the experiment ($t = 1200$ s) and could be reversibly oxidized back to the neutral corannulene. In this presentation, we examine effect of various electron-withdrawing substituents on the electron-acceptor properties of corannulenes, and how advances in synthetic transformations can help contribute to the development of functional materials.



References:

1. Scott, L. T. *Angew. Chem., Int. Ed.* **2004**, *43*, 4994.
2. Parschau, M.; Fasel, R.; Ernst, K.-H.; Groning, O.; Brandemberger, L.; Schillinger, R.; Greber, T.; Seitsonen, A. P.; Wu, Y.-T.; Siegel, J. S. *Angew. Chem., Int. Ed.* **2007**, *46*, 8258.
3. Kuvychko, I.; Dubceac, C.; Deng, S. H. M.; Wang, X.-B.; Granovsky, A.; Popov, A.; Petrukhina, M.; Strauss, S.; Boltalina, O. *Angew. Chem., Int. Ed.* **2013**, *52*, 7505.

Electrochemical activation of graphene nanowalls synthesized by plasma-enhanced chemical vapor deposition for high-voltage organic EDLCs

Da-Je Hsu,¹ Yu-Wen Chi,^{1,2} Kun-Ping Huang,² and Chi-Chang Hu^{1,*}

¹Department of Chemical Engineering, National Tsing Hua University, Hsin-Chu, Taiwan

²Mechanical and Systems Research Laboratories, Industrial Technology Research Institute, Hsinchu,

*Corresponding author, E-mail: cchu@che.nthu.edu.tw

In this work, plasma-enhanced chemical vapor deposition (PECVD) and microwave plasma torch (MPT) techniques were used to produce vertical graphene nanowalls (GNWs). The crystal quality (defects) and layers of GNWs can be controlled by adjusting the flow rate of precursor and the pressure in the CVD chamber. Characterization of materials includes Raman spectroscopy, scanning electron microscopy, X-ray diffraction analysis and Brunauer-Emmett-Teller surface area analysis. We discover that cyclic voltammetry (CV) is an effective tool for activating the charge storage capacity of GNW in 1 M TEABF₄ / PC (propylene carbonate) between 2 and -3 V (vs. Ag / AgNO₃). Therefore, ions in the electrolyte are speculated to be intercalated into the layered structure of graphene at sufficiently positive or negative potential, allowing the space of the graphene layer to be raised. This activation significantly enhances the specific capacitance of the GNW of the negative electrode material and the positive electrode materials of organic EDLC. Several CV parameters (eg, potential window, activation time, etc.) are investigated to achieve the highest specific capacitance. The results (see the following figure) reveal that after the electrochemical activation of 25 mV s⁻¹ from 0 to +2 V and from 0 to -3 V for 2400 seconds, the specific capacitance of most few-layer graphene sheets is almost doubled.

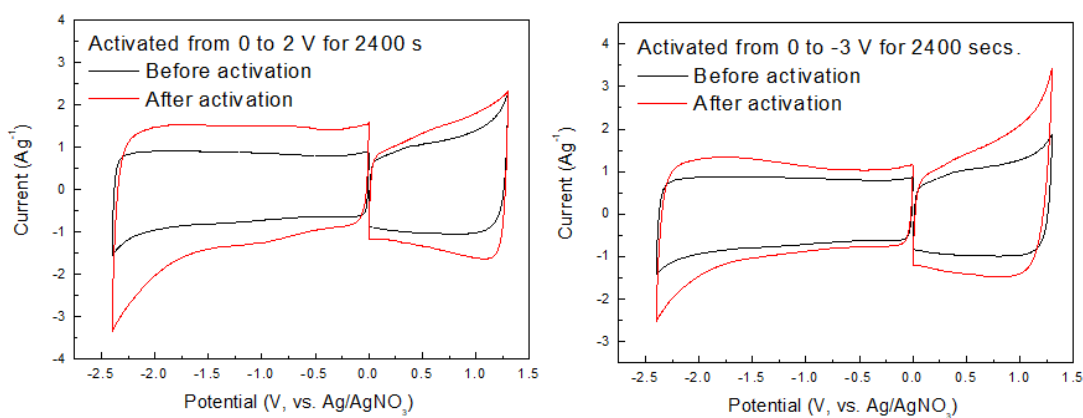


Fig. CV curves of GNWs activated from 0 to +2V and 0 to -3V in 2400 seconds.

Keywords: MPT-PECVD, graphene nanowalls, electrochemical activation, ion intercalation/de-intercalation.

On the applicability of the capillary rise method for determining the internal wettability of gas-diffusion electrodes

Fabian Bienen, Norbert Wagner^a, Dennis Kopljar^c, Armin Löwe^c, Elias Klemm^c, K. Andreas Friedrich^{a,b},

^a*German Aerospace Center (DLR), Institute of Technical Thermodynamics, Pfaffenwaldring 38-40, 70569, Stuttgart, Germany*

^b*University of Stuttgart, Institute for Thermodynamics and Thermal Engineering, Pfaffenwaldring 6, 70569, Stuttgart, Germany*

^c*University of Stuttgart, Institute of Technical Chemistry, Pfaffenwaldring 55, 70569, Stuttgart, Germany*

Fabian.Bienen@dlr.de

Gas-diffusion electrodes are widely used in electrochemical processes which require a large triple phase boundary for the conversion of gaseous reactants to gases, liquids and/or solid soluble products. Obviously, the transport of reactants into the porous electrode and the transport of the products out of this porous system is a crucial parameter for the performance of the electrode. In addition to the structural characteristics of the pore system and the inherent properties of the penetrating liquid and gas, the interaction between liquid, gas and solid in terms of the contact angle determines the wetting behavior of a gas-diffusion electrode [1].

Measuring the contact angle inside a porous system is not a trivial task since the classic drop shape analysis fails. This method is limited to the outer surface of a porous system and affected by surface roughness and liquid penetration. To overcome these issues the flow of a liquid into a porous system is modelled and fitted to experimental capillary penetration data. As a result, the internal contact angle of the porous system can be extracted. This approach can be attributed to Lucas and Washburn and is widely used for the wettability characterization of powders and textiles. Lately, this technique has been used to estimate internal contact angles in fibrous gas-diffusion layers for PEMFC [1-3].

The above-mentioned method has been adapted to measure the contact angle of solvent-free manufactured gas-diffusion electrodes. A simple test set-up has been designed to perform capillary penetration experiments for these gas-diffusion electrodes using different organic solvents as penetrating liquid. The use of organic solvents instead of aqueous liquids is necessary because the testing samples are highly hydrophobic. The testing procedure was optimized to achieve reproducible and reliable results. However, different models based on the macroscopic energy balance of a vertical capillary tube taking surface energy, gravity, viscosity, inertia and friction [4] into account were fitted to the data received from the capillary penetration experiments. Based on these fits, we carefully examined the interaction between the calculated contact angles and the choice of the fitting model. Furthermore, the obtained contact angles are transferred into the two-parameter surface energy model of Owens and Wendt which is then applied to determine the internal contact angle of water in the gas-diffusion electrode.

- [1] V. Gurau, M. Bluemle, E. De Castro, Y. Tsou, J. Mann Jr., T. Zawodzinski Jr., *Journal of Power Sources*, 160, 2, 2006, pp. 1156 – 1162
- [2] A. Alghunaim, S. Kirdponpattara, B. Newby, *Powder Technology*, 287, 2016, pp. 201 - 215
- [3] E. Washburn, *Physical Review*, 17, 1921, pp. 273 - 283
- [4] J. Szekely, A. Neumann, Y. Chuang, *Journal of Colloid and Interface Science*, 35, 2, 1971, pp. 273 - 278

This work is financially supported by the German BMWi (03ET1379A/B)

The Au(111) - Supported Pt Monolayer as the Most Active Electrocatalyst Toward Hydrogen Oxidation and Evolution in Sulfuric Acid

Shuehlin Yau

Department of Chemistry, National Central University

Jhongda Road, Zhongli, Taiwan 320

Yau6017@gmail.com

Platinum (Pt) monolayer deposited on ordered Au(111) substrate is chosen as a model system to understand the structure and property of supported Pt monolayer. We devise a simple method to fabricate a Pt overlayer on Au(111) electrode, where PtCl_6^{2-} complexes are reduced to metallic Pt atoms by CO molecules without potential control. The adsorption of CO molecules first mobilized and rearranged Pt adatoms on Au(111) from disordered Pt aggregates to 0.9 nm wide tortuous stripes, and then to patches of ordered atomic arrays at 0.1 V. The deposition of the Pt film stops at one atom thick. In order to expose the Pt film, the capping CO adlayer is stripped off by pulsing the potential to 0.96 V (vs. hydrogen reversible electrode) for 3 s in H_2 -saturated 0.1 M H_2SO_4 . Atomic resolution STM imaging shows that the Pt adatoms arrange in two hexagonal arrays with different atomic corrugation patterns and a notable difference (5.5 %) in the Pt-Pt distance at 0.1 V. The Pt film with a larger interatomic spacing of 0.287 nm is 2× more active than that of Pt(111), and may be the most active catalyst toward hydrogen evolution and oxidation reactions (HER and HOR) reported thus far.

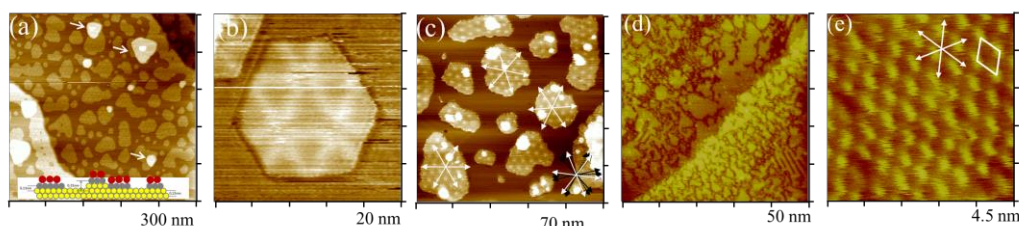


Figure 1. In situ STM acquired with Au(111) pre-dosed with Pt adatoms, whose morphology (a) and atomic structures (b and c) at 0.5 V in 0.1 M H_2SO_4 . Panel d-e show the spatial structure of carbon monoxide molecules adsorbed on the Pt-coated Au(111) at 0.2 V in CO-saturated 0.1 M H_2SO_4 .

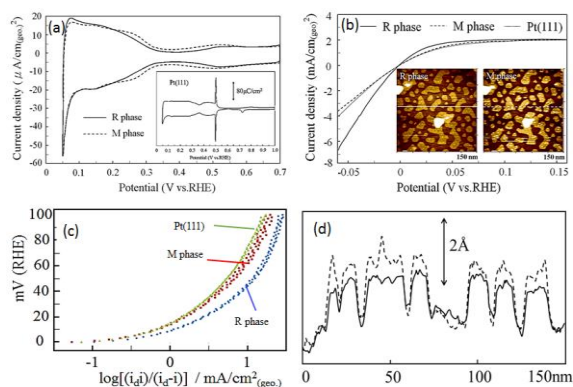


Figure 2. CVs obtained from R phase (solid line) and M phase (broken line) Pt films on Au(111) and Pt(111) (dotted line) in 0.1 M H_2SO_4 saturated with N_2 (a) and H_2 (b). The scan rate and rotating speed were 10 mV/s and 900 rpm. Current density was taken the Au(111) geometric area into account. The Pt coverage was 0.46 ML, as determined from the STM images shown in the inset of panel (b). Panel (c) shows the Tafel plots based on the CV results shown in panel (b). Panel (d) shows two section profiles along the lines marked in panel (b).

References:

1. W. Liao, W. Liao, and S. Yau, *J. Electrochem. Soc.*, 2015, 162, H767-H773.
2. W. Liao and S. Yau, *J. Phys. Chem.*, 2017, 121, 19218.

Correlation between the Interfacial Structure and Carrier Mobility for Electric Double Layer - Organic FET using Ionic Liquid

Daijiro Okaue¹, Sakuroko Ono¹, Ken-ichi Bando¹, Kouta Sakamoto¹, Hiroaki Nato¹, Hiroo Miyamoto¹, Taiki Sato¹, Ichiro Tanabe¹, Yasuyuki Yokota², Jun Takeya³, and Ken-ichi Fukui^{1*}

¹Dept. Mater. Engineer. Sci., Osaka Univ., Machikaneyama, Toyonaka, Osaka 560-8531, Japan

²Surf. Interf. Sci. Lab., RIKEN, Wako, Saitama 351-0198, Japan

³Dept. Adv. Mater. Sci., The Univ. Tokyo, Kashiwa, Chiba 277-8561, Japan

*E-mail: kfukui@chem.es.osaka-u.ac.jp

Ionic liquids (ILs) are promising electrolytes for electrochemical devices such as secondary battery, capacitor, electric double layer (EDL)-FET, etc., due to their high chemical stability with negligible vaporization. Recent progress of frequency modulation AFM (FM-AFM) technique as a highly sensitive force detection tool even in liquid phase enables us to obtain information on degree of structuring of liquid phase molecules at liquid/solid interfaces and at electrochemical interfaces. In this study, we have investigated structuring, dynamics, and electric double layer formation of the interfacial IL faced to organic semiconductor surfaces analyzed by electrochemical FM-AFM (EC-FM-AFM) and electrochemical impedance spectroscopy (EIS) and molecular dynamics (MD) calculations.

Rubrene is a representative p-type organic semiconductor, which shows high hole mobility along the π -stacking direction parallel to the b crystal axis. By using an IL to accumulate high carrier density at the interfaces, very low operating gate voltage less than 0.5 V can be achieved for the EDL-FET.¹⁾ Recently we reported by combining the time lapse carrier mobility measurements for the EDL-FET and corresponding interface structural changes observed by EC-FM-AFM that the self-healing property of the using the BMIM-TFSI (IL) /rubrene interface structure led to the spontaneous improvement of the hole mobility at the interface (Fig.1).²⁻⁴⁾ It is closely related to the soft interface structure of the IL when it is faced to rubrene(001).²⁻³⁾

Instead, by using EMIM-FSI as an IL electrolyte, drastic decrease of the hole mobility was found in a few hours even though no apparent change was observed for the interface structure. These differences will be discussed with the analyses of EIS and MD calculations.

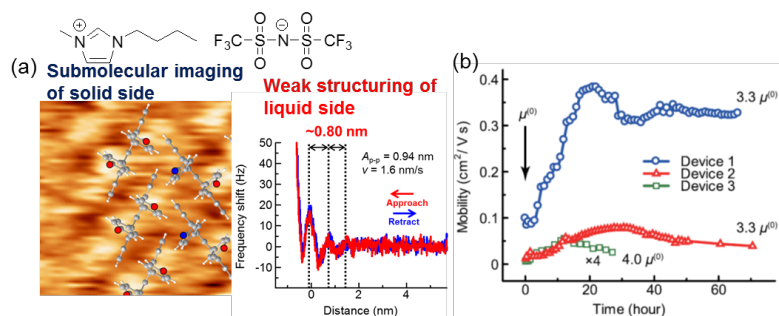


Fig.1 (a) EDL-FET interface (IL(BMI-TFSI) / rubrene(001)) structure analyzed by EC-FM-AFM and (b) time course of the EDL-FET property correlating with the change of the interfacial structure.

References

- 1) S. Ono, S. Seki, R. Hirahara, Y. Tominari, J. Takeya, *Appl. Phys. Lett.* **92**, 103313 (2008).
- 2) Y. Yokota, H. Hara, Y. Morino, K. Bando, A. Imanishi, T. Uemura, J. Takeya, K. Fukui, *Chem. Commun.* **49**, 10596 (2013); *Appl. Phys. Lett.* **104**, 263102 (2014); *Phys. Chem. Chem. Phys.* **17**, 6794 (2015).
- 3) K. Fukui, Y. Yokota, A. Imanishi, *Chem. Rec.* **14**, 964-973 (2014).
- 4) Y. Yokota, H. Hara, Y. Morino, K. Bando, S. Ono, A. Imanishi, Y. Okada, H. Matsui, T. Uemura, J. Takeya, K. Fukui, *Appl. Phys. Lett.* **108**, 083113 (2016).

AN ALTERNATIVE SOLUTION OF INTERNAL SHORT AND SAFETY PROBLEMS IN LITHIUM ION BATTERY

Fu-Ming Wang

Graduate Institute of Applied Science and Technology,
National Taiwan University of Science and Technology,
Taiwan

E-mail: mccabe@mail.ntust.edu.tw

In January 2017, Samsung announced the reason why the Note 7 explodes and losses of more than 5 billion US dollar. According to their explanations, it was caused by the internal short circuit problem in the lithium ion battery. Currently, there is no effectively solution for eliminating the internal short circuit problem owing to the sudden accident.

In this research, a new technology has been developed, which can be used to terminate the thermal runaway and promise the safety performance of lithium ion battery. High voltage Li-excess and Ni-rich layer-type cathode material are employed and combined with this safety electrode additive for investigation. In terms of the results, the new technology LIVING[®] additive significantly enhances the cycle performance at 60°C and high voltage. In addition, the following figures illustrated that the battery containing LIVING[®] technology is stable and passed the nail penetration test. On the other hand, the battery without LIVING[®] cannot be used when the short problem is taking place. The LIVING[®] contains self-polymerized hyper branch structure in order to insulate the directly contact between anode and cathode. This electrode additive not only provides high thermal stability on electrochemical reaction, but the columbic efficiency of charge-discharge is also enhanced.

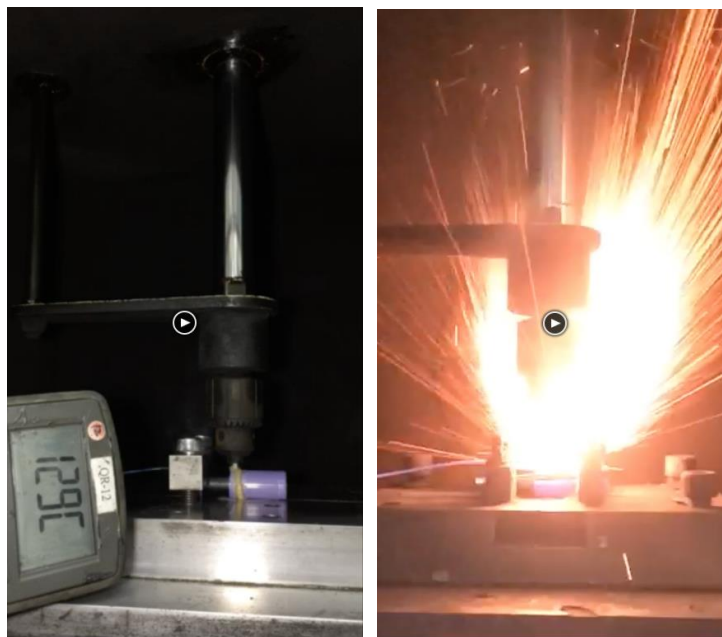


Figure 1 (left) The battery containing LIVING[®] technology and (right) the battery without any modification.

References

- [1] Fu-Ming Wang, J. Membrane Sci. 368 (2014) 165.
- [2] Sunny Hy, J. Am. Chem. Soc. 136 (2014) 999.

Biobased aerogels of different surface charge as electrolyte interface in a quantum dot-sensitized solar cell

Maryam Borghei¹, Kati Miettunen^{1,2}, Luiz G. Greca¹, Aapo Poskela², Janika Lehtonen¹, Sakari Lepikko², Blaise L. Tardy¹, Peter Lund², Vaidyanathan (Ravi) Subramanian^{1,3}, Orlando J. Rojas^{1,2}

¹ Department of Bioproducts and Biosystems, School of Chemical Engineering, Aalto University, Espoo FI-00076, Finland.

² Department of Applied Physics, School of Science, Aalto University, Espoo FI-00076, Finland.

³ Chemical and Materials Engineering, University of Nevada, Reno, Nevada 89557 United States.

maryam.borghei@aalto.fi

Integrating biobased components in solar cell technology received a lot of attention recently for developing sustainable energy generation. In the present effort, biobased aerogels were fabricated and applied as freestanding, porous and eco-friendly electrolyte holding membranes in quantum dot solar cell (QDSC). Bacterial cellulose (BC), cellulose nanofibers (CNF), chitin nanofibers (ChNF) and TEMPO-oxidized CNF (TOCNF) were selected due to their inherently different surface charges, strong fibrillar structure and water-holding capabilities. These aerogels enabled easy handling, effective electrolyte filling and efficient redox reactions while keeping the solar cell performance similar to those of reference cells (with liquid electrolyte). These aerogels were able to maintain all the photocell performance since they take only a very small spatial portion of the electrolyte volume, which allows efficient charge transfer in the electrolyte. In addition, similar performance as the reference cells implies that aerogels were inert and thus did not interfere with the cell operation. This has been approved by investigation of the bio-interphase with the polysulfide-based electrolyte using quartz crystal microbalance (QCM). The electrochemical measurements also suggested that the respective functional groups (hydroxyl, N-acetylglucosamine and carboxyl units) do not interfere with the redox reaction of the polysulfide electrolyte.

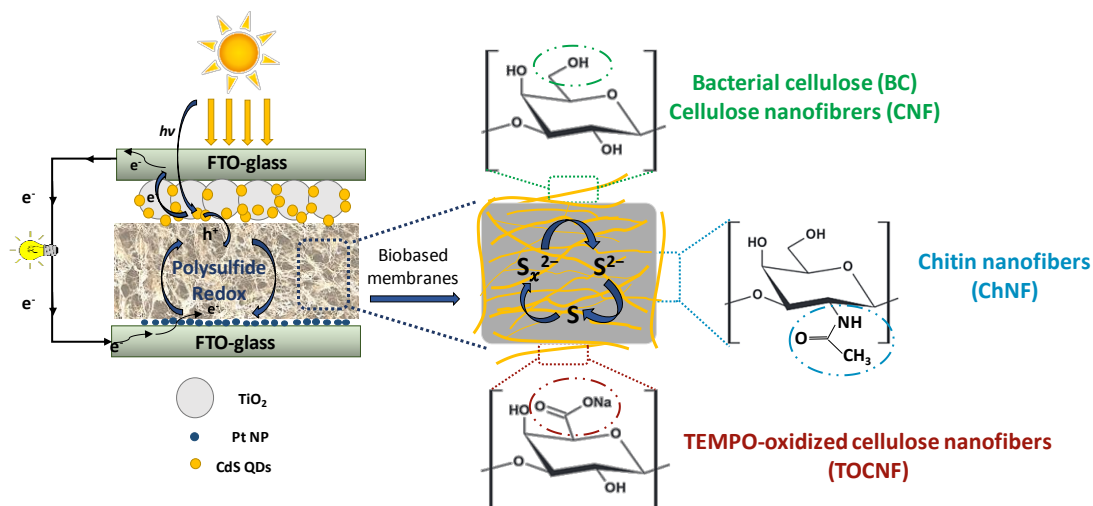


Figure 1. Schematic illustration of biobased aerogels as electrolyte retaining membranes in a QDSC containing CdS-sensitized photoelectrode and Pt counter electrode on fluorine-doped tin oxide (FTO)-glass substrates. The magnified aerogel illustrates the electrolyte redox ions at the interface of nanofibers with different surface charge; hydroxyl groups in BC and CNF, amide groups in ChNF and carboxyl groups in TOCNF.

External Magnetic Field Assisted Electrodeposition of Co-Ru Nanorods for water splitting reaction

I. Dobosz, K. Kołczyk, D. Kutyla, R. Kowalik, P. Zabinski
AGH University of Science and Technology, Faculty of Non-Ferrous Metals,
al. Mickiewicza 30, 30-059 Krakow, Poland
zabinski@agh.edu.pl

The article presents results of tests on potentiostatic electrodeposition of ruthenium and Co-Ru alloys. The tests applying the method of cyclic voltammetry with the use of gold disk electrode (RDE) allowed to define a potentials range in which it is possible to obtain ruthenium and its alloys with cobalt from acid chloride electrolytes.

The influence of electrodeposition parameters and the electrolyte composition on the composition, morphology and structure of the obtained deposits was determined. Co-Ru alloys underwent XRD tests, an analysis with the XRF method and observations using scanning electron microscopy (SEM). Hydrogen evolution tests have been also performed.

Then, cobalt-ruthenium nanorods have been successfully synthesized by electrochemical deposition using an aluminum oxide membrane template with superimposed external magnetic field. The length and average diameter of cobalt alloy nanorods arrays are 4,5 - 9 μm and 100 nm, respectively. For nanorods deposited in applied external magnetic field of 0.6T we observe higher saturation magnetization and slightly higher coercivity field. This method offers a convenient and efficient path to synthesize metal array nanostructures with designed composition.

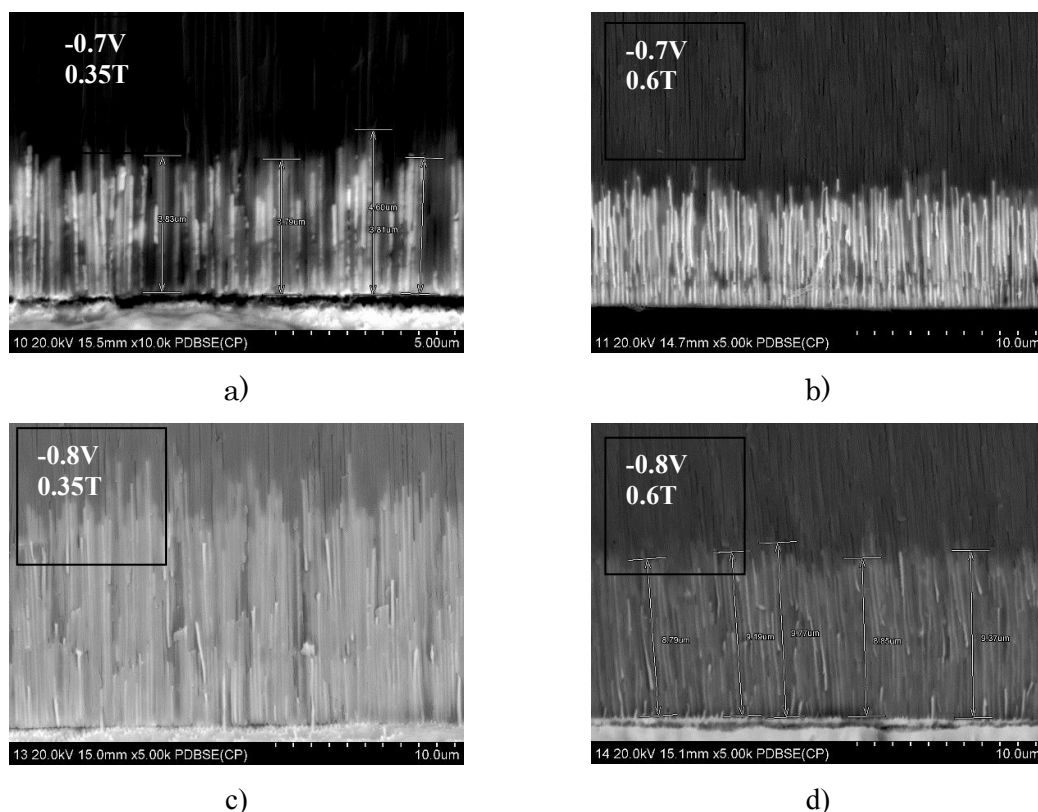


Fig 1. SEM photographs of aluminum membrane crosssection with pore diameter of 100 nm and deposited Co-Ru nanorods at potential of -0,7V and magnetic field 0,35T (a) and 0,6T (b) and -0,8V with applied magnetic field 0,35T (c) and 0,6T (d). Deposition time 60 minutes.

Acknowledgment

The authors would like to thank Polish National Science Centre for the financial support provided by the grants: No UMO-2013/09/B/ST8/00211 and UMO-2016/23/G/ST5/04058.

Quantum-continuum Simulations of High Power Density Oxide Electrodes for Pseudocapacitive Energy Storage

Nathan Keilbart, Yasuaki Okada, Shin'ichi Higai, and Ismaila Dabo
The Pennsylvania State University
N-234 Millennium Science Complex, University Park, PA 16802
ndk123@psu.edu

Pseudocapacitors are energy-storage devices characterized by fast and reversible redox reactions near the surface of an electrode that allows them to store large amounts of energy at fast rates [1]. Much is unknown about these materials due to the complex electrochemical reaction that occurs at the interface between the electrode and solvent. A theoretical modeling approach is developed focusing on ruthenium dioxide (RuO_2), a prototypical pseudocapacitive electrode material, for analyzing the electrochemical response of an electrode under realistic conditions in order to identify the factors that control the performance. Electronic-structure methods are used in combination with a self-consistent continuum solvation model to generate a complete dataset of free energies for varying amounts of proton coverage on the surface. The dataset is used in conjunction with a grand-canonical Monte Carlo sampling technique that computes hydrogen-adsorption isotherms and the charge-voltage response of the system. Close agreement is found with experimental results of the RuO_2 (110) surface under optimal surface charging conditions [2]. It is found that the intrinsic double-layer contribution represents a small fraction of the overall electrochemical response of the electrode but controls to a large extent the onset of pseudocapacitive reactions by influencing the change in the surface dipole. At variance with RuO_2 (110), the double-layer capacitance of RuO_2 (100) is found to vary linearly across a significant portion of the voltage range. This range of variation is also well captured by first-principles calculations of the double-layer capacitance for different coverages. The newly developed model provides a widely applicable computational method to help identify novel pseudocapacitive materials.

[1] V. Augustyn, P. Simon, and B. Dunn, *Energy and Environ. Sci.* **7**, 1597 (2014)

[2] N. Keilbart, Y. Okada, A. Feehan, S. Higai, and I. Dabo, *Phys. Rev. B* **95**, 115423 (2017)

Novel synthesis of nanocrystalline Na₂Ti₃O₇ with improved performance for Na-ion batteries

Marketa Zukalova

J. Heyrovský Institute of Physical Chemistry, Czech Academy of Sciences, v.v.i.

Dolejšková 3, CZ-18223 Prague 8, Czech Republic

marketa.zukalova@jh-inst.cas.cz

The TiO₂-based nanomaterials have triggered great excitement, because of their interesting structural characteristics and potential applications in energy conversion and storage. Among others, monoclinic modification of titanium dioxide (TiO₂B) and Li₄Ti₅O₁₂ spinel were investigated as sodium storage anode materials[1-5]. Na₂Ti₃O₇ was reported as the lowest voltage oxide material for sodium-ion batteries anode[6], with ca. 0.30 V vs. Na⁺/Na on average with two sodium atoms insertion per Na₂Ti₃O₇. This material reached reversible charge capacity of 177-205 mAh g⁻¹. In our work a nanocrystalline Na₂Ti₃O₇ material is prepared by newly developed sol gel procedure. The sol gel made Na₂Ti₃O₇ calcined at 500 °C possesses mesoporous structure and BET surface area of 89 m² g⁻¹. X-ray diffraction and scanning electron microscopy confirm the presence of sintered nanosheets or very small crystals of the size of tens of nanometers exhibiting just short range ordering. Electrochemical behavior of nanocrystalline Na₂Ti₃O₇ is evaluated by cyclic voltammetry of Na insertion and galvanostatic chronopotentiometry at different charging rates. The sol gel made Na₂Ti₃O₇ exhibits improved performance as compared to the microcrystalline Na₂Ti₃O₇ prepared by solid state synthesis. Discharge capacities of optimized material at charging rates 1, 2 and 5C reach 109, 86 and 63 mAh g⁻¹ respectively, with 100% coulombic efficiency and zero capacity drop over 50 cycles after initial conditioning. Hence sol gel made nanocrystalline Na₂Ti₃O₇ represents promising anode material for Na-ion batteries due to its charge capacity and outstanding cycling stability[7].

Acknowledgement:

This work was supported by V4-Japan Joint Research Program, Structure- function relationship of advanced nanooxides for energy storage devices (AdOX) granted from Visegrad fund and Japan Science and Technology Agency (8F15003) and by the Ministry of Industry and Trade of the Czech Republic (contract TRIO FV20471).

- [1] J. Lee, J.K. Lee, K.Y. Chung, H.-G. Jung, H. Kim, J. Mun, W. Choi, Electrochemical Investigations on TiO₂-B Nanowires as a Promising High Capacity Anode for Sodium-ion Batteries, *Electrochim Acta*, 200 (2016) 21-28.
- [2] M. Kitta, K. Kuratani, M. Tabuchi, N. Takeichi, T. Akita, T. Kiyobayashi, M. Kohyama, Irreversible structural change of a spinel Li₄Ti₅O₁₂ particle via Na insertion-extraction cycles of a sodium-ion battery, *Electrochim Acta*, 148 (2014) 175-179.
- [3] J.P. Huang, D.D. Yuan, H.Z. Zhang, Y.L. Cao, G.R. Li, H.X. Yang, X.P. Gao, Electrochemical sodium storage of TiO₂(B) nanotubes for sodium ion batteries, *RSC Adv*, 3 (2013) 12593.
- [4] M. Zukalová, B. Pitřna Lásková, M. Klementová, L. Kavan, Na insertion into nanocrystalline Li₄Ti₅O₁₂ spinel: An electrochemical study, *Electrochim Acta*, 245 (2017) 505-511.
- [5] Y. Sun, L. Zhao, H. Pan, X. Lu, L. Gu, Y.S. Hu, H. Li, M. Armand, Y. Ikuhara, L. Chen, X. Huang, Direct atomic-scale confirmation of three-phase storage mechanism in Li₄Ti₅O₁₂ anodes for room-temperature sodium-ion batteries, *Nat Commun*, 4 (2013) 1870.
- [6] H. Pan, X. Lu, X. Yu, Y.-S. Hu, H. Li, X.-Q. Yang, L. Chen, Sodium Storage and Transport Properties in Layered Na₂Ti₃O₇ for Room-Temperature Sodium-Ion Batteries, *Adv Energy Mater*, 3 (2013) 1186-1194.
- [7] M.P.L. Zukalova, B.; Mocek, K.; Zukal, A.; Kavan, L. , Novel synthesis of nanocrystalline Na₂Ti₃O₇ with improved performance for Na-ion batteries, *J Solid State Electrochem*, submitted.

Electrodeposition of HgTe and related compounds from dichloromethane

D. C. Smith^{1*}, G.P.K. Kissling², M. Aziz¹, W. Zhang², A. Lodge², G. Reid², A. L. Hector², P.N. Bartlett²

¹School of Physics & Astronomy, University of Southampton, Southampton SO17 1BJ, United Kingdom

²School of Chemistry, University of Southampton, Southampton SO17 1BJ, United Kingdom

E-mail: D.C.Smith@soton.ac.uk

HgTe is scientifically and technologically interesting for a number of key reasons. One key technological reason is that it is one of the parent materials of HgCdTe which is still the dominant material in the production of high end IR detectors. However pure HgTe itself has a number of interesting applications. Scientifically it has received huge attention recently as HgTe quantum wells demonstrate topological insulating properties [1]. Another key area of HgTe research is focused on the application of HgTe quantum dots [2]. Colloidal HgTe quantum dots with diameters of less than 10nm are semiconducting and dots with a diameter between 3-6 nm have absorptions in the NIR region, including the telecommunications bands [3]. It has been shown that fast, reasonably high efficiency/detectivity photodetectors (2×10^9 cm Hz^{1/2}/W at 130 K) can be fabricated from thin films of such colloidal dots produced in air [2]. Another application is as an ohmic contact to HgCdTe [4, 5].

Good quality HgTe films can be produced by MBE and CVD although these require a high vapor pressure of Hg in the growth environment and a low growth temperature. Processing the deposited material is not trivial as there is a tendency for Hg to be lost and for interstitial defects due to etching to lead to significant changes in doping. The fragility of HgTe means that etched nanowires are not good quality. In addition, whilst attempts have been made to form HgTe nanowires by the vapor-liquid-solid method [6] this method is much less successful with HgTe than other semiconductors. The existence of high quality colloidal HgTe quantum dots, the low growth temperature required for HgTe and the success of electrodeposition in depositing CdTe for high efficiency solar cells suggest that electrodeposition may be a desirable preparation method for HgTe, particularly for quantum wires.

Whilst electrodeposition of CdTe has received huge attention, more than 500 publications, there is almost no work on the electrodeposition of HgTe with only two groups having worked on this material [7-9]. The most successful of these was Stickney *et al.* [9] who used ECALE to produce 70 nm thick films of crystalline HgTe with reasonable stoichiometry. The second group has published a small number of papers on the electrodeposition of HgTe nanoparticles and the measurement of their optical properties. There are significant reasons for doubting the interpretation of the optical spectra obtained by this group and this casts some doubt on the quality of the electrodeposited material.

We will present a new method for electrodepositing HgTe from dichloromethane using tetrabutylammonium chlorometallate precursors. We will demonstrate that it is possible to deposit crystalline HgTe films onto a range of electrodes with deposition rates much greater than possible with ECALE. We will discuss the determination of the composition of these films using XRF, EDX and ICPMS and in particular the possibility for XRF and EDX to incorrectly report the composition on thin films. We will also present our initial results on the production of HgTe nanowires using templated electrodeposition. If time allows we will discuss the extension of this work to the electrodeposition of HgCdTe.

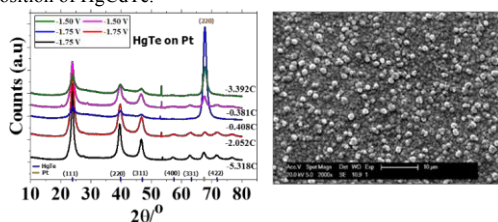


FIG 1: Grazing incident XRD of HgTe deposited at different potentials and thicknesses on Pt/Silicon and SEM image of a similar sample

This work was funded by EPSRC Programme Grant EP/N035437/1, -Advanced Devices by ElectroPlating (ADEPT). The work was carried out by an interdisciplinary team of researchers based at the Universities of Southampton, Nottingham and Warwick, UK.

Refs: [1] König, M. *et al.* Science, 2007. 318(5851): p. 766-770. [2] Keuleyan, S. *et al.* Nature Photonics, 2011. 5(8): p. 489-493. [3] Rogach, A. *et al.* Advanced Materials, 1999. 11(7): p. 552. [4] Chu, T.L. *et al.* Twentieth IEEE Photovoltaic Specialists Conference - 1988, 1-2, p. 1422-1425. [5] Leech, P.W. *et al.* Semiconductor Science and Technology, 1993. 8(12): p. 2097-2100. [6] Haakenaasen, R. *et al.* Journal of Electronic Materials, 2008. 37(9): p. 1311-1317. [7] Rath, S. *et al.* Physical Review B, 2005. 72(20). [8] Rath, S. *et al.* Surface Science, 2006. 600(9): p. L110-L115. [9] Venkatasamy, V. *et al.* Journal of Electroanalytical Chemistry, 2006. 589(2): p. 195-202.

Commenté [CJ1]: This sentence reads oddly – is it worth naming this group as well?

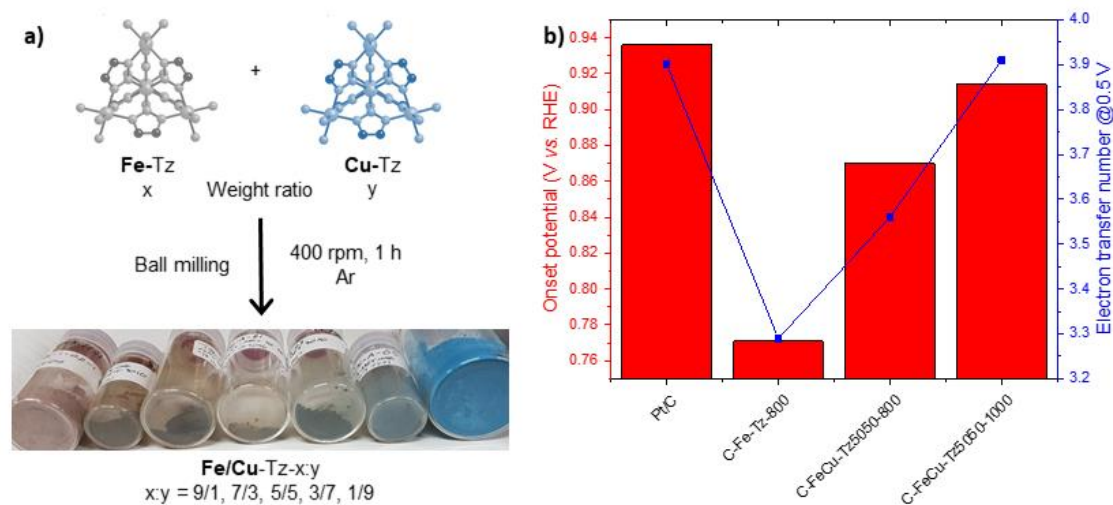
Alloy-Doped Carbons Derived from Porous Coordination Polymers for Oxygen Reduction Reaction

Jet-Sing M. Lee, Susumu Kitagawa, Satoshi Horike
Institute for Integrated Cell- Material Sciences (iCeMS), Kyoto University
Yoshida, Sakyo-ku, Kyoto 606-8501, Japan
jet.lee.42w@st.kyoto-u.ac.jp

With a growing global energy market, rapid depletion of fossil fuels, and the rising problem of environmental pollution, the need to develop efficient, sustainable sources of energy alongside new energy storage technologies is recognized as an urgent priority. Fuel cells, which convert hydrogen and oxygen into electric energy, have been regarded as a promising future technology prescribed to their high efficiency, no environmental pollution, and unlimited sources of reactants. However, a major limitation in the commercialization of this technology is due to the challenges associated with the oxygen reduction reaction (ORR) in the cathode. Due to the sluggish kinetics of ORR, Pt-based catalysts are currently used to achieve a desirable fuel cell performance, however, these are associated with high cost, limited availability, and fast deactivation. Therefore, development of new catalysts by replacing Pt with an abundant and cheap metal is of high priority.

Conventionally, activated carbons have been used as electrode materials due to its affordability, high electric conductivity, and high surface areas for charge storage. Transition metal oxides have also been widely recognized as a highly active electrocatalyst. The combination of both porous carbon and transition metal is a popular strategy to enhance performance for ORR, with recent growing interest in iron and nitrogen co-doped carbons due to their excellent performance and affordability.^[1] These materials can be made by direct carbonization or an organic- and inorganic-containing precursor; such as porous coordination polymers (PCPs).

PCPs (also known as metal-organic frameworks) are completely regular, highly porous, and designable networks made by linking organic and inorganic units with strong bonds.^[2] Recently, it was shown that PCPs containing multiple metals could be made by a simple mechanical milling process of the preformed networks.^[3] By predesigning the PCP, various factors in the resultant metal-doped carbon can be controlled. Here, we show that iron and copper co-doped carbons derived from PCPs show ORR activities outperforming the single-doped carbons and even with performances close to benchmark Pt/C. With over 20,000 different PCPs being reported and studied in the last decade, there is large scope for PCP alloys to be discovered which can form alloy-doped carbons that may surpass those reported here.



- [1] A. Zitolo *et al.*, *Nat. Mat.* **2015**, *14*, 937.
[2] S. Kitagawa *et al.*, *Angew. Chem. Int. Ed.* **2004**, *43*, 2334.
[3] T. Panda *et al.*, *Angew. Chem. Int. Ed.* **2017**, *56*, 2413.

Unraveling the Roles of Point Defects on Carbon Surfaces in Non-Aqueous Lithium-Oxygen Batteries

H.R. Jiang, L. Zeng, J.B. Xu, M.C. Wu, W. Shyy, T.S. Zhao*
*Department of Mechanical and Aerospace Engineering
The Hong Kong University of Science and Technology
Clear Water Bay, Kowloon, Hong Kong SAR, China
Email: hjiangaf@connect.ust.hk*

Non-aqueous lithium-oxygen (Li-O₂) batteries have attracted increasing attention to be used in future electrical vehicles due to their comparable energy density (11682 W h kg⁻¹) with gasoline (13000 W h kg⁻¹). Because the main discharge product Li₂O₂ is in solid state and would accumulate in the cathode, the discharge capacities of non-aqueous Li-O₂ batteries are closely related to the specific surface area and porosity of the cathode. Carbon materials, attributed to their large specific surface area, high porosity, good electronic conductivity and low cost, are therefore widely used to form cathodes in non-aqueous Li-O₂ batteries. However, until now, the mechanistic understanding of carbon materials in non-aqueous Li-O₂ batteries is still limited. Even worse, the roles of carbon surface properties in the discharge and charge processes remains controversial. On the one hand, some researchers found that carbon-based cathodes are not stable during cycling, leading to the formation carbonate and the decomposition of electrolyte, which results in a poor rechargeability [1-3]. On the other hand, some works supported that defective carbon surfaces are effective to increase the discharge capacities, decrease the overpotentials and enhance the cycling performance [4-6]. Although understanding the roles of surface properties on carbon is crucial for the development of non-aqueous Li-O₂ batteries and beneficial to the cathode design, experimental study is difficult to be carried out due to the complexity of non-aqueous system and the difficulty to distinguish various carbon surface properties. Fortunately, first-principles study offers us an effective way to have an in-depth look into surface properties at atomic-level in non-aqueous Li-O₂ batteries.

In this work, starting from point defects, we try to unravel the roles of carbon surface properties in non-aqueous Li-O₂ batteries. Five representative defective structures, including SV (single vacancy), DV5-8-5 (two pentagons and one octagon), DV555-777 (three pentagons and three heptagons), DV5555-6-7777 (four pentagons, one hexagon and four heptagons) and SW (Stone-Wales) defects, are considered. We firstly build the structures of various point defects and calculate the density of state (DOS) to analyze the electrical conductivity. Then, the Li₂O₂ growing pathways on these surfaces are systematically studied and whether the points defects would promote the formation of side product Li₂CO₃ is analyzed. Thirdly, the oxygen reduction reaction (ORR) and oxygen evolution reaction (OER) performances of the point defects in non-aqueous Li-O₂ batteries are evaluated by drawing the free energy diagrams. Finally, the influence of carbon defects on the electrolyte decomposition is investigated. In consideration of all these aspects, results show that some point defects, such as DV5555-6-7777 and SW defects, are beneficial to the battery performance, while others are not. Therefore, the inconsistency of previous experimental results may be attributed to the different contents of various carbon defects. Further computational results will be disclosed at the meeting.

Acknowledgement

The work presented in this meeting was fully supported by a grant from the Research Grants Council of the Hong Kong Special Administrative Region, China (Project No. T23-601/17-R).

References

- [1] D.M. Itkis, D.A. Semenenko, E.Y. Kataev, A.I. Belova, V.S. Neudachina, A.P. Sirotnina, M. Hävecker, D. Teschner, A. Knop-Gericke, P. Dudin, *Nano Lett.* 13 (2013) 4697-4701.
- [2] M.M. Ottakam Thotiyl, S.A. Freunberger, Z. Peng, P.G. Bruce, *J. Am. Chem. Soc.* 135 (2012) 494-500.
- [3] B. McCloskey, A. Speidel, R. Scheffler, D. Miller, V. Viswanathan, J. Hummelshøj, J. Nørskov, A. Luntz, *J. Phys. Chem. Lett.* 3 (2012) 997-1001.
- [4] S. Huang, W. Fan, X. Guo, F. Meng, X. Liu, *ACS Appl. Mater. Inter.* 6 (2014) 21567-21575.
- [5] S. Nakanishi, F. Mizuno, T. Abe, H. Iba, *Electrochemistry.* 80 (2012) 783-786.
- [6] S. Nakanishi, F. Mizuno, K. Nobuhara, T. Abe, H. Iba, *Carbon.* 50 (2012) 4794-4803.

EIS Detection of MUC1 with Two Symmetric Aptamer/Au Electrodes

Chih-Yu Lai and Lin-Chi Chen*

Department of Bio-Industrial Mechatronics Engineering, National Taiwan University
No. 1, Sec. 4, Roosevelt Rd., Taipei 10617, Taiwan (R.O.C.)

*Email: chenlinchi@ntu.edu.tw

Electrochemical impedance spectroscopy (EIS) has been proven as an effective method for ultrasensitive protein and cell detection. Typically, an EIS biosensor is constructed on the basis of a conventional three-electrode system, and an antibody is immobilized on the working electrode for specific affinity binding of the target protein or cell to generate detectable R_{ct} and C_{dl} changes. Although there have been a number of works demonstrating promising integration of EIS biosensors in microfluidic biochips, the tedious three-electrode fabrication and lack of an efficient method for selective deposition of antibodies on the working electrode have hindered EIS biosensors for realistic microscale and multiplex bioanalysis. In this work, we investigated a novel fabrication-favorable EIS approach for detection of mucin 1 (MUC1) using simply two symmetric aptamer-modified Au electrodes ($\phi = 2\text{mm}$). (Note: MUC1 is an important surface glycoprotein over-expressed in several types of cancer cells.) For EIS detection of MUC1, anti-MUC1 aptamers with 5'-thiol linkers were coated to the two Au electrodes in the same way and ferricyanide was employed as a redox reporter. A symmetric duplex Randles circuit (Fig. 1(a)) and a self-defined error mathematical model (Fig. 1(b)) were developed for data fitting and determination of R_{ct} , CPE, and Z_w . Cyclic voltammogram (CV) and EIS responses of two symmetric bare Au electrodes in contact with $[\text{Fe}(\text{CN})_6]^{3-}$ were analyzed to identify the operating sensing voltage (0.70V) that yielded the lowest background R_{ct} (Fig. 1(c)-(e)). With this condition, specific EIS detection of MUC1 (3-200 nM) was successfully performed (Fig. 1(f) and (g)) and a K_D value of 15.92nM for the aptamer-MUC1 binding could be evaluated from the R_{ct} -protein concentration fitting analysis. The above findings can be further extended to symmetric aptamer microelectrodes for both microfluidic applications and K_D measurements.

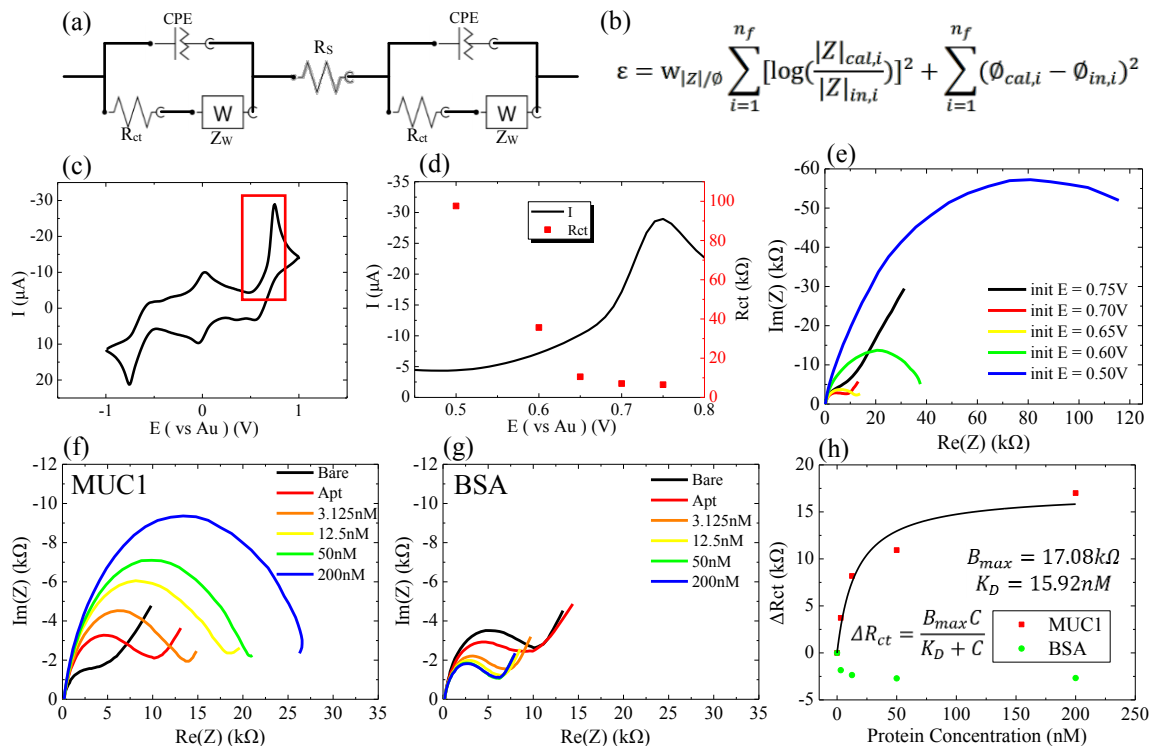


Figure 1. (a) The symmetric Au electrode equivalent circuit. (b) Self-defined error (ϵ) impedance-fitting model. (c) Cyclic voltammogram, (d) magnified area of (c) with R_{ct} data and (e) Nyquist plots obtained at different voltage biases for two bare Au electrodes in contact with $[\text{Fe}(\text{CN})_6]^{3-}$. EIS detection of (f) MUC1 and (g) BSA using the symmetric aptamer/Au electrodes with $[\text{Fe}(\text{CN})_6]^{3-}$. (h) Binding data analysis for MUC1 and BSA detection. Data in (c)~(h) were all obtained with the electrodes immersed in a sample solution of 10mM $[\text{Fe}(\text{CN})_6]^{3-}$ in PBS buffer (0.1M KCl).

Anodization of Ti-Nb-Ta-Zr-O Mixed-oxides Nanotube Arrays: A Promising Alternative Photoelectrode for Solar Conversion

Yi -Hsuan Chiu^{1,2,3}, Chun-Yi Chen^{1,2,*}, Kazunari Ozasa⁵, Mitsuo Niinomi⁶, Kiyoshi Okada⁴, Tso-Fu Mark Chang^{1,2,4}, Nobuhiro Matsushita⁴, Yung-Jung Hsu³, Masato Sone^{1,2,4}

¹Institute of Innovative Research, Tokyo Institute of Technology, Yokohama 226-8503 Japan

²CREST, Japan Science and Technology Agency, Yokohama 226-8503, Japan

³Department of Materials Science and Engineering, National Chiao Tung University,

⁴School of Materials and Chemical Technology, Tokyo 152-8550 Japan
Hsinchu Taiwan 30010 Republic of China

⁵Bioengineering Lab, RIKEN, Saitama 351-0198, Japan

⁶Institute for Materials Research, Tohoku University, Sendai 980-8577, Japan

*chen.c.ac@m.titech.ac.jp

Poor hole-transfer kinetics at the electrode/electrolyte interface has been the primary cause of the mediocre performance for n-type TiO₂ photoelectrodes. By adopting nanotubes as the photoelectrode backbone, light absorption and carrier collection can be spatially decoupled, allowing n-type TiO₂, with its short hole diffusion length, to maximize the use of the available photoexcited charge carriers during operation in photoelectrochemical (PEC) cells. Here, we presented a delicate electrochemical anodization process [1] for the preparation of quaternary Ti-Nb-Ta-Zr-O mixed-oxides (denoted as TNTZO) nanotube arrays and demonstrated their utility in PEC water splitting. For the TNTZO, the introduced Nb, Ta and Zr can induce shallow donor states to increase the carrier concentration and simultaneously cooperate with TiO₂ promoting effective charge transfer. Since the merits of each component can be incorporated, the TNTZO nanotube arrays exhibited superior photoactivity of water oxidation over pristine TiO₂ under AM 1.5G illumination, demonstrating the present TNTZO as a promising, alternative photoelectrode material in various PEC processes. Furthermore, by modulating the water content of the electrolyte employed in the anodization process, the wall thickness of the grown TNTZO nanotubes can be reduced to a size smaller than the depletion layer thickness, realizing a fully-depleted state for charge carriers to further advance the PEC performance, as shown in Figure 1. The fully-depleted TNTZO nanotube arrays may offer a feasible and universal platform for the loading of other semiconductors to construct a sophisticated heterostructure photoelectrode paradigm, in which the photoexcited charge carriers can be entirely utilized for realizing solar-to-fuel conversion.

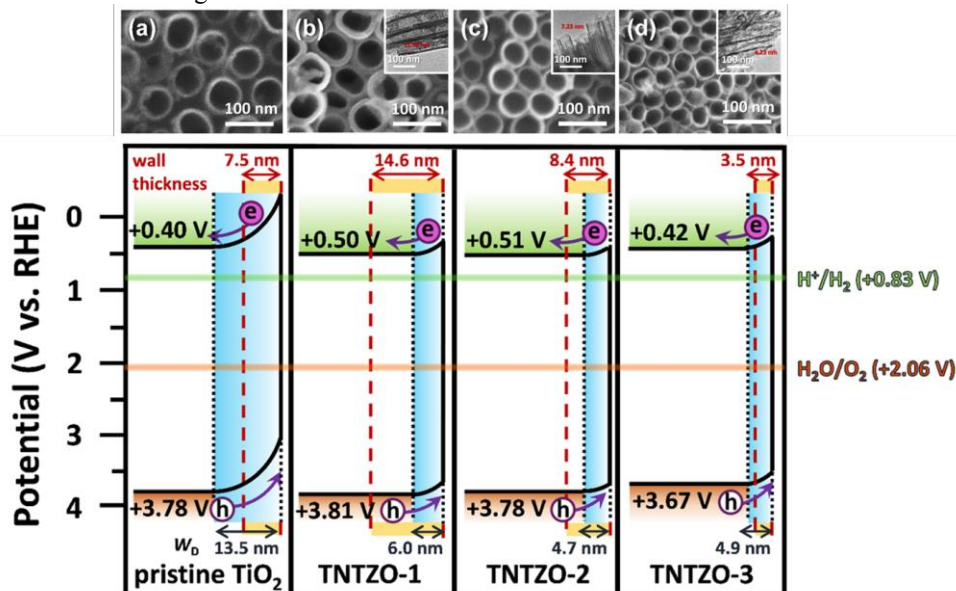


Figure 1. Top-view SEM and TEM images of (a) pristine TiO₂, (b) TNTZO-1, (c) TNTZO-2, (d) TNTZO-3, and plausible band structure for pristine TiO₂ and the three TNTZO electrodes.

Reference:

[1] C.Y. Chen, K. Ozasa, K. Katsumata, M. Maeda, K. Okada, Nobuhiro Matsushita, *Electrochim. Acta*, 153 (2015) 409-415.

Co-deposition of nickel and palladium from ammonia based bath

K. Mech¹, J. P. Chopart², M. Wróbel³, P. Zabiński⁴, and K. Szaciłowski¹

- 1) AGH University of Science and Technology, Academic Centre for Materials and Nanotechnology, al. A. Mickiewicza 30, 30-059 Krakow, Poland
- 2) Laboratoire d'Ingénierie et Sciences des Matériaux (LISM EA 4695), Université de Reims Champagne-Ardenne, UFR Sciences et Naturelles, Bat. 6, Moulin de la Housse BP 1039, Reims Cedex 2, France
- 3) AGH University of Science and Technology, Faculty of Metal Engineering and Industrial Computer Science, al. A. Mickiewicza 30, 30-059 Krakow, Poland
- 4) AGH University of Science and Technology, Faculty of Non-Ferrous Metals, al. A. Mickiewicza 30, 30-059 Krakow, Poland
e-mail: kmech@agh.edu.pl

Water splitting process is an efficient and environment-friendly method of hydrogen generation mainly due to possibility of conversion of energy fabricated by wind power plants, water power plants or solar power stations [1]. Exchange current density versus the enthalpy of hydrogen adsorption ($\text{Log}(i_0)$ - $dG_{\text{Me-H}}$) dependence allows on assumption that material composed of Ni and Pd will exhibit high catalytic properties towards hydrogen evolution reaction (HER). In literature, in spite of its wide application range, few reports exist concerning electrodeposition of NiPd alloys. Existing reports are focused on synthesis of NiPd alloys from sulphate-chloride [2], ethylenediamine [3] and chloride [4] based baths. Crystallites size of Ni-Pd alloys synthesized in acidic chloride electrolytes amounted from 4.1 to 32.5 nm so one order of magnitude larger than resulted in present studies. Kumar et al. reported that crystallites size of alloys deposited in sulfate-ethylenediamine based electrolytes at galvanostatic conditions amounted from 6.8 to 13.8 nm. Ni-Pd alloys reported by Kumar et al. contained from 4.54 to 35.61 at. % of Pd [9] while alloys electrodeposited at potentiostatic conditions from chloride electrolytes contained from 4.38 to 45.47 at. % of Pd [13]. Concentration of Pd in Ni-Pd alloys reported in present work amounted from 6.1 to 83.7 at. % which is much more. In present work authors reported studies focused on electrochemical deposition in alkaline ammonia based system for first time.

Described studies were started from thermodynamic and UV-Vis analysis enabling qualitative description of analysed system. Electrochemistry of $\text{Ni}^{2+} - \text{Pd}^{2+} - \text{Cl}^- - \text{NH}_3 - \text{H}_2\text{O}$ system was analyzed based on results of cyclic voltammetry combined with electrochemical quartz crystal microbalance (EQCM). In further step synthesized alloys were characterized towards their compositions (WD-XRF) and morphology (SEM, AFM) [5].

- [1] M.M. Najafpour, S.I. Allakhverdiev, *Int J Hydrogen Energ*, 37 (2012) 8753-8764.
- [2] K. Chen, Z. Hu, Z. Zhang, D. Yang, *Chinese Journal of Catalysis*, 17 (1996) 352-353.
- [3] K.S. Kumar, P. Haridoss, S.K. Seshadri, *Surface and Coatings Technology*, 202 (2008) 1764-1770.
- [4] K. Mech, M. Wróbel, M. Wojnicki, J. Mech-Piskorz, P. Zabiński, R. Kowalik, *Applied Surface Science*, (2016).
- [5] K. Mech, J.P. Chopart, M. Wróbel, P. Zabiński, K. Szaciłowski, *Journal of the Electrochemical Society*, 164 (2017) D613-D620.

Enhanced Catalytic Performance of Ternary Spinel $\text{Fe}_x\text{Ni}_{1-x}\text{Co}_2\text{O}_4$ / Activated Carbon Composite for the Air Cathode of Rechargeable Zinc-Air Batteries

Yi-Ting Lu, Chi-Chang Hu*

Department of Chemical Engineering, National Tsing Hua University

101, Section 2, Kuang-Fu Road, Hsin-Chu, 30013, Taiwan

*Email address: cchu@che.nthu.edu.tw

Discovering efficient and cost-effective catalysts for rechargeable metal-air batteries is one of the major scientific challenges in future energy storage/conversion technologies because of the sluggish kinetics of the oxygen evolution reaction (OER) and oxygen reduction reaction (ORR). NiCo_2O_4 has been known as bifunctional catalyst for a long time[1] and it has complicated cation occupancy[2], causing the catalytic performance to be various in many cases. Based on the octahedral site preference energy (OSPE) model, engineering the active sites of ternary $\text{M}_{0.1}\text{Ni}_{0.9}\text{Co}_2\text{O}_4$ for the OER and ORR in alkaline solutions is demonstrated in this work. From the X-ray photoelectron spectroscopic (XPS) and OSPE model, Fe-doped NiCo_2O_4 ($\text{Fe}_{0.1}\text{Ni}_{0.9}\text{Co}_2\text{O}_4$, FNCO) provides the highest $\text{Co}^{2+}/\text{Co}^{3+}$ ratio and the lowest $\text{Ni}^{2+}/\text{Ni}^{3+}$ ratio, leading to the enhanced electrocatalytic activities toward both the OER and ORR in alkaline electrolytes in rotating ring-disk electrode (RRDE) tests and full-cell tests. Then we synthesize the FNCO / active carbon composite to enhance the catalytic performance since the active carbon can be supporting substrate with good conductivity, which further enhances the specific activity of the FNCO catalyst. In this research, different amounts of activated carbon are applied to optimize the catalysis, and a series of material analyses are used to explain the reason of enhanced catalytic performance after the carbon material is introduced. The future work will be mainly focused on the investigation of other carbon materials in the rechargeable zinc-air batteries.

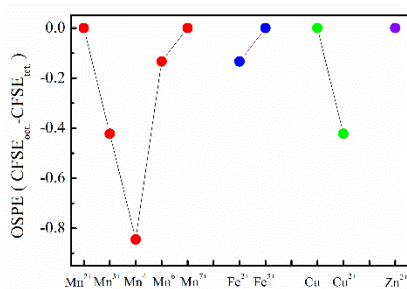


Figure 1. OSPE model is applied to explain the different cation occupancy among all metal-doped NiCo_2O_4 catalysts.

[1] K. S. Kim and Y. J. Park, *Nanoscale Res. Lett.*, 2012, 7, 1–6.

[2] M. Lenglet, R. Guillaumet, J. Durr, D. Gryffroy and R. E. Vandenberghe, *Solid State Commun.*, 1990, 74, 1035–1039.

Hydro-Baric Effect on Cathodic Deposition of Titanium Dioxide and Tin Dioxide

Tso-Fu Mark Chang^{1,2,*}, Yi-Hsuan Chiu^{1,3}, Chun-Yi Chen^{1,2}, Yung-Jung Hsu³, Masato Sone^{1,2}

¹*Institute of Innovative Research, Tokyo Institute of Technology
4259-R2-35 Nagatsuta Midori-ku Yokohama 226-8503 Japan*

²*CREST, Japan Science and Technology Agency,
4259-R2-35 Nagatsuta, Midori-ku, Yokohama 226-8503, Japan*

³*Department of Materials Science and Engineering, National Chiao Tung University
1001 University Road Hsinchu Taiwan 30010 Republic of China*

*chang.m.aa@m.titech.ac.jp

This study reports effects of the applied pressure on cathodic deposition of metal oxides, such as TiO₂ and SnO₂, thin films in an aqueous solution and performance of the TiO₂ thin films in the photoelectrochemical water splitting reaction. Aqueous solutions are often assumed to be incompressible, and the applied pressure is usually considered to have insignificant influence on the properties of the materials fabricated in aqueous solution environment. However, morphology and crystallinity of the TiO₂ [1] and ZnO [2] thin films cathodically deposited at 35 MPa were found to be different from those deposited at atmospheric pressure, shown in Fig. 1. Especially, the crystallinity was improved

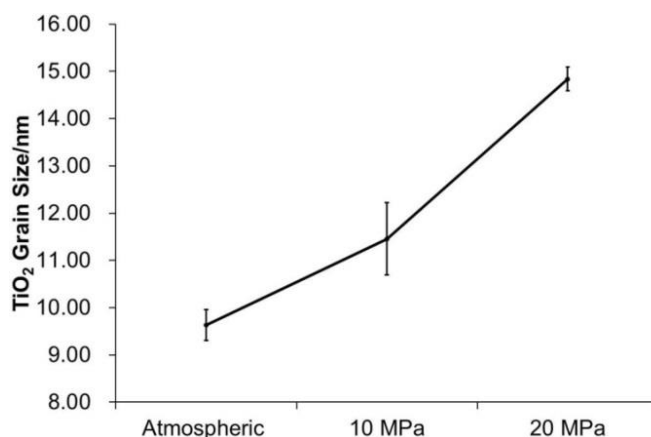


Figure 1. Effect of the applied pressure on average grain size of TiO₂ prepared by cathodic deposition.

with an increase in the applied pressure from atmospheric pressure to 35 MPa, and the as-deposit TiO₂ was found to have anatase crystal phase without any heat treatment process. Because of the effects on the crystallinity, the TiO₂ thin films deposited under high applied pressure exhibited significantly enhanced photocurrent densities of water oxidation reaction under white light illumination. The electrochemical impedance spectra and photovoltage decay data illustrated that the enhanced photoactivity can be attributed to the facilitated charge transfer as a result of the improved crystallinity. Here, “hydro-baric effect” is defined to describe the phenomenon observed from the effect of the high pressure (baric) on the properties of the metal oxides since the cathodic deposition mainly takes place in aqueous solutions (hydro), analogous to the derivative origin of “hydrothermal”. SnO₂ prepared by cathodic deposition is usually amorphous. The hydro-baric effect is also expected to work in cathodic deposition of SnO₂ to improve the crystallinity without addition heat treatment.

This work delivers a sophisticated but efficient preparation method of highly crystalline TiO₂ and SnO₂. Photocatalytic activity for photoelectrochemical water oxidation of the TiO₂ prepared would be evaluated to illustrate advantages of the hydro-baric cathodic deposition method. The effects of the pressure on electrochemical deposition conducted in an aqueous electrolyte can be extended to other solution-phase synthetic systems especially in aqueous solutions, from which highly crystalline metal oxides can be utilized as-prepared without further complicated processing such as post heat treatment or surface modification.

Reference:

- [1] T.F.M. Chang, W.H. Lin, Y.J. Hsu, C.Y. Chen, T.Sato, M. Sone, *Electrochem. Commun.*, **33** (2013) 68.
- [2] W.H. Lin, T.F.M. Chang, Y.H. Lu, T. Sato, M. Sone, K.H. Wei, Y.J. Hsu, *J. Phys. Chem. C*, **117** (2013) 25596-25603.

A Sandwiched Immunosensor for Highly Selective and Sensitive Detection of Alpha-fetoprotein by Using CdTe@SiO₂/GO Electrochemiluminescence Probe

Deng Pan, Yanfei Shen *

Southeast University

No. 87. Ding Bridge, Gulou District, Nanjing, Jiangsu, China

* Yanfei.Shen@seu.edu.cn

Alpha-fetoprotein (AFP), mainly synthesized in fetal liver, was a highly specific and heightened sensitive tumor marker for primary liver cancer. The increase of the AFP concentration in adult serum may be an early sign of some cancer diseases. Therefore, it is necessary to detect its concentration in clinical diagnosis to improve diagnostic accuracy and efficiency. Herein, an ultrasensitive sandwich-type electrochemiluminescence (ECL) biosensor for the analysis of AFP antigen was fabricated based on CdTe doped silica nanoparticles on graphene oxide (CdTe@SiO₂/GO) nanocomposites as carrier to immobilize labeled AFP antibody and chitosan/multi-walled carbon nanotubes (CS/MWCNTs) composite as carrier to immobilize capture AFP antibody. In this project, capture antibodies were immobilized through covalent combination which could catch the target AFP protein as much as possible. High ECL signal could be obtained due to the luminant CdTe@SiO₂/GO produced larges number of the emission photons. Because of its good conductivity and high surface area, the CS/MWCTs composite material, on the one hand, accelerated the electron transfer rate of electrode surface, on the other hand, it improved the loading rate of capture antibody and labeled antibody, thus further obtaining the high ECL intensity and improving the sensitivity of the sensor. In this strategy, under optimized conditions, the ECL intensity increased with the logarithmic values of AFP standard concentrations from 1.0 pg·mL⁻¹ to 100 ng·mL⁻¹ with a detection limit of 0.22 pg·mL⁻¹ (S/N = 3). The ECL immunosensor provided detection method with satisfactory recoveries, excellent reproducibility and stability, indicating that this method had a prospect in the practical application in the clinical diagnosis of AFP.

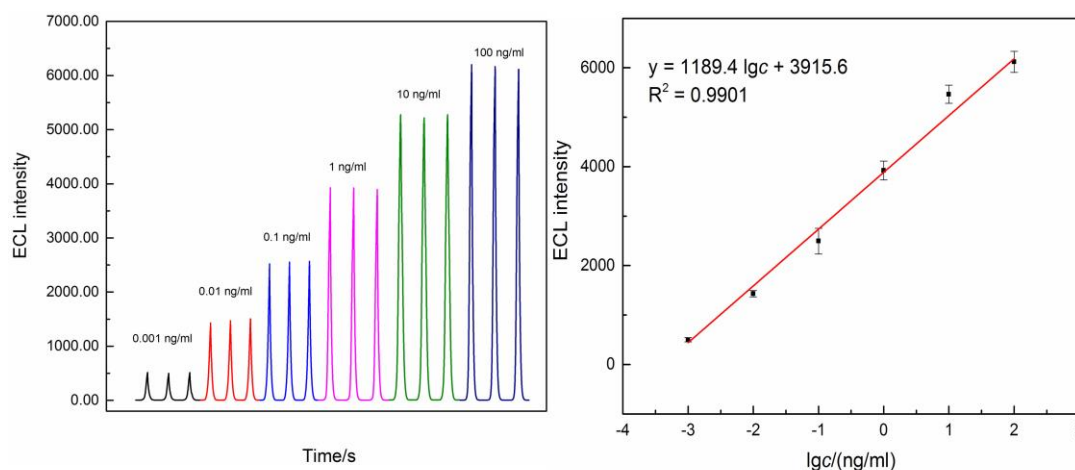


Fig.1 Sensitive detection of different concentrations of AFP by the prepared immunosensor.

References:

- 1) Q. Zhou and Y. F. Shen, *Anal. Chem.*, 88, 9830-9836 (2016),
- 2) Y. H. Yang and M.Y. Gao, *Adv. Matr.*, 17, 2354-2357 (2005),
- 3) Y.F. Shen and T. Nakanishi, *Adv. Optical Mater.*, 7, 925-930 (2015)

Charge separation at electrified semiconductor-solution interfaces

Quinn Campbell, Ismaila Dabo

*Department of Materials Science and Engineering, The Pennsylvania State University
University Park, PA 16802, USA
quinn.campbell@psu.edu*

Solar energy is the most abundant energy source available to humankind; this energy cannot be harnessed on demand, however, due to the variability of sunlight. Artificial photosynthesis offers a sustainable way to overcome this variability through the photocatalytic conversion of solar power into chemical fuels at a semiconductor–electrolyte interface. Although considerable progress has been made in simulating the bulk properties of semiconductors from first principles, much less has been done to address the electrochemical response of semiconductor–electrolyte interfaces under realistic environmental conditions. We present broadly applicable and highly transferable computational techniques to simulate semiconductor–electrolyte interfaces. By introducing a continuum model of the semiconductor and electrolyte regions surrounding the quantum-mechanical interfacial layer, our model enables the self-consistent determination of the electrical response of a semiconductor-solution interface, including the atomistic effects of charge trapping at interfacial surface states. Using this, we develop a new description of the semiconductor-solution interface allowing us to predict the electrical response, stability, and equilibrium Schottky barrier of a photoelectrode as a function of different surface chemistries. This allows researchers to optimize materials selection for both charge transport and stability, leading to more efficient and practical artificial photosynthesis systems.

Reference:

Campbell and Dabo, *Physical Review B* 95, 205308 (2017).

Effect of Activity of Free Solvents in Concentrated Electrolytes on Electrochemical Energy Conversion Reactions

Masayoshi Watanabe, Kazuhide Ueno, Kaoru Dokko
Graduate School of Engineering, Yokohama National University
79-5 Tokiwadai, Hodogaya-ku, Yokohama 240-8501, Japan
e-mail address: mwatanab@ynu.ac.jp

Certain concentrated mixtures of salts and solvents are not simply "solutions" anymore, but they may be described as "solvate ionic liquids", in which the solvents strongly coordinate the cation and/or the anion of the salts to form stable "solvate ions". The new family of ionic liquids can be obtained by simply mixing glyme (triglyme (G3) or tetraglyme (G4)) with lithium bis(trifluoromethylsulfonyl)amide (Li[TFSA]) in a molar ratio of 1:1 [1]. The equimolar complex $[\text{Li}(\text{G3 or G4})_1][\text{TFSA}]$ maintains a stable liquid state over a wide temperature range and can be regarded as a solvate ionic liquid consisting of a $[\text{Li}(\text{glyme})_1]^+$ complex cation and a $[\text{TFSA}]^-$ anion, meaning negligible free solvent activity in these liquids[1].

It is well known that ethylene carbonate is electrochemically compatible with graphite anode because a good SEI layer, which prevents the intercalation of solvents into the graphite, is formed. In contrast, the intercalation of solvents with Li^+ into graphite takes place in other common solvents such as propylene carbonate (PC) and ethers, causing destruction of the graphite crystalline structure. However, it was reported that intercalation of these solvents, namely, PC, dimethoxy ethane, and other solvents into graphite anode can be inhibited by increasing the Li salt concentration and that intercalation of Li^+ into graphite anode occurs reversibly[2]. We also observed the reversible Li^+ intercalation/deintercalation reaction in extremely concentrated triglyme (G3)-Li[TFSA] solution, although the intercalation takes place in the solution containing excess G3 (**Figure 1**)[3]. The electrode potential for the formation of Li^+ intercalated graphite (including desolvation process of $[\text{Li}(\text{G3})]^+$) is expected to increase greatly against the Li salt concentration, because the potential depends on the activity of not only solvate cation but also free solvent ($E = E^0 + 2.303RT/F \log a_{[\text{Li}(\text{G3})]/a_{\text{G3}}}$). On the other hand, the electrode potential for intercalation depends on only the activity of solvate cation, since the reaction does not involve desolvation process. Thus, in the highly concentrated region, the activity of free solvent is very small, and the electrode potential for Li-intercalated graphite formation is higher than that for intercalation, leading to the suppression of intercalation. In this presentation, it will be demonstrated that the activity of the solvent in an electrolyte can be a key factor in controlling electrochemical reactions, especially focusing on the graphite intercalation reactions.

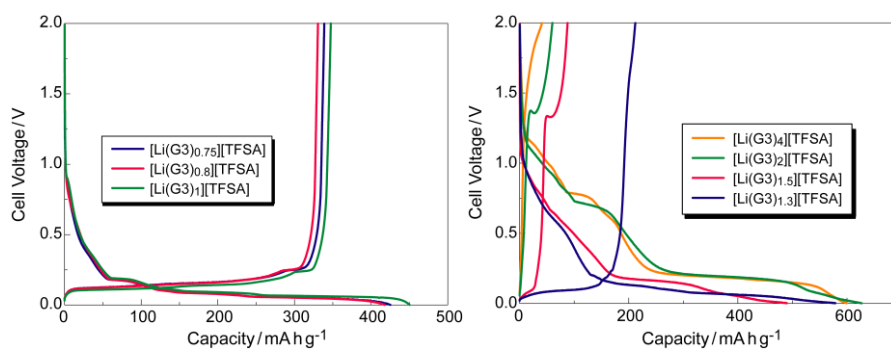


Figure 1 Charge-discharge curves for $[\text{Li}][\text{Li}(\text{G3})_x][\text{TFSA}]/\text{graphite}$ ($x = 0.75\text{--}4.0$) cells measured at 1/20 C rate at 60 °C.

References

- [1] K. Yoshida *et al.*, *J. Am. Chem. Soc.*, **133**, 13121 (2011); K. Ueno *et al.*, *Phys. Chem. Chem. Phys.*, **17**, 8248-8257 (2015).
- [2] S. Jeong *et al.*, *Electrochem. Solid-State Lett.*, **6**, A13 (2003); Y. Yamada *et al.*, *J. Electrochem. Soc.*, **162**, A2409 (2015).
- [3] H. Moon *et al.*, *J. Phys. Chem. C*, **118**, 20246 (2014); H. Moon *et al.*, *J. Phys. Chem. C*, **119**, 3957 (2015).

Potentiometric Carbon Monoxide Sensors Employing Anion-Conducting Polymer Electrolyte and Oxide-Based Sensing Electrodes

Takeo Hyodo, Mari Takamori, Kai Kamada, Taro Ueda, and Yasuhiro Shimizu

Affiliation: Graduate School of Engineering, Nagasaki University

Address: 1-14 Bunkyo-machi, Nagasaki 852-8521, Japan

E-mail address: hyodo@nagasaki-u.ac.jp

Some types of electrochemical CO sensors using sulfuric acid (aq.) or Nafion[®] as an electrolyte and carbon-based electrodes loaded with noble metal (mainly Pt), which can be operated at RT, have been presently commercialized all over the world, but many kinds of oxides are not basically useful as an electrode material of the sensors, due to the lack of chemical stability under the strong acidic environment. On the other hand, anion-conducting polymers (ACP) with large hydroxide-anion conductivity are quite attractive as an alternative electrolyte for the sensors, because most of metal oxides are relatively stable under alkaline environment. We firstly demonstrated that potentiometric gas sensors employing an ACP electrolyte and Pt- or Pd-loaded carbon black electrodes showed relatively large responses to CO₂^{1,2)} and H₂³⁾ respectively, and that the ACP-based sensor using Pd-loaded carbon black electrodes also showed a relatively large response to CO, but the CO selectivity of the sensor against H₂ was much lower than we expected⁴⁾. Subsequently, we reported that SnO₂ and In₂O₃ were quite attractive as a new CO-sensing electrode material for the ACP-based sensors, and the loading of Au or Pt onto these oxides drastically enhanced the magnitude of CO response as well as the CO selectivity against H₂⁵⁻⁷⁾.

In this study, we demonstrated the CO-sensing properties of the ACP-based sensors using a metal oxide (MO) loaded with or without a noble metal (N) as a CO-sensing electrode material (EC(*n*N/MO) or EC(MO), respectively, MO: Bi₂O₃, CeO₂, SnO₂, and so on, *n*: the amount of N loaded onto the oxide (0.5–10 wt%), N: Au, Pt, and so on) and discussed the impacts of the kinds of MO and N and the amount of N loaded onto MO on the magnitude of CO response as well as the CO selectivity against H₂. For example, Fig. 1 shows response transients of typical EC(MO) and EC(2.0N/MO) sensors (N: Au or Pt, MO: Bi₂O₃, CeO₂, or SnO₂) to 500 ppm CO in humidified air (relative humidity (RH): 57%) at 30°C. The EC(Bi₂O₃) sensor showed relatively large CO response and fast response and recovery speeds in comparison with those of EC(CeO₂) and EC(SnO₂) sensors, but even the CO-sensing properties of the EC(Bi₂O₃) sensor were totally insufficient to detect a low concentration of CO practically. However, the loading of 2.0% Au or Pt nanoparticles onto MO was quite effective in improving the CO-sensing properties of only the EC(SnO₂) sensor.

References

- 1) T. Hyodo et al., *Electrochim. Acta*, **82**, pp. 19–25 (2012).
- 2) Y. Shimizu et al., *Japanese Patent*, No. 5787287 (2015).
- 3) T. Hyodo et al., *Reports of the Faculty of Engineering, Nagasaki University*, **42**(79), 42–47 (2012).
- 4) T. Goto et al., *Chemical Sensors*, **29**(B), 94–96 (2013).
- 5) T. Goto et al., *Electrochim. Acta*, **166**, pp. 232–242 (2015).
- 6) Y. Shimizu et al., *Japanese Patent*, No. 6075872 (2017).
- 7) T. Hyodo et al., *J. Electrochem. Soc.*, **163**, pp. B300–B308 (2016).

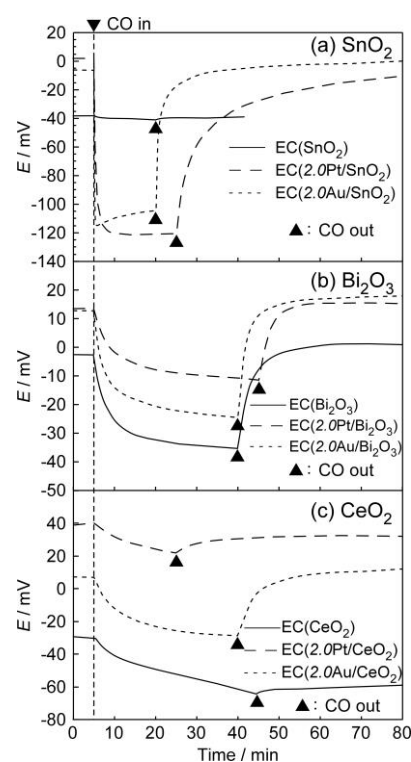


Fig. 1. Response transients of typical EC(MO) and EC(2.0N/MO) sensors to 500 ppm CO in humid air at 30°C (57%RH).

Implications of Transport and pH-Effects on Electrocatalytic CO₂ Reduction

Stefan Ringe, Karen Chan, Jens Nørskov
Department of Chemical Engineering, Stanford University
Stanford, California 94305, United States
sringe@stanford.edu

Electrocatalytic CO₂ reduction has become a highly promising route to sustainable and economical carbon-neutral fuels. So far, however, a basic understanding of the underlying chemical processes is still lacking, mainly due to the highly complex, large reaction network involving a variety of C1 and C2 products. Experimental investigations are additionally aggravated by apparent transport limitations of CO₂ to the surface which are also determined by buffer equilibria in solution. Additionally, pH gradients at the solid-liquid interface can be important to consider, since local pH effects have shown to critically influence product selectivities. Such effects overlay (electro-)chemical kinetics which can be modeled e.g. by Density Functional Theory (DFT) in combination with micro-kinetic modeling approaches. However, in order to utilize these methods for the transport limited regime, these need to be extended by equations governing diffusion and migration effects as well as chemical reactions in the electrolyte. Using a coupled kinetic-transport model based on Poisson-Nernst-Planck theory and ab initio calculations of reaction and activation energies, we show transport limitations to be crucial to determining C2 to C1 product selectivity. We present strategies for catalyst structural design to optimize the selectivity towards higher value C2 products.

Electrochemical Characterization of Semiconducting Oxide Thin Films for Energy Applications: Solar Cells, Fuels, Batteries and Beyond

L. Kavan

*¹J. Heyrovský Institute of Physical Chemistry, v.v.i., Academy of Sciences of the Czech Republic,
Dolejškova 3, CZ-18223 Prague 8, Czech Republic.*

Ladislav.Kavan@jh-inst.cas.cz

The electronic band structure of semiconducting oxides (TiO₂ or SnO₂) is relevant to photo/electrochemistry and energy applications [1]. The position of conduction band (CB) edge controls reductive photocatalytic reactions (e.g. hydrogen formation from water or CO₂-reduction to solar fuels), Li-insertion electrochemistry, recombination blocking in perovskite solar cell (PSC) and open-circuit potential of dye-sensitized solar cell (DSC) [2]. The ALD-grown TiO₂ and SnO₂ layers are useful for electron selective contacts in these solar cells [3]. Amorphous SnO₂ films are pinhole-free for thicknesses down to 2 nm. This allows photoelectrode design with even thinner electron selective layers in PSC, thus minimizing resistance losses. Well-blackening thermally stably TiO₂ (rutile) layers were also developed for these applications [4]. The open-circuit potential (V_{OC}) of DSC is controlled by both the CB position of TiO₂ and by the redox potential of a mediator. The V_{OC} > 1V was demonstrated recently for mediators based on tetra-coordinated Cu(II/I) complexes [5–7]. However, there is a considerable controversy about the position of CB in TiO₂ (anatase, rutile, including the crystals with distinguished facets) [8]. The conflict can be rationalized by taking into account the adsorption of OH⁻ and H⁺ ions from the electrolyte solution on the electrode surface [8]. The facet specific electrochemistry of water splitting on TiO₂ is addressing both the CB position and the electrocatalytic activity of the relevant crystal face [9]. Oxide materials, like TiO₂ and SnO₂ are traditionally regarded semiconductors. Doping of SnO₂ by F⁻ or Sb⁵⁺ provides the quasi-metallic (degenerate semiconductor) material, but little is known about similar doping-induced behavior of TiO₂. We have recently found purely metal-like electrochemical properties of Ta-doped, optically transparent thin films of TiO₂ (anatase) made by pulsed-laser deposition. The quasi-metallic TiO₂ films surprisingly show significant UV-photocurrent of water oxidation, and retain rectifying function for redox couples with highly positive electrochemical potentials [10].

References

- [1] L. Kavan, Chem. Rec. 12 (2012) 131.
- [2] L. Kavan, Curr. Opinion Electrochem. 2 (2017) 88.
- [3] L. Kavan, L. Steier, M. Grätzel, J. Phys. Chem. C 121 (2017) 342.
- [4] S. Kment, H. Krysova, Z. Hubicka, H. Kmentova, L. Kavan, R. Zboril, Appl. Mat. Today 9 (2017) 122.
- [5] L. Kavan, Y. Saygili, M. Freitag, S.M. Zakeeruddin, A. Hagfeldt, M. Grätzel, Electrochim. Acta 227 (2017) 194.
- [6] Y. Saygili, M. Soderberg, N. Pellet, F. Giordano, Y. Cao, A.B. Munoz-Garcia, S.M. Zakeeruddin, N. Vlachopoulos, M. Pavone, G. Boschloo, L. Kavan, J.E. Moser, M. Grätzel, A. Hagfeldt, M. Freitag, J. Am. Chem. Soc. 138 (2016) 15087.
- [7] L. Kavan, H. Krysova, P. Janda, H. Tarabkova, Y. Saygili, M. Freitag, S.M. Zakeeruddin, A. Hagfeldt, M. Grätzel, Electrochim. Acta 251 (2017) 167.
- [8] P. Deak, J. Kullgren, B. Aradi, T. Frauenheim, L. Kavan, Electrochim. Acta 199 (2016) 27.
- [9] K. Minhova-Macounova, M. Klusackova, R. Nebel, M. Zikalova, M. Klementova, I.E. Castelli, M.D. Spo, J. Rossmeisl, L. Kavan, P. Krtil, J. Phys. Chem. C 121 (2017) 6024.
- [10] H. Krysova, P. Mazzolini, C.S. Casari, V. Russo, A. Li Bassi, L. Kavan, Electrochim. Acta 232 (2017) 44.

Advanced Electroplating Technologies for 2.5D and 3D Chip Packaging Fabrication

Wei-Ping Dow*, I-Hsuan Chang, Yi-Yung Chen, Wei-Yang Zeng, Shih-Cheng Chang, Po-Fan Chan,
Chun-Hsiang Lo

*Department of Chemical Engineering, National Chung Hsing University
Taichung 42007, Taiwan*

**dowwp@dragon.nchu.edu.tw*

Abstract

Nowadays, electronic products become smarter and smarter because more IC chips are assembled in the electronic products. However, the basic physical operation mode of MOS (metal-oxide-semiconductor) is still the same as before mode, which means that more MOS need to be fabricated in the chips. This demand forces the chip maker to produce more finer conducting lines in the chips, so that more MOS can be put in the devices and exhibit more functions. In addition, high frequency transmission is also another demand if the functions of these electronic products become more and more. Consequently, 2-dimensional (2D) chip packaging does not meet these criteria anymore. Alternatively, 2.5D and 3D chip packaging technologies are proposed currently and some products do be produced through the 2.5D and 3D packaging technologies.

Herein, we would like to propose two approached to solve two issues, which occur in producing 2.5D or 3D chip packaging. One is packaging substrate and interposer metallization using reduced graphene oxide (rGO) as conducting layer, the other is Kirkendall (KK) void-free copper pillar by electroplating. In the former case, we will present a new metallization approach using rGO to replace electroless copper deposition and then achieve through hole plating, microvia filling, even TSV superfilling with copper and cobalt, respectively. In the latter case, we will present a new copper electroplating formula that can achieve copper foil with ultra-large grain (ULG). Each copper grain is a single crystal with a grain size of 15 ~ 20 μm . The ULG copper foil has few grain boundary, so no KK void is formed after soldering, even at 200°C for 1000 hr. Of course, the IMC (Cu_3Sn and Cu_6Sn_5) is still formed but no KK void occurs at the interface between copper and IMC.

These new copper electroplating processes are characterized by many instruments, such as XRD, HRTEM, FTIR, SEM/EDS, Raman spectroscopy, XPS and AFM. According to the analytical results, a reasonable mechanism is proposed to explain how the rGO and copper plating formula work to exhibit good performance.

Electrocatalytic Applications of Atomically Precise Metal Nanoclusters

Dongil Lee
Department of Chemistry
Yonsei University
Seoul 03722
South Korea
dongil@yonsei.ac.kr

Atomically precise metal nanoclusters containing a few to a few hundreds of atoms have been the focus of recent investigations because of their novel electronic, optical, and catalytic properties. They appear to represent the bulk-to-molecule transition region where electronic band energetics yield to quantum confinement effects and discrete electronic states emerge. In this presentation, the electrocatalytic activities of atomically precise metal nanoclusters for hydrogen evolution reaction (HER) and CO₂ reduction reaction (CO₂RR) are reported. Gold, silver and bimetallic nanoclusters, such as Au₂₅(SR)₁₈, Ag₂₅(SR)₁₈, and PtAu₂₄(SR)₁₈, where SR is alkanethiolate, were synthesized and cast on glassy carbon electrode. Electrocatalytic activities of these clusters for the reduction of CO₂ were compared in an H-type cell. Product analysis using gas chromatography has shown that CO was predominantly produced on Au₂₅(SR)₁₈ and Ag₂₅(SR)₁₈ while H₂ was favorably produced on PtAu₂₄(SR)₁₈.

Highly Durable Electrochemical Capacitors Using Seamless Activated-Carbon Electrode

Soshi Shiraishi, Yoshikiyo Hatakeyama
 Graduate School of Science and Technology, Gunma University
 Kiryu, Gunma 376-8515, Japan
 Hidehiko Tsukada
 AION Co. Ltd.
 Koga, Ibaraki 306-0213, Japan
 soshishiraishi3@gunma-u.ac.jp

The electric double layer capacitor (EDLC) is an electrochemical energy-storage device with high power density. In the EDLC, the higher voltage operation than 3 V is required for the higher energy density and reliability, but electrochemical decomposition during high voltage is the origin of the decrease in the capacitance and the increase in the internal resistance through i) the micropore blocking due to the decomposition products, ii) the gas evolution, or iii) the breakdown of electric network in the electrode.

The conventional EDLC electrode, which is composed of the activated carbon powder, carbon black, and binder (Fig.1(a)), is easily deteriorated by the breakdown of electric network at high voltage charge. Thus, the author's newly proposed the seamless structure of the activated carbon electrode containing no particle-boundaries (Fig.1(b)) to realize high durability against higher voltage charge for the EDLC [1].

The seamless activated carbon electrode (MLpAC) was prepared by pressing, carbonizing, and activating the consecutively macroporous phenolic resin matrix (MICROLITE, AION). The two-electrode cell was assembled by the electrodes and organic electrolyte (1M $(C_2H_5)_3CH_3NBF_4$ /propylene carbonate). The capacitance was measured by the galvanostatic method (80 mA g^{-1} , 0~2.5 V) at 40 °C. The durability test was conducted by the floating condition (3.5 V, 100 h, 70 °C).

The carbon matrix does not have any particle-boundaries to form the seamless structure as shown in Fig.2. The initial capacitance, capacitance retention, and increase in the internal resistance by the durability test are summarized in Table 1. The EDLC using the seamless activated carbon electrodes showed both of the high volumetric-capacitance and durability against 3.5V charging. The durability is due to the stable electric network in the electrode based on binder or particle-boundary-free structure.

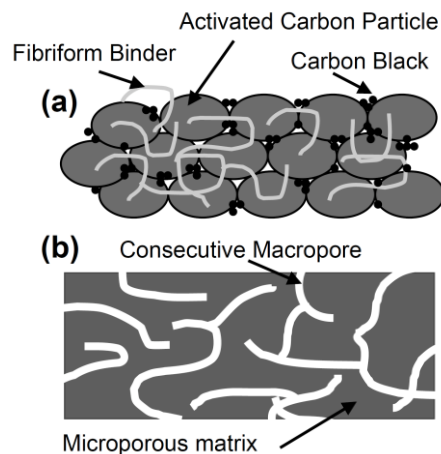


Fig. 1 Schematic model of (a) conventional and (b) seamless activated carbon electrode for EDLC.

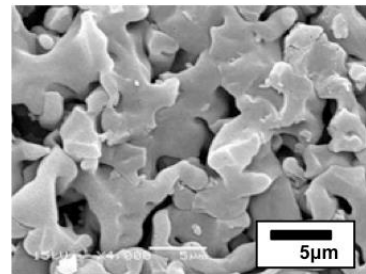


Fig. 2 SEM image of MLpAC.

Table 1 Pore structure, capacitance, and durability (3.5V, 100h, 70°C)

Electrode	S_{BET} [m^2g^{-1}]	V_{micro} [mlg^{-1}]	C_0 [Fcm^{-3}]	C_d/C_0 [%]	R_0 [Ω]	ΔR [Ω]
Seamless (MLpAC)	1530	0.61	17	77	5	13
Composite (YP50F)	1590	0.58	13	12	5	37

Composite: conventional electrode for EDLC, prepared by activated carbon (YP50F, Kuraray Chemical), acetylene black, and PTFE binder.

S_{BET} , V_{micro} : BET specific surface area, micropore volume of activated carbon, C_0 : initial volumetric capacitance, C_d/C_0 : capacitance retention, R_0 : initial internal resistance, ΔR : increase of internal resistance

[1] S. Shiraishi, *Boletín del Grupo Español del Carbón*, **28**, 18–24 (2013).

Acknowledgment A part of this research is supported by JSPS KAKENHI Grant No. 17H03123.

Efficient Direct Formic Acid Fuel Cells (DFAFCs) Anode Derived from Seafood waste: Spillover Mechanism

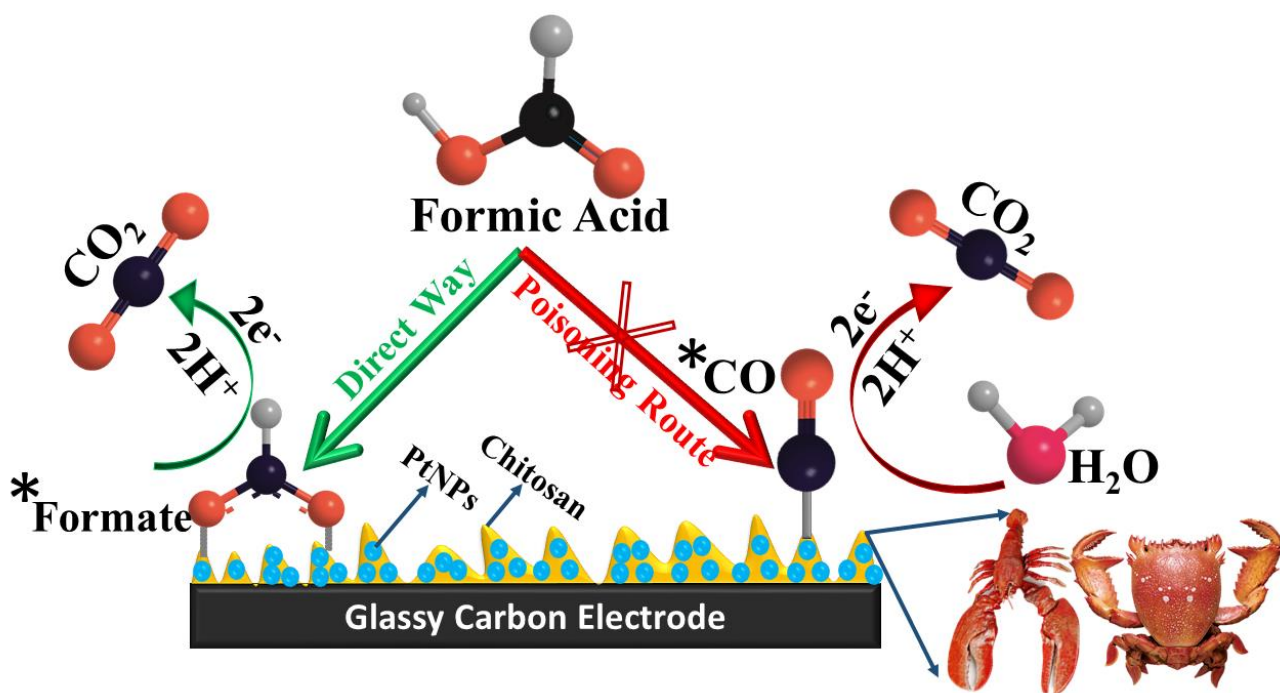
Gumaa A. El-Nagar¹, Iver Lauermann², Christina Roth¹

¹Institute for Chemistry and Biochemistry, FU Berlin, Takustr. 3, D-14195 Berlin, Germany

²Helmholtz-Zentrum Berlin für Materialien und Energie, Hahn-Meitner-Platz 1, 14109 Berlin, Germany

Gumaa.elnagar@fu-berlin.de

Commercial Pt/C anodes of direct formic acid fuel cells (DFAFCs) get rapidly poisoned by in-situ generated CO intermediates. We succeeded in increasing the Pt nanoparticles (PtNPs) stability and activity for formic acid oxidation (DFAFCs anodic reaction) by embedding them inside a chitosan matrix obtained from seafood wastes. Atop the commercial Pt/C, formic acid (FA) is predominantly oxidized via the undesired poisoning dehydration pathway (14 times higher than the desired dehydrogenation route), wherein FA is non-faradaically dissociated to CO resulting in deactivation of the majority of the Pt active-surface sites. Surprisingly, PtNPs chemical insertion inside a chitosan matrix enhanced their efficiency for FA oxidation significantly, as demonstrated by their 27 times higher stability along with ~400 mV negative shift of the FA oxidation onset potential together with 270 times higher CO poisoning-tolerance compared to that of the commercial Pt/C. These substantial performance enhancements are believed to originate from the interaction of chitosan functionalities with both PtNPs and FA molecules helping improving FA adsorption and preventing the PtNPs aggregation, besides providing the required oxygen helping with the poisoning CO oxidative removal at low potentials. Additionally, chitosan induced the retrieval of the Pt surface-active sites by capturing the in-situ formed poisoning CO intermediates via a so-called “Spillover mechanism”.



Sensitive Gold Electrode Biosensors Fabricated on Plastic Substrate

Qingpan Yuan, Wei Lu, Yusheng Wang, Bo Yao

Department of Chemistry, Zhejiang University, Hangzhou 310058, China

E-mail: yaobo08@zju.edu.cn

Up to date, considerable research effort has been focused on sensitive and selective detection of DNA molecules related to variant genetic diseases, among which electrochemical methods are especially popular for its simplicity and low cost. Variety of DNA biosensors have been proposed for electrochemical detection of DNA molecules, for example, enzymatic reaction and gold nano-particle-based signal amplification.

Recently, we developed a novel polystyrene gold electrode (PGE) containing unique nano-scale structure surface which were found having extremely high capacity of DNA immobilization compared with gold electrodes fabricated by standard sputtering based photolithography (figure1)^{1, 2}. When investigated the electrochemical parameters of PGEs, we found significantly improved and interesting electrochemical characteristics of PGEs, for example, split peaks of cyclic voltammetry (CV) and differential-pulse voltammetry (DPV) (figure2). It was proved that Peak I attributed to the redox reaction of $\text{Ru}(\text{NH}_3)_6^{3+}$ diffused to MCH (6-mercapto-1-hexanol) portion in the mixed DNA/MCH monolayers and peak II could be ascribed to $\text{Ru}(\text{NH}_3)_6^{3+}$ electrostatically bound to DNA backbones, which reflected the amount of DNA molecules localized at the electrode surface.

Based on the advantageous electrochemical properties of PGEs, sensitive detection of bio-molecules such as nucleic acids has been developed and PGEs has been proven simple and low-cost biosensor. We believe it provides a practical and alternative technique for fabrication of gold electrode biosensor and it has great potential for wide-spread application, such as point-of-care-testing (POCT).

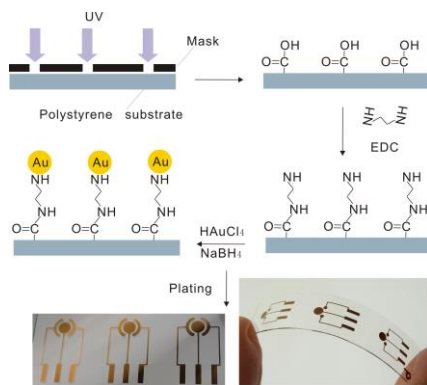


Fig.1 (a) Integrated gold electrodes were fabricated on polystyrene substrate by chemical plating

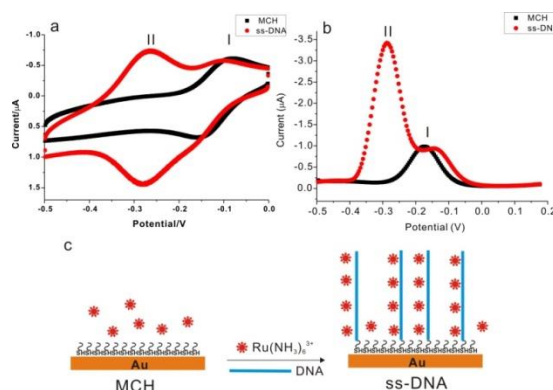


Fig.2 (a) Cyclic voltammogram and (b) differential-pulse voltammetry (DPV) curve of PGE immobilized with MCH and single stranded DNA (c).

This work was supported by the National Natural Science Foundation of China (No. 21375119, 81471750).

References

- [1] Z. Yang, Y. Liu, W. Lu, Q. Yuan, W. Wang, Q. Pu and B. Yao, *Talanta*, 2016, 152, 301-307
- [2] B. Yao, Y. Liu, M. Tabata, H. Zhu and Y. Miyahara, *Chem. Commun.*, 2014, 50, 9704-9706
- [3] W. Lu, Q. Yuan, Z. Yang, B. Yao, *Biosens. Bioelectron.*, 2017, 90(15): 258-263

Electrodeposition of Polyaniline with High Hydrophobicity and Pseudo-capacitance for Multiplex Solid-contact Ion Sensing

Yu-Fu Chen, Ching-Jung Yen, and Lin-Chi Chen*

Department of Bio-industrial Mechatronics Engineering, National Taiwan University

No. 1, Sec. 4, Roosevelt Rd., Taipei 10617, Taiwan (R.O.C.)

*Email: chenlinchi@ntu.edu.tw

Solid-contact ion-selective electrodes (ISEs) are emerging solid-state potentiometric ion sensors that use an electroactive material (e.g., a conducting polymer) as a solid contact (SC) layer to replace an internal reference solution between an ion-selective membrane (ISM) and an electrode. In principle, the SC layer exhibits a field effect of charge-electron separation called “ion-to-electron transduction” (IET) to convert the captured ion concentration into a detectable electrical potential governed by the Nernst equation. Also, an ideal SC layer must be able to resist the permeation of a “water layer” from an analyte solution to avoid non-desired IET attributed to interfering ions. Thus, a SC layer with enhanced hydrophobicity and pseudo-capacitance is favored and needed for improving a number of performance factors, ranging from signal stability, sensitivity, selectivity and detection limit to time response. In this study, we demonstrate a novel idea of electrodeposition of a polyaniline (PANI) film with both high hydrophobicity and pseudo-capacitance on screen printed carbon electrode (SPCE) for enhanced solid-contact ion sensing. As can be seen in Fig. 1(a), the surface structure and contact angle (CA) of a PANI film can be tuned through varying the electrodeposition condition without a significant composition change. From this approach, we successfully grow quasi-superhydrophobic PANI films (CA = 132° for PANI 20, CA = 138° for PANI 10) and observe what condition yields a relatively hydrophilic film (e.g., PANI 100). Moreover, we discover that a quasi-superhydrophobic PANI film has a high pseudo-capacitance as well (see Fig. 1(b): 4.61×10^3 , 2.47×10^3 , 9.46×10^2 , 2.19×10^2 , 4.28×10^1 μF for PANI10, PANI20, PANI50, PANI100, and no PANI, respectively.) When used as a solid contact, the PANI film with both high hydrophobicity and capacitance results in the reduced water layer interference, high potentiometric stability and sensitivity, and improved limit of detection. This advantage is further demonstrated via manufacturing a solid-contact ISE array for multiplex sensing of essential physiological electrolytes Na^+ , K^+ , Cl^- and Ca^{2+} (Fig. 1(c)), showing that the enhanced PANI solid contact is favored for different ion sensors.

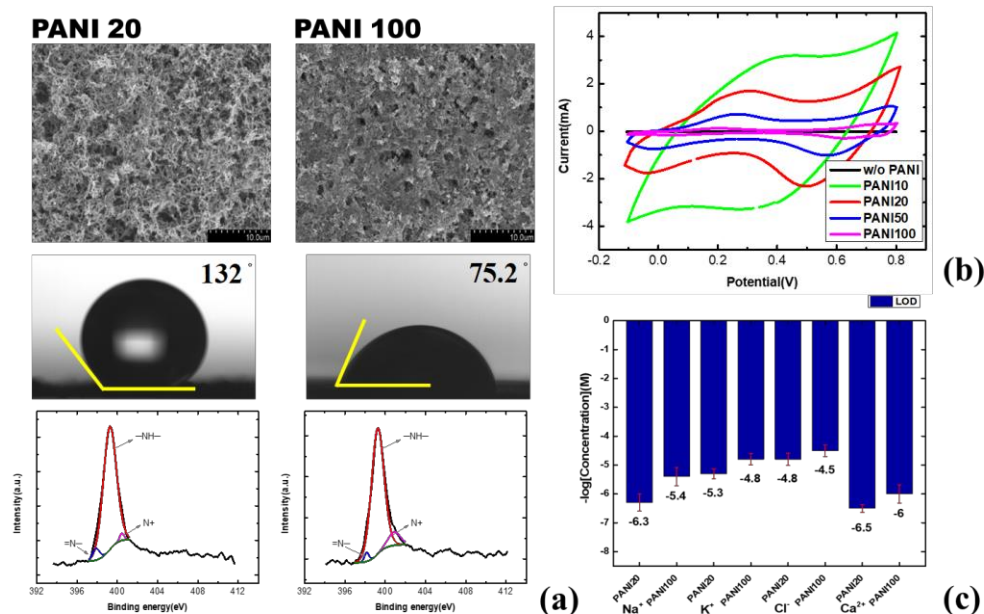


Figure 1. (a) Comparisons of SEMs, contact angles, and XPS data between a hydrophobic (PANI20) and hydrophilic (PANI100) film. (b) Comparisons of the pseudo-capacitances between different PANI films. (c) Application to multiplex solid-contact ion sensing that shows improved LODs (PANI20 vs. PANI100).

Surface morphology and microstructure control of electrodeposited copper foils for high-frequency wireless devices and Li-ion batteries

Chi-Chang Hu*, Chun-Cheng Lin

*Department of Chemical Engineering, National Tsing Hua University
101, Sec. 2, Kuang-Fu Rd., Hsin-Chu 30013, Taiwan*

**e-mail: cchu@che.nthu.edu.tw*

The thickness of Cu foils for the anode current collector of LIBs is required to be thin ($< 10 \mu\text{m}$) to reduce the volume and weight of batteries but the mechanical properties has to remain strong enough to go through the roll-to-roll manufacturing process without fracture. The surface roughness on both sides should be identically smooth and glossy to provide acceptable wettability and adhesion of the graphite coating. On the other hand, Cu foils for the fifth generation (5G) high-frequency wireless devices must be exceedingly smooth because the skin depth of copper caused by the so-called skin effect is merely $0.266 \mu\text{m}$ when the transmitting frequency of signals is up to 60 GHz. Thus, the majority of electric currents passing through the conductor flows extremely near the Cu foil surface. Under such circumstances, the coarse surface roughness shows a significant detrimental effect on the signal loss of wireless communication devices, and consequently, the surface morphology and mechanical properties of copper foils need to be further improved in order to meet the requirements for the next generation electronic devices.

The microstructures of copper fabricated by electrodeposition (ED) strongly depend on the plating parameters, including current density, convection rate of the electrolyte, pulsed/direct current deposition, or using appropriate organic additives to ameliorate the nucleation behavior of Cu from cupric ions. Manufacturing of ED copper foils should be operated at high current densities and high temperatures to promote the yield rate of mass production. In this work, we tailor the microstructure of copper foils by correct selection of additives and demonstrate the copper foil fabricated by high-speed electrodeposition at a current density of 450 mA/cm^2 (average growth rate $> 150 \text{ nm/s}$) from a 54°C bath, which meets the required yield rate for genuine mass-production. The surface morphology of the foil facing the electrolyte side is smooth by our designed additives, and surface roughness values, R_a and R_q , are less than 100 nm , which are as smooth as foils manufactured via the rolling process. In addition, the microstructure of copper can be further tuned by a specially selected additive. The grain size of copper is getting smaller as the concentration of this additive is increased. When the concentration of this additive is up to 800 ppm , the average grain size of copper is shrunk from $3 \mu\text{m}$ to $0.3 \mu\text{m}$, and surprisingly, an extremely unique, nearly single-crystalline, copper texture in the (220) orientation is obtained. Owing to such delicate microstructure, considerable improvement in mechanical properties with more than 40 % increase in tensile strength and 4 times increase in the elongation rate compared to the conventional gelatin-based copper foil is achieved. This single-crystalline texture is able to provide uniform etching rate for the PCB circuit formation process.

To design novel organic additives, developing the corresponding monitor method to quantify the additive concentration is crucial to ensure the long-time quality. There are three major kinds of additives to ameliorate ED copper: brightener, suppressor, and leveler, with different properties toward the Cu electrodeposition. Based on their characteristics, cyclic voltammetric stripping (CVS) is a well-known method to quantify additive concentration. However, to distinguish one concentration out of three additive precisely, several considerations have to be carefully done to provide the result with acceptable reliability. Herein, we introduce a method to isolate the disturbance of suppressor and leveler, and obtain the concentration of brightener within 5 % deviation. The surface morphology and microstructure of copper foil are characterized by scanning electron microscopy, atomic force microscopy, X-ray diffraction, electron back-scattered diffraction, transmission electron microscopy, and tensile testing. How to utilize additives to tailor the structure of copper and to utilize CVS to quantify the additive concentration precisely will be discussed.

Electrochemical Micro/Nano-Machining on Semiconductor Wafers

Dongping Zhan, Lianhuan Han, Zhong-Qun Tian, Zhao-Wu Tian

State Key Laboratory of Physical Chemistry of Solid Surfaces (PCOSS), Collaborative Innovation Centre of Chemistry for Energy Materials (iChEM), and Department of Chemistry, College of Chemistry and Chemical Engineering, Xiamen University
422 Siming South Road, Xiamen 361005, China.
e-mail address: dpzhan@xmu.edu.cn

Micro/nano-machining (MNM) is becoming the cutting-edge of high-tech manufacturing because of the increasing industrial demand for supersmooth surfaces and functional three-dimensional micro/nano-structures (3D-MNS) in ultra-large scale integrated circuits, microelectromechanical systems, miniaturized total analysis systems, precision optics and so on. Taking advantage of no tool wear, no surface stress, environmental friendliness, simple operation, and low cost, electrochemical micro/nano-machining (EC-MNM) has an irreplaceable role in MNM. However, because the thickness of the electrolyte solution between the tool electrode and the workpiece are usually at micro/nano-meter scale, it is a challenge to solve the problems of potential distribution and mass transfer in the ultra-thin layer electrolyte cell. In this presentation, we will introduce our recent work on the external physical field induced electrochemical reactions in which there is no need of 2-electrode or 3-electrode system in the conventional electrochemical system. Figure 1 gives an example on the contact electrification induced electrochemical reactions and its application in nanoimprint lithography.

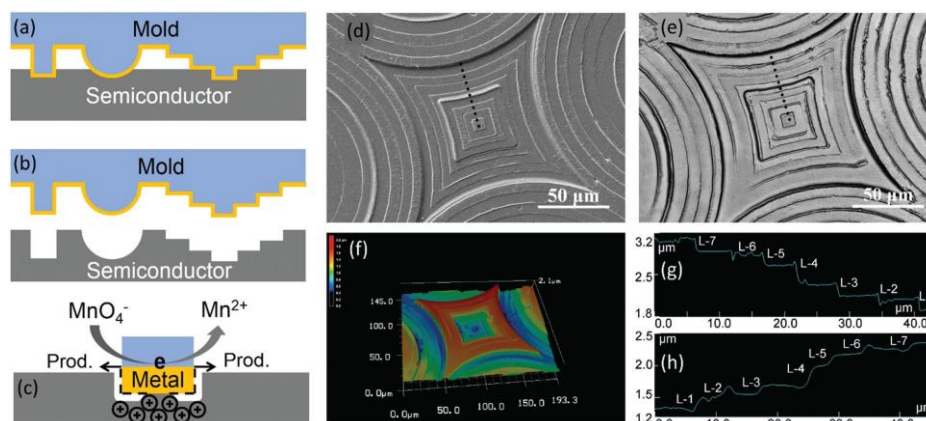


Fig. 1 (a–c) The schematic of ECNL; (d) the SEM image of a diffractive microlens on a catalyst mold. (e) The confocal laser microscopy image of a diffractive microlens fabricated on GaAs. (f) The AFM image of (e). (g and h) The cross-sectional profiles of eight-phase levels on a catalyst mold and GaAs outlined by the black dotted lines, respectively.

Reference:

1. D. Zhan*, L. Han, J. Zhang, Q. He, Z.-W. Tian*, Z.-Q. Tian, Electrochemical micro/nano-machining: principles and practices, *Chem. Soc. Rev.* 2017, 46, 1526-1544.
2. D. Zhan*, L. Han, J. Zhang, S. Kang, J.-Z. Zhou, Z.-W. Tian, Z.-Q. Tian*, Confined Chemical Etching for Electrochemical Machining with Nanoscale Accuracy, *Acc. Chem. Res.* 2016, 49, 2596-2604.
3. J. Zhang, L. Zhang, W. Wang, L. Han, J. Jia, Z.-W. Tian, Z.-Q. Tian, D. Zhan*, Contact electrification induced interfacial reactions and direct electrochemical nanoimprint lithography in n-type gallium arsenate wafer, *Chem. Sci.* 2017, 8, 2407-2412.
4. L. Zhang, J. Zhang, D. Yuan, L. Han, J.-Z. Zhou, Z.-W. Tian, Z.-Q. Tian, D. Zhan*, Electrochemical nanoimprint lithography directly on n-type crystalline silicon (111) wafer, *Electrochem. Commun.* 2017, 75, 1-4.
5. J. Lai, D. Yuan, P. Huang, J. Zhang, J.-J. Su, Z.-W. Tian, D. Zhan*, Kinetic Investigation on the Photoetching Reaction of n-Type GaAs by Scanning Electrochemical Microscopy, *J. Phys. Chem. C* 2016, 120, 16446-16452.

A Neodymium Oxide Nanoparticle-Doped Carbon Felt as Promising Electrode for Vanadium Redox Flow Batteries

Abdulmonem Fetyan^a, Gumaa A. El-Nagar^{a,b}, Igor Derr^a, and Christina Roth^a

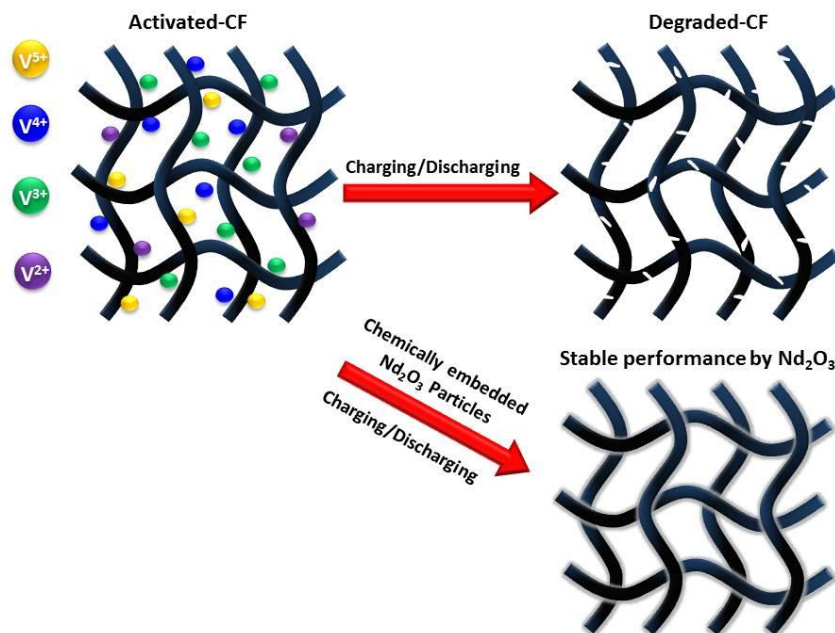
^a Institute for Chemistry and Biochemistry, Freie Universität Berlin, Takustr. 3, 14195 Berlin, Germany

^b Chemistry Department, Faculty of Science, Cairo University, Cairo 12613, Egypt

abdul.fetyan@fu-berlin.de

Commercial rayon and polyacrylonitrile-based carbon felts have been considered as good candidate electrode materials in vanadium redox flow batteries. Despite otherwise favorable properties, these felts still have poor electrochemical activity which limits the power density of the battery. To enhance the electrochemical activity, various treatments, such as electrochemical oxidation [1], acid treatment [2] and thermal treatment [3], are carried out, whereas the obtained improvement is limited and the electrode suffers from degradation [4].

In this work, a powerful electrocatalyst (Nd_2O_3) was chemically embedded on a carbon felt (CF) by a surface precipitation method. Nd_2O_3 particles were decorated on the felts with different concentrations and tested for the application as electrode in vanadium redox flow batteries. Cyclic voltammetry studies confirmed that Nd_2O_3 has a catalytic effect toward both redox couples $\text{V}^{4+}/\text{V}^{5+}$ at the positive side and $\text{V}^{2+}/\text{V}^{3+}$ at the negative side. Scanning electron microscopy, energy dispersive X-ray spectroscopy and X-ray diffraction demonstrated minimum agglomeration and high dispersion of the particles on the fibres. Charge/discharge profiles in battery tester revealed an enhanced performance with higher discharge capacity and energy efficiency for the modified felts when compared to a thermally activated CF. Cycling performance also demonstrated an excellent stability of the modified felt after 50 charge/discharge cycles and after exchanging the electrolyte (after 50 cycles), the felts retained their original performance indicating that less degradation occurred in the modified felts than in the industrial standard and that they maintained their oxygen-donating functionalities on the surface as compared to thermally activated CF.



[1] W. Zhang, J. Xi, Z. Li, H. Zhou, L. Liu, Z. Wu, X. Qiu, *Electrochim. Acta*, 2013, *89*, 429–435.

[2] A. Di Blasi, O. Di Blasi, N. Briguglio, A. S. Arico, D. Sebastian, M. J. Lazaro, G. Monforte, V. Antonucci, *J. Power Sources*, 2013, *227*, 15–23.

[3] C. Flox, M. Skoumal, J. Rubio-Garcia, T. Andreu, J. R. Morante, *Appl. Energy*, 2013, *109*, 344–351.

[4] I. Derr, M. Bruns, J. Langner, A. Fetyan, J. Melke, C. Roth, *J. Power Sources*, 2016, *325*, 351–359.

LiNi_{1/3}Mn_{1/3}Co_{1/3}O₂ submicronic particles to improve the power performances of Li-ion batteries

D. PERALTA, J. SALOMON, A. BOULINEAU, J-F. COLIN, F. FABRE, C. BOURBON, D. BLOCH, S. PATOUX

*Univ. Grenoble Alpes, F-38402 Saint Martin d'Hères, France.
CEA, LITEN, F-38054 Grenoble, France.
david.peralta@cea.fr*

The literature reports the influence of various morphologies of layered oxide materials on their Li-ion batteries performances. In a recent study based on LiNi_{1/3}Mn_{1/3}Co_{1/3}O₂, our group showed that the influence of the agglomerates porosity on the electrochemical performances clearly depends on the densification degree of the secondary particles. In the case of very dense secondary particles, the meaningful scale to discuss the electrochemical process is the agglomerate one.^[1] In this case, opening the porosity of the agglomerate results in reducing the solid state diffusion length and improve the lithium accessibility by reducing the grain boundaries. However, for very porous materials, for example agglomerates of flake-shaped crystallites, increasing the porosity does not necessary lead to an increase of the power performances because the lithium diffusion length is already short and the accessibility of the lithium insertion planes is unchanged. In another publication, we highlight that in porous materials, the electrochemical process is not limited by the lithium solid state diffusion but by ionic charge transfer process.^[2] Consequently, one of the most important levers to improve the power performances consists in tuning the interface between the material and the electrolyte in order to maximize the electroactive surface area.

Production of submicronic and discrete particles could be a solution to limit the loss of electroactive surface due to grain boundaries. Such morphology could open new and important perspectives for cathode materials such as the use of these material for power applications or for applications for which an optimized interface with the electrolyte is required (e.g all solid state battery or polymer battery). However, it is clearly difficult to synthesis this kind of morphology with an inexpensive and scalable process. Submicronic particles with homogenous particles sizes are generally obtained by original and complex synthesis process. Our study aims at increasing the electroactive surface area of LiNi_{1/3}Mn_{1/3}Co_{1/3}O₂ by using a very simple and scalable coprecipitation synthesis. On another hand, we also worked on the cathode formulation process in order to obtain dense cathode electrodes even if submicronic particles are used. At the end we show that the electrochemical behavior of this material is clearly enhanced by using this material (figure1).

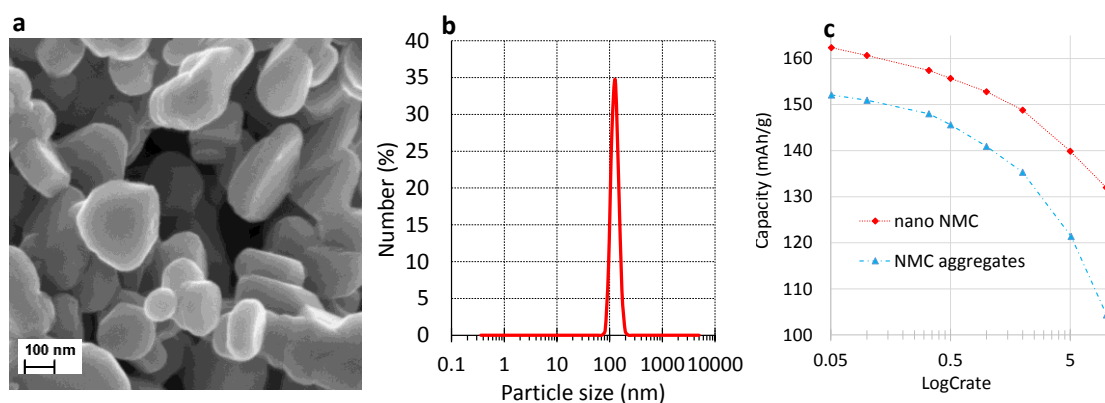


Figure 1: a/ SEM picture of submicronic NMC b/ PSD analysis of the powder c/ Crate behavior of the material

[1] P.-E. Cabelguen, D. Peralta, M. Cugnet, P. Maillet, J. Power Sources 2017, DOI: 10.1016/j.jpowsour.2017.02.025.

[2] P.-E. Cabelguen, D. Peralta, M. Cugnet, J.-C. Badot, O. Dubrunfaut, P. Mailley, Adv. Sustain. Syst. 2017, DOI: 10.1002/adsu.201700078

The synthesis of TiO₂ self-ordering nanocolumns on Al/Ti layers by two-step anodizing process using etidronic acid and their electrochemical study by cyclic voltammetry.

M. Sepúlveda¹, J.G. Castaño^a, F. Echeverría^a,

^a Centro de Investigación, Innovación y Desarrollo de Materiales- CIDEMAT, Universidad de Antioquia UdeA; Calle 70 N° 52- 21, Medellín, Colombia.

lina.sepulveda@udea.edu.co

Abstract

In recent years, the arrangement of the highly-ordered TiO₂ arrays has drawn much attention due to permit directed charge transfer along the length of the TiO₂ arrays to the conductive substrate, thereby reducing the losses incurred by charge-hopping across nanoparticle grain boundaries.[1] The anodization process is adopted to form 0D and 1D nanostructures [2]. Because anodization is a cost-effective process, it has the potential to grow large-scale arrays nanostructures for device applications. TiO₂ nanostructures can be grown inside AAO pores by anodization [3]. The synthesis of dot, rod or wire-like nanostructures from bilayers has been reported for a number of valve metal including Ta [4] and W [5]. In this work, the TiO₂ nanocolumns were fabricated by a two-step anodizing process of an Al/Ti bilayer system and using an electrolyte 0.3 M etidronic acid at 40 °C. TiO₂ nanocolumns of various heights were fabricated by means of a two-step anodizing process at potentiodynamic mode. The surface properties were determined by XRD, Raman, SEM. The experimental results obtained from the voltammetry study at various scan rates suggest that the kinetics of the ion intercalation and oxide reduction process increases, for the different TiO₂ nanocolumns heights. The metal oxides can be developed as biomaterials [6], solar cells [7], fuel cell materials and lithium ion batteries [8].

Keywords: *two-step anodizing process, etidronic acid, titania nanocolumns, nanostructures, anodic alumina membranes*

References

- [1] G.R. Torres, T. Lindgren, J. Lu, C.G. Granqvist, S.E. Lindquist, Photoelectrochemical study of nitrogen-doped titanium dioxide for water oxidation, *J. Phys. Chem. B.* 108 (2004) 5995–6003. doi:10.1021/Jp037477s.
- [2] W. Lee, S.-J.S.S. Park, Porous anodic aluminum oxide: anodization and templated synthesis of functional nanostructures, *Chem. Rev.* 114 (2014) 7487–7556. doi:10.1021/cr500002z.
- [3] L.K. Tsui, N.T. Nguyen, L. Wang, R. Kirchgeorg, G. Zangari, P. Schmuki, Hierarchical decoration of anodic TiO₂ nanorods for enhanced photocatalytic degradation properties, *Electrochim. Acta.* 155 (2015) 244–250. doi:10.1016/j.electacta.2014.12.111.
- [4] A. Mozalev, A. J. Smith, S. Borodin, A. Plihaika, A. W. Hassel, M. Sakairi, H. Takahashi, Growth of multioxide planar film with the nanoscale inner structure via anodizing Al/Ta layers on Si, *Electrochim. Acta.* 54 (2009) 935–945. doi:10.1016/j.electacta.2008.08.030.
- [5] R. Calavia, a. Mozalev, R. Vazquez, I. Gracia, C. Cané, R. Ionescu, E. Llobet, Fabrication of WO₃ nanodot-based microsensors highly sensitive to hydrogen, *Sensors Actuators, B Chem.* 149 (2010) 352–361. doi:10.1016/j.snb.2010.06.055.
- [6] T. Sjöström, G. Lalev, J.P. Mansell, B. Su, Initial attachment and spreading of MG63 cells on nanopatterned titanium surfaces via through-mask anodization, *Appl. Surf. Sci.* 257 (2011) 4552–4558. doi:10.1016/j.apsusc.2010.11.064.
- [7] B. Liu, E.S. Aydil, Growth of oriented single-crystalline rutile TiO₂ nanorods on transparent conducting substrates for dye-sensitized solar cells, *J. Am. Chem. Soc.* 131 (2009) 3985–3990. doi:10.1021/ja8078972.
- [8] T. Fukutsuka, K. Koyamada, S. Maruyama, K. Miyazaki, T. Abe, Ion Transport in Organic Electrolyte Solution through the Pore Channels of Anodic Nanoporous Alumina Membranes, *Electrochim.*

Acta. 199 (2015) 380–387. doi:10.1016/j.electacta.2016.03.049.

Room-temperature Sodium-ion Batteries: Improving the Rate Capability using Porous Carbon Networks

Yan Yu*

*Department of Materials Science and Engineering, University of Science and Technology of China,
230026, Hefei, Anhui, P. R. China.
Email:yanyumse@ustc.edu.cn*

Na-ion batteries (NIBs) have attracted rapidly increasing attention because sodium is abundant resources, low cost and their better safety. However, the development of NIBs is greatly hampered due to the lack of appropriate active materials for both cathodes and anodes, because of the large radius of Na⁺. NASICON-type Na₃V₂(PO₄)₃ (denoted as NVP) has recently been investigated as a promising cathode material for NIBs. While it is difficult to reach high rate performance of Na₃V₂(PO₄)₃ cathode due to the poor electronic conductivity of phosphates. For anode materials, NaTi₂(PO₄)₃ has shown promising electrochemical performance.

Here, we reported electrode materials for NIBs based on porous carbon with excellent rate performance: Carbon-coated nanosized Na₃V₂(PO₄)₃ embedded in the porous carbon matrix.[1] [2-5] The double carbon coating NVP could deliver high rate performance (44 mAhg⁻¹ at 200C). This ultrahigh rate performance is comparable to that of supercapacitor, but with much higher energy density. We also designed NaTi₂(PO₄)₃ particles embedded in micro-sized 3D graphene network to improve its electrochemical performance.

The outstanding electrochemical performance of electrode materials with porous carbon network for NIBs is attributed to the special structure design, which confined a variety of advantages: hierarchical porous channels facilitating fast ions and electrons transport, carbon coated structure resulting in low resistances, good mechanical properties leading to the excellent morphology stability.

References:

- [1] C. Zhu, P. Kopold, P.A. van Aken, J. Maier, Y. Yu*, *Adv. Mater.*, (2016).
- [2] X. Rui, W. Sun, C. Wu, Y. Yu*, Q. Yan*, *Adv. Mater.*, 27 (2015) 6670-6676.
- [3] C. Wu, P. Kopold, Y.-L. Ding, P.A. van Aken, J. Maier, Y. Yu*, *ACS Nano*, 9 (2015) 6610-6618.
- [4] Y. Jiang, Z. Yang, W. Li, L. Zeng, F. Pan, M. Wang, X. Wei, G. Hu, L. Gu, Y. Yu*, *Advanced Energy Materials*, 5 (2015) 1402104.
- [5] C. Zhu, K. Song, P.A. van Aken, J. Maier, Y. Yu*, *Nano Letters*, 14 (2014) 2175-2180.

Nanostructuring Earth Abundant Electrocatalysts for Water Splitting

Chuan Zhao

School of Chemistry, University of New South Wales, Sydney, Australia

E-mail: chuan.zhao@unsw.edu.au

Abstract The increasing demands for clean energy have triggered tremendous research interests on electrochemical energy conversion and storage systems with minimum environmental impact. Electrolytic water splitting holds the promise for global scale storage of renewable energy, e.g., solar and wind in the form of hydrogen fuel, enabling the continuous usage of these diffusive and intermittent energy sources when used together with fuel cells.^{1,2} Nevertheless, the widespread application of water splitting technology has been severely constrained by the use of precious metal catalysts, such as oxides of ruthenium and iridium for the anodic oxygen evolution reaction (OER), and platinum for the cathodic hydrogen evolution reaction (HER). This presentation concerns our recent progress in developing non-precious metal-based, carbon-based and metal-organic framework (MOF)-based water splitting catalysts, as well as our strategies for enhancing the efficiency of these catalysts by nanostructuring to a level comparable to that of precious metal catalysts.³⁻¹⁰

References

1. Smith, R. D. L.; Prevot, M. S.; Fagan, R. D.; Zhang, Z. P.; Sedach, P. A.; Siu, M. K. J.; Trudel, S.; Berlinguette, C. P. *Science* **2013**, 340, 60.
2. Gong, M.; Li, Y. G.; Wang, H. L.; Liang, Y. Y.; Wu, J. Z.; Zhou, J. G.; Wang, J.; Regier, T.; Wei, F.; Dai, H. J. *J. Am. Chem. Soc.* **2013**, 135, 8452.
3. Lu, X.; Zhao, C. *J. Mater. Chem. A*, **2013**, 1, 12053
4. Xiao, C. Lu, X.; Zhao, C. *Chem. Comm.*, **2014**, 50, 10122
5. Lu, X.; Yim, W.; Bryan, B.H.R.; Zhao, C. *J. Am. Chem. Soc.*, **2015**, 137, 2901
6. Lu, X.; Zhao, C. *Nat. Commun.*, **2015**, 6, 6616
7. Xiao, C., Li, Yi. Lu, X. Zhao, C. *Adv. Func. Mater.* **2016**, 26, 3515
8. Li, Y.; Zhao, C. *Chem. Mater.* **2016**, 28, 5659
9. Li, Y.; Zhao, C. *ACS Catal.*, **2017**, 7, 2535
10. Duan, J.; Chen, S.; Zhao, C. *Nat Commun.*, **2017**, 8, 15341.

Unravelling the Role of Oxygen-containing Functional Groups for Vanadium Electrochemistry

Lin Zeng^{ab}, T.S. Zhao^a, Le Shi^a, Jianbo Xu^a, Lei Wei^a

^aDepartment of Mechanical and Aerospace Engineering, ^bHKUST Jockey Club Institute for Advanced Study, The Hong Kong University of Science and Technology, Clear Water Bay, Kowloon, Hong Kong SAR, China. E-mail: zenglinhit@gmail.com

Due to their high electron conductivity and excellent chemical stability, carbon electrodes have been extensively studied as the electrodes for vanadium redox flow batteries that are considered to be competent for the requirements of renewable energy storages [1, 2]. Commonly, the pristine carbon materials are subjected to different surface treatments to enhance the electroactivity. These treatments will modify the physicochemical properties of carbon materials, including the grafted oxygen-containing functional groups and the specific surface area [3, 4]. To explore the mechanism of electroactivity enhancement, the linear sweep voltammetry (LSV) with rotating disc electrode technique was performed to analyze the electroactivity of the model carbon electrodes treated at different conditions. The LSV curves in the corresponding vanadium solution were measured and the kinetic parameters, including exchange current density (i_0) and kinetic rate constants (k_0), were determined. It is quantitatively demonstrated that the grafted functional groups promote the V(II) oxidation and V(III) reduction significantly when the content of OCFGs is higher than 5 wt%, while exhibiting a minute catalytic effect on the V(IV) oxidation and V(V) reduction. Specifically, the V(II) and V(III) prefer to adsorb and react on the grafted functional groups and edge sites of carbon materials. If the functional groups (particularly COOH) are located on the edge sites, the reaction can be further promoted. However, the reactions of V(IV) oxidation and V(V) reduction are not significantly affected by the functional groups. Worse, the electroactivities will be reduced to some extent if the carbon surface is grafted with numerous of functional groups (higher than 8 wt%). The work described in this abstract was fully supported by a grant from the Research Grants Council of the Hong Kong Special Administrative Region, China (Project No. T23-601/17-R).

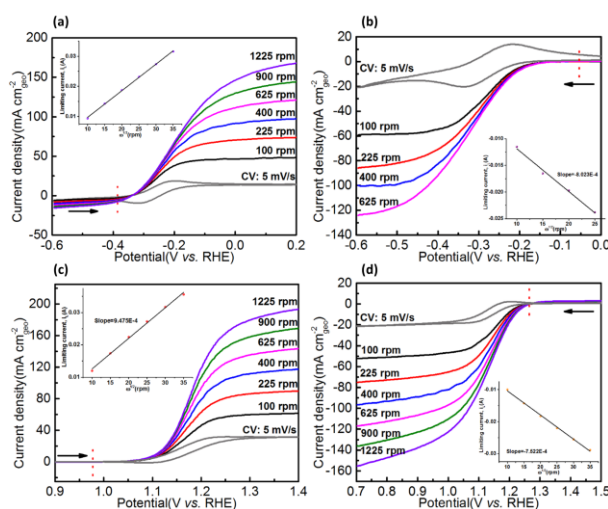


Figure 1 The LSV curves of the model electrodes at various rotation speeds for V(II) oxidation (a), V(III) reduction (b), V(IV) oxidation (c) and V(V) reduction (d). The inset showed the limiting current versus rotating speed. The CV curves without rotating were also respectively measured for the purpose of comparison. The scan rate is 5 mV s⁻¹.

References

- [1] Z. Yang, J. Zhang, M.C.W. Kintner-Meyer, et al., *Chemical Reviews*, 111 (2011) 3577-3613.
- [2] C. Ding, H. Zhang, X. Li, et al., *Journal of Physical Chemistry Letters*, 2013, 4, 1281-1294.
- [3] M. Park, Y.-j. Jung, J. Kim, et al., *Nano Letters*, 13 (2013) 4833-4839.
- [4] C. Flox, J. Rubio-Garcia, M. Skoumal, et al., *Carbon*, 60 (2013) 280-288

Interface Analysis of Si-based Anode in Li-ion Batteries through Electrochemical Impedance Spectroscopy and equivalent electrical circuit analysis

P. Bernard^a, A. Desrues^b, J. P. Alper^{a,b}, N. Dufour^a, C. Haon^a, M. Chandesris^a, N. Herlin-Boime^b

^aUniv. Grenoble Alpes, CEA LITEN, F-38054 Grenoble, France

^bCNRS UMR 3685, NIMBE, IRAMIS, CEA, University Paris Saclay, F-91191 Gif sur Yvette, France

Due to its high capacity compared to graphite, silicon has attracted attention for li-ion battery technology as a promising material for negative electrodes. It is abundant and non-toxic. However, this material is well known to undergo large volume changes upon lithiation and delithiation (up to 320 %). This phenomenon causes particle cracking, instability of the solid electrolyte interphase (SEI) at the interface between solid Si and liquid electrolyte, and finally leads to electrode delamination and battery performance loss. To overcome these problems, several strategies have been proposed such as using submicronic particles (< 150 nm) to mitigate the volume changes and protection of the silicon material with a carbon layer to stabilize the active surface in contact with electrolyte. Combining both strategies, Si@C core-shell nanoparticles synthesized in one step process have recently been proposed as a promising anode material [1]. Specifically, the Si-based nanoparticles are synthesized in a two stage laser pyrolysis reactor, which yields carbon coated silicon nanoparticles in a single step. This approach mitigates material oxidation because there is no air exposure between the synthesis of the core and shell. Additionally, the nanometric size of the particles prevents material pulverization upon cycling. The synthesis technique also allows control of the core crystallinity, and both highly crystalline and amorphous silicon cores have been synthesized. Moreover, the shell thickness can be tuned by changing the flow of carbon precursor.

To optimize the design of composite electrodes based on such active materials, an in-depth understanding of their performance and chemical/mechanical degradation processes remains critical. In this work, the analysis of the electrochemical performances of such Si-based electrodes was performed using several electrochemical techniques to compare crystalline or amorphous Si nanoparticles without shell as well as crystalline Si nanoparticles coated by a thin or a thick layer of carbon (Si@C). The EIS study, carried out at various states of lithiation of Si material, allows tracking the evolution of several critical parameters (for example SEI resistance and charge transfer resistance) of the equivalent electrical circuit describing the electrode electrical behavior. Figure 1a shows typical impedance spectra while Figure 1b shows the evolution of the of charge transfer resistance for the different coated and non-coated materials. A very different behavior is observed as a function of the interface material and carbon thickness. The modification of the interface between electrolyte and Si or Si@C materials is also visible on measured equilibrium potentials and power capabilities. This presentation will be devoted to the analysis of the impact of interfaces between electrolyte and Si or Si@C materials on electrochemical performances.

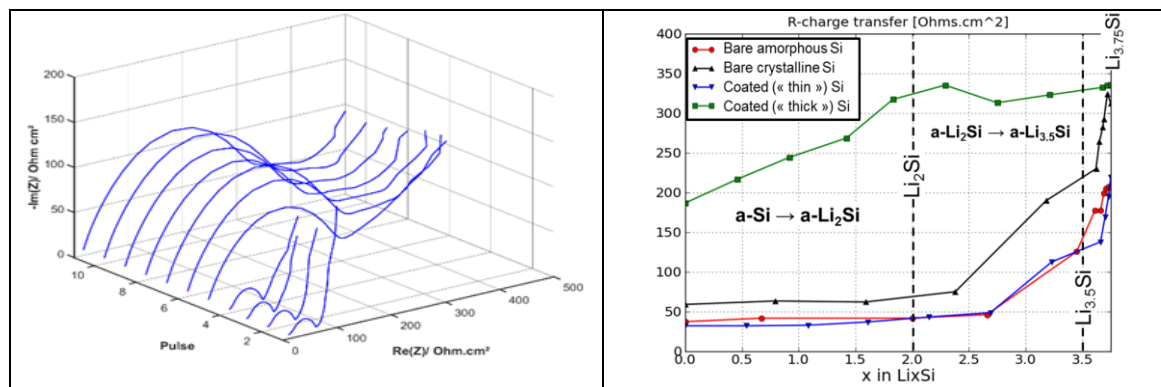


Figure 1: a) example of Impedance spectra during the lithiation in a non-coated crystalline silicon electrode and b) charge transfer resistance calculated from spectra fitting for different materials (i.e bare crystalline or amorphous material and Si coated Si with a C shell and two different C content

Investigation of AuCeO₂/C as electrocatalyst for alkaline fuel cells

Raminta Stagniunaite, Virginija Kepeniene, Daina Upskuvienė, Loretta Tamasauskaite Tamasiunaite, Eugenijus Norkus

*Center for Physical Sciences and Technology
Sauletekio ave. 3, LT-10257 Vilnius, Lithuania
raminta4ka@gmail.com*

A fuel cell is electrochemical cell that converts chemical energy into electrical energy without intermediate of mechanical links. Fuel cells are different from batteries in requiring a continuous source of fuel and oxygen (usually from air) to sustain the chemical reaction, so it is very important to select suitable catalysts for both oxidation of the fuel and reduction of oxygen. Recent research is based on electroactive materials which can change or supplement precious metals. Although Pt is known as the one of the best and commonly used catalysts for fuel cells, but now the purpose is to replace Pt in the catalysts by adding other different materials, such as transitional metals or metal oxides, because of its high cost and the possible poisoning of electrode surface. Rare earth metal oxide, such as CeO₂, is widely used as an additive in preparation of fuel cell catalysts due to its synergetic electronic effect, tolerance to CO poisoning, low price and many other characteristics. Nanoparticles of gold are attractive for their interaction with other compounds and property to attract catalytic active groups. When Au and CeO₂ are combined together, the new catalyst shows greater electrocatalytic properties for the oxygen reduction and ethylene glycol oxidation reaction.

In this paper, we investigated the influence of synthesis method to the electrocatalytic activity of catalyst. Therefore Au nanoparticles were deposited on the CeO₂/carbon substrate using microwave irradiation (AuCeO₂/C-1) and adsorption (AuCeO₂/C-2) methods. The composition, morphology and structure of the prepared catalysts were characterized using Inductively Coupled Plasma Optical Emission Spectroscopy (ICP-OES), Field Emission Scanning Electron Microscopy (FESEM), Transmission Electron Microscopy (TEM) and X-ray diffraction (XRD). The electrocatalytic properties of AuCeO₂/C were investigated towards oxygen reduction and ethylene glycol oxidation in alkaline medium. Oxygen reduction was investigated by using rotating disk electrode (RDE) linear sweep voltammetry (LSV) and ethylene glycol oxidation using cyclic voltammetry (CV).

It has been found that the way of synthesis has influence for electrocatalytic properties. The AuCeO₂/C-1 catalyst, where Au nanoparticles was deposited using microwave irradiation method, showed higher electrocatalytic activity, compare to AuCeO₂/C-2 prepared using adsorption method. In addition to this, ethylene glycol oxidation on AuCeO₂/C-1 started at about 0 V vs. SHE potential values, while ethylene glycol oxidation on the AuCeO₂/C-2 catalyst started on more positive potential values i.e. at about 0.15 V vs. SHE. It has been found that AuCeO₂/C-1 current densities were 1.5 times higher if compare those with AuCeO₂/C-2. Moreover AuCeO₂/C catalysts showed very similar or even higher electrocatalytic activity, more positive onset potentials, as well as higher current in the mixed-kinetic-diffusion region towards oxygen reduction reaction in alkaline medium as compared with that at the bare rotating disk gold electrode or as-prepared carbon based gold catalysts.

Reconstruction of Nanoparticle or Electroactive Nano-Component Distributions in Electrochemical Arrays based on Chronoamperometric Data

Alexander Oleinick, Oleksii Sliusarenko, Irina Svir, Christian Amatore
*Ecole Normale Supérieure-PSL Research University, Département de Chimie;
Sorbonne Universités-UPMC Paris 6; CNRS UMR 8640 PASTEUR
24 rue Lhomond, 75005 Paris, France
oleksandr.oliynyk@ens.fr*

The main scope of this work [1] was to establish and then to test a simple mathematical and numerical procedure for the reconstruction of probability density functions, $f(\rho)$, characterizing the distribution of electroactive or electrocatalytic of near-spherical nano-components present or deposited on a planar electrochemically-inert surface. The reconstruction procedure requires as an entry a time-dependent chronoamperometric current responses of the corresponding electrochemical array. The mathematical and numerical validity of the procedure was established for three types of arrays: one is a regularly periodical, two others are involving random dispersions. Indeed, altogether, these three types represent most frequent surface distributions of electroactive components in electrochemical micro-/nanoarrays used for (bio)analytical or electrocatalytic (viz., using perfectly tailored nanocatalyst crystals) purposes. This work takes advantage of our recent research on regular and randomly distributed micro- and nanodisk electrodes [2, 3].

Proposed reconstruction procedure is easily implementable in the most popular commercial mathematical programs (e.g., Mathematica). Albeit the simplicity of its implementation, it allowed recovering probability density functions with an excellent precision, even when the available time-range experimentally accessible results too short for its rigorous application, being thus perfectly adequate to most experimental purposes.

Acknowledgements:

This work was supported in parts by PSL, Ecole Normale Supérieure, CNRS, and the University Pierre and Marie Curie (UMR 8640). Support by the ANR-NSF bilateral (USA-France) program (ANR grant #ANR-AAP-CE06 “ChemCatNanoTech”) is also greatly acknowledged.

References:

- [1] A. Oleinick, O. Sliusarenko, I. Svir, C. Amatore. *J. Electrochemistry* 23 (2017) 141-158.
- [2] O. Sliusarenko, A. Oleinick, I. Svir, C. Amatore. *Electroanalysis* 27 (2015) 980-991.
- [3] O. Sliusarenko, A. Oleinick, I. Svir, C. Amatore. *ChemElectroChem* 2(2015) 1279-1291.

Carbon Based Cobalt Catalysts for Oxygen Reduction Reaction

Virginija Kepenienė, Raminta Stagniūnaite, Loreta Tamasauskaitė Tamasiūnaite, Eugenijus Norkus

Center for Physical Sciences and Technology

Saulėtekio ave. 3, LT-10257 Vilnius, Lithuania

virginalisk@gmail.com

Lately, the application of electroactive non-noble metal catalysts in fuel cells is in progress. Although platinum is known as one of the most effective catalyst for fuel cells, however because of high price of platinum researchers are working on the creation of modified catalysts by adding the transition metals or metals oxides in the composition of catalysts. It is known that further enhancement in the performance of Pt alloys with limited amounts of another transition metal such as Ni, Co, Fe etc., may be explained by both tuning the interatomic distance as well as providing an increase in the electron density at the catalytic sites. Cobalt is one of the most popular metals used as an additive in the platinum catalysts or even replacing platinum in them.

In this work cobalt(II,III) oxide were deposited on the surface of carbon ($\text{Co}_3\text{O}_4/\text{C}$). Synthesis was performed by combining the two methods. At first, the reaction mixture containing cobalt(II) nitrate as cobalt precursor and β -cyclodextrine as a reducing agent was stirred for the Co_3O_4 adsorption on the surface of carbon powder. Then, the reaction mixture was heated using microwave irradiation. The composition, morphology and structure of $\text{Co}_3\text{O}_4/\text{C}$ was characterized by Inductively Coupled Plasma Optical Emission Spectroscopy (ICP-OES), Field Emission Scanning Electron Microscopy (FESEM), Transmission Electron Microscopy (TEM) and X-ray diffraction (XRD). The electrocatalytic properties of $\text{Co}_3\text{O}_4/\text{C}$ towards the reduction of oxygen were carried out in alkaline medium by using rotating disk electrode (RDE) linear sweep voltammetry (LSV).

It has been determined that using β -cyclodextrin as a reducing agent the Co_3O_4 was successfully deposited on the surface of carbon powder. The $\text{Co}_3\text{O}_4/\text{C}$ catalyst shows very similar or even higher electrocatalytic activity, more positive onset potentials, as well as higher current in the mixed-kinetic-diffusion region towards oxygen reduction reaction in alkaline medium as compared with that at the bare rotating disk platinum electrode or as-prepared carbon or graphene based platinum catalysts.

Electrochemistry in superconcentrated aqueous electrolytes

Laura Coustan and Daniel Bélanger

*Département de Chimie, Université du Québec à Montréal, Case Postale 8888 succursale Centre-Ville,
Montréal (Québec) Canada H3C 3P8*

E-mail: belanger.daniel@uqam.ca

Highly concentrated aqueous electrolytes have recently attracted a lot of interest in the field of electrochemistry, more specifically in energy storage systems such as rechargeable batteries (1) and electrochemical capacitors (2). Highly concentrated (also called superconcentrated) aqueous solutions include salt such as lithium bis(trifluoromethylsulphonyl)imide (LiTFSI). The initial report about such solutions consists of a 5 M LiTFSI solution, which contains 21 moles of LiTFSI in 1 kg of water (21 m) (1). In the latter solution characterized by a H₂O/ Li⁺ molar ratio of 2.6, the number of water molecules is insufficient for full solvation of all Li⁺ cations. Nonetheless, a significant fraction (about 15%) of free water molecules is still present in the electrolyte (1). On the other hand, hydrate melt electrolytes have been shown to have negligible amount of free water (3)

It can be anticipated that superconcentrated aqueous solutions cannot only be used in energy storage systems. Therefore, in order to determine their potential usefulness in other electrochemical technologies, recent investigations focused on the study of the electrochemical behavior of various electrode materials in highly concentrated electrolytes (4). In the latter report, a significant increase of the electrochemical stability window has been observed and attributed to a shift to more negative and positive potential of the onset of hydrogen and oxygen evolution.

In this talk, the electrochemical behavior of superconcentrated aqueous solutions will be presented. In addition, their behavior in various electrochemical systems will be also presented and discussed.

References

- 1) L. Suo, O. Borodin, T. Gao, M. Olguin, J. Ho, X. Fan, C. Luo, C. Wang, K. Xu, "Water-in-salt" electrolyte enables high-voltage aqueous lithium-ion chemistries, *Science* 350 (2015) 938.
- 2) A. Gambou-Bosca, D. Bélanger, Electrochemical characterization of MnO₂-based composite in the presence of salt-in-water and water-in-salt electrolytes as electrode for electrochemical capacitors, *J. Power Sources* 326 (2016) 595.
- 3) Y. Yamada, K. Usui, K. Sodeyama, S. Ko, Y. Tateyama, A. Yamada, *Nature Energy*, 1 (2016) 16129.
- 4) L. Coustan, G. Shul, D. Bélanger. Electrochemical behavior of platinum, gold and glassy carbon electrodes in water-in-salt electrolyte, *Electrochem. Commun.*, 77 (2017) 89.

Enhanced Performance of Li-Ion Battery Cathodes by Polymeric Artificial Solid-Electrolyte-Interphase Coatings

Nae-Lih Wu

Department of Chemical Engineering, National Taiwan University

Taipei, Taiwan

nlw001@ntu.edu.tw

The development of advanced Li-ion battery (LIB) cathodes has been directed toward high capacity, high voltage and good cycle life. The ability for high-temperature operation is also desired for certain applications, such as electric vehicles. The cycle stability of typical LIB cathodes deteriorates rapidly either under high voltage or high temperature because of strong chemical interactions at the interface of the solid active material and electrolyte causing rapid formation of passivation films and dissolution of the transitional metal ions of the cathode oxides. Particularly at elevated temperatures, the LiPF_6 based electrolyte can readily decompose and reacts with residual water in the electrolyte to generate HF, which readily attacks the cathode surface causing side reactions and cathode dissolution. To solve these problems, researchers in the past have proposed to apply oxide coatings, such as MgO , TiO_2 , ZrO_2 , ZnO , Al_2O_3 , etc., to reduce direct contact of the cathode with the electrolyte solution. Unfortunately, these approaches also lead to additional drawbacks, such as the crack of oxide layers, decrease of ion-conductivity, or involve more complex high temperature calcination steps, which may increase the processing costs. In this presentation a novel approach using polymeric artificial solid-electrolyte interphases (SEIs) to modify the surface of cathode materials for enhancing the cyclic and rate performance and safety properties of the Li-ion batteries is described. The results show that polymeric SEIs can substantially suppress the parasitic reactions between the electrolyte and electrode at high temperature and high operating potentials, improve the structural stability and decrease the polarization of the material during the electrochemical operations. Comparing to the pristine cell, the modified cells show better performance both in cycle life and rate capability, maintaining lower cell impedance due to the reduced electrolyte decomposition and enhanced structure stability. In addition, the polymeric artificial SEI also improved the safety of the cathode material by delaying the decomposition of the cathodes at high temperatures. The underlying mechanisms leading to the improvement are discussed.

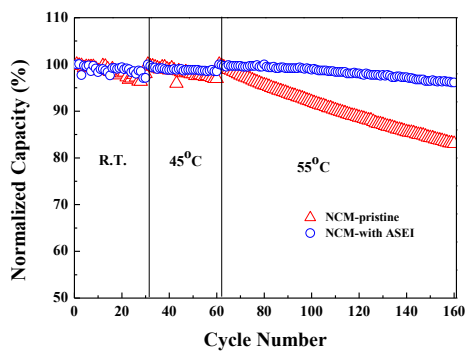


Figure 1. Improved cycle stability of NCM cathode by polymeric artificial SEI (ASEI) coating

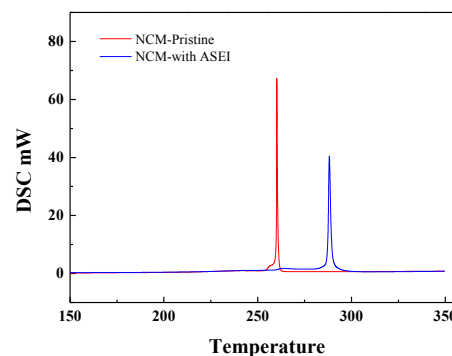


Figure 2. Delayed decomposition of NCM cathode by polymeric artificial SEI (ASEI) coating

Synthesis and Electrochemical Characterization of Transition Metal Doped $\text{Li}_2\text{Fe}_{0.975}\text{M}_{0.025}\text{P}_2\text{O}_7/\text{C}$ (M=Co, Ni, or Cu)

Heechan Jang^a, Izumi Taniguchi^b

^a Department of Chemical Engineering, Tokyo Institute of Technology, Tokyo 152-8552, Japan

^b Department of Chemical Science and Engineering, Tokyo Institute of Technology, Tokyo 152-8552, Japan

itaniguc@chemeng.titech.ac.jp

1. Introduction

In 2010, $\text{Li}_2\text{FeP}_2\text{O}_7$ was introduced as 3.5 V class cathode material for lithium-ion battery with structural study and experimental result [1]. However, like the LiFePO_4 system, it also has struggled with lower electrical conductivity and Li diffusivity even though better safety and stability with excellent cycle retention performance than another system of cathode materials [2]. In this study, transition metal doped $\text{Li}_2\text{Fe}_{0.975}\text{M}_{0.025}\text{P}_2\text{O}_7/\text{C}$ (M=Co, Ni, or Cu) were prepared by spray pyrolysis (SP) followed by ball milling process. Periodically adjacent transition metal of Co, Ni, and Cu with a fixed amount in composition was well deposited into pure- $\text{Li}_2\text{FeP}_2\text{O}_7$. Rietveld method was performed on pure $\text{Li}_2\text{FeP}_2\text{O}_7$ composition, and the strain of lattice constant was observed and compared with each doped substance. Electrochemical performances for each sample were investigated at various current rate conditions.

2. Experimental

LiH_2PO_4 (99%, Aldrich) and $\text{Fe}(\text{NO}_3)_3 \cdot 9\text{H}_2\text{O}$ (99%, Wako) were introduced to distilled water in a stoichiometric ratio. Ascorbic acid (99.6%, Wako) and citric acid (98%, Wako) were dissolved in solution as a reduction agent for Fe^{3+} and incorporated carbon source, respectively. 2.5 mol % of transition metal substituted to Fe-site by dissolving with $\text{Co}(\text{NO}_3)_2 \cdot 6\text{H}_2\text{O}$ (98%, Wako), $\text{Ni}(\text{NO}_3)_2 \cdot 6\text{H}_2\text{O}$ (98%, Wako), and $\text{Cu}(\text{NO}_3)_2 \cdot 3\text{H}_2\text{O}$ (>99%, Wako) for preparing the precursor solution. An ultrasonic nebulizer with the frequency of 1.7 MHz atomized precursor solution, and the generated droplet passed through a tube furnace, which was fixed at 400 °C using carrier gas. The converted solid particles were captured into an electrostatic collector that operated at 150 °C of temperature as-prepared powder. The entire SP system was maintained under the inert atmosphere using 3 % of $\text{H}_2\text{-N}_2$ mixed gas with a flow rate of 2 L min^{-1} due to prevent the oxidation of iron composition.

3. Results and discussion

X-ray diffraction patterns for all of the doped $\text{Li}_2\text{FeP}_2\text{O}_7/\text{C}$ are shown in Fig. 1. All of the patterns were indexed pure crystalline $\text{Li}_2\text{FeP}_2\text{O}_7/\text{C}$ without any impurities. Based on those of patterns, the lattice parameter of each sample were refined. The capacity and coulombic efficiency for various transition metal doped $\text{Li}_2\text{Fe}_{0.975}\text{M}_{0.025}\text{P}_2\text{O}_7/\text{C}$ are shown in Fig. 2. In order to evaluate the electrochemical performance at high current density, the capacity retention was carried out at a current rate of 1 C for 50 cycles. The initial discharge capacities of samples were 76, 65, 69, and 60 mAh g^{-1} for Co, Ni, pristine, and Cu, respectively. After 15 cycles, the discharge capacities of all the sample stabilized to approximately 70, 60, 63, and 50 mAh g^{-1} as the previous orders in rate capability. While the similar electrochemical properties between Co and Ni-doped sample were shown in the rate capability, a remarkable difference of the performances revealed in capacity retention at a current rate of 1 C. For all samples, near 98 % of coulombic efficiencies were exhibited during 50 cycles.

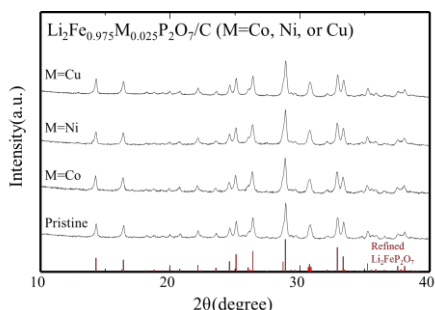


Fig. 1. X-ray diffraction patterns of $\text{Li}_2\text{Fe}_{0.975}\text{M}_{0.025}\text{P}_2\text{O}_7/\text{C}$ (M=Co, Ni, and Cu)

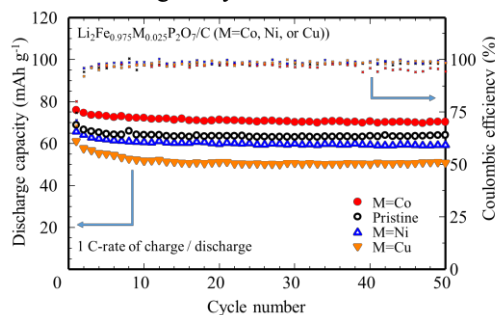


Fig. 2. Capacity retention and coulombic efficiency of $\text{Li}_2\text{Fe}_{0.975}\text{M}_{0.025}\text{P}_2\text{O}_7/\text{C}$ (M=Co, Ni, and Cu)

References

- [1] S. Nishimura *et al.* (2010) *J Am Chem Soc* 132:13596–13597
- [2] P. Barpanda *et al.* (2012) *Adv Energy Mater* 2:841–859

Fouling behavior of electrooxidation-membrane bioreactor (EO-MBR) coupled with non-woven fabric pre-filter

Chong Min Chung¹, Kangwoo Cho^{2}, Kazuo Yamamoto²*

¹Department of Urban Engineering, The University of Tokyo, 7-3-1 Hongo, Bunkyo, Tokyo 113-8656, Japan

²Environmental Science Center, The University of Tokyo, 7-3-1 Hongo, Bunkyo, Tokyo 113-0033, Japan

³Division of Environmental Science and Engineering, Pohang University of Science and Technology (POSTECH), Pohang 37673, Korea

This study experimentally demonstrates that an in-situ electrolytic chlorine generation coupled with non-woven fabric filters can effectively mitigate the fouling in membrane bioreactors (MBRs) for high-salinity wastewater treatment. The performance of electro-oxidation(EO)-MBR modified with non-woven fabric media as a means of pre-filter was investigated under variable design parameters of importance. Under intermittent current density of 5 mA/cm² (“30 s on, 2 min 30 s off” mode), the modified EO-MBR process showed retarded increases of transmembrane pressure (TMP) so that a prolonged operation cycle was expected when compared to the control EO-MBR configuration under open circuit. The alleviation of membrane fouling observed in the modified EO-MBR was largely due to the free chlorine species, electrochemically generated on the Ti/IrO₂ anode, which reduced the protein foulants and physically irremovable membrane fouling. In addition, the novel process was found to show an improved ammonium nitrogen removal efficiency via breakpoint chlorination. Despite moderate shift in the microbial community in the modified EO-MBR, the wastewater treatment efficacy in terms of total organic carbon removal remained unchanged throughout the operation period. The energy consumption of the modified EO-MBR was approximately 0.028 kWh/m³ permeate.

Fabrication and evaluation of light-addressable electrodes for the integration in lab-on-a-chip systems

R. Welden¹, M.J. Schöning^{1,2}, P. Wagner³, T. Wagner^{1,2}

¹ *FH Aachen, Campus Jülich, Institute of Nano- and Biotechnologies (INB), 52428 Jülich, Germany*

² *Research Center Jülich, Institute of Complex Systems (ICS-8, Bioelectronics), 52425 Jülich, Germany*

³ *KU Leuven, Department of Physics and Astronomy, 3001 Leuven, Belgium*
torsten.wagner@fh-aachen.de

Electrodes are often embedded in lab-on-a-chip (LOC) devices. They function for example as actuators for the stimulation of cells or to modify the pH value within a microfluidic channel. Conventional electrodes for those systems have a rigid arrangement and the shape and location is defined during the design and manufacturing process. Particularly biological components in a LOC system might require to adapt the electrode area and location in situ, as the binding position and activity of those components is not always predictable. To increase the adaptability of electrodes within LOC devices, light-addressable electrodes can be used. A semiconducting layer on a transparent conductive substrate forms the top layer of the electrode and stays in direct contact with the analyte solution. For these electrodes, the active area can be defined by illumination with a precise light beam. Due to the photoelectric effect the conductivity will increase spatially resolved by several orders of magnitude. The non-illuminated area remains non-conductive and therefore can be considered inactive. Hence, it is possible to change in situ the geometry and the location of the active area of the electrode.

In this work, titanium dioxide TiO₂ was deposited on a transparent conductive oxide (ZnO) layer by means of different sol-gel processes or by pulsed laser deposition (PLD). Protocols were established to achieve a dense layer with a smooth and self-contained surface. The quality of the layer and its surface is of importance, as it stays in direct contact with the analyte solution. Impurities and cracks would lead to a faster degradation over time and contribute to electric short circuits. As a consequence, applying a dc bias voltage across the analyte solution and electrode substrate, will result in a high leakage current among the entire electrode area. However, a high ratio between the leakage current and the photocurrent is of importance, to achieve high spatial resolutions. To evaluate and to optimize the electrode performance, electrochemical measurements will be presented to determine the ratio between the leakage current and the illuminated photocurrent. Multiple step responses, to demonstrate the function as an electrode and investigations of the spatial resolution and the long-term stability will be shown.

Effect of Supporting Electrolyte on Electrochemical Production of Cu Nanoparticles

Mikiko Saito¹, Tomohiro Ishii², Hidemichi Fujiwara², and Takayuki Homma^{1,3}

¹Research Organization for Nano & Life Innovation, Waseda University, 513, Wasedaturumaki-cho, Shinjuku, Tokyo 162-0041, Japan

²Furukawa Electric Co. LTD., 500, Kiyotaki-cho, Nikko, Tochigi 321-1493, Japan

³Department of Applied Chemistry, Waseda University, 3-4-1, Okubo, Shinjuku, Tokyo 169-8555, Japan
mikiko@waseda.jp

Metal nanoparticles are widely applied featuring their unique properties, and various approaches have been attempted for their production [1-3]. We have proposed the production of the nanoparticles using electrochemical processes [4]. In this study, synthesis of metal nanoparticles under the control of solid-liquid interface with focusing supporting electrolyte such as sodium acetate, calcium acetate, and magnesium acetate was investigated.

Au or Pt seed layers were deposited on Si(111) wafers by sputtering. The thickness was 100 nm. Electrochemical synthesis of the Cu nanoparticles was carried out using an electrochemical analyzer (HZ-7000, Hokuto Denko) with a bath composition shown in Table 1. A constant potential of -3.0 V vs. Ag/AgCl was applied to the electrode. The deposition duration was ranged from 20 to 600 s. The Cu nanoparticles were prepared from copper acetate solutions by collecting particles dispersed in the solution after the electrochemical reduction. The surface morphology of the nanoparticles was observed using scanning electron microscopy with a field emission source (FE-SEM, S-4800, Hitachi). Zeta potential measurements were performed using a zeta potential and particle analyzer system (ELS-8000, Otsuka Electronics). Chemical structure of the deposits was analyzed using Raman microscopy (Nanofinder 30, Tokyo Instruments).

From the analyses of the structure and morphology of the initial electrodeposits and dispersed nanoparticles, the formation of Cu₂O or Cu(OH)₂ at the cathode was confirmed. Hydrogen evolution at the interface of the cathode might induce the alkaline environment followed by the presence of Cu₂O or Cu(OH)₂. These existence of Cu₂O or Cu(OH)₂, which are non-conductive species, suppress the current supply for further growth, enhancing the detachment of the deposited particles to be separated from the cathode surface. It was confirmed that the deposits formed with the supporting electrolyte became uniform particle size compared to that of formed without the supporting electrolyte, suggesting that the alkaline environment at the interface is stabilized by supporting electrolyte. The nanoparticles formed with sodium acetate to the bath indicated the smallest size particles among the examined samples. In the case of calcium acetate, the Raman peak of Ca(OH)₂ was obtained at the cathode electrodeposits. The current density for the formation of nanoparticles with calcium acetate was smaller than that with sodium acetate, followed by the particle size. The quantity of hydroxides at the interface of the cathode might affect the size of nanoparticles. It was considered that alkaline metal and earth-alkaline metal could induce the alkaline environment near the cathode followed by the promoting the formation of nanoparticles. It was suggested that high potential, high pH, the use of supporting electrolyte, and addition of PVP to the bath are resulted in the formation of nanoparticles with uniform particle formation.

Table 1 Bath composition.

Chemicals	Composition	pH
(CH ₃ COO) ₂ Cu	0.1 M	
(CH ₃ COO) ₂ Ca	0.005 M	5.51
(CH ₃ COO) ₂ Mg	0.005 M	5.50
CH ₃ COONa	0.01 M	5.48
CH ₃ COOH	0.01 M	5.27
PVP M. W. 3500	5 g/L	

References.

- [1] M. Tanaka and T. Watanabe, *Thin Solid Films*, **516**, 6645 (2008).
- [2] C. Hayashi, *Mater. Sci. Forum*, **246**, 153 (1997).
- [3] T. Yonezawa, *J. Surf. Finish. Soc. Jpn.*, **59**, 712 (2008).
- [4] T. Ishii, H. Fujiwara, M. Saito, T. Homma, *Journal of Japan Institute of Copper*, **55**, 101 (2016).

Electrochemical Synthesis of Mesoporous Nickel Films by Using Polymeric Micelles

Daisuke Baba,^{1,2} Yusuke Yamauchi,^{1,2,3} and Toru Asahi¹

¹School of Advanced Science and Engineering, Waseda Univ., Okubo, Shinjuku, Tokyo 169-8555, Japan

²MANA, National Institute for Material Science, Namiki, Tsukuba, Ibaraki 305-0044, Japan

³School of Chemical Engineering, Univ. of Queensland, Brisbane QLD 4072 Australia

yamauchi.yusuke@nims.go.jp; tasahi@waseda.jp

Mesoporous metal films are attractive materials due to interesting features such as large surface area derived from porous structure, and high electric conductivity and superior catalytic activity derived from metallic frameworks. They can provide abundant ideal reaction sites which are quite different from bulky metals. Generally, they can be synthesized through an electrochemical process by using soft-templates and they have been utilized in a wide range of applications, such as electrodes, batteries, and catalysts.^[1] Unfortunately, the compositions of mesoporous metals have been mostly limited in noble metals, such as Pt, Pd, Au, and Rh.^[2-4] Compared to noble metals, it is quite difficult to synthesize mesoporous non-noble metals because of their low reduction potentials, high susceptibility upon exposure to oxygen, and uncontrollable deposition behavior. To further develop the research of 'mesoporous metals', we need to focus on Earth abundant non-noble metals. Recently, we reported a synthesis of mesoporous copper (Cu) by an electrodeposition method in the solutions including stable polymer micelles.^[5]

In this study, we focus on nickel (Ni) as another non-noble metals to prepare mesoporous Ni films, by taking advantage of stable polymer micelles made of diblock copolymer polystyrene-*b*-poly-(oxyethylene). From TEM images of the solution including polymer micelles and nickel ion, it is revealed that spherical micelles with approximate 50 nm in size are formed. As shown in **Figure 1a**, the film electrodeposited under the optimal condition at -1.4 V vs. Ag/AgCl shows porous architecture with uniformly sizes pores. The pore size is approximate 50 nm which is similar size of the used polymeric micelles. Thus, the polymeric micelles can serve as the template. The film thicknesses of the mesoporous Ni films can be linearly increased with increase of the deposition times. When the deposition time is 60 min, the film thickness is approximate 500 nm from a cross-sectional scanning electron microscope image (**Figure 1b**). Using X-ray photoelectron spectroscopy, the surface of mesoporous Ni films was characterized carefully. It is found that the Ni surface are partially oxidized. Finally, we demonstrate an electrochemical supercapacitor application using the obtained mesoporous Ni films. Cyclic voltammetric and charge-discharge curves were measured in KOH solution. Compared with nonporous Ni prepared without polymeric micelles, our mesoporous Ni films show superior electrochemical features and the detailed results will be reported in this presentation.

References:

- [1] V. Malgras, H. Atae-Esfahani, H. Wang, B. Jiang, C. Li, K. C. W. Wu, J. H. Kim, Y. Yamauchi, *Adv. Mater.* 2016, **28**, 993
- [2] C. Li, O. Dag, T. D. Dao, T. Nagao, Y. Sakamoto, T. Kimura, O. Terasaki, Y. Yamauchi, *Nat. Commun.* 2015, **6**, 6608
- [3] B. Jiang, C. Li, Ö. Dag, H. Abe, T. Takei, T. Imai, M. S. A. Hossain, M. T. Islam, K. Wood, J. Henzie, Y. Yamauchi, *Nat. Commun.* 2017, **8**, 15581.
- [4] M. Iqbal, C. Li, K. Wood, B. Jiang, T. Takei, Ö. Dag, D. Baba, A. S. Nugraha, T. Asahi, A. E. Whitten, M. S. A. Hossain, V. Malgras, Y. Yamauchi, *Chem. Mater.* 2017, **29**, 6405.
- [5] D. Baba, C. Li, V. Malgras, J. Bo, H. R. Alamri, Z. A. Allothman, M. S. A. Hossain, Y. Yamauchi, T. Asahi, *Chem. Asian J.* 2017, **12**, 2467.

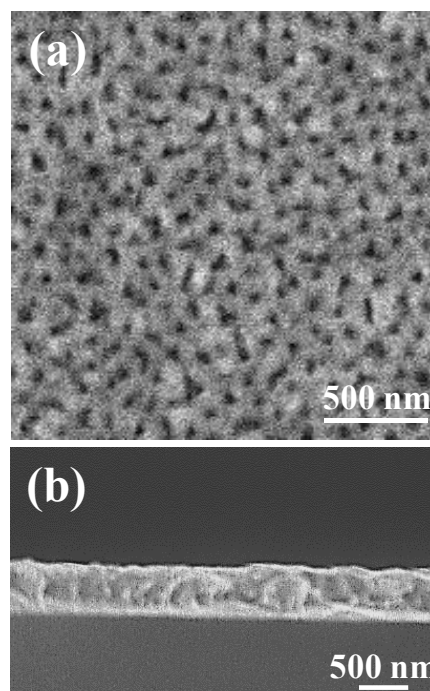


Figure 1 (a) Top-surface and (b) cross-sectional SEM images of the obtained mesoporous Ni films.

Improvement of lithium ion transportation at interface between LiFePO₄ and electrolyte by surface-nitrided treatment

Yoshiharu Uchimoto¹, Kentaro Yamamoto¹, Tomoki Uchiyama¹,
Takahiro Yoshinari¹, Eri Kato¹, Yuki Orikasa²

¹ Graduate School of Human and Environmental Studies, Kyoto University,
Yoshida-honmachi, Sakyo, Kyoto 606-8501, Japan

² Department of Applied Chemistry, Ritsumeikan University,
1-1-1 Noji-higashi, Kusatsu, Shiga 525-8577, Japan

uchimoto.yoshiharu.2n@kyoto-u.ac.jp

Lithium ion batteries (LIBs) are a kind of key device to realize sustainably energy society grid system because of the highest energy density among commercially available batteries, and further improvement of the performance is demanded. LiFePO₄, which is one of the most promising cathode materials of LIBs, shows large capacity available at high rates of charge and discharge. Lithium-ion intercalation proceeds through a two-phase reaction divided into LiFePO₄ and FePO₄. The volume change between two phases is slightly large, 6.81% [1]. These characteristics suggest the nucleation occurs at the cathode/electrolyte interface and would limit the rate performance [2]. Recently, it is reported that surface modification of LiFePO₄ with nitrogen improves the rate capability [3]. However, the origin of improvement in rate performance still has not been understood clearly. This is because it is difficult to analyze the interfacial reaction using composite electrodes, which have complex structures of mixture with active material, carbon, and binder. In this study, we prepared surface modified LiFePO₄ thin-film electrode with nitrogen and discuss the correlation between the surface modification and reaction kinetics of LiFePO₄ using electrochemical and surface-sensitive X-ray absorption spectroscopy (XAS) measurements.

The LiFePO₄ thin film was prepared by pulsed laser deposition method at 650°C. The surface-nitrided treatment was conducted to anneal the as-prepared LiFePO₄ thin-film at 600°C under NH₃ atmosphere for 10min. Charge-discharge measurements were performed by using three-electrode cells. We investigated the surface electronic and local structure by soft X-ray absorption spectroscopy (N K and O K-edge) and depth-resolved XAS (Fe K-edge) at SPring-8 BL 27SU and BL37XU.

The surface-nitrided LiFePO₄ shows the higher capacity than the bare LiFePO₄, 123% (10C) and 150% (10C) in discharge processes. The surface-nitrided treatment improves both charge/discharge kinetics. In N K-edge XAS spectra, no spectrum was observed in the bare LiFePO₄, whereas a spectrum having a sharp peak was observed in the surface-nitrided LiFePO₄, which means that nitrogen species exist in the surface-nitrided LiFePO₄. O K-edge XAS measurements via total electron yield mode observed that the intensity of the pre-edge in the surface-nitrided LiFePO₄ was higher than that of the pre-edge in the Bare-LiFePO₄, and the peak position was lower than the peak position in the Bare-LiFePO₄. These results indicate that nitrogen species introduced into the surface of LiFePO₄ by surface-nitrided treatment formed new hybridized states with the Fe 3d and O 2p orbitals. and decreases the total barrier for the charge transfer kinetics, which leads to better rate performance.

Reference

- [1]. Padhi, A. K.; Nanjundaswamy, K. S.; Goodenough, J. B., *J. Electrochem. Soc.* **1997**, 144, 1188–1194.
- [2]. Delmas, C.; Maccario, M.; Croguennec, L.; Le Cras, F.; Weill, F. *Nat. Mater.* **2008**, 7, 665-671.
- [3]. Park, K. S.; Xiao, P. H.; Kim, S. Y.; Dylla, A.; Choi, Y. M.; Henkelman, G.; Stevenson, K. J.; Goodenough, J. B. *Chem. Mater.* **2012**, 24, 3212-3218.

TMV nanoparticles as enzyme carriers for biosensor applications

M. Jablonski¹, A. Poghossian^{1,3}, C. Koch², C. Wege², M.J. Schöning^{1,3}

¹ *FH Aachen, Campus Jülich, Institute of Nano- and Biotechnologies (INB), 52428 Jülich, Germany*

² *Institute of Biomaterials and Biomolecular Systems, University of Stuttgart, 70569 Stuttgart, Germany*

³ *Research Center Jülich, Institute of Complex Systems (ICS-8, Bioelectronics), 52425 Jülich, Germany
schoening@fh-aachen.de*

Among the multitude of concepts and different types of chemical sensors and biosensors discussed in literature, the strategy to integrate chemical or biological recognition elements together with semiconductor-type field-effect devices is one of the most attractive approaches. In this context, the immobilization of the biological recognition element on top of the transducer structure is one of the key challenging techniques to end up with reliable and highly sensitive biosensors.

In this study, we present a new immobilization strategy based on tobacco mosaic virus (TMV) nanotubes as enzyme nanocarriers. TMV scaffolds enable a dense immobilization of precisely positioned enzymes with retained activity. Two examples that take benefit from those nanocarriers will be discussed and compared with current state-of-the-art technologies: The generic approach has been demonstrated by realizing amperometric glucose sensors combining an array of platinum electrodes loaded with glucose oxidase (GOD)-modified TMV nanotubes and coat protein aggregates as a model system. The second example describes a TMV-modified capacitive field-effect penicillin biosensor. Both sensor types – the amperometric and potentiometric one – possess a high glucose and penicillin sensitivity, respectively, and a low detection limit. In case of the penicillin biosensor, the long-term stability has been investigated over a time period of about 1 year, and it has been successfully tested for the penicillin detection in diluted milk samples.

Fabrication of plasmon sensor with Ag@TiO₂ core-shell nanoparticles for surface-enhanced Raman scattering

Yuka Kashimata¹, Yuta Sato¹, Masahiro Kunimoto², Masahiro Yanagisawa², Takayuki Homma^{1,2}

1. Dept. of Applied Chemistry, Waseda Univ. 3-4-1 Okubo, Shinjuku, Tokyo, Japan

2. Research Organization for Nano & Life Innovation, Waseda Univ. Wasedaturumakicho, Shinjuku, Tokyo 162-0041, Japan.

t.homma@waseda.jp

Surface-enhanced Raman scattering (SERS) is a well-known spectroscopic effect to enhance Raman-scattered light, which originates from electric field enhancement caused by localized plasmonic resonance at the surface of metal nanostructures. The effect is utilized for highly sensitive analyses of chemical behaviors of molecules that are relevant to various chemistry fields, such as surface chemistry and biochemistry. To make this strategy more practicable, we have developed a handy optical element that provides SERS effect [1]. This element is made of transparent materials, such as glass or poly (dimethylsiloxane) (PDMS) resin and holds nano particles of SERS active metals, such as Ag or Au, on its surface, which is called “plasmon sensor”. The sensor located on the measurement object allows us to obtain an enhanced Raman spectrum from the surface of the object, without forming metal nanostructures directly on it.

In order to develop the plasmon sensor applicable to much wider area, durability of the nanoparticles needs to be improved. For example, the bare Ag nanoparticles are not able to stick on the sensor in strong alkaline solution, which is often used as battery electrolyte. In this study, the plasmon sensor with Ag nanoparticles covered with TiO₂ shell, Ag@TiO₂ is developed. TiO₂ shows strong chemical resistance to prevent core Ag nanoparticles from being inactivated. PDMS film with microlens array (MLA) structure is selected as a base material of the sensor so that it can be attached onto many points of specimens.

First, PDMS was spin-coated on a template with pyramid-shaped pit array (pit size: 30 μm, pitch length: 60 μm, pit depth: 21 μm), which led to the sharpened MLA structures on the sensor base. Ag nanoparticle was modified to the MLA sensor via self-assembled monolayer of (3-Aminopropyl) triethoxysilane (APTES), followed by immersion in a titanium oxide acetylacetonate (TOAA) solution to be coated by TiO₂. This PDMS MLA sensor with Ag@TiO₂ nanoparticle was finished by annealing in vacuum condition. The chemical resistance of the fabricated Ag@TiO₂ nanoparticles was evaluated by Raman measurement after immersing it in 4.0 mol/L KOH as a strong alkaline solution. Raman spectrum was measured by irradiating excitation laser through the fabricated sensor located on the 4-mercaptobenzoic acid (pMBA) modified Au substrate.

SEM image of PDMS MLA sensor showed successfully fabricated Ag@TiO₂ nanoparticle modified on its surface. Raman spectrum of pMBA modified Au substrate with the Ag@TiO₂ sensor attached clearly identified the signal from pMBA, whereas the signal could not be seen in the case of the sensor with the bare Ag nanoparticles. It should be noted that both sensors were located on the substrate after immersion in KOH solution. These results suggest that chemical resistance of the Ag nanoparticle modified on PDMS MLA sensor has been improved by TiO₂ shell coating.

This research was financially supported in part by “Development of Systems and Technology for Advanced Measurement and Analysis” program from JST.

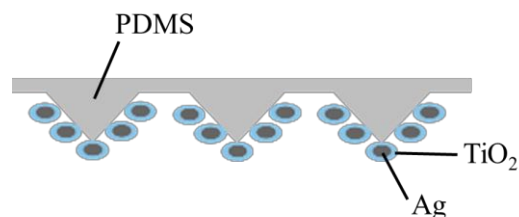


Fig. 1. Schematic image of Ag@TiO₂ nanoparticle modified on PDMS MLA sensor

[1] M. Yanagisawa, M. Saito, M. Kunimoto, T. Homma, *Appl. Phys. Express*, **9** (2016), 122002.

Electrodeposition of Ti Films in Water-Soluble KF–KCl Molten Salt

Yutaro Norikawa¹, Kouji Yasuda^{2,3}, Koma Numata⁴, Tomoyuki Awazu⁴,
Masatoshi Majima⁴, Toshiyuki Nohira^{1,*}

¹ Institute of Advanced Energy, Kyoto University, Uji 611-0011, Japan

² Agency for Health, Safety and Environment, Kyoto University, Kyoto 606-8501, Japan

³ Graduate School of Energy Science, Kyoto University, Kyoto 606-8501, Japan

⁴ Sumitomo Electric Industries, Ltd., Itami 664-0016, Japan

*nohira.toshiyuki.8r@kyoto-u.ac.jp

Titanium metal exhibits corrosion resistance, heat resistance, etc. However, the high production cost and poor workability have been preventing its wide use. Plating metallic titanium on general substrates is a promising approach to utilize the superior properties of titanium. Further, plating on substrates with complicated shapes is possible in electrodeposition. A number of studies have been conducted for the electrodeposition of Ti from molten salts [1–4]. In previous studies, chloride [1], fluoride [2,3] and fluoride-chloride [4] molten salts have been used as electrolytes. Generally, compact and smooth Ti films were obtained from fluoride melts such as LiF–NaF–KF [2,3] and fluoride-chloride melts such as NaCl–KCl–NaF [4]. However, one of the problems using fluoride-based molten salts in the previous studies was the difficulty in removing the salt adhered to the deposited Ti due to low solubility of LiF and NaF in water. Recently, we have proposed the new electrodeposition process of Ti using molten KF–KCl [5]. Since both KF and KCl are highly soluble in water, the adhered salt can be easily removed by washing with water. In the present study, we investigated the electrodeposition of Ti in molten KF–KCl to which K_2TiF_6 and sponge Ti were added.

Fig. 1 shows optical and SEM images of the sample obtained by galvanostatic electrolysis on a Ni plate electrode at 923 K. The electrolysis was carried out at current density of 100 mA cm^{-2} for 5 min. As seen from the optical image in Fig. 1(A), the deposits have metallic luster. XRD analysis revealed that the deposits were metallic titanium. From the surface SEM image in Fig. 1(B), the film is densely packed with compact crystal grains. From the cross-sectional SEM image in Fig. 1(C), the film has smooth surface and constant thickness around $10 \mu\text{m}$. The components of the molten salt electrolyte (K, F, and Cl) were not detected on the surfaces of Ti films by EDX analysis. Thus, the adhered salt on the Ti films were successfully removed only by water washing.

References

- [1] G. M. Haaberg, W. Rolland, A. Sterten, J. Thonstad, *J. Appl. Electrochem.*, **23**, 217 (1993).
- [2] A. Robin, R.B. Ribeiro, *J. Appl. Electrochem.*, **30**, 239 (2000).
- [3] J. De Lepinay, J. Bouteillon, S. Traore, D. Renaud, M. J. Barbier, *J. Appl. Electrochem.*, **17**, 294 (1987).
- [4] V. V. Malyshev, D. B. Shakhnin, *Mater. Sci.*, **50**, 91 (2014).
- [5] Y. Norikawa, K. Yasuda, T. Nohira, *Mater. Trans.*, **58**, 390 (2017).

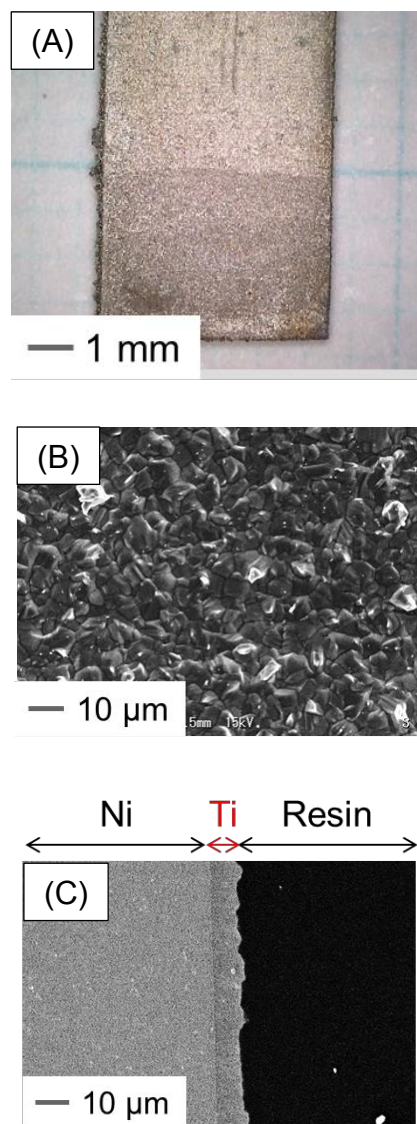


Fig. 1. (A) An optical image, (B) surface and (C) cross-sectional SEM images of the sample obtained by galvanostatic electrolysis of a Ni plate electrode at -100 mA cm^{-2} for 5 min in molten KF–KCl after the addition of K_2TiF_6 (2.0 mol%) and sponge Ti (1.3 mol%) at 923 K.

Electrocatalytic Activity for Oxygen Reduction Reaction of Nitrogen-containing Carbon Composites synthesized via Solution Plasma Process

Hoonseung Lee^a, Yuta Wada^b, Amane Kaneko^b, Camelia Miron^c, Takahiro Ishizaki^{c,d*}

^aFunctional and Control Engineering, Faculty of Engineering, Shibaura Institute of Technology, Koto, Tokyo, 135-8548, Japan. E-mail: i041214@shibaura-it.ac.jp

^bGraduate School of Materials Science and Engineering, Faculty of Engineering, Shibaura Institute of Technology, Koto, Tokyo 135-8548, Japan

^cSIT Research Laboratories, Shibaura Institute of Technology, Koto, Tokyo, 135-8548, Japan.

^dDepartment of Materials Science and Engineering, College of Engineering, Shibaura Institute of Technology, Koto, Tokyo 135-8548, Japan

i041215@sic.shibaura-it.ac.jp, *ishizaki@shibaura-it.ac.jp

Oxygen reduction reaction (ORR) is one of the most important reactions for fuel cells and Li-air batteries. Recently, heteroatom-doped carbon materials have attracted much attention because they have been reported to show high electrocatalytic activity for ORR. The composite of different carbon materials can be an effective means to further improve the catalytic performance. In this study, we aimed to synthesize nitrogen-containing carbon composite materials.

In order to obtain nitrogen-containing carbon composites, acrylonitrile (nitrogen precursor; >99.5 %, Kanto chemical) and ketjenblack (KB; EC600JD) were used as raw materials. 100 ml volume of acrylonitrile was set in insulated reactor, and then 100 mg of KB was introduced into the reactor under magnetic stirring condition. Electric discharge was generated in the mixed solution between high purity tungsten electrodes (99.999%, Nilaco) by using a bipolar pulse power supply (MPP-HV04, Kurita) operated at a voltage of ~1.5 kV, a frequency of 50 kHz, and a pulse width of 0.5 μ s. After 20 min of discharge, synthesized carbon composite was separated by filtering through the polytetrafluoroethylene (PTFE; JWVP04700, Merck Millipore) membrane filter of 100 nm diameter and dried in oven at 100 °C for 24 h. After that, dried carbon composite (KB+AN) was heated at 900 °C for 1hr under argon atmosphere (KB+AN_HT). Morphology and chemical composition of the carbon composites were characterized by scanning electron microscope (SEM), X-ray diffraction (XRD), and X-ray photoelectron spectroscopy (XPS). Surface area and pore structures were analyzed by using Nitrogen absorption-desorption method (BET). Electrocatalytic activity for oxygen reduction reaction (ORR) of the synthesized carbon composites were investigated by using electrochemical analyzer.

Nitrogen-containing carbon composites were successfully synthesized by *in-situ* solution plasma process. The catalytic activities for ORR of the carbon composites were changed depending on the surface area and nitrogen-bonding states. Especially, the limiting current density and onset potential for ORR were clearly improved after heat treatment. The effect of composites and heat treatment on catalytic performance for ORR was discussed.

Acknowledgement: This work was partly supported by Grant-in-Aid for Scientific Research (C) (No. 17K06822) from Japan Society for the Promotion of Science.

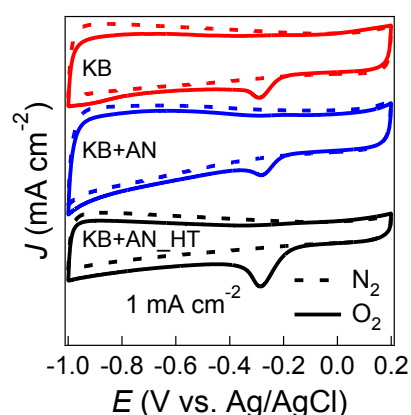


Fig. 1 CV curves of various catalysts in N₂ and O₂ saturated 0.1 M KOH solution at a scan rate of 50 mV s⁻¹.

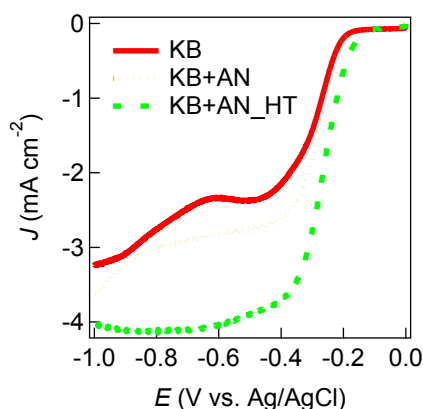


Fig. 2 LSV curves of various catalysts in O₂ saturated 0.1 M KOH solution at a scan rate of 10 mV s⁻¹ and rotation speed of 1500 rpm.

Visualization of the barrier function of an epithelial cell layer by chemical imaging sensor and its future application

Ko-ichiro Miyamoto¹, Daisuke Suzuki², Carl Frederik Werner¹,
Yuhki Yanase³, Shigeyasu Uno⁴, Tatsuo Yoshinobu^{1,2}

1) Department of Electronic Engineering, Tohoku University

2) Department of Biomedical Engineering, Tohoku University

6-6-05 Aramaki Aza Aoba, Aoba-ku, Sendai, Miyagi, Japan

3) Department of Dermatology, Hiroshima University,

1-2-3, Kasumi, Minami-ku, Hiroshima, Japan

4) Department of Electrical and Electronic Engineering, Ritsumeikan University

1-1-1 Noji-Higashi, Kusatsu, Shiga, Japan

k-miya@ecei.tohoku.ac.jp

A layer of epithelial cells, which are tightly connected, covers the whole surface of human body to form a barrier against foreign substances. As an index of the barrier function of the epithelial cell layer, “trans-epithelial electrical resistance (TEER)” has been used [1]. However, the TEER, conventionally measured using a couple of electrodes, offers only an averaged value over the cell layer, and the spatial distribution of the barrier function within a cell layer cannot be evaluated.

To overcome the problem, we have proposed to utilize the chemical imaging sensor [2], which is a semiconductor-based chemical sensor and capable of visualizing the distributions of ion concentration / impedance without label molecules. Figure 1a shows a schematic diagram of the chemical imaging sensor comprising the sensor plate, scanning optics and measurement circuit. In our previous study [3], a defect in a cell layer (of human intestinal cells) cultured on a permeable membrane was successfully visualized. However, the spatial resolution of the obtained image was poor due to the separation between the sensor surface and the cell layer.

In this study, a cell layer was directly cultured on the sensor surface. In advance of cultivation, a thin film of collagen was spin-coated on the sensor surface to improve the adhesion of the cell layer. After forming a confluent cell layer, it was mechanically scratched as shown in Figure 1b. Figure 1c shows the obtained photocurrent image. The distribution of the photocurrent clearly corresponds to the shape of the defect in the cell layer.

The visualization of the barrier function of the epithelial cell layer has a potential to develop a novel cell-based assay. Combination of the proposed method with other paradigms such as surface plasmon resonance imaging (SPRI) and electrical impedance spectroscopy (EIS) will be a prospective strategy to acquire complementary information of the barrier function in a cell layer.

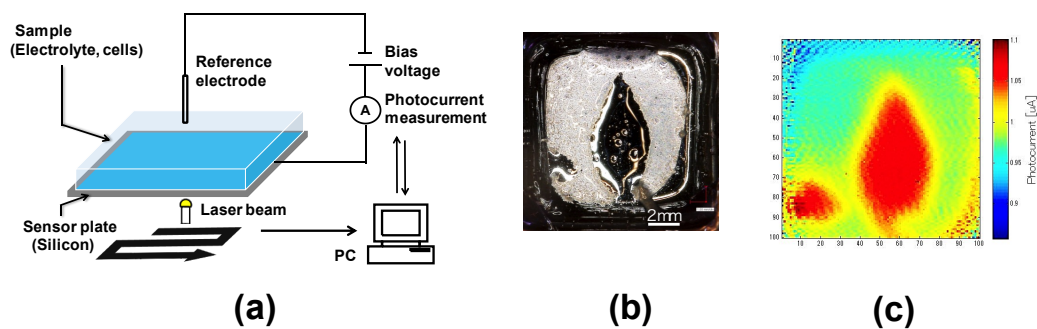


Figure 1. (a) Schematic diagram of the measurement system of the chemical imaging sensor. (b) A defect in a cell layer on the sensor surface. (c) Obtained photocurrent image corresponding to the defect in (b).

[1] J. Han, H. Isoda, T. Maekawa, *Cytotechnology*, **40**, 93-98 (2002).

[2] K. Miyamoto, B. Yu, H. Isoda, T. Wagner, M.J. Schöning, T. Yoshinobu, *Sens. Act. B* **236**, 965-969 (2016).

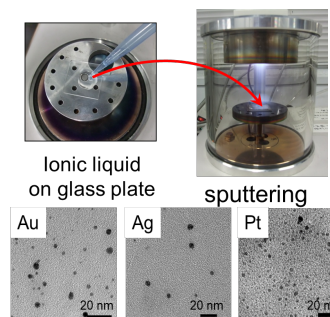
[3] T. Yoshinobu, K. Miyamoto, T. Wagner, M.J. Schöning, *Sens. Actuators B* **207**, 926-932 (2015).

Real-time observation of Au nanoparticles formation process using ionic liquid-sputtering method

Tomoya Sasaki¹, Tetsuya Tsuda¹, Taro Uematsu¹, Tsukasa Torimoto², Susumu Kuwabata¹

¹Graduate School of Engineering, Osaka University
2-1 Yamada-oka, Suita, Osaka 565-0871, Japan
e-mail address t_sasaki@chem.eng.osaka-u.ac.jp

Ionic liquids (ILs) are a subset of molten salts with melting point below 100°C, which have many unique properties like the negligible low vapour pressure. In hence, the IL is allowed to enter into the vacuum instruments. In addition, ILs have attracted much attention as a solvent for the inorganic nanoparticles preparation since they can stabilize the surface of the inorganic nanoparticles. We have recently developed a clean metal nanoparticles preparation method, which is conducted by sputtering onto IL without adducts such as surface stabilizing and reducing agents (Fig. 1). To clarify the mechanism of nanoparticles formation, previous studies have focused on the kind of cation and anion of ILs¹ and condition of sputtering² as the factors affecting the size and the distribution of metal nanoparticles. However, it is still hard to observe the formation process of nanoparticles during the sputtering procedure. In this research, the color changes caused by the surface plasmon resonance of Au nanoparticles was recorded by video to illustrate the growing process of them. We succeeded in real-time observing appearance of Au nanoparticles.



Au nanoparticles were prepared by magnetron sputtering into 1-butyl-3-methylimidazolium bis (trifluoromethanesulfonyl) amide ([C4mim] [TFSA]) for 5 min. The sputter conditions were that the puresure of Ar gas was 5 Pa, the current was 40 mA. Real-time observations were performed in three directions, a frontal view and an obliquely downward view, a view from underneath. Fig. 2 shows three direction, (a), (b), and (c), respectively. In a frontal view and an obliquely downward view (Fig. 2(a), (b)), a glass container filled with [C4mim] [TFSA] until slitting was sputtered. In obosevation from underneath (Fig. 2 (C)), a slide glass with ionic liquid was placed on a sample table made of glass plates and mirror inclined at 45 ° was placed under the sample table, and the ionic liquid surface during Au sputtering was observed directly.

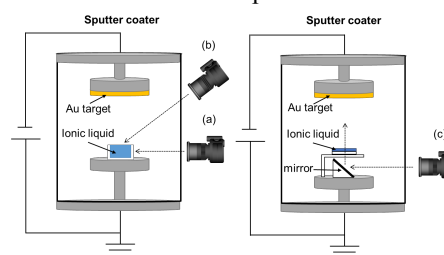
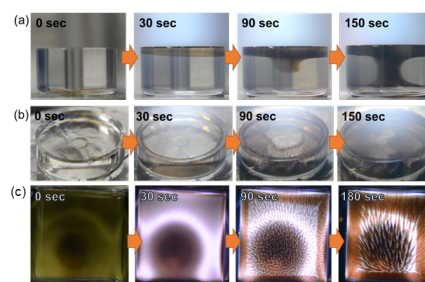


Fig. 3 show the appearance during Au sputtering. As shown in Fig.3 (a), (b), convection of IL was found in the sputtering process. It is assumed that there are two types of convection which are caused by the change of temperature and density varying. In addition, during sputtering into ionic liquid, not only convection of IL occurred but also the unique pattern on the surface was observed, which could be attributed to ununiform concentration distribution of Au nanoparticles colored brown by surface plasmon resonance. Au exists in IL as two kinds of states: Au nanoparticles and clusters. The later one is a several atoms group separated from the Au target early before touching IL, which is unstable and easy to aggregate after entering IL. Since this aggregation could lead to the ultra-high concentration area of dark color, it would be partly reason for the pattern formation. These phenomena can be a hint to elucidate the process of nanoparticle formation in the ionic liquid-sputtering method.



1. Y. Hatakeyama, K. Judai, K. Onishi, S. Takahashi, S. Kiumura, K. Nishikawa, *Phys. Chem. Chem. Phys.*, 18, 2339 (2016).
2. Y. Hatakeyama, K. Onishi, K. Nishikawa, *RSC Advances*, 1, 1815 (2011)

Effect of light intensity towards the signal of a light-addressable potentiometric sensor

Carl Frederik Werner¹, Ko-ichiro Miyamoto¹, Torsten Wagner³,
Michael J. Schöning³, Tatsuo Yoshinobu²

¹Department of Electronic Engineering, Tohoku University, Sendai, Japan

²Department of Biomedical Engineering, Tohoku University, Sendai, Japan

³Institute of Nano- and Biotechnologies (INB), FH Aachen, Jülich, Germany

werner@ecei.tohoku.ac.jp

To study chemical and biological processes, the determination of concentrations of one or more analyte species on a defined position is of distinct interest. With a light-addressable potentiometric sensor (LAPS) spatially resolved measurement of analyte concentrations on the sensor surface can be performed utilizing a modulated light spot. This allows spatiotemporal measurements of e.g., local chemical reactions or diffusion processes [1]. Therefore, LAPS can be applied to monitoring cellular activities or to microfluidic devices. A schematic of the LAPS principle is depicted in Figure 1. One important parameter is the light intensity of the light spot, as it affects the signal-to-noise ratio and the lateral resolution of the LAPS. Therefore, this study investigates the effect of the light intensity towards the LAPS signal by means of a semiconductor device simulator.

The modulated light beam generates charge carriers inside the semiconductor. These charge carriers diffuse to the semiconductor-insulator interface and will be separated by the electric field inside the space-charge region, leading to an externally measurable photocurrent. Lateral diffusion of the charge carriers results in a larger measurement spot than the original light spot size. Since the photocurrent amplitude depends on the local thickness of the space-charge region, the signal can be correlated with the local analyte concentration on the sensor surface. To investigate the effect of the light intensity, semiconductor device simulations with “Sentaurus TCAD” from Synopsys were performed utilizing a two dimensional, rotation symmetric LAPS model.

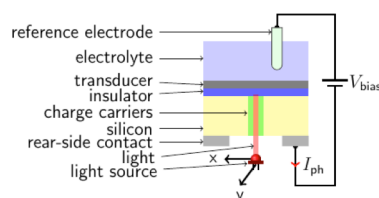


Figure 1: Schematic of LAPS principle

Figure 2 (left) shows photocurrent/bias voltage (I/V) curves for different light intensities. A higher light intensity results in a larger photocurrent amplitude and therefore a higher signal-to-noise ratio. However, higher light intensities lower the slope of the I/V curve due to the additional charge carriers. This also affects the lateral resolution as shown in Figure 2 (right). Here various radii of circular regions with lower surface potential were placed on the sensor surface to investigate the lateral resolution of the LAPS. As can be seen, decreasing of the light intensity results in a better lateral resolution.

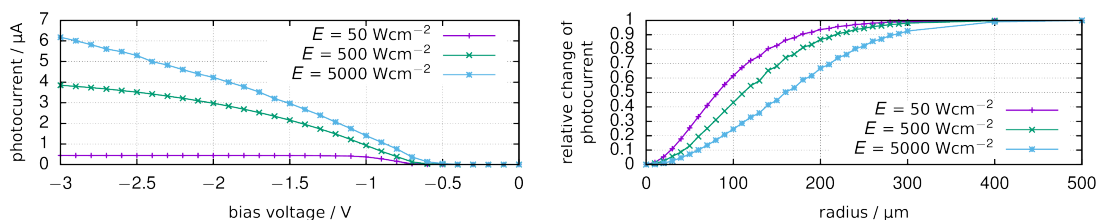


Figure 2: Photocurrent/bias voltage curve (left) and relative change of photocurrent for various radii of circular regions with lower surface potential (right) for different light intensities.

The light intensity affects the signal-to-noise ratio and the lateral resolution of LAPS in a contrary way. This information is important to improve the performance of LAPS.

Acknowledgment

This work is supported by VDEC, The University of Tokyo in collaboration with Synopsys Corp.

References

- [1] Yoshinobu, T.; Iwasaki, H.; Ui, Y.; Furuichi, K.; Ermolenko, Y.; Mourzina, Y.; Wagner, T.; Näther, N.; Schöning, M. J.; *Methods* **2005**, doi: 10.1016/j.ymeth. 2005.05.020

Developments of novel semiconductor nanoparticles stabilized with metal-organic frameworks (MOFs)

Kohei Kumagai,¹ Taro Uematsu,¹ Tsukasa Torimoto,² and Susumu Kuwabata*¹

¹Osaka University,² Nagoya University

Osaka University 1-1 Yamadaoka Suita Osaka 565-0871 Japan

k_kumagai@chem.eng.osaka-u.ac.jp

Semiconductor nanoparticles, or quantum dots (QDs), have attracted much attention as next generation light emitting materials due to their size-dependent optical properties. Surface modification of semiconductor nanoparticles by proper organic ligands, e.g. amines or thiols, is essential to obtain strong photoluminescence. Therefore, the photoluminescence quenching is often occurred by desorption of the ligands, implying the necessity of more robust protecting layers which are bound on the surface of nanoparticles. In this study, we focused on Metal Organic Frameworks (MOFs) as novel protecting agents of semiconductor nanoparticles. Band gap engineering of MOFs achieved by the combination of metal ions and organic linkers are one of the great advantages as surface modification agents^[1]. We examined the conditions for the growth of MOFs on semiconductor nanoparticles and investigated the changes of their optical properties brought by MOFs.

Oleylamine-capped CdSe/CdS core/shell nanoparticles, which were monodispersed and showed strong emission at visible light region, were used for modification by MOFs. The surface ligands of core/shell nanoparticles were exchanged to pyridine for solubilizing in polar solvents, and they were mixed with zinc nitrate hexahydrate and 2-methylimidazole (MOFs precursors) in methanol at room temperature. After 24 h, Zeolitic imidazolate framework-8 (ZIF-8)-modified CdSe/CdS core/shell nanoparticles were obtained in powder form. We investigated change in morphology and photoluminescence properties by TEM observation and photoluminescence spectroscopy, respectively.

Figs. 1a and 1b show the photographs of CdSe/CdS@ZIF-8 NPs under room light and UV light, respectively. The bright photoluminescence in solid state indicates that ZIF-8 was working as an appropriate surface protecting agent like amines and thiols. TEM images of pyridine-capped CdSe/CdS core/shell nanoparticles and CdSe/CdS@ZIF-8 NPs are shown in Figs. 1c and 1d, respectively. Without MOFs, nanoparticles were almost aggregated because pyridine could not keep the distance between the particles due to its weak binding force to the surface. The modification by ZIF-8, however, dispersed the nanoparticles with keeping the distance between the particles. Interestingly, CdSe/CdS@ZIF-8 showed higher photoluminescence quantum yields (36%) than the same nanoparticles before the ZIF-8 treatment (7.0%). Increase in photoluminescence quantum yield was remarkable because it often decreases by solidification. The MOFs seems to have significant effects on the surface conditions of nanoparticles and we are investigating this point with other types of MOFs.

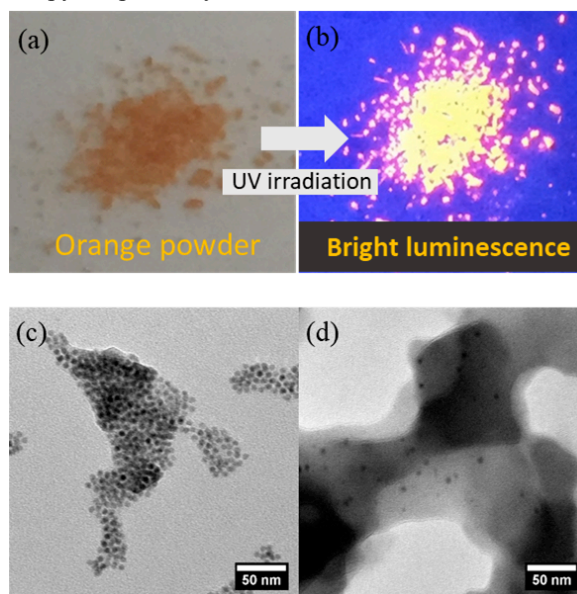


Figure 1. Photograph of CdSe/CdS@ZIF-8 NPs under room light (a) and UV light (b). TEM images of CdSe/CdS core/shell NPs capped with pyridine (c) and stabilized with ZIF-8 (d).

[1] Aron Walsh et al. *Appl. Mater. Interfaces* **2014**, 6, 22044–22050

Si-O-C powders with ultra-long cycle ability as anode materials in lithium ion batteries

Seongki Ahn^a, Toshiyuki Momma^{a,b,c}, Tokihiko Yokoshima^a, Hiroki Nara^a, and Tetsuya Osaka^{a,b,c}

^aResearch Organization for Nano and Life Innovation, Waseda University
Wasedaturumakicho, Shinjuku-ku, Tokyo 162-0041, Japan

^bFaculty of Science and Engineering, Waseda University,
3-4-1, Okubo, Shinjuku-ku, Tokyo 169-8555, Japan

^cKagami Memorial Research Institute for Materials Science and Technology, Waseda University
2-8-26, Nishiwaseda, Shinjuku-ku, Tokyo, 169-0051, Japan

momma@waseda.jp

Silicon-based materials have attracted as promising alternative anode material for high energy density lithium ion batteries due to their higher theoretical capacity than graphite anode, which is employed as an anode so far ($\text{Li}_{4.4}\text{Si}$: 4200 mAh g^{-1} , Li_6C : 372 mAh g^{-1}). However, the silicon-based materials suffer volume change up to $\sim 400\%$ during lithiation/de-lithiation, resulting in poor electrochemical performance. To reduce this critical problem, we reported the Si-O-C film synthesized by electrodeposition in an organic solvent. The Si-O-C film demonstrated an outstanding cycle ability for 7200th cycle with good discharge capacity. The reason for good electrochemical performance is that the co-deposited materials containing with oxygen and carbon act as buffer matrix to reduce internal stress during volume change of silicon. Despite these exceptional results, it is difficult to apply full-cell configuration because of low adhesion strength between Si-O-C film and copper substrate, which causes exfoliation of Si-O-C layer at high passing charge over $15 \text{ coulomb cm}^{-2}$ during electrodeposition.

Herein, we introduce a new way to obtain a silicon-based anode material by electrodeposition harvesting method. The Si-O-C composite could be obtained by peeling off after electrodeposition technique with ball milling process and it comes in powder. To fabricate electrode, the obtained Si-O-C powder was mixing with a carbon material and a polymer binder in N-Methyl-2-pyrrolidone. This new type Si-O-C anode shows a super cycle ability for 10,000 cycles at 2 C-rate, good C-rate performance from 0.1 to 10.0 C-rate, and higher areal capacity of over 0.3 mAh cm^{-2} than Si-O-C film, which has areal capacity of 0.1 mAh cm^{-2} . In addition, it shows higher areal capacity than Si-O-C film, indicating that Si-O-C powder can offer enough areal capacity as much as cathode needs for full-cell configuration. To figure out the reason of these outstanding results, material and electrochemical characteristics are examined by scanning electron microscope (SEM), inductively coupled plasma atomic emission spectroscopy (ICP-AES), charge/discharge measurements, and so on.

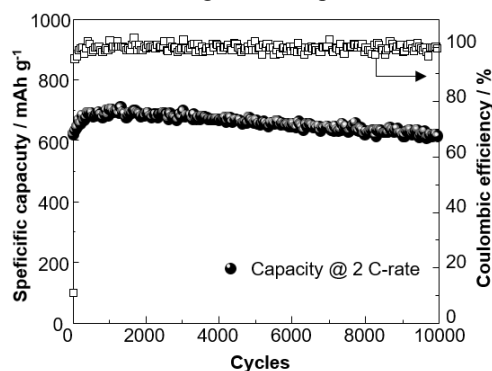


Figure 1. Long cycle ability of Si-O-C anode prepared by electrodeposition harvesting method for 10,000 cycles at 2 C-rate.

To figure out the reason of these outstanding results, material and electrochemical characteristics are examined by scanning electron microscope (SEM), inductively coupled plasma atomic emission spectroscopy (ICP-AES), charge/discharge measurements, and so on.

Acknowledgement

This work is partly supported by Advanced Low Carbon Technology Research and Development Program Special Priority Research Area “Next-generation Rechargeable Battery” (ALCA-Spring) from the Japan Science and Technology Agency (JST), Japan.

References

- [1] H. Nara, T. Yokoshima, T. Momma, T. Osaka, *Energ. Environ. Sci.*, 5, (4) 6500-6505 (2012).
- [2] T. Osaka, H. Nara, T. Momma, T. Yokoshima, *J. Mater. Chem. A*, 883-896 (2014).
- [3] S. Ahn, M. Jeong, T. Yokoshima, H. Nara, T. Momma, T. Osaka, *J. Power Sources*, 336, 203-211 (2016).

Morphology Control of Electrodeposited ZnO Patterns for Micro Thermoelectric Devices

Koichiro Yoshitoku¹, Hinako Matsuo¹, Mikiko Saito², Hidefumi Takahashi³,
Ichiro Terasaki⁴, Takayuki Homma^{1,2}

1. Department of Applied Chemistry, Waseda University, Okubo, Shinjuku, Tokyo 169-8555, Japan

2. Research Organization for Nano & Life Innovation, Waseda University, Wasedatsurumakicho,
Shinjuku, Tokyo 162-0041, Japan

3. Department of Applied Physics, The University of Tokyo, Tokyo 113-8656, Japan

4. Department of Physics, Nagoya University, Furocho, Chikusa, Nagoya 464-8602, Japan
t.homma@waseda.jp

Micro thermoelectric devices are attractive for power generation method which can directly convert heat energy into electric energy even with small heat source [1]. For fabrication of these devices, patterned formation of thermoelectric materials is needed. For this, electrodeposition has numbers of advantages, such as high deposition rate, precise controllability, deposition selectivity, etc. Among thermoelectric materials, ZnO is known to be applicable at higher temperature region, and electrodeposition of ZnO using zinc nitrate based electrolytes has been widely investigated. However, some drawbacks in the films deposited from these bath systems have still remained, for example, rough and non-uniform surface was formed mainly due to gas evolution derived from nitrate ion, such as nitrogen [2], which are obstacles to deposit thick and uniform patterns. In order to solve these problems, the zinc acetate bath which has a merit of no gas evolution is proposed. Hence, in this study, we attempted to form electrodeposited ZnO patterns from zinc acetate bath.

Experimental condition is shown in Table 1. Electrodeposition of ZnO was carried out using a three-electrode system with a stirring paddle or ultrasonic agitation. A glass substrate coated with 100 nm Au/10 nm Cr layers was used as working electrode, Pt plate as counter electrode, and Ag/AgCl as reference electrode, respectively. Electrolytes were aqueous solution, containing 0.01 mol/L of $\text{Zn}(\text{CH}_3\text{COO})_2 \cdot 2\text{H}_2\text{O}$ and 0.02 mol/L of H_2O_2 . The size of p-n legs in the device is 200 μm diameter and 15 μm thick. Ni was used as dummy patterns for p-type to evaluate thermoelectric properties of devices with n-type ZnO. Patterned substrates for the selective deposition were formed by using photolithography [3]. The morphology and crystallinity of samples were characterized by field emission scanning electron microscope (FESEM) and x-ray diffraction (XRD). The thermoelectric performances of samples were evaluated by heating the surface around 200 °C, using focused light from a halogen lamp. The current and voltage of the devices were measured using a multimeter with a constant current source.

First, ZnO films were electrodeposited from zinc acetate bath with stirring paddle. As a result, films with uniform and smooth surface were obtained, however, non-uniform ZnO patterns were formed. Thus, ultrasonic agitation was conducted to prepare uniform ZnO patterns. As a result, smooth and compact deposits were obtained in the patterns with 200 μm diameter and 15 μm thick. For application of ZnO patterns obtained in this study, thermoelectric micro-device was fabricated, and power curves were measured. The maximum power of the device with n-type ZnO and dummy Ni, was 6.1 nW, which increased from previous study [3]. These results indicated, ZnO films from zinc acetate bath with ultrasonic agitation, smooth and compact deposits were obtained in the patterns, and resulting in high thermoelectric performance of the devices.

$\text{Zn}(\text{CH}_3\text{COO})_2 \cdot 2\text{H}_2\text{O}$	0.01 M
H_2O_2	0.02 M
Temperature	65 - 70 °C
pH	pH6.2
Potential	-1.2 V
Time	60 min
Stirring	Stirring paddle or Ultrasonic agitation
W.E.	Au/Cr/Glass
C.E.	Pt plate
R.E.	Ag/AgCl

[1] G.J. Snyder, J.R. Lim, C.K. Huang, J.P. Fleurial, *Nat. Mater.*, **2**, 528–531 (2003).

[2] H. Matsuo, K. Yoshitoku, D. Furuyama, M. Saito, T. Homma, *ECS Trans.*, **75**, 143-148 (2017).

[3] K. Uda, Y. Seki, M. Saito, Y. Sonobe, Y-C. Hsieh, H. Takahashi, I. Terasaki, T. Homma, *Electrochim. Acta*, **153**, 515-522 (2015).

Electrochemiluminescent Chemodosimetric Sensors for Selective Detection of Homocysteine

Hoon Jun Kim and Jong-In Hong

Department of Chemistry, Seoul National University, Seoul 08826, Korea

*jihong@snu.ac.kr

Elevated levels of plasma homocysteine (Hcy) are an independent risk factor for cardiovascular disease. Herein, we report a chemodosimetric approach for one-step analysis of Hcy levels based on the electrochemiluminescence (ECL).[1] A rationally designed cyclometalated iridium(III) complex possessing a phenylisoquinoline main ligand underwent a selective ring-formation reaction with Hcy to generate a binding adduct, which enabled producing highly luminescent excited states, and yielded strong ECL signals on the surface of electrode without any use of enzymes or antibodies. The level of Hcy was successfully monitored by the ECL increment with a linear correlation between 0–40 μM in 99.9% aqueous media. The approach required neither sample preparation nor bulky instrument, suggesting the point-of-care testing of Hcy levels, and is potentially useful for routine, cost-effective, and precautionary diagnosis of various cardiovascular diseases.

Reference

1. H. J. Kim, K.-S. Lee, Y.-J. Jeon, I.-S. Shin, and J.-I. Hong, *Bios. Bioelec.* 91, 497-503 (2017).

Gas-Imaging Sensor Based on Metal Oxide and Field Effect Structure

Mengyun Wang, Hoang Anh Truong, Carl Frederik Werner, Koichiro Miyamoto, Tatsuo Yoshinobu
Department of Electronic Engineering, Tohoku University
6-6-05 Aramaki Aza Aoba, Aoba-ku, Sendai, Miyagi 980-8579, Japan
m-wang@ecei.tohoku.ac.jp

Metal-oxide gas sensors are widely used in many applications, expanding from conventional areas of gas leak detectors into diverse and targeted areas such as breath analysis for health monitoring. However, they still remain a challenge when it comes to gas imaging, or visualization of gas distribution. One possible approach is to use an array of sensors for spatially resolved measurement of gas concentration. The light-addressable potentiometric sensor (LAPS) [1,2] and the scanning photo-induced impedance microscopy (SPIM) [3] offer a platform for spatially resolved measurement of analytes. They both have the same field effect structure on a Si substrate, in which the measurement spots on the sensing surface can be arbitrarily defined by a scanning light beam. While the photocurrent signal induced by a scanning light beam responds to the local potential on the sensing surface in a LAPS, the photocurrent signal of a SPIM responds to the local impedance on the sensing surface. In this study, a gas-imaging sensor based on a gas-sensitive metal-oxide layer deposited on the field effect structure is proposed.

To fabricate a gas-sensitive LAPS/SPIM, a tin dioxide (SnO_2) film was deposited on the sensing surface (Si_3N_4) by vacuum evaporation. This film consisted of nanoparticles with diameter of 50–100 nm (Fig. 1a). To read out the photocurrent signal, a suspended-gate structure with an air gap [4] was employed. The suspended-gate structure was fabricated by the following process. A 100-nm-thick thermal oxide was formed on another Si plate, and a part of the oxide layer was removed to form a 100-nm-deep groove structure. Then a gate electrode (Ti and Au) was evaporated at the bottom of the groove and the oxide surface was directly bonded with the sensing surface to form an air gap by annealing at 400 °C for 3 hours. A schematic of the fabricated structure is shown in Fig. 1b.

The SnO_2 layer deposited on the sensing surface was used as an active area of LAPS/SPIM. The sensor was illuminated by a focused laser beam modulated at 4 kHz. The amplitude of the photocurrent signal for air and ethanol vapor was plotted as a function of the bias voltage applied to the sensor in Fig. 1c. The difference of the photocurrent observed at negative bias suggests a lowering of the impedance of the SnO_2 layer exposed to ethanol vapor.

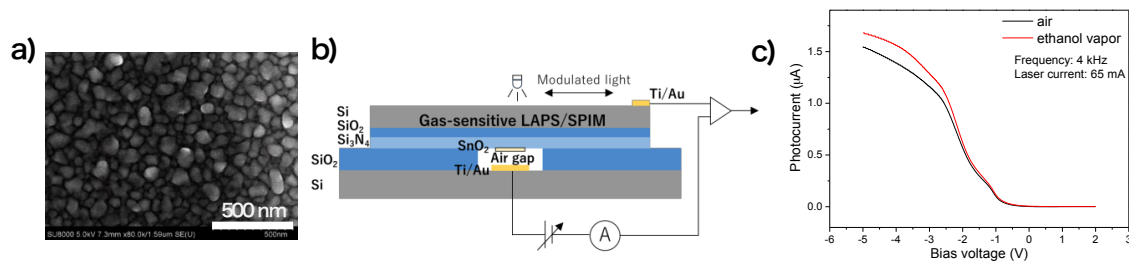


Figure 1. a) SEM picture of the prepared SnO_2 ; b) Schematic structure of gas-sensitive LAPS/SPIM; c) I-V curves measured for air and ethanol vapor

Due to the light-addressability, the gas-sensitive LAPS/SPIM can be applied to spatially resolved measurement of the gas concentration on the sensing surface. Another possible application is a multi-analyte gas sensor, in which more than one kind of gas-sensitive materials are deposited on the sensing surface and individually addressed. The imaging and multi-analyte gas sensing are expected to have potential applications such as breath analysis, food security, process control and air quality monitoring.

Reference

- [1] D. G. Hafeman, J. W. Parce and H. M. McConnel, *Science*, 240 (1988) pp.1182-1185.
- [2] T. Yoshinobu, K. Miyamoto, C. F. Werner, A. Poghossian, T. Wagner and M. J. Schöning, *Annu. Rev. Anal. Chem.*, 10 (2017) pp.225-246.
- [3] S. Krause, H. Talabani, M. Xu, W. Moritz and J. Griffiths, *Electrochim. Acta*, 47 (2002) pp.2143-2148.
- [4] T. Sato, M. Shimizu, H. Uchida and T. Katsube, *Sens. Actuators B*, 20 (1994) pp.213-216.

Effect of Metal Additives on Electrodeposited Bi-Sb-Te Films for Micro Thermoelectric Devices

Misaki Sugie¹, Mikiko Saito², Hidefumi Takahashi³, Ichiro Terasaki⁴, Takayuki Homma^{1,2}

1. Department of Applied Chemistry, Waseda University, Okubo, Shinjuku, Tokyo 169-8555, Japan

2. Research Organization for Nano & Life Innovation, Waseda University, Wasedaturumakicho, Shinjuku, Tokyo 162-0041, Japan

3. Department of Applied Physics, The University of Tokyo, Tokyo 113-8656, Japan

4. Department of Physics, Nagoya University, Furocho, Chikusa, Nagoya 464-8602, Japan
t.homma@waseda.jp

Micro thermoelectric devices can directly convert heat energy into electric energy by Seebeck effect with various heat sources^[1]. To prepare thermoelectric materials, electrodeposition is advantageous for the micro devices owing to patterned formation of micro structures by selective deposition and so on. Among the materials, Bi-Te is the best-known because of high performance at room temperature, and we have fabricated micro thermoelectric devices using electrodeposited Bi-Te films^[2]. We have attempted to improve their performance, and identified that Cu addition to p-type Bi-Sb-Te films effectively prevented an increase in resistivity after annealing, resulting in high performance of the devices. In this study, effect of Cu on the electrodeposited Bi-Sb-Te films was analyzed by comparing addition of Cu and other metal species.

P-type Bi-Sb-Te films was electrodeposited using a three-electrode system with a stirring paddle at room temperature. A glass substrate coated with 100 nm Au/10 nm Cr layers was used as working electrode, Pt as counter electrode, and Ag/AgCl as reference electrode, respectively. Electrolyte contained 1.0 mmol/L Bi(NO₃)₃·5H₂O, 6.0 mmol/L TeO₂, 10 mmol/L Sb₂O₃, 0.10 mol/L C₄H₆O₆, 1.0 mol/L HNO₃, and 0.50 mmol/L of metal species were added to the electrolyte. Cu(NO₃)₂·3H₂O, HAuCl₄·4H₂O, and AgNO₃ were chosen as the metal species. Deposition potential and duration were -80 mV for 30 min or -120 mV for 25 min. The deposited films were annealed at 230 °C or 300 °C for 120 min in Ar+H₂(4%) atmosphere. The resistivity was measured by four-point probe method. The morphology was characterized by field emission scanning electron microscopy (FESEM). The elemental mapping was conducted by energy dispersive X-ray spectroscopy (EDS) after focused ion beam (FIB) processing.

First, p-type Bi-Sb-Te films were electrodeposited with metal additives, followed by annealing. Then, their properties before and after the annealing were evaluated. As a result, it turned out that the increase in resistivity after the annealing was significantly suppressed for Au added films, not only for Cu added films. On the other hand, the resistivity of Ag added films was considerably increased after the annealing similar to those of additive free condition. From SEM images, change of the morphology after the annealing was confirmed for additive free condition, however little change was observed for both Cu and Au added condition. Hence, elemental mapping was performed to those films. As a result, it was suggested that elemental diffusion after the annealing was significantly affected by metal species of both Cu and Au.

In conclusion, it was suggested that the reason why Cu addition to Bi-Sb-Te films suppressed the increase in resistivity was because the elemental diffusion after the annealing was prevented by Cu.

We would like to thank Dr. Y. Sonobe for his kind advices. This research was partially supported by a Grant-in-Aid for Scientific Research from MEXT, Japan.

References

[1] G.J. Snyder, J.R. Lim, C.K. Huang, J.P. Fleurial, *Nature Materials*, **2**, 528-531 (2003).

[2] K. Uda, Y. Seki, M. Saito, Y. Sonobe, Y-C. Hsieh, H. Takahashi, I. Terasaki, T. Homma, *Electrochimica Acta*, **153**, 515-522 (2015).

Distribution of Water inside Thin Nafion Film Analyzed by Neutron Reflectivity under Controlled Temperature and Humidity

Tepppei Kawamoto,¹ Makoto Aoki,² Taro Kimura,³

Takako Mizusawa,⁴ Norifumi L. Yamada,⁵ Junji Inukai^{1,3}

¹Fuel Cell Nanomaterials Center, University of Yamanashi, 6-43 Miyamae-cho, Kofu 400-0021, Japan

²Division of Life, Medical, Natural Sciences and Technology, Organization for Advanced and Integrated Research, Kobe University, 1-1 Rokkodai-cho, Nada-ku, Kobe 658-8501, Japan

³Clean Energy Research Center, University of Yamanashi, 4-3-11 Takeda, Kofu 400-8501, Japan

⁴Comprehensive Research Organization for Science and Society Neutron Science and Technology Center162-1 Shirakata, Tokai, Ibaraki 319-1106, Japan,

⁵Institute of Materials Structure Science, High Energy Accelerator Research Organization, 203-1 Shirakata, Tokai, Ibaraki 319-1106, Japan

e-mail address: jinukai@yamanashi.ac.jp

Introduction: Three-dimensional structures of polymer electrolyte membranes and binders, as well as the concentration of water molecules in the electrolyte, are important for designing ion-conductive membranes and binders for fuel cells. Neutron reflectivity is suitable for analyzing the nanometer-scale structures of thin films.¹⁾ In this study, we investigated the distribution of water molecules absorbed inside a thin Nafion[®] film on Si(100) in an environment-controlled chamber.

Experimental: Thin Nafion film was prepared by spin-coating an alcohol dispersion of Nafion on Si(100) with the thickness of approximately 100 nm (under the dry condition). The sample was placed in an environment-controlled chamber continuously purged with humidified nitrogen at the relative humidities (RHs) of 30% and 80% and the temperature of 80 °C. Neutron reflectivity measurements were carried out using a horizontal-type reflectometer at the beamline BL16 of J-PARC.

Result and Discussion: Neutron reflectivity curves at 30%RH and 80%RH on a Nafion film on Si(100) are shown in Fig. 1. Experimental data sets are shown by symbols, and fitted reflectivity curves are shown by the solid lines. The curves are vertically offset for clarity. In a higher Q region ($Qz > 0.2$ / Å^{-1}), a reflectivity abruptly increased. The characteristic bumps observed in Fig. 1 at both relative humidities can be explained by the existence of a layer with much different scattering length density from that of Nafion. A four-layer model structure was employed inside a Nafion film for curve-fitting: Topmost layer, Second layer, Third layer, and Interfacial layer. We numerically fitted the reflectivity data (Fig. 1) based on the model. Thus-obtained thicknesses of and the water uptakes inside four layers of the Nafion film on a Si substrate at 30%RH and 80%RH are shown in Fig. 2. Bumps seen in Fig. 1 were originated from highly-humidified Interfacial layers at the Si substrates even at 30%RH. Now, we have prepared thin Nafion films also on different substrates to elucidate the interfacial structures between the catalysts and the ionomers in the catalyst layer of polymer electrolyte fuel cells.

1) Y. Ogata, D. Kawaguchi, N. L. Yamada, and K. Tanaka, *ACS Macro Lett.*, **2**, 856-859 (2013).

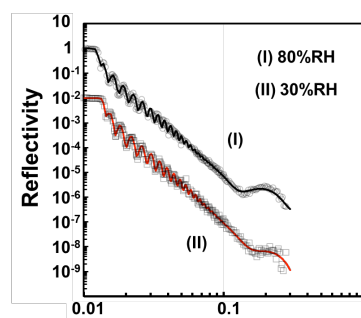


Figure 1. Neutron reflectivity curves for 100-nm Nafion film formed on silicon substrate at 80%RH (I) and 30%RH (II).

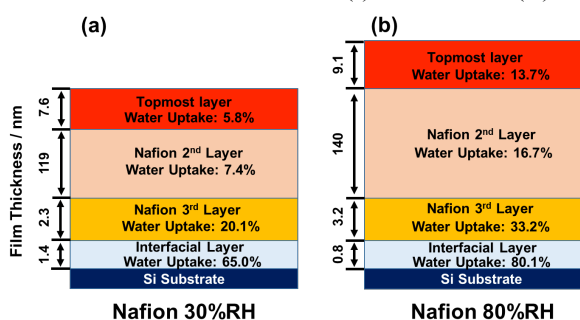


Figure 2. Thicknesses and water uptakes of four layers of Nafion/Si(100), (a)30 %RH, (b)80%RH

This work was supported by the SPer-FC project from NEDO, Japan. The neutron experiments at the Materials and Life Science Experimental Facility of the J-PARC was performed under a user

program (2016A0246).

Influences of ZnO Formation on Morphological Evolution of Zn Negative Electrode

Tomohiro Otani^a, Masato Nagata^b, Yasuhiro Fukunaka^c, Takayuki Homma^{a,b,c,*}

^a Department of Advanced Science and Engineering, Waseda University,
Shinjuku, Tokyo 169-8555, Japan

^b Department of Nanoscience and Nanoengineering, Waseda University,
Shinjuku, Tokyo 169-8555, Japan

^c Research Organization for Nano & Life Innovation, Waseda University,
Shinjuku, Tokyo 162-0041, Japan

*t.homma@waseda.jp

Zn is one of the promising negative electrode materials for secondary batteries featuring its low cost, abundant resources and compatibility with aqueous electrolyte. However, shape change of the electrode during charge-discharge cycles is major drawback for the application. During discharge of the electrode, ZnO forms on the electrode surface, which significantly affects reversibility of the electrode [1]. Although the zinc electrodeposition (charging) behaviors from alkaline zincate solution have been widely studied in past, deposition behavior with the presence of ZnO on the electrode surface is not well understood yet. In this study, morphological evolution during Zn electrodeposition was investigated after forming ZnO by anodic dissolution (discharge). In order to reversibly reduce ZnO to metal Zn, effects of Li⁺ addition on ZnO formation process was investigated.

Oxidation and reduction of Zn were performed in alkaline zincate solution containing 4.0 mol/L KOH + 0.25 mol/L ZnO. As an additive to the electrolyte, 0.50 mol/L LiOH was also added. Working electrode was Zn plate with mirror-like surface. Counter and reference electrodes were Zn and Hg/HgO, respectively. Working electrode was horizontally upward faced to counter electrode. Discharge and charge of the electrode (oxidation and reduction) were galvanostatically performed at 20 mA cm⁻². Morphology of films was analyzed by optical microscope and scanning electron microscope (SEM). In addition, oxidation and reduction behaviors were observed *in situ* by CCD camera. For this analysis, Zn wire was embedded in epoxy resin and the measurements were performed on edge of 500 μmφ Zn wire.

Zn electrodeposition behavior was analyzed after forming ZnO by anodic dissolution. First, to investigate influence of ZnO formation on following reduction, oxidation was stopped at different dissolution time. One was at 1100 s and the other was at 1300 s (potential reaching to -1.2 V, passivation state). In the latter case, ZnO was thought to fully cover the electrode surface. Under this condition, very rough and fragile deposits appeared soon after the reduction started. In contrast, when oxidation was stopped at 1100 s, no significant roughening of the surface was observed in reduction. In other words, ZnO formed at passivation conditions resulted in the non-uniform deposition behavior in following reduction step.

To suppress such a non-uniform deposition even after forming ZnO, LiOH was added to the electrolyte since Li⁺ was known to suppress ZnO crystal growth [2]. When oxidation and reduction were performed at the presence of Li⁺ in electrolyte, formation of the rough deposits was not observed even after passivating electrode in oxidation step. To understand different ZnO growth behaviors, surface morphology was analyzed by SEM after oxidation step. When ZnO was formed without LiOH, acicular structures were observed. When LiOH was added, shape of ZnO became particulate and size of each particle decreased. Thus, dominant ZnO growth in oxidation step resulted in non-uniform deposition behavior in following reduction. LiOH addition was effective to suppress the crystal growth of ZnO during oxidation, and this resulted in uniform Zn electrodeposition in following reduction.

This work was partly supported by the “Research & Development Initiative for Scientific Innovation of New Generation Batteries (RISING 2)” from the New Energy and Industrial Technology Development Organization (NEDO) of Japan. T.O. acknowledges the Leading Graduate Program in Science and Engineering, Waseda University from MEXT, Japan.

References

- [1] H.-I. Kim, E.-J. Kim, S.-J. Kim, H.-C. Shin, *J. Appl. Electrochem.* **45** (2015) 335.
- [2] N. Uekawa, R. Yamashita, Y. J. Wu, K. Kakegawa, *Phys. Chem. Chem. Phys.* **6** (2004) 442.

Effect of Water on Cu Electrodeposition from a Water-containing Deep Eutectic Solvent

Priscila Valverde Armas^a, Todd Green^b, Sudipta Roy^c

^{a,b,c}Department of Chemical and Process Engineering, Strathclyde University

James Weir building, 75 Montrose Street, 4th Floor, Scotland-United Kingdom, G1 1XJ

^apriscila.valverde-armas@strath.ac.uk, ^btodd.green@strath.ac.uk, ^csudipta.roy@strath.ac.uk

Ionic Liquids (ILs) have been proposed as alternative electrolytes for metal electrodeposition. Deep Eutectic Solvents (DESs) are a novel type of ILs tolerant to water. Moreover, DESs formulated from quaternary ammonium salts and hydrogen bond donors are promising electrolytes since they are water tolerant and they are available at a reasonable cost. Although DESs are hygroscopic and absorb water from the atmosphere, earlier studies to plate Cu have concentrated on low-water containing DESs (<0.5 wt% H₂O). However, for DESs to become exploitable, metal deposition from water-containing electrolytes requires to be investigated.

In this work, we have endeavoured to establish a quantitative correlation that might explain the effect of water content on the electrolyte and on Cu deposition process. The intrinsic concentration of water in the electrolyte was measured using Karl Fischer titration. Thereafter, to quantify the electrolyte uptake of water a time-dependant test was conducted. After adding various concentration of water to the electrolyte determined from the time-dependant experiment (3 to 15 wt%), the influence of water content was examined with polarisation experiments collected using a rotating disc electrode. Finally, Cu deposition was carried on steel substrata from electrolytes containing different weight percentages of water. Cu deposits were characterised with Scanning Electron Microscopy (SEM) (Figure 1) and Energy Dispersive X-ray Spectroscopy (EDS).

Different water contents in the electrolyte reduced the viscosity of the liquid which promotes the diffusivity of Cu²⁺ ions in the liquid. As a result, the limiting currents of the process increased. Higher water content changed the morphology of Cu films. Even at low water content (~3 wt%), the current distribution on the deposits is non-uniform. Furthermore, adding H₂O worsens the already uneven current distribution leading to less uniform Cu deposits.

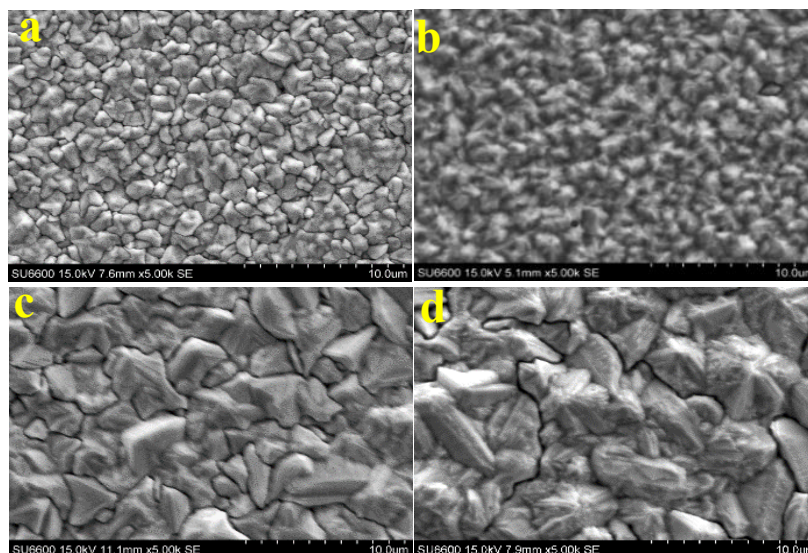


Fig 1. Micrographs of Cu deposits electroplated using an inert anode at 25 °C, rotation speed of 700 rpm from water-containing electrolytes (a) 1 wt%, (b) 3wt%, (c) 6wt% and (d) 10 wt% total H₂O.

Investigation of Electrochemical Activity of Cobalt-Manganese-Boron Catalysts Towards Ethanol and Borohydride Oxidation

K. Antanaviciute, Z. Sukackiene, A. Balciunaite, J. Vaiciuniene, L. Tamasauskaite Tamasiunaite,
A. Naujokaitis, E. Norkus

*Center for Physical Sciences and Technology
Sauletekio Ave. 3, LT-10257, Vilnius, Lithuania
kornelija.antanaviciute@gmail.com*

Fuel cells are promising, environmentally friendly and clean energy source, which generates electric power without any mechanical link. It is known that gold and platinum are very effective catalysts towards ethanol or sodium borohydride oxidation. High price of noble metals is the main reason why development and investigation of non-noble catalysts is important. In this study we present electrochemical activity investigation of low-cost cobalt alloys (cobalt-manganese-boron) catalysts towards ethanol and sodium borohydride oxidation. Cobalt alloys catalysts were prepared via electroless plating on copper surface when morpholine borane was used as a reducing agent. Cobalt-manganese-boron/copper catalysts were prepared using manganese (II) sulphate and potassium permanganate. Composition and morphology of catalysts surface was determined by using Field Emission Scanning Electron Microscopy (FESEM) and Inductively Coupled Plasma Optical Emission Spectroscopy (ICP-OES). The electrochemical activity of cobalt-manganese-boron/copper catalysts towards ethanol and sodium borohydride oxidation was determined by using cyclic voltammetry and chronoamperometry.

Acknowledgment

This research was funded by a grant (No. M-ERA.NET-1/2016) from the Research Council of Lithuania.

The Double Layer Capacitance of Room Temperature Ionic Liquids and the Influence of Water

Jochem Friedl, Ulrich Stimming

Chemistry - School of Natural and Environmental Sciences, Newcastle University
Bedson Building, Newcastle upon Tyne, NE1 7RU, United Kingdom
ulrich.stimming@newcastle.ac.uk

Room temperature ionic liquids (RTILs) have properties in between solid electrolytes and electrolyte solutions with a number of potential applications in electrochemical systems. One of their main advantages is their large potential window, in some cases 4.5-6V^{1,2}. The presence of water may reduce the width of this potential window. The adsorption of water at electrodes has only recently been investigated theoretically³ and experimentally^{2,4}. Feng et al. studied humid imidazolium-based ionic liquids and the adsorption of water at a carbon-like electrode using molecular dynamics simulations³. Motobayashi and Osawa used Surface Enhanced Infrared Absorption Spectroscopy (SEIRAS) as a tool to detect the presence of water in the electrochemical double layer (ECDL) of a humid imidazolium-based RTIL at an Au electrode⁴. They confirmed that water accumulates at the electrode even at low concentrations and that the adsorption is more pronounced at potentials positive of the p.z.c..

In this study we employ electrochemical impedance spectroscopy to determine the electrochemical double layer capacity C_{DL} of 1-butyl-1-methylpyrrolidinium bis[(trifluoromethyl)sulfonyl]imide (PyrTFSI) in contact with an Au(111) electrode. The water content of PyrTFSI is carefully adjusted and monitored. Recorded Nyquist spectra are fitted to three equivalent circuits and we give a detailed physical explanation for the single circuit elements.

Our experimentally obtained C_{DL} vs. potential curves are compared to curves calculated by mean-field theory (Fig. 1). Together, experiment and theory yield a conclusive understanding of the influence of water on the electrode-RTIL interface:

1. Our results show potential-dependent agglomeration of water in the ECDL;
2. Theoretical predictions regarding the sensitivity of C_{DL} of RTILs towards water are confirmed³;
3. Theoretical tools such as mean-field theory calculations with the compactness parameter γ of RTILs⁵ are shown to be able to reproduce experimental data. From the parameters used in the calculation properties of RTILs, like the preferred interaction of water with anions, can be deduced.

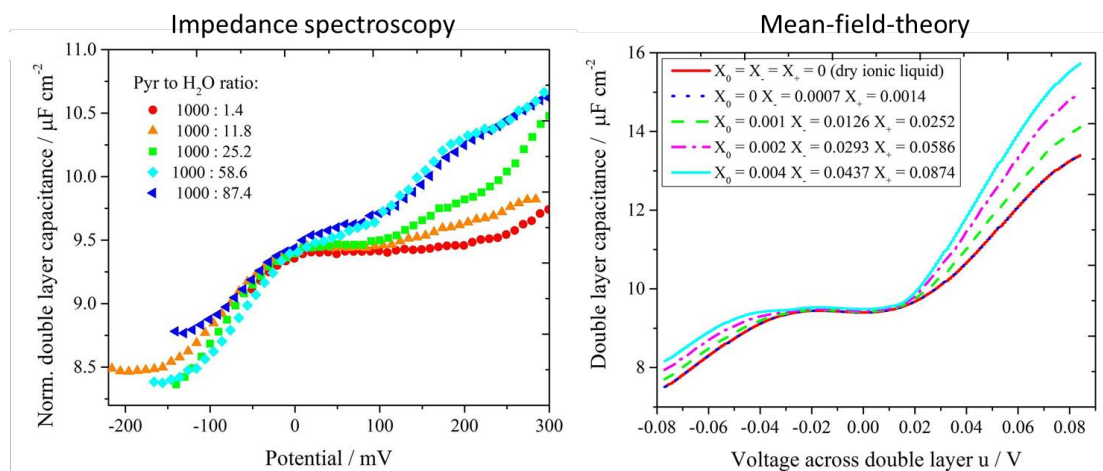


Figure 1: (left) Normalized double layer capacitance over potential of PyrTFSI with various contents of water obtained from electrochemical impedance spectroscopy. (right) Double layer capacitance over potential calculated from mean field theory².

- 1 M. C. Buzzeo, C. Hardacre and R. G. Compton, *ChemPhysChem*, 2006, **7**, 176–180.
- 2 J. Friedl, I. I. E. Markovits, M. Herpich, G. Feng, A. A. Kornyshev and U. Stimming, *ChemElectroChem*, 2016, **71**, 311–315.
- 3 G. Feng, X. Jiang, R. Qiao and A. A. Kornyshev, *ACS Nano*, 2014, **8**, 11685–11694.
- 4 K. Motobayashi and M. Osawa, *Electrochem. commun.*, 2016, **65**, 14–17.
- 5 A. A. Kornyshev, *J. Phys. Chem. B*, 2007, 111, 5545–5557.

Heterogeneous and homogenous catalysis in an All-Vanadium Flow Battery

Matthäa V. Holland-Cunz, Jochen Friedl, Ulrich Stimming

Chemistry - School of Natural and Environmental Sciences, Newcastle University

Bedson Building, Newcastle upon Tyne, NE1 7RU, United Kingdom

ulrich.stimming@newcastle.ac.uk

Redox Flow Batteries (RFBs) can be described as a hybrid between fuel cells and batteries. The aqueous RFB concept has many intrinsic advantages, like non-flammable electrolytes, independent scalability of energy and power, high life-time and high efficiencies. Unfortunately, it also inherits the two disadvantages of fuel cells and batteries: Energy density is low, like in a battery, and electrode kinetics are slow, as in fuel cells. Those two short-comings lead to electricity storage costs that are much higher than the current goal of the ARPA-e, which is 100 US\$ per kWh.

In this work, we describe our efforts to increase the power density of the All-Vanadium RFB (VRB) by heterogenous catalysis of the V^{2+}/V^{3+} and the VO^{2+}/VO_2^+ redox reactions¹⁻³. A newly developed procedure based on electrochemical impedance spectroscopy was employed to unambiguously determine the rate of electron transfer on porous carbon structures such as multi-walled carbon nanotubes and carbon felts¹. Combining these results and x-ray photoelectron spectroscopy, we show that surface functional groups such as hydroxyl, carbonyl and carboxyl increase the wetted surface area A^{wet} , increase the rate constant k_0 for the V^{2+}/V^{3+} -redox reaction but decrease the rate constant k_0 for the VO^{2+}/VO_2^+ -redox reaction². Either half-cell can exhibit the higher normalized rate constant, depending on the amount of hydroxyl on the electrode surface. Reaction mechanisms based on these results are discussed.

Because heterogeneous catalysis of the VO^{2+}/VO_2^+ -redox reaction was unsuccessful, we investigated homogeneous catalysis. Phosphoric acid is often added to VRB electrolytes to improve the stability of the VO_2^+ in solution at high (>45 °C) temperatures⁴. We show that the rate constant of the VO^{2+}/VO_2^+ -redox reaction is 63 times higher in 1 M H_3PO_4 than it is in 1 M H_2SO_4 (see Fig. 1). Therefore, phosphoric acid has not only a stabilizing effect, but also a catalytic effect. Solution ^{51}V NMR indicated that the chemical composition of the V(V) species depends on the anions (PO_4^{3-} or SO_4^{2-}) present in the electrolyte. The reaction mechanism in both electrolytes is discussed in detail.

In conclusion, we present a (heterogeneous) catalyst for the V^{2+}/V^{3+} redox reaction, and a (homogeneous) catalyst for the VO^{2+}/VO_2^+ redox reaction. In combination, it might be possible to produce a high power VRB.

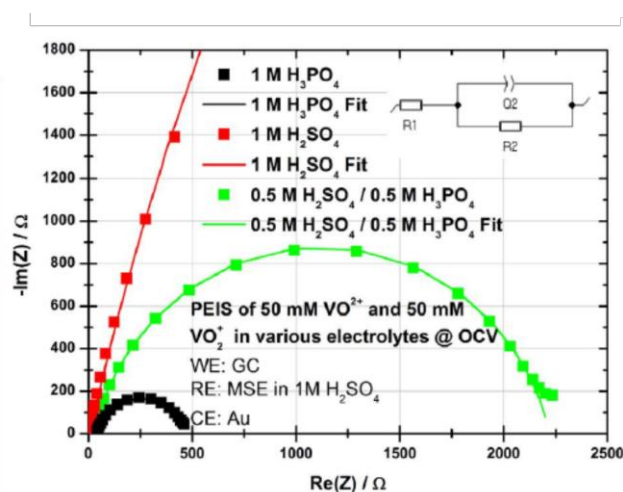


Figure 1: Nyquist plot of 50mM VO^{2+} and 50 mM VO_2^+ in 1M H_3PO_4 (black), 1M H_2SO_4 (red) and a mixture of the two acids (green). The data points were fitted to the Randles circuit shown in the inset. From ref. ⁴

Bibliography:

- 1 J. Friedl, C. M. Bauer, A. Rinaldi and U. Stimming, *Carbon*, 2013, **63**, 228–239.
- 2 H. Fink, J. Friedl and U. Stimming, *J. Phys. Chem. C*, 2016, **120**, 15893–15901.
- 3 J. Friedl and U. Stimming, *Electrochim. Acta*, 2017, **227**, 235–245.
- 4 M. V. Holland-Cunz, J. Friedl and U. Stimming, *J. Electroanal. Chem.*, DOI:10.1016/j.jelechem.2017.10.061.

Electrochemical and Spectroelectrochemical Analysis of Pyridine Derivatives as Materials for Optoelectronic Applications

Przemysław Data,^{1,2,3} Marharyta Vasylieva,¹ Piotr Pander.²

¹ *Silesian University of Technology, Faculty of Chemistry, Department of Physical Chemistry and Technology of Polymers, 44-100 Gliwice, Strzody 9, Poland*

² *Durham University, Department of Physics, South Road, DH1 3LE, Durham, United Kingdom*

³ *Centre of Polymer and Carbon Materials of the Polish Academy of Sciences, Zabrze, Poland*
przemyslaw.data@polsl.pl

Many of organic materials can already be encountered in prototypical, and commercial, chemical sensors, photovoltaic cells and AMOLED display devices. Their major advantage is the possibility to tailor their properties, including the colour of emitted light, by modifying their molecular structure. The optimum operation of OLEDs based on luminescent polymers requires maintaining a balanced distribution of injected charge carriers, positive (holes) and negative (electrons). This ensures the effective recombination of these individual charges and consequently significantly improves OLED efficiency. However, a large energy gap, a high ionization potential, or low electron affinity often lead to disruption of the desired equilibrium. The control of these characteristics is achieved by influencing the effective conjugation length as well as the introduction of electron-donating or electron-accepting substituents to the chromophore.

We would like to present several pyridine derivatives where the pyridine was the acceptor and carbazole, phenoxazine or phenothiazine as the donor for D-A and D-A-D type molecule design. The subject of the study was mono- (3 or 4 position) and di-substituted (3,5 positions) pyridine with phenothiazine or phenoxazine substituents. Electrochemical and UV-Vis, ESR spectroelectrochemical studies allow determining the effects of excitation states and the impact of charged units. These compounds have proved themselves to be good donors, and they have a low value of HOMO energy level. ESR measurements were shown, that cation radicals and isolated diradical dication are localized on nitrogen atom upon phenothiazine/phenoxazine moiety. We observed doublet-triplet ESR spectrum in planar mono-substituted phenoxazine derivatives. The twist angles between both donors and acceptor are smaller in triad contains phenothiazine in lateral position too. This is confirmed by cyclic voltammetry, with close oxidation peaks recorded for the two oxidation steps and UV-Vis absorption spectra typical for dication. This state, however, is paramagnetic, but the reduced g-factor indicates electron interaction between both lateral groups via central acceptor unit.



Donor-Acceptor Light Emitting
EXCIplexes as Materials for Easy-to-
Tailor Ultra-efficient OLED LIGHTing
H2020-MSCA-ITN-2015/ 674990



Effect of electrolyte flow on the evolution of microsteps during zinc electrodeposition

Yuta Masuda^a, Tomohiro Otani^b, Yasuhiro Fukunaka^c, Takayuki Homma^{a, b, c, *}

^a Department of Applied Chemistry, Waseda University, Shinjuku, Tokyo 160-8555, Japan

^b Department of Advanced Science and Engineering, Waseda University, Shinjuku, Tokyo 160-8555, Japan

^c Research Organization for Nano & Life Innovation, Waseda University, Shinjuku, Tokyo 162-0041, Japan

*t.homma@waseda.jp

Zinc is one of the promising candidates for negative electrode material of a flow-assisted batteries because of compatibility with aqueous electrolyte and low cost. The charge-discharge cycle for this system is Zn deposition and dissolution directly onto current collector under electrolyte flow. Despite these simple reactions, it is difficult to perform reversible cycles due to evolution of non-uniform Zn electrodeposits, called mossy structures. Electrodeposition behavior of mossy structures is very characteristic to Zn deposition because they appear even under flowing electrolyte conditions or at low overpotential, which are generally effective ways to obtain uniform deposition. In this study, to understand the conditions which initiates the formation of mossy structures under electrolyte flow, influences of electrolyte flow on the Zn electrodeposition process were analyzed by two types of rotating disk electrode (RDE). Furthermore, the electrodeposition behavior was also investigated in the flow cell and deposition behavior was compared with that with the RDE.

Zn electrodeposition was performed under galvanostatic conditions from alkaline zincate solution ($6.0 \text{ mol dm}^{-3} \text{ KOH} + 0.50 \text{ mol dm}^{-3} \text{ ZnO}$). To investigate effects of electrolyte flow, two types of RDEs were used; One embedded substrate at the bottom of cavity (RDE1) and the other exposed electrode surface directly to electrolyte (RDE2). Electrochemical measurements were performed with three electrodes, Cu working (diameter = 0.80 cm), Zn counter and Hg/HgO reference electrodes. Cu W.E. was downward faced to Zn counter. To examine the detail of Zn deposition at initial stages under conditions close to flow-assisted batteries, fluidic device was fabricated by 3D printer. In this case, Cu W.E. was vertically faced to Zn C.E. and electrolyte flow rate was controlled by peristaltic pump from 0 to 200 mL/min.



Fig.1 two types of RDEs

First, in order to understand the electrodeposition behavior of zinc by RDE1, the morphology was investigated at a rotation speed from 0 to 1800 rpm at -5 mA/cm^2 . Although compact deposits were obtained at the center of the W.E., mossy structures were preferentially formed at the edge of RDE1. Since such a non-uniform distribution of mossy structures was not observed in static condition (0 rpm), non-uniform deposition was thought to be caused by flow geometry of the electrolyte; the flow was suppressed at the edge of RDE1, resulting in preferential formation of mossy structures. In order to verify this, the other type of RDE was introduced. When deposition was performed on RDE2, non-uniform distribution of mossy structure was not observed. Accordingly, mossy structures formation was promoted by non-uniform electrolyte flow on the electrode surface. Furthermore, in order to understand the behavior of nucleation and growth under electrolyte flow, especially at the initial stages of mossy structures formation, microstructures of Zn deposits were investigated by SEM. Here, flow cell was used to investigate the behaviors under conditions close to practical operation. As a result, unclear microsteps were formed under electrolyte flow at initial stages. It was reported that intensive and continuous nucleation on the microsteps could cause formation of mossy structure in previous study [1]. Therefore, it was proposed the mossy structure could be suppressed through forming unclear microsteps by flowing electrolyte. From these results, it was suggested that the rotating electrode and flowing electrolyte itself could suppress the formation of mossy structure by making the microsteps unclear. However, partial inhibition of electrolyte flow could promote the formation of mossy structure, which caused the non-uniform distribution of Zn electrodeposits.

This work was partly supported by the “Research & Development Initiative for Scientific Innovation of New Generation Batteries (RISING 2)” from the New Energy and Industrial Technology Development Organization (NEDO) of Japan.

[1] T. Mitsuhashi, Y. Ito, Y. Takeuchi, S. Harada, T. Ujihara, Non-uniform electrodeposition of zinc on the (0001) plane, *Thin Solid Films* 590 (2015) 207.

First-Principles Study of Reaction Mechanism of Reducing Agents on Ni and Cu in Electroless Deposition Processes

Yusuke Onabuta^a, Masahiro Kunimoto^b, Hiromi Nakai^c and Takayuki Homma^{a,b}

^aDepartment of Applied Chemistry, ^bResearch Organization for Nano & Life Innovation

and ^cDepartment of Chemistry and Biochemistry,

^{a, c}Waseda University, Shinjuku-ku, Tokyo 169-8555, Japan

and ^bWaseda University, Shinjuku-ku, Tokyo 162-0041, Japan

t.homma@waseda.jp

Electroless deposition process has been applied to various industrial fields as one of the element technologies to fabricate metal thin films. To improve the controllability of this process, investigation of the detailed reaction mechanism is essential. The catalytic activity of metal surfaces for each reducing agent reaction is, in particular, one of the important aspects to be understood. For systematic analyses of such properties of metals, theoretical calculation can be employed as a powerful tool. Our previous theoretical studies, in which the metal surface is modeled by a cluster, reveal that the dehydrogenation should be a rate-determining step in the all elementary steps and the catalytic activities of Pd for hypophosphite are attributed to its d-band structure [1,2]. However, the simulation using such a cluster model often encounters difficulties in modeling many of transition metal surfaces with more complex d-band, such as Ni or Pt, due to the edge effect and the limited size. In this work, the dehydrogenation reactions of formaldehyde and hypophosphite on Ni surfaces, which are hard to be modeled by clusters, are analyzed and compared to the reactions on Cu by density functional theory (DFT) using a slab model to explore the predominant factor to determine the catalytic activity of each metal surface.

All calculations were carried out by using Vienna Ab initio Simulation Package (VASP). The cutoff energy for the plane wave basis set was set at 400 eV. The core electrons were described by pseudopotentials constructed with the Projector Augmented Wave (PAW). The exchange-correlation energies were evaluated with the Perdew, Burke and Ernzerhof (PBE) functional. Metal surfaces were modeled as a periodic (4 x 4) surface unit cell with three layers, whose orientation was set (111). The bottom two layers were fixed. The oxidation reactions of formaldehyde and hypophosphite consist of adsorption, dehydrogenation and oxidation, as elementary steps. In particular in this study, the dehydrogenation step was focused on, because it was considered to be the rate-determining step for the whole process[1]. Assuming that the process is employed in high pH solution, the molecular structures of formaldehyde and hypophosphite were modeled as $\text{H}_2\text{CO}(\text{OH})^-$ and H_2PO_2^- , respectively.

Both reductants were assumed to adsorb on metal surfaces via H atoms (Fig. 1), based on previous results which had suggested that O atoms had been oriented to the bulk due to the strong interaction with solvent molecules[2]. The reaction energy profiles of dehydrogenation on Cu(111), obtained from the geometry optimization of adsorption structure, clearly show the trend of its catalytic activity for each agent that corresponds to experimentally observed phenomena: the activation energy for dehydrogenation of formaldehyde turned out to be lower than that of hypophosphite. On Ni(111), the bond lengths between the center atom (C or P) and H tend to be much longer than on Cu, which might indicate the relatively stronger catalytic activity of Ni surface for each. Density of state results indicate that this difference derives from the electronic structural properties from each metal. These results suggest that slab model is capable to analyze the catalytic activity of metal surface with much complex electronic structure in the electroless processes.

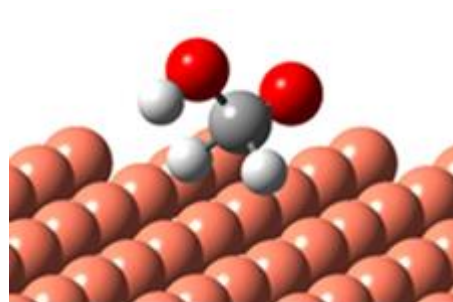


Figure 1. The adsorption structure of formaldehyde on Cu(111)

[1] M. Kunimoto, T. Shimada, S. Odagiri, H. Nakai, T. Homma, *J. Electrochem. Soc.*, **158**, D585-D589 (2011).

[2] M. Kunimoto, K. Seki, H. Nakai, T. Homma, *Electrochemistry*, **80** (4), 222-225 (2012).

Porous Nanocomposite for Highly Sensitive Pressure Sensor

Fu-Ren Xiao, Chun-Hao Su and Ying-Chih Liao*

Department of Chemical Engineering, National Taiwan University, Taipei, Taiwan

No. 1, Sec. 4, Roosevelt Rd., Taipei 10617, Taiwan (R.O.C.)

e-mail: liao@ntu.edu.tw

There are many advantages for porous and flexible pressure sensors, including light weight, good flexibility, great heat resistance, high mechanical strength, and shock prevention. Among many pressure sensing materials, piezo-resistive materials have been widely used due to its unique electrical properties and mechanical behavior. In this study, a novel nanocomposite material with porous structure is synthesized for pressure sensing. Single-wall carbon nanotubes as the conductive filler is embedded in fluoro-rubber G801 to form a piezo-resistive nanocomposite. To enhance the sensitivity, a foaming agent, AIBN, is added in the synthetic process and is heated to create porous structures. The larger contact areas of these pores result in better resistance/force sensitivity. The relationship between the external force on the composite formulation and the resulted electrical resistance will be carefully examined to understand the conduction pathway in the composite materials. Moreover, the mechanical strength and stability of the nanocomposite material will also be investigated. Finally, several examples, such as vibration detectors or heart-beat sensor, will be demonstrated to show the potential of this nanomaterials for flexible sensing applications.

Three-Dimensional Ordered Macro/Meso Porous Composite Materials in Electrode Array
Configuration for Gas Sensing Applications

Yu-Szu Chou, Pei-Sung Hung, Guang-Ren Wang, Chuan-Jyun Wang, Pu-Wei Wu*
Department of Materials Science and Engineering, National Chiao Tung University
Hsinchu 300, Taiwan, ROC
*ppwu@mail.nctu.edu.tw

Breath sample analysis has drawn much attention recently due to increasing demand for rapid and non-invasive early detection as affordable personal care products. Several prototypes for these devices have been developed and tested. Nevertheless, performances regarding to sensitivity and response/recovery time usually fall behind the requirements for practical applications. Herein, we demonstrate a facile method for the fabrication of 3D inverse opaline structures to utilize the limited real estate on the electrode arrays. Through the construction of a well-ordered and interconnect porous scaffold, increase amount of sensor materials could be employed with a larger surface area and sufficient mechanical strength as compared to conventional nanostructured films. In addition to structural design, selective composite materials for enhanced sensitivity with the aid of heterojunction formation are introduced in the skeleton construction. Several oxides are made into nanoparticles with controlled size, or are fabricated as the backbone of inverse opaline films. Processing parameters and material combinations are studied, evaluated, and optimized for enhanced sensor performance. Structural characterizations of these composite porous films are conducted by SEM and TEM examination, and XRD and XPS methods are employed for compositional analysis.

Analysis of Interface Behavior of Room-temperature Ionic Liquids / Air Electrodes in Lithium-Air Secondary Batteries

Koichi Ui, Yushi Sato, Toshihiko Mandai, and Tatsuya Takeguchi

Department of Frontier Materials and Function Engineering,
Graduate School of Engineering, Iwate University,
4-3-5 Ueda, Morioka, Iwate 020-8551, Japan
kui@iwate-u.ac.jp

Introduction Lithium-air secondary batteries (LABs) have attracted attention owing to the outstanding energy density. The open atmospheric system and violent reactivity of the discharge intermediates however strongly limit the electrolyte choice applicable to LABs. Ionic liquid (IL)-based electrolytes are promising electrolytes for LABs because of the low volatility and high chemical/electrochemical stabilities. In the IL-based electrolyte, the carbon particles air electrodes retained an original size, whereas lithium alkyl carbonates were found in the organic solvent-based counterpart¹. However, the influence of the components of the electrolyte on the interface behavior has not yet been clarified. In this study, we analyzed the interfacial behavior of IL-based electrolytes/air electrodes in LABs.

Experimental Ketjen black was used to make an air electrode. A CR2032 coin-type cell, which consists of the air electrode, a lithium metal foil, 1 mol dm⁻³ Li-TFSA/P₁₃-TFSA (IL-based electrolyte), and a glass fiber filter separator, was used for the electrochemical measurements. For comparison, 1 mol dm⁻³ LiCF₃SO₃/TEGDME was used as an organic solvent-based electrolyte. Surface morphology was observed using a field-emission scanning electron microscope (FE-SEM). The electrochemical impedance spectroscopy was performed to analyze the electrochemical behaviors at the interface between electrolytes and air electrodes.

Results and Discussion Fig. 1 shows the cycle performance of air electrodes. The cycle performance for the IL-based electrolyte was stable over 100 cycles, whereas the discharge capacity suddenly decreased around 50 cycles for the organic solvent-based electrolyte. In the organic solvent-based electrolyte, severe cracks were observed on the surface of air electrode even after initial discharge. In contrast, in the IL-based electrolyte, no crack was found on the surface, indicating that the components of electrolytes have a significant impact on the surface morphology of the air electrode during discharging.

Nyquist plots of air electrodes after 30 and 55th charge were measured. In the organic solvent-based electrolyte, the interface resistance increased from 30 to 55th charge. In contrast, in the IL-based electrolyte, there was no significant change in the interface resistance. Owing to the small change in the interface resistance, it is considered to exhibit good cycle performance in the IL-based electrolyte. Degradation of cycle performance would be caused by an increase in the interface resistance due to the decomposition products.

Based on these results, the suitable choice of electrolytes can improve the electrochemical characteristics of LABs.

Reference

1) F. Mizuno, et al., *J. Power Sources*, **228**, 51 (2013).

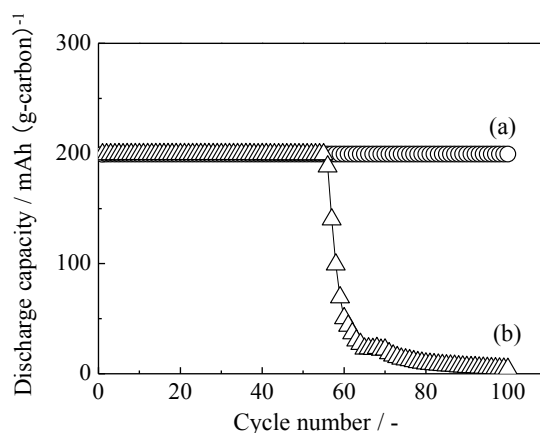


Fig. 1. Cycle performance of air electrodes at 25 °C; carbon amount: 0.5 mg cm⁻², discharge capacity: 200 mAh (g-carbon)⁻¹, current density: 100 mA (g-carbon)⁻¹; (a) Li-TFSA/P₁₃-TFSA and (b) LiCF₃SO₃/TEGDME.

Anodic Electrodeposition of Tungsten Oxide Hydrate Films from Tungstate-Citrate Complex Solutions

Junji Sasano, Yuya Kojima, Takuya Sakai, Kentaro Nishiyama, Seiji Yokoyama, Masanobu Izaki
Toyohashi University of Technology
1-1 Hibarigaoka, Tempaku-cho, Toyohashi, Aichi, 441-8580, Japan
sasano@me.tut.ac.jp

Tungsten oxide is an n-type semiconductor with a bandgap of about 2.5-3.5 eV, and it shows characteristic electrochromic responses under electric current application. As an efficient formation process of thin films of this material we have developed an anodic electrodeposition method. Under the application of anodic electrode potential, water solvent is oxidized to produce oxygen, leading to decrease in pH of the solution in the vicinity of electrodes; then tungsten oxide hydrates ($\text{WO}_3 \cdot (\text{H}_2\text{O})_n$), which are stable in acidic condition, deposit on the electrode surface. We have revealed the conditions of the solution, especially concentration of tungstate ions, affect the morphology and crystal structure of the deposited films, as well as their bandgap energy.¹ Moreover, combining these films with other anodically electrodeposited films of mixtures of tin dioxide and hydroxide ($\text{Sn}(\text{O},\text{H})_x$), we have demonstrated a simple formation method of a solid-state electrochromic device.² Since the method of anodic electrodeposition itself is similar to conventionally used electroplating of metal films, it is suitable to industrial production. The anodic electrodeposition of $\text{WO}_3 \cdot (\text{H}_2\text{O})_n$, however, is not as easily to control as normal electrodeposition of metal due to its sluggish electrode reaction. One reason for the obstacle is the pH buffering effects due to the formation of polytungstate ions. To overcome this obstacle we investigated anodic electrodeposition of tungsten oxide hydrate from the baths containing tungstate-citrate complex ions.

Before starting electrochemical measurements, we surveyed the solution chemistry of electrolytes containing sodium tungstate dihydrate ($\text{Na}_2\text{WO}_4 \cdot 2\text{H}_2\text{O}$) and citric acid. Molar ratio of citrate to tungstate ions in solution was varied from 0 to 5, and each solution was titrated with sulfuric acid; then, the transmittance of each solution was measured with a spectrophotometer. From the transmission spectra the pH value where precipitation starts to occur in each solution was determined. As the results, we found that the solution containing 0.1 mol/L $\text{Na}_2\text{WO}_4 \cdot 2\text{H}_2\text{O}$ and 0.1 mol/L citric acid showed the highest pH value for precipitation, and we chose the solution to be used for successive electrochemical measurements.

Electrochemical measurements were performed using a three-electrode electrochemical cell with glass substrates coated with fluorine-doped tin oxide (FTO) films, an Ag/AgCl electrode, and a Pt plate as working, reference, and counter electrodes, respectively. Anodic electrodeposition of $\text{WO}_3 \cdot (\text{H}_2\text{O})_n$ was conducted at various electrode potentials between 2.0 and 3.0 V vs. Ag/AgCl. Scanning electron microscope (SEM) observation revealed that the obtained films have platelet structures. (Fig. 1)

Further details will be discussed in the presentation.

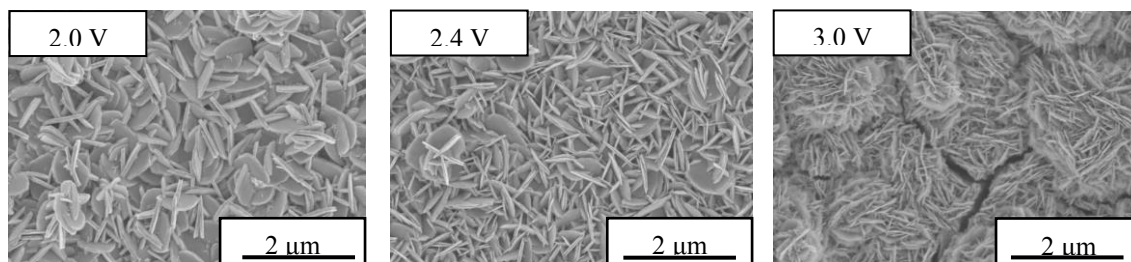


Fig. 1 SEM images of tungsten oxide hydrate films deposited by anodic electrodeposition at 2.0 V (left), 2.4 V (center), and 3.0 V (right) vs. Ag/AgCl from the solution containing tungstate-citrate complex ions.

References

- 1) K. Nishiyama, J. Sasano, S. Yokoyama, and M. Izaki, *Thin Solid Films*, **625**, 29, (2017).
- 2) K. Nishiyama, R. Matsuo, J. Sasano, S. Yokoyama, and M. Izaki: *AIP Advances*, **7**, 035004, (2017).

LiFePO₄/C Composite Cathode Materials with Different Types of Graphene Oxides and Its Performance

Ya-Ru Li¹ and Chun-Chen Yang^{1,2,*}

¹ Department of Chemical Engineering, Ming Chi University of Technology (MCUT)

² Battery Research Center of Green Energy, Ming Chi University of Technology (MCUT)

#84 Gungjuan Rd., Taishan Dist., New Taipei City 24301, Taiwan, R.O.C.

*ccyang@mail.mcut.edu.tw

Abstract

The work reported preparation of LiFePO₄/C (LFP/C) with 2 different types of graphene oxides (GOs) by a sol-gel method. In order to enhance the electrochemical performance of LFP/GO/C, we prepared the as-prepared GO and 3D-GO additives for LFP/C. In Figure 1 and 2, The 3D-GO additive was prepared by using PMMA polymer sphere as the template. The characteristic properties were examined by scanning electron microscopy (SEM), transmission electron microscopy (TEM), X-ray diffraction (XRD), the galvanostatic charge-discharge method, AC impedance method and cyclic voltammetry method. It was found that the discharge capacities of LFP/C material are 139.68, 137.92, 127.08, 116.25, 96.25, 85.42, 65.21 mAhg⁻¹ at 0.1C, 0.2C, 0.5C, 1C, 3C, 5C and 10C, respectively. In contrast, Table 1 and Figure 3 was revealed that the discharge capacity of LFP/1%3D-GO composite material shows 151.57, 143.25, 139.20, 132.74, 119.47, 109.14, 96.98 mAhg⁻¹ at 0.1C to 10C, respectively. In term of the long-term cycling performance, we found that the discharge capacities at 0.1C achieved around 150.19 mAh g⁻¹, then decline to 147.16 mAh g⁻¹ after 30 cycles. It shows excellent charge retention ca. 97.7%. Moreover, it was found that discharge capacities at 1C start at 129.17 mAh g⁻¹, then gradually decline to 121.59 mAh g⁻¹ after 100 cycles; it shows good charge retention ca. 94.1%. The diffusion coefficient of lithium ion (D_{Li+}) was measured by the AC impedance and CV methods. It found that the D_{Li+} of LFP/1%3D-GO/C (1.53×10⁻¹³ cm² s⁻¹) has higher than that of pure LFP/C (1.38×10⁻¹⁴ cm² s⁻¹) by an AC impedance method. By comparison, we also found that the D_{Li+} of LFP/1%3D-GO (7.71×10⁻¹⁰ cm² s⁻¹) has better D_{Li+} than that of pure LFP/C (4.32×10⁻¹⁰ cm² s⁻¹) by a CV method. We found that our homemade 3D-GO additive can effectively improve electrochemical performance of LFP/C composite material.

Keywords: LiFePO₄/C (LFP/C), Sol-gel method, Graphene oxide (GO), 3D-GO, Lithium ion Diffusion coefficient

Table.1 Comparisons of LFP/GO/C cathodes

Rate : 5C	LFP/C	LFP/GO	LFP/3DGO
Capacity _{Avg} /mAh g ⁻¹	90.53	68.92	108.65
ΔQ /%	0.00	-23.87 %	+20.02 %
Rate : 10C	LFP/C	LFP/GO	LFP/3DGO
Capacity _{Avg} /mAh g ⁻¹	75.14	57.39	95.63
ΔQ /%	0.00	-23.63 %	+27.26 %

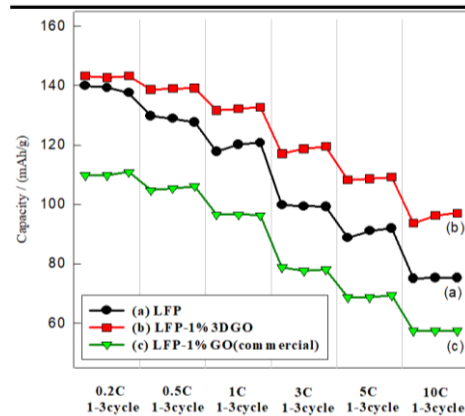


Figure 3. Comparisons of LFP/GO/C cathodes

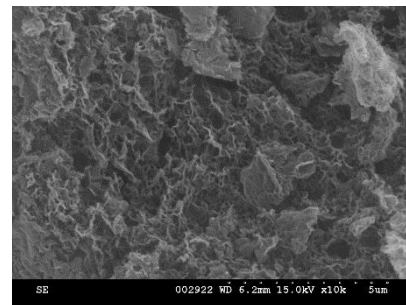


Figure 1. SEM image of 3D-GO

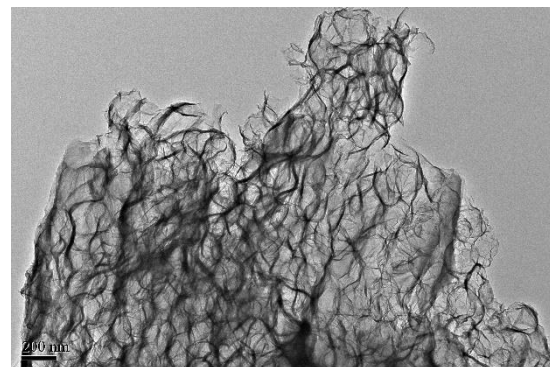


Figure 2. TEM image of 3D-GO

Electrodeposited MnO₂//Polyaniline on Electrospun Carbon Nanofibers for Asymmetric Electrochemical Capacitor in Water Desalination

Jingting Huang, Chia-Hung Hou

Graduate Institute of Environmental Engineering, National Taiwan University

No. 1, Sec. 4, Roosevelt Rd., Taipei 10617, Taiwan

r05541204@ntu.edu.tw

Technologies of water desalination have become concerned since rapidly growing popularity and gradually exhausted resource. Capacitive deionization (CDI) is an emerging electrochemical water desalination technology with several advantages of low energy input, easy regeneration and environmental friendliness. In CDI, anions and cations are electrostatically removed from saline water by applying an external electrical field between two porous electrodes, and thereby the ions can be temporarily immobilized. There are two major mechanisms of charge storage in capacitors: (1) the electrical double-layer (EDL) capacitance from a pure electrostatic interaction; and (2) the pseudocapacitance based on Faradaic redox reaction. Typically, porous carbon electrodes that remove salt ions based on EDL formation may have limited salt adsorption capacity. Noteworthy, pseudocapacitors, using fast, reversible redox reactions on the active materials (i.e., transition-metal oxides and conducting polymers) could significantly enhance the charge storage capacity. For the adsorption of cation, manganese oxide (MnO₂) is a common type of transition-metal oxides materials due to its high theoretical capacitance (>1000 F g⁻¹), eco-friendly characteristic and well stability. For the adsorption of anion, polyaniline (PANI) is one of the earliest known conducting polymers which has the virtue of high conductivity, easy synthesis and low cost. However, the large electrical resistance of MnO₂ could limit the Faradaic charge-transfer for storing salt ions in CDI application. Furthermore, electrospinning is a simple process to generate continuous electrospun nanofiber webs. After stabilization and activation, the electrospun nanofiber web will turn into a porous and high conductivity activated nanofiber web (ANF), which also stand for an excellent material as a base of pseudocapacitor mentioned above. In this study, MnO₂ and PANI will be electrodeposited on ANFs to form hybrid materials. The electrochemical water desalination based on the asymmetric capacitor, in which the PANI/ANF and MnO₂/ANF were used as anode and cathode, respectively, is expected to demonstrate high amount of salt adsorption capacity. To begin with, electrospun fabricated by 10 wt% polyacrylonitrile (PAN) dissolved in dimethylacetamide (DMAc) is activated and carbonated to form ANF. After scanned by cyclic voltammetry (CV) and galvanostatic charge-discharge (GC), high specific capacitance (70 F g⁻¹), low iR drop and stable electric property are obtained. ANF electrodeposited with different loading of pseudocapacitive materials (MnO₂ on the cathode and PANI on the anode) will be employed in an asymmetric electrochemical capacitor. Furthermore, the salt adsorption capacity is investigated by batch-mode experiments in asymmetric electrochemical capacitor. It is believed that the electrodeposited MnO₂//PANI on ANF for asymmetric electrochemical capacitor is a potential water deionization system for offering high-performance desalination.

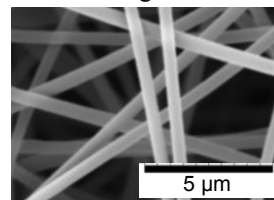


Figure 1. SEM images of the ANF

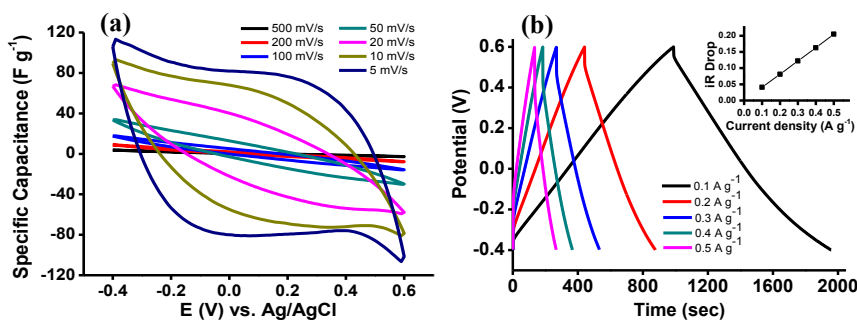


Figure 2. (a) CV curve of the ANF electrode at various scan rates. (b) GC curves of the ANF electrode at various current density (inset showing iR drops of the electrodes as a function of current density). CV and GC curves were obtained in 1 M NaCl aqueous solution.

Effects of Atomic Diffusion on Electroless Ni-P Film/Epitaxial Gold Nanoparticles/Silicon Wafer Interface

Yuichi Takasaka¹, Ryo Fujii¹, Kotaro Higashi¹, Susumu Sakamoto^{1,2}, Ayumu Matsumoto¹, Naoki Fukumuro¹, Shinji Yae^{1,*}

¹) Department of Chemical Engineering and Materials Science, Graduate School of Engineering, University of Hyogo 2167 Shosha, Himeji, Hyogo 671-2280, Japan

²) Nippon Oikos Co., Ltd., 3-6-16 Mitsusadadai, Yahatanishi, Kitakyushu, Fukuoka 807-0805, Japan

*yae@eng.u-hyogo.ac.jp

Formation of adhesive metal film on silicon (Si) wafers is important to obtain infallible electrical contacts for various devices. Autocatalytic electroless deposition has several advantages, e.g. simplicity of process, uniformity of deposited films, and covering on complicated structures. However, adhesion of metal films obtained on Si substrates using conventional pretreatments is much lower than that required for the devices. We recently developed a new surface-activation process for the direct electroless deposition of adhesive metal films on Si substrates [1–3]. This process consists of two steps: Step 1) formation of gold (Au) nanoparticles by electroless displacement deposition; and Step 2) metal film formation by autocatalytic electroless deposition. As shown in Fig. 1, we reported that single crystalline Au nanoparticles are epitaxially deposited on Si substrates [3] and Au-Si alloy is formed at the Au-Si interface [2,3]. The epitaxially grown Au nanoparticles cause high adhesion of the deposited films [3]. In this study, we investigate effects of aging on nickel-phosphorus (Ni-P) alloy films electrolessly deposited on Si substrates using Au nanoparticles.

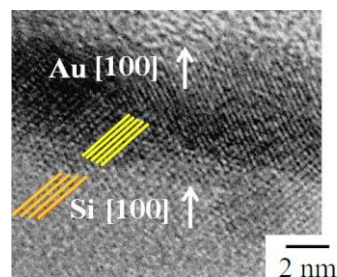


Fig. 1 Cross-sectional TEM image of Au/Si interface.

The Au nanoparticles were deposited on p-Si (100) substrates by immersing in a 0.5 mM HAuCl₄ solution containing 0.15 HF at 278 K. The Ni-P films were formed on the Si substrates using a solution containing 0.1 M NiSO₄ and 0.3 M NaPH₂O₂ at 343 K. The adhesion of deposited films was examined by a tape test based on JIS H8504 corresponding to ISO 2819 after room temperature aging at atmospheric ambient.

Fig. 2 shows the percentage of the area of the Ni-P films that remained on the Si substrate after the tape test as a function of the film thickness. No peeling occurred for the films thinner than 0.8 μm immediately after the film deposition. The starting point of peeling increased with aging time and reached at 1.7 μm after aging for 7 days. Since the starting point increased with the square root of aging time, we consider that the improvement in adhesion is due to the atomic diffusion of Au into Si at room temperature.

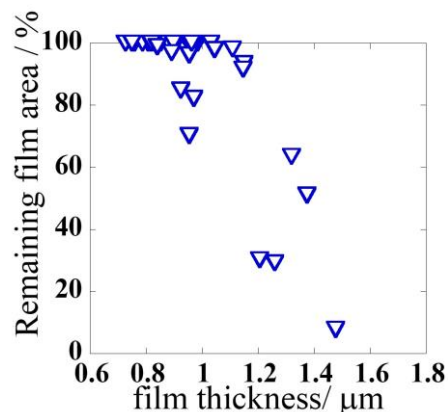


Fig. 2 Remaining area of Ni-P films immediately after the deposition on Si vs. film thickness.

Acknowledgement

This work was partly supported by JSPS KAKENHI Grant Number JP26289276.

References

1. S. Yae, M. Enomoto, H. Atsushiba, A. Hasegawa, N. Fukumuro, S. Sakamoto, and H. Matsuda, *ECS Trans.*, **53**(6), 99 (2013).
2. H. Atsushiba, Y. Orita, S. Sakamoto, N. Fukumuro, and S. Yae; *ECS Trans.*, **61**(10), 9 (2014).
3. N. Yamada, H. Atsushiba, S. Sakamoto, N. Fukumuro, and S. Yae. *ECS Trans.*, **69**(39), 59 (2015).

How Sodium Storage Depends on Hard Carbon Structure?

Ronald Väli, Meelis Härmas, Riinu Härmas, Thomas Thomberg, Tavo Romann, Alar Jänes, Enn Lust
University of Tartu, Institute of Chemistry
Ravila 14A, 50411, Tartu, ESTONIA
ronald.vali@ut.ee

Sodium-ion batteries have attracted great deal of attention due to sodium's abundance and lower price compared to lithium and cobalt. Negatively charged electrode characteristics (anode during discharge) are a major obstacle that prevents sodium-ion batteries going to a mass-scale. Graphite is currently the best negative electrode material for high-voltage lithium-ion batteries, but does not intercalate sodium reversibly, because sodium ions prefer prismatic or octahedral coordination sites [1].

In our previous works, we focused on the synthesis and electrochemical characterization of glucose-derived hard carbon electrodes in Li- and Na-based electrolytes [2,3] and compared Li, Na and K insertion processes into/on hard carbon electrodes using electrochemical impedance spectroscopy [4].

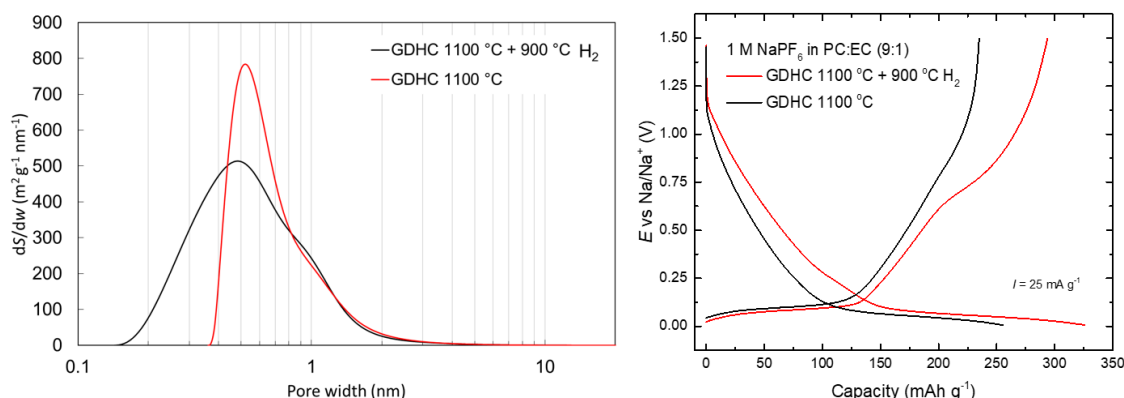


Fig 1. NLDFT pore size distribution graph from CO₂ sorption data (left) and galvanostatic charge-discharge graphs (right) of D-glucose derived hard carbon (GDHC) material/electrodes.

The right graph in Fig. 1 shows typical hard carbon charge-discharge plots. Although, capacities over 300 mAh/g can be reached at 1.5 V vs Na/Na⁺, the usable capacity in a two-electrode single cell is below 0.2 V vs Na/Na⁺ (the plateau). As seen from the pore size distribution graph (Fig. 1, left), reduction with H₂ increases microporosity of the material (SSA of both materials is $\sim 400 m^2 g^{-1}$) which manifests itself on E – capacity graph as decreased slope at $0.6 < E < 0.85 V$.

This presentation will introduce new ideas of evaluating hard carbon structure using Raman, gas sorption and EIS measurements.

Acknowledgements

This research was supported by the EU through the European Regional Development Fund (Centers of Excellence, TK141 2014-2020.4.01.15-0011 and TK117 3.2.0101-0030, TeRa project SLOKT12026T, Higher education specialization stipends in smart specialization growth areas 2014-2020.4.02.16-0026, Graduate School of Functional materials and technologies in University of Tartu and NAMUR project 3.2.0304.12-0397). This work was partially supported by Estonian Research Council Institutional Research Grant IUT20-13 and personal research grant PUT1033. R. Väli thanks Estonian Students Fund in USA and University of Tartu Foundation for financial support.

References

1. J. Qian, X. Wu, Y. Cao, X. Ai, and H. Yang, *Angew. Chem. Int. Ed.*, 52 (2013) 4633.
2. R. Väli, A. Jänes, T. Thomberg, and E. Lust, *J. Electrochem. Soc.*, 163 (2016) A1619.
3. R. Väli, A. Jänes, T. Thomberg, and E. Lust, *Electrochim. Acta*, 253 (2017) 536.
4. R. Väli, A. Jänes, and E. Lust, *J. Electrochem. Soc.*, 164 (2017) E3429.

Influence of Electrolysis Conditions on Anodic Exfoliation of Graphite in Sulfuric Acid

Yusuke Muramatsu, Hideki Hashimoto, Hidetaka Asoh*

Department of Applied Chemistry, School of Advanced Engineering, Kogakuin University,
2665-1 Nakano, Hachioji, Tokyo 192-0015, Japan.

*Corresponding author. E-mail address: asoh@cc.kogakuin.ac.jp

Two-dimensional sheet structured materials have been intensively studied from the fields of electronics, information technologies, and environments as novel functional materials that contribute continuous development of humankind due to their excellent electronic, magnetic, optical, and chemical properties, and extraordinary high surface area. Among them, graphene having infinitely expanding two-dimensional honeycomb structure of carbon atoms with one-atom-thin structure is attracted much attention from the materials scientist interests as a next-generation innovative material due to its high possibility of mass production and high controllability of its surface structure. Top-down preparation methods based on the exfoliation of graphite are generally applied when a large amount of graphene is required. In terms of simple and inexpensive methods, electrochemical exfoliation approaches have also attracted considerable attention as a key fabrication method [1–3]. Using ion intercalation under cathodic or anodic voltage in proper electrolytes, the expansion and subsequent delamination of graphite electrode occur.

Here we investigated the influence of electrolysis conditions on anodic exfoliation of graphite in sulfuric acid. A graphite and a platinum were used as anode and cathode, respectively. Constant voltage or current was applied to exfoliate graphite. The exfoliated samples were mainly characterized by X-ray diffractometry and electron microscopy. The effect of voltage, current, and electrolyte concentration on the anodic exfoliation of graphite was discussed.

[1] C.T.J. Low, F.C. Walsh, M.H. Chakrabarti, M.A. Hashim, M.A. Hussain, *Carbon*, **54**, 1–21 (2013).

[2] S. Yang, M.R. Lohe, K. Mullen, X. Feng, *Adv. Mater.*, **28**, 6213–6221 (2016).

[3] J.I. Paredes, J.M. Munuera, *J. Mater. Chem. A*, **5**, 7228–7242 (2017).

Photo-electrochemical Characteristics of Porphyrin Containing Metal Organic Frameworks on Solid Surfaces

Eika Tomizawa, Yuri Kondo, Haruka Terasaki, and Toshihiro Kondo
Division of Chemistry, Graduate School of Humanities and Sciences, Ochanomizu University
2-1-1, Ohtuka, Bunkyo-ku, Tokyo 112-8610, Japan
g1740635@edu.cc.ocha.ac.jp (E. Tomizawa)

Metallo-porphyrins have planar structure and effectively absorb visible-light normal to the ring plane. Thus, they can be applied to artificial photosynthetic systems and photovoltaic cells when the porphyrin ring was adsorbed parallel to the solid surface [1].

Si is one of the most basic and important semiconductor materials and used to the crystal Si-based solar cell. Si mainly absorbs infrared-light and cannot absorb visible-light. On the other hand, TiO₂ is a widely used semiconductor material and strongly absorbs ultraviolet-light. Furthermore, Au is one of the most useful metal substrate for the construction of the molecular layers and does not absorb any visible light. Because most of the sunlight is in a visible-light region, combination of Si, TiO₂, and/or Au substrates with metallo-porphyrin should be required in order to construct the solar-active devices. However, the interaction between the Si, TiO₂, and Au substrate surfaces and metallo-porphyrin is very weak. Thus, we have to construct the self-assembled monolayers (SAMs), with a binding group such a carboxylate group to metallo-porphyrin, on the Si, TiO₂, and Au surfaces as a first and then the metallo-porphyrin layers were constructed on them as a layer-by-layer fashion like a metal organic framework (MOF)

In this study, we constructed 5,10,15,20-tetracarboxyphenyl-porphyrin (TCPP) in a planar array on the Si(111), TiO₂(110), and Au(110) single-crystal substrates through the carboxy-terminated SAM and investigated photo-electrochemical characteristics for the visible-light active photodevices.

Ester-terminated SAMs of methyl acrylate (MA) and ethyl undecylenate (EU) SAMs were self-assembled on the hydrogen terminated Si(111) substrate by heating. After the SAM preparation on the Si surface, the terminated ester groups of the SAMs were hydrolyzed by the immersion into a hot HCl solution [2,3]. Carboxylate-terminated TiO₂ surface was prepared just by dipping the pre-cleaned TiO₂(110) substrate into an ethanol solution containing saturated 1,4-benzenedicarboxylic acid (BDC) for overnight. The SAM of 4-mercaptobenzoic acid (4-MBA) was constructed on the Au(110) surface. These carboxylate-terminated Si(111), TiO₂(110), and Au(110) substrates were dipped into the ethanol solution containing TCPP. In each step, structure, orientation, and surface coverage of the molecular layers were estimated by attenuated total reflection Fourier transformed infrared spectroscopy (ATR-FTIRS), x-ray photoelectron spectroscopy (XPS), and scanning tunneling microscopy (STM) in order to determine the optimum condition. Finally, the photo-electrochemical characteristics of the constructed porphyrin molecular layers on Si(111), TiO₂(110), and Au(110) were investigated in the electrolyte solution containing electron donor and/or acceptor with and without Xe lamp irradiation.

From the results of ATR-FTIRS, XPS, and STM [4,5], it was found that the longer the dipping time of each SAM-modified Si(111), TiO₂(110), and Au(110) substrates, the more the absorbed amount of TCPP. On all the surfaces, potential-dependent anodic photocurrent was observed by visible-light irradiation. Excited energy dependence is now under investigation.

References

- [1] D. Dolphin, "The Porphyrins", Academic Press, New York (1978).
- [2] H. Asanuma, E. M. Bishop, and H.-Z. Yu, *Electrochim. Acta*, 52 (2007) 2913.
- [3] K. Rück-Braun, M. Å. Petersen, F. Michalik, A. Hebert, D. Przyrembel, C. Weber, S. A. Ahmed, S. Kowarik, and M. Weinelt, *Langmuir*, 29 (2013) 11758.
- [4] D. H. Karweik and N. Winograd, *Inorg. Chem.*, 15 (1976) 2336.
- [5] M. Hase, W.-J. Chun, and T. Kondo, *ECS Trans.*, 75 (2017) 49.

Analysis of Hydrogen Adsorption and Incorporation during Electrodeposition of Platinum Films

Takeshi Kinoshita, Ayano Yokoyama, Ayumu Matsumoto, Naoki Fukumuro, Shinji Yae
Department of Chemical Engineering and Materials Science,
Graduate School of Engineering, University of Hyogo
2167 Shosha, Himeji, Hyogo 671-2280, Japan
yae@eng.u-hyogo.ac.jp

Hydrogen incorporation into electrodeposited metal films is largely influenced by the depositing conditions. We previously reported that a large amount of hydrogen (content in atomic ratio: H/Pt = 0.1) is incorporated in the electrodeposited platinum (Pt) films [1]. In this study, we investigate the adsorption and incorporation of hydrogen during the electrodeposition of Pt films using electrochemical quartz crystal microbalance (EQCM) method [2, 3] and thermal desorption spectroscopy (TDS) [3].

Pt films were potentiostatically deposited on a gold foil from a solution containing $0.024 \text{ mol dm}^{-3} \text{ K}_2\text{PtCl}_4$ at pH of 0.8. For an EQCM measurement, a gold coated quartz crystal electrode (resonant frequency: 10 MHz), an Ag/AgCl electrode, and a Pt wire were used as the working, reference, and counter electrodes, respectively. The hydrogen in samples was measured by TDS (300~1100K).

Figure 1 shows the current density (j) and mass increase rate (dm/dt) as a function of electrode potential (U). A shoulder at around 0 V and a peak at around -0.2 V for the current density and mass increase rate were observed. These potentials are more positive than reversible hydrogen electrode (RHE, -0.25 V vs. Ag/AgCl). Each of the potential corresponds to the underpotential deposition of hydrogen (UPD-H) on the Pt surface [2, 4]. The large decrease of mass increase rate at around -0.3 V which is more negative than RHE corresponds to the overpotential deposition of hydrogen (OPD-H) [2, 4].

The total amount of desorbed hydrogen from potentiostatically deposited Pt films (+0.1 ~ -0.3 V) at various thickness is summarized in Fig. 2. The amount of hydrogen was nearly 0 at +0.1 V (Fig. 2 ●) and hardly changed against the Pt film thickness at 0 V (Fig. 2 ◇). For the Pt films deposited at -0.1 and -0.2 V, a positive correlation was observed between the amount of hydrogen and the film thickness (Fig. 2 ○ and △). The positive correlation indicates that hydrogen was uniformly contained in the Pt films. For the Pt films deposited at -0.3 V, the slope was much greater than that at -0.1 and -0.2 V, and the hydrogen content of the films was estimated to be H/Pt = 0.11 (Fig. 2 □).

These results indicate that the hydrogen incorporation into the Pt films depends on the change in hydrogen adsorption state by the applied potential. Further, a certain amount of hydrogen was contained in the initial deposits of Pt films at the potential of UPD-H and OPD-H.

Acknowledgements

The present work was partly supported by JSPS KAKENHI (JP26289276) and (JP17K06864).

References

- [1] N. Hisanaga, N. Fukumuro, S. Yae, H. Matsuda, ECS Trans., 50(48) (2013) 77.
- [2] T. Hagihara, K. Yaori, K. Iwakura, N. Fukumuro, S. Yae, Electrochim. Acta., 176 (2015) 65.
- [3] A. Yokoyama, S. Karatsu, M. Sumikawa, N. Fukumuro, S. Yae, ECS Trans., 75(52) (2017) 55.
- [4] G. Jerkiewicz, Electrochim. Acta., 55 (2010) 179.

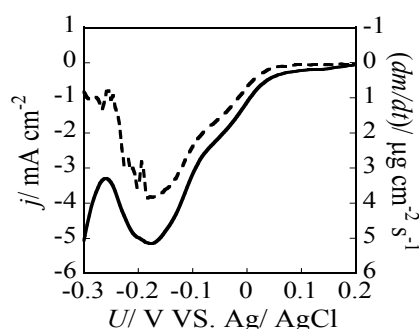


Fig. 1 Current density (j) (solid line) and Pt deposition rate (dm/dt) (broken line) vs. potential (U) curves.

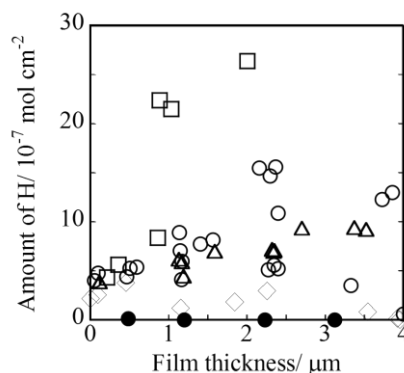


Fig. 2 Total amount of desorbed hydrogen from Pt films potentiostatically deposited at +0.1 (●), 0 (◇), -0.1 (○), -0.2 (△), and -0.3 (□) V vs. Ag/AgCl.

Solid-state Planar Amperometric CO Gas Sensor Based on Nafion[®]/Porous Pd/Au(Sputtering)/Al₂O₃

Ying-Fang Xu¹, Ming-Liao Tsai¹, Jing-Shan Do^{*1,2}

¹Department of Chemical and Materials Engineering, National Chin-Yi University of Technology
Taichung, Taiwan

No.57, Sec. 2, Zhongshan Rd, Taiping Dist, Taichung 41170, Taiwan (R.O.C.)

²College of Materials Science and Engineering, Xi'an University of Science and Technology
No.58, Yen-Ta Rd, Xi'an, China

E-mail: [cijh9910624@gmail.com](mailto:cjih9910624@gmail.com), jsdo@ncut.edu.tw

Carbon monoxide sensor plays an important role in the industrial processes and environmental monitoring [1]. Most of CO gas sensors are conductometric type based on metal oxide semiconductors sensing materials [1-2], which are generally operated at a relative higher temperature with energy consuming. Using C-loaded PdCl₂-CuCl₂ as sensing material, the sensitivity and detecting limit of amperometric CO gas sensor operated at room temperature are found to be 0.35 μA ppm⁻¹ and 1 ppm, respectively [3]. The porous Pd electrodeposited with hydrogen bubble dynamic template (HBDT) method on the working electrode of the planar three-electrode pattern, which is prepared by the microfabrication technique, is used as the sensing electrode of the amperometric CO gas sensor. The surface morphologies and crystallographic information of as-prepared electrodes are characterized by field-emission scanning electron microscopy (FE-SEM) and X-ray diffraction (XRD), respectively. The electrochemical properties of Nafion[®]/porous Pd/Au (sputtering)/Al₂O₃ electrodes are studied with cyclic voltammetry (CV) and polarization methods. The porous structure with spherical cavities caused by the hydrogen bubble evolved within the electrodeposition of Pd are found from the SEM images. The electroactive surface area (ESA) and roughness of porous Pd electrodeposited in 0.02 M PdCl₂ with current density and charge passed of 0.068 A cm⁻² 7.5 C are obtained by CV to be 103.64 cm² and 411.6, respectively. Using Nafion[®]/porous Pd/Au (sputtering)/Al₂O₃ cast with 10 μl 5 wt% Nafion[®] solution as sensing electrode, increasing the potential from 0 to 0.2 V (vs. Au) the anodic oxidation of 20 ppm CO is increased from 2.418 to 5.564 μA, which is controlled by the kinetic on the electrode surface. Furthermore, the anodic oxidation of CO is controlled by the mass transfer from the gas bulk phase to the electrode at the potential of 0.45 - 0.55 V (vs. Au) due to the slight change of current (11.2644 - 11.384 μA). The sensitivity and detect limit of amperometric planar CO gas sensor based on homemade Nafion[®]/porous Pd/Au (sputtering)/Al₂O₃ are found to be 0.23 μA ppm⁻¹ for 1 - 20 ppm, and less than 1 ppm, respectively.

References:

- [1] A. Debararaja, D. W. Zulhendri, B.-Y. Nugrah, Hiskia and B. Sunendar, Investigation of Nanostructured SnO₂ Synthesized with Polyol Technique for CO Gas Sensor Applications, *Procedia Engineering* 170 (2017) 60 – 64.
- [2] N. H. Ha, D. D. Thinh, N. T. Huong, N. H. Phuong, P. D. Thach and H. S. Hong, Fast response of carbon monoxide gas sensors using a highly porous network of ZnO nanoparticles decorated on 3D reduced graphene oxide, *Applied Surface Science* 434 (2018) 1048–1054.
- [3] X. Li, T. Xuan, G. Yin, Z. Gao, K. Zhao, P. Yan, and D. He, Highly sensitive amperometric CO sensor using nanocomposite C-loaded PdCl₂-CuCl₂ as sensing electrode materials, *Journal of Alloys and Compounds* 645 (2015) 553-558.

Formation of Porous Alumina Films by DC-Bipolar Anodization

Tadashi Mori, Hideki Hashimoto, Hidetaka Asoh*

*Department of Applied Chemistry, School of Advanced Engineering, Kogakuin University,
2665-1 Nakano, Hachioji, Tokyo 192-0015, Japan.*

**Corresponding author. E-mail address: asoh@cc.kogakuin.ac.jp*

Recently, surface modification of electrodes and the development of functional materials based on the principles of bipolar electrochemistry have attracted considerable attention because of the simple process without the need for a physical connection between the conductive bipolar electrode and an external power supply. When an electric field is applied to the outer two electrodes, an inhomogeneous reaction field similar to a potential difference or localized pH gradient is generated between them.

For anodization of light metals, Loget et al. demonstrated that TiO₂ nanotube gradients with a tunable length and diameter were formed on titanium, which acted as a bipolar electrode, based on the difference in polarization established between the electrolyte and bipolar titanium electrode under a DC electric field [1]. Saqib et al. reported similar results on the bipolar anodization of titanium [2].

In our previous study, we successfully formed porous alumina films by indirect oxidation under an AC electric field without a direct electrical connection [3]. Our approach has the following features: i) the aluminum can be oxidized indirectly in aqueous solutions via wireless treatment under an AC electric field; ii) AC electrolysis is not used to form asymmetrical objects or surfaces but to form symmetrical objects or uniform coatings; and iii) numerous small objects can be treated simultaneously.

In the present study, we focused on the differences between the use of DC and AC electric fields to obtain a better understanding of the effect of an external electric field on oxide film formation on a wireless aluminum electrode. The thickness and uniformity of the films were evaluated using a spectrophotometric analysis and scanning electron microscopy. The composition and morphology of nanoporous films were also discussed.

- [1] G. Loget, S. So, R. Hahn and P. Schmuki, *J. Mater. Chem. A* **2**, 17740 (2014).
- [2] M. Saqib, J. Lai, J. Zhao, S. Li and G. Xu, *ChemElectroChem* **3**, 360 (2016).
- [3] H. Asoh, M. Ishino and H. Hashimoto, *RSC Adv.* **6**, 90318 (2016).

Catalyst coated membrane for efficient alkaline water electrolysis

Jaromír Hnát, Michaela Plevová, Jan Žitka, Monika Drakselová, Karel Bouzek
University of Chemistry and Technology Prague
Technická 5, 166 28, Prague 6-Dejvice, Prague, Czech Republic
hnatj@vscht.cz

Alkaline water electrolysis represents promising technology for production of the green hydrogen. It can subsequently act as an energy vector in the energy conversion and storage processes. Advantage of the alkaline water electrolysis over the competitive technologies, such as polymer electrolyte membrane (PEM) or high temperature water electrolysis, is multifold. Between main of them belongs: (i) it is a technology well established in industry, (ii) it does not require precious Pt group metals to be used as electrocatalysts of the electrode reactions and (iii) availability of the construction materials. On the other hand, this technology does not achieve intensity and flexibility of the operation comparable to the PEM water electrolysis. This is due to the absence of the membrane based on anion selective polymer material able to ensure sufficient ionic contact between the electrodes and separation of produced gasses at the same time. Utilization of the anion selective polymer electrolyte membrane would allow not only to use zero gap arrangement (the electrodes are pressed directly to the surface of the membrane), but even to deposit electrocatalytic layer directly on the surface of the membrane. Although in the PEM water electrolysis such approach provides results superior to the catalyst coated electrode due to the improved ionic contact of the catalyst particles to the membrane, in alkaline process such approach has not yet been used. This is due to the absence of an appropriate polymer electrolyte utilizable as both a polymer electrolyte, as well as a binder. The main aim of this contribution is to verify advantages of such approach.

In this study anion selective polymer membrane based on the block copolymer of styrene-ethylene-butylene-styrene (PSEBS) with 1,4-diazabicyclo[2.2.2]octane (DABCO) functional groups is used. The 5wt.% solution of the chloromethylated PSEBS (PSEBS-CM) in chloroform was used as a polymer binder of the catalytic layer. Non platinum mixed oxides with spinel structure NiCo_2O_4 and NiFe_2O_4 were used as an anode and cathode catalysts respectively. In order to gain information fundamental for development of technique of membrane coating by the catalyst, TGA and DSC of the bare membrane (PSEBS-CM) and functionalized membrane (PSEBS-CM-DBC) were performed. Chemical stability of the PSEBS-CM-DBC membrane in Cl^- form was evaluated at temperatures ranging up to 200 °C. Catalyst coated membrane (CCM) was prepared using PSEBS-CM membrane as well as PSEBS-CM-DBC. CCM PSEBS-CM was subsequently functionalized by DABCO. Both CCM were tested in laboratory alkaline water electrolyzer coupled with electrochemical impedance spectroscopy measurement. Morphology of the CCM was investigated by scanning electron microscopy. Results confirm good adhesion of the catalytic layer to the membrane and performance of the alkaline water electrolysis comparable to the industrial units achieved under milder conditions of 50 °C and concentration of circulating electrolyte 10wt.%.

Acknowledgement

Financial support of this research by Grant Agency of the Czech Republic under project No. 16-20728S is gratefully acknowledged.

Development of Third Generation Glucose Biosensors Based on Organic Metal Particles of In Situ Synthesis

Jia-De Yan¹, Yu-Fen Kuo², Ching-Chou Wu^{*}

¹Department of Bio-industrial Mechatronics Engineering, National Chung Hsing University

²Metal Industries Research & Development Centre, Tainan, Taiwan

No.145, Xingda Road, Taichung 402, Taiwan, ROC

ccwu@dragon.nchu.edu.tw

Abstract

Background: Diabetes is one of the most popular chronic diseases in 21st century. If diabetic cannot control their blood glucose concentration well, they would be murdered by the serious complications such as cardiovascular diseases, nephropathy, or neuropathy. To avoid complications, diabetic should often detect blood glucose and accept insulin therapy. For this reason, glucose biosensors have become the most important products of the in vitro diagnostics market. However, the commercialized blood glucose strips are based on the use of electroactive mediators, called 2nd generation glucose biosensors, which are easily affected by hematocrit factor. This disadvantage limits the development of 2nd generation glucose biosensors. Therefore, in order to solve the problem, this research utilized Prussian blue particles to develop a 3rd generation glucose biosensor.

Method: This research used screen print carbon electrodes (SPCE) as the electrode substrate. Glucose oxidase (GOx) and ϵ -Poly-L-lysine (PLL) were dissolved in a PBS buffer (pH 7.0). Then, the mixture of glucose, ferricyanide (FIC) and KCl solution was dripped into the GOx/PLL solution for synthesizing the Prussian blue (PB) particles in situ. After EC clean and peroxidation, SPCE would be more hydrophilic to adsorb the GOx/PLL/PB complex. The GOx/PLL/PB-containing solution would be dripped on the SPCE and dried in the oven for 15 minutes at 30°C. Finally, Nafion would be coated as a membrane to protect the sensing layer.

Result: The phenomenon of direct electron transfer (DET) was an important feature for 3rd generation glucose biosensors. The GOx/PLL/PB-modified SPCE showed an obvious redox peak at the -0.5 V as shown in Fig.1. This cyclic voltammogram implies that the PB particles were synthesized at the neighborhood of GOx redox center to perform DET. The linear range of the glucose detection was from 0.5 mM to 3 mM and the sensitivity was $17.955 \mu\text{A mM}^{-1} \text{cm}^{-2}$.

Conclusion: This research used a simple and low cost method for synthesizing PB particles close to the redox center of GOx. The DET phenomenon between GOx and the SPCE electrode is obvious and good response to the glucose concentration. This fabricating method has great promise for the development of 3rd generation glucose biosensors.

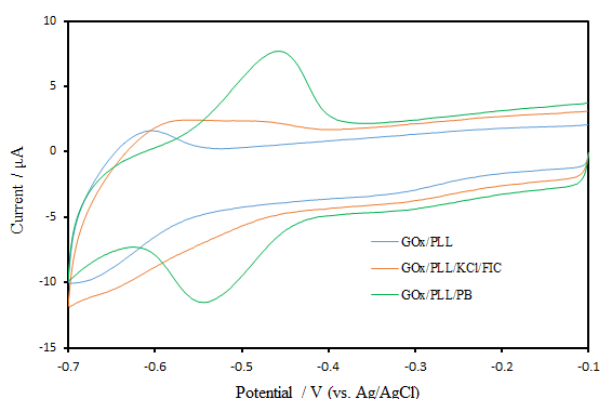


Figure 1. The cyclic voltammograms of GOx/PLL, GOx/PLL/KCl/FIC and GOx/PLL/PB-modified SPCEs measured in PBS (pH 7.0).

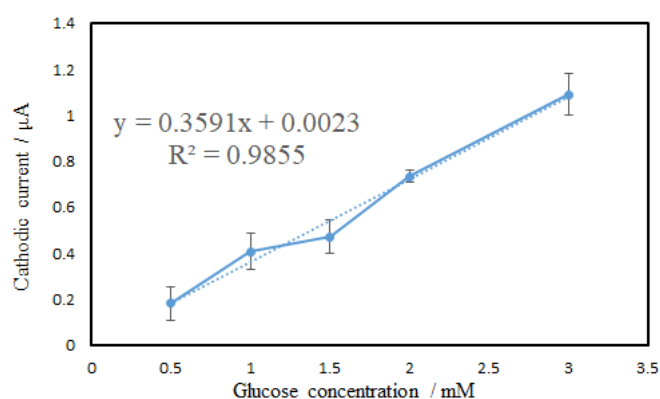


Figure 2. The linear range of glucose detection measured by GOx/PLL/PB-modified SPCE.

Improved dispersion of Co₃O₄ nanoparticles on platelet carbon nanofibers for oxygen reduction reaction

Naohito Yamada¹, Yuki Sato¹, Damian Kowalski², Chunyu Zhu^{1,2}, Yoshitaka Aoki^{1,2}, Hiroki Habazaki^{1,2}

¹Graduate School of Chemical Sciences and Engineering, Hokkaido University, Sapporo, Japan

²Division of Applied Chemistry, Faculty of Engineering, Hokkaido University, Sapporo, Japan
Email address: naohi0206@eis.hokudai.ac.jp (N. Yamada).

1. Introduction

For practical application of fuel cells and metal-air secondary batteries, highly active electrocatalysts for oxygen reduction reaction (ORR) is necessary. Pt nanoparticles supported on carbon materials have been often used for the efficient ORR catalyst. However, because of the high cost and scarcity of platinum resource, platinum-free electrocatalysts with high activity is awaited. Cobalt oxide supported on carbon materials is one of the candidates. To obtain the high activity, the cobalt oxide nanoparticles must be highly dispersed on carbon. Platelet carbon nanofibers (pCNFs) are promising carbon materials for the support of electrocatalyst nanoparticles since the side wall of pCNFs consists of the edge plane of carbon, where nanoparticles would be more strongly supported in comparison with the basal plane of carbon. In fact, it was demonstrated that Pt nanoparticles were uniformly dispersed on pCNFs and the Pt/pCNFs exhibited the improved durability for ORR¹. In this study, we used pCNFs as a support of cobalt oxide nanoparticles for ORR electrocatalyst and the ORR activity was examined in alkaline KOH solution.

2. Experimental method

The pCNFs were prepared by a template-assisted liquid phase carbonization of polyvinylchloride (PVC) powders². After heating a mixture of the porous anodic alumina template and PVC at 600°C in an Ar atmosphere, the template was dissolved in alkaline solution. The obtained pCNFs (pCNF600) were further heat-treated at 1100°C (pCNF1100) and 1500°C (pCNF1500) under an Ar atmosphere. Co₃O₄/carbon catalysts were prepared by immersing the pCNFs in a mixed aqueous solution containing cobalt acetate, ammonia and ethanol and heating at 80°C for 12 h. The carbon materials used in this study were pCNF1100, pCNF1500, commercially available multiwall carbon nanotubes (MW). Electrochemical measurements were carried out by using a rotating disk electrode with a normal three electrode system. Pt wire and Ag/AgCl was used as a counter electrode and reference electrode, respectively. The electrolyte used was oxygen-saturated 0.1 mol dm⁻³ KOH aqueous solution.

3. Results and Discussion

TEM observations of the Co₃O₄/carbon showed that Co₃O₄ with a particle size of 10-20 nm were well dispersed on the pCNF1100. The less uniform dispersion of Co₃O₄ was found on the pCNF1500, probably because of the change in the structure of the edge plane of carbon. Poorest dispersion of Co₃O₄ was on MW such that the basal plane of carbon was not suitable for the uniform dispersion of the oxide nanoparticles. The thermogravimetric analysis in air indicated that the loading amount of oxide decreases in the following order: pCNF1100 > pCNF1500 > MW.

The polarization curves for ORR revealed that the onset potential for ORR was largely dependent upon the carbon support. The Co₃O₄/pCNF1100 shows highest onset potential, which was more than 150 mV higher than those of Co₃O₄/pCNF1500 and Co₃O₄/MW. The Koutecky-Levich analysis also indicated that the electron transfer number for ORR is higher for the Co₃O₄/pCNF1100 in comparison with the other two electrodes. Findings suggest the importance of the Co₃O₄ dispersion and the structure of the edge plane of carbon for ORR activity.

References

- 1) E. Tsuji, T. Yamasaki, Y. Aoki, S.-G. Park, K. Shimizu, H. Habazaki; *Carbon*, **87**, 1 (2015).
- 2) H. Konno, S. Sato, H. Habazaki, M. Inagaki; *Carbon*, **42**, 2756 (2004).

Electrochemically Gating of Low Molecular Weight Analytes through Self-Doped TiO₂ Nanotubes

Felipe F. Hudari, Guilherme G. Bessegato, Flávio C. Bedatty Fernandes, Paulo R. Bueno, Maria V. Boldrin Zanoni*

Institute of Chemistry, São Paulo State University (UNESP), Araraquara, São Paulo, Brazil
Rua Prof. Francisco Degni, 55, 14800-060
*boldrinv@iq.unesp.br

Highly ordered nanomaterials such as TiO₂ nanotubes (TiO₂NT), can be easily prepared by electrochemical anodization and are known to be vastly employed in photoelectrochemical applications such as oxidation of contaminants [1]. However, TiO₂NT electrodes are little used as anode sensors because it is a *n*-type semiconductor. In this work, a self-doped TiO₂NT electrode (SD-TiO₂NT) was proposed by means of a cathodic polarization for partial conversion of Ti⁴⁺ to Ti³⁺. The TiO₂ nanotube electrodes (TiO₂NT) were prepared by electrochemical anodization and the self-doped titania nanotubes (SD-TiO₂NT) electrodes were prepared by cathodic polarization using a three-electrode cell with an Autolab PGSTAT302N potentiostat, an Ag|AgCl (KCl 3 mol L⁻¹) as reference electrode and a dimensionally stable anode (DSA®, De Nora) as counter electrode. The electrolyte was 0.1 mol L⁻¹ KH₂PO₄ buffer pH 10, and TiO₂NT electrode was submitted to -2.5 V for 5 min [2]. Using electrochemical capacitance spectroscopy (ECS), a 286-fold increase in the capacitance of SD-TiO₂NT compared to TiO₂NT was observed, which is explained by the accessible quantum levels created by auto-doping (Figure 1a). In addition, the material resistance decreased from 1.47 MΩ cm⁻² (TiO₂NT) for 25.6 Ω cm⁻² (SD-TiO₂NT), showing that the creation of Ti³⁺ states increases the conductivity of the material. The application of the SD-TiO₂NT was made comparing the techniques of cyclic voltammetry (CV) and ECS for the determination of the triamterene diuretic. Figure 1b shows a comparison between the analytical curves using CV and ECS where the best results were obtained for ECS using the immittance function (C''/C'), finding a linear range between 5 × 10⁻⁷ to 1 × 10⁻⁴ mol L⁻¹ with limit of detection of 2.04 × 10⁻⁷ mol L⁻¹.

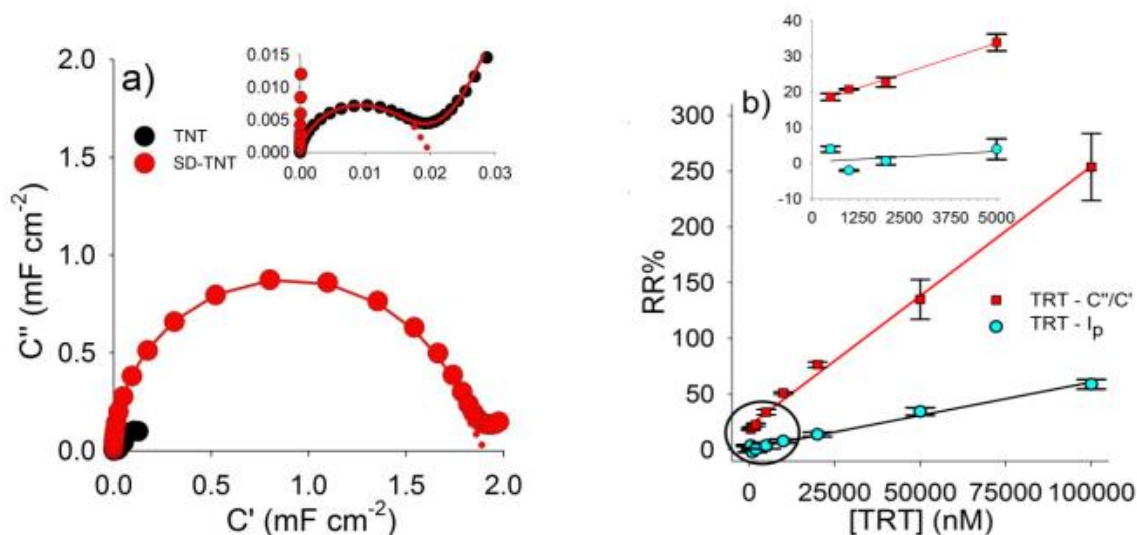


Figure 1. a) Immittance function response, herein represented by impedance derived to capacitance, to TiO₂NT and SD-TiO₂NT in the Nyquist plot. Measurements recorded in 0.10 mol L⁻¹ B-R buffer solution (pH 2.0) in the range of 10⁶ – 0.03 Hz, with a 10 mV rms sinusoidal modulation and applying potential of +1.80 V. b) Comparison between peak current (I_p) and C''/C' responses for TRT target.

References

- [1] G.G. Bessegato, J.C. Cardoso, B.F. da Silva, M.V.B. Zanoni, Appl. Catal. B Environ. 180 (2016) 161–168.
- [2] Bessegato, G. G.; Hudari, F. F.; Zanoni, M. V. B. Electrochim. Acta 2017, 235, 527–533.

Development of Silica Microlens Array Sensor for *in situ* SERS Analysis of Electrode Reaction Processes

Asuka Hayashi¹, Yuta Sato¹, Masahiro Kunimoto², Masahiro Yanagisawa², Takayuki Homma^{1,2}

1. Dept. of Applied Chemistry, Waseda Univ. 3-4-1 Okubo, Shinjuku, Tokyo, Japan

2. Research Organization for Nano & Life Innovation, Waseda Univ. Wasedatsurumakicho, Shinjuku, Tokyo 162-0041, Japan.
t.homma@waseda.jp

Surface-enhanced Raman spectroscopy (SERS) measurement is a highly sensitive and nondestructive method to analyze the interfacial state of materials, electrodes, bio systems, etc. While the conventional SERS measurement needs directly formed nanostructures on analytes, our novel optical element, which is called “plasmon sensor”, is capable to provide enhanced Raman signal from the species at the interfacial area without undesirable influence from nanostructures that often arises in the conventional setups [1]. This sensor element is made of highly transparent materials, on the surface of which nano particles of SERS active metals, such as Ag or Au, are deposited. Irradiation of the excitation laser onto the contact point of sensor and specimen should bring the enhanced Raman signal from the interface. In this study, to improve the spatial resolution of this technique, we newly designed and fabricated the sensor structure with microlens array (MLA). Furthermore, the fabricated sensor is applied to *in situ* measurement to monitor electrode reactions.

As a base material for MLA sensor, silicon substrate is chosen, for its microstructures are highly controllable by wet processes. Pyramid type pits, whose height, width, and pitch are $\sim 20 \mu\text{m}$, $50 \mu\text{m}$, $100 \mu\text{m}$, respectively, were prepared on the substrate, using photolithography and anisotropic alkaline etching. Ag nano particles were electrolessly deposited on the pits. The spatial resolution of this sensor was examined by scanning Raman mapping measurement around the area, in which the pits of the sensor contact to the Au substrate that holds 4-Mercapropbenzoic acid (pMBA) as a label molecule on the surface.

The scanning electron microscope (SEM) image depicted that Ag nanoparticles with diameter of $\sim 60 \text{ nm}$ were successfully deposited at the tip of the prepared silica MLA sensor, which should be suitable for SERS measurement. Scanning Raman mapping on the pMBA modified Au substrate with the sensor attached showed that the enhanced signal from pMBA was detected only in the area of $0.5 \mu\text{m} \times 0.5 \mu\text{m}$, which was attributed to the tip of the sensor. This result suggests that the sensor has high spatial resolution and sensitivity.

As a case example of its application, the surface pH changes on the working electrode during ZnO electrodeposition was monitored *in situ*, which is crucial for the discussion about its reaction mechanism [2]. It should be noted that pMBA, which is the pH-responsive molecule, was modified to the Ag nano particles on the silica MLA sensor. pH changes around the interfacial area can be detected by receiving SERS signal from modified pMBA on the sensor that is located on the working electrode (Fig. 1); changes in the Raman peak intensity at $\sim 1400 \text{ cm}^{-1}$ that is attributed to COO⁻ of pMBA indicates pH changes. The measurement was performed for the Zn working electrode in the electrodeposition bath containing 0.02 M zinc acetate, 0.01 M hydrogen peroxide and acetic acid. The time-dependent changes in the signal from 1400 cm^{-1} clearly showed pH increase during ZnO deposition. In addition, different pH behavior was observed, depending on the presence of Zn^{2+} . These data suggest that the fabricated MLA plasmon sensor is quite practical and applicable to the *in situ* analyses of the interfacial phenomena.

This research was financially supported in part by “Development of Systems and Technology for Advanced Measurement and Analysis” program from JST.

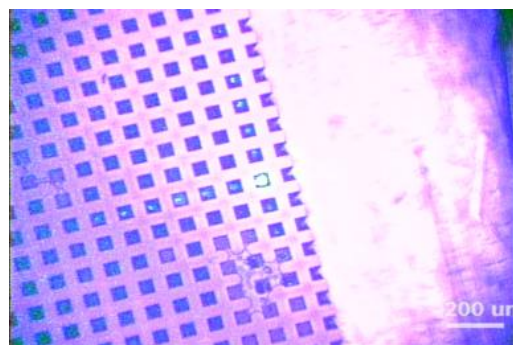


Fig.1. Optical microscope image of the MLA sensor located on the working electrode during measurement

[1] M. Yanagisawa, M. Saito, M. Kunimoto, T. Homma, *Appl. Phys. Express*, **9** (2016), 122002.

[2] M. Skompska, K. Zarebska, *Electrochimica Acta*, **127** (2014), 467-488.

Corrosion Resistance of Boehmite Based Films Prepared on Al-Mg-Si Alloy by Steam Coating

Kohei Watanabe¹, Takahiro Ishizaki², Ai Serizawa²

¹ Graduate School of Engineering and Science, Shibaura Institute of Technology
3-7-5 Toyosu, Koto-ku, Tokyo 135-8548 Japan

² Department of Materials Science and Engineering, Shibaura Institute of Technology
3-7-5 Toyosu, Koto-ku, Tokyo 135-8548 Japan
serizawa@shibaura-it.ac.jp

1. Introduction

Al alloys have an excellent physical and mechanical properties such as a low density, high electrical conductivity, high specific strength, and good ductility. However, their low corrosion resistance has limited their application in corrosive environments, especially Al alloys is used as outer materials for transportation parts. There is a need, therefore, for a novel coating technology capable of improving the corrosion resistance of Al alloys.

In this presentation, steam coating was applied to an Al-Mg-Si alloy [1]. Then, the resultant film was characterized and evaluated by electrochemical measurements. In particular, pitting corrosion behavior was investigated because this property of the alloys is particularly significant when they are applied as structural materials. The objective of the present study is to develop a new coating technology that is environmentally friendly, and which thus contributes to the creation of a sustainable society.

2. Experimental procedure

Al-Mg-Si alloy was used as the substrate. The cleaned substrates were set in an autoclave with ultrapure water as the steam source and processed using different temperatures and holding times, resulting in the formation of anticorrosive films on the alloy. The surface morphologies of the anticorrosive films on the Al-Mg-Si alloy substrates were observed using a field emission scanning electron microscope (FE-SEM). The crystal phase of the obtained film was identified using an X-ray diffraction (XRD). The corrosion resistance was estimated by electrochemical measurements. All the electrochemical measurements were performed using a 5 mass% NaCl aqueous solution. An immersion corrosion test was conducted to evaluate the corrosion resistance of the specimens subjected to the steam coating.

3. Results and discussion

FE-SEM images of the film surfaces showed that plate-like nanocrystals were densely formed over the entire surface. XRD patterns indicated that the film was composed mainly of AlOOH crystals. The potentiodynamic polarization curves revealed that the corrosion current density of the film-coated substrates significantly decreased, and that the pitting corrosion was completely suppressed, indicating that the corrosion resistance of the Al-Mg-Si alloy was improved by the film formed by means of steam coating. The appearance of the surface of the film-coated specimen exhibited no damage at all, even after saltwater immersion for 48 h. In contrast, considerable pitting corrosion was observed on the as-received specimen. Even after immersion in a NaCl solution for 48 h, the pitting corrosion did not occur on the Al-Mg-Si alloy that had been film coated using the steam coating method.

4. Conclusions

A novel means of preparing an AlOOH film on an Al alloy by steam coating was successfully established. The corrosion resistance of the film-coated Al-Mg-Si alloy was improved compared to that of the bare alloy due to the formation of the composite film via steam coating. This would enable the wider application of the alloy in the automotive, building, power transmission, and heat transfer industries.

Reference

[1] T. Ishizaki, N. Kamiyama, K. Watanabe, A. Serizawa, *Corros. Sci.*, 92, 76-84 (2015).

Acknowledgment - This research was supported by Japan Science and Technology Agency (JST) under Industry-Academia Collaborative R&D Program "Heterogeneous Structure Control: Towards Innovative Development of Metallic Structural Materials" (No. 20100120).

In-situ analysis for interaction of additives for electrodeposition in through silicon via using surface enhanced Raman scattering

Tetsuya Yasuda¹, Futa Yamaguchi¹, Masahiro Kunimoto², Masahiro Yanagisawa², Takayuki Homma^{1,2}

1. Dept. of Applied Chemistry, Waseda Univ. 3-4-1 Okubo, Shinjuku, Tokyo, Japan

2. Research Organization for Nano & Life Innovation, Waseda Univ. Wasedaturumakicho, Shinjuku, Tokyo 162-0041, Japan.

t.homma@waseda.jp

For the large-scale, three-dimensional packaging, copper through silicon via (Cu-TSV), is one of the key techniques and precise process for its formation should be established. Since TSV shows high aspect ratio in several hundred micrometers of scale, Cu electrodeposition process for defect-free filling is significant. For this, several additives are synergistically applied, in which the control of the concentration distribution and adsorption state of each additive is a key factor.

In this study, a novel approach to directly observe the diffusion and adsorption behaviors of the additives in the via structure is developed using surface enhanced Raman spectroscopy (SERS). Here, the horizontally lying transparent via structure is attached on the substrate with Cu nano dot array so that the bottom part, as one of the side walls of the via, can exhibit SERS effect with high uniformity for the detection of trace amount of additives. Excitation laser can reach the bottom part to obtain the SERS signal (Fig.1)[1]. Then the method is applied to in situ monitoring of interactive behaviors of Cl⁻ and bis(3-sulfopropyl)disulfide (SPS), which are contained simultaneously in the widely studied bath composition.

Cu nano dot array substrate was fabricated by electrodeposition to the dot structures prepared by nanoimprint lithography. The diameter and pitch of the nano dot array was 150 nm and 300 nm, respectively. The transparent via structure was made of polydimethylsiloxane (PDMS) by molding process: liquid PDMS was poured on the horizontal via-shaped silicon mold, followed by heating. Width, height, and horizontal depth of the via were 40 μm, 30 μm, and 400 μm, respectively. The finished transparent via structure was attached on the Cu nano dot array substrate. In the SERS measurement, the fabricated PDMS via was firstly filled with pure water, followed by dropping 20 μl of analyte solutions that contained each additive. Concentration of Cl⁻ (added as HCl) was 100 ppm and that of SPS was 300 ppm. After dropping the solution, excitation laser (633 nm) which penetrated the transparent wall was irradiated at the proper spot on the Cu nano dot array and time-dependent Raman spectroscopy for the diffusing species was performed.

The time-dependent Raman spectrum, in which the diffusion of Cl⁻ and SPS were individually measured, from the bottom side of the via (400 μm deeper from the entrance, as depicted in Fig. 1) shows that the detection of Cl⁻ on that spot is earlier than that of SPS. This suggests that the diffusion of Cl⁻ into the deeper side of the via is faster than that of SPS due to its smaller molecular mass. In the case of mixture of Cl⁻ and SPS, longer duration was needed for reaching to adsorption equilibrium of SPS due to the presence of Cl⁻ in the solution. This indicates the replacement of preabsorbed Cl⁻ with SPS. The bond between Cl⁻ and Cu should be broken as a result of interaction with SPS. These results show the capability of this method to perform in situ analysis of the interaction among the diffusing species inside the TSV structure during the via filling.

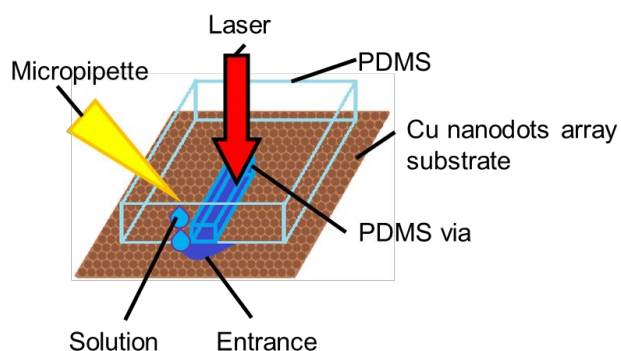


Fig.1. In situ measurement setup for TSV

This research was financially supported in part by “Development of Systems and Technology for Advanced Measurement and Analysis” program from JST.

[1] T. Homma, A. Kato, M. Kunimoto, M. Yanagisawa, *Electrochem. Commun.*, submitted.

Electrochemical and Spectroelectrochemical Properties of Phosphorus-Containing Organic Materials

S. Pluczyk¹, H. Higginbotham², P. Data^{1,2}, Y. Takeda³, S. Minakata³

¹*Faculty of Chemistry, Silesian University of Technology,
M. Strzody 9, 44-100 Gliwice, Poland*

²*Physics Department, Durham University,
South Road, Durham DH1 3LE, United Kingdom*

³*Department of Applied Chemistry, Graduated School of Engineering, Osaka University,
Yamadaoka 2-1, Suita, Osaka 565-0871, Japan*

E-mail: sandra.pluczyk@polsl.pl-e-mail address

Organophosphorus compounds have very recently been found as a promising building block for organic functional materials for optoelectronic applications. Organophosphorus materials exhibit hyperconjugation which lowers the LUMO levels, making them particularly attractive as electron-acceptor materials for n-type as well as ambipolar organic semiconductors. Their optoelectronic properties (e.g., HOMO/LUMO energies, photo-absorption/emission properties, etc.) can be effectively tailored by (C–P) σ^* - π^* electronic interaction and chemical P-functionalization [1,2]. One of the greatest advantage of these materials is the reactivity of phosphorus which easily allows for synthesis of series of derivatives with different physical characteristics.

In this work we present the photophysical, electrochemical and spectroelectrochemical characterization of new electron withdrawing phosphorus-containing compounds for organic optoelectronics. The comparison between phosphorus-containing and nitrogen analogues will be presented. Investigations show the effect of changing the nitrogen to a phosphorus atom. Results confirmed tunability of properties by changing the amount of incorporated phosphorus atoms. Photophysical and electrochemical analysis revealed that in this way the tailoring of the triplet energy as well as LUMO level is possible. The phosphorous analogue exhibits higher reduction potential than nitrogen one, hence develop of such type of compounds seems to be valuable stream in research on new materials with stable electron accepting properties.



Acknowledgements:

We thanks to the networking action funded from the European Union's Horizon 2020 research and innovation programme under grant agreement No 691684.

References:

- [1] Y. Takeda, K. Hatanaka, T. Nishida, S. Minakata, Chem. - A Eur. J., 22, 10360 (2016).
- [2] Y. Takeda, T. Nishida, S. Minakata, Chem. - A Eur. J., 20, 10266 (2014).

Investigation of Biocompatible Electrode Materials for Powering Ingestible Electronic Medical Devices

Sven Stauss, Naoki Tazawa, and Itaru Honma

*Research Center for Sustainable Science & Engineering, Institute of Multidisciplinary Research for Advanced Materials, Tohoku University
2-1-1 Katahira, Aoba-ku, Sendai, Miyagi 980-8577 Japan
stauss@tagen.tohoku.ac.jp*

Ingestible electronic medical devices and smart pills hold promise for a wide range of applications: Controlled drug release, pH, temperature, and pressure monitoring, and remote endoscopy, possibly enabling early detection and treatment of gastrointestinal diseases and diabetes [1]. So far, for powering such electronic devices, mainly primary or secondary batteries that consist of electrode materials and electrolytes also employed in consumer electronic devices have been used. Consequently, they often contain toxic materials, which could be harmful in case of battery leakage. Because of this, they require special encapsulation, leading to bulky form factors, thereby increasing the risk of retention in the gastrointestinal tract. Moreover, self-discharge limits the shelf life of these batteries.

In recent years, ingestible batteries that are powered by using gastric fluid as electrolyte have been demonstrated [2,3]. Compared to conventional primary or secondary battery systems, their shelf life is not limited, as they become activated by the gastric fluid after ingestion. However, current solutions are hampered by low cell voltages and relatively low capacities, enabling operation of only a few hours at most, or they are based on expensive electrode materials, which would limit their use for daily health care products.

To address some of the limitations in present ingestible battery systems, the main goal of this work was to investigate biocompatible electrode materials that could potentially be used in small-scale batteries for powering ingestible sensor devices.

Mg/AgCl and Zn/AgCl so-called macrocells were realized using Mg and Zn ribbons (thickness 25 μm and 240 μm , respectively), and Ag foils (thickness 20 μm), the AgCl cathodes being realized by anodisation in 1 M KCl solutions. The electrodes (nominal active surfaces $\sim 2 \times 2$ to $\sim 2 \times 10 \text{ mm}^2$) were fixed on laminate sheets and formed into small pockets, into which simulated gastric fluid (nominal pH 1.2) was introduced before sealing the macrocells. The volumes of the macrocells realized in this manner had nominal volumes of 1–5 μL . The voltages of the of the Mg/AgCl macrocells reached values of $\sim 1.2 \text{ V}$, while in the case of Zn/AgCl outputs of the order of ~ 0.9 – 1.0 V were achieved. In both cases, this would be sufficient for powering a temperature sensor and a wireless transmitter. Compared to the Mg/AgCl macrocells, Zn/AgCl showed a higher stability, possibly a consequence of the more rapid oxidation of the Mg anodes [4]. By varying the output current between 100 and 2 μA , operating times between 0.5 and 24 h could be achieved for the Zn/AgCl macrocells. More details and discussion of the potential of Zn/AgCl for use as biocompatible batteries in ingestible electronic medical devices will be discussed at the meeting.

References

- [1] C.J. Bettinger, Materials Advances for Next-Generation Ingestible Electronic Medical Devices, Trends Biotechnol. 33 (2015) 575–585..
- [2] H. Jimbo, N. Miki, Gastric-fluid-utilizing micro battery for micro medical devices, Sensors Actuators, B Chem. 134 (2008) 219–224.
- [3] H. Hafezi, T.L. Robertson, G.D. Moon, K.Y. Au-Yeung, M.J. Zdeblick, G.M. Savage, An ingestible sensor for measuring medication adherence, IEEE Trans. Biomed. Eng. 62 (2015) 99–109.
- [4] P. Nadeau, D. El-Damak, D. Glettig, Y.L. Kong, S. Mo, C. Cleveland, L. Booth, N. Roxhed, R. Langer, A.P. Chandrakasan, G. Traverso, Prolonged energy harvesting for ingestible devices, Nat. Biomed. Eng. 1 (2017) 1–8.

Electrochemical Impedance Spectroscopy Study of Lithium–Sulfur Batteries: Effects of Electrolyte/Sulfur Ratios

Jie Fang¹, Samson H. S. Cheng^{1,2}, S. Ghashghaie¹, H.K. Shahzad¹, L.W. Ma², C.Y. Chung¹

¹Department of Materials Science and Engineering, City University of Hong Kong

Hong Kong SAR, P. R. China

²Department of Mechanical and Aerospace Engineering, The Hong Kong University of Science and Technology, Hong Kong, China

Email: Jiefang5-c@my.cityu.edu.hk

Lithium–sulfur (Li–S) batteries are promising beyond lithium-ion battery technology. However, in order to compete with lithium-ion cells on a specific energy (Wh/kg) basis, it is critical to decrease the E/S ratio to a smaller value ($\leq 11 \mu\text{l/mg}$) [1]. The typical ether-based liquid electrolytes are known to have high polysulfides solubility which promote the electrochemical reaction. A low E/S ratio, which have polysulfide concentration close to or exceeding the maximum polysulfides solubility of the electrolyte, will however cause limited capacity and slow kinetics [2]. Electrochemical impedance spectroscopy (EIS) is a powerful tool for exploring properties of electrode/electrolyte interfaces [3]. Here, we carried out the EIS measurements on Li–S cell with a specially designed three-electrode configuration (Figure 1). This new configuration enables the separation of cathode and anode impedance contributions in a complete Li–S cell. In this study, impedance information of the electrolyte, electrode and their interfaces were collected at different depths of discharge (DOD) in the first cycle. Due to the electrodeposition of polysulfides, the electrolyte resistance decreases after reaching a maximum value and, simultaneously, interfacial resistance become more noticeable. In order to understand the effect of E/S ratio on the properties of electrolyte and interfaces, electrodes of three ratio values are being tested and compared. It is found that both interfacial and electrolyte resistances increase with decreasing E/S ratio. The rate-determining step during discharge process, which has the highest resistance, has been proposed. Reducing the E/S ratio significantly enlarges the electrode polarization, leading to insufficient utilization of sulfur and low output potential. The results measured from our newly developed three-electrode configuration can provide valuable information about the electrochemistry between electrolyte and interfaces, which are important for high energy density Li–S batteries design.

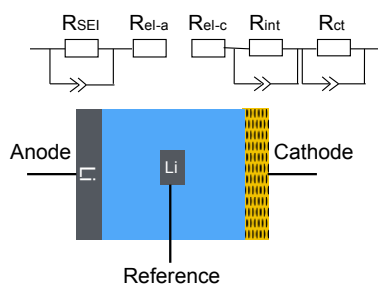


Figure 1. Three electrode set-up and typical equivalent circuit.

References

- [1] B.D. McCloskey, J. Phys. Chem. Lett. 6 (2015) 4581–4588.
- [2] F.Y. Fan, Y.-M. Chiang, J. Electrochem. Soc. 164 (2017) A917–A922.
- [3] S. Drvarič Talian, J. Moškon, R. Dominko, M. Gaberšček, ACS Appl. Mater. Interfaces 9 (2017) 29760–29770.

Hydrothermal Synthesis of Copper Oxide and Carbon Nanotube (CuO/CNT) Nanocomposite to Enhance Supercapacitor Electrodes Performance

Julistian-Ade, An-Ya Lo*

*Department of Chemical and Materials Engineering, National Chin-Yi University of Technology, Taiwan
No.57, Sec. 2, Zhongshan Rd., Taiping Dist., Taichung 41170, Taiwan (R.O.C.)
ade_julistian@yahoo.com, aylo@ncut.edu.tw**

Supercapacitors (SCs) are great candidate for energy storage compared to batteries because its have higher power capability and longer cycle life [1]. Hybrid-supercapacitor is made by a combination of metal oxide and carbon materials. The purpose of combining this two materials is to acquired both advantages of each materials [1-2]. In this study, copper oxide and carbon nanotubes (CuO/CNT) nanocomposite was synthesized by hydrothermal method. The optimum condition was obtained by adjusting reaction time, temperature, and concentration of copper acetate solution. The electrochemical properties were tested by half-cell in a three-electrode configuration; stainless steel was used as the working electrode, platinum wire as the counter electrode and Ag/AgCl electrode as the reference electrode with saturated ammonium sulfate ((NH₄)₂SO₄) as the electrolyte. The surface morphologies and crystallographic informations of CuO/CNT was analyzed by the SEM and XRD. The experimental results showed that the optimum conditions to synthesized CuO/CNT nanocomposite were 5 mmol copper acetate concentration for 30 mg CNT, 12 h reaction time, and the temperature was maintained at 180 °C in the hydrothermal process. The maximum specific capacitance of CuO/CNT nanocomposite could reach 621 F/g at a charging current of 1 A/g, which is 10-times higher than typical carbon nanotubes composite for supercapacitor electrode. EDS mapping for 10 minutes indicated that the weight ratio was 1, 1, 4.5 for copper, oxygen, and carbon, respectively. Thus, performance enhancement of supercapacitor electrode can be acquired by combining copper oxide and carbon nanotube.

References

- [1] Mao-Sung Wu*, Ya-Ping Lin, Chun-Hao Lin, Jyh-Tsung Lee, Formation of Nano-Scaled Crevices and Spacers in NiO-Attached Grapheme Oxide Nanosheets for Supercapacitors, *J. Mater. Chem.* (2012) 22:2442
- [2] Nagesh Kumar, Yun-Cheng Yu, Yi Hsuan Lu, Tseung Yuen Tseng, Fabrication of Carbon Nanotube/Cobalt Oxide Nanocomposites via Electrophoretic Deposition for Supercapacitor Electrodes, *J. Mater. Sci.* (2016) 51:2320-2329

Cobalt-Boron-Iron/Copper Catalysts for Low-Temperature Fuel Cells

Zita Sukackiene, Kornelija Antanaviciute, Aldona Balciunaite, Jurate Vaiciuniene, Arnas Naujokaitis,
Loreta Tamasauskaite Tamasiunaite, Eugenijus Norkus
Center for Physical Sciences and Technology
Saulėtekio ave. 3, LT-10257, Vilnius, Lithuania
zitaja@gmail.com

Low-temperature fuel cells, such as direct borohydride (DBFC), methanol (DMFC), ethanol (DEFC) are promising and environmentally friendly energy sources for electric vehicles and distributed energy generation both for mobile, portable and stationary applications because of their high efficiency and low CO₂ emission. DBFC and DEFC have higher specific energy theoretical voltage and faster anodic kinetics compared with those for direct hydrogen or methanol fuel cells. Since sodium borohydride and ethanol are used as fuels, the search of an efficient non-noble anode materials is industrially vital as well as the evaluation of electrocatalytic activity of these materials.

In this study, the electrocatalytical properties of non-noble catalyst - cobalt-boron-iron/copper were investigated towards the oxidation of sodium borohydride and ethanol using cyclic voltammetry and chronoamperometry. The cobalt-boron-iron/copper catalysts were deposited on the copper surface using morpholine borane as a reducing agent. Iron (II) sulfate and iron (III) chloride have been used as the source of iron ions. The morphology and composition of the cobalt-boron-iron/copper catalysts were studied using Field Emission Scanning Electron Microscopy and Inductively Coupled Plasma Optical Emission Spectroscopy.

Data for the electrocatalytical activity of the cobalt-boron-iron/copper catalysts towards the oxidation of ethanol and borohydride were compared and discussed on the basis of electrochemical data.

Acknowledgment

This research was funded by a grant (No. M-ERA.NET-1/2016) from the Research Council of Lithuania.

Electrochemical Mapping of Transmission Spectra for Electron Transporting through Single-Molecule Junctions

Chun-hsien Chen, Chih-Hsun Lin,¹ Geng-Min Lin,¹ Ching-Hwa Ho,¹ Er-Chien Horng,¹ Han Hsiao,¹ Wei-Chen Yen,² Tsai-Hui Wang,² Wei-Ling Hua,² Hsu-Fu Hsu^{2,*}

¹*Department of Chemistry and Centre for Emerging Material and Advanced Device, National Taiwan University, Taipei, Taiwan 10617.*

²*Department of Chemistry, Tamkang University, New Taipei City, Taiwan 25137.
chhchen@ntu.edu.tw*

In this poster presentation, an electrochemical approach is employed to reveal the transmission function of an electrode-molecule-electrode (EME) junction. Single-molecule electric devices represent the ultimate miniaturization of organic devices. Their electrical performance is measured by applying bias voltages across the rudimentary configuration of EME junctions. Typically, the junction conductance is ascribed to the degree of energy-level alignment, the difference between the Fermi level of electrodes (E_{Fermi}) and the frontier molecular orbitals (*viz.*, HOMO or LUMO). A higher degree of energy-level alignment renders a superior junction conductance. To acquire the conductance (G) of the single-molecule junction, the applied E_{bias} is small and presumably within the ohmic range where the current is linearly proportional to E_{bias} and passes through the origin (*viz.*, zero bias, E_{bias}). The i/E_{bias} ratio yields G . The mechanism features the inversely exponential relationship between conductance and molecular dimensions by $G = G_{\text{contact}} \exp(-\beta L)$ where G , G_{contact} , β and L represent the conductance across the single-molecule junction, the conductance at the contact, the tunneling decay constant, and the length of the molecule (or the distance of the junction). At a large bias, a variety of transport mechanisms may take place collectively and complicate the interpretation. Accordingly, the intrinsic effects of E_{Fermi} on G cannot be unsophisticatedly extracted from this prevalent 2-electrode experimental scheme. Herein, this problem is lifted by integrating conductance measurements with an electrochemical bipotentiostat which keeps E_{bias} constant and concurrently drives chemical potentials of the two working electrodes against that of a reference electrode (explicitly, $\mu = E_{\text{wk}} = E_{\text{Fermi}}$). Therefore, the contribution of the chemical potentials and E_{bias} to G can be decoupled. The transmission spectrum which describe the efficiency of electron transport as a function of E_{Fermi} (or E_{wk}) can be experimentally explored.

Effect of Carbon-Based Cathode Materials on Charge-Discharge Performance of Aprotic Li-O₂ Battery

Kensuke Fujiwara^a, Hoonseung Lee^a, Amane Kaneko^a, Takahiro Ishizaki^b

^aGraduate School of Materials Science and Engineering, Shibaura Institute of Technology

^bDepartment of Materials Science and Engineering, Shibaura Institute of Technology

3-5-7 Toyosu, Koto-ku, Tokyo, JAPAN

ishizaki@shibaura-it.ac.jp

Li-O₂ batteries are promising for electric-vehicle applications because their high theoretical energy density is five times higher than that of Li-ion batteries. The Li-O₂ battery performance can be affected by morphologies and crystal structures of Li₂O₂ formed on cathode electrode after discharge. It has been reported that the morphologies and crystal structures of Li₂O₂ changed depending on the electrolytes, electrolytic solutions, and electrode materials.[1–3] Previous studies have shown that the characteristics of carbon as cathode materials such as pore size, surface area, and pore volume can affect the Li-O₂ battery performance.[4–6] Thus, it is very important to reveal the relationship between Li-O₂ battery performance and the characteristics of various carbon materials. In this study, we aimed to investigate the relationship between the Li-O₂ battery performance and the characteristics of various carbon materials various carbon materials.

Various carbons such as KB, and super P were used as active materials of cathode electrode for Li-O₂ battery. Li metal sheet and 1M LiTFSI in TEGDME were used as anode electrode and electrolyte, respectively. The charge-discharge performance of Li-O₂ battery was investigated using a Swagelok type cell. The physicochemical properties for various carbons were characterized by FESEM, TEM, and BET.

Figure 1 shows discharge profiles of Li-O₂ batteries using various carbons as cathode materials. The discharge performance changed depending on the types of carbon materials. The difference in the discharge performance could be due to the difference in the surface functional groups and surface area of the carbon materials. The relationship between the Li-O₂ battery performance and the characteristics of various carbon materials various carbon materials will be reported.

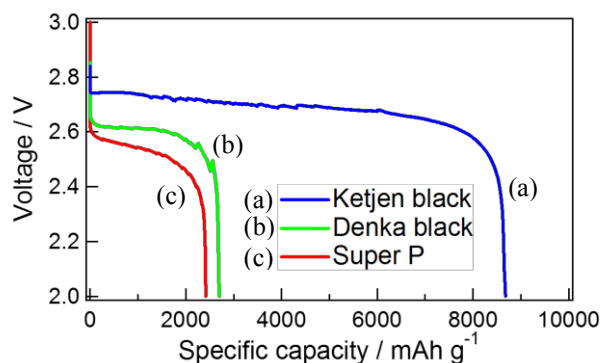


Fig. 1 Discharge profiles of Li-O₂ batteries using various carbons as cathode materials.

References

- [1] L. Johnson, C. Li, Z. Liu, Y. Chen, S.A. Freunberger, P.C. Ashok, et al. *Nat Chem.* 6 (2014) 1091–9.
- [2] D. Sharon, D. Hirsberg, M. Salama, M. Afri, A. Frimer, M. Noked, et al. *Acs Appl Mater Interfaces.* 8 (2016) 5300–5307.
- [3] N. Aetukuri, B. McCloskey, J. García, L. Krupp, V. Viswanathan, A. Luntz. *Nature Chemistry.* 7 (2015) 50–56.
- [4] J. Xiao, D. Wang, W. Xu, D. Wang, R. Williford, J. Liu, et al. *J Electrochem Soc.* 157 (2010) A487–A492.
- [5] C. Tran, X.-Q. Yang, D. Qu. *J Power Sources.* 195 (2010) 2057–2063.
- [6] N. Ding, S. Chien, A.T. Hor, R. Lum, Y. Zong, Z. Liu. *Journal of Materials Chemistry A.* 2 (2014) 12433–12441.

Acknowledgement: This work was partly supported by Grant-in-Aid for Scientific Research (C) (No. 17K06822) from Japan Society for the Promotion of Science.

Evaluation of Anode-Supported Solid Oxide Fuel Cells using Lanthanum Tungstate as a Proton-Conducting Solid Electrolyte Membrane

Gen Kojo¹, Hiroshi Tadokoro¹, Yoshio Matsuzaki², Junichiro Otomo^{1*}

¹ Department of Environment Systems, Graduate School of Frontier Sciences, The University of Tokyo
5-1-5 Kashiwanoha, Kashiwa, Chiba 277-8563, Japan

² Tokyo Gas Co., Ltd. Fundamental Technology Dpt.,
1-7-7 Suehiro, Tsurumi, Yokohama, Kanagawa 230-0045, Japan

*otomo@k.u-tokyo.ac.jp

Lanthanum tungstate ($\text{La}_{28-x}\text{W}_{4+x}\text{O}_{54+3x/2}\text{V}_{2-3x/2}$: LWO) is one of the promising candidate materials for proton-conducting solid electrolyte. LWO shows high proton conductivity at intermediate temperature (around 500°C) because of its intrinsic oxygen vacancies. Also, the concentration of oxygen vacancies in LWO can be controlled by La/W ratio [1]. In our previous study, LWOs were synthesized successfully in a single phase with high La/W ratios ($6.3 \leq \text{La/W} \leq 6.7$) and proton conductivity was increased with an increase in La/W ratio [2]. The application of LWOs as a solid electrolyte membrane for proton-conducting solid oxide fuel cells (p-SOFC) was also examined. Total conductivity measurements as a function of oxygen partial pressure ($p\text{O}_2$) showed that the transport number of proton was almost unity and hole and electron conduction were well suppressed with high La/W ratio. The relationship between calculated power generation efficiency and transport properties of LWOs was investigated. The result indicated that LWOs can realize high power generation efficiency with ca. ten micrometer of thickness of electrolyte because of its low hole and electron conductivities [3]. Table 1 shows the estimated power generation efficiencies and relevant parameters. Based on the results, we fabricated anode-supported single cells using LWOs as thin electrolyte membranes. The chemical stability of the interfaces between electrolyte and electrodes was evaluated using SEM-EDX and fuel cell operation was also tested. The SEM-EDX results showed that there was no diffusion of cation at the interfaces between electrolyte and electrodes. Fuel cell operation was performed at 600°C. The open circuit voltage (OCV) was 1.00 V, which mostly agreed with that of a theoretical value. This result indicated the suitability of LWOs for highly efficient p-SOFCs.

Table 1 Estimated maximum efficiencies and relevant parameters used for the calculations*.

Materials	$\sigma_{\text{hole}}(\text{S cm}^{-1})$	$\sigma_{\text{ion}}(\text{S cm}^{-1})$	Efficiency	References
LWO67	1.20×10^{-3}	1.70×10^{-5}	0.942	[3]
$\text{BaZr}_{0.9}\text{Y}_{0.1}\text{O}_{3-\delta}$ (BCZY09)	2.48×10^{-3}	1.66×10^{-3}	0.728	[4]
$\text{BaCe}_{0.2}\text{Zr}_{0.7}\text{Y}_{0.1}\text{O}_{3-\delta}$ (BCZY27)	2.32×10^{-3}	1.89×10^{-3}	0.740	[4]
$\text{BaCe}_{0.6}\text{Zr}_{0.3}\text{YO}_{3-\delta}$ (BCZY63)	1.22×10^{-3}	2.33×10^{-3}	0.790	[4]
$\text{BaCe}_{0.9}\text{Y}_{0.1}\text{O}_{3-\delta}$ (BCZY90)	4.01×10^{-3}	1.17×10^{-2}	0.813	[4]
$\text{BaZr}_{0.5}\text{Ce}_{0.3}\text{Y}_{0.2}\text{O}_{3-\delta}$	2.06×10^{-4}	4.51×10^{-3}	0.905	[5]

* Electrolyte thickness: 20 μm

Acknowledgements

This work was supported by the Center of Innovation Program (COI) of Japan Science and Technology Agency, JST, the Ministry of Education, Culture, Sports, Science and Technology (MEXT) KAKENHI Grant 17H00801.

References

- [1] A. Magrasó *et al.*, *J. Mater. Chem. A.*, **22**, 12630-12641, 2014.
- [2] G. Kojo *et al.*, *J. Solid State Chemistry*, **248**, 1-8, 2017.
- [3] G. Kojo *et al.*, *Solid State Ionics*, **306**, 89-96, 2017.
- [4] S. Ricote *et al.*, *J. Power Sources*, **193**, 189-193, 2009.
- [5] J. Bu *et al.*, *Ceramics International*, **42**, 4393-4399, 2016.

Influence of Ionomer Content on Cell Performance and Load Cycle Durability of Membrane-Electrode Assemblies Using Pt/Nb-SnO₂ Cathode Catalyst Layers

Ryo Kobayashi^{a,b}, Katsuyoshi Kakinuma^b, Akihiro Iiyama^b, Makoto Uchida^b

^a Interdisciplinary Graduate School of Medicine and Engineering, University of Yamanashi, 4 Takeda, Kofu 400- 8511, Japan

^b Fuel Cell Nanomaterials Center, University of Yamanashi, Miyamae 6-43, Kofu 400-0021, Japan
kkakinuma@yamanashi.ac.jp

Polymer electrolyte fuel cells (PEFCs) are promising power generation devices that are being applied in vehicles owing to their high energy density, energy efficiency and reduction of carbon dioxide emissions. Present candidate cathode catalysts, Pt supported on carbon (Pt/C), undergo serious corrosion during startup/shutdown (1.0-1.5 V), which is a problem that should be overcome to improve the performance. In our previous research, Pt supported on Nb-doped SnO₂ (Pt/Nb-SnO₂) showed higher mass activity and startup/shutdown cycle durability compared to Pt supported on graphitized carbon black (Pt/GCB).¹⁻³ In this research, we evaluated the cell performance using a Pt/Nb-SnO₂ cathode catalyst with various ionomer contents, and the durability under load cycling conditions.

A Pt/Nb-SnO₂ (Pt loading amount: 13.1 wt%, particle size 2.9 ± 0.5 nm) cathode catalyst layer (CL) with various ionomer contents and a Pt/CB anode CL were formed on a Nafion[®] membrane (NRE212, thickness 50 μm, DuPont, USA). The volume ratio of ionomer to support is denoted as I/S. The cell performance of each cell was evaluated at 80 °C, 80% RH, with H₂ and O₂ or air supplied. A load cycle durability test (LDT) was evaluated up to 50,000 potential step cycles (0.6~1.0 V vs. RHE; holding time, 3 s at each potential, Fuel Cell Commercialization Conference of Japan (FCCJ)). Cross-sectional images of the catalyst-coated membranes (CCMs) before and after the durability test were obtained with scanning transmission electron microscopy (STEM, HD2700 Hitachi High Technologies Co., Japan).

Initial apparent mass activity@0.80 V (MA_{app} at 0.80 V) of Pt/Nb-SnO₂ CL increased with decreasing I/S ratio (Fig. 1), and the maximum MA value at I/S = 0.12 was twice that of the Pt/GCB CL (Pt particle size 3.5 ± 0.8 nm; I/S was optimized at I/S = 0.67). The initial values of electrochemical surface area (ECA) for the Pt/Nb-SnO₂ CLs were ca. 60 m² g⁻¹, which were nearly the same in all CLs with different I/S ratios. The ECA was also three times larger than that of the Pt/GCB cathode CL (Fig. 2). ECA values of Pt/Nb-SnO₂ with all I/S ratios remained higher than that of Pt/GCB throughout the LDT. After the LDT, no Pt band appeared in any of the membranes of CCMs using the Pt/Nb-SnO₂ cathode with different I/S ratios. The ionomer coverages on the hydrophilic surface of Pt/Nb-SnO₂ were found to be uniform, whereas it was nonuniform on the hydrophobic surface of Pt/GCB. The ionomer coverage strongly affected the cell performance, along with the Pt utilization and load cycle durability.

This work was supported by funds for the “SPer-FC” project of the New Energy and Industrial Technology Development Organization (NEDO) of Japan.

- 1) Y. Senoo, K. Kakinuma, M. Uchida, H. Uchida, S. Deki, and M. Watanabe, RSC Adv. 4 (2014) 32180.
- 2) Y. Chino, K. Taniguchi, Y. Senoo, K. Kakinuma, M. Hara, M. Watanabe, and M. Uchida, J. Electrochem. Soc. 162 (2015) F736.
- 3) Y. Chino, K. Kakinuma, D.A. Tryk, M. Watanabe, and M. Uchida, J. Electrochem. Soc. 163 (2016) F97.

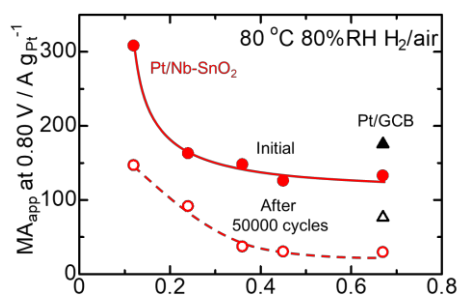


Fig. 1 Apparent MA_{app} at 0.80 V of Pt/Nb-SnO₂ CLs and Pt/GCB CL initially and after 50,000 cycles.

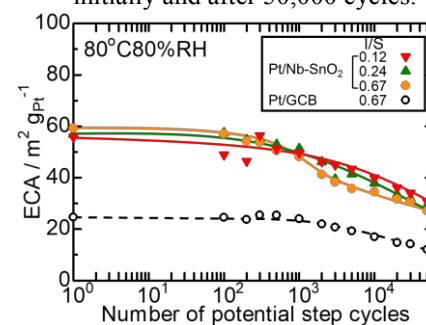


Fig. 2 Load cycle durability test of Pt/Nb-SnO₂ CLs and Pt/GCB CL.

Electrochemical Sensing of Cathepsin L Activity via H3-functionalized Biosensor

Tae Wha Seong¹, Jungmok Seo^{1,2}, and Kwan Hyi Lee^{1,2}

¹*Center for Biomaterials, Korea Institute of Science and Technology (KIST)*

²*Division of Bio-Medical Science & Technology, KIST School, Korea University of Science and Technology (UST), Seoul 02792, Republic of Korea*

5 Hwarangro 14-gil, Seongbuk-gu, Seoul 02792, Republic of Korea

kwanhyi@kist.re.kr

Extracellular proteolytic Cathepsin L (CTSL) serves an important role in regulating the metastatic potential of cancer. In this research, biotinylated full length histone H3 (BFLH3) treated extended gate (EG) field effect transistors (FETs) were used to detect extracellular activity of CTSL with 104 times the sensitivity of fluorometric CTSL activity assays. The treated BFLH3 is cleaved after amino acid 21 upon active reaction by CTSL, inducing a significant change in charge on the EG surface due to the large size and charge of the cleaved BFLH3. FET can detect the change in EG surface charge, allowing the quantification of proteolytic extracellular CTSL activity. Furthermore, self-normalized quantification of CTSL activity was possible in heterogeneous LNCaP and PANC-1 cultured cell media, which accurately demonstrated higher CTSL levels in LNCaP derived from metastatic lesion of human prostatic adenocarcinoma. EG FET allows multiple measurements of CTSL activity with one FET and further investigation is possible to detect other proteolytic enzymes for cancer diagnosis and prognosis.

Electrodeposition of Li at Propylene Carbonate / Ga(l) Interface

Yuta Suzuki¹, Yoshihide Sakanaka¹, Yasuhiro Fukunaka², Takuya Goto^{1*}

¹ Department of Science of Environment and Mathematical Modeling, Graduate School of Science and Engineering, Doshisha University, Kyotanabe, Kyoto 610-0321, Japan

²Nanotechnology Research Institute, Waseda University, Shinjuku-ku, Tokyo 162-0041, Japan

*tgoto@mail.doshisha.ac.jp

Electrochemical nucleation and crystal growth is an important process for understanding the metal deposition, and determining the characteristics of electrodeposits such as morphology, crystallinity, and texture etc. Many researches have studied the initial stages of metal deposition on solid metals as substrates which have crystal imperfections that exhibit preferred nucleation sites. In order to eliminate the influence of inhomogeneities, we focused on liquid metal as substrates. Recently, electrodeposition of metals on liquid metal substrates has been attracting attention^[1,2]. The electrodeposition mechanism of metal on liquid metal substrates is necessary to be examined in detail, nevertheless much less work has been done. In this study, we investigated electrodeposition mechanism of Li at propylene carbonate / Ga(l) interface.

Electrochemical behavior of Li ion on a Ga(s) and Ga(l) in PC-LiClO₄ at 25 / 40°C was investigated by electrochemical measurements. The cyclic voltammograms for Ga(s) at different scan rates showed the current density peaks which attributed to the reduction of Li ion were the linear correlation with respect to the scan rate, indicating the reduction of Li ion on a Ga(s) in a diffusion-limited process. However, there is no relevance between the current density peaks and scan rates on Ga(l), indicating the behavior of reduction of Li ion on Ga(l) was almost different from on Ga(s). The current-time transients curves obtained by potentiostatic polarization also showed the different electrochemical behavior. The current density peaks which ascribed to the nucleation and growth of Li were observed on Ga(s). On the other hand, in the case of using Ga(l), no current density peaks were observed at any potential on Ga(l) substrates.

In order to reveal the electrodeposition mechanism of Li on Ga(l), the interfacial behavior of Ga(l) during potentiostatic polarization was investigated. With proceeding potentiostatic operation, the shape of substrate had been changed from protruded to flat entirely. This phenomenon can be discussed in terms of interfacial tension, that is, the tension of a Ga(l) was changed with the reaction of Li ion reduction. This consideration was supported by Ga-Li phase diagram and electrochemical measurements. This electrodeposition mechanism by using Ga(l) will make a contribution to material science.

[1] S. Maldonado et.al., *J. Am. Chem. Soc.*, **139**, 6960 (2017).

[2] T. Ouchi, D. R. Sadoway, *J. Power Sources*, **357**, 158 (2017).

Non-Polluting Process for Plastic Metallization

S. Ben Jadi¹, M. Bouabdallaoui², A. El Jaouhari¹, Z. Aouzal², A. El Guerraf², E.A. Bazzaoui², R. Wang³,
M. Bazzaoui¹

¹ LME, Faculty of sciences, Ibn Zohr University, 80 000 Agadir, Morocco

² LCM, Faculty of sciences, Mohammed 1^{er} University, 60 000 Oujda, Morocco

³ Department of Mechanical Systems Engineering, Faculty of Engineering, Hiroshima Institute of
Technology, 2-1-1 Miyake, Saeki-ku, Hiroshima 731-5193, Japan
e-mail address: sanabenzadi@gmail.com

Metallization of insulator materials can combine all their properties. The metal carries its conductivity to the insulator while the latter acts as thermal barrier and supports machinery. In particular, plastic metallization is broadly applied in various fields such as electronic housing, automotive and computer body and others.

Conventionally processes for plastic metallization, whether in solid, liquid or gaseous phases have obvious disadvantages. Firstly multi-steps are often required with heavy equipment and precious metal catalysts. In addition, highly toxic compounds, such as salts of tin and chromium are used with pollution as human carcinogen. This brings about large negative impact on the environment and human health.

In this work, a simple eco-friendly process is applied to metalize poly(methyl methacrylate) (PMMA) based on the utilization of conductive polymer. This process consists firstly to modify PMMA surface with polypyrrole (PPy) by chemical polymerization. The PPy coating makes PMMA conductive enough for metal deposition. Secondly, different thicknesses of copper coating on PPy/PMMA were obtained by electrodeposition. High adherence and quality of copper coating were proved by normal sellotape test, microscopic and spectroscopic analysis techniques.

Keywords: Metallization, PMMA, Conducting polymer,

Detection of Mental Stress Biomarker by Aptamer-Immobilized Field-Effect Transistor Sensor

Shigeki Kuroiwa^a, Ryota Takibuchi^b, Sho Hideshima^a, Naoto Kaneko^c, Katsunori Horii^c, Hiroataka Minagawa^c, Iwao Waga^c, Takuya Nakanishi^a, Keishi Ohashi^a, Toshiyuki Momma^{a,b}, Tetsuya Osaka^{a,b}

^a Research Organization for Nano and Life Innovation, Waseda University
513 Wasedatsurumakicho, Shinjuku-ku, Tokyo 162-0041, Japan

^b Graduate School of Advanced Science and Engineering, Waseda University
3-4-1, Okubo, Shinjuku-ku, Tokyo, 169-8555, Japan

^c Innovation Laboratory, NEC Solution Innovators, Ltd.
1-18-7, Shinkiba, Koto-Ku, Tokyo 136-8627, Japan
osakatets@waseda.jp

120 million people are depressed all over the world. The lifetime prevalence of depression is 10-15%¹. In severe cases depression may cause suicide. Mental disorders such as depression are often caused by mental stress. Several biomarkers related to mental stress have been proposed. Detection of biomarkers in the body is very effective for diagnosis of disease and monitoring of human health status. However, blood sampling of mental stress markers is stressful to those who want to check only their own stress levels. We need to measure stress markers non-invasively in our daily lives. Saliva is an ideal biological sample that is sampled non-invasively. Since individual differences in stress response are large, it is important to simultaneously detect multiple markers and evaluate the stress level.

In this study, we attempted to fabricate field effect transistor (FET) biosensors using aptamers against stress biomarkers known to be contained in saliva, α -amylase, cortisol, secretory immunoglobulin A (sIgA), and chromogranin A (CgA)^{2,3}. The aptamers against the above biomarkers were obtained after eight rounds of selection by SELEX method from an initial DNA library, respectively. The gate insulator (SiO₂) of FET was modified with 3-aminopropyltriethoxysilane, followed by addition of glutaraldehyde⁴. Each of the four aptamers terminated with amino groups was immobilized on the thus-prepared surface of insulator. We detected α -amylase, sIgA, CgA, and cortisol in phosphate buffer using each biosensor. Increases in the magnitude of response were observed with increases of the biomarkers' concentration in the range between 1 nmol/dm³ and 100 nmol/dm³, 3 pmol/dm³ and 3 nmol/dm³, 2 nmol/dm³ and 200 nmol/dm³, 1 μ mol/dm³ and 1 mmol/dm³, for α -amylase, sIgA, CgA, and cortisol, respectively. FET sensor responded as a gate voltage shift to the change in charge on the gate insulator surface (Figure 1). The observed responses suggested to be the binding of negatively charged α -amylase (isoelectric point (pI) = 6.34), sIgA (pI = 4.8-6.5), CgA (pI = 4.6-4.9) to the corresponding aptamers. Though cortisol is an electrically neutral molecule, a similar behavior toward the increase of negative charge or the decrease of positive charge was observed. The phosphate groups of DNA aptamers and their counter ions have an electrical charge on the gate insulator. This suggests that the cortisol aptamer contracted and its negative charge penetrated Debye length or that the counter ion bound to the aptamer beforehand was removed after the association of cortisol. The quantitative detection of α -amylase, sIgA, CgA and cortisol using aptamer-immobilized FET sensor was achieved. This sensor is sensitive to a structural change of aptamer induced by the combination with target molecules. It was in this way proved that the detection of neutral target molecules was realized.

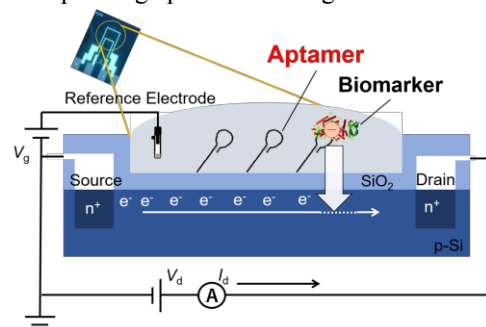


Figure 1 Schematic illustration of detection of biomarker using aptamer-immobilized FET

References

- [1] Lépine, J.-P. and Briley, M., *Neuropsychiatr. Dis. Treat.*, **7**(Suppl 1), 3–7 (2011).
- [2] Kirshbaum, C., and Hellhammer, D.H., *Psychoneuroendocrinology*, **19**, 313-333 (1994).
- [3] Chatterton, R.T., Vogelsong, K.M., Lu, Y., Ellman, A.B., Hudgens, G.A., *Clin. Physiol.*, **16**, 433-448 (1996).
- [4] Wustoni, S., Hideshima, S., Kuroiwa, S., Nakanishi, T., Mori, Y., and Osaka, T., *Sens. Actuators B*, **230**, 374-379 (2016).

Electrodeposited Pt Alloy Cathode Catalysts for High Temperature PEMFC

Hyanjoo Park, Hoyoung Kim, Dong-Kwon Kim, Seonhwa Oh, Soo-Kil Kim*

*School of Integrative Engineering, Chung-Ang University,
84 Heukseokno, Dongjak-gu, Seoul, 06974, Republic of Korea*

* *sookilkim@cau.ac.kr*

A high temperature PEMFC (HT-PEMFC) operates at over 150°C and uses a PBI-based membrane containing phosphoric acid (PA) as an electrolyte [1]. The high operating temperature has the advantages of tolerance to poisons such as carbon monoxide, which is often contained in hydrogen fuel [2]. However, flooding of PA and subsequent phosphate poisoning of the catalyst severely blocks the active sites of the catalysts, resulting in deteriorated performance [3]. As a solution for this, platinum-based alloy (Pt-M) catalysts resistant to phosphate poisoning and have high catalytic activity for ORR [4-5] have been studied. In this study, a variety of transition metals such as Fe, Co, Ni, Cu, Zn and etc. have been alloyed with Pt for testing the PA-resistance and ORR activity.

Alloy catalysts were fabricated by electrodeposition method. It has the advantages of being relatively simple, easy control, low cost, and high throughput compared to the conventional chemical synthesis. Pt-M catalysts with various alloy compositions were electrodeposited on glassy carbon (GC) by controlling the precursor concentrations. The fabricated Pt-M catalysts were analyzed through FE-SEM and EDS for surface morphologies and composition, XRD for the crystallinity and degree of alloying, and XPS to identify the electron structures. The activities to ORR were evaluated both in the presence and absence of PA for evaluation of the PA resistance. The effects of alloying in terms of changes in the electronic structures affecting the adsorption of PA and oxygenated species have been interpreted and will be introduced.

[1] S. S. Araya, F. Zhou, V. L., S. L. Sahlin, J. R. Vang, S. Thomas, X. Gao, C. Jeppesen and S. Knudsen Kær, *Int. J. Hydrogen Energy*, 41 (2016) 21310-21344.

[2] Q. Li, R. He, J. -A. Gao, J.O. Jensen and N.J. Bjerrum, *J. Electrochem. Soc.*, 150 (2003) A1599-A1605.

[3] E. Heider, N. Ignatiev, L. Jörissen, A. Wenda and R. Zeis, *Electrochem. Commun.*, 48 (2014) 24-27.

[4] M.-k. Min, J. Cho, K. Cho and H. Kim, *Electrochim. Acta*, 45 (2000) 4211-4217.

[5] V. Stamenkovic, B. S. Mun, K. J. Mayrhofer, P. N. Ross, N. M. Markovic, J. Rossmeisl, J. Greeley and J. K. Norskov, *Angew. Chem. Int. Ed.*, 45 (2006) 2897-2901.

Highly Porous Non-precious Cathode Catalysts for Proton Exchange Membrane Water Electrolyzer

Hoyoung Kim, Hyanjoo Park, Dong-Kwon Kim, Seonhwa Oh, and Soo-Kil Kim*
School of Integrative Engineering, Chung-Ang University
84 Heukseok-ro, Dongjak-gu, Seoul, 06974, Republic of Korea
**sookilkim@cau.ac.kr*

Water electrolysis is a promising method to produce hydrogen (H₂) with high purity [1,2]. As a catalyst for water electrolysis, platinum (Pt) group materials have usually been used because of their high performance and excellent durability [3], in spite of the high price. To overcome the cost issues, particularly for the cathode where H₂ evolution occurs with relatively fast kinetics, non-Pt materials have been continuously investigated to replace Pt. Among the non-Pt catalysts, Ni, Co, Fe, Mo and W based catalysts which have reasonable performances than others have been studied [4,5]. However, the catalytic activities of these materials are still significantly lower than that of Pt, there have been many trials to enhance the activity using porous structures having large surface areas [6,7]. In this sense, Cu which has moderate activity and relatively positive standard reduction potential would be a promising candidate for this purpose [8].

In this study, Cu nanowires arrays (Cu NAs) with large surface area were fabricated by electrodeposition with modification of Ni overlayer. The catalytic activity of the prepared catalysts to H₂ evolution was evaluated in aqueous sulfuric acid solution according to the changes in the surface morphologies, crystal structures and the electronic structures. The structural characteristics of Ni-modified Cu NA as well as the fairly good activity to the H₂ evolution would be introduced.

References

- [1] M.G. Walter, E.L. Warren, J.R. McKone, S.W. Boettcher, Q. Mi, E.A. Santori, N.S. Lewis, *Chem. Rev.*, 110 (2010) 6446-6473.
- [2] J.H. Williams, A. DeBenedictis, R. Ghanadan, A. Mahone, J. Moore, W.R. Morrow, S. Price, M.S. Torn, *Science* 335 (2012) 53-59.
- [3] J. Greeley, T.F. Jaramillo, J. Bonde, I.B. Chorkendorff, J.K. Norskov, *Nat. Mater.*, 5 (2006) 909-913.
- [4] M.H. Miles, M.A. Thomason, *J. Electrochem. Soc.*, 123 (1976) 1459-1461.
- [5] C.C.L. McCrory, S. Jung, I.M. Ferrer, S.M. Chatman, J.C. Peters, T.F. Jaramillo, *J. Am. Chem. Soc.*, 137 (2015) 4347-4357.
- [6] Y.-H. Chang, C.-T. Lin, T.-Y. Chen, C.-L. Hsu, Y.-H. Lee, W. Zhang, K.-H. Wei, L.-J. Li, *Adv. Mater.*, 25 (2013) 756-760.
- [7] H. Zhou, Y. Wang, R. He, F. Yu, J. Sun, F. Wang, Y. Lan, Z. Ren, S. Chen, *Nano Energy* 20 (2016) 29-36.
- [8] M.E. Bjorketun, A.S. Bondarenko, B.L. Abrams, I. Chorkendorff, J. Rossmeisl, *Phys. Chem. Chem. Phys.*, 12 (2010) 10536-10541.

Electrochemical Impedance Spectroscopy for Detection of Single Nucleotide Polymorphism by Using S1 Nuclease

Yu-Sheng Chuang, Hao-Yu Yen, Ching-Chou Wu*

Department of Bio-industrial Mechatronics Engineering, National Chung Hsing University
No.145, Xingda Road, Taichung 402, Taiwan, ROC
ccwu@dragon.nchu.edu.tw

Abstract

Background: *Geminiviridae* can cause severe infection in economic plants in tropical and subtropical regions. Infected plants would grow poorly, dwarf and die. If the infected plant are not detected immediately, it will be easily to spread by insects, causing large-range infection. Real-time polymerase chain reaction (RTPCR) is a common diagnostic method in specific gene detection, but it is difficult to distinguish the gene mutation by the PCR process. Geminivirus has a high-degree variability in genomes. The variation of single nucleotide occurs at a specific position in the genome, called single nucleotide polymorphism (SNP). Therefore, developing fast and accurate method for the detection of geminivirus SNP is an important issue. In this study, electrochemical impedance spectroscopy (EIS) was used to detect the hybridization of single nucleotide-mismatched target DNA with the cleavage of S1 nuclease.

Method: The position-varied single mismatched target geminivirus DNA (smtDNA) fragments were synthesized to demonstrate the feasibility of SNP detection. The smtDNAs were hybridized with a thiolated probe DNA (pDNA) to form a double-stranded structure in a PBS solution. The mismatch position of the double-stranded DNA (dsDNA) is cut by S1 nuclease. Afterwards, the thiolate-containing dsDNA was immobilized on a cleaned thin-film gold electrode via the formation of Au-S bond. The dsDNA-modified electrodes were applied a -0.2 V pulse in the 6-mercapto-1-hexanol (MCH) solution for the surface blocking and the prevention of nonspecific adsorption. Afterwards, EIS was used to measure the impedance of the dsDNA/MCH-modified electrode for the estimation of SNP.

Result: The target DNA fragments of single mismatched base positioned at 5th, 11th, 16th form 5' end were hybridized with thiolated pDNA and then acted with S1 nuclease. The length of dsDNA immobilized on the Au electrodes was measured by EIS. The corresponding ΔR_{et} increment is shown in Figure 1. The ΔR_{et} values of 5th, 11th, 16th-positioned mismatch dsDNA were respectively 75%, 58% and 42% of ΔR_{et} values of the complete complementary dsDNA. Furthermore, the ΔR_{et} presents a good linearity with the dsDNA concentration in the range of 1 pM- 10 nM and exhibit a detection limit of 1 pM, as shown in Figure 2.

Conclusion: The detection strategy and analysis method can improve the resolution of single-mismatch target DNA. Single-mismatch base position can be directly measured without expensive fluorescent reagents and PCR equipment of precise temperature control.

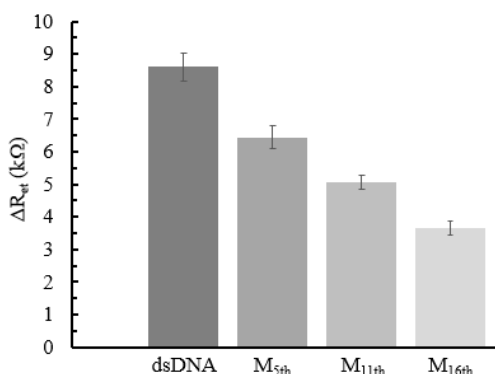


Figure 1. The change in electron transfer resistance (ΔR_{et}) after modifying the different single-mismatch base positions dsDNA.

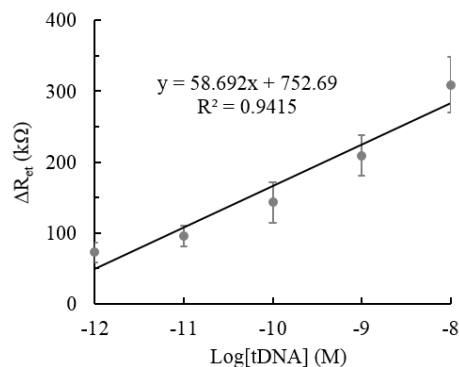


Figure 2. The ΔR_{et} value as a function of each hybridization concentration.

Evaluation of Unsupported Pt₃Ni Aerogels as PEFC Anode Catalysts under Hydrogen Starvation Conditions

Ryo Shimizu,^a Sebastian Henning,^b Juan Herranz,^b Thomas J. Schmidt,^{b,c} Laura Kühn,^d Alexander Eychmüller,^d Katsuyoshi Kakinuma,^e and Makoto Uchida^e

^a Interdisciplinary Graduate School of Medicine and Engineering, University of Yamanashi, 4-4-37Takeda, Kofu, 400-8510, Japan, ^bElectrochemistry Laboratory, Paul Scherrer Institut, 5232 Villigen, Switzerland, ^c Laboratory of Physical Chemistry, ETH Zurich, 8093 Zurich, Switzerland, ^d Physical Chemistry, Technische Universität Dresden, Bergstr. 66b, 01062 Dresden, Germany, ^e Fuel Cell Nanomaterials Center, University of Yamanashi, 6-43 Miyamae, Kofu, 400-0021, Japan.

E-mail: uchidam@yamanashi.ac.jp

Polymer electrolyte fuel cells' (PEFCs) successful commercialization depends crucially on further cost reductions. These could be achieved using catalysts with higher durability, therefore allowing a lower Pt use. In this respect, anode catalysts with high stability in case of gross hydrogen starvation events constitute a pressing need. The latter fuel starvation events are caused by the blockage of the hydrogen gas flow in an anode flow field by water droplets, and lead to an anode potential increase from ≈ 0 V to ≥ 1.5 V.¹ At these potentials, significant corrosion of the carbon support in commercial Pt on carbon black (Pt/CB) catalysts and concomitant performance decreases have been reported.² Motivated by our previous study in which unsupported Pt₃Ni aerogel demonstrated remarkable corrosion stability as PEFC cathode catalyst,³ in this work the applicability of the former material on the anode side was investigated.

Pt₃Ni aerogel catalyst was synthesized according to the steps described in reference 4, and a commercial Pt/CB catalyst (47wt% Pt, TKK, TEC10E50E) was used as a benchmark. The hydrogen starvation events were simulated by an accelerated stress test (AST) performed at 80 °C, 100 % RH, ambient pressure, and H₂ / N₂ flows of 100 ml/min at cathode and anode, respectively. Under these conditions, 250 potential cycles in a square wave voltammetry pattern between 0 and 1.5 V with a holding time of 10 s were applied to the anode side.

Figure 1 shows polarization curves of membrane electrode assemblies (MEAs) utilizing Pt₃Ni aerogel or Pt/CB as anode catalysts (with loadings of ≈ 0.05 mg_{Pt}/cm²_{anode}) at beginning and end-of-life (BOL, EOL). The agreement of the BOL data indicates that the performance attained with the aerogel CLs is identical to the one with a commercial benchmark catalyst. Interestingly, the AST caused large performance deterioration for the MEA using Pt/CB at the anode, whereas the cell using Pt₃Ni was not affected at all. This contribution will report a detailed investigation of the reasons for the former degradation, which were investigated using electrochemical impedance spectroscopy and hydrogen pump tests to decouple the overpotential contributions to the materials' BOL and EOL performance. Ultimately, this approach leads to the conclusion that the majority of the performance losses are related to changes in the anodic CLs' mass transport properties, and illustrates the superiority of Pt₃Ni aerogel vs. Pt/CB as a PEFC anode catalyst.

This work was carried out in the Electrochemistry Laboratory of Paul Scherrer Institute and funded by the Swiss National Science Foundation (20001E_151122/1), the German Research Foundation (EY 16/18-1) and the European Research Council (ERC AdG 2013 AEROCAT).

References

- 1) P. Rodriguez, T.J. Schmidt, Encyclopedia of Applied Electrochemistry, Springer New York, New York, NY, 1606-1617 (2014).
- 2) J. Speder, A. Zana, I. Spanos, J.J.K. Kirkensgaard, K. Mortensen, M. Hanzlik, M. Arenz, J. Power Sources 261, 14-22 (2014).
- 3) S. Henning, J. Herranz, H. Ishikawa, B.J. Kim, D. Abbott, L. Kühn, A. Eychmüller, T.J. Schmidt, J. Electrochem. Soc. 164, F1136-F1141 (2017).
- 4) S. Henning, L. Kühn, J. Herranz, J. Durst, T. Binninger, M. Nachtgeal, M. Werheid, W. Liu, M. Adam, S. Kaskel, A. Eychmüller, T.J. Schmidt, J. Electrochem. Soc. 163, F998-F1003 (2016).

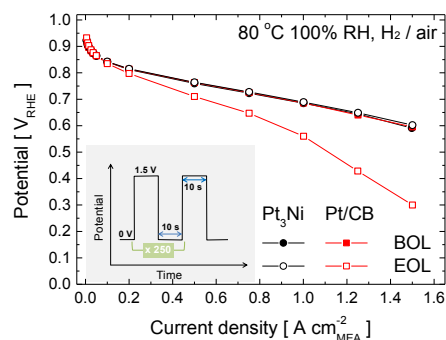


Figure 1. BOL and EOL I/E curves at 80 °C, 100 % RH in H₂/air at 1.5 bar_{abs} for MEAs with Pt₃Ni aerogel and Pt/CB anodes (with ≈ 0.05 mg_{Pt}/cm²_{MEA}), respectively. The inset illustrates the performed accelerated stress test protocol.

Analysis of Electrodeposition Process of $L1_0$ -Ordered FePtCu Nanodot Arrays

Mana Kambe^a, Siggi Wodarz^a, Shogo Hashimoto^a, Giovanni Zangari^b, Takayuki Homma^a

^a Department of Applied Chemistry, Waseda University, Shinjuku, Tokyo 169-8555, Japan

^b Department of Materials Science and Engineering and CESE, University of Virginia, Charlottesville, VA 22904-4745, USA

e-mail address: t.homma@waseda.jp

$L1_0$ -ordered FePt alloy has been considered as one of the most promising candidates for use in ultra-high density magnetic recording media, such as heat assisted magnetic recording (HAMR) and bit-patterned media (BPM) [1], due to its high uniaxial crystal magnetic anisotropy, which enables recording density well beyond several Tbit/in². We have developed a fabrication process of ferromagnetic nanodot arrays by using lithography techniques and electrodeposition for BPM applications [2]. In a previous study, we have succeeded to fabricate FePt nanodot arrays with areal density of 0.5 Tbit/in² (distance between nanodots is 35 nm), however, the degree of $L1_0$ ordering of nanodot arrays was not sufficient; enhancement of $L1_0$ ordering was therefore strongly needed. In order to solve this problem, in this work, we fabricated uniform $L1_0$ -FePt nanodot arrays with Tbit/in²-level recording density by synthesizing a FePtCu ternary alloy to accelerate the ordering process of FePt under lower annealing temperature or heating time requirements.

Nanopore patterned substrates with 15 nm in diameter and 35 nm in pitch were fabricated by electron beam lithography onto n-Si(100) wafers covered with 60 nm Ru/5 nm Ti. Electrodeposition of FePtCu was conducted in a three-electrode system with the nanopore patterned substrate as working electrode, a Pt mesh as counter electrode and Ag/AgCl as reference electrode, respectively. The composition of FePtCu alloy was optimized by varying the applied potential and concentration of CuSO₄ in the electrolyte [2]. The deposited continuous film and nanodot arrays were then annealed in Ar+H₂ atmosphere using rapid thermal annealing system to achieve the $L1_0$ ordering.

In a previous report, sputter-deposited (Fe_{100-x}Cu_x)Pt₄₅ showed $L1_0$ structure when the Cu fraction was under 25 at% [3]. In order to achieve FePtCu with Cu composition of ~25 at%, we further optimized the composition of FePtCu by controlling the CuSO₄ concentration and the applied potential. Based on the linear sweep voltammetry (LSV) of the FePtCu electrolyte, electrodeposition was carried out with -0.95, -1.0, -1.05 V under different CuSO₄ concentration (0.025~0.05 mM); LSV showed that Pt and Cu deposited at around -0.5 V and Fe deposited at -0.85 V. From these results the composition of each metal species changed approximately linearly with applied potential and the Cu content increased with higher CuSO₄ concentration as expected. At less negative potential, the composition was close to the ideal composition, i.e. ~25 at% Cu, 40~50 at% Pt, and FePtCu film with composition of Fe:Pt:Cu=30:46:24 was obtained at -0.95 V with 0.025 mM CuSO₄. To investigate the phase transformation of this film, as deposited continuous films were annealed at 450 °C for 1 h. XRD of annealed FePtCu films showed (001), (110), and (200) peaks of the $L1_0$ -ordered structure, which were not observed with the annealed FePt binary alloy. In addition, the (001) peak shifted to higher 2θ angle compared to that of FePt binary alloy, suggesting the promotion of $L1_0$ ordering by addition of Cu. Along with the phase transformation magnetic hardening was observed with FePtCu film and its perpendicular coercivity increased up to 6.0 kOe, whereas FePt film did not exhibit magnetic hardening (1.0 kOe). Furthermore, in order to fabricate nanodot arrays with $L1_0$ structure, FePtCu was electrodeposited in nanopore array, substrate with 15nm in diameter and 35 nm pitch under the same deposition condition as continuous film. The fabrication of FePtCu nanodot arrays was successfully carried out with the optimum annealing condition being 650 °C and ramp rate 1950 °C/min, where significant deformation of nanodots did not occur. After annealing, TEM imaging and diffraction of FePtCu nanodot arrays showed that nanodot arrays were single crystal with a (111) crystal orientation. In addition, lattice constant was calculated to be 0.210 nm, which was close to the value of (111) plane of $L1_0$ structure (=0.219 nm), indicating a successful fabrication of FePt nanodot arrays with $L1_0$ -ordered structure by Cu addition.

[1] B. D. Terris and T. Thomas, J. Phys. D: Appl. Phys., 38, (2005) R199-R222.

[2] T. Homma, S. Wodarz, D. Nishiie, T. Otani, G. Zangari, and T. Homma, Electrochem. Soc. Trans., 64, (2015) 1-9.

[3] D. C. Berry and K. Barmak, J. Appl. Phys., 102, (2007) 024912-1-9.

Local Cyclic Voltammogram Mapping on Silicon-Carbon Composite Negative Electrodes for Lithium-ion Batteries

Y. Sato¹, A. Kumatani^{1,2}, Y. Takahashi^{3,4}, K. Kubota⁵, H. Shiku⁶, S. Komaba⁵ and T. Matsue¹

1. Graduate School of Environmental Studies, Tohoku University, Japan.

2. Advanced Institute for Materials Research (AIMR), Tohoku University, Japan.

2. Graduate School of Environmental Studies, Tohoku University, Japan.

3. Division of Electrical Engineering and Computer Science, Kanazawa University, Kanazawa, Japan.

4. Precursory Research for Embryonic Science and Technology (PRESTO),
Japan Science and Technology Agency (JST), Japan.

5. Department of Applied Chemistry, Tokyo University of Science, Japan.

6. Department of Applied Chemistry, Graduate School of Engineering, Tohoku University, Japan.

e-mail address: kumatani@bioinfo.che.tohoku.ac.jp, matsue@bioinfo.che.tohoku.ac.jp

Recent progress of high performance lithium-ion batteries (LIBs) is remarkable for practical application to electric/hybrid vehicles. For realization of higher energy capabilities in LIBs, one of approach is to make active materials with micro-/nano-meter size in the electrodes for enhancement of functionalities and cycle abilities or to use materials with higher compatibilities such as silicon nanoparticles for negative electrodes. Although the size of active materials are miniaturized, their electrochemical performance is evaluated under conventional bulk measurement. As other characterization technique, scanning probe microscopies such as scanning tunneling microscopy and conductive atomic force microscopy can be available as atomic level analyses, but their information are mainly obtained from electronic conduction. It is therefore required to develop a spatially resolved electrochemical analysis at microscopic scale for understanding their electrochemical properties to lead optimized electrode structures. In this study, we have investigated the local electrochemical properties on silicon-carbon composite negative electrodes by scanning electrochemical cell microscopy with a nanopipette, i.e. SECCM [1]. The SECCM is able to analyze *in-situ* local electrochemical performance through a meniscus created between sample and nanopipette. By SECCM analysis, we have investigated local electrochemical properties on the composite negative electrodes in LIBs.

The negative composite electrodes were prepared with 100 nm diameter silicon (Si) nanoparticles with graphite planers conjugated by a polyacrylate based binder [2]. The morphology of the electrode surface was observed by scanning electron microscopy in Fig. 1 (a). Si nanoparticles and graphite showed good dispersion because of a polyacrylate binder was covered with them. For SECCM analysis, a 100 nm diameter nanopipette was filled with organic electrolyte and a lithium quasi-reference counter electrode. The pipette was used as a probe, and the cell was utilized to measure the local electrochemical reaction once the meniscus was created between pipette and sample surface as a nanoscale electrochemical simulator cell. Through the cell a local electrochemical analysis was applied (cyclic voltammograms (CVs) with a scan rate of 100 mV/s). By hopping the pipette to measure the local electrochemical information ($7 \times 7 \mu\text{m}^2$ with $1 \mu\text{m}$ intervals), the CV results were classified with regard to delithiation process. Further, the results was mapped, suggesting where the delithiation was occurred from silicon or/and graphite. The information would be important to confirm the dispersion of active materials, the performance of each particle on composite electrodes for practical purpose.

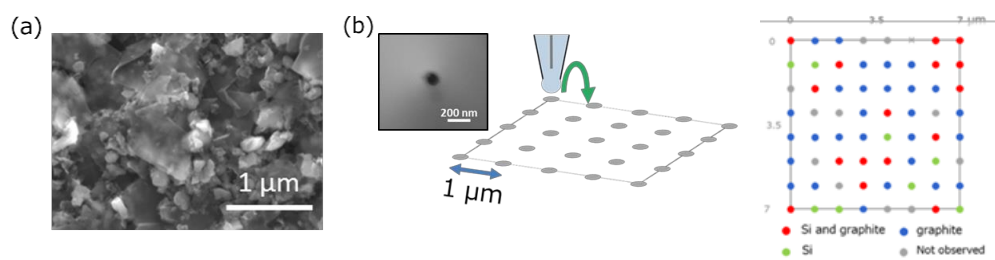


Fig.1 (a) An SEM image and (b) a local CV mapping results on lithium-ion delithiation (from Si and/or graphite) for investigation of the dispersion state of Si-graphite negative electrodes.

Reference:

[1] Y. Takahashi *et al.*, Nat. Commun. 5:6450 (2014).

[2] Z.-J. Han *et al.*, Energy Environ. Sci., 5, 9014 (2012).

Respiration Assay of Co-culture Cell Spheroid Using an LSI-based Electrochemical Device

Hao-Jen Pai, Takehiro Onodera, Kosuke Ino, Hitoshi Shiku

Graduate School of Engineering, Tohoku University, Aramaki Aoba 6-6-11, Sendai 980-8579, Japan

Email: pai.hao-jen.p5@dc.tohoku.ac.jp (H. J. Pai)

Abstract:

Recently, three-dimensional (3D) cell spheroid has been used as an *in vitro* model in the field of cancer theory and drug delivery research. Comparing to two-dimensional (2D) monolayers, which inadequately reflects tumor growth, extra-cellular interaction and gene expression, Three-dimensional (3D) cell spheroid structure is able to recapitulate many environmental factor *in vivo* such as oxygenation and nutrition gradients, hypoxia and necrosis. The limit of spheroid diffusion is about 150-200 μm . In larger cell spheroid, the outer layer continuously proliferates while hypoxia and necrosis appears at inner layer of spheroid. For better imitation of tumor, angiogenesis, which is the formation of new blood vessels, was introduced by co-culturing Human Umbilical Vein Endothelial Cells (HUVEC) with HepG2 to develop capillary structure in 3D spheroid. In the present study, the effect of co-culture of HUVECs on HepG2 spheroids was investigated using an LSI-based electrochemical device.

Large-scale integration (LSI) is an effective tool for bio-imaging and bio-sensor. It has been used as enzyme activity sensor and real time monitor of electroactive molecules such as neurotransmitters and oxygen of single cell and cell aggregate through local redox reaction. Previously, we developed an LSI-based electrochemical device, which is called as Bio-LSI, and the device was used to detect cell activities of neuron-like cells and embryonic stem cells, such as dopamine release, respiration activity and alkaline phosphate activity. In the present study, the device was applied for evaluation of the co-culture, based on respiration assay. The detection scheme is shown in Fig. 1.

To increase the oxygen concentration and decrease hypoxia effect on inner spheroid, HepG2 cell was tested by co-cultured with HUVEC in different ratios. HUVEC was stained with CellTracker Green to observe capillary structure. Respiration ability of spheroid was monitored by O_2 reduction current through LSI-based device. 5000 cells per spheroid were cultured through hanging drop method. Five ratios of HepG2 cell and HUVEC (1:0, 2:1, 1:1, 1:2, and 0:1) were cultured and respiration ability was tested at the 3rd and 7th day of hanging drop. Cell spheroids were introduced on LSI device by using micropipette. Voltage was set to be -0.5V. $\Delta\text{Current}$, calculated by subtracting background and peak current, was used as discussion of respiration ability and effects of HUVEC co-culture. Figure 2 shows optical image and electrochemical image of four cell ratios co-cultured for 3 days. In future work, electrochemical graphic of 7th day culturing and HepG2: HUVEC =0:1 will further be done. The calculation of $\Delta\text{current}$ will be use for discussion of the influence of co-culturing with HUVEC cells.

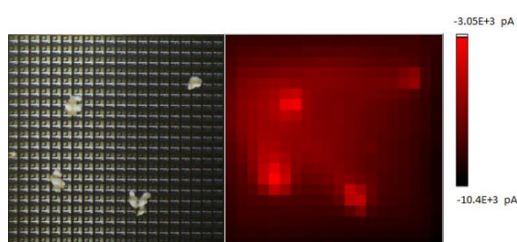


Figure 1 Optical image of spheroid and electrochemical image detected by LSI device.

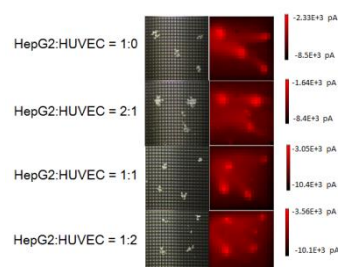


Figure 2 Optical and electrochemical image of co-culture cell spheroid

References:

1. Y. Kanno, K. Ino, H. Abe, C. Sakamoto, T. Onodera, K. Y. Inoue, A. Suda, R. Kunikata, M. Matsudaira, H. Shiku, T. Matsue, *Anal. Chem.* 2017.
2. K. Y. Inoue, M. Matsudaira, M. Nakano, K. Ino, C. Sakamoto, Y. Kanno, R. Kubo, R. Kunikata, A. Kira, A. Suda, R. Tsurumi, T. Shioya, S. Yoshida, M. Muroyama, T. Ishikawa, H. Shiku, S. Satoh, M. Esashi, T. Matsue, *Lab Chip*, 15, 848, 2015.

Electrochemical characterization of solution-processed TMD thin films

Gyeong Sook Bang, Tae In Kim, Jae Eun Lee, Sung-Yool Choi

*School of Electrical Engineering, Center for Advanced Materials Discovery for 3D Display,
Graphene/2D Materials Research Center, KAIST, Daejeon 34141, Republic of Korea*

smilegs@kaist.ac.kr, sungyool.choi@kaist.ac.kr

Transition metal dichalcogenides (TMDs, MX_2 ; M = Mo and W, X = S and Se), belong to the family of layered materials, whose crystal structures are built up of covalently bonded X-M-X single-layers that interact by van der Waals forces as graphite [1]. Each single layer consists of two X atom layers and a layer of metal atoms sandwiched between two layers of chalcogens. This has been taken much attention in a variety of applications including catalyst, energy storage, solar cell, and sensing devices. Li-intercalated exfoliation approaches have been proposed to produce 2D-TMDs nanoflakes and are among the most effective methods for the mass production of exfoliated MX_2 nanoflakes [2]. Despite their application as energy material, there are not many reports on study of electrochemical properties of 2D-TMDs nanoflakes prepared by Li-intercalated exfoliation.

We present an electrochemical characterization of the 2D-TMDs nanoflake films prepared by Li-intercalated exfoliation. These 2D-TMDs films show a low sheet resistance and their conductivity change by oxidative electrochemical treatment. The 2D-MoSe₂ film shows about 200 mV lower oxidation potential than 2D-MoS₂ film. These properties may give important information on their use for energy-related devices.

References

1. A. K. Geim; I. V. Grigorieva, *Nature* 499, 419 (2013).
2. Eda, G.; Yamaguchi, H.; Voiry, D.; Fujita, T.; Chen, M.; Chhowalla, M. *Nano. Lett.* **2011**, *11*, 5111-5116.

Nanoscale Electrochemical Imaging of Redox Activities on Metallic and Semiconducting Single-Walled Carbon Nanotubes

M. Shimura¹, A. Kumatani^{1,2}, C. Miura¹, Y. Takahashi^{3,4}, T. Okada⁵, H. Ida¹,
H. Shiku⁶, S. Samukawa^{2,5} and T. Matsue¹

1. Graduate School of Environmental Studies, Tohoku University, Japan.

2. Advanced Institute for Materials Research (AIMR), Tohoku University, Japan.

3. Division of Electrical Engineering and Computer Science, Kanazawa University, Kanazawa, Japan.

4. Precursory Research for Embryonic Science and Technology (PRESTO),
Japan Science and Technology Agency (JST), Japan.

5. Institute for Fluid Science (IFS), Tohoku University, Japan.

6. Department of Applied Chemistry, Graduate School of Engineering, Tohoku University, Japan.

e-mail address: kumatani@bioinfo.che.tohoku.ac.jp, matsue@bioinfo.che.tohoku.ac.jp

Single walled carbon nanotubes (SWNTs), whose structure is a rolled monolayer of graphene into a cylinder shape, behaves both metallic/semiconducting properties depending upon how they are rolled up. Their physical properties are well-known such as high electronic mobility for semiconducting nanotubes as expected future nanocarbon-based devices. For realization of nanotube-based devices (e.g. thin film transistors with semiconducting nanotubes), there is still an issue to remove some amount of metallic nanotubes inside semiconducting nanotube films, which will affect to their total performance in transistors. Recently, Tanaka and his research group introduced a gel-based technique for separation between metallic and semiconducting SWNTs with large production (~90%) [1]. Although the technique is an effective, it is required to detect a trace amount of metallic nanotubes for the application purpose.

In this research, we have challenged to develop a sensitive characterization technique to detect either between semiconducting and metallic nanotubes by using a difference between semiconducting and metallic nanotubes in redox activities as nanoscale electrochemical imaging. For the imaging, we have applied a scanning electrochemical cell microscopy (SECCM) [2]. The SECCM can create a confined electrochemical cell at nanoscale as a meniscus between pipette and sample surface. A 190 nm diameter glass pipette was used as a probe filled with 5 mM $\text{Ru}(\text{NH}_3)_6^{3+/2+}$ in deionized water and an Ag/AgCl quasi-reference counter electrode. For the sample, both semiconducting and metallic thin films were prepared by a dried droplet of high purity SWNT solutions (Meijo Nano Carbon). Once the pipette was contacted at the sample surface by meniscus, the cyclic voltammetry (CV) was measured at a scan rate of 10 mV/s. The Fig. 1 (a) shows CV results from both films, showing that there is about 100 mV difference to induce the $\text{Ru}(\text{NH}_3)_6^{3+/2+}$ redox reaction. Using the difference, both SWNT thin films were visualized as nanoscale electrochemical imaging by SECCM as shown in Fig 1 (b). Those results suggested that SECCM could be applicable for sensitive detection between semiconducting and metallic nanotubes.

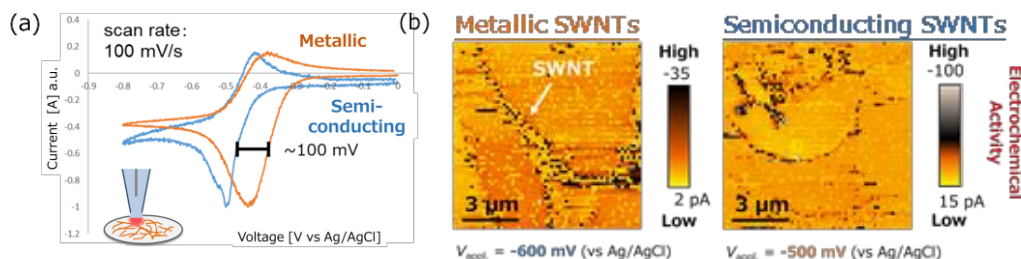


Fig.1 (a) CV results and (b) electrochemical imaging on both semiconducting and metallic SWNTs films

Reference:

[1] T. Tanaka *et al.*, Nano Lett. 9, 1497 (2009).

[2] Y. Takahashi *et al.*, Nat. Commun. 5:6450 (2014).

Screening of Indium Cadmium Sulfur-based Photocatalysts and Characterization of Efficient Photocatalysts

Yu-Ching Weng, Ke-Jih Ciou

Feng Chia University

Department Chemical Engineering, Feng Chia University, Taichung 40724, Taiwan

ycweng@fcu.edu.tw

The utilization of solar energy for the production of hydrogen from water using semiconductor photocatalysts is of great significant due to the global problems in energy and environment. To develop visible-light-driven photocatalysts is important for enhancing the efficiency of solar light conversion. CdS was one of the promising photocatalysts due to its narrow band gap, a sufficiently negative flat band potential and low cost. However, it is prone to photo corrosion. In addition, the fast recombination of photogenerated electrons and holes results in low photocatalytic efficiency. Therefore, to discovery of new type of visible-light-driven photocatalysts is urgently required. In this study, an $M_x-(In_{0.2}Cd_{0.8})_{1-x}S$ based photocatalyst array was prepared by pico-liter piezoelectric dispensing system. The arrays was then rapidly screened by scanning electrochemical microscopy (SECM) with an optical fiber in Na_2SO_4/Na_2SO_3 solution. The photocatalytic activity of the spots was measured via photocurrents at the substrate of the array for water splitting. The optimal photocatalysts were further characterized by X-ray diffraction (XRD), X-ray photoelectron spectrometry (XPS), UV-vis spectroscopy and electrochemical impedance spectroscopy (EIS). The photochemical properties of the bulk film photoelectrode were also investigated and compared with the $In_{0.2}Cd_{0.8}S$.

Bimetallic Pt-based Sensor for Oxygen Detection

Yu-Ching Weng, Wei Peng

Feng Chia University

Department Chemical Engineering, Feng Chia University, Taichung 40724, Taiwan

ycweng@fcu.edu.tw

Carbon-supported bimetallic Pt-M (Co, Ni, Y and Ga) electrocatalyst were prepared and characterized for oxygen detection. These bimetallic Pt-based electrocatalysts were fabricated by chemical reduction method at low temperature and then were sprayed on the Nafion membrane as working electrode. The surface morphology, loading weight, elemental composition and crystalline of electrocatalysts were characterized by transmission electron microscopy (TEM), thermogravimetric analysis (TGA), energy dispersive spectroscopy (EDX) and high-resolution X-ray diffraction analyzer (HRXRD). Analytic methods such as linear sweep voltammetry, rotating ring-disk electrode (RRDE) and tafel curves were used to determine the initial potential, electron transfer number and kinetic parameters of the electrocatalysts for oxygen reduction reaction (ORR). Among electrocatalysts prepared in the work, Pt₃-Ni₁/C electrocatalysts have best catalytic activity for ORR. All these electrocatalysts possess face-centered cubic structure with the average particle size less than 5 (nm). The electron transfer number of bimetallic Pt-based electrocatalysts is close to 4. It indicates that oxygen can be directly reduced to water on the Pt-based electrocatalysts. The performances of the oxygen sensor including sensitivity, selectivity, stability as well as the response and recovery times have been examined.

Novel approaches to Synthesize S-PAN/FeS₂ Electrocatalyst for Hydrogen Evolution Reaction

Na-Jung Kuo¹, Min-Hsin Yeh², Yi-Ying Tsai³, Chun-Hong Kuo², Bing-Joe Hwang^{3,4*},
Wei-Nien Su^{1*}

¹*Graduate Institute of Applied Science and Technology, National Taiwan University of Science and Technology, Taipei 10607, Taiwan*

²*Institute of Chemistry, Academia Sinica, Taipei, Taiwan.*

³*Nanoelectrochemistry Laboratory, Department of Chemical Engineering, National Taiwan University of Science and Technology, Taipei 10607, Taiwan*

⁴*National Synchrotron Radiation Research Center, Hsin-Chu 30076, Taiwan*

**Email: bjh@mail.ntu.edu.tw; wsu@mail.ntust.edu.tw*

Abstract

Environmental issues and depletion of fossil fuels have motivated intense research on alternative clean and sustainable energy carriers. Hydrogen has been regarded as a promising energy carrier by virtue of its high energy density and zero-emission. For harvesting the hydrogen from nature, electrocatalytic hydrogen evolution reaction (HER) is one of the most appealing approaches to extract molecular hydrogen from water. Currently, Pt-based materials are regarded as the most efficient electrocatalysts for HER. However, the low abundance and high cost limit their widespread applications. Providing a promising replacement to the Pt-based electrocatalysts became an exciting issue in this field. Recently, transition metals chalcogenides had been studied as an alternative to replace the precious metal catalysts for HER. However, poor conductivity for transition metal dichalcogenides may limit its HER performance. In this study, novel sulfurized polyacrylonitrile derived FeS₂ (S-PAN/FeS₂) composite has been proposed and synthesized by different approaches (physical coating on carbon paper, hydrothermal process and electrochemical process, etc.). After structural and electrochemical characterizations, as-prepared S-PAN/FeS₂ electrocatalyst has shown promising HER activities.

Keywords: sulfurized polyacrylonitrile, FeS₂, non-precious metal, transition metal dichalcogenides.

Measurement of Tin Oxide Thickness with Sequential Electrochemical Reduction Analysis

Hiroyuki Saito

Tokyo Denki University

5 Senju-Asahi-Cho Adachi Tokyo Japan

h.saito3110@mail.dendai.ac.jp

Introduction

The author measured tin oxide thickness formed on pure tin solder plate with Sequential Electrochemical Reduction Analysis (SERA). SERA is a variation of cathodic reduction analysis and is developed by D. M. Tench¹⁾. Though the SnO₂ SnO Sn transition is observed with XPS analysis²⁾ or TEM & EDS observation³⁻⁴⁾, the growth rate of those oxides was unclear. Researchers report that the oxide thickness affect the wetness of solder¹⁻⁵⁾.

Experimental

The 99.9% pure tin plates are exposed at TDU building in Tokyo, Japan. The room temperature is controlled around 300K. Humidity is not controlled. 180 days exposure test was carried out. During exposure, periodically the oxide thickness is measured by SERA. The schematic illustration of SERA apparatus⁵⁾ is shown in Fig.1.

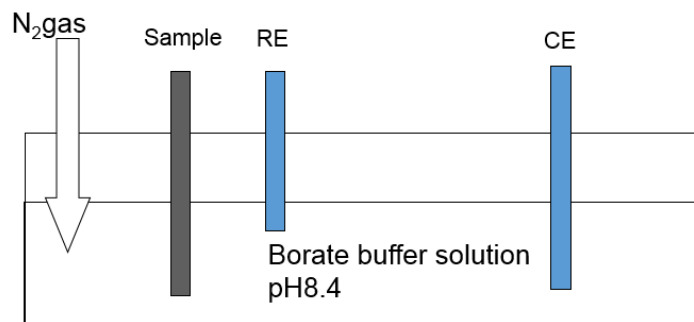


Fig.1 Schematic illustration of apparatus

Results and Discussion

Figure 2 shows the oxide growth during exposure test. The SnO layer is formed on Sn in early stage of oxidation. The thickness of SnO₂ layer is increased, though that of SnO layer does not change⁵⁾. This is because that the redox potential of SnO₂ is lower than SnO.

On the other hand, the grows rate of SnO₂ layer seems to behave as parabolic or logarithmic to the exposed time. This shows that the controlling process of this oxidation is diffusion of oxygen or mobility of electron through the barrier, such as SnO layer..

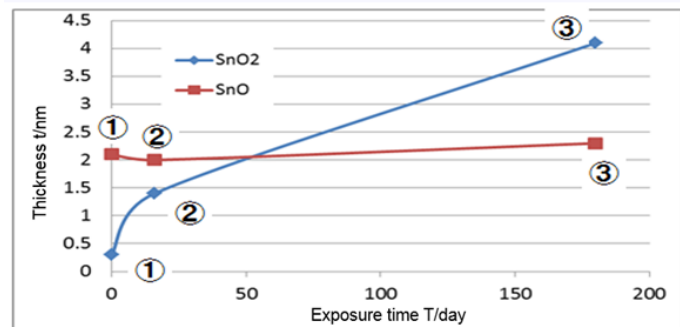


Fig.2 Relation between thickness of oxides and exposure time

Acknowledgment

The author thanks Mr. M. Kumakura, Mr. K. Yamada, students of Tokyo Denki University for his help of the experiment. The author thanks Dr. S. Mitani for the sample preparation.

References

- 1) D.M. Tench, et.al. "Solderability assessment via sequential electrochemical reduction analysis" *Journal of Applied Electrochemistry*, 24, (1994), 18-29.
- 2) T. Hetschel et.al. "Wettability of immersion tin final finishes with lead free solder" *IEEE 2nd Electronics System Integration Technology conference*, (2008), 561-566.
- 3) H. Saito, M. Kumakura, and S. Mitani, "Measurement of the thickness of oxide film formed on tin exposed to the air," *Journal of Material Testing Research Association of Japan*, (2015), pp.250-251.
- 4) M. Kumkura, H. Saito, and S.Mitani, "Effect of oxide films foemed on tin surface on wettability," *JSME annual conference*, (2016), J0250302
- 5) H.Saito, "Study of tin oxidation film growth in atmosphere with cathodic reduction" *ECSJ Spring meeting*,(2015), 1D26.

Nitrogen-containing Porous Carbon Electrocatalyst for Efficient Oxygen Reduction Reaction

Cheong Kim¹, Chunyu Zhu², Yoshitaka Aoki², Hiroki Habazaki²

¹Graduate School of Chemical Sciences and Engineering, Hokkaido University, Sapporo, Hokkaido 060-8628, Japan

²Division of Applied Chemistry, Faculty of Engineering, Hokkaido University, Sapporo, Hokkaido 060-8628, Japan
cjddl90@naver.com

Metal-air batteries and fuel cells are promising energy storage and conversion systems, and their practical use is highly dependent on the development of efficient electrocatalysts to improve the slow oxygen reduction reaction (ORR) occurring at the air electrode. Precious metal-based catalysts are generally used for ORR, but their intrinsic drawbacks, such as high cost and scarcity of precious metals, crossover deactivation, and poor durability, limit their wide commercialization. Therefore, it is desirable to develop non-precious metal electrocatalysts for ORR with high catalytic activity. Porous carbon with nitrogen doping is one of the promising candidates because of the low cost, good thermal and chemical stability, high electrocatalytic activity and remarkable methanol tolerance. To obtain the highly active air electrode, it is desirable that the nitrogen-doped carbon has high surface area to increase the number of active sites and also hierarchical porous morphology is preferable in terms of mass transport. In this study, nitrogen-containing porous carbon with hierarchical pore structure has been successfully synthesized by a solution combustion synthesis method and the ORR activity of the carbon materials have been examined in KOH solution.

The nitrogen-containing porous carbon was prepared by a novel exothermic process in which urea (nitrogen source) and cotton (1g, carbon source) were pyrolyzed in the presence of magnesium nitrate (2.56 g, oxidant and template). The molar ratio of urea to magnesium nitrate was 0:1 or 2:1. After calcination at high temperatures (700-1100°C) under an Ar atmosphere, acidic leaching of the in situ generated MgO was conducted to construct a macro-, meso- and microporous structure. The samples prepared at different temperatures and ratios are denoted as Mg_xUr_yCot1g-x00, where x represents the magnesium nitrate molar ratio, y represents urea molar ratio and x00 represents the calcination temperature (x00 = 700, 800, 900, 1000 or 1100).

The structure of obtained samples was characterized by X-ray diffraction (XRD), which showed the broad peaks of carbon. The scanning/transmission electron microscopy (SEM/TEM) were used to characterize the morphologies of the Mg_xUr_yCot1g-x00, which showed multi-porous structure after acid leaching (Fig. 1a). The samples also showed high specific surface area of larger than 1000 m² g⁻¹. X-ray photoelectron spectroscopy (XPS) analysis indicated that the content of N species decreased with the calcination temperature. Even if urea was absent in the mixed precursor, the nitrogen was incorporated in carbon, so that the nitrate and/or cotton may also be source of nitrogen.

The electrocatalytic performances of Mg_xUr_yCot1g-x00 were measured using a rotation-disk electrode system in 0.1 M KOH solution (Fig. 1b). The Mg₁₀Ur₂₀cot1g-1000 showed the high activity for ORR. The experimental results demonstrate that the remarkable performance of Mg₁₀Ur₂₀cot1g-1000 toward ORR originates from the combined effect of nitrogen concentration, graphitization degree, and surface area. Thus, the calcination temperature and urea concentration affect largely the ORR activity.

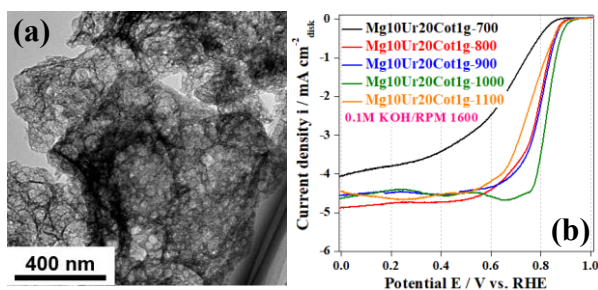


Figure 1. (a) TEM image of Mg₁₀Ur₂₀Cot1g-1000 and (b) ORR activity; effect of calcination temperature.

Effect of Glyme/Li Salt Molar Ratios on Charge-Discharge Behavior of High Sulfur Loading Lithium-Sulfur Batteries

Masato Yanagi, Ayumi Ando, Azusa Nakanishi, Kenzo Obata, Yoshiharu Matsumae, Kazuhide Ueno, Kaoru Dokko, Masayoshi Watanabe

Yokohama National University, Department of Chemistry and Biotechnology
79-5 Tokiwadai, Hodogaya-ku, 240-8501, Yokohama, Japan
E-mail address: yanagi-masato-kh@ynu.jp

1. Introduction

One of the challenges for practical application of Li-S battery is to control dissolution/precipitation of sulfur (S_8)/lithium polysulfides (Li_2S_x) active species during charge-discharge reactions with mitigating rapid capacity fade and low Coulombic efficiency. In addition, high sulfur loading and lean electrolyte conditions are other key factors for achieving high energy density Li-S cells. In a typical organic electrolyte where Li_2S_x are highly soluble, the capacity becomes significantly lower under lean electrolyte conditions with high sulfur loading cathode [1]. We reported that Li_2S_x solubility can be reduced to 1/100 or less in a solvate ionic liquid (SIL)-based electrolyte, $[Li(G4)][TFSA]$ diluted with a hydrofluoroether (HFE), and cycle life and coulombic efficiency of the Li-S cell could be improved with this electrolyte [2]. Therefore, the SIL-based electrolytes have a potential to achieve high energy density Li-S cells with no concern for the dissolution/precipitation issue. In this work, we prepared a high sulfur loading cathode using an Al-foam 3D current collector, and attempted to optimize the electrolyte composition of the SIL-based electrolyte for high energy density Li-S cells operating under lean electrolyte conditions.

2. Experiments

The sulfur/carbon (Ketjen black) composite (S/C) was prepared by melt-diffusion method [2]. The S/C was dispersed in a carboxymethyl cellulose (CMC) aqueous solution with sulfur : carbon : CMC = 6 : 3 : 1 (wt. ratio). The obtained slurry was infiltrated into an Al-foam 3D current collector. Charge-discharge properties of Li-S cells were evaluated with 2032 type coin cells. The coin cells were assembled in an Ar-filled glovebox. The charge-discharge test was carried out at $50 \mu A cm^{-2}$ in voltage range of 1.0-3.3 V.

3. Results and Discussion

The mixed electrolytes, $[Li(G4)_x][TFSA]/yHFE$ ($x = 0.8, 1, 1.2, 1.5$), were prepared using G4 and HFE, where concentration of $LiTFSA$ was adjusted to 1 M. The sulfur loading was $3.1 \sim 4.2 mg cm^{-2}$. The ratio of electrolyte volume and sulfur loading (E/S [$\mu L_{-electrolyte} mg_{-sulfur}^{-1}$]) was $20 \mu L mg^{-1}$. 1st discharge capacity exceeds $1000 mAh g^{-1}$ with $x = 0.8$ and 1.5 , while the Li-S cells shows low capacity with the other compositions (Fig. 1A). In addition, high discharge capacity was obtained only with $x = 0.8$ at the 2nd cycle (Fig. 1B). These results suggest that G4/Li molar ratio in the electrolytes would influence the discharge capacity (utilization of the sulfur cathode) and reversibility of the electrode reactions. We will discuss the effect of the G4/Li molar ratio on the charge-discharge behavior in terms of Li_2S_x solubility and electrolyte properties such as ionic conductivity.

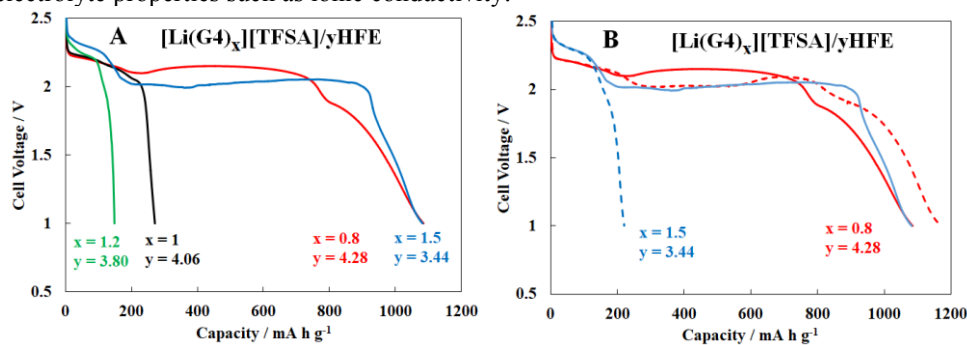


Fig. 1 (A) 1st discharge curves using 1 M $[Li(G4)_x][TFSA]/yHFE$ ($x = 0.8, 1, 1.2, 1.5$). (B) 1st (solid line) and 2nd (dashed line) discharge curves using 1 M $[Li(G4)_x][TFSA]/yHFE$ ($x = 0.8, 1.5$)

4. Acknowledgement

This research was supported by JST ALCA-SPRING.

5. Reference

- [1] M.Hagen *et al.*, *J. Power Sources*, **2014**, 264, 30-34.
- [2] K.Dokko *et al.*, *J. Electrochem. Soc.*, **2013**, 160, A1304.

Influences of Lithium Species and Additional Cesium Ion on the Morphology of Lithium Deposited in Ionic Liquid Electrolytes

Kazuki Kitta,¹ Naoki Tachikawa,¹ Kazuki Yoshii,¹ Nobuyuki Serizawa,¹ Toshihiro Takekawa,² Hideto Imai,³ Tetsuo Nishida,⁴ and Yasushi Katayama¹
(Keio Univ.,¹ Nissan Motor Co., Ltd.,² Nissan Arc, Ltd.,³ Stella Chemifa,⁴)
¹3-14-1 Hiyoshi, Kohoku-ku, Yokohama, Kanagawa 223-8522, Japan
kkitta@ec.applc.keio.ac.jp

Lithium metal has been expected as an ideal anode material because of a high theoretical capacity and low redox potential. However, Li metal is likely to deposit as whiskers or needles, leading to low coulombic efficiency and internal short-circuit during charge-discharge cycles. Therefore, it is important to control the morphology of Li deposits in order to improve the reliability and safety of the Li anode. Ionic liquids are composed of only cation and anions without any molecular solvent. Among various ionic liquids, MOMMPTFSA (1-methoxymethyl-1-methylpyrrolidinium bis(trifluoromethylsulfonyl) amide) is known to have relatively low viscosity and high cathodic stability [1]. In order to use MOMMPTFSA as the electrolytes for rechargeable Li batteries, Li ions have to be introduced by dissolving Li salts. LiTFSA is the typical Li salt which is often used for the TFSA⁻-based ionic liquids. However, formation of the Li complex with TFSA⁻, [Li(TFSA)₂]⁻, often results in an increase in the viscosity and low transference number of the Li species. In addition, MOMMP⁺ is the only cationic species, that is expected to be accumulated at the electrode surface in order to compensate the negative charge on the anode. In the present study, the influence of the dissolved states of Li species on the morphology of Li deposits was investigated in MOMMPTFSA containing LiTFSA with and without triglyme (G3), which has been known to coordinate Li ion to form a stable complex, [Li(G3)]⁺ [2]. Furthermore, addition of an additional cationic species, which is not reduced at the potential more positive than the deposition potential of Li, was attempted to control the structure of the interface between the anode and electrolytes.

1 M LiTFSA/MOMMPTFSA, 1 M [Li(G3)]TFSA/MOMMPTFSA and 1 M [Li(G3)]TFSA/0.05 M CsTFSA/MOMMPTFSA, were prepared and used as the electrolytes. The electrochemical measurements were performed with a three electrode cell. Cu or Li was used as a working electrode. Li was used as a reference and counter electrode. Li deposits obtained by galvanostatic electrodeposition were characterized by scanning electron microscope (SEM) without exposure to air. The electrochemical impedance spectroscopy of the Li anode was performed at the reversible potential with the frequency range of 20 kHz to 100 mHz.

Figure 1 shows the SEM images of the Li deposits in the different electrolytes. Whisker-like Li deposits were obtained in LiTFSA/MOMMPTFSA containing [Li(TFSA)₂]⁻. On the other hands, fine and granular Li deposits were obtained in [Li(G3)]TFSA/MOMMPTFSA, probably because the cationic species, [Li(G3)]⁺, was accumulated in addition to MOMMP⁺ on the anode surface and reduced to form the Li nuclei uniformly. The overpotential for Li deposition in [Li(G3)]TFSA/MOMMPTFSA was larger than that in LiTFSA/MOMMPTFSA, suggesting the promotion of nucleation under the large overpotential led to deposition of Li with fine and granular morphology. On the other hand, fine and granular Li deposits were also obtained in [Li(G3)]TFSA/MOMMPTFSA with addition of 0.05 M CsTFSA. An increase in the interfacial resistance with addition of CsTFSA suggested the participation of Cs⁺ in formation of the electric double layer at the interface. However, the morphological differences were not remarkable in the electrolytes with and without Cs⁺.

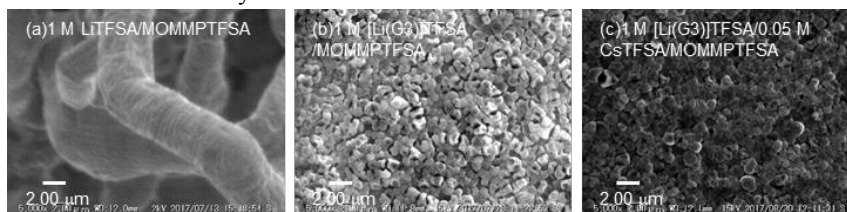


Fig. 1 SEM images of the electrodeposits obtained by galvanostatic cathodic reduction on a Cu electrode in (a) 1 M LiTFSA/MOMMPTFSA, (b) 1 M [Li(G3)]TFSA/MOMMPTFSA and (c) 1 M [Li(G3)]TFSA/0.05 M CsTFSA/MOMMPTFSA. Current density : -0.1 mA cm^{-2} . Electric charge : 3.6 C cm^{-2} .

[1] T. Nishida, K. Nishikawa, M. Rosso, and Y. Fukunaka, *Electrochim. Acta*, **100** (2013) 333-341.

[2] Y. Katayama, S. Miyashita, and T. Miura, *J. Power Sources*, **195** (2010) 6162-6166.

Nitrogen-Doped Carbon with Hierarchical Porous Structure as Electrocatalyst for Oxygen Reduction Reaction

Manami Takata, Cheong Kim, Chunyu Zhu, Yoshitaka Aoki, and Hiroki Habazaki
Hokkaido University, Sapporo, Hokkaido, Japan
micub0901@gmail.com

Recently, with the increasing demand for renewable energies, the development of fuel cells and metal air batteries have drawn attentions as the next-generation energy devices. In these devices, electrochemical oxygen reduction reaction (ORR) plays crucial role. Presently, Pt-based compounds are recognized as the most efficient ORR catalysts, but their wide applications are hampered by the high-cost and scarcity of platinum. Additionally, Pt-based catalysts suffer from poor durability and sensibility to crossover effect. Therefore, it is important to search for cost-effective, highly efficient and stable ORR catalysts as alternatives to Pt-based materials. Among various Pt-free ORR catalyst candidates, nitrogen doped carbon is promising due to its high ORR activity and good stability. In this study, we aim to synthesize nitrogen-doped porous carbon (NPC) by a facile glycine-nitrate method. The NPC has a well-developed hierarchical porous structure and high surface area, which shows high ORR activity.

NPC was prepared in the following procedures. First, 5 mmol magnesium nitrate and 10, 12.5 and 15 mmol glycine (with a molar ratio 1:n, n=2, 2.5 and 3, named with NPC-n2 for example) were dissolved in Milli-Q water and stirred at 100 °C to evaporate water to obtain gel precursors. The gel raw materials were preliminarily heated to 500 °C under Ar atmosphere with a heating rate of 10 °C min⁻¹. The pyrolyzed precursors (MgO@C) were then calcined at 800, 900, 1000, and 1100 °C (named with NPC-n2-1000 for example) for 2 hours, followed by which were finally washed with HCl aqueous solution to dissolve MgO. After washing and with Milli-Q water, filtered and dried to get the final NPC products were obtained. The obtained samples were analyzed by TG, XRD, Raman, BET, SEM, TEM, and XPS. The oxygen reducing ORR property was evaluated by the rotating disc electrode method in a typical three-electrode system, in which a glassy carbon electrode loaded with different catalysts was used as working electrode, a Ag/AgCl electrode and a platinum foil as reference and counter electrode, respectively. A 0.1 mol dm⁻³ KOH solution was served as the electrolyte.

The pyrolysis of glycine-nitrate gel is a vigorous exothermic reaction, which generates a lot of gases, so as to produce numerous meso (2-50 nm) and macropores (>50 nm) in the pyrolyzed precursor. In this study, since magnesium nitrate was used, MgO nanoparticles were introduced as a template to be dispersed in the calcined carbon matrix. After acid washing to remove MgO templates, additional micropores (<2 nm) and mesopores were further created. As shown in Fig. 1, a lot of pores with diverse sizes are observed by TEM observation analysis. It was also confirmed from the nitrogen adsorption experiment that NPCs feature hierarchical porous structure with high specific surface area (>1000 m²g⁻¹). As for the calcination temperature factor, NPC-1000 showed better ORR activity than NPC-800, NPC-900 and NPC-1100. It is well known that the nitrogen content in carbon decreases with increasing calcination temperature. Thus, This is because of that there is a trade-off relationship between the conductivity requiring a higher calcination temperature and inevitable concurrent nitrogen leaching effect at higher calcination temperature. On the other hand, the molar ratio factor was found to affect the hierarchical porous structure and

specific surface area. As the decrease of molar ratio of glycine to magnesium nitrate, the specific surface area of NPC become larger. Actually, NPC-n2-1000 showed a BET specific surface area of 1838 m²g⁻¹ and resulted in higher ORR activity than NPC-n2.5-1000 and NPC-n3-1000, as presented in Fig. 2. The highly active NPC-n2-1000 catalyst afforded an onset potential of 0.94 V, together with great durability. This superior performance was ascribed to the balance of good conductivity, optimized nitrogen amount and ratio, the hierarchical porous structure, and high specific surface area.

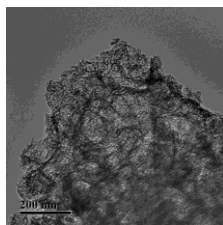


Fig. 1 Typical TEM image of NPC.

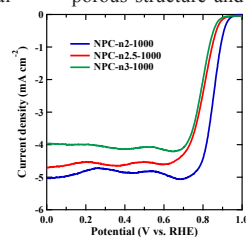


Fig. 2 LSV curves of NPC-1000 samples at 1600 rpm.

Mis en forme : Non Exposant/ Indice

Mis en forme : Non Exposant/ Indice

Mis en forme

[1] [W. Xia et al., Angew. Chem., Int. Ed., 2016, 55, 2650.](#)

HCP Metal Electrodeposition from Concentrated Aqueous Solution using a Hydrophobic Anion

Shota Inoguchi*, Atsushi Kitada, Kazuhiro Fukami, Kuniaki Murase
Department of Materials Science and Engineering, Kyoto University
Yoshidahonnmachi, Sakyo, Kyoto 606-8501, Japan
* inoguchi.shota.34v@st.kyoto-u.ac.jp

Zinc (Zn) is widely used for the anode material of zinc-air batteries and corrosion protection coating. The electrodeposition of Zn is involved in the charge reaction, so it is important. Zn has HCP structure. It was reported that by increasing the rate of *c*-axis orientation, the surface roughness of Zn film decreased and the corrosion resistance increased [1, 2]. The surface morphology and the orientation of Zn films are controlled by electrodeposition conditions. The mechanism of changing these surface properties has been investigated in many researches. However, few researches have focused on the hydration state around cation, and its effect still remains unknown. In this study, we used hydrophilic / hydrophobic anions to control the hydration state around and Zn^{2+} cations by adjusting the concentration of aqueous solution. In addition, we investigated solution properties and electrodeposition behavior with the change of hydration state. We also perform same research using cadmium (Cd) which has HCP structure and similar properties to Zn.

Two types of aqueous solutions were prepared using SO_4^{2-} as a hydrophilic anion and bis[(trifluoromethyl)sulfonyl]amide (Tf_2N^- ; $Tf = CF_3SO_2$) as a hydrophobic anion, with the concentration adjusted to 0.1 - 3.5 mol kg^{-1} . All experiments were performed at room temperature. The Open Circuit Potential (OCP) was measured using the target metal plate as working electrode and Ag/AgCl electrode as reference electrode. The behavior of water molecules and the state of hydrophobic anion were examined by Fourier transform infrared spectroscopy (FT-IR) and Raman spectroscopy, respectively. Electrodeposition was carried out on Cu working electrode at -0.2 V vs. Zn with a coulomb amount of about 8 C. The orientation of the electrodeposits was characterized by X-ray diffraction (XRD) and using this result, the *c*-axis orientation index of Zn deposits was calculated by the method of Willson *et al.* [3].

As the result of FT-IR, it is turns out that only in the case of the concentrated aqueous solution using the hydrophobic anion, the “free” water, i.e., water that is not coordinated with other species, decreases and hydrogen-bonded network is broken. The Raman spectra also indicated that the cation was not coordinated with the hydrophobic anion. In addition, using the hydrophobic anion, the OCP moved more positive than expected from the salt concentration change as shown in Table.1. ($Zn^{2+} + 2e = Zn$ $E^\circ = -0.76$ V vs. SHE). Therefore, it is cleared that by broken the hydrogen-bonded network structure and decreasing the amount of “free” water, the activity coefficient of the metal cation increases more than 1 and the activity of water decreases. These results were similar in the case of Cd electrodeposition. Fig. 1 shows the *c*-axis orientation index of Zn deposits from $Zn(Tf_2N)_2$ and $ZnSO_4$ aqueous solutions at each concentration, By using the hydrophobic anion, it was found that the deposit's *c*-axis orientation (001 relative intensity) is more significant than the case of using the hydrophilic anion. Therefore, it is suggested that the change of the hydration state affects the electrodeposition behaviors.

[1] H. Nakano *et al.*, *Tetsu-to-Hagane* (in Japanese), **88**, 8 (2002).

[2] D. Abayarathna *et al.*, *Corros. Sci.*, **32**, 755 (1991).

[3] K. S. Willson *et al.*, *Tech. Proc. Amer. Electroplaters Soc.*, **51**, 92 (1964).

Table. 1 OCPs of $Zn(Tf_2N)_2$ aqueous solutions at each concentration.

Concentration (mol kg^{-1})	OCP (V vs. SHE)
0.1	-0.78
0.5	-0.76
1.0	-0.73
2.0	-0.69
3.5	-0.61

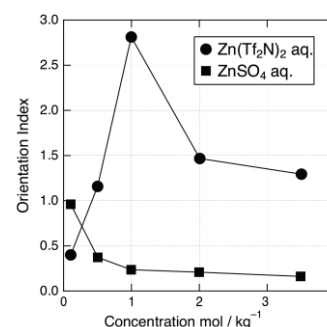


Fig. 1 The *c*-axis orientation index of electrodeposits obtained from $Zn(Tf_2N)_2$ and $ZnSO_4$ aqueous solutions at each concentration.

Effect of Photoisomerization Reaction in Electric Double Layer Transistor Using Photoresponsive Ionic Liquid

Satoshi Saito^a, Tatsuhiro Horii^a, Caihong Wang^a, Kazumoto Miwa^b, Shimpei Ono^b,
Yumi Kobayashi^a, Hisashi Kokubo^a, Masayoshi Watanabe^a

^aDepartment of Chemistry and Biotechnology, Yokohama National University, 79-5 Tokiwadai,
Hodogaya-ku, Yokohama 240-8501, Japan

^bCentral Research Institute of Electric Power Industry, 2-6-1 Nagasaka, Yokosuka 240-0916, Japan

E-mail address: saito-satoshi-cn@ynu.jp

Intensive attention has been paid to ionic liquids (ILs) because of their unique and advantageous properties.^[1] Given a wide variety of ions available, incorporating various functional groups into the component ions not only reserves the inherent properties of ILs but also affords a feasible and efficient method to explore novel functionalized ILs. Azobenzene molecule as a reversible photochromic functional group has been introduced into IL to afford light responsive properties.^[2] We synthesized a photoresponsive IL, 1-butyl-3-phenyl-azobenzylimidazolium bis(trifluoromethanesulfonyl)amide ([Azobim][NTf₂]), which changes its geometrical structure by light stimulation resulting in polarity of the IL as well (Fig. 1). The photo-isomerization reaction of [Azobim][NTf₂] is expected to induce changes in the electrochemical properties. Several studies relating to the application of ILs to electric double layer transistors (EDLTs) as the gate materials have been reported. A threshold voltage and mobility of the EDLT were decreased with an increase in the capacitance of the IL.^[3] Therefore, the performance of the EDLT can be controlled by changing the capacitance of the IL. In this study, we investigated the electrochemical properties and the effect of the photoisomerization reaction with UV and visible (vis) light irradiation on the performance of EDLT using [Azobim][NTf₂]. Fig. 2 shows galvanostatic charge-discharge curves and discharge capacitance of [Azobim][NTf₂] measured after UV and vis light irradiation for 30 min. The discharge capacitance was increased after irradiation with UV and decreased after irradiation with vis light. We will discuss the effect of electrical and electrochemical properties of [Azobim][NTf₂] on performances of the EDLTs in detail.

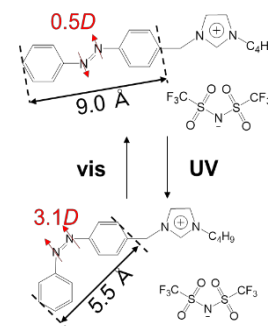


Fig. 1 Chemical structure of [Azobim][NTf₂] and its changes in the molecular structure and dipole moment induced by photo irradiation.

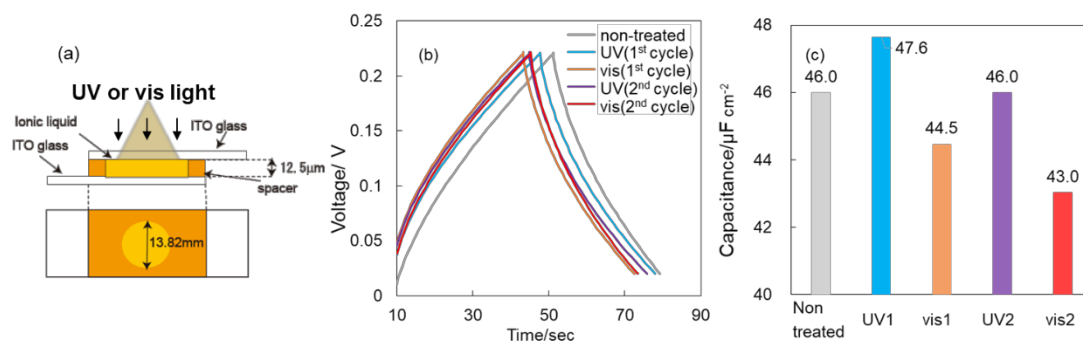


Fig. 2 (a) Schematic image of the electrochemical cell for photo-irradiation, (b) Charge-discharge curves of [Azobim][NTf₂] at 30 °C after UV and vis light irradiation for 30 min at the 2nd cycle at a constant current of 0.1 μA, (c) Changes in the discharge capacitance of [Azobim][NTf₂] with UV and vis light irradiation.

Reference:

- [1] J. D. Holbrey *et al.*, *Clean Prod. Process.*, **1999**, *1*, 223-236.
- [2] C. Wang, *et al.*, *Macromolecules*, **2017**, *50*, 5377-5384.
- [3] S. Ono, *et al.*, *Appl. Phys. Lett.*, **2009**, *94*, 063301.

Pre-potential Cycling Effects of Lithium Deposition/Dissolution Processes Studied by Electrochemical Quartz Crystal Microbalance

Ayano Ohama, Kumar Sai Smaran, Asako Niida, and Toshihiro Kondo
Division of Chemistry, Graduate School of Humanities and Sciences, Ochanomizu University
2-1-1, Ohtuka, Bunkyo-ku, Tokyo 112-8610, Japan
g1740627@edu.cc.ocha.ac.jp (A. Ohama)

Much higher theoretical specific capacity of lithium (3860 mA h g^{-1}) makes lithium one of the most desirable anode materials of future lithium-based batteries such as lithium-air battery (LAB). During charging, the dendrite, which further leads to poor performance and short circuit, forms on a lithium anode surface. In addition with the dendrite, solid electrolyte interphase (SEI), generated by decomposition of electrolytes and/or solvents, accumulates on the anode surface. In order to avoid dendrite formation, an ideal SEI layer is expected to be higher conductive for lithium ion and lower conductive for electron. Moreover, it should be flexible and should have a relatively flat surface without any defects [1].

On the other hand, electrochemical quartz crystal microbalance (EQCM) technique provides us not only mass change (Δm) [2,3], but also resonance resistance change (ΔR) which shows surface area change (ΔA) and/or density and viscosity change ($\Delta \rho$ and $\Delta \eta$, respectively) [4,5]. Thus, in this study, cyclic voltammetry (CV) and EQCM techniques were employed to study the electrodeposition and dissolution process of lithium utilizing 1 M LiPF₆, 1 M LiTFSI, and 1 M LiFSI in tetraglyme (G4). Additional pre-potential-cycling resulted in the accumulation of a pre-SEI layer over the native SEI layer. Based on the potential dependences of Δm and ΔR (Fig. 1), benefits of such pre-SEI layer in lithium deposition/dissolution processes are discussed.

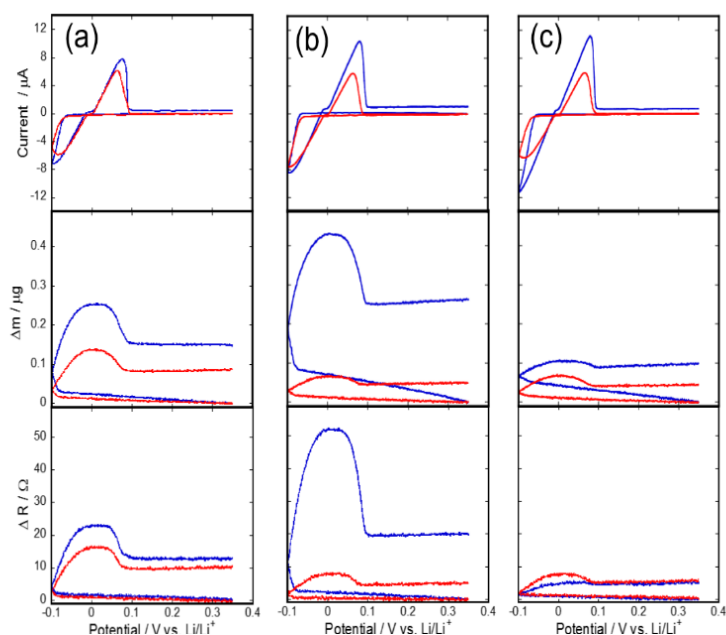


Fig. 1 Cyclic voltammograms and potential dependences of Δm and ΔR with (red) and without (blue) pre-SEI, measured in (a) 1 M LiPF₆, (b) 1 M LiTFSI, and (c) 1 M LiFSI in G4.

References

- [1] X.-B. Cheng, R. Zhang, C.-Z. Zhao, F. Wei, J.-G. Zhang, *Adv. Sci.* **3**, 1500213 (2016).
- [2] K. Kanamura, S. Shiraishi, Z. Takehara, *J. Electrochem. Soc.* **147**, 2070 (2000).
- [3] D. Aurbach, M. Moshkovich, Y. Cohen, A. Schechter, *Langmuir* **15**, 2947 (1999).
- [4] K. Naoi, M. Mori, Y. Naruoka, W. M. Lamanna, R. Atanasoski, *J. Electrochem. Soc.* **146**, 462 (1999).
- [5] N. Serizawa, S. Seki, K. Takei, H. Miyashiro, K. Yoshida, K. Ueno, N. Tachikawa, K. Dokko, Y. Katayama, M. Watanabe, T. Miura, *J. Electrochem. Soc.* **160**, A1529 (2013).

Fabrication of Fully Screen-printed Reference Electrode using Silica Gel Inks

Masato Komoda¹, Yoshinao Hoshi¹, Isao Shitanda^{1,2}, Masayuki Itagaki^{1,2}

¹ Department of Pure and Applied Chemistry, Faculty of Science and Technology, Tokyo University of Science, Noda, Chiba 278-8510, Japan

² Research Institute for Science and Technology Tokyo University of Science, Noda, Chiba 278-8510, Japan

E-mail address: shitanda@rs.noda.tus.ac.jp (I.Shitanda)

A printed-type reference electrode is a promising for suitable to miniaturize and applying to wearable device and other equipment [1-3]. However, a reference electrode, having short set-up time with in a minutes and long lifetime over a days, has never been reported. In this research, we newly prepared two silica gel inks to develop a high performance printed-type reference electrode, which has silica liquid junction and electrolyte layers fabricated by screen-printing.

0.8 g of polyvinylidene difluoride (PVdF) powder and 1g of nonion surfactant (Triton X) were dissolved in 8.2 g of N-methyl-2-pyrrolidone (NMP). Then, 1.5g of micro silica gel was mixed with the NMP solution and homogenized by ultrasonic homogenizer to be prepared an ink for forming the liquid junction. In the case of an ink for electrolyte layer, 1 g of silica gel and 4 g of KCl powder was mixed with the NMP solution. Figure 1 shows a schematic illustration of the electrode structure. Silver and silver-silver chloride inks were printed on a poly imide substrate, successively. Then, the liquid junction ink and electrolyte ink were printed. Finally, resist ink was printed to protect the electrolyte layer and control the geometric surface area of the liquid junction area [1].

The potential difference between the present reference electrode and a commercially available glass-type silver/silver reference electrode was measured (Fig. 2). The setup time was about 5 minutes, and lifetime was about 10 days.

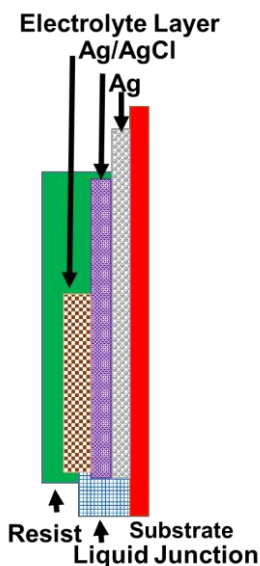


Fig.1 Structure of screen-printed reference electrode

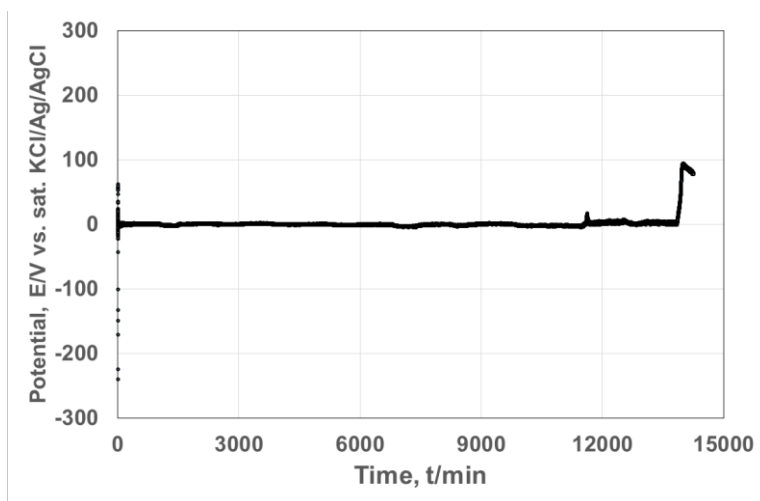


Fig. 2 Time-Potential curve of fabricated reference electrode

References

- [1] M. Komoda, Y. Hoshi, I. Shitanda, M. Itagaki *Chemical Sensors (Supplement A)*, 33 (2017) 61.
- [2] I. Shitanda, H. Kiryu, M. Itagaki, *Electrochim. Acta*, 58(2011) 528.
- [3] L. Tymecki, Z. Zwierkowska and R. Koncki, *Anal. Chim. Acta*, 526(2004) 3.

Immobilization of Nanocarbons and Glucose Oxidase by Electrodeposition Method for Glucose Sensor Fabrication

H. P. Jhong^{1,2}, M. Uchimaru¹, S. Isoai¹, M. Kurashina¹, M. Yasuzawa^{1,*},
C. H. Wang², W. H. Chiang², Y. Fuchiwaki³, T. Harada⁴

¹*Tokushima University, Tokushima 770-8506, Japan*

²*National Taiwan University of Science and Technology, Taipei 106, Taiwan*

³*Health Research Institute, AIST, Takamatsu, Kagawa 761-0395, Japan*

⁴*Kondo Chemical Industry, Higashiosaka, Osaka 578-0932, Japan*

e-mail: yasuzawa@tokushima-u.ac.jp

During the glucose measurement, there are several items must be considered. First of all, enzyme immobilization plays the significant role to decide the efficiency of detection. Hence, there are various ways of enzyme immobilization be developed and used in biosensor field, such as cross-linking, covalent coupling, entrapment and so on. Herein, the novel immobilized method has been established by the electrochemical deposition and polymerization procedures. Afterward, the high-density of enzymes will be immobilized onto the electrode based on this method.

Second, the nanocarbons (NCs) which can provide the high conductivity and enhance the electron transfer rate are been included. Consequently, the multi-walled carbon nanotubes (MWCNTs) that suggest the strongest tensile strength and owing to the above properties are been adopted in this research. Nevertheless, the well-dispersed ability of solution should also be concerned simultaneously before doing the electrode deposition. In order to have the excellent disperse property, a kind of anionic polysaccharide gellan gum is been induced to do the modification during the process.

Finally, the solution which contained the glucose oxidase (GOx) and MWCNTs are carried out with a gelling agent gellan gum in this work. The above solution followed by applying the specific potential (vs. Ag/AgCl) and using the Pt wire as the counter electrode to get the successful immobilization of enzyme. The CNT/GOx immobilized electrode demonstrates a high sensitivity and efficiency when doing the glucose measurement.

Design of Combined Scanning Ion Conductance and Atomic Force Microscope Investigation of Lithium Iron Phosphate

T. Enright, Y. Miyahara, A. Mascaro, C. Aiken, P. Grutter
McGill University
3600Rue University
Montreal, QC H3A 2T8
Canada
tyler.enright@mail.mcgill.ca

In this study we aim to create a scanning probe measurement device capable of studying the charging characteristics of battery materials. While Scanning Ion Conductance Microscopy (SICM) allows for local probing of conductance characteristics of materials, the poor spatial resolution of this technique limits its use to flat samples. By combining SICM with Atomic Force Microscopy we may overcome these issues and produce spatially resolved ionic conductance measurements in real time. This can be used to coordinate the charging characteristics of lithium iron phosphate battery materials with conformational changes which occur through charging events.

Title in Times Roman 14 point – Upper and Lower Case

Presenting author, Co-Authors

Affiliation

Address

e-mail address

These instructions are an example of what a properly prepared meeting abstract should look like. Proper column and margin measurements are indicated.

The abstract **should not exceed ONE PAGE** of text, references, tables and figures. Abstracts exceeding this limit may be cut without consideration of content after the first page.

Type the title single-spaced in 14-point Times Roman bold, upper and lower case and NOT in ALL CAPITAL letters.

Type the author(s) name(s) single-spaced in 10-point Times Roman regular.

Type the affiliation(s) and address(es) single-spaced in 10-point Times Roman italic.

Type the body of the abstract text (including references and tables) single-spaced in 10-point Times Roman regular.

Paper Size: A4 (21.0 x 29.7 cm)

Margins

Top: 30.0 mm

Bottom: 30.0 mm

Sides: 30.0 mm

Glucose-oxygen Biofuel Cell Based on Anodizing Mesoporous Carbon as Support for Immobilizing Enzymes

Kuan-Hua Liao¹, Ming-Liao Tsai¹, Jing-Shan Do^{*1,2}

¹Department of Chemical and Materials Engineering, National Chin-Yi University of Technology
Taichung, Taiwan

No.57, Sec. 2, Zhongshan Rd., Taiping Dist., Taichung 41170, Taiwan (R.O.C.)

²College of Materials Science and Engineering, Xi'an University of Science and Technology

No. 58, Yen-Ta Rd., Xi'an, China

E-mail: girl950682121@gmail.com, *jsdo@ncut.edu.tw

MOST 105-2221-E-167-032-MY3

Abstract

Biofuel cells (BFCs) are directly convert renewable fuels (such as sugars, alcohols) to the electrical energy catalyzed by the microorganisms or enzymes. Due to the enzyme reaction have advantages such as high specificity, environmental compatibility, and the ability to operate at room temperature, hence the enzymatic biofuel cells (EBFCs) can be constructed without membrane. For the development of high performance EBFCs, four bottlenecks needed to be overcome include enzyme immobilization, efficient electron transfer between the enzyme active site and electrode surface, efficient fuel supply, and the lifespan of EBFCs [1-2]. The porous gold current collector prepared by the electrodeposition with hydrogen bubble dynamic template (HBDT) technique, and the mesoporous carbon (MC) support modified by the anodizing method are used to promote the performance of glucose-oxygen EBFCs. The electrochemical surface area of Au current collector prepared by HBDT technique is obtained to be 12.94 cm², which is 15.98 folds of sputtering Au current collector. As a result, replacing the sputtering Au current collector of bioanode with the electrodeposition Au the current is effectively promoted from 3.82 to 17.95 μ A at 0.2 V vs. Ag/AgCl/3M NaCl_(aq). The increase in hydrophilicity MC support modified with the anodizing treatment results in the increase in the performances and stability of the bioelectrodes due to the facility of enzyme immobilization and the transfer of reactants to the enzymatic active sites. Using Chitosan/GOx/TMPD (*N,N,N',N'*-tetramethyl-*p*-phenylenediamine)/MC/Au (deposition)/Au (sputtering)/Al₂O₃ as bioanode, increasing the anodizing time for modifying MC from 0 to 180 s the current for anodic oxidation of glucose at 0.2 V vs. Ag/AgCl/3M NaCl_(aq) is increased from 17.95 to a maximum value of 35.73 μ A at 37°C in pH 7 buffer solution containing 30 mM glucose. The current is decreased to 24.94 μ A by further increasing the anodizing time to 300 s. The performances of home-made membraneless glucose/O₂ biofuel cell based on the bioelectrodes with electrodepositing Au current collector and anodizing MC support for immobilizing enzymes are also investigated in this work.

References

- [1] M. Holzinger, A. L. Goff and S. Cosnier. Carbon nanotube/enzyme biofuel cells, *Electrochim. Acta* 82 (2012) 179–190.
- [2] X. Yang, W. Yuan, D. Li and X. Zhang. Study on an improved bio-electrode made with glucose oxidase immobilized mesoporous carbon in biofuel cells, *RSC Adv.* 6 (2016) 24451–24457.

Highly Sensitive Amperometric Formaldehyde Gas Sensor Based on Nafion[®]/Pt/Au/Al₂O₃ Electrode: Optimizing Electrode Preparation

Nurpratama-Aditya Febry¹, Ming-Liao Tsai¹, Jing-Shan Do*^{1,2}

¹Department of Chemical and Materials Engineering, National Chin-Yi University of Technology
No.57, Sec. 2, Zhongshan Rd., Taiping Dist., Taichung 41170, Taiwan (R.O.C.)

²College of Materials Science and Engineering, Xi'an University of Science and Technology
No. 58, Yen-Ta Rd., Xi'an, China

pratamaa104@gmail.com, *jsdo@ncut.edu.tw
MOST 105-2221-E-167 -032 -MY3

Abstract

Formaldehyde is a harmful volatile organic compound (VOC) due to its toxic, allergenic and also a human carcinogen with a maximum legal level in indoor air of 80 ppb for 30 min exposure limit [1]. The electrochemical detection of formaldehyde based on amperometric gas sensor by using gold and platinum electrodes has been studied and showed a linear response and low detection limit characteristics [2-3]. In this study, an amperometric formaldehyde gas sensors by using porous Pt deposited with hydrogen bubble dynamic template (HBDT) technique, and cast with Nafion[®] film as the solid polymer electrolyte was fabricated and operated at room-temperature. The conditions for electrodeposition porous Pt was optimized to achieving high sensitivity of amperometric formaldehyde gas sensor. The surface morphologies and crystallographic information of as-prepared electrode materials are analyzed by the FESEM and XRD, respectively. The electrochemical properties are investigated by the cyclic voltammetry (CV). Using Nafion[®]/Pt/Au/Al₂O₃ as sensing electrode, a linear relationship of the amperometric formaldehyde gas sensor is obtained in the concentration range of 0.04 - 5 ppm at room temperature. The sensitivity, response time (t_{90}), and detection limit of the amperometric formaldehyde gas sensor are obtained to be 1.79 $\mu\text{A ppm}^{-1}$, 300 s and 40 ppb, respectively. Base on the cyclic voltammogram of formaldehyde gas on the sensing electrode, the intermediates of anodic oxidation of formaldehyde, such as CO_{abs} and formic acid, are found in the reverse of scan.

References

- [1] T. Salthammer, S. Mentese and R. Marutzky, Formaldehyde in the indoor environment, *Chem. Rev.* 110 (2010) 2536–2572.
- [2] R. Knake, P. Jacquinet and P. C. Hauser, Amperometric Detection of Gaseous Formaldehyde in the ppb Range, *Electroanalysis* 13 (2001) 631–634.
- [3] C.-H. Chou, J.-L. Chang and J.-M. Zen, Effective analysis of gaseous formaldehyde based on a platinum-deposited screen-printed edge band ultramicroelectrode coated with Nafion as solid polymer electrolyte, *Sensors and Actuators B* 147 (2010) 669–675.

Highly Concentrated Mixed-Li Salt Electrolytes for High-Voltage Lithium-ion Batteries

Yosuke Ugata, Jingjun Zhang, Daiki Watanabe, Shoshi Terada, Kazuhide Ueno, Kaoru Dokko and Masayoshi Watanabe

Department of Chemistry and Biotechnology, Yokohama National University
79-5 Tokiwadai, Hodogaya-ku, Yokohama 240-8501, Japan
ugata-yosuke-zk@ynu.jp

Highly concentrated lithium bis(trifluoromethanesulfonyl)amide (Li[TFSA]) based electrolyte solutions have unique properties that are not observed in lower concentration electrolytes. Our group has reported that an equimolar mixture of Li[TFSA] and triglyme (G3) with high lithium salt concentration ($\approx 3 \text{ mol dm}^{-3}$) shows a reversible Li^+ intercalation reaction into graphite electrode.¹⁾ In addition, oxidative stability was enhanced in the highly concentrated Li[TFSA]/G3 electrolyte where HOMO energy level of glymes was lowered by the strong coordination with the lithium cation²⁾. These properties can be expected in other solvents and their highly concentrated electrolytes could be the candidate for the electrolyte of high-voltage batteries. A crucial problem associated with the use of Li[TFSA] based organic electrolytes at high voltage is a severe corrosion of an aluminum current collector at positive electrodes.³⁾ However, this parasitic side reaction could be suppressed by addition of a Li-salt that forms protective AlF_3 layer on aluminum surface or by increasing Li[TFSA] concentration.^{4,5)} In this work, the effect of a “co-salt” in highly concentrated Li[TFSA]/sulfolane (SL) electrolytes on electrochemical properties was studied.

Figure 1 shows chronoamperograms of an aluminum electrode polarized at 4.8 V vs Li/Li^+ in Li[TFSA]:SL=1:2 (molar ratio) and LiBF_4 :Li[TFSA]:SL=0.5:0.5:2 electrolyte with Li metal as counter and reference electrode. The anodic current in Li[TFSA]:SL=1:2 electrolyte continuously increased and was higher than $10 \mu\text{A cm}^{-2}$ after 24 hours, indicating the severe Al corrosion. On the other hand, the anodic current of $2.5 \mu\text{A cm}^{-2}$ is much lower in LiBF_4 :Li[TFSA]:SL=0.5:0.5:2 after 24 hours, indicating the suppression of Al corrosion by addition of the co-salt, LiBF_4 . The battery application of the above electrolytes to high-voltage operating cathode materials will be also reported.

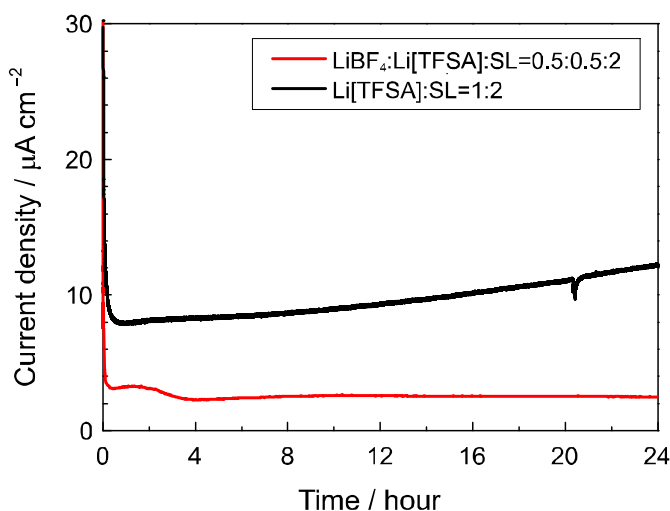


Figure 1. Chronoamperograms of an aluminum electrode at 4.8 V in Li[TFSA]:SL=1:2 (molar ratio) and LiBF_4 :Li[TFSA]:SL=0.5:0.5:2

References

- (1) H. Moon *et al.*, *J. Phys. Chem. C*, **118**, 20246-20256 (2014).
- (2) K. Yoshida *et al.*, *J. Am. Chem. Soc.*, **133**, 13121-13129 (2011).
- (3) R Atanasoski *et al.*, *J. Power Sources*, **68**, 320-325 (1997).
- (4) S Zhang *et al.*, *J. Power Sources*, **109**, 458-464 (2002).
- (5) K. Matsumoto *et al.*, *J. Power Sources*, **231**, 234-238 (2013).

Establishing ionic tunnels with WPU-PAAK GPE in electrode materials for supercapacitor

Jeng-An Wang, Chen-Chi M. Ma, Chi-Chang Hu*

National Tsing Hua University

No. 101, Section 2, Kuang-Fu Road, Hsinchu, Taiwan 30013, R.O.C.

cchu@che.nthu.edu.tw

In this study, the sticky copolymer polyurethane - potassium poly(acrylate) (WPU-PAAK) which can act not only as an electrolyte in supercapacitor but also as a binder in the electrode materials has been successfully synthesized from potassium poly(acrylate) (PAAK) backbone cross-linked by polyurethane (PU). WPU-PAAK binder in substitution for PVDF binder can enhance the specific capacitance of active electrode about 12 % in current density of 1 A/g. In the high current density of 10 A/g, it can even enhance over 30 % in specific capacitance. Furthermore, the areal specific capacitance of active electrode, which used the WPU-PAAK binder, was increasing with increased mass loading in the same ratio. The symmetrical device of AC//WPU-PAAK-K//AC after charge balance demonstrated excellent potential window of 1.4 V and specific capacitance. The specific capacitances of each device were 45.48, 89.78 and 136.59 mF/cm² in the mass loading of activated carbon (ACS 25) which were 1.07, 2.14 and 3.21 mg/cm², respectively.

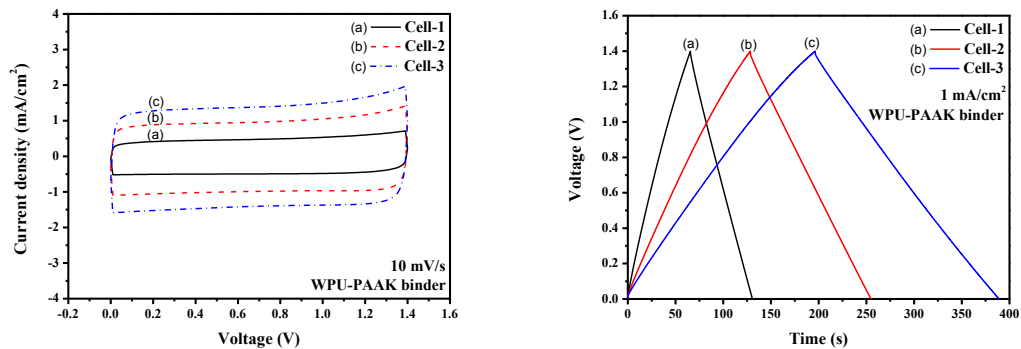


Figure 1. (a) Cyclic voltammetry in scan rate of 10 mV/s and (b) Galvanic charge-discharge curves in power density of 1 mA/cm² recorded from different mass loading cells.

Structural Study of Pt Ultra-thin Film on Ni Substrate Surface Prepared by Galvanic Replacement

Risa Yoshioka, Sayumi Sakai, and Toshihiro Kondo

Division of Chemistry, Graduate School of Humanities and Sciences, Ochanomizu University
2-1-1, Ohtuka, Bunkyo-ku, Tokyo 112-8610, Japan
g1740642@edu.cc.ocha.ac.jp (R. Yoshioka)

It is well-known that ultra-thin precious metal layers formed on the foreign metal substrates often have a relatively high electro-catalytic activity [1]. Platinum (Pt) is one of the most powerful electro-catalysts for the various catalytic reactions, especially a cathode reaction for polymer electrolyte membrane fuel cell (PEMFC), *i.e.*, oxygen reduction reaction (ORR). However, electro-catalytic activity of polycrystalline Pt for ORR is not enough for actual operation of PEMFC, and moreover, Pt is the expensive and precious metal, leading that the commercially available PEMFC is still too expensive, unfortunately. One of the candidate as a cheaper electro-catalyst for ORR in PEMFC is expected to Pt ultra-thin film covered with low cost metal surface. We have succeeded to electrochemically synthesize the Ni core Pt shell (Ni@Pt) nanoparticles and proved its high electro-catalytic activity for ORR (Fig. 1) [2-6]. In these studies, we employed the galvanic replacement technique to prepare such Pt thin layer covered Ni nanoparticles.

There are many methods to prepare the Pt ultra-thin film on the foreign metal surface. Among them, a galvanic replacement technique is one of the best candidates to easily prepare such Pt ultra-thin film, but there were few reports to structurally investigate the galvanic replacement process at an atomic level.

In this report, we structurally investigate the galvanic replacement process of Ni substrate surface under several conditions by using the electrochemical measurements and angle-resolved x-ray photoelectron spectroscopy (AR-XPS).

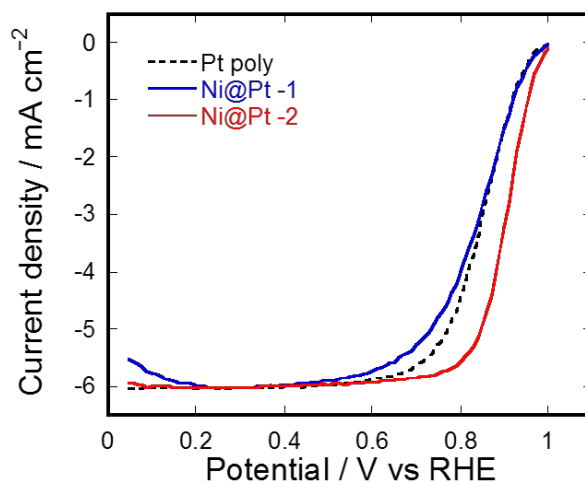


Fig. 1 Linear sweep voltammograms of the GCE electrodes modified with the Ni@Pt nanoparticles, which were prepared in the typical conditions, and polycrystalline Pt electrode, measured in the oxygen saturated 0.1 M HClO₄.

References

- [1] G. A. Somorjai, *Surface Chemistry and Catalysis*, John Wiley & Sons (1990).
- [2] T. Kondo, M. Shibata, N. Hayashi, H. Fukumitsu, T. Masuda, and K. Uosaki, *Electrochim. Acta*, **55**, 8302 (2010).
- [3] T. Kondo, C. Song, N. Hayashi, T. Sakurai, M. Shibata, H. Notsu, and I. Yagi, *Chem. Lett.*, **40**, 1235 (2011).
- [4] M. Shibata, N. Hayashi, t. Sakurai, A. Kurokawa, H. Fukumitsu, T. Masuda, K. Uosaki, and T. Kondo, *J. Phys. Chem. C*, **116**, 26464 (2012).
- [5] H. Nagai, H. Aso, M. Kawabuchi, and T. Kondo, *ECS Trans.*, **58**, 27 (2014).
- [6] M. Ueda and T. Kondo, *ECS Trans.*, **75**, 43 (2017).

Electrochemical Synthesis of Mesoporous Gold-Copper Alloy Films with Vertical Mesochannels

Asep Sugih Nugraha,¹ Yusuke Yamauchi,^{1,2,3} Toru Asahi¹

¹School of Advanced Science and Engineering, Waseda University, 3-4-1 Okubo, Shinjuku, Tokyo 169-8555, Japan

²MANA, National Institute for Material Science (NIMS), 1-1 Namiki, Tsukuba, Ibaraki 305-0044, Japan

³School of Chem. Eng., Univ. of Queensland, Brisbane QLD 4072, Australia

y.yamauchi@uq.edu.au; tasahi@waseda.jp

Precise detection of glucose concentration is very important to monitor glucose level in the human blood. Among the various techniques to detect glucose concentration such as coulometric measurement, capacitive detection and optical technique, the glucose sensing based on non-enzymatic electrochemical method have attracted great interest due to rapid and simple detection method. Architecting porous electrode with high surface area and abundant catalytic sites is playing the key role in this method. Owing to these unique properties as well as fairly stable and highly conductive frameworks, mesoporous metal films with controllable pore structures and compositions are very promising materials for facilitating the direct electro-oxidation of glucose.¹

In this study, we report an electrochemical synthesis of mesoporous AuCu bimetallic alloys in electrolyte solutions containing polymeric micelles. The obtained mesoporous AuCu alloy films were characterized by using several techniques such as scanning electron microscopy (SEM), X-ray diffraction (XRD), X-ray photoelectron spectroscopy (XPS), induced coupled plasma (ICP) analysis, transmission electron microscopy (TEM) and cyclic voltammetry (CV). Interestingly, mesoporous architectures are changed depending on the electrolyte compositions. From cross-sectional SEM image, vertically aligned mesochannels are standing on the substrate in the typical compositions (**Figure 1a**). This structure is favorable for the optimization of mass- and ion-transfer to the mesopores which can enhance the diffusion of electroactive species in the electrochemical process.² The catalytic activities of mesoporous AuCu films were evaluated in the alkaline solution at the suitably applied potential where the current signal of glucose oxidation was maximized while the current signals of the other interference species were minimized. As seen in **Figure 1b**, the linear relationship between the current response and the glucose concentration was observed in the wide range of concentration. Compared to nonporous Au₄₉Cu₅₁ film and mesoporous Au film, mesoporous Au₄₉Cu₅₁ film showed superior catalytic performance toward glucose electro-oxidation. Thus, it is revealed that the mesoporous AuCu film with the synergistic effect of alloying and vertical mesopores has a great potential for the electrochemical glucose sensing application.

Reference

1. A.S. Nugraha, C. Li, J. Bo, M. Iqbal, S. M. Alshehri, T. Ahmad, V. Malgras, Y. Yamauchi and T. Asahi, *ChemElectroChem*. **2017**, 4, 2571-2576.
2. C. Li, J. Bo, N. Miyamoto, J. H. Kim, V. Malgras, Y. Yamauchi, *J. Am. Chem. Soc.* **2015**, 137, 1158-11561.

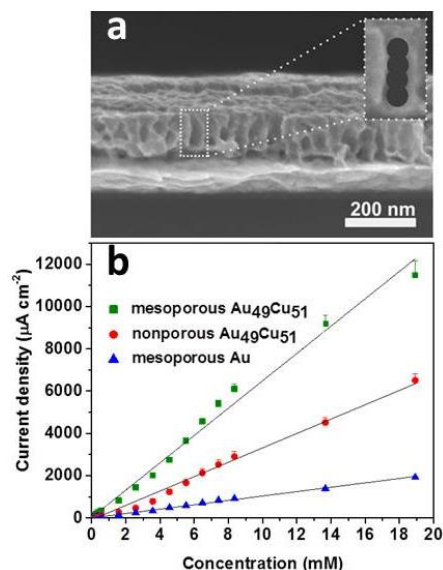


Figure 1. (a) Cross-sectional SEM image of the obtained mesoporous Au₄₉Cu₅₁ film and (b) current response for various glucose concentrations by using mesoporous Au₄₉Cu₅₁ alloy, mesoporous Au and nonporous Au₄₉Cu₅₁ alloy films.

Effects of Anion Doping on the Surface Hydrophobicity and Pseudo-capacitance of a Poly(3,4-ethylenedioxythiophene) Solid Contact

Li-Cheng Ho, Chi-Han Lu, and Lin-Chi Chen*

Department of Bio-industrial Mechatronics Engineering, National Taiwan University
No. 1, Sec. 4, Roosevelt Rd., Taipei 10617, Taiwan (R.O.C.)

*Corresponding author: chenlinchi@ntu.edu.tw

Ion-selective electrodes (ISEs) apply a potentiometric sensing method to determine the concentrations of target ions and have been widely used in environmental and biomedical fields. To miniaturize an ISE, a solid contact (SC) material, which serves as an ion-to-electron transducer (IET), is used to replace the conventional inner reference solution between the ion-selective membrane (ISM) and electrode, recently. The mostly used SC materials are the electroactive materials with a high redox pseudo-capacitance (e.g., conducting polymers, CPs), and it is known that the hydrophobicity of an SC is important for minimizing water-layer interference effect. Many papers reported that the CPs electrodeposited with different anions and charge capacities would exhibit distinct morphology and conductivity properties and might thus exert a different effect on an SC's IET performance. In this study, we fabricated a flexible screen-printed carbon electrode (SPCE)/PET substrate with a working area 0.28 cm² and electrodeposited poly(3,4-ethylenedioxythiophene) (PEDOT) on the SPCE as an SC for K⁺ sensing. From the experiments, we find that the hydrophobicity of an electrodeposited PEDOT film is dependent on its doped anion, as can be seen from the contact angle (CA) data in Fig. 1(a) (CA = 92.05° for PEDOT/Cl⁻, CA = 80.46° for PEDOT/ClO₄⁻, CA = 101.65° for PEDOT/SO₄²⁻, CA = 77.97° for PEDOT/BF₄⁻). In addition, PEDOT solid contacts with different pseudo-capacitances were fabricated via varied deposition methods and anion dopants: e.g., C = 1.552 mF, 2.839 mF, and 0.9576mF for PEDOT/Cl⁻ prepared by 1.2V/300s, 1.2V/600s, and CV deposition, respectively; 4.778mF, 7.729mF, and 4.495mF for PEDOT/ClO₄⁻; 1.693mF, 1.610mF, and 0.9544mF for PEDOT/SO₄²⁻; 4.310mF, 5.320mF, and 3.371mF for PEDOT/BF₄⁻ (see Fig. 1(b)). The capacitance of PEDOT with a constant deposited charge still differs when the dopant ion varies, as shown in Fig. 1(c), indicating a clear effect of anion doping on PEDOT's capacitance. Fabricated into a solid-contact K⁺ ISE (Fig. 1(d)), PEDOTs doped with different anions are compared for their K⁺ sensing performance (Fig. 1(e)), in which BF₄⁻ doping tends to result in a high sensitivity for its higher capacitance. Effect of the anion doping on the ISE water layer interference is under investigation.

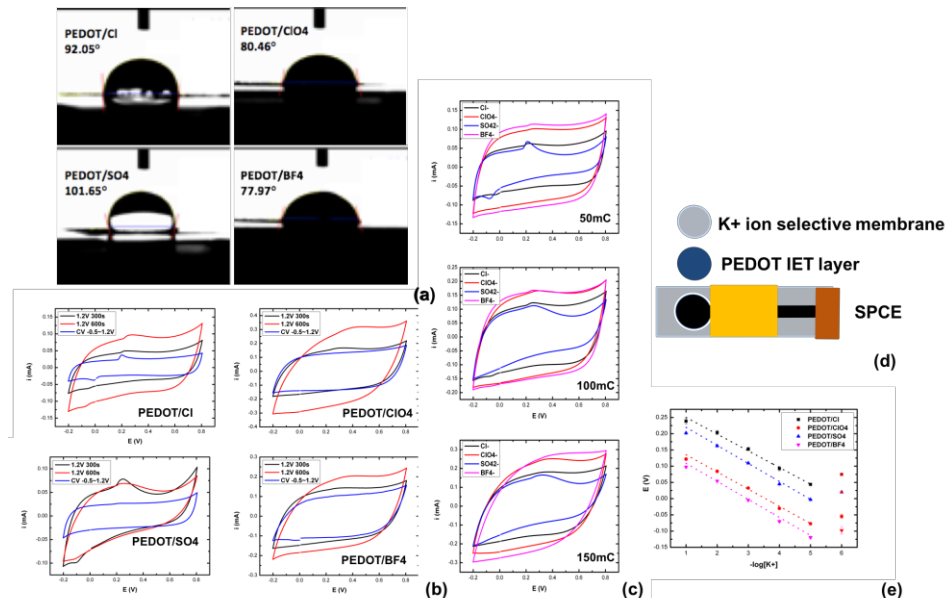


Figure 1. (a) Comparison of the contact angles of different anion-doped PEDOTs. (b) Comparison of the capacitance performance of anion-doped PEDOTs prepared by constant-potential and CV deposition. (c) Comparisons of the capacitance performance of anion-doped PEDOTs prepared with the same deposited charges. (d) Scheme of an K⁺ SC-ISE. (e) Dose-dependent responses of the ISEs with different PEDOTs.

Effect of Divalent Cation in Highly Concentrated Aqueous Electrolytes for Li-Ion Batteries

Shinji Kondo, Shoshi Terada, Kazuhide Ueno, Kaoru Dokko, Masayoshi Watanabe
Department of Chemistry and Biotechnology, Yokohama National University,
79-5 Tokiwadai, Hodogaya-ku, Yokohama 240-8501, Japan
kondo-shinji-sg@ynu.jp

1. Introduction

H₂O is an attractive solvent for electrolytes of Li-ion batteries owing to numerous advantages such as non-flammability, high ionic conductivity, environmental friendliness and low cost. In recent years, significant improvements in oxidative and reductive stability of aqueous electrolytes by increasing salt concentration were reported.^{1,2)} In this work, we investigated the additive effect of Mg[TFSA]₂ (TFSA: N(SO₂CF₃)₂) or Ca[TFSA]₂ in highly concentrated Li[TFSA]/H₂O electrolyte on electrochemical stability and aqueous lithium secondary battery performance.

2. Experimental

Li[TFSA], Mg[TFSA]₂, and Ca[TFSA]₂ were dissolved in water at molar ratios of Li[TFSA]:Mg[TFSA]₂:H₂O=1:0.03:2.6 and Li[TFSA]:Ca[TFSA]₂:H₂O=1:0.05:2.6. Linear sweep voltammetry was carried out at a scan rate of 1 mV s⁻¹ using a three-electrode cell at 30 °C. Al was used as working electrode to evaluate the reductive stability of electrolytes. The counter electrode was Pt coil, and the reference electrode was Ag/AgCl in saturated KCl aqueous solution. To investigate the reductive decomposition product, XPS was performed on the Al electrode. The samples were prepared by conducting LSV to -1.8 V vs. Ag/AgCl and then switching to chronoamperometry (-1.8 V vs. Ag/AgCl for 16 h) in each electrolyte followed by washing with DME.

3. Results and Discussion

Fig. 1 shows the reductive stability of Li[TFSA]:H₂O=1:2.6, Li[TFSA]:Mg[TFSA]₂:H₂O=1:0.03:2.6, and Li[TFSA]:Ca[TFSA]₂:H₂O=1:0.05:2.6. In the Li[TFSA]:H₂O electrolyte, the reductive current was observed at about -1.5 V vs. Ag/AgCl. However, in the presence of Mg[TFSA]₂ or Ca[TFSA]₂, the voltage at which the reductive current started to flow shifted more than 1 V to negative side. Therefore, the reductive stability was enhanced by adding Mg[TFSA]₂ or Ca[TFSA]₂.

Fig. 2 and 3 show the XPS of Al electrode after LSV and chronoamperometry in Li[TFSA]:Mg[TFSA]₂:H₂O=1:0.03:2.6 or Li[TFSA]:Ca[TFSA]₂:H₂O=1:0.05:2.6. It is reported that in the saturated Li[TFSA]/H₂O electrolyte, LiF-rich interphase formed by decomposition of [TFSA]⁻ suppresses the reduction of water.¹⁾ However, by adding Mg[TFSA]₂ or Ca[TFSA]₂, such LiF-derived peaks disappeared and the peaks of MgF₂, CaCO₃, CaF₂ were observed instead. The solubility of MgF₂, CaCO₃, and CaF₂ in water is 2 or 3 orders of magnitude lower than LiF.³⁾ This suggests that the reduction of water was further suppressed by the formation of an insoluble inorganic layer due to decomposition of Mg[TFSA]₂ or Ca[TFSA]₂ on the electrode surface. Further discussion will be made with Raman spectroscopy, LSV and XPS. In addition, Li secondary battery performance with the electrolytes will be presented.

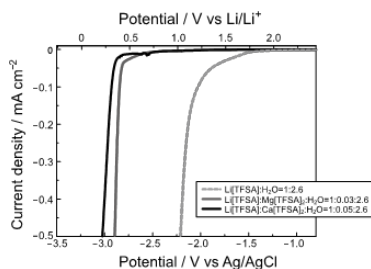


Fig. 1 Linear sweep voltammograms of Li[TFSA]:H₂O=1:2.6, Li[TFSA]:Mg[TFSA]₂:H₂O=1:0.03:2.6 and Li[TFSA]:Ca[TFSA]₂:H₂O=1:0.05:2.6.

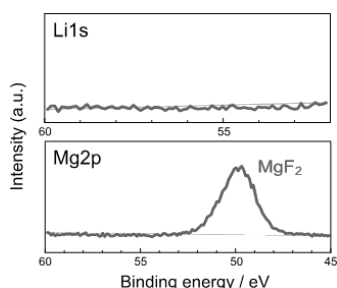


Fig. 2 XPS (Li 1s, Mg 2p) of Al electrode after chronoamperometry (-1.8 V vs. Ag/AgCl for 16 h) in Li[TFSA]:Mg[TFSA]₂:H₂O=1:0.03:2.6.

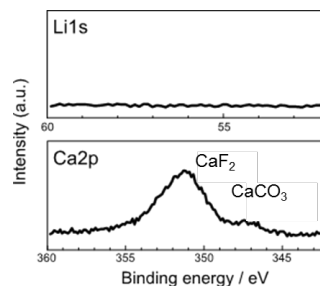


Fig. 3 XPS (Li 1s, Ca 2p) of Al electrode after chronoamperometry (-1.8 V vs. Ag/AgCl for 16 h) in Li[TFSA]:Ca[TFSA]₂:H₂O=1:0.05:2.6.

References: [1] L.Suo *et al.*, *Science*, **350**, 938-943 (2015). [2] Y.Yamada *et al.*, *Nat. Energy*, **1**, 16129 (2016). [3] D. R. Lide ed., *Handbook of Chemistry and Physics*, 73th (1993).

Electro-catalysts used in Direct Ammonia Fuel Cell

Hsin-Wen Huang and Andrew S. Lin*

Department of Chemical and Materials Engineering, Chang Gung University,
Taoyuan, TAIWAN 333

*Andrew@mail.cgu.edu.tw

By using ammonia as a liquid fuel for a direct fueled fuel cell, direct ammonia fuel cell can be a polymer electrolyte fuel cell by using alkaline membrane or by using Nafion of sodium form. As a no-carbon fuel and a mass production chemicals, ammonia is a liquid fuel for fuel cell having similar energy density(5500-6000 W/kg) in comparison to direct methanol fuel cell without carbon dioxide emission.

Electrocatalysts used for electrochemical oxidation of ammonia can be platinum and platinum alloy, such as Pt-Zn alloy and the strongly adsorbed intermediates with carbon-nitrogen bond causing retardation of oxidation potentials. Platinum-gold alloy are the alternatives electro-catalysts were used at electrochemical reaction of ammonia. Further study of the single cell measurements are carried by using carbon supported metal clusters in membrane electrode assembly. The comparison of various catalysts will be demonstrated.

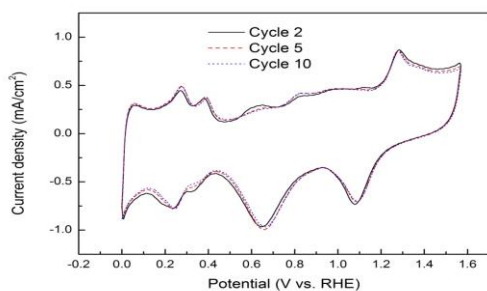


Fig.1: Cyclic voltammety of platinum and gold metal clusters on glassy carbon in 1M KOH.

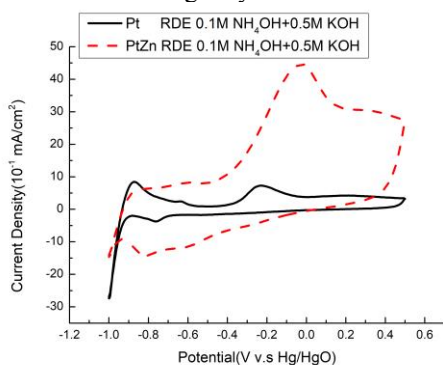


Fig.3 Cyclic voltammety of electrochemical oxidation of ammonia at platinum and platinum-zinc metal clusters deposited on glassy carbon at 0.1M NH₄OH in 0.5M KOH.

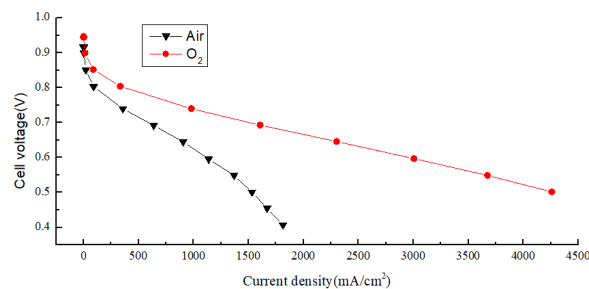


Fig.2: Current-voltage loading curves of catalysts coated membrane by using air and oxygen at the cathode for hydrogen and oxygen polymer electrolyte fuel cell.

References

- [1] Ahmed Afif, Nikdalila Radenahmad, Quentin Cheok, Shahriar Shams, Jung H. Kim, Abul K. Azad, Renewable and Sustainable Energy Reviews. 60(2016)822.
- [2] J. C. M. Silva, S. G. da Silva, R. F. B. De Souza, G. S. Buzzo, E. V. Spinacé, A. O. Neto and M. H. M. T. Assumpção, Applied Catalysis A: General 490 (2015) 133.
- [3] H.Moller, P.C. Pistorius, Journal of Electroanalytical Chemistry 570 (2004) 243.

Electrodeposition of Ni-Ru alloys from chloride solutions – morphology and catalytic study

Dawid Kutyla, Karolina Kołczyk, Anna Kwiecińska, Remigiusz Kowalik and Piotr Żabiński
Department of Physical Chemistry and Metallurgy of Non-Ferrous Metals, AGH University of Science and Technology in Kraków
Al. A. Mickiewicza 30, 30-059 Kraków - Poland
e-mail: kutyla@agh.edu.pl

Nickel alloys are used in fuel and electrolytic cells for industrial production of hydrogen and oxygen. Literature indicates that the addition of Co, W, Mo and platinoids into nickel electrodes can decrease the overpotential of hydrogen evolution process and also increase corrosion resistance in sodium hydroxide solutions which is widely used in industrial process. Properties of plated cobalt or nickel – platinoids alloys are similar to the pure platinum-group elements, but their cost are significantly lower.

The work comprises the results of the electrochemical synthesis of nickel-ruthenium alloys from chloride solutions. The studies were preceded by the UV-vis absorbance analysis of electrolytes and their stability. Electrochemical investigations were performed by CV-measurements onto polycrystalline golden electrode. Obtained results show the mechanism of co-deposition of nickel-ruthenium alloys.

Moreover, alloys with varied composition were deposited onto copper substrates under potentiostatic conditions. Nickel and ruthenium concentration in alloys were estimated by the XRF analysis. Structural changes of obtained materials were discussed according to X-ray diffraction measurements.

Electrochemical characterization of coatings were examined in 1M NaOH solutions. The catalytic activity and Electrochemical Active Surface Area (ECSA) have been estimated.

Acknowledgments: This work was supported by the Polish National Center of Science under the grant UMO-2016/21/N/ST8/00222.

Metallization of 3D prints by magnetic coatings in electroless and electrodeposition processes

Karolina Kolczyk, Wojciech Zborowski, Dawid Kutyla, Anna Kwiecińska, Remigiusz Kowalik, Piotr Żabiński

*AGH University of Science and Technology, Faculty of Non-Ferrous Metals
al. Mickiewicza 30, 30-059 Krakow, Poland
kkolczyk@agh.edu.pl*

3D printing is one of the newest method of precise elements production. One of advantages of this technique is possibility of production elements with any geometry and very good tolerance of dimensions. Materials very often used in this method are plastics which are easy formable, cheap and non-toxic.

To obtain special properties the prints can be coated by magnetic layers. This operation gives the plastic elements new properties like electric and thermal conductivity or magnetism. As a results of this combination, elements with mix of plastic and metallic properties are obtained. It allows to increase the number of application of these elements. Depending on the material, the plastics covered by metallic coatings can find application in many field of technology like medicine, automotive, metallurgy or energy industry.

In this work it will be presented process of metallization of 3D prints from light-hardened resins. The metallization is a few steps process demanding precise parameters. The prints are coated by bimetal coating containing copper and nickel. This method combines electroless deposition of copper and electrodeposition of nickel. Also, the nickel coatings are obtained in electroless deposition.

In results of this work the optimum parameters of metallization processes are obtained. Variation of many parameters like duration time of every steps, composition of electrolytes, current density were analyzed. Additionally, the influence of magnetic field on the coatings was investigated. The magnetic field can significantly change the morphology of obtained surfaces.

The presented work is the preliminary studies to manufacture composite micro elements. It is planned to coat the 3D prints by metallic layers to obtain precise parameters of more detailed elements and possibility to control their movement them by magnetic field.

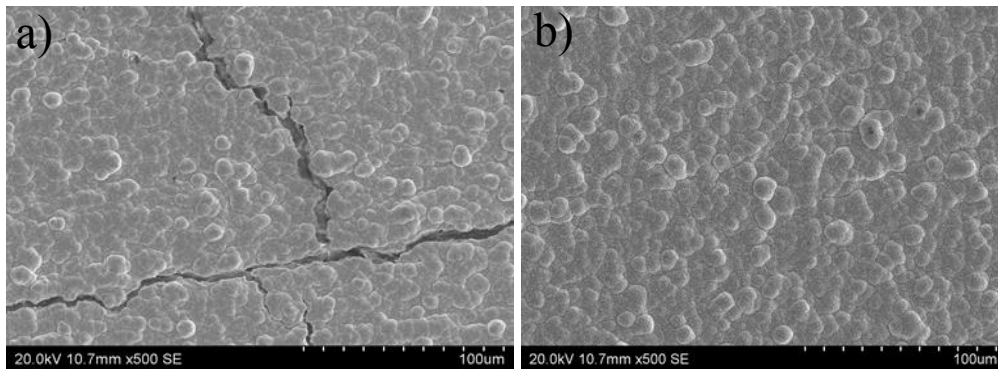


Fig. 1 SEM microstructure of nickel electrodeposited coatings onto plastic in a) 10 and b) 30 min

The financial support from National Science Center Poland under grant number UMO-2017/25/N/ST8/01721 is gratefully acknowledged.

Electrochemical Preparation of Roughened Current Collectors and Their Application to Sn Negative Electrode for Na-ion Batteries

Masahiro Shimizu^{1,2}, Ryosuke Yatsuzuka¹, Masaomi Horita³, Susumu Arai^{1,2}

¹ Department of Materials Chemistry, Faculty of Engineering, Shinshu University

² Institute of Carbon Science and Technology, Faculty of Engineering, Shinshu University

³ Technical Division, Faculty of Engineering, Shinshu University

4-17-1 Wakasato, Nagano, 380-8553, Japan

shimizu@shinshu-u.ac.jp, araisun@shinshu-u.ac.jp

The use of high capacity electrode materials such as Sn and P based on alloying and dealloying reactions with Na is very effective for improving energy density of batteries. However, their application brings on electrical isolation such as detachment of the electrode mixture layer from a current collector, causing rapid capacity fading. We previously found that Cu electrochemically grows in sheet form by electroplating in a CuSO₄-based aqueous solution with polyacrylic acid (PAA).¹⁻³ In the present study, optimized the sheet thickness by controlling PAA concentration and current density during Cu electroplating, and applied the roughened Cu substrate as a current collector of a Sn negative electrode for Na-ion batteries to upgrade cycling performance.

The working electrode was formed on the substrate by using a slurry composed of 70 wt.% Sn powder (diameter: 70–500 nm, EMJapan Co., Ltd.), 15 wt.% acetylene black (AB; Denka Co., Ltd.), 10 wt.% carboxymethyl cellulose (CMC, Mw = 90000; Sigma-Aldrich), and 5 wt.% styrene butadiene rubber (SBR; JSR Corporation). Methanol (150 μ L) was used as a dispersant of the Sn powder. The electrode thickness was adjusted by a doctor blade to 10 μ m in dry conditions, and the mass loading of the Sn active material powder was approximately 0.7–1.1 mg cm⁻².

Figure 1 displays surface and cross-sectional FE-SEM images of roughened Cu substrates in which PAA concentration was set to 1.0×10^{-5} , 5.0×10^{-5} , and 1.0×10^{-4} M. As for 1.0×10^{-4} M PAA, Cu grew as a sheet on the substrate to a height of about 3 μ m, and sheets formed the space capable of accommodating an active material layer. In fact, after slurry casting, it was confirmed that the Cu sheets extended to inside the active material layer, like a support pillar.

Figure 2 shows charge–discharge curves of roughened-Cu/Sn and flat-Cu/Sn electrodes operated at the potential range of 0.005–0.650 V (vs. Na/Na⁺) in 1 M NaPF₆/EC:DEC with 5 vol.% FEC. Although the initial reversible capacities of flat-Cu/Sn and roughened-Cu/Sn electrodes were comparable, the developed Cu substrate (1.0×10^{-4} M PAA) delivered a noticeable increase in the reversible capacity by 210 mA h g⁻¹ from the first to the second cycle, whereas the flat-Cu remained the increase by 100 mA h g⁻¹. In addition, the roughened-Cu substrate suppressed the detachment of the active material layer to maintain a high capacity of 685 mA h g⁻¹ with good capacity retention of more than 90% by the anchor effect. These results demonstrate that the roughened-Cu substrate prepared in the present work is a promising candidate as a current collector for rechargeable batteries.

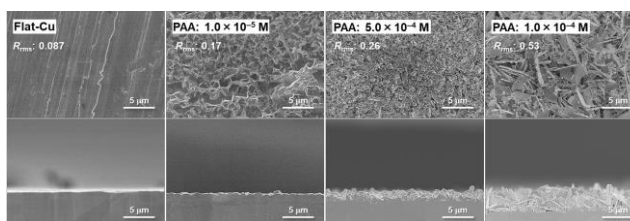


Fig. 1 Surface and cross-sectional FE-SEM images of roughened Cu current collectors prepared by an electroplating method using PAA with various concentration.

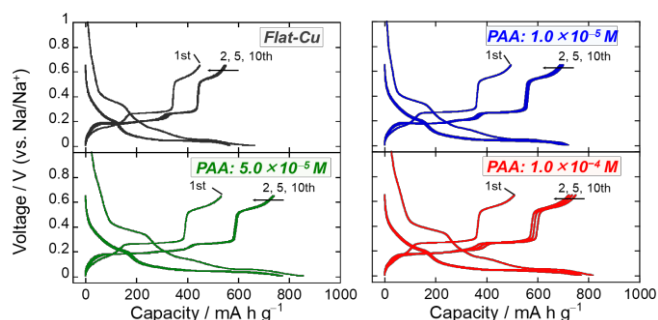


Fig. 2 Charge–discharge (Na-insertion/extraction) profiles of Sn electrodes using flat-Cu and roughened-Cu substrates.

- 1) S. Arai *et al.*, *ECS Electrochem. Lett.*, **3** (5) (2014) D7.
- 2) M. Shimizu, S. Arai *et al.*, *J. Appl. Electrochem.*, **47** (2017) 727.
- 3) M. Shimizu, S. Arai *et al.*, *J. Phys. Chem. C*, (2017) *in press*.

Corrosion Behavior of 3C-SiC with Irradiation-Induced Defects

Yuki Maeda¹, Kazuhiro Fukami¹, Sosuke Kondo², Tatsuya Hinoki², Atsushi Kitada¹
and Kuniaki Murase¹

¹Department of Materials Science and Engineering, Kyoto University, Kyoto 606-8501, Japan

²Institute of Advanced Energy, Kyoto University, Kyoto 611-0011, Japan

maeda.yuki.38a@st.kyoto-u.ac.jp

Silicon Carbide (SiC) has attracted attention as an alternative material for core components of a fuel cladding because of its high sublimation point, strength and chemical stability. At present, zircaloy (zirconium alloy) is used for a fuel cladding. However, it reacts with high temperature steam to generate hydrogen, and its strength decreases in a high temperature environment such as an accident. In this situation, some authors reported that SiC has a high tolerance against corrosion in reactor environments [1]. However, in a nuclear reactor many lattice defects are induced by a neutron-irradiation. Kondo et al. reported that corrosion of SiC is accelerated by irradiation-induced defects [2]. But its mechanism has not been clarified so far. In the present study, we mimicked the defect formation in a single crystalline 3C-SiC by an ion irradiation, and the electrochemical behavior of the SiC with lattice defects was investigated in order to understand the corrosion mechanism.

We used n-type highly doped 3C-SiC (111) on Si (111) substrate. The dopant was nitrogen and the thickness of SiC was 2.5 μm . By using Dual-beam facility for Energy Science and Technology (DuET) in Kyoto university, 5.1 MeV Si^{2+} ions were irradiated to SiC samples at 400 $^{\circ}\text{C}$ in order to produce lattice defects. The irradiation time was from 0.3 min to 100 min. For the electrochemical measurement, we used a three-electrode cell and the electrolyte contained 21 mM HF, 12 mM NH_4F and 0.967 M NH_4Cl . Since it is not easy to realize the actual reactor environments (in a hot water at 300 $^{\circ}\text{C}$ and 20 MPa), we used HF solution as the electrolyte to accelerate some reactions even at room temperature and the ambient air pressure. All measurements were carried out in the dark. The working, counter and reference electrodes were SiC, Pt rod and Ag/AgCl sat. KCl electrode, respectively. We measured cyclic voltammograms (CVs) ranging from -0.4 V to 1.0 V vs. Ag/AgCl sat. KCl. The scan rate was 10 mV / s.

Figure 1 shows Evans diagrams of irradiated SiC. The corrosion potential shifted to positive when the irradiation time was increased from 0.3 min to 3 min. On the other hand, when the irradiation time was prolonged from 10 min to 100 min, the corrosion potential in turn shifted to negative. In order to determine that these changes in the corrosion potential is related to the irradiation-induced defects, we measured CV of a sample annealed for 30 min at 1000 $^{\circ}\text{C}$ after irradiation. This result is shown in Figure 2. The corrosion potential in the positive returned to negative. This result suggests that the change in the corrosion potential is caused by lattice defects.

[1] D. Tanaka *et al.*, *Zairyo-to-Kankyo (in Japanese)*, **42**, 585 (1993).

[2] S. Kondo *et al.*, *Corros. Sci.*, **112**, 402 (2016).

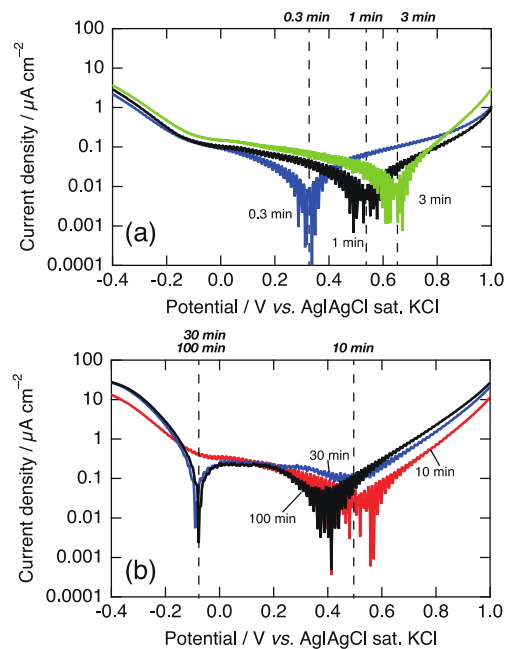


Figure 1. Evans diagrams of SiC irradiated for (a) 0.3 min, 1 min, 3 min, (b) 10 min, 30 min, and 100 min.

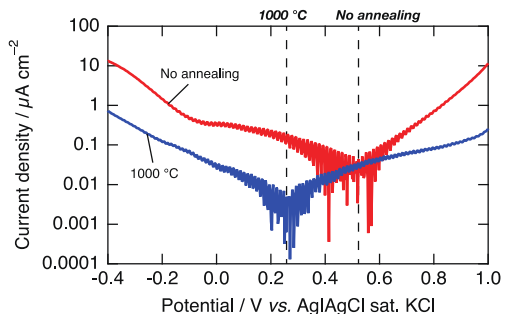


Figure 2. Evans diagrams of SiC irradiated for 10 min and annealed at 1000 $^{\circ}\text{C}$ after irradiation.

Determination of As(III) at Nanoporous Gold Electrode by Square Wave Voltammetry

Minji Seo, Jongwon Kim*

*Department of Chemistry, Chungbuk National University
1, Chungdae-ro, Cheongju, Chungbuk, Korea
9022323@naver.com*

Nanoporous gold (NPG) has a much larger surface area than the bare gold electrode and is widely used because of its unique physical and chemical properties. In this experiment, when the As (III) detection was performed, it was observed how the electrochemical behavior and sensitivity at NPG electrode were enhanced compared to the bare gold electrode. Furthermore, it was observed how the electrochemical behavior and sensitivity of the As (III) detection changes when the surface area of the NPG electrode is controlled. NPG electrode was prepared by anodization of Au surfaces. Arsenic (III) detection was carried out by using a square wave voltammetry (SWV) technique at an NPG electrode, and the electrochemical behavior was observed by varying the deposition time and deposition potential to find the optimum condition. Under the optimized experimental conditions, observation of the electrochemical behavior of the Arsenic (III) peak at the NPG electrode showed that the peak was negatively shifted and had greater sensitivity than the bare gold electrode. This suggests that the NPG electrode with a large surface area and high sensitivity could be used as a very useful electrode sensor for the detection of Arsenic (III) by square wave voltammetry (SWV).

References

1. *Langmuir*, **2014**, *30*, 4844 – 4851
2. *Int. J. Electrochem. Sci.*, **2017**, *12*, 8345 – 8356

Co-deposition of Ni–P and P25 on Silk Textile by Supercritical CO₂ Promoted Electroless Plating for Flexible Photocatalyst Applications

*Wan-Ting Chiu^{1,2}, Chun-Yi Chen^{1,2}, Tso-Fu Mark Chang^{1,2}, Tomoko Hashimoto³, Hiromichi Kurosu³, Masato Sone^{1,2}

¹ Institute of Innovative Research, Tokyo Institute of Technology, Yokohama, Japan

² CREST, Japan Science and Technology Agency, Yokohama, Japan

³ Department of Clothing Environmental Science, Nara Women's University, Nara, Japan

*chiu.w.aa@m.titech.ac.jp

The global market of wearable devices is foreseen to keep prospering in the future [1]. In the meanwhile, the wearable devices are diversified into various functions such as the photovoltaics and photocatalytic devices due to a range of requirements in the next-generation technology. This study therefore demonstrated co-deposition of metal oxide/metal composite on a flexible substrate to meet the aforementioned demands. Electroless plating [3] is a promising method for deposition of materials onto non-conductive substrate. Electroless plating consists of a pretreatment step to clean the substrate, a catalyzation step to activate the substrate, and a metallization step to metallize the substrates. In the conventional catalyzation step, the catalyst is only inlaid on the substrate surface due to the polar property of aqueous solution. Supercritical carbon dioxide (sc-CO₂) was introduced to the electroless plating system to solve these problems [4]. Since sc-CO₂ owns the properties in the midway of gas and liquid, and affinity to non-polar material, it thus can carry the metal-organic complex catalysts to go into the textile and remains the substrate intact. In this way, the adhesive property can be enhanced due to embedment of the catalyst in the substrate. Sc-CO₂ assisted electroless plating were carried out in this study to co-deposit the metal and metal oxide to functionalize the flexible substrate for applications in wearable devices.

Since a small disturbance from the rigid component in the wearable devices can be annoyance to the users. Silk, a common clothing material, was chosen in this study due to its flexibility and stretchability. Ni–P was chosen due to its high corrosion resistance and low cost. P25 TiO₂ which has attracted widespread interest due to its high photocatalytic activity, was selected as the co-deposition material.

The surface morphology, cross-section and compositions were examined by an OM, SEM, and EDX. The crystal structures and phases were identified by an XRD. Electrical resistance was measured by a four-point probe. The photoelectrochemical measurement was conducted in a three electrode cell consisting of a Pt counter electrode, Ag/AgCl reference electrode, and a piece of the Ni–P/P25 on silk as the working electrode. 0.5 M Na₂SO₄ solution was used as the electrolyte.

Here we reported a facile fabrication process to prepare a functional composite material toward application into wearable devices. With the assistance of sc-CO₂, smooth, strong adherence, and uniform coverage of Ni–P/P25 was successfully electroless plated on the silk. The coatings on the silk have been confirmed to be Ni–P phase and P25 through the XRD pattern and compositional analysis. Chronoamperometric I–t curves collected at 0 V vs Ag/AgCl show positive tendency of P25 amount and photocatalytic activity. Photocatalytic activity was improved significantly (Fig. 1).

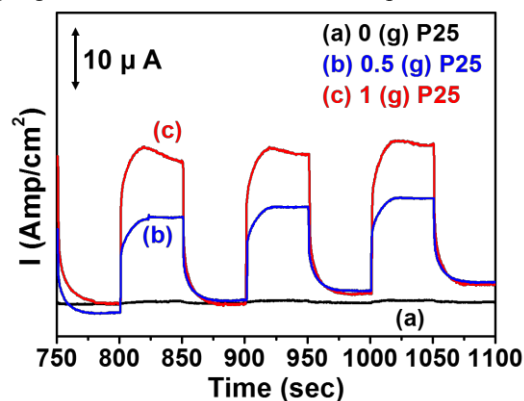


Fig. 1 Photocatalytic activity of Ni–P+P25

References:

- [1] T. Page, *Int. J. Technol. Diffus.* 6 (2015) 18.
- [2] G.O. Mallory and J.B. Hajdu, *Electroless Plating: Fundamentals and Applications* (Elsevier, Amsterdam, 1990).
- [3] W.-T. Chiu, Y. Tahara, C.-Y. Chen, T.-F.M. Chang, T. Hashimoto, H. Kurosu, M. Sone, *Microelectron. Eng.* 175 (2017) 34-37.

N-doped Carbons Directly Synthesized from Protic Salts for Sodium Secondary Battery

Yukihiro Okamoto,^a Shoshi Terada,^a Mahfuzul Hoque,^a Kazuhide Ueno,^a Kaoru Dokko,^{a,b}
Masayoshi Watanabe^a

^a Department of Chemistry and Biotechnology, Yokohama National University
79-5 Tokiwadai, Hodogaya-ku, Yokohama 240-8501, Japan

^b Unit of Elements Strategy Initiative for Catalysts and Batteries (ESICB), Kyoto University, Japan
1-30, Goryo-Ohara, Nishikyo-ku, Kyoto 615-8245, Japan
okamoto-yukihiro-ny@ynu.jp

1. Introduction

Our group have been focusing on N-doped carbons (NDCs) derived from protic salts or protic ionic liquids which contain N atoms. NDCs produced from protic salts have advantages such as simple synthetic procedure through neutralization of the precursors followed by carbonization without catalyst or pre-polymerization, tunable carbon structure by changing conditions of carbonization, and high electric conductivity.¹⁾ On the other hand, our group have applied unique electrolytes called “solvate ionic liquids” (SIL) for the electrolyte of sodium secondary batteries.²⁾ The SILs are a molten salt complex of glymes (G_n : $\text{CH}_3\text{O}(\text{CH}_2\text{CH}_2\text{O})_n\text{CH}_3$) and certain sodium salts, having high thermal stability and moderate ionic conductivity. In addition, the ionic conductivity of the SIL can be enhanced by adding low viscosity solvent and that improves the battery performance.³⁾ Here we report electrochemical properties of the protic salt-derived NDCs as an anode material for sodium batteries with the SIL electrolyte.

2. Experimental

A protic salt [pPDA][2HSO₄] (*p*-phenylenediammonium dibisulfate) was prepared according to the previously reported procedure.^{1), 4)} The NDC was synthesized by carbonizing the obtained [pPDA][2HSO₄] at 700, or 900 °C for 2 h under Ar atmosphere. Then the NDC were ball milled and X-ray diffraction patterns (XRD) were collected. The electrochemical sodiation/de-sodiation of the NDC was investigated. The composite electrode was fabricated by mixing NDC:acetylene black:CMC = 90:5:5(wt%) and pasted on to Al foil. The sodium metal was used as the counter electrode. The electrolyte was prepared by mixing Na[FSA] (sodium bis(flurosulfonyl)amide), G5, and HFE (hydrofluoroether, 1,1,2,2-tetrafluoroethyl 2,2,3,3-tetrafluoropropyl ether) at 1:1:4 molar ratio in an Ar atmosphere glove box.

3. Results and Discussion

Figure 1 shows the XRD patterns of NDC carbonized at 700 °C, and 900 °C. From the figure, (002) (100) peaks derived from graphitic structure are observed in all NDCs. The peak intensity increased by increasing carbonization temperature, indicating the more pronounced graphitic structure at higher carbonization temperature. **Figure 2** shows charge-discharge curves of NDC carbonized at 700 °C or 900 °C. [pPDA][2HSO₄]-700 exhibited higher capacity above 0.9 V than [pPDA][2HSO₄]-900. The capacity in this region is reported to be the uptake of Na⁺ by defect sites on the carbon surface.⁵⁾ Therefore, the [pPDA][2HSO₄]-700 having lower graphitization degree is expected to have more defect sites and results in higher capacity. Further characterization of the NDCs and correlation between the carbon structure and charge-discharge behavior will be reported.

4. References

- 1) S. Zhang et al., *Chem. Mater.* **2014**, *26*, 2915–2926
- 2) S. Terada et al., *Phys. Chem. Chem. Phys.* **2014**, *16*, 11737–1174
- 3) S. Terada et al., *J. Phys. Chem. C* **2016**, *120*, 23339–23350
- 4) S. Zhang et al., *J. Am. Chem. Soc.* **2014**, *136*, 1690–1693
- 5) B. Zhang et al., *Adv. Energy Mater.* **2016**, *6*, 1501588

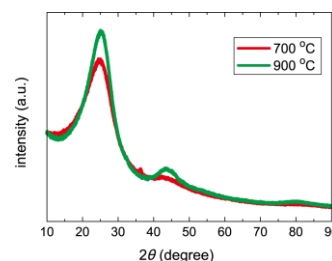


Figure 1. XRD pattern of NDCs carbonized at various temperatures.

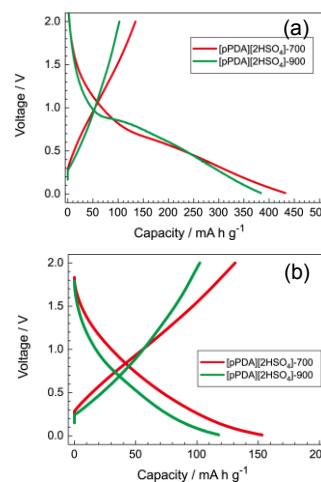


Figure 2. (a) 1st (b) 2nd cycle charge-discharge behavior of NDCs carbonized at various temperatures.

Redox-Active Solvate Ionic Liquids with Halide/Polyhalide Redox Couples

Shigenobu Keisuke, Azusa Nakanishi, Kazuhide Ueno, Kaoru Dokko and Masayoshi Watanabe
Department of Chemistry and Biochemistry, Yokohama National University
79-5 Tokiwadai, Hodogaya-ku, Yokohama, Kanagawa 240-8501, Japan
shigenobu-keisuke-xm@ynu.jp

1. Introduction

Ionic liquids (ILs) are molten salts having melting points below 100 °C^[1]. They have remarkable properties, such as low-flammability, negligible volatility and high ionic conductivity^[2]. Among subclasses of ILs, solvate ILs are a new family of ILs composed of long-lived, stable complex ions in the molten state^[3]. Solvate ILs reported so far are mostly based on metal complex cations, and a typical example of solvate ILs, [Li(G4)][TFSA], is shown in Fig. 1. Besides [TFSA] anion, other anions such as trifluoroacetate and NO₃⁻ have been considered; however, only limited combinations of multidentate glyme and Li salt having bulky and weakly coordinating anions were found to yield a stable solvate IL^[4]. Owing to high Li ion conductivity and electrochemical stability, the lithium solvate ILs are applicable as IL-based electrolyte for lithium secondary batteries. In this study, we prepared novel solvate ILs consisting solely of 'complex' ions, where halide/polyhalide redox couples (Fig. 2) were employed as redox-active complex anions for the solvate ILs. Physicochemical and electrochemical properties of the redox-active solvate ILs were studied.

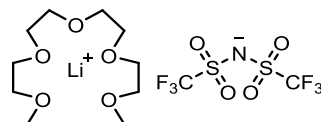


Fig. 1 Chemical structure of [Li(G4)][TFSA].

Besides [TFSA] anion, other anions such as trifluoroacetate and NO₃⁻ have been considered; however, only limited combinations of multidentate glyme and Li salt having bulky and weakly coordinating anions were found to yield a stable solvate IL^[4]. Owing to high Li ion conductivity and electrochemical stability, the lithium solvate ILs are applicable as IL-based electrolyte for lithium secondary batteries. In this study, we prepared novel solvate ILs consisting solely of 'complex' ions, where halide/polyhalide redox couples (Fig. 2) were employed as redox-active complex anions for the solvate ILs. Physicochemical and electrochemical properties of the redox-active solvate ILs were studied.



Fig. 2 Preparation of [Li(glyme)][trihalide] solvate IL.

2. Experimental

[Li(G4Et)]I₃ were prepared by simply mixing tetraethylene glycol ethylmethylether (G4Et) and lithium iodide (LiI) at 1:1 molar ratio in an Ar-filled glove box. [Li(G4Et)]I was further mixed with equimolar of iodine (I₂) to obtain [Li(G4Et)]I₃ in the same atmosphere.

3. Results and Discussion

Fig. 3 shows Raman spectra of G4Et, [Li(G4Et)]I, and [Li(G4Et)]I₃ in the range of 700-1000 cm⁻¹ (left) and diluted [Li(G4Et)]I₃ solution in the range of 100-300 cm⁻¹ (right). Formation of the complex ions can be confirmed from characteristic Raman bands around 870 cm⁻¹ for crown ether-like complex cations (left) and 125 cm⁻¹, 155 cm⁻¹ and 180 cm⁻¹ for triiodide anions (right), respectively. Thermal, physicochemical, and electrochemical properties of the solvate ILs will also be reported in detail.

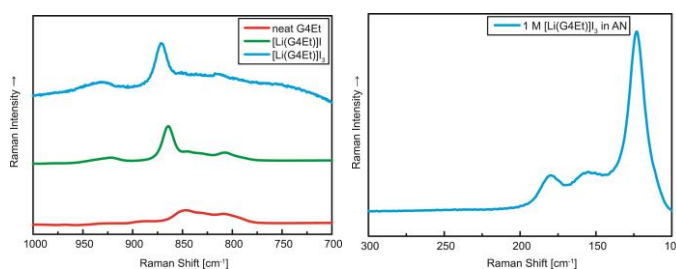


Fig. 3 Raman spectra of G4Et, [Li(G4Et)]I and [Li(G4Et)]I₃ (left) of 1 mol dm⁻³ [Li(G4Et)]I₃ in acetonitrile (right).

4. References

- [1] J. D. Holbrey, K. R. Seddon, *Clean Prod. Process*, 1, 223 (1999).
- [2] A. Lewandowski, A. Swiderska-Mocek, *J. Power Sources*, 194, 601-609 (2009).
- [3] C. A. Angell, Y. Ansari, Z. Zhao, *Faraday Discuss.*, 154, 9-27 (2012).
- [4] K. Ueno, K. Yoshida, M. Tsuchiya, N. Tachikawa, K. Dokko, M. Watanabe. *J. Phys. Chem. B*, 116, 11323-11331 (2012).

Performance Evaluation of Anion Exchange Membrane Fuel Cells Using Hydrocarbon Polymer Electrolytes

Kanji Otsuji^a, Manai Shimada^b, Naoki Yokota^b, Natsumi Yoshimura^b, Kenji Miyatake^{c,d}, Makoto Uchida^d

^a Integrated Graduate School of Medicine, Engineering and Agricultural Sciences, University of Yamanashi, ^b Takahata Precision Japan Co., Ltd., ^c Clean Energy Research Center, University of Yamanashi, ^d Fuel Cell Nanomaterials Center, University of Yamanashi,

^a 4-4 Takeda, Kofu 400-8510, Japan, ^b 390 Maewada, Sakaegawatyou, Fuefuki 406-0843, Japan,

^c 4-4 Takeda, Kofu 400-8510, Japan, ^d 6-43 Miyamae, Kofu 400-0021, Japan

E-mail: uchidam@yamanashi.ac.jp

Anion exchange membrane fuel cells (AEMFCs) are expected to proliferate due to their use of non-noble metal catalysts.¹ Many anion exchange membranes (AEMs) have been recently developed; however, there has been few studies of ionomers as binders for catalyst layers.

In our previous research, we developed two kinds of alcohol-soluble hydrocarbon polymer electrolytes (QPAF-1², QPAF-4³) which were different in molecular structure (Fig. 1) and stability in alkaline solution (Fig. 2). In this work, the power generation performance and durability of cells using these ionomers as the cathode binders were evaluated.

A201 (IEC=1.7 meq/g) membrane and AS-4 (IEC=1.4 meq/g) ionomer, which were supplied from Tokuyama Corp., were used as the electrolyte membrane and the binder on the anode side, respectively.

QPAF-1 and QPAF-4 were dissolved in alcohol and applied to the cathode side. The IECs of QPAF-1 and QPAF-4 used in this work were 1.2 meq/g and 1.4 meq/g, respectively. Pt loaded on carbon black (Pt/CB, TEC10E50E, supplied from TKK Japan) was used as the electrocatalyst for both electrodes. The catalyst layer areas and Pt loading amounts were 4.4 cm² and 0.2 mg_{Pt}/cm², respectively.

Current-voltage (I-V) curves of these cells were measured at 40 °C under 100% RH and gas-flow rates of both H₂ (100 mL/min, anode) and O₂ (100 mL/min, cathode). Thereafter, the cathode gas was changed to N₂ (100 mL/min), and the cell voltages decreased to about 0.1 V; the cathode gas was then stopped, and cyclic voltammograms (CVs) were measured at a sweep rate of 10 mV/s. These I-V curves and CVs were alternately measured three times, and the performances were compared.

In Fig. 3, the cell using QPAF-1 showed higher initial performance than that using QPAF-4. In comparison with the first and third I-V, however, the current density at 0.6 V of QPAF-1 decreased significantly, by 77%, but that using QPAF-4 decreased only 14%. In addition, the retention of the electrochemically active surface area (ECA) for the cell using QPAF-1, which was calculated from the hydrogen adsorption electric charge in the CV, was 54%. In contrast, that using QPAF-4 was 99%. From these results, it was found that the stability of the power generation performance of the cell was able to be improved by using an electrolyte binder with high alkali stability such as QPAF-4.

This work was supported by the Japanese Science and Technology Agency (JST), CREST.

References

- 1) K. Asazawa et al., *Angew. Chem. Int. Ed.*, 46, 8024 (2007)
- 2) H. Ono et al., *J. Mater. Chem. A*, 3, 21779 (2015)
- 3) H. Ono et al., *J. Mater. Chem. A*, 5, in press (2017)

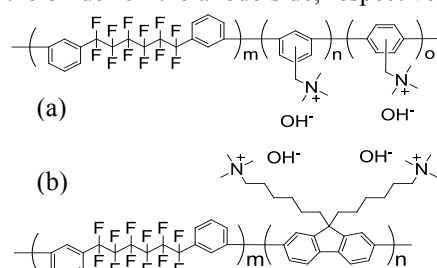


Fig. 1 Chemical structures of quaternized poly(arylene perfluoroalkyl)s, QPAF-1(a) and QPAF-4(b).

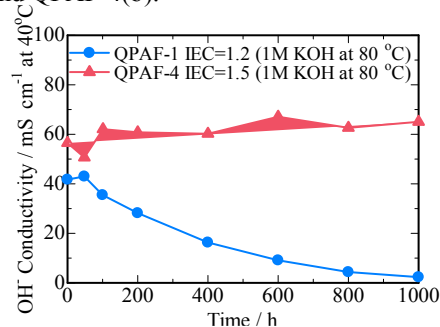


Fig. 2 Alkaline stability test of QPAF-1 and QPAF-4 membranes.

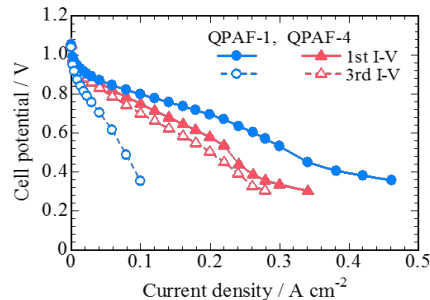


Fig. 3 I-V curves at 40 °C 100%RH; anode H₂ (100 mL/min); cathode O₂ (100 mL/min).

Interfacial Structure of Hydrophobic Cations Activating Oxygen Reduction Reaction on Pt(111) Electrode

Tomoaki Kumeda, Nagahiro Hoshi, Masashi Nakamura
Chiba University
Yayoi-cho 1-33, Inage-ku, Chiba 263-8522, Japan
aaaa2605@chiba-u.jp

The enhancement of the activity of cathode catalysts for the oxygen reduction reaction (ORR) is important for the widespread use of polymer electrolyte fuel cells at low cost. The ORR activity of Pt(111) electrode is influenced by specifically and non-specifically adsorbed ions. There is a correlation between the catalytic activity of Pt(111) electrode and the hydration energy of the alkali metal cations[1]. In-situ X-ray diffraction and infrared spectroscopy measurements revealed the interfacial structure of Pt(111) in alkaline electrolytes, which suggests that the non-specifically adsorbed cations affect the surface oxidation of the Pt[2]. The hydration structures differ between hydrophilic cations (alkali metals) and hydrophobic cations (tetraalkylammonium)[3].

We evaluated the ORR activities of Pt(111) electrode in acidic solutions containing hydrophobic cations with various lengths of alkyl chains: tetramethylammonium (TMA^+), tetraethylammonium (TEA^+), tetrabutylammonium (TBA^+), and tetrahexylammonium (THA^+). The interfacial structures were determined using surface X-ray diffraction (SXRD).

Fig. 1 shows the ORR voltammograms of Pt(111) in 0.1 M HClO_4 containing TBA^+ and THA^+ . The ORR current density at 0.9 V increases as the alkyl chains of the cation become longer, and the activity in the solution containing THA^+ is 5 times as high as that without hydrophobic cations. Fig. 2 shows the specular CTR profiles of the Pt(111) in 0.1 M HClO_4 and 0.1 M HClO_4 containing THA^+ at 0.9 V. As a result of structural optimization, the formation of adsorbed OH species was restrained in the solution containing THA^+ . The hydration shell of the hydrophobic cation destabilizes adsorbed OH and activates the ORR.

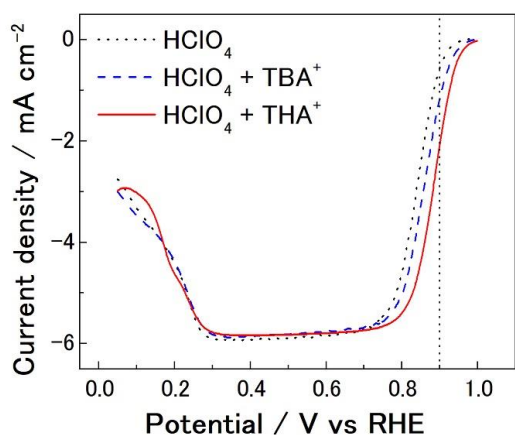


Fig.1 ORR voltammograms of Pt(111) in 0.1 M HClO_4 (dotted), 0.1 M HClO_4 + 10^{-5} M TBA^+ (broken), and 0.1 M HClO_4 + 10^{-6} M THA^+ (solid) saturated with O_2 . The scanning rate is 0.01 V s^{-1} .

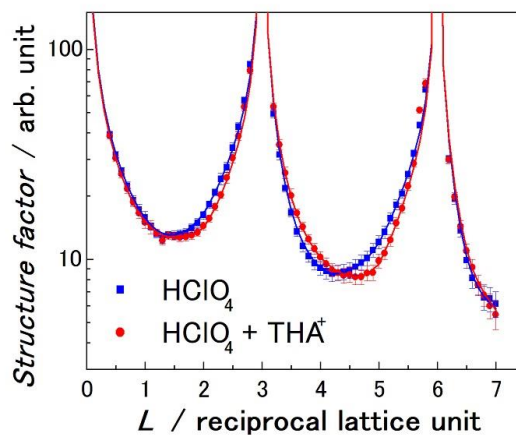


Fig.2 Specular CTR profiles of the Pt(111) in 0.1 M HClO_4 (square) and 0.1 M HClO_4 + 10^{-6} M THA^+ (circle) at 0.9 V. Solid lines are the calculated structure factors.

[1] D. Strmcnik, K. Kodama, D. van der Vliet, J. Greeley, V. R. Stamenkovic, N. M. Markovic, *Nat. Chem.*, 1, 466 (2009).

[2] M. Nakamura, Y. Nakajima, N. Hoshi, H. Tajiri, O. Sakata, *ChemPhysChem*, 14, 2426 (2013).

[3] A. Yamakata, M. Osawa, *J. Phys. Chem. Lett.*, 1, 1487 (2010).

Acknowledgement

This work was supported by New Energy and Industrial Technology Development Organization (NEDO).

Highly Thermal Stable Acetonitrile based Gel Polymer Electrolyte for 3.0 V Supercapacitor

Habin Park¹, Hansol Yong¹, Jongwon Jung¹, Sanghyeon Lee^{1,2}, Cheolsoo Jung^{1*}

¹Department of chemical engineering, University of Seoul, ²Skychem Co.

¹163 Seoulsirip-daero, Dongdaemun-gu, Seoul 02504, Korea

²215 Galmachi-ro, Jungwon-gu, Seongnam-si, Gyeonggi-do 13217, Korea

csjung@uos.ac.kr*

Supercapacitors, also called electrochemical double layer capacitors (EDLCs), have lower energy density than lithium ion batteries (LIBs), but are characterized by their high power density and outstanding cycle life. Acetonitrile (AN) based liquid electrolytes are mostly used in supercapacitors, which can pull off high ionic conductivity than propylene carbonate (PC) or sulfolane (SL) based electrolytes [1-2]. Nevertheless, the AN based liquid electrolytes have a few drawbacks, such as unstable operation at high temperature, due to its low boiling point, and deteriorated electrochemical performances at 2.5 ~ 2.7 voltage range, due to reactions of a little trace of water in AN and functional groups in electrode surfaces [3-5].

Our group developed a novel AN based gel polymer electrolyte (GPE), which can be stable even at 80 °C and 3.0 V, while maintaining advantage of high conductivity of AN based electrolytes, and the application technology into activated carbon (AC) supercapacitors. This GPE can well suppress the vaporization of the AN, which was found in thermogravimetric analysis (TGA), and improve the electrochemical stability and performances of the AN based electrolyte on AC surfaces. Analyzing electrochemical impedance spectroscopy (EIS) of the GPE cells, interfacial resistances, such as R_{ct} and R_f were found to extremely decrease after long cycle tests at 3.0 V, 80 °C, compared to the AN based liquid electrolyte cell. Although, mass gas evolution of the AN based liquid electrolyte was observed during 3.0 V, 80 °C cycle tests, the novel GPE showed well suppressed amount of gas evolution, in other words the highly stable electrochemical stability.

Acknowledgement: This research was supported by X-mind Corps program of National Research Foundation of Korea (NRF) funded by the Ministry of science, ICT (NRF-2017H1D8A1030582)

[1] P. Liu, M. Verbrugge, S. Soukiazian, Journal of Power Sources, 156, **2006**, 712-718

[2] V. Chaudoy, F. Tran Van, M. Deschamps, F. Ghanmouss, Journal of Power Sources, 342, **2017**, 872-878

[3] P. Azaïs, L. Duclaux, P. Florian, D. Massiot, M. Lillo-Rodenas, A. Linares-Solano, J. Peres, C. Jehoulet, F. Béguin, Journal of Power Sources, 171, **2007**, 1045-1053

[4] P. Kurzweil, M. Chwistek, Journal of Power Sources, 176, **2008**, 555-567

[5] Y. Lee, J. Chung, C. Jung, Electrochimica Acta, 253, **2017**, 59-67

Measurement of Deuterium Isotope Separation Factor By Combined Electrolysis Fuel Cell

Risako Tanii, Ryota Ogawa, Hisayoshi Matsushima, and Mikito Ueda
Faculty of Engineering, Hokkaido University,
Kita-13, Nishi-8, Kita-ku, Sapporo, Hokkaido 060-8628, Japan
r_tanii@eis.hokudai.ac.jp

1. Introduction

The heavy hydrogen isotopes, deuterium (D) and tritium (T) are important materials in the field of nuclear energy. Particularly in recent years, development of new effective separation method is required because of tritium water accumulated in Fukushima Daiichi Nuclear Power Station. The most general separation method is combined electrolysis and catalytic exchange (CECE). In this system, water electrolysis has disadvantage of consuming enormous electricity. To solve this point, we have investigated the novel hydrogen isotope separation system: Combined Electrolysis Fuel Cell (CEFC) [1]. In this system, hydrogen and oxygen produced by electrolysis are reused for power generation in fuel cell. The electric energy can be saved and further isotope separation in fuel cell can be expected. We reported that both Polymer Electrolyte Membrane Fuel Cell (PEMFC) and Alkaline Membrane Fuel Cell (AMFC) could enrich deuterium in the produced water when the mixture gases of H₂ and D₂ were supplied [2][3]. In this study, we investigate the total separation factor and energy consumption of CEFC system.

2. Experimental

Water electrolysis was carried out in small scale electrolyzer (Y5390, Pelmelec Electrode Ltd., Japan). Pure Ni electrodes were used as anode and cathode. Both electrodes were mesh shape and the apparent surface area was 35 cm². They sandwiched a thin porous membrane filter to separate anolyte and catholyte. Potassium hydroxide (1 M KOH) was used as electrolyte. Deuterium concentration of 10 at.% was adjusted by heavy water (99.9% D₂O, Sigma-Aldrich, Japan).

JARI standard cell (FC Development Corp., Japan) was used as PEMFC. The membrane electrode assembly (50×50 mm) was composed of a Nafion electrolyte (NRE-212) and two catalytic layers loaded with platinum catalyst (Pt 0.50 mg cm⁻²). The hydrogen gas was supplied from electrolyzer directly. The pure oxygen was supplied from gas bottle as cathode gas.

3. Results

It is expected that a synergy separation effect can be obtained by using multiple fuel cells which is set to an appropriate fuel utilization. Here several fuel cells are used. Table 1 shows the total separation factor and energy consumption at each PEMFC number. The total power currents of fuel cells were set at 1.9 A. Thus, the amount of consumed hydrogen gas is the same in any PEMFC number. In the table, the number of fuel cell 0 means the result of electrolysis only. Apparently the separation factor increased with the number of fuel cells. The separation factor of 78.3 was marked in CEFC, which was corresponding to 10 times larger than the result of water electrolysis. Regarding to the total energy consumption, it could be reduced by about 22%. The present study confirmed that the high separation factor and efficient energy consumption could be achieved by the introduction of PEMFC.

Table 1 Total separation factor and energy consumption at each PEMFC number.

Number of fuel cells	0	1	2	3
Power current of each fuel cells	-	1.8 A	0.9 A	0.6 A
Total amount of the power currents	-	1.8 A	1.8 A	1.8 A
Separation factor	6.9	29.4	54.1	78.3
Energy consumption	5.9 W	4.8 W	4.7 W	4.6 W

References

- [1] H. Matsushima, T. Nohira, T. Kitabata, Y. Ito, *Energy*, **30** (2005) 2413.
- [2] S. Shibuya, H. Matsushima, M. Ueda, *J. Electrochem. Soc.*, **163** (2016) F704.
- [3] R. Ogawa, H. Matsushima, M. Ueda, *Electrochem. Commun.*, **70** (2016) 5.

Pulse Current Electrodeposition of Ultrahigh Strength Nanocrystalline Au–Cu Alloys

Haochun Tang^(a,b), Chun-Yi Chen^(a,b), Tso-Fu Mark Chang^(a,b), Daisuke Yamane^(a,b), Toshifumi Konishi^(a,b,c), Katsuyuki Machida^(a,b), Kazuya Masu^(a,b), Masato Sone^(a,b)

^(a) Institute of Innovative Research, Tokyo Institute of Technology, Japan

^(b) CREST, Japan Science of Technology Agency, Japan

^(c) NTT Advanced Technology Corporation, Japan

tang.h.ab@m.titech.ac.jp

Electroplating of Au-based electronic components applied in micro-electrical-mechanical system (MEMS) devices has been developed to replace the conventional Si-based components for further improving the performance and miniaturization of the devices [1]. However, the mechanical strength of Au is relatively low when compared with other metallic materials. Although the grain refinement in pure Au is effectively on the strengthening [2], further improvement is still necessary for applying in practical MEMS devices. To overcome these predicaments, forming the Au-based alloys is expected to further enhance the strength according to the solid solution hardening mechanism [3]. In this work, we focused on the Au–Cu alloys and investigated the mechanical properties by pillar micro-compression tests.

Au–Cu films were electroplated from the sulfite-based electrolyte with the pH value of 7.5. The pulse parameters including pulse current density (J_p), pulse on-time (t_{on}), and pulse off-time (t_{off}) were varied. The crystalline structure and chemical composition were characterized by X-ray diffraction and energy-dispersive X-ray spectroscopy, respectively. The Au–Cu micro-pillars were fabricated by focus ion beam with the dimension of $10 \times 10 \times 20 \mu\text{m}^3$. The mechanical properties were evaluated using a test machine equipped with a flat-ended diamond indenter [4].

A wide copper concentration (w_{Cu}) in the Au–Cu alloys ranging from 3.5 to 26.7 wt% was obtained. An increase in the w_{Cu} was observed by using either or both of a high pulsed current density and a short current off-time. The smallest d_g of ca. 4.40 nm was achieved in films having the w_{Cu} ranged from 13 to 16 wt%. Grain refinement was achieved with a high J_p , and promoting the displacement reaction could also reduce the d_g . A high J_p would cause roughening of the surface, and enhancing the displacement reaction lead to a surface smoothing effect. Deformation behavior of the Au–Cu micro-pillar was affected by the w_{Cu} , which brittle fraction was observed when the w_{Cu} was higher than 20 wt%. An ultrahigh yield strength at 1.38 GPa was obtained in the micro-pillar having the w_{Cu} of 14.2 wt% and the grain size of 4.68 nm, which is a result of synergistic effects of the grain boundary strengthening and solid solution strengthening mechanisms. The present study demonstrated the simplicity (by the pulse current electrodeposition) and the versatility in controlling properties of the Au–Cu alloys for applications in design and fabrication of micro-components in micro-electronic devices.

References

- [1] D. Yamane, T. Konishi, T. Matsushima, K. Machida, H. Toshiyoshi, K. Masu, *Appl. Phys. Lett.*, **104** (2014) 074102.
- [2] H. Tang, C.-Y. Chen, T. Nagoshi, T.-F.M. Chang, D. Yamane, K. Machida, K. Masu, M. Sone, *Electrochem. Commun.*, **72** (2016) 123–130.
- [3] R. Labusch, *Phys. Stat. Sol.*, **41** (1970) 659–669.
- [4] T. Nagoshi, T.-F.M Chang, T. Sato, M. Sone, *Microelectron. Eng.*, **110** (2013) 270–273.

Designing binary Ru-Sn oxides with optimized performances for the air electrode of rechargeable zinc-air batteries

Ting-Hsuan You, Chi-Chang Hu*

Department of Chemical Engineering, National Tsing-Hua University

101, Section 2, Kuang-Fu Road, Hsin-Chu 30013, Taiwan

*Email: cchu@che.nthu.edu.tw

Due to the sluggish kinetics of the oxygen evolution reaction (OER) and oxygen reduction reaction (ORR), binary ruthenium-tin oxides synthesized by a hydrothermal method with post annealing at 450°C for 2 h as a bifunctional catalyst for these two reactions on the air electrode of rechargeable zinc-air batteries. Ru-Sn oxide nanoparticles have been characterized by X-ray diffraction, transmission electron microscopic images, and N₂ adsorption-desorption isotherms analysis. From the TEM images, the particle size of Ru-Sn oxide nanoparticles is less than 10 nm. The binary Ru-Sn oxides in various compositions show the typical oxide solid solution in the rutile phase. Among all binary Ru-Sn oxides, RuSn73 (70 at.% RuO₂ and 30 at.% SnO₂) and RuSn37 (30 at.% RuO₂ and 70 at.% SnO₂) show the highest catalytic activities towards the OER and ORR, respectively. The electro-catalytic activities were conducted by linear sweep voltammetry using a rotating ring-disk electrode. Consequently, a novel design of the air electrode consisting of a RuSn37 coating on the carbon paper and a RuSn73-coated Ti mesh (denoted as RuSn(37-C|73-Ti)) is proposed to possess the optimal charge-discharge performances. A unique cell employing such an air electrode has been demonstrated to exhibit a very low charge-discharge cell voltage gap of 0.75 V at 10 mA cm⁻². This cell with a peak power density of 120 mW cm⁻² at the current density of 235 mA cm⁻² also shows an outstanding charge-discharge stability over 80 h.

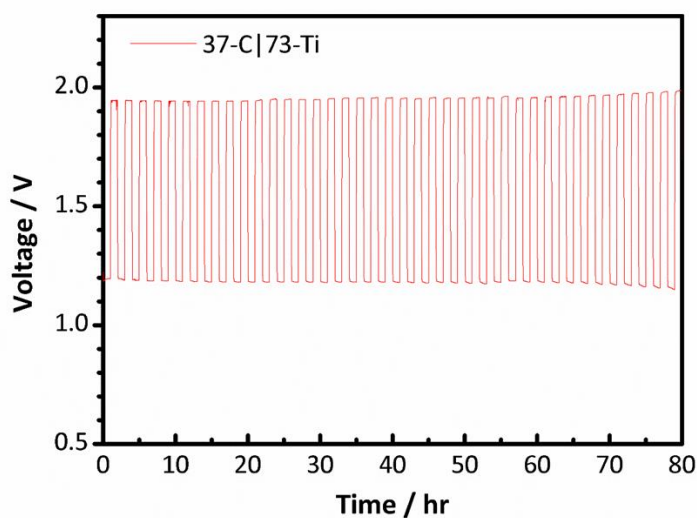


Figure 1. The discharge/charge profile in galvanostatic (10 mA cm⁻², 2 hour per cycle) mode for a Zn-air battery using the RuSn(37-C|73-Ti) air electrode in 6 M KOH and 0.2 M Zn(CH₃COO)₂ in ambient air.

Solid Polymer Electrolyte for Flexible Secondary Zinc–Air Batteries

Pemika Teabnamang, Soraya Hosseini, Soorathep Kheawhom
Department of Chemical Engineering, Faculty of Engineering, Chulalongkorn University
254 Phayathai Rd. Patumwan Bangkok 10330 Thailand
Soorathep.k@chula.ac.th

Recently, various types of flexible batteries have been successfully demonstrated. Among these, zinc-air batteries have attracted tremendous attention because of their high energy density, low-cost and safety. Besides, the batteries use zinc anode which is rather safe and non-toxic. Also, solid polymer electrolytes (SPEs) have been developed and implemented. These SPEs facilitate physical flexibility of the batteries whilst prevent the issue of electrolyte leakage.

The aim of this work focuses on the development of SPE for secondary zinc-air batteries. The use of Carbopol® 940, a synthetic poly(acrylic acid) derivative carbomer known to have excellent ionic conductivity, is examined. Nevertheless, Carbopol® 940 exhibits poor mechanical characteristics and low film-forming properties, so that its incorporation into a matrix of a film-forming agent such as poly(vinyl acetate) (PVAc) is necessary. Herein, different ratios of Carbopol® 940 to PVAc were systematically investigated and discussed. Also, this work examined zinc deposition and stripping as well as the effects of PVAc/Carbopol® 940 on charge-discharge characteristics of a flexible zinc-air battery. Carbopol® 940/PVAc exhibited a promising electrochemical performance and stability. A higher ratio of Carbopol® 940 enhanced the ionic conductivity and leading to better battery performance. Also, it permitted a quasi-reversible zinc deposition/stripping. Besides, we demonstrated that the formation of zinc dendrite was significantly diminished. PVAc/Carbopol® 940 plays a significant role in controlling zinc ions transport. Thus, zinc deposition rate is diffusion controlled.

Functionalized Conducting Polymer Electrodes for Cardiac Troponin I Aptasensor Fabrication

Jou-Hsuan Chu and Lin-Chi Chen*

Department of Bio-industrial Mechatronics Engineering, National Taiwan University

No. 1, Sec. 4, Roosevelt Rd., Taipei 10617, Taiwan (R.O.C.)

*Email: chenlinchi@ntu.edu.tw

Human cardiac troponin I (hcTnI) is a clinical biomarker for rapid *in vitro* diagnosis of acute myocardial infarction (AMI) as well as an important monitoring index for the patients after heart-related surgery. Thus, more and more electrochemical troponin biosensors have been developed recently. However, there are several challenges encountered, such as the need of an additional redox reporter reagent and chemical instability of antibodies. To tackle the challenges, we aim to develop an electrochemical troponin sensor based on a conducting polymer electrode to eliminate the need of an extra redox reporter and using a stable DNA aptamer to replace an antibody for hcTnI recognition. In this work, we investigated *in situ* carboxylation of polyaniline (PANI) and polypyrrole (PPy) through co-electrodeposition of a polymer or a carbon nanomaterial carrying $-\text{COOH}$ group, e.g., poly(acrylic acid) (PAA), carboxylated carbon nanotube (COOH-CNT), and carboxylated graphene (COOH-Gr). From FTIR spectra (Fig. 1(a)), it was found that both PANI and PPy electrodes were successfully *in situ* functionalized with $-\text{COOH}$ groups through co-electrodeposition of PAA, COOH-CNT or COOH-Gr, with which a FTIR $\text{C}=\text{O}$ stretching peak at 1700 cm^{-1} was observed as the evidence. From contact angle measurements (Fig. 1(b)), we observed that carboxylation with PAA would result in a hydrophilic polymer surface, while carboxylation with CNT or Gr tended to increase surface hydrophobicity. In addition, while PAA was non-electroactive and played an inert effect on the redox behaviors of PANI and PPy, it was discovered that CNT contributed a larger pseudo-capacitance as compared to Gr (Fig. 1(c)). The above effects on the aptamer sensing is under investigation, and the functionalized PANI and PPy electrodes are ready for surface covalent grafting with amino-modified anti-hcTnI aptamers (Fig. 1(d)) for troponin sensing.

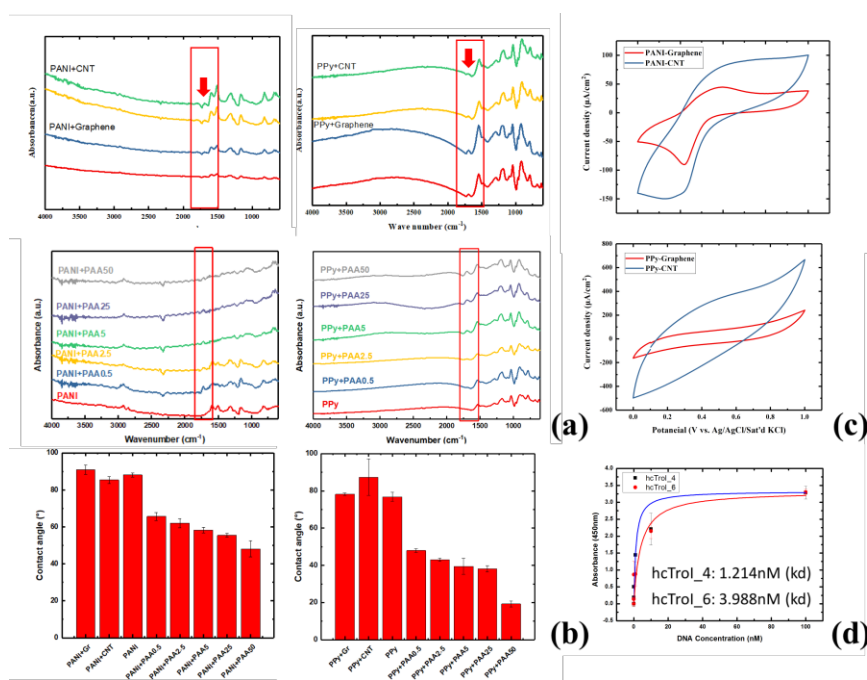


Figure 1. (a) Comparison of the FTIR spectra of the PANI and PPy electrodes *in situ* functionalized with carboxylated CNT, graphene, and PAA. (b) Comparison of the contact angles of the functionalized PANI and PPy electrodes. (c) CVs of PANI and PPy functionalized with carboxylated graphene and CNT measured in a neutral buffer saline. (d) ELONA assays of anti-troponin I aptamers.

Silver nanowire based flexible electrodes with improved optical properties

Chang Su Kim

*Advanced Functional Thin Films Department, Korea Institute of Materials Science (KIMS), Changwon,
Gyeongnam 51508, South Korea
cskim1025@kims.re.kr*

Transparent electrodes have been widely used in electronic devices such as solar cells, displays, and touch screens. Transparent electrodes are especially desired for the development of next generation flexible electronic devices. Currently indium tin oxide (ITO) is the most commonly used material for the fabrication of transparent electrodes, its brittleness and growing cost limit its utility for flexible electronic devices. Therefore, the need for new transparent conductive materials with superior mechanical properties is clear and urgent. Ag nanowire (AgNW) has been attracting much attention because of its effective combination of electrical and optical properties.

However, it still suffers from several drawbacks including low transmittance due to the plasmonic resonance. Also AgNW film typically has a yellowish appearance corresponding to B^* value of 1.0~1.5 in the sheet resistance of 50~150 ohm/sq. To overcome this problem, we treated a solution of hydrazine with a suitable refractive index on the AgNW electrode. It has been derived a higher transmittance and lower yellowish index.

In this study, AgNW electrode with the improved transparence and lower yellowish index by hydrazine treatment is expected to be applied to the next generation of electronic devices such as solar cells and the OLED.

Effect of nanoporous structure and Ir modification on electrocatalytic oxygen evolution reaction

Yumi Wang, Jongwon Kim*

Department of Chemistry, Chungbuk National University

*Department of Chemistry, Chungbuk National University, 1, Chungdae-ro, Cheongju, Chungbuk, Korea
dball1414@naver.com*

Oxygen evolution reaction (OER) is used in electrochemical devices that store the energy of electricity or light as chemical energy. At this time, there is a problem that OER requires high overpotential because the reaction is more sluggish than hydrogen evolution reaction (HER). Therefore, researching on OER has been investigated to reduce its overpotential. In this study, NPG with uniform and very large surface area was used. The NPG is applied to a lot of research because the structure is electrochemically stable and show a high catalytic activity in a variety of reactions. However, no significant OER activity was observed with NPG itself. In this study, Pt was modified on NPG through atomic layer electrodeposition (Pt ALD) to form a porous Pt structure, and then OER activity was observed. Also, it was observed that Ir, which is known as a metal with excellent electrochemical catalytic activity, was spontaneously replaced with Au and Pt. As a result, a porous Ir structure was prepared, and the OER activity of the porous Ir substrate was observed. A total of four types of NPG, NPG @ Pt, NPG @ Ir and NPG @ Pt / Ir substrates were fabricated and the OER activity was compared using these electrodes.

References

1. *Langmuir* **2014**, *30*, 4844-4851.
2. *ChemCatChem* **2014**, *6*, 2219-2223.

Effects of Current Density on Mechanical Properties of Electroplated Nickel with High Speed Sulfamate Bath

Takahiro Yamamoto^{1,2,*}, Chun-Yi Chen^{1,2}, Tso-Fu Mark Chang^{1,2}, Daisuke Yamane^{1,2}, Toshifumi Konishi^{1,2,3}, Katsuyuki Machida^{1,2}, Kazuya Masu^{1,2}, Masato Sone^{1,2}

¹*Institute of Innovative Research, Tokyo Institute of Technology
4259-R2-35 Nagatsuta-cho Midori-ku Yokohama 226-8503 Japan*

²*CREST, Japan Science and Technology Agency,
4259-R2-35 Nagatsuta-cho, Midori-ku, Yokohama 226-8503, Japan*

³*NTT Advanced Technology Corporation, Kanagawa, 243-0124, Japan
yamamoto.t.bn@m.titech.ac.jp*

Electroplating is a key technology in fabrication of components in electronic devices. Properties of the electroplated materials can be easily manipulated through control of the electroplating parameters. Among nickel electroplating baths, the sulfamate bath has the advantage of high growth rate, low internal stress, high current efficiency, and etc. Hence, nickel sulfate baths are often applied in decoration of complicate surfaces and fabrication of 3D materials with precise control on the dimensions.

Reliability of the electronic components is highly dependent on the mechanical property, and mechanical properties of a metallic material is related to its average grain size according to the Hall-Petch relationship, where the strength is inversely proportional to square root of the average grain size. On the other hand, in electroplating of metallic materials, the average grain size can be controlled by the applied current density. Therefore, the effect of current density on average grain size and Vickers hardness of nickel films electroplated with sulfamate bath was evaluated in this study. For applications of the electroplated nickel as micro-components in miniaturized electronic devices, mechanical properties of micro-specimens composed of the electroplated nickel were also evaluated.

Nickel films with a thickness at about 50 μm were electroplated on Cu substrates. The electrolyte was a commercially available nickel sulfamate bath (NS-160) provided by Showa Chemical Co., Ltd., and the composition was 600 g/L $\text{Ni}(\text{SO}_4\text{NH}_2)_2 \cdot 6\text{H}_2\text{O}$, 10 g/L $\text{NiCl}_2 \cdot 6\text{H}_2\text{O}$, and 40 g/L H_3BO_3 . The bath temperature was 60 $^\circ\text{C}$. The applied current density was ranged from 10–50 mA/cm^2 . The counter electrode was a platinum plate. The electroplating was conducted under stirring at 250 rpm using a cross shape magnetic stirrer. The crystalline structure was characterized by X-ray diffraction (XRD), and the average grain size was calculated using the XRD results and the Scherrer equation. The mechanical properties were evaluated using Vickers hardness measurement. The loading was 0.025 kg. Micro-pillars having dimensions of $10 \times 10 \times 20 \mu\text{m}^3$ were fabricated from the nickel films by focus ion beam for evaluation of the micro-mechanical properties.

As shown in Fig.1, the average grain size reduced from 21.5 to 14.0 nm when the current density increased from 10 to 20 mA/cm^2 . The grain size is highly dependent on the cathodic overpotential. Based on the Butler-Volmer equation, the cathodic overpotential increases as the current density increases. Therefore, it is expected to see a reduction in the grain size as the current density increases. On the other hand, an increase in the grain size was observed as the current density increased beyond 20 mA/cm^2 . Increasing the current density also promotes the side reaction(s), such as hydrogen evolution. Cathodic overpotential of the main reaction would be lowered when the side reaction is promoted. Fig. 2 shows relationship between the average grain size and the Vickers hardness. The maximum Vickers hardness obtained was 371 HV, which was the film with the finest average grain size. The nickel film showed an ultra-high yield stress at 2.6 GPa from micro-compression test of the micro-pillar. The hardness and the

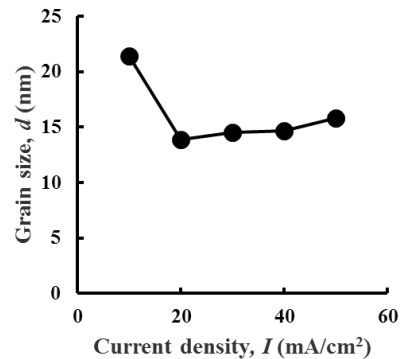


Fig. 1 Effect of the current density on the grain size

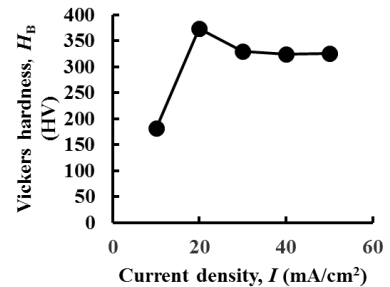


Fig. 2 Effect of the current density on the Vickers hardness

yield stress were all higher than conventional nickel mostly because of the Hall-Petch relationship.

Application of Holographic Interferometric Microscope for Cu^{2+} Concentration Profile during Cu Electrodeposition in Magnetic Field

Hisayoshi Matsushima¹, Takaki Saitoh¹, Kei Nishikawa², Mikito Ueda¹

¹Faculty of Engineering, Hokkaido University,
Kita 13 Nishi 8, Sapporo, Hokkaido 060-8628, Japan.
matsushima@eng.hokudai.ac.jp

²National Institute for Materials Science,
1-1 Namiki, Tsukuba, Ibaraki 3050044, Japan.

In late years the highly precise control of the plating film is demanded. This is very important technique for ultra-microstructure production and high-speed process. One of major factors causing the film roughness is the inhomogeneity of the diffusion layer of the metal ions near the electrode [1]. Especially when the ion consumption rate during the electrodeposition exceeds the supply one by the mass transportation by the diffusion and convection, the ion concentration on the cathode surface is close to zero where dendrite growth is induced.

As one of the solutions, we have investigated the stirring effect by using the magnetic field [2]. When the electrodeposition is conducted in a magnetic field, Lorentz force can act on the motion of the ions so that a magnetic convection (MHD convection) is generated. Since the MHD convection stirs an electrolyte unlikely to a normal forced convection, it is expected that a uniform plating film should be provided. In this study, Cu is electrodeposited in a magnetic field and the concentration profile of Cu^{2+} ion near the cathode is in-situ observed by holographic laser interference microscope.

The working and counter electrodes were thin Cu film with 50 μm thickness. The side areas were used as the electrodes. They were polished by emery paper and then washed in acid solution. The electrolyte was 0.3 M CuSO_4 solution. The Cu was electrodeposited at the constant current density of 10 mA cm^{-2} at room temperature. The magnetic field was generated by the permanent magnet (NEOMAX). The magnetic intensity was 0.3 T and applied perpendicular to the working surface. The Cu^{2+} ion profile was observed by holographic laser interference microscope (Lyncee Tec, DHM- T1000).

Figure 1 shows phase distribution interferometry near cathode surface after 40 s Cu electroplating in a magnetic field. The phase variation is explained by the change of the optical pass length which depends on Cu^{2+} concentration. It was found that Cu^{2+} concentration clearly decreased during the electrodeposition. At 40 s after starting the electrodeposition, the diffusion layer of 400 μm thickness was formed towards the left (cathode) from the right (bulk) side. Figure 2 shows transient behavior of Cu^{2+} concentration with (red symbol) and without a magnetic field (white symbol). The Cu^{2+} concentration on cathode surface became zero after 60 s and the dendrite formation was observed when the magnetic field was not superimposed. In the magnetic field, mass transfer of Cu^{2+} was promoted by MHD convection. The surface concentration reached the steady state value of about 0.05 mol L^{-1} . The surface morphology of the film was more uniform than in no magnetic field.

REFERENCES

- [1] K. Nishikawa, Y. Fukunaka, E. Chassaing, M. Rosso, *Electrochim. Acta*, **100** (2013) 342.
[2] H. Takahashi, H. Matsushima, M. Ueda, *J. Electrochem. Soc.*, **164** (2017) H5165.

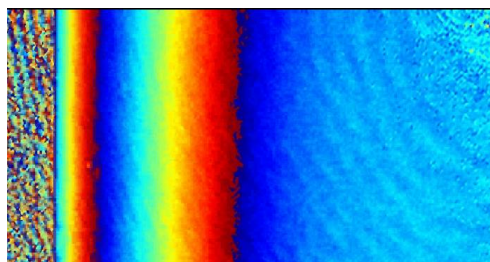


Fig.1 Phase profile of interferometry in vicinity of cathode surface after 40 s electrodeposition in a magnetic field.

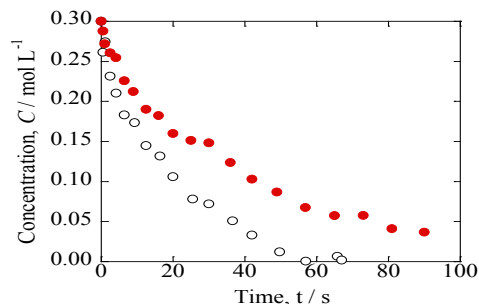


Fig. 2 Time dependency of Cu^{2+} surface concentration with (red symbol) and without a magnetic field (white symbol).

Controllable Construction of Core-Shell Polymer@Zeolitic Imidazolate Frameworks Fiber Derived Heteroatom-doped Carbon Nanofiber Network for Efficient Oxygen Electrocatalysis

Yingxuan Zhao,^a Qingxue Lai,^a Junjie Zhu,^a Jia Zhong,^a Zeming Tang,^a Yan Luo,^a Yanyu Liang,^{*a, b}
^(^aJiangsu Key Laboratory of Materials and Technology for Energy Conversion, College of Materials Science and Technology, Nanjing University of Aeronautics and Astronautics, Nanjing 211106, E-mail: lianggy403@126.com; ^bJiangsu Collaborative Innovation Center for Advanced Inorganic Function Composites, Nanjing 210009)

Rechargeable metal-air battery with the features of high energy density and flat discharge voltage has been chosen as one of the most promising energy conversion and storage devices. The major bottleneck of this technology is the sluggish kinetics of oxygen reduction reaction (ORR) and oxygen evolution reaction (OER). Recently, heteroatom-doped carbon nanomaterials derived from metal-organic frameworks (MOFs) have been chosen as inexpensive and efficient non-noble metal bifunctional catalysts for ORR/OER since their tunable structures at molecular level and highly porous characteristics. However, direct carbonization of dissociative MOFs cannot form consecutive electric conductive networks and make the most of active sites, which hinder the actual catalytic performances of MOFs-based carbon materials in ORR/OER. Rationally designing the structure of MOFs as precursor to achieve a high-performance bifunctional catalyst is highly desirable but challenging.

In this work, we developed an in-situ growth method to achieve one dimensional structure-controllable zeolitic imidazolate frameworks (ZIFs)/polyacrylonitrile (PAN) core/shell fiber (PAN@ZIFs). Subsequent pyrolysis of this precursor can obtain heteroatom-doped carbon nanofiber networks as an efficient bifunctional oxygen electrocatalyst. The electrocatalytic performance of derived carbon nanofiber was dominated by the structures of PAN@ZIFs fiber, which was facily regulated by efficiently controlling the nucleation and growth process of ZIFs on the surface of polymer fiber as well as optimizing the components of ZIFs. Benefit from the synergistic effect of distinctive core-shell structures, in terms of fast electron/ions transport and abundant multi-active sites, the as-prepared catalysts shown brilliant bifunctional ORR/OER catalytic activity ($\Delta E = 0.88$ V) and durability. Finally, the rechargeable Zn-air battery assembled from the optimized catalyst displayed a peak power density of 140.1 mW cm^{-2} , energy density of $878.9 \text{ Wh kg}_{\text{Zn}}^{-1}$ and excellent cyclic stability over 150 h.

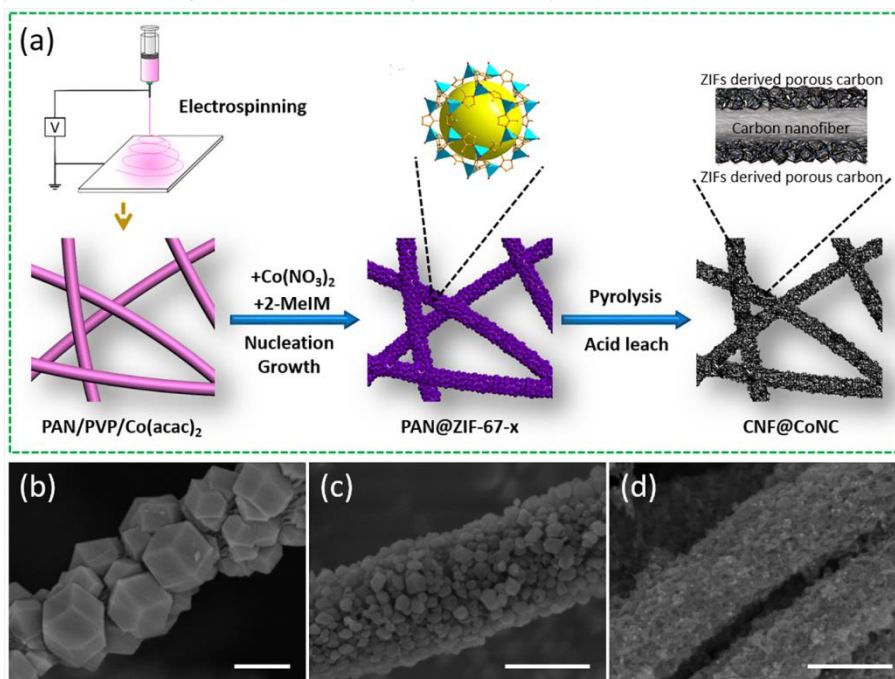


Figure.1 a) Schematic illustration of the synthesis of heteroatom-doped carbon nanofiber derived from core-shell PAN@ZIF-67 fiber; SEM image of b) large-sized PAN@ZIF-67 fiber, c) small-sized PAN@ZIF-67 fiber and d) CNF@CoNC-100. (scale bar: 500 nm)

This work was supported by the National Natural Science Foundation of China 21771107), Natural Science Foundation of Jiangsu Province (BK20161484), Fundamental Research Funds for the Central Universities (NE2015003),.

Reference:

- [1] G. Wu, A. Santandreu, et al. *Nano Energy*, 2016, 29: 83.
- [2] W. Xia, C. Qu et al. *Nano lett.*, 2017, 17(5): 2788.
- [3] J. Shui, C. Chen et al. *Proc. Natl. Acad. Sci.*, 2015, 112(34): 10629.

Graphene Electrodes Modification with an Elastic Structure by Partially Neutralized Acrylic Acid-Based Copolymer for Organic Supercapacitors

Tien-Yu Yi, Chi-Chang Hu*

*Department of Chemical Engineering, National Tsing Hua University
101, Section 2, Kuang-Fu Road, Hsin-Chu, 30013, Taiwan*

**Email address: ychu@che.nthu.edu.tw*

KOH neutralized acrylic acid-based copolymer is examined as a binder for graphene negative electrode for supercapacitors in organic phase, and acrylic acid is copolymerized with polyurethane(PUPAA). Capacitor using carbon electrodes stores electrical energy by separation of charges in double layers at the interface between the surface of electrode and electrolyte, called electric double-layer capacitors(EDLC). It is found that supporting electrolyte would intercalate into the space between graphene layers on high potential that may improve the performance of energy storage of capacitor depending on the structure of carbon materials, called electrochemical activation[1]. Polyvinylidene fluoride (PVdF) is a binder commonly used in electrode preparation; however, electrode with PVdF would declines during test with a few cycles because its elasticity is too weak to bear the expansion by activation. The comparison between PVdF and sodium-neutralized poly(acrylic acid) ($\text{PAH}_x\text{Na}_{1-x}$) as binder in Li-ion batteries has been studied[2], and it is reported that $\text{PAH}_x\text{Na}_{1-x}$ will help electrodes to endure the volume expansion. To investigate the performance improvement of graphene electrodes, PVdF, $\text{PAH}_x\text{Na}_{1-x}$ were compared together. Further, we copolymerized PAA with PU and neutralized it with KOH, to examine if there was an improvement between $\text{PAH}_x\text{Na}_{1-x}$ and $\text{PUPAH}_x\text{K}_{1-x}$. It is found that $\text{PAH}_x\text{Na}_{1-x}$ and $\text{PUPAH}_x\text{K}_{1-x}$ were more uniformly coated on the surface of graphene materials than PVdF. Therefore, an improved capacitance, approximately 70F/g was obtained, with $\text{PUPAH}_x\text{K}_{1-x}$ serving as a binder for graphene negative electrodes.

- [1] H. K. Bok and S. M. Oh, *Journal of The Electrochemical Society*, vol. 155, no. 9, pp. A685-A692, 2008.
- [2] Z.-J. Han, N. Yabuuchi, K. Shimomura, M. Murase, H. Yui, and S. Komaba, *Energy & Environmental Science*, vol. 5, no. 10, pp. 9014-9020, 2012.

Voltammetric Study and Electrodeposition of Copper with Electrocatalytic Activity to Nitrate Reduction from a Hydrophobic Brønsted Acidic Amide-Type Ionic Liquid Using Copper Oxides as the Copper Source

Yi-An Shao, Po-Yu Chen*

Department of Medicinal and Applied Chemistry, Kaohsiung Medical University
No.100, Shih-Chuan 1st Road, Kaohsiung, 80708, Taiwan (R.O.C.)
pyc@kmu.edu.tw

Voltammetric behavior and electrodeposition of copper was studied in a hydrophobic Brønsted acidic ionic liquid (protonated betaine bis(trifluoromethyl)sulfonyl)amide; IL [Hbet][TFSI]/water mixture¹ under an ambient atmosphere at 40°C using cupric oxide (CuO) and cuprous oxide (Cu₂O) as the sources of copper. According to the voltammetric and spectroscopic studies, both copper sources produced the same Cu(II) species in the mixed electrolytes, indicating that the cuprous ion was oxidized by air to cupric ion. At glassy carbon electrode (GCE), two reductive waves coupled with a single oxidative stripping wave were observed regardless of CuO or Cu₂O used as the copper source. At stainless-steel electrode (SSE), however, a single redox couple was observed. The corresponding cyclic voltammograms (CVs) are shown in Figure 1. The reductive *c*₁ and *c*₂ waves resulted from the reduction of Cu(II) + e⁻ → Cu(I) and Cu(I) + e⁻ → Cu, respectively. The anodic wave *a* was due to a two electron oxidation of Cu → Cu(II) + 2e⁻. A disproportionation reaction of 2Cu(I) → Cu(II) + Cu was found at wave *c*₁. Highly pure copper with a preferable (111) facet could be obtained by potentiostatic electrodeposition from the mixed electrolyte, and their surface morphologies significantly depended on the applied potentials.

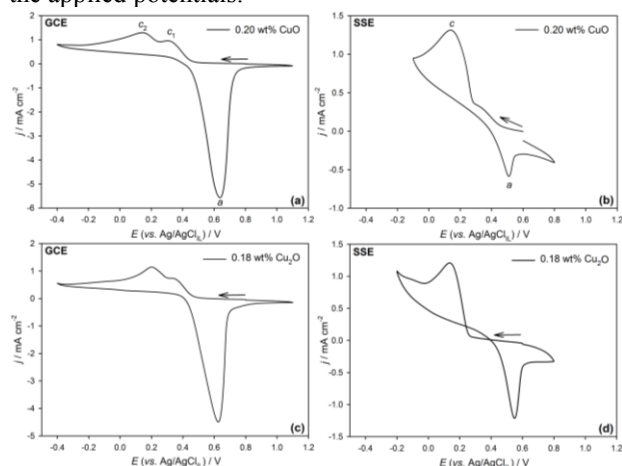


Fig. 1 CVs recorded at the indicated electrodes in [Hbet][TFSI]/H₂O mixture containing CuO or Cu₂O as indicated at 40°C. Scan rate: 50 mVs⁻¹.

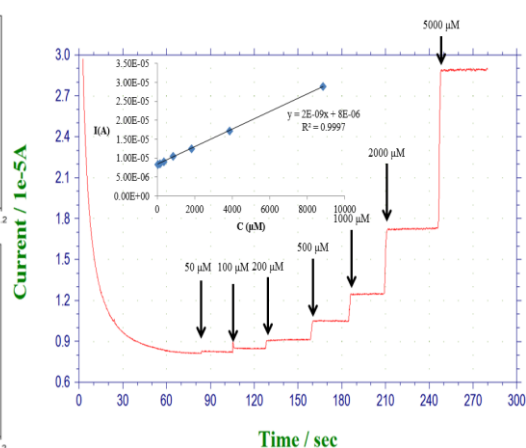


Fig. 2 HCA recorded on a Cu-deposited electrode at -0.65 V with successive injection of nitrate standard solution.

The electrodeposited copper electrodes showed electrochemical activities towards the reduction of nitrate anion (NO₃⁻), and the electrode performance is highly dependent on the surface morphologies of the Cu electrodeposits. The hydrodynamic chronoamperogram (HCA) recorded on a selected Cu-electrodeposited electrode at -0.65 V in pH 7.0 PBS with successive injection of nitrate solution is shown in Figure 2. The relevant calibration curve of nitrate is shown in the inset. Based on the experimental results, the Cu-electrodeposited electrodes probably exhibit the potential to be a nitrate sensor.

Reference:

1. Yi-Han Chen, Hsing-Wen Yeh, Nai-Chang Lo, Chen-Wei Chiu, I-Wen Sun, Po-Yu Chen, *Electrochimica Acta*, 2017, **227**, 185-193.

Dependence of surface adsorption status on electrode potentials for electrocatalytic reduction of CO₂ on Pd nanoparticles

Ren Hau Guo, Chi-Chang Hu*
Department of Chemical Engineering National Tsing-Hua University
101, Section 2, Kuang-Fu Road, Hsin-Chu 30013, Taiwan
cchu@che.nthu.edu.tw

Electrochemical reduction of CO₂ in aqueous media is one of the most effective methods for reusing of greenhouse gas CO₂ in the atmosphere. This technology can generate valuable chemicals from water and unwanted CO₂ which serve as the hydrogen and carbon sources, respectively. Also, the reaction rate and product selectivity of CO₂ reduction can be controlled and optimized with proper materials and structure of catalyst. Therefore, understanding the mechanism of CO₂ reduction on electrocatalysts is important and desirable in designing effective catalysts with high product rate selectivity.

Although the effects of the CO* binding energy and pH on the electrochemical behavior of CO₂ reduction have been discussed, the dependence of surface adsorption status on catalysts and applied potential are unclear. This study focuses on the adsorption/absorption responses of hydrogen and intermediate, such as COOH* or CO*, on palladium nanoparticles (NPs) via electrochemical reduction of CO₂, since palladium generally shows excellent H adsorption/absorption ability and good adsorption capability of CO. We have found that the departure of CO* is the key step for high faradaic efficiency and high current density of CO formation.

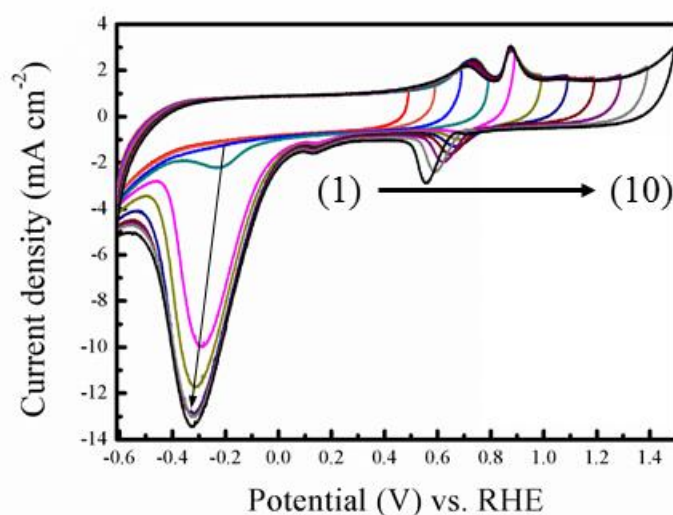


Figure 1. CV curves of a Pd/XC72-coated GDE measured in 0.5 M KHCO₃ under CO₂ atmosphere at 25 mV s⁻¹ (a) between -0.6 V and (1) 0.6, (2) 0.7, (3) 0.8, (4) 0.9, (5) 1.0, (6) 1.1, (7) 1.2, (8) 1.3, (9) 1.4, and (10) 1.5 V.

Keywords: Pd nanoparticles, carbon monoxide, CO₂ reduction

One-Pot Fabrication of Nanoporous Pd-Au via Electrochemical Alloying/Dealloying in Chlorozincate Ionic Liquid

Hau-Yu Chiu^a, Yi-Chen Liu^a, Yi-Ting Hsieh^b, Nai-Chang Lo^a, I-Wen Sun^{a*}
^a Department of Chemistry, National Cheng Kung University, Tainan 701, Taiwan
^b Department of Chemistry, Soochow University, Taipei, 11102, Taiwan
*iwsun@mail.ncku.edu.tw

Abstract

In this study, nanoporous Pd-Au was fabricated via electrochemical alloying/dealloying of commercial Pd/Au wire in Lewis acidic ZnCl₂-1-ethyl-3-methylimidazolium chloride (ZnCl₂-EMIC) ionic liquid^{1,2}. Dealloying process was done by utilizing two different electrochemical methods; constant potential electrolysis and multi-cycle voltammetry with varies of working temperature and show significant effect on porous structure of Pd-Au. Finer Pd-Au nanostructure can be obtained by using constant potential electrolysis, and a higher working temperature can result in a more apparent porous structure which shows an excellent performance for the electrooxidation of glucose in alkaline solution.

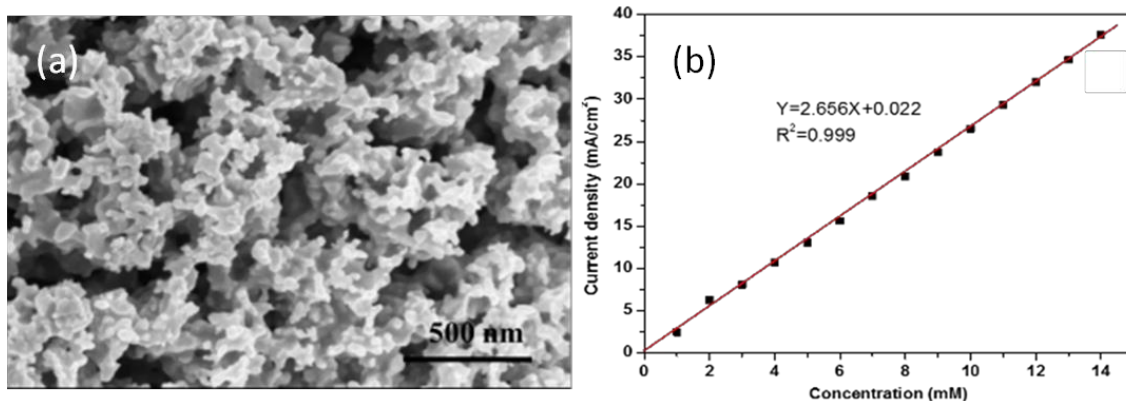


Fig. (a) SEM image of nanostructure Pd-Au samples that electrodeposited with 10 Ccm⁻² of Zn at -0.2 V and dealloyed at 1 V at 150°C. (b) Calibration curve of glucose by using the electrode shown in fig a. in 1 M NaOH.

Reference

- (1) Hsieh, Y.-T.; Sun, I. W. *Chem. Commun. (Cambridge, U. K.)* **2014**, 50, 246-248.
- (2) Hsieh, L.-Y.; Wang, P.-K.; Chang, C.-C.; Sun, I. W. *J. Electrochem. Soc.* **2017**, 164, D752-D757.

Electrochemical Reduction Reaction of Carbon Dioxide on the Exfoliated Single-Crystal Copper Membranes

Hiroki Saito, Naoki Yoshihara*, Masaru Noda
Department of Chemical Engineering, Fukuoka University
Fukuoka, 8-19-1 Nanakuma, Jonan-ku, Japan
nyoshihara@fukuoka-u.ac.jp

The electrochemical reduction reaction of carbon dioxide (CO₂) enables to produce hydrocarbons, which are widely utilized as fuels or industrial feedstock, at ambient pressure and room temperature. In addition, due to the improved power generation technology using renewable energy sources such as solar and wind, CO₂ electrochemical reduction reaction has attracted a great deal of interest as a novel technique to realize a sustainable carbon cycle [1-2]. Our previous work achieved that the single-crystal copper membranes epitaxially deposited on support substrates preferably converted CO₂ to hydrocarbons [3]. However, the fabrication of the large-area and free-standing single-crystal copper membranes with a well-defined atomic arrangement is much difficult. In this study, we succeeded to peeling the free-standing single-crystal copper membranes from support substrate, investigated CO₂ electrochemical reduction reaction on these copper membranes.

The fabrication of single-crystal copper membranes was demonstrated to sputter on c-plane sapphire (Al₂O₃) substrates. It is suggested that the copper atoms are epitaxially deposited on the crystal arrangement of the sapphire substrate because the atomic distance between oxygen atoms on the sapphire substrate and copper (111) atoms is mismatch. These copper membranes were easily peeled off the support substrates and enabled to the repeatable growth on the similar support substrate.

Table 1 showed the current efficiency for CO₂ electrochemical reduction reaction on the exfoliated single-crystal copper membranes. The current efficiency of hydrocarbon products, such as methane (CH₄) and ethylene (C₂H₄), indicated 36.1% and 12.3% at -20 mA/cm², respectively. However, the current efficiency of hydrocarbon products tended to decrease with increasing potential. These results suggested that the proton (H⁺) reduction on our copper membrane was promoted more than that of dissolved CO₂ in an electrolyte solution

Table 1. Current efficiency for CO₂ electrochemical reduction reaction on the exfoliated single-crystal copper membranes.

Current density [mA/cm ²]	Potential [V vs. RHE]	Current efficiency			Total [%]
		H ₂	[%] CH ₄	C ₂ H ₄	
-20	-1.41	51.4	36.1	12.3	99.8
-40	-1.92	59.5	35.1	1.9	96.5
-60	-2.35	65.7	32.0	1.2	98.9
-80	-2.74	74.6	25.9	1.0	101.5

References:

- [1] Y. Hori, I. Takahashi, O. Koga, and N. Hoshi, *Journal of Molecular Catalysis A: Chemical*, 199, 39–47 (2003).
- [2] K. J. P. Schouten, E. P. Gallent, and M. T. M. Koper, *ACS Catal.*, 3(6), 1292–1295 (2013).
- [3] N. Yoshihara, and M. Noda, *ECS trans.*, 75, 33-38 (2017).

Partial Exfoliation of Graphite and its Integration with Pseudocapacitive Materials for Supercapacitor

Yu Song, Cai Xiang, Xiaoxia Liu
Chemistry Department, Northeastern University
3-11 Wenhua Road, Shenyang, 110819, China
xxliu@mail.neu.edu.cn

Graphene has been received great attention as electrode materials for supercapacitor due to its high electrical conductivity, large surface area and perfect porosity effects. However, low capacitance of carbon-based materials limits their applications. In addition, pristine graphene is easy to restack. Incorporation of pseudocapacitive materials with graphene sheets is a good way to fabricate high performance supercapacitor electrodes. However, in the composites made by in situ deposition of conducting polymers or inorganic oxides in suspensions of graphene sheets, connections between graphene sheets might be blocked by aggregations of the pseudocapacitive materials, so its effect on improving electric conductivity for the composites may be weakened.

We will present a facile electrochemical method to prepare partially exfoliated graphite (FEG) with functionalized graphene sheets anchoring on the graphite substrates via a two-step partial exfoliation (Figure 1).

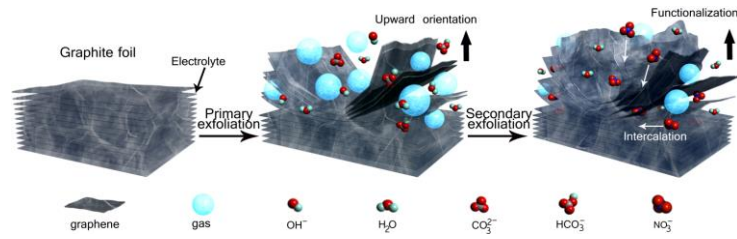


Figure 1 Scheme of two-step partial-exfoliation process.

Nanosheets of Ni-Co double hydroxide (Ni-Co DH) and MnO_2 , as well as thin films of polypyrrole (PPy) were electrochemically in situ grown on surfaces of graphene sheets in FEG.

The obtained composites of FEG/Ni-Co DH, FEG/ MnO_2 and FEG/PPy displayed excellent charge storage behaviors. The assembled asymmetric supercapacitors of FEG/PPy//FEG/ Ni-Co DH and FEG/PPy//FEG/ MnO_2 displayed high energy densities of 61.3 W h/kg at 0.65 kW/kg and 75 W h/kg at 1 kW/kg, respectively. Especially, the FEG/PPy//FEG/ MnO_2 supercapacitor demonstrated an exceptional stability with capacitive retention rate of 97% after 10,000 galvanostatic charge/discharge cycles.

Acknowledgments

We gratefully acknowledge financial supports from National Natural Science Foundation of China (project number: 21673035).

Optimization of Alkali ion-intercalated Manganese Oxide for Asymmetric Supercapacitors

Po-Yu Chen, Chi-Chang Hu*

Department of Chemical Engineering, National Tsing Hua University, Hsinchu, Taiwan

**E-mail address: cchu@che.nthu.edu.tw*

Abstract

This work investigates the preparation and characterization of alkali cation pre-intercalated manganese oxides for the asymmetric super-capacitor application. In the first part of this study, effects of the pH value in the precursor solution on the textural and electrochemical characteristics of Na-intercalated manganese oxides are investigated. The textural characteristics are examined by the X-ray diffractometer (XRD), scanning electron microscope (SEM), transmission electron microscope (TEM), X-ray photoelectron spectroscope (XPS), inductively coupled plasma-mass spectrometer (ICP-MS), Raman spectroscope (Raman), and N₂ adsorption/desorption isotherms for specific surface area and pore size distribution. The capacitive performances of these Na-intercalated manganese oxides were evaluated in sulfate electrolytes containing various cations (Li⁺, Na⁺, K⁺, Mg²⁺, Al³⁺, etc.) by cyclic voltammetry (CV) and chronopotentiometry (CP). From the textural and electrochemical results, the Na-intercalated manganese oxide synthesized at pH = 12.3 shows poor crystalline and hydrous properties, leading to an excellent capacitive performance (specific capacitance obtained at 1000 mV/s and 200 A/g are respectively equal to 194 and 203 F/g in 0.5 M Na₂SO₄).

Keywords : supercapacitor, cation-doped manganese oxides, cation intercalation/de- intercalation and aqueous electrolyte

Electrocatalytic Hydrogenation of Toluene in a PEM Reactor: Influence of Catalyst Materials on the Process

¹Atsushi Fukazawa, ¹Ken Takano, ¹Yoshimasa Matsumura, ²Kensaku Nagasawa, ²Shigenori Mitsushima, ¹Mahito Atobe

¹ Graduate School of Environment and Information Sciences, Yokohama National University
79-7, Tokiwadai, Hodogaya-ku, Yokohama 240-8501, Japan

² Graduate School of Engineering, Yokohama National University
79-5, Tokiwadai, Hodogaya-ku, Yokohama 240-8501, Japan
fukazawa-atsushi-cw@ynu.jp

Chemical conversion of toluene (TL) to methylcyclohexane (MCH) has been examined to develop a novel organic chemical hydride system. One of the most promising hydrogen storage techniques relies on the organic chemical hydride because of its safety and feasible handling. This chemical hydride system is consisted of reversible hydrogenation and dehydrogenation reactions. When the energy is required, the hydrogen is extracted from the organic chemical hydride by dehydrogenation. Because the candidates for the organic chemical hydride are liquid state under ordinary environment, their handling risk is regarded as almost same level with that of gasoline.

Methylcyclohexane is one of the promising organic chemical hydride due to its availability, melting point, and toxicity. Therefore, in our previous work, we chose methylcyclohexane as an organic hydride. To produce methylcyclohexane effectively, we investigated electrochemical hydrogenation of toluene using PEM (Proton Exchange Membrane) reactor with various catalysts (Figure 1) and found that PtRu/C catalyst afforded excellent current efficiencies for the hydrogenation. However, it has not been made clear whether by-products such as methylcyclohexadienes and methylcyclohexenes are produced in the hydrogenation of toluene. In this work, we demonstrated a systematic study on the electrocatalytic hydrogenation of toluene to methylcyclohexane in order to clarify the above question.

MEA (Membrane Electrode Assembly) of the PEM reactor was consisted of noble metal catalysts, nafion membrane, ionomer, and diffusion layer. We chose Pt/C, Ru/C, PtRu/C as cathode catalysts in this work. Pt was used for an anode catalyst (0.5 mg cm^{-2}), and Pt, Ru, PtRu alloy were used for a cathode catalyst (0.5 mg cm^{-2}). We conducted electrochemical hydrogenation with constant current method (12.5 mA cm^{-2}).

These instructions are an example of what a properly prepared meeting abstract should look like. Proper column and margin measurements are indicated.

As shown in Table 1, methylcyclohexane was obtained as a main product with high current efficiencies in all cases. However, small amounts of the partially hydrogenated product such as 1-methyl-1-cyclohexene (1-ene) was also produced. Among the all tested catalysts, the use of PtRu catalyst gave better selectivity and higher current efficiency for the desired product like methylcyclohexane. Hence, it can be stated that PtRu is the most suitable catalyst for the electrochemical hydrogenation of toluene.

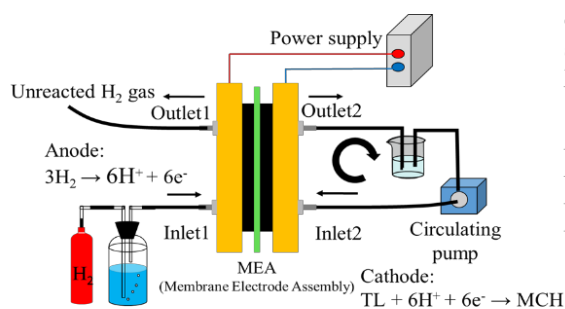


Figure 1. Schematic representation of PEM reactor.

Table 1. Current efficiency for MCH and 1-ene generation and selectivity for MCH in the electrochemical hydrogenation of toluene using various cathode catalysts

Metal catalyst	Current efficiency (MCH)/%	Current efficiency (1-ene)/%	1-ene selectivity
Pt	81	0.05	0.1
Ru	93	5.6	5
PtRu	>99	0.3	0.3

^a Experimental condition: anode, Pt (loading was 0.5 mg cm^{-2}); cathode, (loading was 0.5 mg cm^{-2}), cell temperature, r.t.; flow rate of toluene, 0.25 mL min^{-1} ; flow rate of hydrogen, 30 mL min^{-1} .

^b Determined by GC.

Au@g-C₃N₄ Decorated TiO₂ Nanotube Arrays: Visible-Light Triggered Photoelectrochemical Platforms for H₂O₂ Sensing

Yanyan Song, Yongfang Qu, Xiaoxia Jian, Zhida Gao
Department of Chemistry, Northeastern University,
Wenhua Road 3-11, Shenyang 110004, China
e-mail address: yysong@mail.neu.edu.cn

Graphitic carbon nitride (g-C₃N₄) has attracted considerable attention as a potential visible light photocatalyst owing to its visible-light band-gap at 2.69 eV and its high stability. However, the photocatalytic performance of g-C₃N₄ is limited by the low quantum efficiency for this pristine semiconductor. To resolve this problem, many attempts have been carried out to improve the photocatalytic performance of g-C₃N₄, such as nonmetal doping, preparation of nano/porous C₃N₄, and formation of heterojunction between C₃N₄ and other materials. The highest occupied molecular orbital (HOMO) of the g-C₃N₄ is located more negative than the conduction band (CB) of several common wide band-gap semiconductor photocatalysts such as TiO₂, ZnO, and BiPO₄. Thus, by constructing heterojunctions with g-C₃N₄, these wide band-gap semiconductors can be sensitized by g-C₃N₄ and a visible light response can be obtained. Here, we explore the feasibility to decorate and activate TiO₂ nanotube arrays by g-C₃N₄. We integrated the synthesis of g-C₃N₄ and decoration of TiO₂ nanotubes (TiNTs) using a one-step chemical vapor deposition technique. Compared with g-C₃N₄/TiNTs, Au@g-C₃N₄/TiNTs showed improved photochemical response under visible light. The g-C₃N₄ loaded anatase TiNTs were then further functionalized with Au nanoparticles by proton-AuCl₄⁻ exchange approach. Under visible-light irradiation, g-C₃N₄ can generate the electron-hole pair, delivering the excited electrons to the AuNPs, and then to the conduction band (CB) of TiNTs. Detection of low levels of Hydrogen peroxide (H₂O₂) is of great importance for modern medicine and environmental protection. H₂O₂, as the electron donor, could increase the photocurrent of Au@g-C₃N₄/TiNTs composite. The enhanced photocurrent of Au@g-C₃N₄/TiNTs is linear with the H₂O₂ concentrations from 0.03 to 18 mmol L⁻¹ with the detection limit of 6.86 nmol L⁻¹, indicating the great application potential of Au@g-C₃N₄/TiNTs in biosensing. The proposed Au@g-C₃N₄/TiNTs sensing platform is promising in the analysis of other significant proteins or enzymatic related reaction in the future.

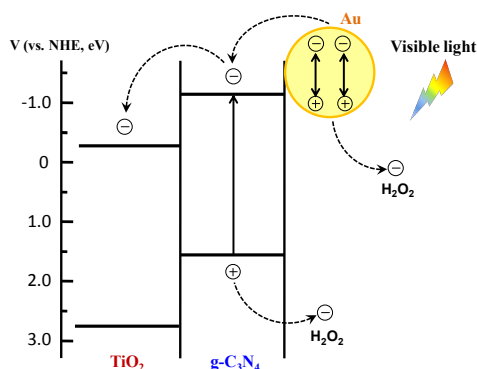


Figure 1. Proposed mechanism for photoelectrochemical sensing under visible-light irradiation.

Reference

1. I. Paramasivam, H. Jha, N. Liu, P. Schmuki, *Small*, **2012**, 8, 3073.
2. Y. Y. Song, F. Schmidt-Stein, S. Bauer, P. Schmuki, *Journal the American Chemistry Society*, **2009**, 131, 4230.
3. A. L. Linsebigler, G. Lu, J. T. Yates, *Chemical Review*, **1995**, 95, 735.
4. M. R. Hoffmann, S. T. Martin, W. Choi, D. W. Bahnemann, *Chemical Review*, **1995**, 95, 69.
5. Z. -D. Gao, Y.-F. Qu, X. Zhou, L. Wang, Y.-Y. Song, P. Schmuki, *ChemistryOpen*, **2016**, 5, 197.

Synthesis and Characterization of Carbon Modified $\text{Li}_2\text{MnP}_2\text{O}_7/\text{C}$ Composites Prepared by Spray Pyrolysis

Heechan Jang^a, Izumi Taniguchi^b

^a Department of Chemical Engineering, Tokyo Institute of Technology, Tokyo 152-8552, Japan

^b Department of Chemical Science and Engineering, Tokyo Institute of Technology, Tokyo 152-8552, Japan

itaniguc@chemeng.titech.ac.jp

1. Introduction

In recent years, structural properties of the $(\text{P}_2\text{O}_7)^{3-}$ framework employed $\text{Li}_2\text{MnP}_2\text{O}_7$ composite has been investigated since the $\text{A}_2\text{MP}_2\text{O}_7$ composition has proposed with no ionic conductivity property by Adam et al. [1]. The pure phase of $\text{Li}_2\text{MnP}_2\text{O}_7/\text{C}$ composite was prepared via spray pyrolysis followed by heat treatment in this study. Two of approaches for carbon modification in particles were carried out to enhancing the electrochemical property. Citric acid was used as a carbon source in the precursor solution to enhance the electrochemical properties. Synthesis conditions influenced the amount of residual carbon in the prepared particle and lattice parameters. An additional carbon coating was carried out by wet ball milling process to surpass the carbon limitation by citric acid. Evaluation of electrochemical properties investigated appropriate conditions of synthesis and ball milling process, and the limitations of the process were discussed.

2. Experimental

The precursor solution was prepared by dissolving the LiH_2PO_4 (99%, Aldrich) and $\text{Mn}(\text{NO}_3)_2 \cdot 9\text{H}_2\text{O}$ (99%, Wako) in distilled water with a stoichiometric ratio. The solution was atomized to droplet by ultrasonic nebulizer which has the frequency of 1.7 MHz and was passed to a tubular furnace by the carrier gas. Heat treatment was conducted under same gas atmosphere with spray pyrolysis for 2 hours. Wet-ball milling process was employed to enhance the electrical conductivity of the optimized sample. After wet ball milling process, samples were dried and annealed at 650 °C for 2 hours under the atmosphere of 3 % of $\text{H}_2\text{-N}_2$ mixture gas flow in a tubular furnace.

3. Results and discussion

Fig. 1. displays X-ray diffraction pattern of bare- $\text{Li}_2\text{MnP}_2\text{O}_7$ prepared by spray pyrolysis followed by an annealing process. Refined lattice parameters for $\text{Li}_2\text{MnP}_2\text{O}_7$ single crystal were $a=11.1580$ Å, $b=9.8069$ Å, $c=9.8947$ Å, $\beta=102.509$ °, and $V=1057.03$ Å³. Unit cell parameters are close to those reported previously [2]. Besides the indexed X-ray diffraction pattern verified a pure crystalline of $\text{Li}_2\text{MnP}_2\text{O}_7$ peaks without any impurities. **Fig. 2.** exhibits that the initial charge-discharge profiles of bare and ball-milled $\text{Li}_2\text{MnP}_2\text{O}_7/\text{C}$ samples cycled at ambient temperature and higher temperature of 60 °C. At ambient temperature, both of samples showed almost inactive electrochemical performance and delivered approximately 10 mAh g⁻¹ of discharge capacity. While as increasing the temperature, the apparent plateau revealed which represents a redox couple of $\text{Mn}^{3+}/\text{Mn}^{2+}$ at 4.1 V vs. Li^+ as well as the enhancement of capacity that was attributed to improved electrical conductivity by carbon coating. Bare and ball milled $\text{Li}_2\text{MnP}_2\text{O}_7/\text{C}$ samples delivered a discharge capacity of 37 and 60 mAh g⁻¹ at 60 °C, respectively.

Reference

[1] L. Adam et al. (2008) *J. Solid State Chem* 181:3110-3115

[2] N. V. Kosova et al. (2015) *Electrochim Acta* 174:1278-1289

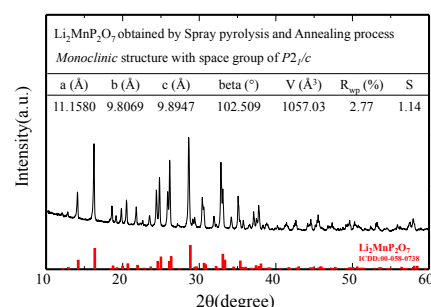


Fig. 1. X-ray diffraction pattern and refined lattice parameters of $\text{Li}_2\text{MnP}_2\text{O}_7$ prepared by spray pyrolysis followed by annealing process.

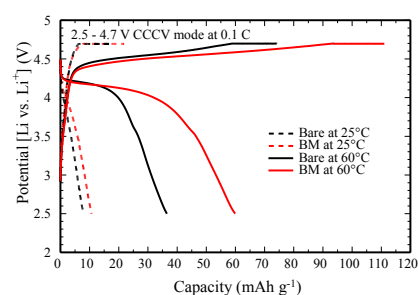


Fig. 2. Initial charge-discharge profiles of bare and ball-milled sample at 25 and 60 °C.

Asymmetric supercapacitors based on electrospun carbon nanofiber/sodium-pre-intercalated manganese oxide electrodes with high power and energy densities

Sheng-Chi Lin, Chen-Chi M. Ma* and Chi-Chang Hu *

Department of Chemical Engineering

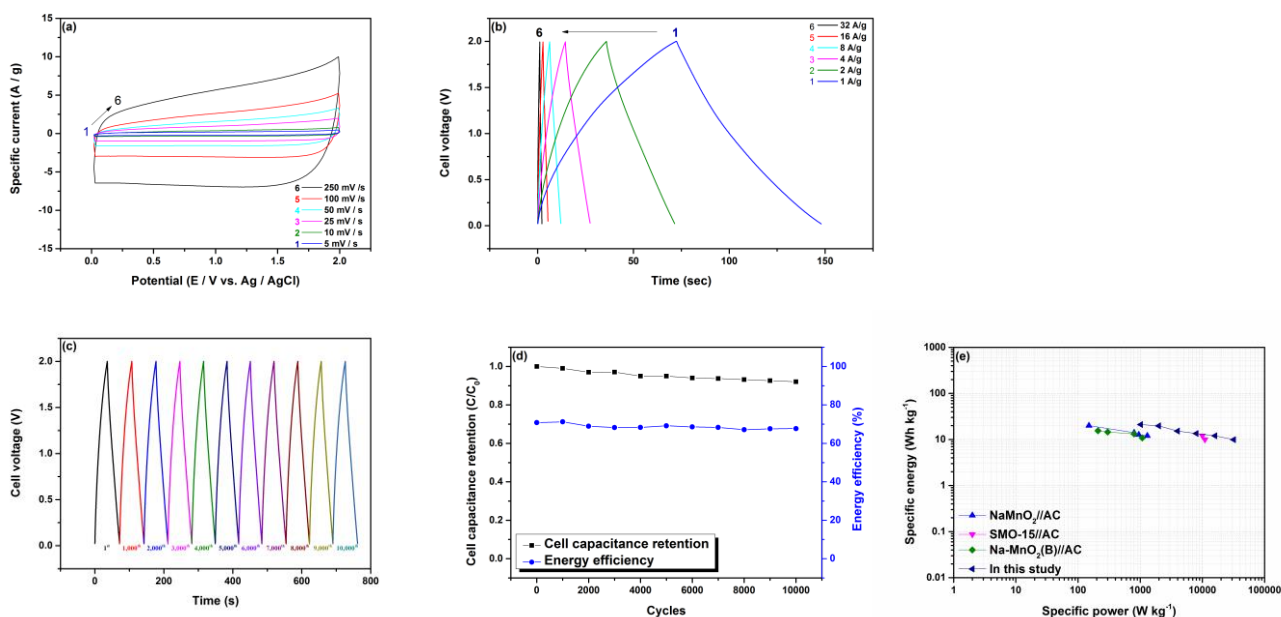
National Tsing-Hua University

101, Section 2, Kuang-Fu Road

Hsin-Chu 30013, Taiwan

ccma@che.nthu.edu.tw, cchu@che.nthu.edu.tw

The sodium-preintercalated δ -MnO₂ is grown on carbon nanofiber (denoted as CNF@SM) via a simple, low cost synthesis method for the application of asymmetric supercapacitors. The pre-intercalation of Na ions into layered structure of δ -MnO₂ reduces the crystallinity, beneficial for Na⁺ diffusion into/out the interlayer structure and pseudocapacitive utilization of MnO₂. This CNF@SM nanocomposite with desirable pseudocapacitance from sodium-preintercalated δ -MnO₂ and high electric conductivity from CNF network shows a high specific capacitance of 325 F g⁻¹ at 5 mV s⁻¹ with ca. 82 % capacitance retention from 5 to 250 mV s⁻¹. An ASC cell consisting of this nanocomposite and activated carbon as the positive and negative electrodes can be reversibly charged and discharged to a cell voltage of 2.0 V in 1 M Na₂SO₄ and 4 mM NaHCO₃ with specific energy and power of 21 Wh kg⁻¹ and 1 kW kg⁻¹, respectively. This ASC also shows excellent cell capacitance retention (7 % decay) in the 2V, 10,000-cycle stability test, revealing superior performance.



Reference

- [1] T.-M. Ou, C.-T. Hsu, C.-C. Hu, *Journal of The Electrochemical Society*, 162 (2015) A5124-A5132.
- [2] Q.T. Qu, Y. Shi, S. Tian, Y.H. Chen, Y.P. Wu, R. Holze, *Journal of Power Sources*, 194 (2009) 1222-1225.
- [3] A. Radhiyah, M.I. Izwan, V. Baiju, C.K. Feng, I. Jamil, R. Jose, *RSC Advances*, 5 (2015) 9667-9673.

Electroplating of Gold on Titanium Substrate: Method to Deposit Defect-Free Film

Ken Hashigata^{1,2,*}, Haochun Tang^{1,2}, Tso-Fu Mark Chang^{1,2}, Chun-Yi Chen^{1,2}, Daisuke Yamane^{1,2}, Toshifumi Konishi^{1,2,3}, Katsuyuki Machida^{1,2}, Kazuya Masu^{1,2}, Masato Sone^{1,2}

¹*Institute of Innovative Research, Tokyo Institute of Technology
4259-R2-35 Nagatsuta-cho Midori-ku Yokohama 226-8503 Japan*

²*CREST, Japan Science and Technology Agency,
4259-R2-35 Nagatsuta, Midori-ku, Yokohama 226-8503, Japan*

³*NTT Advanced Technology Corporation, Kanagawa, 243-0124, Japan*

*hashigata.m.aa@m.titech.ac.jp

Gold is a promising material for micro-electro-mechanical (MEMS) devices owing to its high mass density [1,2]. Components composed of gold could maintain a high enough weight even when it is miniaturized to reduce the Brownian noise. However, gold is known for its weak mechanical properties with a yield stress of 55-200 MPa in bulk [3], and the low mechanical strength could cause a problem in terms of the structure stability. In a previous study, enhancement in the structure stability of micro-cantilevers using a Ti/Au two-layer structure was reported using finite element method [4]. The structure stability was quantified by the level of defection at tip of the micro-cantilevers. On the other hand, it is still necessary to perform real mechanical test to provide critical information needed for design of the MEMS components.

In order to further enhance the mechanical properties, the grain refinement mechanism [5] was utilized by depositing nano-grained gold on titanium by constant current electrodeposition with a sulfite-based gold electrolyte. However, there is not many reports on electrodeposition of gold on titanium. In addition, from a preliminary experiment, poor adhesion problem between the two metals was discovered. Therefore, electrodeposition of defect-free gold on titanium becomes the first task to allow mechanical property evaluation of specimens using the Ti/Au two-layer structure.

Oxides formed on surface of the titanium substrate was suspected to be the cause of the poor adhesion problem. This oxide layer might inhibit or obstruct the reduction of gold on the substrate. To prove this hypothesis, a pre-treatment involving immersion of the titanium substrate in 9 M HCl at 80°C for 30 minutes was carried out. X-ray diffraction (XRD) patterns of the titanium substrate before and after acid treatment were taken for comparisons. The gold electrodeposition was conducted on an as-received titanium substrate and an acid treated titanium substrate to reveal effects of the acid treatment. In order to test the adhesion properties, an adhesion test comprising tapping a piece of 3M tape on the gold film and then peeled the tape off from the surface was conducted.

From the XRD results, signals from titanium oxides were observed for the as-received titanium substrate, and only signals from metallic titanium were observed after the acid treatment. Regarding the adhesion test, the gold deposited on the as-received titanium substrate was easily peeled-off along with the tape, where the gold coating on the acid treated titanium was perfectly fine after the peeling-off process. In addition, defects were observed on surface of the gold deposited on the as-received titanium substrate using an optical microscope. On the other hand, the gold on the acid treated substrate yielded a very homogenous surface with no defect. The acid treatment was confirmed to be effective in allowing deposition of defect-free gold on titanium substrate, and oxides formed on the titanium substrate was the root-cause of the poor adhesion problem.

Reference:

- [1] D. Yamane, T. Konishi, T. Matsushima, K. Machida, H. Toshiyoshi, K. Masu, *Appl. Phys. Lett.* **104** (2014) 074102.
- [2] S.T. Patton, J.S. Zabinski, *Tribol. Lett.* **18** (2005) 215-230.
- [3] H. D. Espinosa, B. C. Prorok, and B. Peng, *J. Mech. Phys. Solids* **52** (2004) 667-689.
- [4] M. Teranishi, T.F.M. Chang, C.Y. Chen, T. Konishi, K. Machida, H. Toshiyoshi, D. Yamane, K. Masu, M. Sone, *Microelectron. Eng.* **159** (2016), 90-93.
- [5] H.C. Tang, C.Y. Chen, T. Nagoshi, T.F.M. Chang, D. Yamane, K. Machida, K. Masu, M. Sone, *Electrochem. Commun.* **72** (2016) 126-130.

A Novel Graphene/Nafion Screen-Printed Electrode for the Simultaneous Determination of Fat-Soluble Vitamins by Square-Wave Voltammetry

Jeerakit Thangphattharungruang¹, Aroonsri Ngamaroonchote², Rawiwan Laocharoensuk², Chuleekorn Chotsuwan^{2,*}, and Weena Siangproh^{1,**}

¹Department of Chemistry, Faculty of Science, Srinakharinwirot University, Sukhumvit 23, Wattana, Bangkok 10110, Thailand

²Nanostructures and Functional Assembly Laboratory, National Nanotechnology Center, National Science and Technology Development Agency, Klong Luang, Pathumthani 12120, Thailand

*e-mail: chuleekorn@nanotec.or.th

**e-mail: weena@g.swu.ac.th

A novel electrochemical sensor was developed for the simultaneous determination of fat-soluble vitamins (A, D, E, K) using a graphene/nafion screen-printed electrode. The electrochemical oxidations of fat-soluble vitamins have been studied in mixed ethanol/sodium perchlorate monohydrate solution using square-wave voltammetry (SWV). To enhance sensitivity, the various experimental variables such as the effects of proportions ethanol, potential increment, amplitude, frequency, and quiet time were investigated. Under the optimal conditions, the relationship between oxidative currents and concentrations of fat-soluble vitamins ranged from 0.1 $\mu\text{g mL}^{-1}$ to 5 $\mu\text{g mL}^{-1}$ for vitamin A, 0.08 $\mu\text{g mL}^{-1}$ to 5 $\mu\text{g mL}^{-1}$ for vitamin D and E, and 0.2 $\mu\text{g mL}^{-1}$ to 1.6 $\mu\text{g mL}^{-1}$ for total vitamin K, with the limits of detection of 0.018, 0.013, 0.012 and 0.004 $\mu\text{g mL}^{-1}$, respectively. This developed method provides highly sensitive and potential to apply for the simultaneous determination of fat-soluble vitamins in dietary supplements or biological samples.

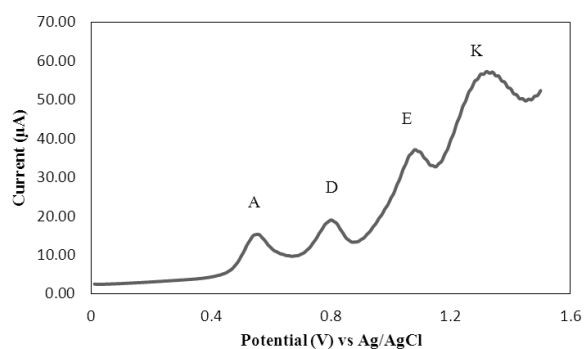


Figure. Square-wave voltammogram of 5 $\mu\text{g mL}^{-1}$ of each fat-soluble vitamin in ethanol/sodium perchlorate monohydrate solution

Acknowledgments

This work was financially supported by conference grant from Graduate School of Srinakharinwirot University for the fiscal year 2018, The Thailand Research Fund (TRF) and Thailand Graduate Institute of Science and Technology (TGIST). The author would also like to acknowledge Nanostructures and Functional Assembly Laboratory, National Nanotechnology Center (NANOTEC), National Science and Technology Development Agency (NSTDA) for supporting the facilities which enable this work to be carried out.

High mobility transparent conductive Al-doped ZnO thin films grown by atomic layer deposition

Man-Ling Lin, Jenh-Yih Juang and Hsin-Yi Lee
 Scientific Research Division, National Synchrotron Radiation Research Center,
 101 Hsin-Ann Road, Hsinchu Science Park, Hsinchu 300, Taiwan
 hylee@nsrrc.org.tw

The effects of growth temperature on the microstructure, transport and optoelectronic properties of a series of Al-doped ZnO (AZO) films with thickness of 20-30 nm deposited on polished silicon-(100) and glass substrates by the atomic layer deposition (ALD) were investigated. Effective Al-doping was achieved by an in-situ doping-growth scheme with the growth temperature ranging from 100 °C to 300 °C. Experimental results showed that, in general, increasing the growth temperature would result in much improved film crystallinity as shown in Figure 1 and carrier mobility, with the average transmittance in the visible wavelength range being exceeding 95% in all cases. In particular, for AZO films grown at 300 °C, although the resistivity of $6 \times 10^{-4} \Omega\text{-cm}$ is still slightly higher than that of some highly-doped ZnO ($\rho \approx 2 \sim 4 \times 10^{-4} \Omega\text{-cm}$) prepared by sputtering method, an unprecedented mobility of $136 \text{ cm}^2\text{V}^{-1}\text{s}^{-1}$, comparing to the typical values of $50\text{-}60 \text{ cm}^2\text{V}^{-1}\text{s}^{-1}$ reported previously, was obtained. Figure 2 show the electrical properties and the average transmittance of the AZO films. The secondary ion mass spectroscopy (SIMS) analyses revealed that hydrogen incorporation is the key in reducing the charge trap density and, hence, resulting in much enhanced carrier mobility. The present results promise a keen competitiveness of AZO with the indium tin oxide (ITO) film for thin-film-transistor (TFT) as well as in photovoltaic device applications.

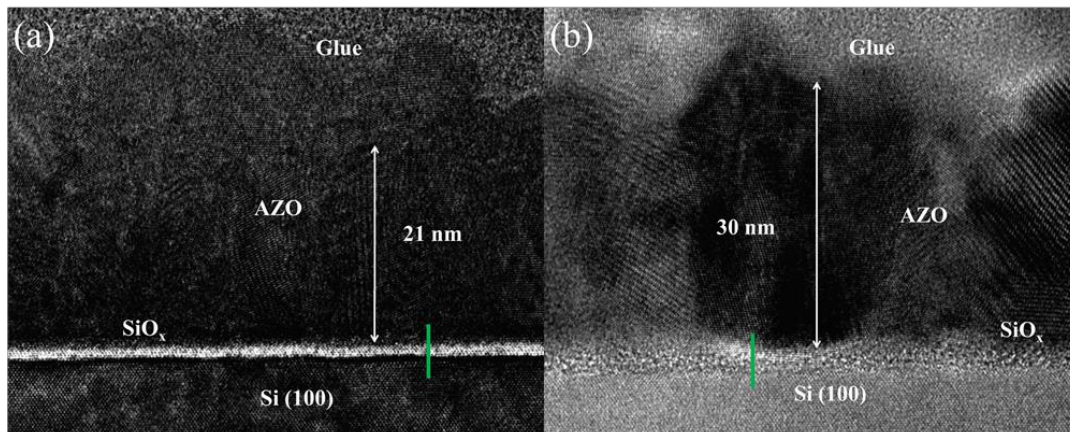


Figure 1. High-resolution cross-sectional transmission electron microscope (HR-XTEM) images of the AZO thin films grown at (a) 150 °C and (b) 300 °C.

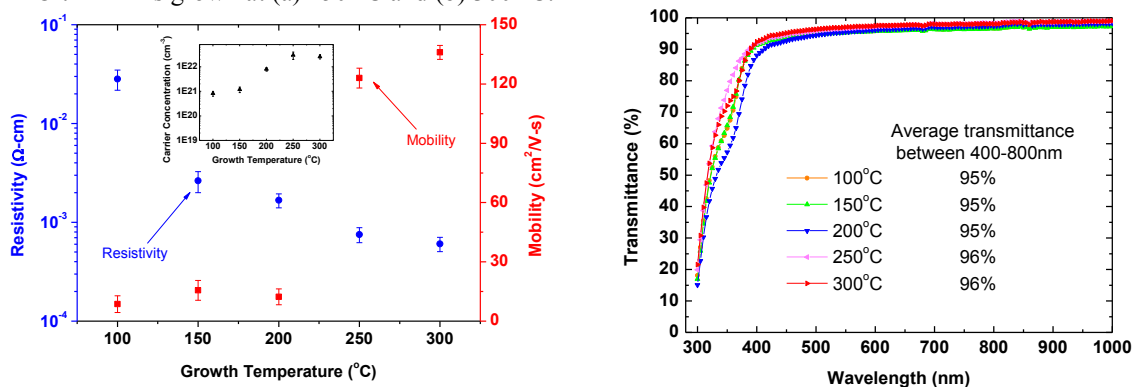


Figure 2. The electrical properties of the AZO films grown at the various temperatures. The inset shows the carrier concentration in the respective AZO films (left). UV-Vis spectra of the AZO films grown on glass. The inset shows the average transmittance of visible region from 400-800nm (right).

Rhenium Complexes Based on 2-Pyridyl-1,2,3-Triazole Ligands: a New Class of CO₂ Reduction Catalysts

H.Y. Vincent Ching,¹⁻³ Xia Wang,¹ Menglan He,² Noemi Perujo Holland,² Régis Guillot,⁴ Cyrine Slim,³ Sophie Griveau,³ Hélène C. Bertrand,² Clotilde Policar,² Fethi Bedioui,³ and Marc Fontecave¹

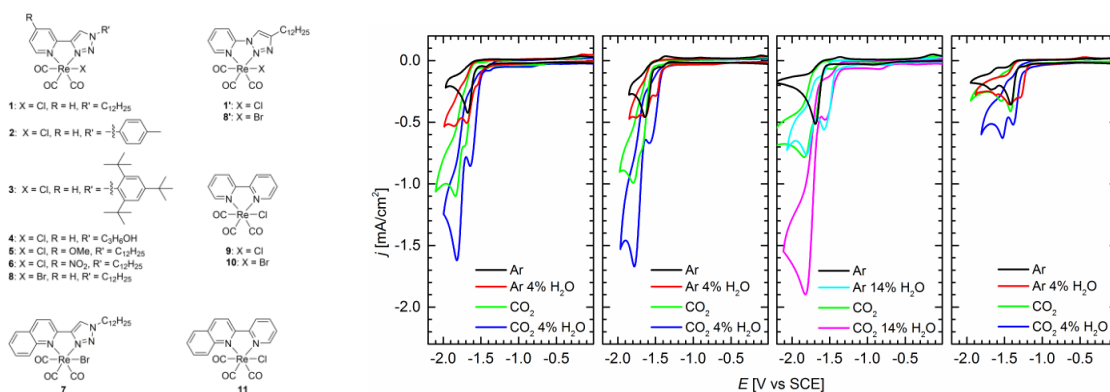
1. *Laboratoire de Chimie des Processus Biologiques, PSL Research University, Collège de France, CNRS 8229, Université Pierre et Marie Curie, Paris, France.*

2. *Département de Chimie, Ecole Normale Supérieure, PSL Research University, UPMC Univ Paris 06, CNRS, Laboratoire des Biomolécules, Paris, France.*

3. *Chimie ParisTech, PSL Research University, Unité de Technologies Chimiques et Biologiques pour la Santé, CNRS 8258, INSERM 1022, Univ. Paris Descartes, Paris, France*

4. *Institut de Chimie Moléculaire et des Matériaux d'Orsay, Université Paris-Sud, UMR CNRS 8182, Université Paris-Saclay, Orsay, France*

A series of [Re(N^N)(CO)₃(X)] (N^N = diimine and X = halide) complexes based on 4-(2-pyridyl)-1,2,3-triazole (pyta) and 1-(2-pyridyl)-1,2,3-triazole (tapy) diimine ligands have been prepared and electrochemically characterized. The first ligand-based reduction process is shown to be highly sensitive to the nature of the isomer as well as to the substituents on the pyridyl ring, with the peak potential changing by up to 700 mV. The abilities of this class of complexes to catalyze the electroreduction and photoreduction of CO₂ were assessed for the first time. It is found that only Re-pyta complexes that have a first reduction wave with a peak potential at around -1.7 V vs SCE are active, producing CO as the major product, together with small amounts of H₂ and formic acid. The catalytic wave that is observed in the CVs is enhanced by the addition of water or trifluoroethanol as a proton source. Long-term controlled potential electrolysis experiments gave total Faradaic yield close to 100%. In particular functionalization of the triazolyl ring with a 2,4,6-tri-tert-butylphenyl group provided the catalyst with a remarkable stability.



(Right) : Structure of rhenium complexes synthesized and investigated in this study. (left) : cyclic voltammograms of 1 mM of compounds 1, 2, 3, and 1' (left to right panels) in MeCN with 0.1 M Bu₄NPF₆ under argon or CO₂ and with or without water recorded at 0.1 V · s⁻¹ at a glassy carbon disk electrode at room temperature.

H.Y. V. Ching et al. *Inorg. Chem.* 56 (2017) 2966–2976.

We acknowledge PSL Research University (“PSL-Chimie” Project CATAcarb) for funding The China Scholarship Council for a CSC scholarship for MH. The authors would like to thank Dr P. Simon (College de France) for assistance with gas and ion chromatography, and Dr V. Mougél (College de France) and T. Forgeron (College de France) for fruitful discussions.

Synthesis of Graphene Oxide Nanoribbons and Their Photoelectrochemical Measurements

Chia-Liang Sun^{1,2*}, Chia-Heng Kuo¹, Cheng-Hsuan Lin¹

¹Department of Chemical and Materials Engineering, Chang Gung University, Guishan, Taoyuan 33302, Taiwan

²Department of Neurosurgery, Linkou Chang Gung Memorial Hospital, Guishan, Taoyuan 33305, Taiwan

e-mail address: sunchialiang@gmail.com

We demonstrated the microwave-assisted synthesis of graphene oxide nanoribbons (GONRs) from the unzipping of multiwalled carbon nanotubes (MWCNTs) and their applications since 2011. [1-11] A core-shell MWCNT/GONR-modified carbon electrodes were used to electrochemically detect ascorbic acid, dopamine, and uric acid. [1, 5, 9] The specific capacitance is 252.4 Fg⁻¹ for the supercapacitor electrode with the MWCNT@GONR. [2] We also modified GONRs with phospholipid-polyethylene glycol (PL-PEG) to prepare PEGylated GONRs for biodistribution and drug delivery studies. [3] The reduced GONR was further used as the catalytic film of the counter electrode of a dye-sensitized solar cell (DSSC) with an efficiency of 6.91 %. [4] GONR/cobalt oxide composites were prepared for OER and ORR reactions. [6] On the other hand, the detection of TNT [7, 10] and visible light [8] was also investigated. More recently, scanning electrochemical microscopy has been used to create maps of the biodistribution of GONRs in mouse livers. [11] On the other hand, the collaboration work on a solution gate GONR transistor would be mentioned. Finally, our research on the ZnCl₂-treated GONRs and their photoelectrochemical measurement results will be discussed. Briefly, our papers since 2011 will be all presented in this conference.

References

- [1] C. L. Sun *et al.* ACS Nano 5 (2011) 7788.
- [2] L. Y. Lin *et al.* J. Mater. Chem. A 1 (2013), 11237.
- [3] Y. J. Lu *et al.* Carbon 74 (2014) 83.
- [4] M. H. Yeh *et al.* J. Phys. Chem. C 118 (2014) 16626.
- [5] C. L. Sun *et al.* Biosens. Bioelectron. 67 (2015) 327.
- [6] X. Lu *et al.* J. Mater. Chem. A 3, (2015) 13371.
- [7] R. Zhang *et al.* Anal. Chem. 87, (2015) 12262.
- [8] Y. W. Lan *et al.* Nano Energy 27, (2016) 114.
- [9] C. H. Su *et al.* ACS Omega 2(8), (2017) 4245.
- [10] R. Zhang *et al.* Carbon 126, (2018) 328.
- [11] T. E. Lin *et al.* Angew. Chem. Int. Ed. (in press) DOI: 10.1002/anie.201709271.

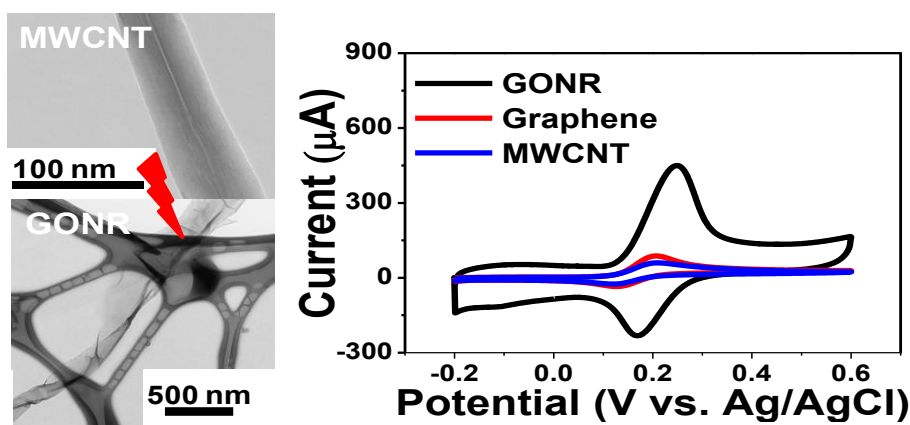


Fig. 1. Microwave-assisted synthesis of core-shell MWCNT/GONR heterostructure for electrochemical detection of ascorbic acid, dopamine, and uric acid. [1]

Simultaneous Removal of COD and Total Nitrogen for Wastewater Treatment Using Electrochemical Method

Jiachao Yao, Jiade Wang*

College of Environment, Zhejiang University of Technology,
18, Chaowang Road, Hangzhou, China
E-mail: jdwang@zjut.edu.cn

Electrochemical method, an environmental friendly process, has been gradually used to treat industrial wastewater containing biorefractory compounds. In this work, a divided electrolysis cell with porous reticulated electrodes was used to simultaneously remove COD and total nitrogen (TN, including ammonia, nitrate and nitrite) for pharmaceutical wastewater treatment. In the process, NO_3^- and NO_2^- could be reduced to N_2 on cathode, while the COD and ammonia could be oxidized to CO_2 and N_2 on anode respectively.

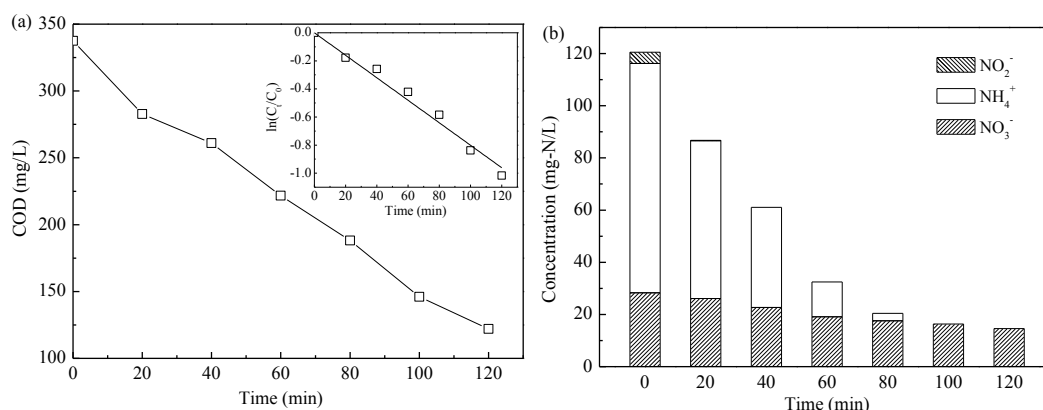


Fig. 1 The removal of COD (a) and TN (b) in pharmaceutical wastewater treatment

Main operating variables, such as current density ($5\text{--}15\text{ mA/cm}^2$) and flow rate ($50\text{--}300\text{ mL/min}$), for simultaneous removal of COD and TN was studied. Experimental results showed that the electrochemical method could effectively remove COD and TN in wastewater. The degradation of COD followed pseudo first-order kinetics. The current density and flow rate had an effect on COD and TN removal, and the effect on ammonia removal was more significant than that on COD removal. Under the optimal conditions of current density of 10 mA/cm^2 and flow rate of 300 mL/min , COD and TN decreased from 337.57 mg/L and 120.53 mg-N/L to 122.05 mg/L and 14.61 mg-N/L after 120 min electrolysis, respectively. No ammonia and nitrite were detected, while nitrate removed from 28.33 mg-N/L to 14.61 mg-N/L . All the results indicated that it's feasible and capable for electrochemical method to simultaneously remove COD and TN in wastewater.

References:

- [1] V. Díaz, R. Ibáñez, P. Gómez, A.M. Urtiaga, I. Ortiz, *Water Res.* 45 (2011) 125.
- [2] J. Ding, Q.L. Zhao, Y.S. Zhang, L.L. Wei, W. Li, K. Wang, *Water Res.* 74 (2015) 122.
- [3] M. Li, C.P. Feng, Z.Y. Zhang, Y.N. Yang, R.Z. Chen, N. Sugiura, *J. Hazard. Mater.* 171 (2009) 724.
- [4] A. Fernandes, M.J. Pacheco, L. Ciriaco, A. Lopes, *Appl. Catal. B: Environ.* 176 (2015) 183.
- [5] W. Li, C.W. Xiao, Y. Zhao, Q.Q. Zhao, R. Fan, J.J. Xue, *Catal. Lett.* 146 (2016) 2585.

Fabrication of Ag/SnO₂/TiO₂ Nanotube Films for Photoelectrochemical Cathodic Protection of Stainless Steel

Haipeng Wang, Zichao Guan, Xia Wang, Ronggui Du*

Department of Chemistry, College of Chemistry and Chemical Engineering, Xiamen University,

Xiamen 361005, China

E-mail: rgdu@xmu.edu.cn

In recent years, a potential method so-called photoelectrochemical cathodic protection (or photocathodic protection) to suppress metal corrosion has drawn significant attention of corrosion researchers because it is an environmentally friendly technique without consumption of electrical energy or sacrificial anode materials. TiO₂ is the most frequently used photoanode material in photoelectrochemical protection systems due to its good photosensitivity, high physical and chemical stability, low toxicity and low cost. However, TiO₂ can only absorb ultraviolet light because it is a wide band gap semiconductor. In addition, the photo-induced electron-hole pairs in a TiO₂ photoanode are easy to recombine, which may decrease its photoelectric conversion efficiency. For these reasons, many methods have been established to prepare composite TiO₂ photoanode materials for improving their photoelectrochemical properties. In this work, a composite Ag/SnO₂/TiO₂ nanotube film was prepared on a Ti substrate by anodization combined with hydrothermal and pulsed electrodeposition methods for photoelectrochemical protection of 403 stainless steel.

The Ti foils with sizes of 15 mm × 10 mm × 0.1 mm were used as specimens. A TiO₂ nanotube array film was prepared on the Ti specimen surface by anodization in a two-electrode cell with 0.5 wt% HF solution at 20 V for 30 min at room temperature, with the Ti specimen as the working electrode and a Pt sheet as the counter electrode. Afterwards, the as-prepared sample was annealed at 450 °C for 2 h in air to obtain a crystallized anatase TiO₂ nanotube array film.

A hydrothermal method was used for the preparation of SnO₂ quantum dots on the TiO₂ nanotube film. The specimen with TiO₂ nanotube film was immersed in an ethanol solution with SnCl₄ and hydrazine hydrate at 150 °C for 3 h, and then the specimen with a SnO₂/TiO₂ composite film was annealed at 500 °C for 2 h. Ag nanoparticles were deposited on the SnO₂/TiO₂ film by pulsed electrodeposition from a mixed solution containing AgNO₃ and NaNO₃ in a two-electrode cell with the SnO₂/TiO₂ composite film as the working electrode and a Pt sheet as the counter electrode. Then, the specimen with a Ag/SnO₂/TiO₂ film was rinsed with deionized water and dried in air.

The prepared films were characterized by surface analyses and photoelectrochemical measurements. The results showed that the pure TiO₂ film prepared by the anodization was composed of the ordered nanotube arrays. The nanotubes were perpendicular to the Ti substrate, and their average inner diameter and length were about 100 nm and 400 nm, respectively. The surface analyses indicated that a Ag/SnO₂/TiO₂ composite film was obtained after deposition of SnO₂ quantum dots and Ag nanoparticles onto the TiO₂ film, and the ordered nanotube structure was retained for the composite film. Compared with the pure TiO₂ nanotube film, the absorption band edge of the Ag/SnO₂/TiO₂ composite film showed a significant red shift in the optical response, and its light absorption intensity in the visible region and photocurrent density were considerably enhanced. The potential of 403 stainless steel in a 0.5 M NaCl solution decreased by 475 mV when it was coupled with the Ag/SnO₂/TiO₂ composite film under white light irradiation, indicating that the composite film could provide a good photoelectrochemical cathodic protection effect on the steel. After the light source was cut off, a certain cathodic protection effect on 403 stainless steel was maintained in darkness for more than 22.5 h resulting from the charge storage capability of the composite film.

Acknowledgements

We acknowledge financial support from the National Natural Science Foundation of China (Grant Nos. 21573182, 21621091, and 21173177).

Mechanical Activation by Polishing of Screen-Printed Electrodes

Loanda R Cumba^{a,b*}, Robert Forster^a, and Craig Banks^b

a School of Chemical Sciences, National Centre for Sensor Research, Dublin City University, Collins Avenue, Dublin 9, Ireland.

b Faculty of Science and Engineering, School of Science and the Environment, Division of Chemistry and Environmental Science, Manchester Metropolitan University, Chester Street, Manchester M1 5GD, UK.

*Loanda.cumba@dcu.ie

The mechanical activation (polishing) of screen-printed electrodes (SPEs) is explored and shown to exhibit an improved voltammetric response (in specific cases) when polished with either commonly available alumina slurry or diamond spray. Proof-of-concept is demonstrated for the electrochemical sensing of nitrite (Figure 1) where an increase in the voltammetric current is found using both polishing protocols, exhibiting an improved limit of detection (3σ) and a two-fold increase in the electroanalytical sensitivity compared to the respective un-polished counterpart. It is found that mechanical activation/polishing increases the C/O ratio which significantly affects inner-sphere electrochemical probes only (whereas outer-sphere systems remain unaffected). Mechanical activation/polishing has the potential to be a simple pre-treatment technique that can be extended and routinely applied towards other analytes for an observable improvement in the electroanalytical response^{1,2}.

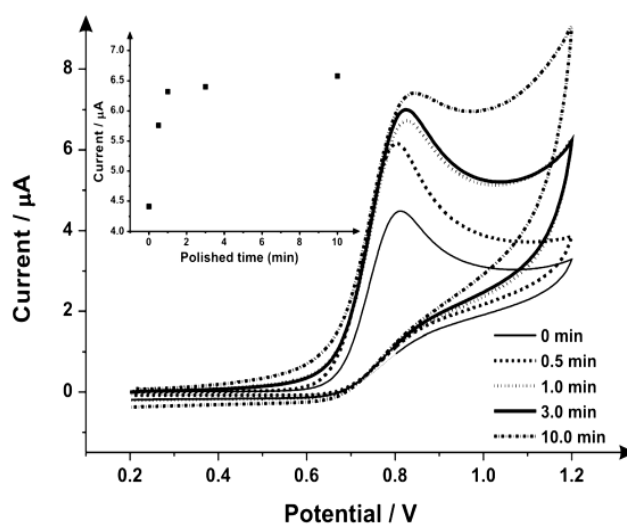


Figure 1 - Cyclic voltammetric study of the variation of mechanical activation/polishing times recorded in $50 \mu\text{mol L}^{-1}$ sodium nitrite/PBS (pH 7) using SPEs (different SPE per experiment). Inset: a plot of current as a function of mechanical activation/polishing time (with alumina slurry) variation. Scan rate: 50 mV s^{-1} vs. SCE.

References

1. Cumba, L. R. *et al.* Can the mechanical activation (polishing) of screen-printed electrodes enhance their electroanalytical response? *Analyst* **141**, 2791–2799 (2016).
2. Metters, J. P., Kadara, R. O. & Banks, C. E. New directions in screen printed electroanalytical sensors: an overview of recent developments. *Analyst* **136**, 1067–1076 (2011).

Investigation of Hydrogen Generation on Cobalt-Manganese-Boron and Cobalt-Iron-Boron Catalysts from Borohydride Solution

K. Antanaviciute, Z. Sukackiene, L. Sumskas, A. Naujokaitis, J. Vaiciuniene, L. Tamasauskaite
Tamasiunaite, E. Norkus

*Center for Physical Sciences and Technology
Sauletekio Ave. 3, LT-10257, Vilnius, Lithuania
kornelija.antanaviciute@gmail.com*

Hydrogen fuel cells are energy source, which generates electric power without any mechanical link. These fuel cells are environmentally friendly and clean energy sources. It is known that noble metals, such as platinum and gold are effective catalysts for hydrolysis of sodium borohydride. Expensiveness of such catalysts is one of the reasons why development of non-noble catalysts is very important. In this study we present low-cost cobalt alloys (cobalt-manganese-boron/copper, cobalt-iron-boron/copper) catalysts which show catalytic activity towards hydrogen generation from sodium borohydride solution. Cobalt alloys catalysts were prepared by electroless plating method on copper surface when morpholine borane was used as reducing agent. Cobalt-iron-boron/copper catalyst were prepared using iron (III) chloride or iron (II) sulphate and cobalt-manganese-boron/copper catalysts were prepared using manganese (II) sulphate or potassium permanganate. Morphology and composition of catalysts surface was determined by using Field Emission Scanning Electron Microscopy (FESEM) and Inductively Coupled Plasma Optical Emission Spectroscopy (ICP-OES). The catalytic activity of cobalt alloys catalysts towards hydrolysis of sodium borohydride were determined by measuring the amount of generated hydrogen. Alkaline sodium borohydride hydrolysis was performed under different conditions. It was determined that the highest hydrogen evolution rate was obtained using cobalt-manganese-boron/copper catalysts when temperature was 343 K and the lowest evolution rate was obtained using cobalt-iron-boron/copper catalyst at the temperature of 313 K. The highest activation energy was obtained by using cobalt-iron-boron/copper catalysts. The lowest activation energy was received using cobalt-manganese-boron/copper catalyst which were made using potassium permanganate.

Acknowledgment

This research was funded by a grant (No. M-ERA.NET-1/2016) from the Research Council of Lithuania. The author's research was performed in cooperation with the University of Tartu (Estonia), Latvian State Institute of Wood Chemistry (Latvia) and Horizon Pulp&Paper Ltd (Estonia).

Investigation of Hydrogen Generation from Borohydride Solution on Noble-Metal-Free Cobalt Catalysts

Zita Sukackiene, Jurate Vaiciuniene, Arnas Naujokaitis, Loreta Tamasauskaite Tamasiunaite, Eugenijus Norkus

*Center for Physical Sciences and Technology
Saulėtekio ave. 3, LT-10257, Vilnius, Lithuania
zitaja@gmail.com*

Hydrogen fuel cells are an environmentally friendly energy source, and they are a promising alternative for the development of clean-energy technologies. It is well known that noble metals catalysts like platinum and other its alloys effectively catalyze the catalytic hydrolysis of sodium borohydride. However, such catalysts are very expensive and its application is not viable. In this study we present low-cost, promising cobalt alloys (cobalt/copper, cobalt-boron/copper, cobalt-molybdenum-boron/copper) catalysts which are also show promising catalytic activities for hydrogen generation from the sodium borohydride solution. The cobalt alloys catalysts have been successfully prepared by the electroless plating method on the copper surface using morpholine borane as a reducing agent. The surface morphology and composition of the samples have been characterized using Field Emission Scanning Electron Microscopy (FESEM) and Inductively Coupled Plasma Optical Emission Spectroscopy (ICP-OES). The catalytic activity of the cobalt and its alloys catalysts towards the hydrolysis of alkaline sodium borohydride solution has been investigated under different conditions by measuring the amount of hydrogen generated.

It was found that the highest hydrogen evolution rate was obtained on the cobalt-molybdenum-boron/copper catalyst at the temperature of 343 K and is equal to 53.5 ml min⁻¹ as compared with that of cobalt-boron/copper and cobalt/copper catalysts. The lowest activation energy was received on the cobalt-molybdenum-boron/copper catalyst and it is about 27 kJ mol⁻¹. Addition of molybdenum to the cobalt or cobalt-boron films results in enhanced hydrogen generation rates as compared with those on bare cobalt or cobalt-boron.

Acknowledgment

This research was funded by a grant (No. M-ERA.NET-1/2016) from the Research Council of Lithuania. The author's research was performed in cooperation with the University of Tartu (Estonia), Latvian State Institute of Wood Chemistry (Latvia) and Horizon Pulp&Paper Ltd (Estonia).

Fabrication of Porous Electrodes with a Picosecond Pulsed Laser and Improvement of the Rate Performance of a Porous Graphite Anode, LiFePO₄ and LiFePO₄/Activated Carbon Cathodes

Takashi Tsuda¹, Nobuo Ando², Naoto Mitsuhashi¹, Toyokazu Tanabe¹, Kaoru Itagaki³, Naohiko Soma³, Susumu Nakamura⁴, Narumi Hayashi⁵, Futoshi Matsumoto¹

¹ Department of Materials and Life Chemistry, Kanagawa University, 3-27-1, Rokkakubashi, Kanagawa-ku, Yokohama, Kanagawa 221-8686, Japan

² Research Institute for Engineering, Kanagawa University, 3-27-1, Rokkakubashi, Kanagawa-ku, Yokohama, Kanagawa 221-8686, Japan

³ Wired Co., Ltd. (1628 Hitotsuyashiki shinden, Sanjo, Niigata 959-1152, Japan)

⁴ Department of Electrical and Electronic Systems Engineering, National Institute of Technology, Nagaoka College (888 Nishikataki, Nagaoka, Niigata 940-8532, Japan)

⁵ Industrial Research Institute of Niigata Prefecture (1-11-1 Abuminishi, Chuo-ku, Niigata-shi, Niigata, 950-0915, Japan)

e-mail address fmatsumoto@kanagawa-u.ac.jp

Recently we have examined the fabrication of porous current collector and porous electrodes for lithium-ion battery to improve the battery performance such rate performance, pre-lithiation and charge/discharge cycle ability. In this study, after preparing LiFePO₄ (LFP) and activated carbon (AC) layers on each face of an aluminum current collector, through-holes with the pore diameter of 22 μm and opening rate of 0.5 % were formed on the electrode. A half-cell was fabricated with the electrode and two lithium (Li) metal electrodes. The half-cell exhibited much improvement of rate performance. Because the LFP/AC electrode having no through holes and LFP electrode did not exhibit the improvement, it was considered that energy and Li⁺ transfer occurred between LFP and AC layers, and Li⁺ passed through the holes from AC to LFP (Fig. 1).

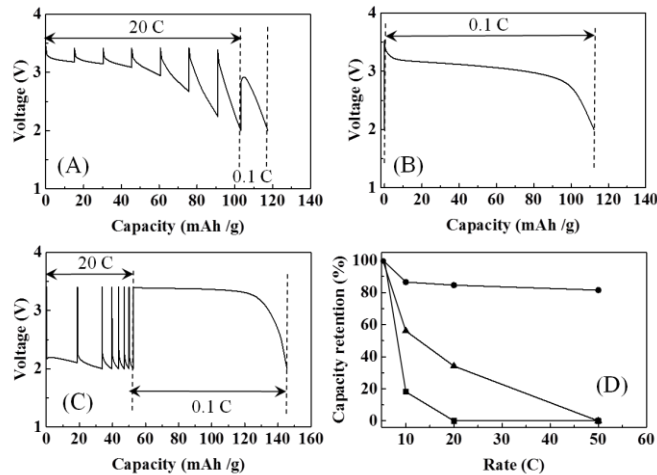


Fig. 1 Discharge curves of LFP/AC electrodes with 0.5 (A) and 0 % (B) of the opening rate of hole and 22 μm of average hole diameter, and LFP electrode (C) at 20 C, where the discharge of 20 mAhg⁻¹ was repeated by 7 times and then the cells were finally discharged at 0.1 C, and the open circuit time (5 min) was inserted between discharge processes. (D) Total discharge capacity observed after 7 times-discharge/open circuit processes vs. the discharge rate. ●: LFP/AC electrode with 0.5 % of the opening rate, ▲: LFP/AC electrode with 0 % of the opening rate, ■: LFP electrode.

Relationship between d-band center of Dealloyed PtPb Ordered Intermetallic Nanoparticle Deposited on TiO₂/ Cup-Stacked Carbon Nanotube and ORR Activity in Acidic Aqueous Media

Fuma Ando ¹, Takashi Tsuda ¹, Toyokazu Tanabe ¹, Takeo Ohsaka ², Futoshi Matsumoto ¹

¹ Department of Materials and Life Chemistry, Kanagawa University, 3-27-1, Rokkakubashi, Kanagawa-ku, Yokohama, Kanagawa 221-8686, Japan

² Research Institute for Engineering, Kanagawa University, 3-27-1, Rokkakubashi, Kanagawa-ku, Yokohama, Kanagawa 221-8686, Japan
e-mail address fmatsumoto@kanagawa-u.ac.jp

The development of fuel cells that convert chemical energy to electric energy with high efficiency are one of key factor to solve energy issues. In order to widespread the fuel cells to our daily life, various technologies for the fuel cells have been developed with much effort of researchers and engineers. Now, electric cars (EV) powered by electricity which is produced by fuel cells are put on the market. However, it will take a long time before it becomes widespread because from the viewpoints of performance, durability and cost, many unsolved problems are still piled. One of the unsolved problems is sluggish kinetics of oxygen reduction reaction (ORR) even on the surface of platinum (Pt). Although, theoretically, the onset potential of ORR is 1.23 V vs. NHE, due to large overpotential for ORR, the onset potential can be seen around 1 V even on Pt surface which is the best ORR catalyst in acidic aqueous solutions among catalysts composed of single elements. Pt-based alloys, core-shell structures and Pt on metal oxide have been proposed as promising catalysts in many papers. Many results on the enhancement of ORR have been reported. The important principle at the bottom of the ORR enhancements is modification of the electric state of Pt atoms on the catalyst surfaces where oxygen molecules adsorb to start the ORR. In the discussion on the enhancement of ORR and electronic modification of Pt atoms, *d*-band center theory is often used [1, 2]. The theory has become a popular language in the community of electrocatalysis, especially ORR. In this study, in each electrodes treated by the potential cycling, ORR activity was measured with rotating ring-disk electrode method and change of the surface structure and the composition of Pb atoms on the PtPb ordered intermetallic NP surface [3] treated by the potential cycling was analyzed with transmission electron microscope (TEM). In addition, the *d*-band center of the Pt atoms on the treated PtPb NPs was evaluated with X-ray photoelectron spectroscopy (XPS). The volcano plot mentioned above for ORR was tried to make with the ORR activities and *d*-band center obtained with the electrochemically treated PtPb NPs. It was made clear that the NP surfaces prepared by gradual electrochemical dissolution of Pb atoms exhibited the shift of *d*-band center and that the shift of *d*-band center controlled the ORR activity on the dealloyed Pt-Pb NP surfaces.

[1] J. Greeley *et al.*, "Alloys of platinum and early transition metals as oxygen reduction electrocatalysts", *Nature Chemistry*, **1**, 552-556(2009).

[2] E. Toyoda *et al.*, "The *d*-band structure of Pt nanoclusters correlated with the catalytic activity for an oxygen reduction reaction", *J. Phys. Chem. C*, **115**, 21236–21240 (2011).

[3] F. Ando *et al.*, "Improvement of ORR activity and durability of Pt electrocatalyst nanoparticles anchored on TiO₂/cup-stacked carbon nanotube in acidic aqueous media", *Electrochimica Acta*, **232**, 404-413(2017).

Carbon-Supported Gold Catalysts for Ethanol Oxidation Reaction

Virginija Kepeniene, Daina Upskuviene, Algirdas Selskis, Loreta Tamasauskaite Tamasiunaite,
Eugenijus Norkus

*Center for Physical Sciences and Technology
Sauletekio ave. 3, LT-10257 Vilnius, Lithuania
virginalisk@gmail.com*

The development and investigation of various materials used in fuel cells is a major challenge in the scientific community. Literature describes many various supports, metals, methods, which are able to enhance the electrocatalytic activity of the new created catalysts. The nano-sized gold nanoparticles (GNPs) have been known from the very beginning of human civilization, but systematic scientific investigations were performed much later. One of the most popular and thoroughly studied methods for GNPs' synthesis developed by Turkevich is the citrate method. Recently, formation of new composites by adsorption of gold nanoparticles on carbon has attracted interest due to their physical properties and applications in catalysis, electrochemical energy storage or electrochemical sensor.

In this study gold nanoparticles (GNPs) were synthesized by using mentioned Turkevich method and additional amount of halides. Gold nanoparticles were obtained by reducing of Au^{3+} (HAuCl_4) to Au^0 with trisodium citrate ($\text{Na}_3\text{C}_6\text{H}_5\text{O}_7$) in an aqueous solution. In addition, KI, KBr and KCl were added to the solution. Further GNPs' were deposited on carbon surface (Au/C) by adsorption using stirring.

The composition, morphology and structure of the Au/C catalysts was characterized by Inductively Coupled Plasma Optical Emission Spectroscopy (ICP-OES) and Field Emission Scanning Electron Microscopy (FESEM). The electrocatalytic properties of Au/C towards the oxidation of ethanol were investigated in alkaline medium by using cyclic voltammetry (CV).

It has been found that adding of halides enhanced electrocatalytic activity of Au/C catalysts as compare to that with the Au/C catalyst obtained by using Turkevich method without additives. The highest electrocatalytic activity showed Au/C catalyst, where KCl additive were used. In general, the Au/C catalysts, for which synthesis the halides were used showed 2-3 times higher electrocatalytic activity as compared to the Au/C catalyst synthesized without the use of additives.

Synthesis, Photocatalytic Properties and Langmuir-Blodgett Film Photoelectrochemical Behavior of CdS and CdSe Nanoparticles of Hydrophilic or Hydrophobic Organic Shell

Momoka Nagamine¹, Magdalena Osial², Pawel Krysiński², Justyna Widera-Kalinowska¹,

¹ *Department of Chemistry, Adelphi University, USA*

² *Faculty of Chemistry, University of Warsaw, Poland*

¹ *1 South Avenue, Garden City, NY 11530*

² *1 Pasteura Street, 02-093 Warsaw, Poland*

momokanagamine@mail.adelphi.edu

Quantum-dot-sensitized solar cells have gained growing attention as an alternative to existing photovoltaic technologies (1). In this research, n-type cadmium sulfide (CdS) and cadmium selenide (CdSe) nanoparticles with varying stabilizing shells were successfully synthesized, thus providing them with hydrophilic or hydrophobic properties. The as-synthesized nanoparticles with those properties were studied by SEM, DLS, and FT-IR analysis. Aqueous suspension of the hydrophilic nanoparticles was used for band gap evaluations and photocatalytic activity studies in the presence of methylene blue by means of UV-Vis spectroscopy. It is concluded that the synthesized nanoparticles catalyzed the degradation process of methylene blue under the UV light irradiation. Hydrophobic nanoparticles were spread onto the free aqueous interface of the Langmuir trough with subsequent Langmuir-Blodgett (2) transfer on the ITO surface. Photoelectrochemistry of such layers was then studied in relation to the number of transferred layers, and compared to the drop-casted nanoparticle samples. The results showed the increase of the current density with the increase of the transferred layers of nanoparticles.

References

- (1) Jin, H.; Choi, S.; Lee, H. J.; Kim, S. **2013**.
- (2) Osvaldo N.; Oliveira Jr.. **1992**, 22 (2).

Optimization of Calcination Temperature in Preparation of a High Capacity Li-rich Solid-Solution $\text{Li}[\text{Li}_{0.2}\text{Ni}_{0.18}\text{Co}_{0.03}\text{Mn}_{0.58}]\text{O}_2$ Material and Its Cathode Performance in Lithium Ion Battery

Fumihiro Nomura ¹, Takashi Tsuda ¹, Toyokazu Tanabe ¹, Takeo Ohsaka ², Futoshi Matsumoto ¹

¹ Department of Materials and Life Chemistry, Kanagawa University, 3-27-1, Rokkakubashi, Kanagawa-ku, Yokohama, Kanagawa 221-8686, Japan

² Research Institute for Engineering, Kanagawa University, 3-27-1, Rokkakubashi, Kanagawa-ku, Yokohama, Kanagawa 221-8686, Japan
e-mail address fmatsumoto@kanagawa-u.ac.jp

In previous paper [1], it has been reported that $\text{Li}[\text{Ni}_{0.208}\text{Li}_{0.183}\text{Co}_{0.033}\text{Mn}_{0.575}]\text{O}_2$ Li-rich solid-solution layered oxide (LLO) cathode (Li_2MnO_3 (55%) - $\text{LiNi}_{0.5}\text{Mn}_{0.5}\text{O}_2$ (35%) - $\text{LiNi}_{1/3}\text{Co}_{1/3}\text{Mn}_{1/3}\text{O}_2$ (10%)) exhibited the best performance as cathode material among the examined LLO cathode material of Li_2MnO_3 - $\text{LiCo}_{1/3}\text{Ni}_{1/3}\text{Mn}_{1/3}\text{O}_2$ - $\text{LiNi}_{0.5}\text{Mn}_{0.5}\text{O}_2$ for lithium ion battery. In order to improve its cathode performance more, calcination temperature was optimized. The cathode performance is sensitive to calcination temperature. The increase in the calcination temperature improved the discharge capacity, its discharge capacity retention and rate capability. However, upper 1000°C, the cathode performance was degraded. The structural analysis with transmission electron microscope (TEM, Fig. 1) and Rietveld analysis of XRD patterns indicated that the cation mixing between Li^+ on the 2c site and Ni^{2+} ions on the 2b site of the layered oxide structure was reduced at calcination temperature of 1000°C and ordering of Li^+ ions on the transition metal layer was improved, resulting in the improvement of cathode performance such as charge/discharge capacities, stability of charge/discharge capacities and rate capability. The other LLOs having near different composition were also prepared and tested. Even after optimal calcination was extracted, the discharge capacity of $\text{Li}[\text{Ni}_{0.208}\text{Li}_{0.183}\text{Co}_{0.033}\text{Mn}_{0.575}]\text{O}_2$ is the highest among all LLOs examined in this study.

[1] T. Tsuda, H. Kokubun, Y. Asaoka, K. Miyamoto, Y. Mochizuki, T. Gunji, T. Tanabe, S. Kaneko, T. Ohsaka, F. Matsumoto, ECS Transactions, 75(20) (2017) 173–187.

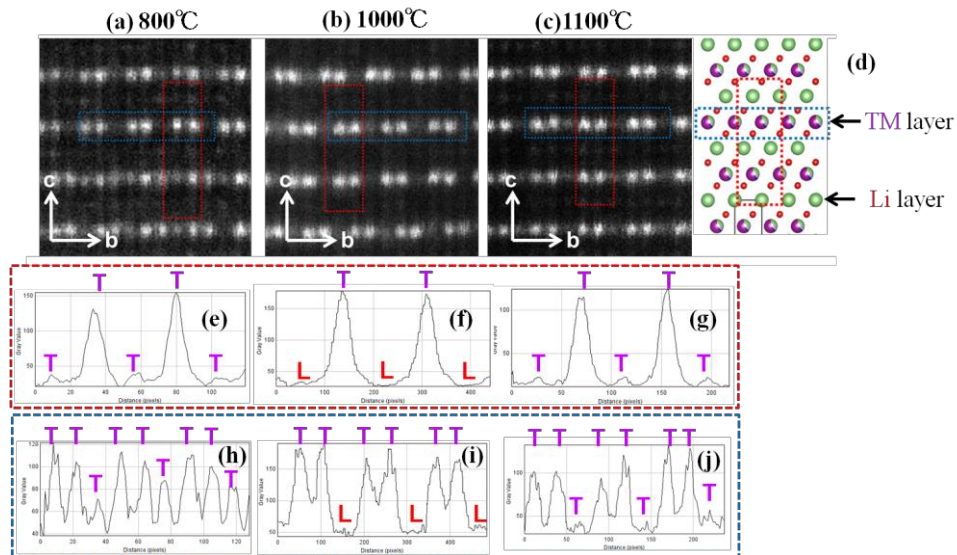


Figure 1 STEM-HAADF images of $\text{Li}[\text{Li}_{0.2}\text{Ni}_{0.18}\text{Co}_{0.03}\text{Mn}_{0.58}]\text{O}_2$ samples prepared at the calcination temperature of (a) 800, (b) 1000 and (c) 1100 °C. (d) Crystal structure of $\text{Li}[\text{Li}_{0.2}\text{Ni}_{0.18}\text{Co}_{0.03}\text{Mn}_{0.58}]\text{O}_2$ corresponding to the obtained STEM-HAADF images. (e-j) Intensity profiles corresponding to the dotted red and blue sections shown (e, h) in panel (a), (f, i) in panel (b) and (g, j) in panel (c).

Two Important Examples of Accurate Simulation of Complex Electrochemical Problems by KISSA-software

Irina Svir, Alexander Oleinick, Christian Amatore

*Ecole Normale Supérieure-PSL Research University, Département de Chimie, Sorbonne Universités-UPMC Paris 6, CNRS UMR 8640 PASTEUR
24 rue Lhomond, 75005 Paris, France
irina.svir@ens.fr*

KISSA-software (KISSA-1D for 1D- and KISSA-2D for 2D-electrode geometry) developed in our group, provides a general framework to treat electrochemical problems (by providing mechanism, rate constant, diffusion coefficients etc.) of any complexity in a user-friendly environment and returns the simulations results without any intervention into numerical part from the user side [1]. The accuracy of the numerical solution is guaranteed in KISSA by employment of a non-uniform and adaptive grid. The latter is constructed on the basis of a kinetic criterion (rather than on a gradient-based one as in other programs) and provides a high dynamic resolution at the acute reaction fronts which are automatically detected and followed by the program.

The efficiency of this strategy was proved by addressing such sophisticated problems as 1) simulation of reaction mechanisms leading to the emission of electrochemiluminescence (ECL) and 2) including the reactive dynamic adsorption.

In first example we consider the ECL systems which are possess extremely sharp reaction fronts since some reaction constants are close to the diffusion limit (either cation/anion radicals annihilation reactions or luminophor/co-reactant reaction). More precisely, for the ECL co-reactant system, such as alkyl amines / transition metal(II) complexes, it was shown via simulations with KISSA-1D that changes in ECL intensities emitted by these systems are much more dependent on the relative diffusivities of the two co-reactants than on the range of thermodynamic and kinetic rate constants that are possible to explore and vary [2].

In second example we present the electrochemical system with the reactive dynamic adsorption. The traditional views that contrast the important areas of electrocatalysis and molecular electrochemistry are challenged. By extending Laviron's seminal concept, we show that these two domains only represent idealized limits of a much broader continuum. More importantly, we show that electrochemical systems that apparently behave experimentally as if under diffusion control (i.e. systems that obey the founding molecular electrochemistry paradigm) may be controlled by electrocatalytic steps, that is, in which the activation of electroactive substrates exclusively occurs through adsorbed intermediates. This analysis is supported through quantitative experimental and theoretical investigations on the reduction of benzyl chloride at silver electrodes. At silver cathodes, the reduction wave of benzyl chloride as monitored at the usual scan rates is dramatically shifted to more positive potentials by about 0.5 V versus that at inert (e.g. glassy carbon) electrodes. This approach, which is based on the use of fast-scan cyclic voltammetry and simulations (KISSA-1D) [3], combined with our previous results from surface-enhanced Raman spectroscopy (SERS) and density functional theory (DFT) analysis, allow us to fully unravel the mechanistic origin of this dramatic effect and quantitatively validate this mechanism, which has eluded many research groups until now. In practice, this example provides a missing link between the traditional areas of electrocatalysis and molecular electrochemistry.

References:

[1] KISSAgroup: <http://kissagroup.com/>

[2] I. Svir, A. Oleinick, O.V. Klymenko, C. Amatore *ChemElectroChem* 2(2015) 811-818.

[3] O.V. Klymenko, O. Buriez, E. Labbe, D.P. Zhan, S. Rondinini, Z.Q. Tian, I Svir, C. Amatore. *ChemElectroChem* 1(2014) 227-240.